

	Preface	i
	Contents	iii
	Introduction	vi
	Experimental information	viii




Chapter 1

Discovery of the tube radial distribution phenomenon (TRDP) and development of tube radial distribution chromatography (TRDC)	1
---	---

	1.1 Novel capillary chromatography based on tube radial distribution of aqueous-organic mixture carrier solvents
---	--






Chapter 2

Observation and characterization of tube radial distribution phenomenon (TRDP)	11
--	----

	2.1 Observation and characterization of TRDP with fluorescence microscope-CCD camera system
	2.2 Observation and characterization of TRDP with various flow rates and capillary tube lengths
	2.3 Observation and characterization of TRDP with various inner diameters of capillary tubes

Chapter 3

Consideration of tube radial distribution phenomenon (TRDP)	46
---	----

	3.1 Experimental consideration through the phase diagram in TRDC and TRDP
	3.2 Experimental consideration through the phase diagram including solubility curves at different temperatures in TRDC and TRDP
	3.3 Experimental consideration through the phase diagram including tie lines and solubility curves in TRDC and TRDP
	3.4 Experimental consideration through the estimation of the dimensionless Weber number in TRDP
	3.5 Experimental consideration through the inner and outer phase formation in TRDP using various types of mixed solvent solutions

Chapter 4

Development of tube radial distribution chromatography (TRDC) 89

- ➔ 4.1 Analytical conditions and separation performance in TRDC
- ➔ 4.2 Influences of analyte injection volumes and concentrations in TRDC
- ➔ 4.3 Investigation of the composition for a ternary mixed solvent system in TRDC using PTFE capillary tube
- ➔ 4.4 Investigation of the composition for a ternary mixed solvent system in TRDC using fused-silica capillary tube
- ➔ 4.5 Fundamental experiments for tentative comparison of TRDC and capillary zone electrophoresis

Chapter 5

Effects of inner wall characteristics of capillary tubes on tube radial distribution chromatography (TRDC) 138

- ➔ 5.1 Effects of the inner-wall characteristics of the fused-silica capillary tube on TRDC
- ➔ 5.2 Effects of inner-wall-modified capillary tubes on TRDC
- ➔ 5.3 Effects of the inner wall materials of capillary tubes on TRDC

Chapter 6

Detection methods in tube radial distribution chromatography (TRDC) 158

- ➔ 6.1 Introduction of fluorescence and chemiluminescence detection to TRDC

Chapter 7

Microchip-tube radial distribution chromatography (microchip-TRDC) 168

- ➔ 7.1 Microchip-TRDC with chemiluminescence detection

Chapter 8

Examination of various types of analytes with tube radial distribution chromatography (TRDC) 179

- ➔ 8.1 Examination of carboxylated polymer particles as analytes with TRDC using a polyethylene capillary tube
- ➔ 8.2 Examination of polymer compounds as analytes with TRDC using a fused-silica capillary tube
- ➔ 8.3 Examination of metal compounds as analytes with TRDC

- ➔ 8.4 Examination of biomolecules as analytes with TRDC
- ➔ 8.5 Examination of lambda-DNA molecules as analytes with TRDC
- ➔ 8.6 Examination of metal ions as analytes with TRDC using an absorption reagent
- ➔ 8.7 Examination of dansyl-DL-amino acids as analytes with TRDC using cyclodextrin

➔ Chapter 9

Consideration of tube radial distribution chromatography (TRDC) 229

- ➔ 9.1 Experiments and consideration through temperature effect in TRDC
- ➔ 9.2 Experiments and consideration through adding surfactants to an analyte solution in TRDC
- ➔ 9.3 Theoretical consideration through outer phase formation in TRDC
- ➔ 9.4 Considerations through computer simulation in TRDC

➔ Chapter 10

Development of tube radial distribution extraction (TRDE) 258

- ➔ 10.1 TRDE using a microchip that has triple-branched microchannels
- ➔ 10.2 TRDE using a device having double tubes of different inner diameters

➔ Chapter 11

Development of tube radial distribution mixing (TRDM) 272

- ➔ 11.1 TRDM using a microchip having three-to-one line microchannels

➔ Chapter 12

Development of tube radial distribution reaction (TRDR) 284

- ➔ 12.1 TRDR featuring the liquid-liquid interface created with TRDP

➔ Chapter 13

Two-phase separation systems of mixed solutions and TRDP 296

- ➔ 13.1 Two-phase extraction of metal ions using a ternary water-acetonitrile-ethyl acetate mixed solution
- ➔ 13.2 TRDP created with an aqueous ionic liquid mixed solution
- ➔ 13.3 TRDP created with an aqueous non-ionic surfactant mixed solution
- ➔ 13.4 TRDP created with a fluorocarbon and hydrocarbon organic solvent mixed solution

- ➔ 13.5 TRDP created with a water-acetonitrile containing sodium chloride mixed solution

➔ Chapter 14

Applications and related techniques with microfluidic behavior of mixed solvent solutions 337

- ➔ 14.1 TRDP in bent and wound microchannels on microchips
- ➔ 14.2 Introduction of double tubes having different inner diameters to TRDC system
- ➔ 14.3 Capillary chromatography using an annular and sluggish flow in the ternary water–acetonitrile–ethyl acetate mixed solution
- ➔ 14.4 Microfluidic inverted flow of aqueous and organic solvent mixed solution in a microchannel

➔ Conclusions 366

➔ A list of the TRDP-related manuscripts reported by the author's group in chronological order 366

Investigation of
Tube **R**adial **D**istribution **P**henomenon
(**TRDP**)
and **I**ts **F**unction **A**pppearance

Kazuhiko Tsukagoshi



Preface

My laboratory has mainly investigated microflow analysis systems, such as microflow injection analysis, capillary chromatography using coated-capillary tubes, capillary electrophoresis, microchip capillary electrophoresis, and microchip flow analysis systems since 1995 in Doshisha University. I have been especially interested in chemiluminescence detection that are introduced into microflow analysis systems. I have done extensive research in this area especially for 20 years with my students in my laboratory. First of all, looking back upon very happy days in my laboratory, I greatly appreciate all my students; bachelor, master, and doctoral course students, as well as my co-workers in Doshisha University and in other universities, research institute centers, and companies.

Herein I describe a specific microfluidic behavior exhibited by mixed-solvent solutions in a microspace, coined as the tube radial distribution phenomenon (TRDP). The related manuscript was first reported in 2009. The specific fluidic behavior was observed in the following solution systems: ternary water–hydrophilic/hydrophobic organic solvents, water–surfactant, water–ionic liquid, water–hydrophilic solvents containing salts, and fluoruous/organic solvents. When the mixed homogeneous solutions were delivered into a microspace under certain conditions, the solvent molecules were radially distributed in the microspace, generating inner and outer phases with a kinetic liquid-liquid interface. The TRDP was fundamentally evaluated by fluorescence microscopy, phase diagram construction, and the elution behaviors of solutes in a capillary tube. A TRDP-based capillary chromatography, referred to as tube radial distribution chromatography (TRDC); where the outer phase serves as a pseudo-stationary phase under laminar flow conditions, has been developed as one of the applications of TRDP. We have also investigated TRDP-based extraction, chemical reaction, and mixing processes, coined as tube radial distribution extraction (TRDE), tube radial distribution reaction (TRDR), and tube radial distribution mixing (TRDM), respectively. The concept and experimental findings regarding TRDP, TRDC, TRDE, TRDR, and TRDM are described in this book.

In 2011 the author established “tube radial distribution phenomenon (TRDP) research center” in Doshisha University together with co-workers. In 2012, the manuscript (Y. Masuhara, et al., *Analytical Sciences*, **2012**, 28, 439) with the title “The Micro-Flow Reaction System Featured the Liquid-Liquid Interface Created with Ternary Mixed Carrier Solvents in a Capillary Tube”, was given an award of Hot Article Award Analytical Sciences. The review of the TRDP and the TRDP-related technologies that was written in Japanese and was published in 2013 (K. Tsukagoshi, *Bunseki Kagaku*, **2013**, 29, 393). Also, in 2013, the manuscript (M. Murakami, et al., *Analytical Sciences*, **2011**, 27, 793) of the title, Tube Radial Distribution Phenomenon of Ternary Mixed Solvents in a Microspace under Laminar Flow Conditions, was given the award

of Most Cited Paper Award of Analytical Sciences-2012. In January 2014, an English review of each of paper was invited to be included in the 30th anniversary publication of Analytical Sciences (K. Tsukagoshi, *Analytical Sciences*, **2014**, 30, 65). My students, 10 bachelors, 10 masters, and 2 doctorates, as well as my co-workers in and outside Doshisha University have begun this academic year's, 2014, research into, TRDP and other related studies.

Once again, I would like to offer my heartfelt thanks to all my students and co-workers for their experimental support and data, as well as the useful and helpful discussions regarding TRDP and it's related studies.



A handwritten signature in black ink that reads "K. Tsukagoshi". The signature is written in a cursive style with a large, sweeping initial "K".

Professor Kazuhiko Tsukagoshi

October 20, 2014

Professor Kazuhiko Tsukagoshi

*Department of Chemical Engineering and Materials Science, Doshisha University,
Kyotanabe, Kyoto 610-0321, Japan*

*Tube Radial Distribution Phenomenon Research Center, Doshisha University,
Kyotanabe, Kyoto 610-0321, Japan*

E-mail: ktsukago@mail.doshisha.ac.jp Tel & Fax: +81-75-462-4636

Contents

Preface	i
Contents	iii
Introduction	vi
Experimental information	viii

Chapter 1

Discovery of the tube radial distribution phenomenon (TRDP) and development of tube radial distribution chromatography (TRDC)	1
1.1 Novel capillary chromatography based on tube radial distribution of aqueous-organic mixture carrier solvents	

Chapter 2

Observation and characterization of tube radial distribution phenomenon (TRDP)	11
2.1 Observation and characterization of TRDP with fluorescence microscope-CCD camera system	
2.2 Observation and characterization of TRDP with various flow rates and capillary tube lengths	
2.3 Observation and characterization of TRDP with various inner diameters of capillary tubes	

Chapter 3

Consideration of tube radial distribution phenomenon (TRDP)	46
3.1 Experimental consideration through the phase diagram in TRDC and TRDP	
3.2 Experimental consideration through the phase diagram including solubility curves at different temperatures in TRDC and TRDP	
3.3 Experimental consideration through the phase diagram including tie lines and solubility curves in TRDC and TRDP	
3.4 Experimental consideration through the estimation of the dimensionless Weber number in TRDP	
3.5 Experimental consideration through the inner and outer phase formation in TRDP using various types of mixed solvent solutions	

Chapter 4

Development of tube radial distribution chromatography (TRDC)	89
4.1 Analytical conditions and separation performance in TRDC	
4.2 Influences of analyte injection volumes and concentrations in TRDC	
4.3 Investigation of the composition for a ternary mixed solvent system in TRDC using PTFE capillary tube	

- 4.4 Investigation of the composition for a ternary mixed solvent system in TRDC using fused-silica capillary tube
- 4.5 Fundamental experiments for tentative comparison of TRDC and capillary zone electrophoresis

Chapter 5

- Effects of inner wall characteristics of capillary tubes on tube radial distribution chromatography (TRDC) 138
- 5.1 Effects of the inner-wall characteristics of the fused-silica capillary tube on TRDC
 - 5.2 Effects of inner-wall-modified capillary tubes on TRDC
 - 5.3 Effects of the inner wall materials of capillary tubes on TRDC

Chapter 6

- Detection methods in tube radial distribution chromatography (TRDC) 158
- 6.1 Introduction of fluorescence and chemiluminescence detection to TRDC

Chapter 7

- Microchip-tube radial distribution chromatography (microchip-TRDC) 168
- 7.1 Microchip-TRDC with chemiluminescence detection

Chapter 8

- Examination of various types of analytes with tube radial distribution chromatography (TRDC) 179
- 8.1 Examination of carboxylated polymer particles as analytes with TRDC using a polyethylene capillary tube
 - 8.2 Examination of polymer compounds as analytes with TRDC using a fused-silica capillary tube
 - 8.3 Examination of metal compounds as analytes with TRDC
 - 8.4 Examination of biomolecules as analytes with TRDC
 - 8.5 Examination of lambda-DNA molecules as analytes with TRDC
 - 8.6 Examination of metal ions as analytes with TRDC using an absorption reagent
 - 8.7 Examination of dansyl-DL-amino acids as analytes with TRDC using cyclodextrin

Chapter 9

- Consideration of tube radial distribution chromatography (TRDC) 229
- 9.1 Experiments and consideration through temperature effect in TRDC
 - 9.2 Experiments and consideration through adding surfactants to an analyte solution in TRDC
 - 9.3 Theoretical consideration through outer phase formation in TRDC
 - 9.4 Considerations through computer simulation in TRDC

Chapter 10

- Development of tube radial distribution extraction (TRDE) 258
- 10.1 TRDE using a microchip that has triple-branched microchannels
 - 10.2 TRDE using a device having double tubes of different inner diameters

Chapter 11

- Development of tube radial distribution mixing (TRDM) 272
- 11.1 TRDM using a microchip having three-to-one line microchannels

Chapter 12

- Development of tube radial distribution reaction (TRDR) 284
- 12.1 TRDR featuring the liquid-liquid interface created with TRDP

Chapter 13

- Two-phase separation systems of mixed solutions and TRDP 296
- 13.1 Two-phase extraction of metal ions using a ternary water-acetonitrile-ethyl acetate mixed solution
 - 13.2 TRDP created with an aqueous ionic liquid mixed solution
 - 13.3 TRDP created with an aqueous non-ionic surfactant mixed solution
 - 13.4 TRDP created with a fluorocarbon and hydrocarbon organic solvent mixed solution
 - 13.5 TRDP created with a water-acetonitrile containing sodium chloride mixed solution

Chapter 14

- Applications and related techniques with microfluidic behavior of mixed solvent solutions 337
- 14.1 TRDP in bent and wound microchannels on microchips
 - 14.2 Introduction of double tubes having different inner diameters to TRDC system
 - 14.3 Capillary chromatography using an annular and sluggish flow in the ternary water–acetonitrile–ethyl acetate mixed solution
 - 14.4 Microfluidic inverted flow of aqueous and organic solvent mixed solution in a microchannel

Conclusions 366

A list of the TRDP-related manuscripts reported by the author's group in chronological order 366

Introduction

Microfluidic behaviors of solvents, confined in a microspace, e.g., microchannels in a microchip or capillary tubes, have been investigated since the nineteenth century, and are known to generate interesting and useful physical or hydrodynamic phenomena, such as electroosmotic and laminar flows. Electroosmotic flow was first reported in 1809 by Reuss along with electrophoresis [1]. In the last century, capillary electrophoresis [2], micellar electrokinetic chromatography [3], and capillary electrochromatography [4] were developed on the basis of electroosmotic flow. Such flow is instigated under high-applied voltages. Laminar flow was reported by Hagen in 1839 [5] and Poiseuille in 1841 [6]. Reynolds later studied turbulent and laminar flows and formulated a dimensionless parameter, known as the Reynolds number, in fluid mechanics [7]. In the last century, the application of laminar flow led to the development of hydrodynamic chromatography [8], wide-bore hydrodynamic chromatography [9], and field flow fraction chromatography [10].

Recently, the microfluidic behavior of solvents, based on electroosmotic and laminar flows, has been examined through the use of varied channel configurations, solvent flow rates, aqueous–organic solvent mixtures, and by introducing specific obstacles into the microchannel [11–13]. The fluidic behavior of solvents in the microchannel is related to the separation, diffusion, and reaction of the solutes. The development of novel uses for the microfluidic behaviors of solvents is both important and useful for designing microreactors or micro-total analysis systems [14,15]. We have reported an interesting, and unique, microfluidic behavior based on a mixed-solvents system confined in a microspace, which we named: the tube radial distribution phenomenon (TRDP). TRDP was observed in various types of mixed solutions, namely, ternary water–hydrophilic/hydrophobic organic solvents, water–surfactant, water–ionic liquid, water-hydrophilic solvents containing salts, and fluoruous/organic solvents. TRDP induces the formation of a kinetic liquid–liquid interface in a microfluidic flow, leading to the development of inner and outer phases.

A capillary chromatography system, operating under TRDP, where the outer phase functions as a pseudo-stationary phase under laminar flow conditions, has been developed. Such a system is referred to as tube radial distribution chromatography (TRDC). We have also applied TRDP to the extraction, chemical reaction, and mixing processes. The respective TRDP-based processes are coined as tube radial distribution extraction (TRDE), tube radial distribution reaction (TRDR), and tube radial distribution mixing (TRDM). Since the development of TRDP in 2009, the latter has been widely investigated in several areas pertaining to microfluidics. This book mainly reviews the development and application of TRDP, TRDC, TRDE, TRDR, and TRDM in a specific water–acetonitrile–ethyl acetate ternary system.

References

[1] F. F. Reuss, *Proceedings of the Imperial Society of Naturalists of Moscow*, **1809**, 2,

327.

- [2] J. W. Jorgenson and K. D. Lukacs, *Anal. Chem.*, **1981**, *53*, 1298.
- [3] S. Terabe, K. Otsuka, K. Ichikawa, A. Tsuchiya, and T. Ando, *Anal. Chem.*, **1984**, *56*, 111.
- [4] T. Tsuda, *Anal. Chem.*, **1987**, *59*, 521.
- [5] G. Hagen, *Ann. Phys. Chem.*, **1839**, *46*, 423.
- [6] R. B. Bird, W. E. Stewart, and E. N. Lightfoot, “*Transport Phenomena*”, 2nd ed., **2002**, Chapter. 2, (Wiley, Toronto, Canada).
- [7] O. Reynolds, *Phil. Trans. R. Soc.*, **1883**, *174*, 935.
- [8] H. Small, *J. Colloid Interface Sci.*, **1974**, *48*, 147.
- [9] M. Harada, T. Kido, T. Matsudo, and T. Okada, *Anal. Sci.*, **2005**, *21*, 491.
- [10] J. C. Giddings, M. N. Myers, G.-C. Lin, and M. Martin, *J. Chromatogr., A*, **1977**, *142*, 23.
- [11] Y. Kikutani, H. Hisamoto, M. Tokeshi, and T. Kitamori, *Lab Chip*, **2004**, *4*, 328.
- [12] A. Hibara, M. Tokeshi, K. Uchiyama, H. Hisamoto, and T. Kitamori, *Anal. Sci.*, **2001**, *17*, 89.
- [13] N. Kaji, Y. Okamoto, M. Tokeshi, and Y. Baba, *Chem. Soc. Rev.*, **2010**, *39*, 948.
- [14] H. Nakamura, Y. Yamaguchi, M. Miyazaki, H. Maeda, and M. Uehara, *Chem. Commun.*, **2002**, 2844.
- [15] H. Kawazumi, A. Tashiro, K. Ogino, and H. Maeda, *Lab Chip*, **2002**, *2*, 8.
- [16] N. Jinno, M. Hashimoto, and K. Tsukagoshi, *Anal. Sci.*, **2009**, *25*, 145.

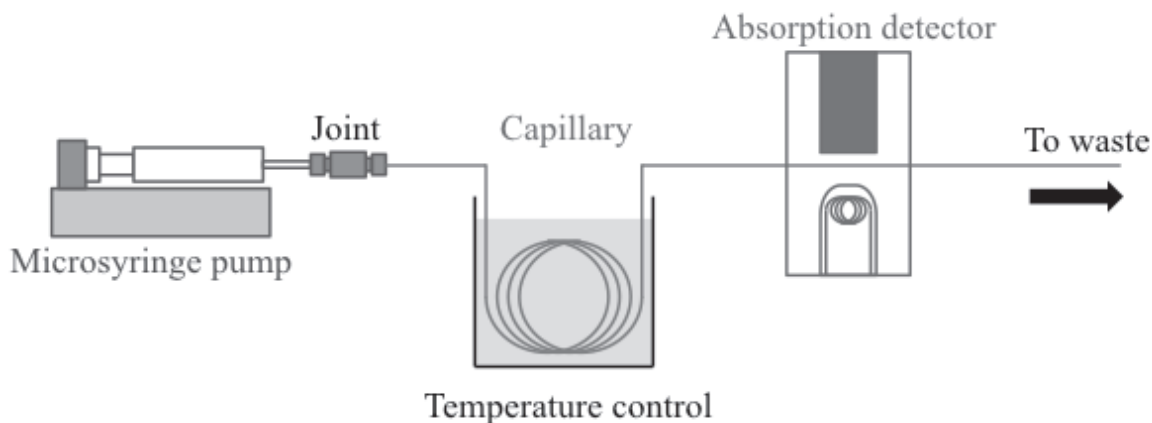
Experimental information

Water and reagents: Water was purified with an Elix 3 UV (Millipore Co., Billerica, MA). All reagents used were commercially available and of analytical grade.

Capillary tubes: A fused-silica capillary tube, a high-density polyethylene (PE) capillary tube, a polytetrafluoroethylene (PTFE) capillary tube, and a copolymer of (tetrafluoroethylene-perfluoroalcoxyethylene) (PTFE-PFAE) capillary tube were purchased from GL Science (Tokyo, Japan), Natume Co. (Tokyo, Japan), Yasaka Industries, Inc. (Tokyo, Japan), and Iwase Co. (Tokyo, Japan), respectively.

Microchips: A microchip made of glass and incorporating microchannel lines was acquired from Microchemical Technology (Kanagawa, Japan).

Tube radial distribution chromatography (TRDC) system: The system comprised a microsyringe pump (MF-9090; Bioanalytical Systems, Inc., West Lafayette, IN, USA) and an absorption detector (modified SPD-10AV spectrophotometric detector; Shimadzu Co., Kyoto, Japan), a fluorescence detector (modified RF-535 fluorescence detector; Shimadzu Co.), or a chemiluminescence (CL) detection (Model EN-21, Kimoto Electric Co., Ltd.) as main devices. The following figure shows a schematic diagram of typical TRDC system.

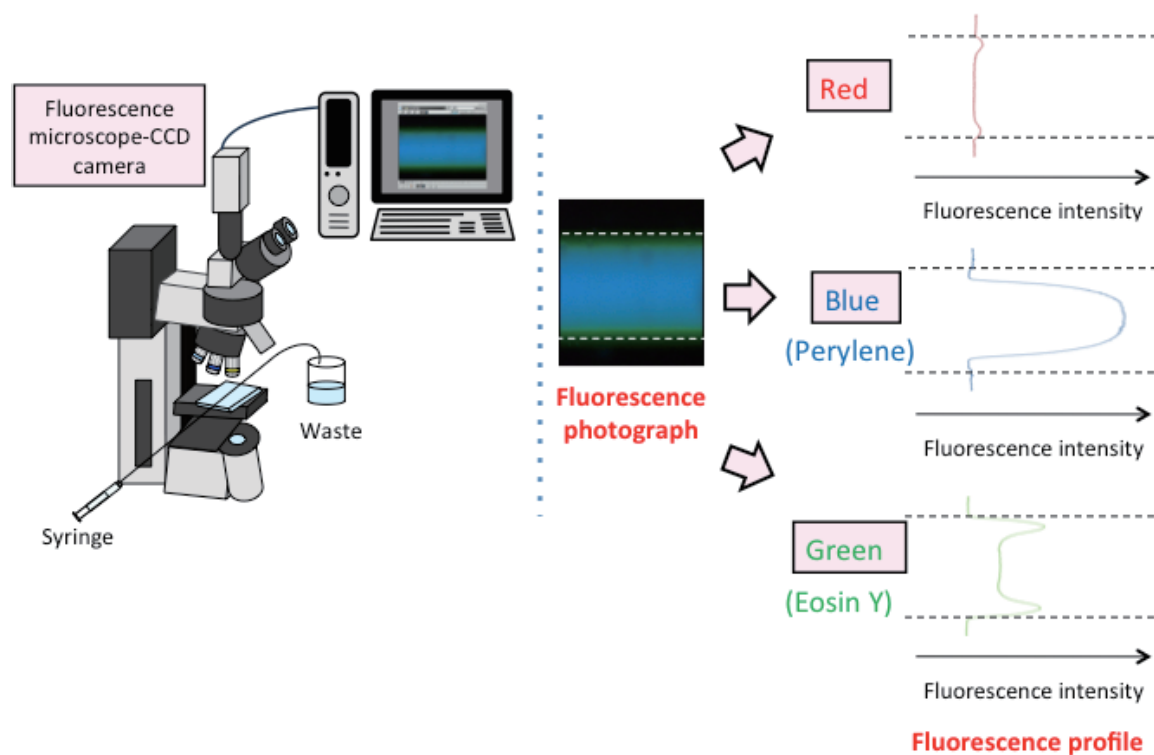


Fluorescence microscope-CCD camera system: A fluorescence microscope (BX51; Olympus, Tokyo, Japan) equipped with an Hg lamp and a filter (U-MWU2, ex 330–385 nm, em. >420 nm) and CCD camera (JK-TU53H; Toshiba, Tokyo, Japan) was operated in the system.

Fluorescence profiles: The obtained fluorescence images were transformed into line drawings in order to evaluate the color depth using a computer. The observed colors included red, green, and blue (RGB). The images principally consisted of blue and green because perylene and Eosin Y emit light at approximately 470 nm and 550 nm

respectively. The blue and green color depths were numerically expressed as digital data on a computer (with BMP2CSV free-software), after which the numbers were standardized to line drawing data to give fluorescence profiles (with Microsoft Excel).

The following figure shows a schematic diagram of fluorescence microscope-CCD camera and the transformation of fluorescence photograph to fluorescence profile through the computer.



Chapter 1 Discovery of the tube radial distribution phenomenon (TRDP) and development of tube radial distribution chromatography (TRDC)

The discovery of the tube radial distribution phenomenon (TRDP) and the development of tube radial distribution chromatography (TRDC), that is, TRDP-based capillary chromatography, were first reported in 2009. As this discovery was not confirmed by visual data, such as a fluorescence photograph through a fluorescence microscope-CCD camera system, strictly speaking, the hypothesis of TRDP might be a more suitable expression than the discovery, at least for the moment. The part of this chapter is reconstructed and rewritten based on the related manuscripts that have been published.^{1,2)}

1.1 Novel capillary chromatography based on tube radial distribution of aqueous-organic mixture carrier solvents

A capillary chromatography system was newly developed using open capillary tubes made of fused-silica, polyethylene, or poly(tetrafluoroethylene), and an aqueous-organic mixture (water-acetonitrile-ethyl acetate mixture) as a carrier solution. Model analyte mixture solutions, such as 2,6-naphthalenedisulfonic acid and 1-naphthol, Eosin Y and perylene, bis[*N,N*-bis(carboxymethyl)aminomethyl]fluorescein and 1,1-bi-2-naphthol, and 2,7-naphthalenedisulfonic acid and *p*-nitroaniline, were introduced into the capillary tube by gravity. The analyte solutions were subsequently delivered through the capillary tube with the carrier solution by a micro-syringe pump. The system worked under laminar flow conditions. The analytes were separated through the capillary tube and detected on-capillary by an absorption detector. For example, 2,6-naphthalenedisulfonic acid and 1-naphthol were detected in this order with a carrier solution of water-acetonitrile-ethyl acetate (volume ratio 15:3:2), but this order was reversed when a carrier solution of water-acetonitrile-ethyl acetate (volume ratio 2:9:4) was used. The other analyte solutions were similarly separated by the system and their elution times could be easily reversed by changing the component ratio of the solvents in the carrier solution.

Introduction

Capillary chromatography including capillary electrochromatography [1,2], micellar electrokinetic capillary chromatography [3,4], and capillary high-performance liquid chromatography using packed and monolithic capillary columns [5,6] have attracted a lot of attention in the analytical chemistry field as well as in separation science ever

since the last century. Most capillary chromatography systems feature rapid measurements, easy procedures, inexpensive and small apparatus, small sample volumes, and low costs. However, only a few new concepts concerned with capillary chromatography have been proposed in the last decade. In one example, wide-bore hydrodynamic chromatography [7,8] was carried out using an open capillary tube of fused-silica. Diffusive and non-diffusive analytes showed quite different elution behavior in the capillary tube under laminar flow conditions. However, these analytes were not completely separated using the principle of the method, i.e., the diffusive and non-diffusive analytes were overlapped on the chromatogram. In a second example, Tabata et al. have recently reported a capillary chromatography system based on the microphase separation of mixed solvents [9]. They described that when an acetonitrile-water mixture with suitable salt concentration was pumped into a fused-silica capillary with a negatively charged inner wall due to the dissociation of its silanol group, microphase separation occurred near the capillary wall, resulting in a water-enriched aqueous phase attached to the capillary inner wall. The mixture of hydrophilic and hydrophobic analytes was separated in this order using chromatography.

Here, a capillary chromatography system using open capillary tubes made of either fused-silica, polyethylene, or poly(tetrafluoroethylene) (PTFE), and a salt-free water-hydrophilic-hydrophobic organic solvent mixture carrier solution is described. In our previous communication,¹⁾ we briefly described the results of a fused-silica or polyethylene capillary tube that was applied to the system, and here we mainly report on the results concerning a PTFE capillary tube. Four analyte solution mixtures of hydrophilic and hydrophobic molecules (2,6-naphthalenedisulfonic acid and 1-naphthol, Eosin Y and perylene, bis[*N,N*-bis(carboxymethyl)aminomethyl]fluorescein and 1,1-bi-2-naphthol, and 2,7-naphthalenedisulfonic acid and *p*-nitroaniline) were examined in the present system and were found to separate well. Separation in the capillary chromatography system was performed without the use of any specific packed capillary tubes, additions of gels; surfactants; or salts, or high-voltage supply devices. Furthermore, the elution order of the analytes could be changed easily by altering the component ratio of the solvents in the carrier solution. The separation performance of the system is discussed based on the results obtained using fused-silica, polyethylene, and PTFE capillary tubes. The elution behavior of the analytes in the system provided some novel information that will be useful in separation science.

Experimental

A fused-silica capillary tube (50 μm i.d., 150 μm o.d.), a high-density polyethylene capillary tube (200 μm i.d., 500 μm o.d.), and a PTFE capillary tube (100 μm i.d., 200 μm o.d.) were used. The present capillary chromatography system was comprised of an open capillary tube, a micro-syringe pump, and an absorption detector. A fused-silica or

polyethylene capillary tube, 120 cm in length (effective length: 100 cm), and a PTFE capillary tube, 90 cm in length (effective length: 70 cm), were placed at room temperature in the system. Water-acetonitrile-ethyl acetate mixtures with volume ratios of 15:3:2, 4:7:9, 2:5:9, 2:7:4, and 2:9:4 were used as carrier solutions. Analyte solutions were prepared with the carrier solutions.

The analyte solution was introduced directly into the capillary inlet side for 20 s from a height of 20 cm for the fused-silica tube, for 5 s from a height of 20 cm for the polyethylene tube, or for 5 s from a height of 20 cm for the PTFE tube by the gravity method. After analyte injection, the capillary inlet was connected through a joint to a micro-syringe. The syringe was set on a micro-syringe pump. The carrier solution was fed in the capillary tube at a flow rate of $0.2 \mu\text{L min}^{-1}$ for fused-silica, $8.0 \mu\text{L min}^{-1}$ for polyethylene, or $0.8 \mu\text{L min}^{-1}$ for PTFE under laminar flow conditions. On-capillary absorption detection (232, 254, or 280 nm) was performed with the detector.

Results and discussion

Properties of PTFE capillary tube Although a PTFE capillary tube is useful and available for micro-flow separation systems because of its inert inner surface and flexibility [10,11], it should be noted that the crystallinity of the PTFE causes light scattering. Therefore, we first examined the optical properties of the PTFE capillary tube in the manner that follows. The PTFE capillary was fixed to the modified absorption detector. The capillary was filled with water, and absorption in the capillary tube was examined at 200-650 nm. The obtained results are shown in Fig. 1. The capillary showed maximum absorption at 200 nm which decreased with increasing wavelength. Absorption detection in the capillary chromatography system, particularly in the ultraviolet region, was disturbed by the innate light scattering properties of PTFE. However, by adjusting the apparent absorption due to the scattering of the tube to a baseline for measuring the absorption profile, compounds with absorption behavior such as the analytes used here were detected without any problems at wavelengths of 232, 254, or 280 nm.

Effects of the component ratio of the carrier on separation In our communication,¹⁾ a solution of 2,6-naphthalenedisulfonic acid (hydrophilic) and 1-naphthol (hydrophobic) was analyzed using the capillary chromatography system with open capillary tubes made of fused-silica or polyethylene. When using a water-rich carrier solution of water-acetonitrile-ethyl acetate with a volume ratio of 15:3:2 for both capillary tubes, the mixture of 2,6-naphthalenedisulfonic acid and 1-naphthol was separated through the open capillary tube and were detected in this order. On the other hand, using an organic solvent rich-carrier solution of water-acetonitrile-ethyl acetate with a volume ratio of 2:7:4 or 2:5:9 for fused-silica or polyethylene, respectively, they were detected with inverse elution times, i.e., 1-naphthol and 2,6-naphthalenedisulfonic were detected in this

order (data not shown). A solution of 2,6-naphthalenedisulfonic acid and 1-naphthol was also analyzed using the present system with an open PTFE capillary tube and an aqueous-organic carrier solution. The obtained absorption profiles are shown in Fig. 2 using three carrier solutions of water-acetonitrile-ethyl acetate with volume ratios of 15:3:2, 4:7:9, and 2:9:4. When using a water-rich carrier solution of water-acetonitrile-ethyl acetate with a volume ratio of 15:3:2, 2,6-naphthalenedisulfonic acid and 1-naphthol were separated through the open capillary tube and detected at ca. 6.8 and 8.5 min, respectively (Fig. 2 a). The components of the analytes, 2,6-naphthalenedisulfonic acid and 1-naphthol, in the profile were confirmed with individual absorption signals. Confirmation was performed for all experimental data shown in Figs. 2-4. On the other hand, using the organic solvent-rich carrier solution of water-acetonitrile-ethyl acetate with volume ratios of 4:7:9 and 2:9:4, the analytes were detected with inverse elution times. 1-Naphthol and 2,6-naphthalenedisulfonic acid were detected in this order at ca. 7.0 and 8.3 min for the carrier with a volume ratio of 4:7:9 (Fig. 2 b) and at ca. 7.1 and 8.9 min for the carrier with a volume ratio of 2:9:4 (Fig. 2 c). The separation behavior of the mixture of 2,6-naphthalenedisulfonic acid and 1-naphthol, including the reversibility of the elution times by changing the component ratio of the solvents in the carrier solution, was observed for fused-silica, polyethylene, and PTFE capillary tubes. Based on the obtained results, the properties of the capillary tube material, i.e., fused-silica, polyethylene, and PTFE, seemed to have little influence on the separation behavior of the analytes in the current capillary chromatography system.

Separation of the other analyte mixtures using a PTFE capillary tube Other mixtures of Eosin Y and perylene, bis[*N,N*-bis(carboxymethyl)aminomethyl]fluorescein and 1,1-bi-2-naphthol, as well as 2,7-naphthalenedisulfonic acid and *p*-nitroaniline were subjected to separation with the present system using the PTFE capillary tube using a water-rich carrier solution of water-acetonitrile-ethyl acetate (volume ratio 15:3:2). The obtained absorption profiles are shown in Fig. 3. In each profile, the hydrophilic Eosin Y, bis[*N,N*-bis(carboxymethyl)aminomethyl]fluorescein, or 2,7-naphthalenedisulfonic acid was eluted first, followed by the hydrophobic perylene, 1,1-bi-2-naphthol, or *p*-nitroaniline, with good separation. In addition, these mixtures were subjected to separation using the present system with an organic solvent-rich carrier solution of water-acetonitrile-ethyl acetate (volume ratio 2:9:4). The obtained absorption profiles are shown in Fig. 4. In each profile, the hydrophobic perylene, 1,1-bi-2-naphthol, or *p*-nitroaniline was eluted first, followed by the hydrophilic Eosin Y, bis[*N,N*-bis(carboxymethyl)aminomethyl]fluorescein, or 2,7-naphthalenedisulfonic acid, with good separation.

Elution times of the two analytes in the mixture A similar separation behavior for a mixture of 2,6-naphthalenedisulfonic acid and 1-naphthol was observed when open capillary tubes made of fused-silica, polyethylene, or PTFE were used. In addition, the four mixed analyte solutions, i.e., 2,6-naphthalenedisulfonic acid and 1-naphthol, Eosin Y and perylene, bis[*N,N*-bis(carboxymethyl)aminomethyl]fluorescein and 1,1-bi-2-naphthol, and 2,7-naphthalenedisulfonic acid and *p*-nitroaniline, were confirmed to be similarly separated with the capillary chromatography system using the PTFE capillary tube. That is, in all of the experiments using the three different types of capillary tubes and four different analyte mixtures, when a water-rich carrier solution, such as water-acetonitrile-ethyl acetate (volume ratio 15:3:2) was used, the hydrophilic compound was eluted earlier than the hydrophobic compound. Conversely, when a carrier solution with a large organic solvent component, such as water-acetonitrile-ethyl acetate (volume ratio 2:9:4) was used, the hydrophobic compound was eluted earlier than the hydrophilic compound. Thus, the elution order can be reversed easily by changing the component ratio of the solvents in the carrier solution in the three capillary tubes. The Reynolds number was estimated to be roughly < 1 under the present analytical conditions, confirming that the system worked under laminar flow conditions. Under these conditions, the linear velocity of the fluid in the capillary tube showed a parabolic curve; the linear velocity showed a maximum value around the middle of the capillary tube and decreased approaching the inner wall of the tube. Solutes that are diffusive or of low molecular weight are eluted from the tube with an average linear velocity and a Gaussian distribution [7,8]. The average linear velocities using the fused-silica, polyethylene, and PTFE capillary tubes were estimated to be 1.7, 4.2, and 1.7 mm s^{-1} , respectively, under the corresponding analytical conditions. As shown in Figs. 2-4 and discussed in our communication¹⁾, the elution times for the first peaks in the fused-silica, polyethylene, and PTFE capillary tubes were ca. 9.6, 4.0, and 6.9 min, respectively, showing no change in the carrier solution for the same capillary tube. Moreover, the elution times of the first peaks nearly corresponded to those calculated with the average linear velocities, and the second peaks were eluted with smaller velocities than the average linear velocities.

Consideration of separation performance Tabata et al. [9] reported a capillary chromatography system using an open fused-silica capillary tube, in which the inner wall was negatively charged due to the dissociation of silanol groups, and a water-acetonitrile mixture including sodium chloride with high concentration as the carrier. Although they separated the hydrophilic and hydrophobic molecules in this order, but could not change the order of elution, we have demonstrated the separation of a mixture of hydrophilic and hydrophobic molecules by capillary chromatography using open capillary tubes made of fused-silica, polyethylene, or PTFE, and a salt-free water-hydrophilic-hydrophobic organic solvent mixture carrier solution. Thus, we

determined that the negative charge due to the silanol groups on the inner wall plays no major role in creating a water-rich phase near the inner wall, at least in our present system. Furthermore, the elution times of the analytes in the present system can be easily reversed by changing the component ratio of the carrier solvents in all types of capillary tubes. In addition such a salt-free solvent mixture is easy to use in a capillary tube without any problems of salt deposition. Based on our results, we proposed that separation in the present capillary chromatography system was performed using the tube radial distribution of the aqueous-organic mixture solvents under laminar flow conditions, referred to here as a tube radial distribution chromatography (TRDC) system. Possible separation performance in the TRDC system using an open capillary tube and an aqueous-organic solvent mixture carrier solution is described as follows and illustrated in Fig. 5 (water-rich case in 5a and organic solvent-rich case in 5b). The linear velocity of the fluid in the capillary tube under laminar flow conditions is expressed as a parabolic curve in Fig. 5; however, the results in a water-organic solvent mixture carrier solution may deviate from an ideal parabolic curve. Water and organic solvents in the carrier solution are not dispersed uniformly in the capillary tube. Relative to the internal volume, the inner wall of the tube features an extremely large specific surface area. This leads to the generation of a water-rich phase and an organic solvent-rich phase based on a tube radial distribution of the aqueous-organic solvent mixture under laminar flow conditions. A major solvent phase forms around the middle of the tube, while a minor solvent phase forms near the inner wall. When a water-rich carrier solution is used, a major solvent phase or a water-rich phase forms around the middle of the tube (Fig. 5a). However, when an organic solvent-rich carrier solution is used, a major solvent phase or an organic solvent-rich phase forms around the middle of the tube (Fig. 5b). Such tube radial distribution of the solvent molecules in the carrier solution must be caused through a specific flow in the capillary tube under the laminar flow conditions. The specific microfluidic behavior of the solvents is called tube radial distribution phenomenon (TRDP). Subsequently, as the analyte mixtures consisted of typical hydrophilic and hydrophobic molecules, the former (2,6-naphthalenedisulfonic acid, Eosin Y, bis[*N,N*-bis(carboxymethyl)aminomethyl]fluorescein, and 2,7-naphthalenedisulfonic acid) is mainly dissolved or dispersed in the water-rich phase, while the latter (1-naphthol, perylene, 1,1-bi-2-naphthol, and *p*-nitroaniline) is dissolved in the organic solvent-rich phase, leading to tube radial distribution of analyte molecules in the capillary tube. In the case of a water-rich carrier solution, the hydrophilic analyte, which is dispersed in the water-rich phase of the major solvent phase (around the middle of the capillary tube), is eluted at a nearly average linear velocity. The hydrophobic analyte, which is dispersed in the organic solvent-rich phase of the minor solvent phase near the inner wall of the tube (pseudo-stationary phase), is eluted at a lower than average linear velocity (Fig. 5a). In the case of an organic solvent-rich carrier solution, the hydrophobic analyte dispersed in the organic solvent-rich phase of the major solvent

phase (around the middle of the capillary tube) is eluted with nearly average linear velocity. The hydrophilic analyte dispersed in the water-rich phase of the minor solvent phase near the inner wall of the tube (pseudo-stationary phase) is eluted with a lower than average linear velocity (Fig. 5 b). Therefore, the elution times of the analytes can be easily reversed by altering the component ratio of the solvents in the carrier solution. The separation in the TRDC was performed without using any special materials such as packed and monolithic capillary tubes or applying a high voltage for electrophoresis, as it is done in conventional capillary chromatography.

In conclusion, we developed a capillary chromatography system using an open capillary tube and an aqueous-organic mixture carrier solution that worked under laminar flow conditions. In contrast to conventional capillary electrochromatography, capillary electrophoresis, and capillary liquid chromatography, separation in this system was performed without the use of any specific materials such as packed capillary tubes, additives such as gels, surfactants, host molecules or salts, or high-voltage supply devices. We examined various mixtures consisting of hydrophilic and hydrophobic molecules in this chromatography system using fused-silica, polyethylene, or PTFE capillary tubes and a water-acetonitrile-ethyl acetate mixture carrier solution. The analytes were well separated through the capillary tubes and detected on-capillary by an absorption detector, and the elution times of the components could be reversed easily by changing the component ratio of the solvents in the carrier solution. The separation performance in the system was explained based on the tube radical distribution of the aqueous-organic mixture carrier solvents under laminar flow conditions.

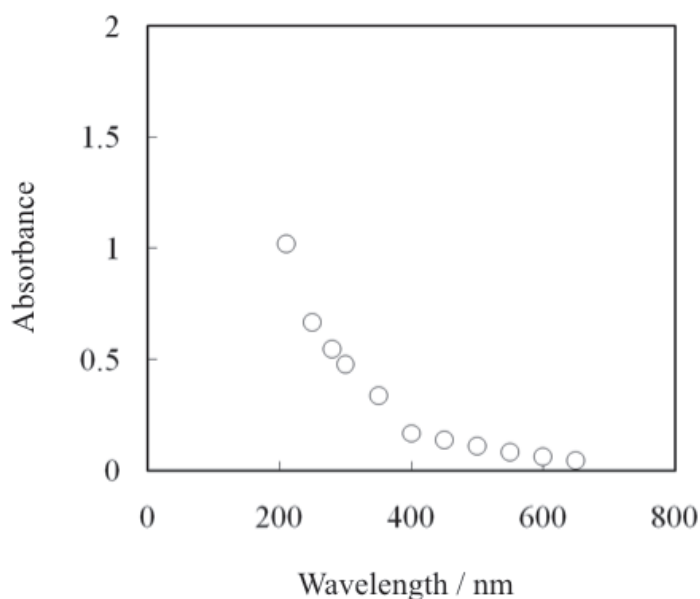


Figure 1. Relationship between detection wavelength and absorption in the PTFE capillary tube.

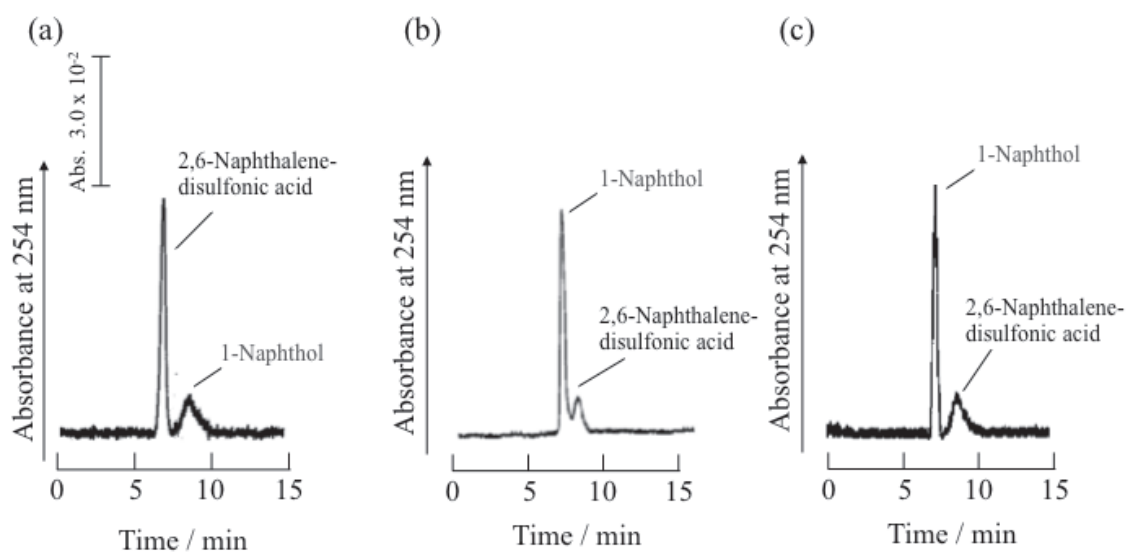


Figure 2. Absorption profiles of a mixture of 2,6-naphthalenedisulfonic acid and 1-naphthol by the current system using a PTFE capillary tube. Conditions: Capillary tube, 90 cm (effective length: 70 cm) of 100 μm i.d. PTFE; carrier, a) water-acetonitrile-ethyl acetate (15:3:2) mixture solution, b) water-acetonitrile-ethyl acetate (4:7:9) mixture solution, and c) water-acetonitrile-ethyl acetate (2:9:4) mixture solution; sample injection, 20 cm height (gravity) \times 5 s; flow rate, 0.8 $\mu\text{L min}^{-1}$; and analyte concentration, 1 mM each.

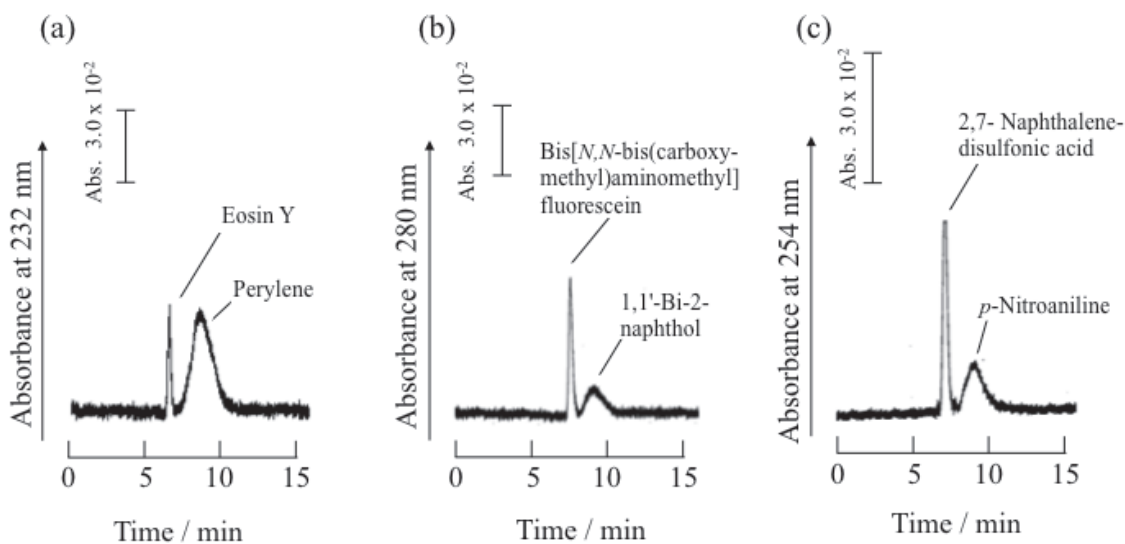


Figure 3. Absorption profiles of the mixtures using the current system with a water-rich carrier solution. a) Eosin Y and perylene, b) bis[*N,N*-bis(carboxymethyl)aminomethyl]fluorescein and 1,1-bi-2-naphthol, and c) 2,7-naphthalenedisulfonic acid and *p*-nitroaniline. Conditions: Capillary tube, 90 cm (effective length: 70 cm) of 100 μm i.d. PTFE; carrier, water-acetonitrile-ethyl acetate (15:3:2) mixture solution; sample injection, 20 cm height (gravity) \times 5 s; flow rate, 0.8 $\mu\text{L min}^{-1}$; and analyte concentration, 1 mM each.

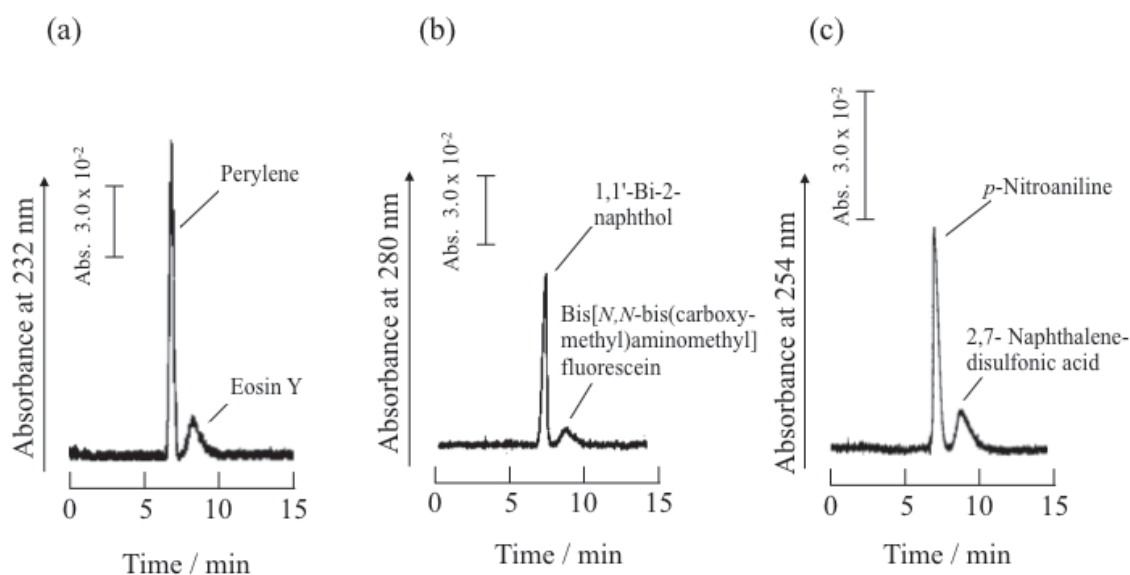
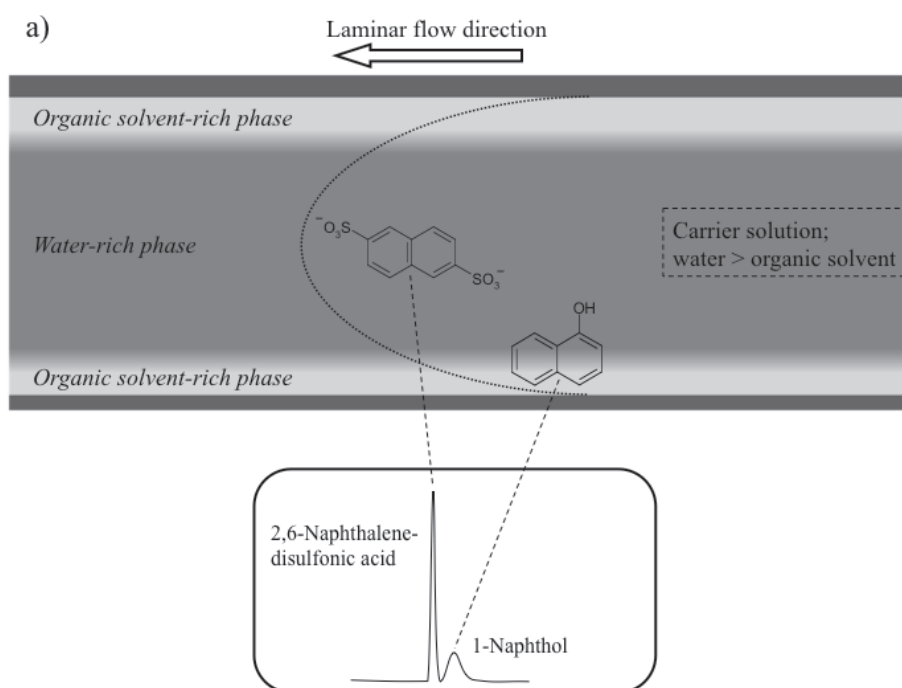


Figure 4. Absorption profiles of the mixtures using the current system with an organic solvent-rich carrier solution. a) Eosin Y and perylene, b) bis[*N,N*-bis(carboxymethyl)aminomethyl]fluorescein and 1,1-bi-2-naphthol, and c) 2,7-naphthalenedisulfonic acid and *p*-nitroaniline. Conditions: Capillary tube, 90 cm (effective length: 70 cm) of 100 μm i.d. PTFE; carrier, water-acetonitrile-ethyl acetate (2:9:4) mixture solution; sample injection, 20 cm height (gravity) \times 5 s; flow rate, 0.8 $\mu\text{L min}^{-1}$; and analyte concentration, 1 mM each.



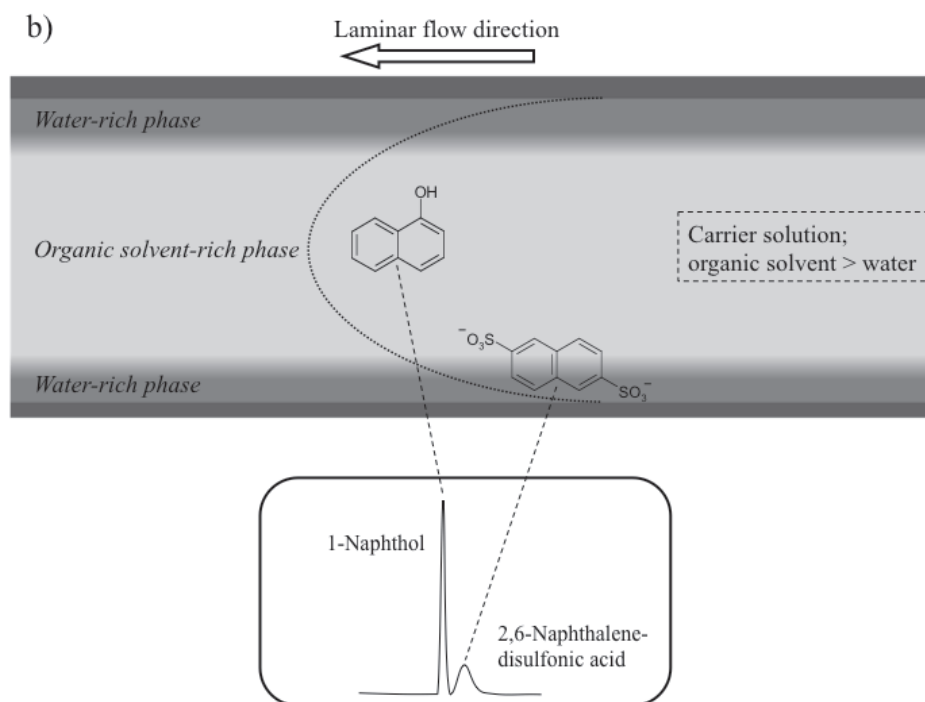


Figure 5. Illustration of separation performance in the capillary chromatography system. a) Water-rich carrier solution and b) organic solvent-rich carrier solution.

References

- [1] M. C. Breadmore, J. R. E. Thabano, M. Dawod, A. A. Kazarian, J. P. Quirino, and R. M. Guijt, *Electrophoresis*, **2009**, *30*, 230.
- [2] I. Miksik and P. Sedlakova. *J. Sep. Sci.*, **2007**, *30*, 1686.
- [3] M. Silva, *Electrophoresis*, **2009**, *30*, 50.
- [4] S. K. Poole and C. F. Poole, *J. Chromatogr. A*, **2008**, *1182*, 1.
- [5] M. C. Jung, N. Munro, G. Shi, A. C. Michael, and S. G. Weber., *Anal. Chem.*, **2006**, *78*, 1761.
- [6] J. Urban and P. Jandera, *J. Sep. Sci.*, **2008**, *31*, 2521.
- [7] M. Harada, T. Kido, T. Masudo, and T. Okada, *Anal. Sci.*, **2005**, *21*, 491.
- [8] K. Tsukagoshi, S. Ishida, and R. Nakajima, *J. Chem. Eng. Jpn.*, **2008**, *41*, 130.
- [9] M. Tabata, Y. G. Wu, T. Charoenraks, and S. S. Samarantunga, *Bull. Chem. Soc. Jpn.*, **2006**, *79*, 1742.
- [10] M. Macka, W-C. Yang, P. Zakaria, A. Shitangkoon, E. F. Hilder, P. Andersson, P. Nesterenko, and P. R. Haddad, *J. Chromatogr. A*, **2004**, *1039*, 193.
- [11] K. Tsukagoshi, S. Ishida, Y. Oda, K. Noda, and R. Nakajima, *J. Chromatogr. A*, **2006**, *1125*, 144.

Chapter 2 Observation and characterization of tube radial distribution phenomenon (TRDP)

Tube radial distribution phenomenon (TRDP), including inner and outer phase formation, was created in various types of microspaces, such as microchannels on a microchip and capillary tubes, under laminar flow conditions. The TRDP was observed with fluorescence photographs through a fluorescence microscope-CCD camera system, and mainly characterized with the elution behavior of analytes in the TRDP-based chromatographic separation system, that is, tube radial distribution chromatography (TRDC). The part of this chapter is reconstructed and rewritten based on the related manuscripts that have been published.^{6,14,17,38)}

2.1 Observation and characterization of TRDP with fluorescence microscope-CCD camera system

We developed a capillary chromatography system by using an open capillary tube made of fused silica, polyethylene, or polytetrafluoroethylene, and a water-hydrophilic/hydrophobic organic mixture carrier solution, called tube radial distribution chromatography (TRDC) system. Comparing with chromatograms obtained via the TRDC system, fluorescence photographs and profiles of the fluorescent dyes dissolved in the carrier solvents in capillary tubes were observed under laminar flow conditions. The chromatograms were obtained for a model mixture analyte consisting of 1-naphthol and 2,6-naphthalenedisulfonic acid with the TRDC system, by using a fused-silica capillary tube and a water–acetonitrile–ethyl acetate carrier solution. By altering the carrier flow rates, we were able to examine the fluorescence both the photographs as well as the profiles of the dyes, perylene and Eosin Y, which were dissolved in the carrier solvents in the capillary tube with the use of a fluorescence microscope equipped with a CCD camera. As confirmed by fluorescence observations, the major inner and minor outer phases generated in the capillary tube were based on the tube's radial distribution of the carrier solvents. We designed and manufactured a microchip incorporating microchannels in which three narrow channels combined to form one wide channel. When the carrier solvents containing the dyes were fed into the channels, the inner and outer phase generations were also observed in the narrow and wide channels, supporting our previous conclusions concerning the tube radial distribution phenomenon (TRDP) of the solvents.

Introduction

Analytical methods using capillary tubes, usually composed of fused silica, have attracted great interest over the last century. Well-known methods include capillary electrophoresis [1,2], capillary electrochromatography [1,3], micellar electrokinetic capillary chromatography [4,5], and high-performance liquid capillary chromatography using packed and monolithic columns [3,6]. However, only a few new concepts concerning capillary chromatography have been reported in the last decade [7,8]. Related research has been discussed in detail in our papers.^{2,10)} We have developed a capillary chromatography system using an open capillary tube and a water-hydrophilic/hydrophobic organic mixture carrier solution. This system works under laminar flow conditions and requires no packed reagents in the capillary tube, nor does it require the application of high voltage to the ends of the tube. Such a system is called a tube radial distribution chromatography (TRDC) system.

The experimental device and data in the TRDC system have the following features: (1) various usable types of capillary tubes, including fused-silica, polyethylene, and polytetrafluoroethylene; (2) an aqueous-organic (homogeneous) carrier solution in which water, hydrophilic, and hydrophobic organic solvents must be delivered into the capillary tube under laminar flow conditions; (3) easily reversible elution times of hydrophobic and hydrophilic analytes, changed by the component ratios of the carrier solvents, e.g., an organic solvent-rich carrier solution (water–acetonitrile–ethyl acetate, 3:8:4 volume ratio) and a water-rich carrier solution (water–acetonitrile–ethyl acetate, 15:3:2 volume ratio); and (4) a first peak with nearly the average linear velocity and with subsequent peaks eluted with velocities at lower than the average linear velocity under laminar flow conditions in both the organic solvent-rich and the water-rich carrier solutions.

We delivered carrier solvents containing fluorescent dyes into a microchannel in a microchip, and observed the fluorescence photographs of the dyes using a fluorescence microscope equipped with a CCD camera.⁶⁾ We found that the dyes dissolved in the carrier solution were distributed radially, based on their hydrophilic or hydrophobic natures in the microchannel in the microchip. However, fluorescence photographs in capillary tubes that were actually used in the TRDC system have yet to be examined. As more information concerning the TRDC system is necessary to confirm and further discuss the TRDP of the carrier solvents in a capillary tube, direct fluorescence observations in the capillary tube in which the TRDC mode is being undertaken would provide visible information, so together with chromatographic data, it would be very beneficial to the TRDC investigation.

Here, we examined separation performances in the TRDC system from the chromatograms obtained for model mixture analytes, and the fluorescence photographs and profiles obtained through a fluorescence microscope equipped with a CCD camera in a fused-silica capillary tube that was used under the TRDC separation mode. Furthermore, we redesigned the microreactor, incorporating

microchannels. The distribution phenomena of the carrier solvents that were fed into the channels under laminar flow conditions were examined with a fluorescence microscope equipped with a CCD camera.

Experimental

Materials Fused-silica capillary tubes (75 μm i.d.) were used. Fig. 1 illustrates the microchip that we designed. The three narrow channels (each 100 μm -wide \times 40 μm -deep) combined to form one wide channel (300 μm -wide \times 40 μm -deep) in the microchip. Herein, we designate these channels as channels N1–N3 and channel W, respectively. Also, the combining points are designated as points 1 and 2, respectively, as shown in Fig. 1.

TRDC system with absorption detection An open, fused-silica capillary tube (75 μm i.d., 120 cm length; 100 cm effective length), a microsyringe pump, and an absorption detector made up the TRDC system with absorption detection.^{2,10} The tube temperature was controlled by immersing the capillary tube in water maintained at 15 °C in a stirred beaker. We used water–acetonitrile–ethyl acetate mixtures in volume ratios of 3:8:4 and 15:3:2 as carrier solutions. We prepared analyte solutions, including 1-naphthol and 2,6-naphthalenedisulfonic acid, with the carrier solutions. The analyte solution was introduced directly into the capillary inlet side via the gravity method (20 cm height for 30 s). After analyte injection, the capillary inlet was connected through a joint to a microsyringe. The syringe was set on the microsyringe pump. The carrier solution was fed into the capillary tube at a controlled flow rate (0.8 $\mu\text{L min}^{-1}$) under laminar flow conditions. We performed on-capillary absorption detection (254 nm) with the detector.

Fluorescence microscope equipped with a CCD camera system We set up a fused-silica capillary tube the same size (75 μm i.d., 120 cm length) as that of the TRDC system with absorption detection, and a microchip incorporating the microchannels for the fluorescence microscope-CCD camera system. The fluorescence in the capillary tube was mainly monitored at approximately 100 cm from the capillary inlet (the focus depth, ca. 6.1 μm , under the present conditions in the microscope device was adjusted to the center of the capillary tube), and the fluorescence in the microchannel was monitored around the combining points using a fluorescence microscope equipped with an Hg lamp and a filter and CCD camera. The organic solvent-rich carrier solution (water–acetonitrile–ethyl acetate; 3:8:4 volume ratio) contained 0.1 mM perylene and 1 mM Eosin Y, while the water-rich carrier solution (water–acetonitrile–ethyl acetate; 15:3:2 volume ratio) contained 1 mM Eosin Y (perylene was little dissolved in this solution). We delivered the carrier

solution into the capillary tube, or into the microchannel at a definite flow rate using the microsyringe pump. The fluorescence photographs thus obtained were also transformed into line drawings to assess color depth using a computer. The colors observed on the photographs were divided into red, green, and blue (RGB). The photographs mainly consisted of blue and green because perylene and Eosin Y emit light at approximately 470 and 550 nm, respectively. Blue and green color depths were expressed numerically as digital data on a computer, and finally, the numbers were standardized to the line drawing data to give the fluorescence profiles.

Results and discussion

Chromatograms obtained with the TRDC system with absorption detection

We analyzed a model mixture solution of 1-naphthol and 2,6-naphthalenedisulfonic acid by using the present TRDC system with absorption detection. Fig. 2 shows the obtained chromatograms. Fluorescence photographs and profiles in the capillary tubes are examined under the same analytical conditions as those acquired using the TRDC system in the following sections. By using the organic solvent-rich carrier solution of water–acetonitrile–ethyl acetate in a volume ratio of 3:8:4, the mixture of 1-naphthol and 2,6-naphthalenedisulfonic acid was separated through the open capillary tube and detected in the stated order (Fig. 2a). In contrast, using the water-rich carrier solution of water–acetonitrile–ethyl acetate in a volume ratio of 15:3:2, the mixture solution was separated and detected with inverse elution times, i.e., 2,6-naphthalenedisulfonic acid and 1-naphthol were detected in this order (Fig. 2b). We confirmed the components of the analytes on the chromatograms from their individual absorption signals. In both chromatograms, we detected the first peaks with elution times roughly corresponding to the average linear velocities under laminar flow conditions, and the second peaks were eluted with velocities below the average linear velocities. When we used the organic solvent-rich carrier solution, the comparatively hydrophobic analyte was eluted first. In contrast, when we used the water-rich carrier solution as the carrier solution, the comparatively hydrophilic analyte was eluted first. That is, the chromatograms clearly indicated reversible elution times, by altering the component ratio of the solvents in the carrier solution. The results shown in Fig. 2 are consistent with the tube radial distribution behavior of the carrier solvents in the TRDC system that we proposed in our reports earlier. In addition, as mentioned in the Introduction, the outer phase in the TRDC system works as a stationary phase in the usual chromatography. But the outer phase in the TRDC is very specific as a stationary phase; it comprises the carrier solvents, organic solvent-rich or water-rich. So, the outer phase in the system features large diffusion coefficient and large thickness of μm order, compared to the usual stationary phase in chromatography. The large diffusion coefficient and thickness of the outer phase that works as a stationary phase in the TRDC system might lead to

the broadening in the second peaks as shown in Fig. 2.

Fluorescence photographs and profiles of the dyes in a capillary tube We examined the fluorescence photographs and profiles of the fluorescent dyes dissolved in the aqueous-organic solvent mixture carrier solution in the microchannels (the cross-sectional view was a rectangle, 100 μm -wide \times 40 μm -deep) in a microchip through the fluorescence microscope equipped with a CCD camera. We reported the preliminary data in our communication.⁶⁾ Here, we attempted to examine the fluorescence photographs and profiles in the fused-silica capillary tube, although the cross section of the tube (circular) made it difficult to observe them compared to the microchannels (rectangular). The experiment using the fluorescence-CCD camera system with the fused-silica capillary tube was performed under the same analytical conditions, including the capillary tube length, the tube inner diameter, and the flow rate, as the TRDC system with absorption detection to give the chromatograms shown in Fig. 2. Fig. 3 depicts the fluorescence photographs and profiles observed for the fused-silica capillary tube in which the dye-containing aqueous-organic solvent mixture carrier solutions were delivered. These solutions were observed in the capillary tube using the TRDC analytical mode. Fluorescence photographs and profiles for the organic solvent-rich carrier solution showed that the hydrophobic perylene molecule (blue) was distributed around the center of the capillary tube and away from the inner wall of the tube, while the hydrophilic Eosin Y molecule (green) was distributed near the tube's inner wall (Fig. 3a). In contrast, fluorescence photographs and profiles for the water-rich carrier solution showed that Eosin Y was distributed around the center of the capillary tube (Fig. 3b). Due to the low solubility of perylene, we were unable to obtain any information regarding its behavior in a water-rich carrier solution. We could not obtain any information regarding the behavior of perylene in the water-rich carrier solution because of its very low solubility in that solution. The tube radial distribution of perylene and Eosin Y present in the carrier solution thus confirmed the partition reversal between the organic solvent-rich and water-rich carrier solutions in the fused-silica capillary tube (Fig. 3). Furthermore, using the same analytical conditions, we tried to observe the fluorescence photographs and profiles from other parts of the capillary tube (effective lengths of 30 and 60 cm). Under the same analytical conditions. The obtained fluorescence photographs and profiles obtained from this further inquiry are shown in Fig. 4. These data allowed us to confirm the tube radial distribution of the fluorescence dyes in the capillary tube at the effective lengths of 30, 60 and even 100 cm. The distribution behavior observed for the fluorescent dyes dissolved in the carrier solution in the capillary tube was consistent with the tube radial distribution of the solvent molecules proposed for the TRDC system. That is to say, the distribution of perylene and Eosin Y at the center

of the capillary tube, or near its inner wall supports the non-uniform dispersion of the aqueous and organic components of the carrier solutions in the capillary tube in the TRDC system. They each generate a major inner phase (organic solvent-rich or water-rich) and a minor outer, or capillary wall phase (water-rich or organic solvent-rich) in the capillary tube. As a result, the analytes are distributed between the inner and outer phases depending on their natures and are separable via chromatography, corresponding to the chromatograms shown in Fig. 2. In our paper,¹¹⁾ we examined the mixture solution of perylene and Eosin Y as an analyte solution using the TRDC system equipped with a fluorescence or chemiluminescence detector. Perylene and Eosin Y were separated and detected in this order with the organic solvent-rich carrier solution, and were eluted in the reverse order with the water-rich carrier solution. The chromatograms data also verified that perylene and Eosin Y acted as hydrophobic and hydrophilic molecules, respectively, in the ternary mixed carrier solutions in the TRDC system.

Effects of flow rates on the tube radial distribution of the dyes in the capillary tube

We examined the effects of flow rate on the tube radial distribution of the dyes in the capillary tube using an organic solvent-rich carrier solution containing perylene and Eosin Y. The fluorescence photographs and profiles were observed for the capillary tube where the dye-containing organic solvent-rich carrier solution was delivered at flow rates varying from 0.5 to 3.0 $\mu\text{L min}^{-1}$. Fig. 5 summarizes these images. The observed fluorescence photographs and profiles showed that the hydrophobic perylene molecule (blue) was distributed around the center of the tube, while the hydrophilic Eosin Y molecule (green) was distributed near the tube's inner wall over the flow rates between 0.5 and 2.0 $\mu\text{L min}^{-1}$. In contrast, we did not observe such a tube radial distribution of the dyes dissolved in the carrier solution at flow rates of 2.5 and 3.0 $\mu\text{L min}^{-1}$. The fluorescence photographs and profiles clearly confirmed that the carrier solution in the capillary tube was heterogeneous for flow rates 0.5 – 2.0 $\mu\text{L min}^{-1}$ and homogeneous for flow rates of 2.5 and 3.0 $\mu\text{L min}^{-1}$. The degree of the flow rate or pressure in capillary tubes under laminar flow conditions together with the component ratios of the carrier solvents must have important roles in determining the tube radial distribution of the carrier solvents in the TRDC system.

Fluorescence photographs and profiles of the dyes dissolved in the water–acetonitrile mixture carrier solution without ethyl acetate

We confirmed that the analytes were not separated on the chromatograms using any water–acetonitrile mixture carrier solutions that did not include ethyl acetate in all types of capillary tube, i.e., fused silica, polyethylene, or polytetrafluoroethylene. Here, fluorescence photographs and profiles of the dyes dissolved in the water–acetonitrile carrier

solution without ethyl acetate were also examined through the fluorescence microscope equipped with a CCD camera under the same analytical conditions as those in Figs. 2 and 3. We did not observe the tube radial distribution of the carrier solvents for the water–acetonitrile carrier solution without ethyl acetate at any flow rate. Fig. 6 shows a typical fluorescence photograph and profile. The hydrophobic organic solvent ethyl acetate was necessary for the preparation of an aqueous-organic mixture carrier solution in the TRDC system.

Fluorescence photographs of the dyes in the microchip

The organic solvent-rich carrier solution (water–acetonitrile–ethyl acetate, 3:8:4 volume ratio) containing Eosin Y and perylene was delivered into a newly designed microchip, from the channels (N1–N3) to the one wide channel, channel W, at a flow rate of $5.0 \mu\text{L min}^{-1}$ for each channel N1–N3. We observed the fluorescent dyes dissolved in the aqueous-organic solvent mixture in the microchannels, and monitored them with the microscope-CCD camera system. Fig. 7a depicts the obtained fluorescence photograph of the dyes in the channel together with its analytical conditions. The photograph proves that in each narrow channel, channel N1–N3, perylene molecule (blue) was distributed around the center of the channel and away from the channel inner wall, while Eosin Y molecule (green) was distributed near the channel's inner wall. The distribution phenomena of the carrier solvents fed into the microchannels clearly existed under laminar flow conditions in each narrow channel, channels N1–N3. The flow rate of $5.0 \mu\text{L min}^{-1}$ (the linear velocity of 125 cm min^{-1}) in the microchannels were larger than the flow rate of $2.5 \mu\text{L min}^{-1}$ (the linear velocity of 57 cm min^{-1}) in the capillary tube that did not provide the formation of the inner and outer phases in the tube. The phase formation must be influenced by cross sectional view, flow rate (or linear velocity), and pressure in a channel or tube. Actually we confirmed that flow rates larger than $50 \mu\text{L min}^{-1}$ in the microchannels could not form stable phase formations including the inner and outer phases in the microchannels. We observed an interesting behavior for the minor outer phases in channel N2 and for the minor outer phases in channels N1 and N3, which were close to channel N2. The minor outer phases in channel N2 combined with the minor outer phases in channels N1 and N3 at points 1 and 2, respectively. That is, the two minor outer phases, combining channel N1 and channel N2, or channel N2 and channel N3, combined at respective combining points, point 1 and point 2. These combined minor outer phases were consecutively delivered into the wide channel under laminar flow conditions, as they were diffused in channel W step by step. Finally, the combined minor outer phases disappeared at a distance around ca. 10 mm from the points 1 and 2 in channel W. The organic solvent-rich carrier solution containing the dyes was also delivered into the microchip at a low flow rate

of $2.0 \mu\text{L min}^{-1}$ for each channel N1–N3. We observed the fluorescent dyes dissolved in the aqueous-organic solvent mixture in the microchannels, and monitored them with the microscope-CCD camera system. Fig. 7b shows the obtained fluorescence photograph of the dyes in the channels. The observed fluorescence photograph obtained at a flow rate of $2.0 \mu\text{L min}^{-1}$ was similar to that at a flow rate of $5.0 \mu\text{L min}^{-1}$, except for the combination of the minor outer phases around the combining points. Both of the minor outer phases in channel N2 were combined with the minor outer phases in channels N1 and N3 that were close to channel N2 at points 1 and 2, respectively. After the two minor outer phases were, respectively, combined at their combining points, the combined phases formed oval balls at points 1 and 2, as shown in Fig. 7b. After a time, the balls were released from the points and were delivered into channel W under laminar flow conditions. They diffused into channel W and finally disappeared. The fluorescence photographs of the dyes dissolved in the solvents strongly supported the fact that the tube radial distribution of the ternary mixed carrier solvents was carried out in micro-spaces such as the capillary tubes and microchannels, under laminar flow conditions.

In conclusion, the inner and outer phase formation, based on the tube radial distribution of the carrier solvents, was considered through the elution behavior of the analytes on the chromatograms, and the distribution of the dyes dissolved in the aqueous-organic solvent mixture carrier solution in the capillary tube. We observed the tube radial distribution of the solvents, TRDP, through the fluorescent dyes in the real capillary tubes under various analytical conditions. Furthermore, when the carrier solvents containing the dyes were fed into the microchannels in the microchip, we also observed the distribution phenomena of the carrier solvents, TRDP, in the microchannels, including both the narrow and wide scales. The fluorescence data obtained experimentally were consistent with the separation performance based on the tube radial distribution of the carrier solvents. Such visual data of fluorescence in the capillary tube and the microchannels should be a useful, effective, and powerful tool for TRDP and TRDC study.

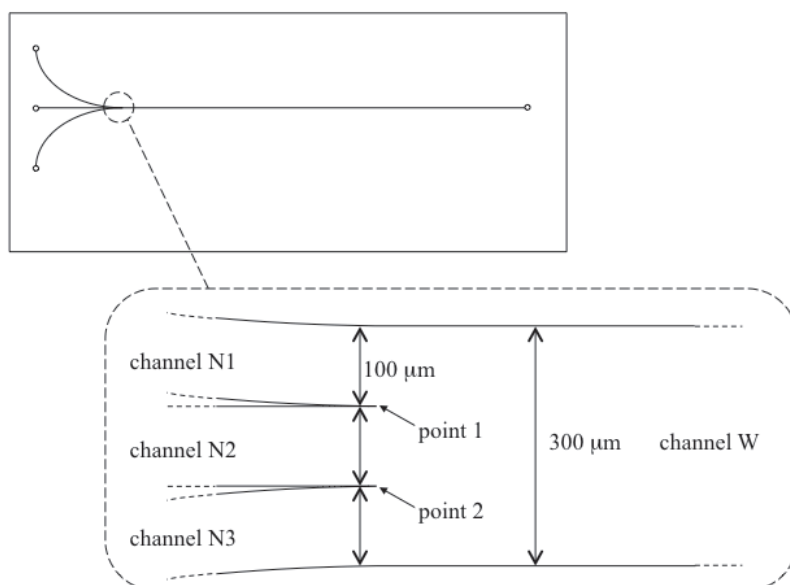


Figure 1. Illustration of a newly designed microchip incorporating microchannels.

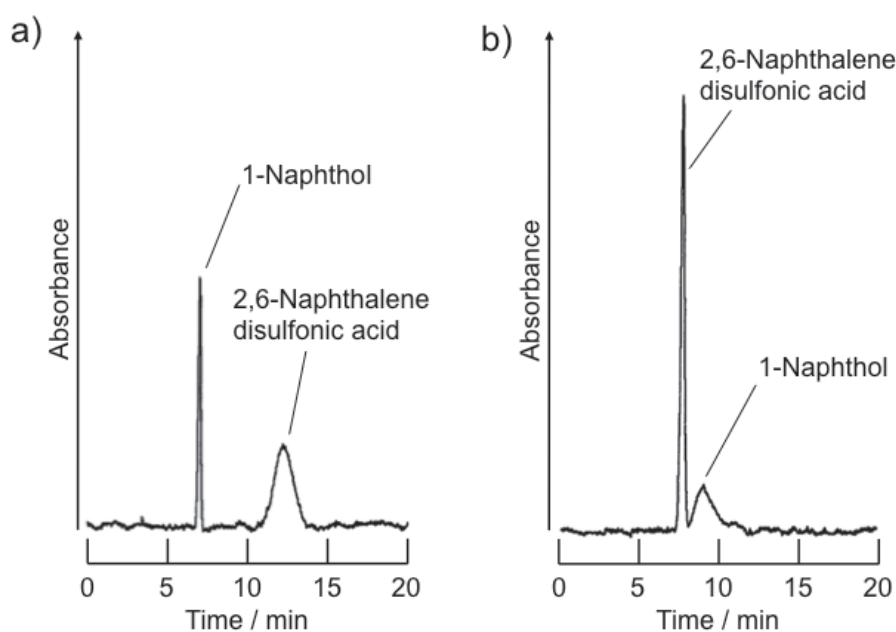


Figure 2. Chromatograms of a mixture of 1-naphthol and 2,6-naphthalenedisulfonic acid obtained by the TRDC system via absorption detection. Conditions: Capillary tube, 120 cm (effective length: 100 cm) of 75 μm i.d. fused-silica; carrier, (a) water–acetonitrile–ethyl acetate (3:8:4 v/v/v) mixture solution and (b) water–acetonitrile–ethyl acetate (15:3:2 v/v/v) mixture solution; sample injection, 20 cm height (gravity) × 30 s; flow rate, 0.8 μL min⁻¹; tube temperature, 15 °C; and analyte concentration, 1 mM.

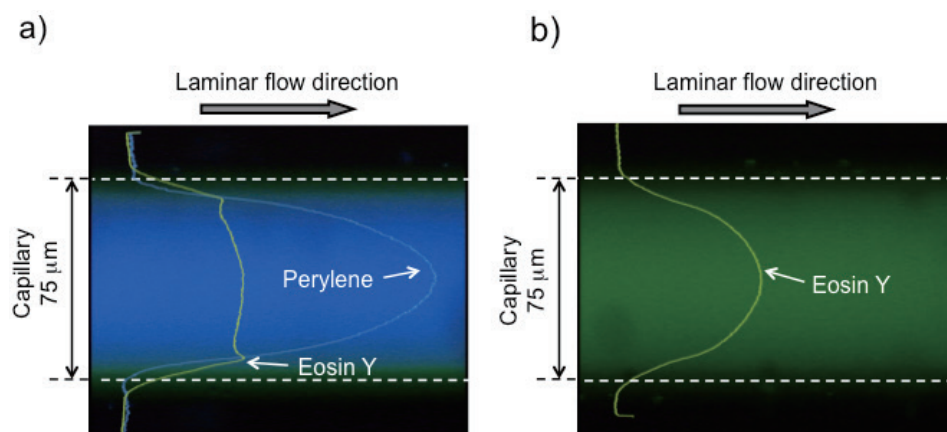


Figure 3. Fluorescence photographs and profiles of the fluorescent dyes dissolved in the aqueous-organic solvent mixture carrier solution in a fused-silica capillary tube. Conditions: Capillary tube, 120 cm (effective length: 100 cm) of 75 μm i.d. fused-silica; carrier, (a) water–acetonitrile–ethyl acetate (3:8:4, v/v/v) mixture, including 0.1 mM perylene and 1 mM Eosin Y and (b) water–acetonitrile–ethyl acetate (15:3:2, v/v/v) mixture, including 1 mM Eosin Y; and flow rate, 0.8 $\mu\text{L min}^{-1}$.

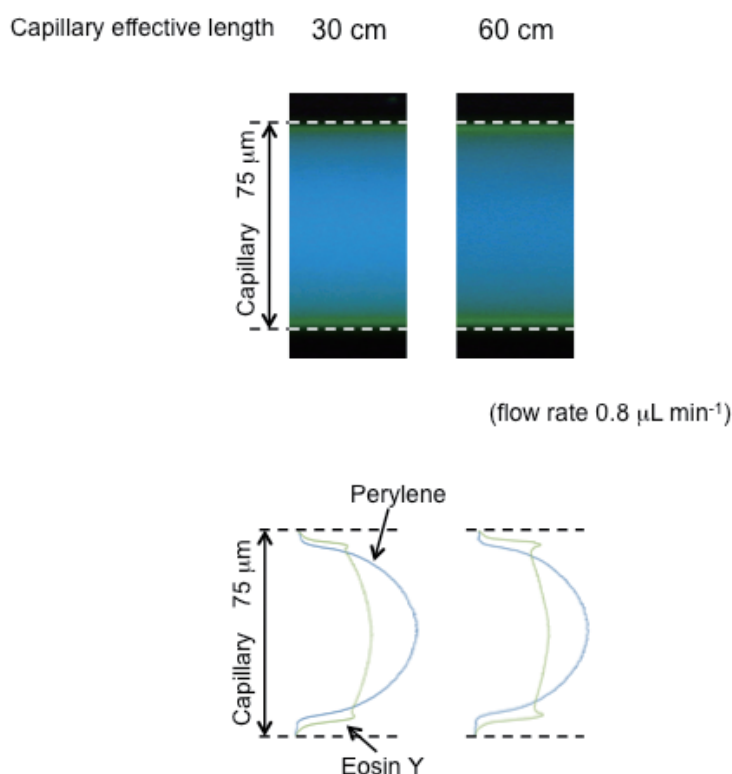


Figure 4. Fluorescence photographs and profiles of the fluorescent dyes at effective lengths of 30 and 60 cm in fused-silica capillary tubes. Conditions: Capillary tube, 120 cm (effective length: 30 and 60 cm) of 75 μm i.d. fused-silica; carrier, water–acetonitrile–ethyl acetate (3:8:4, v/v/v) mixture, including 0.1 mM perylene and 1 mM Eosin Y; and flow rate, 0.8 $\mu\text{L min}^{-1}$.

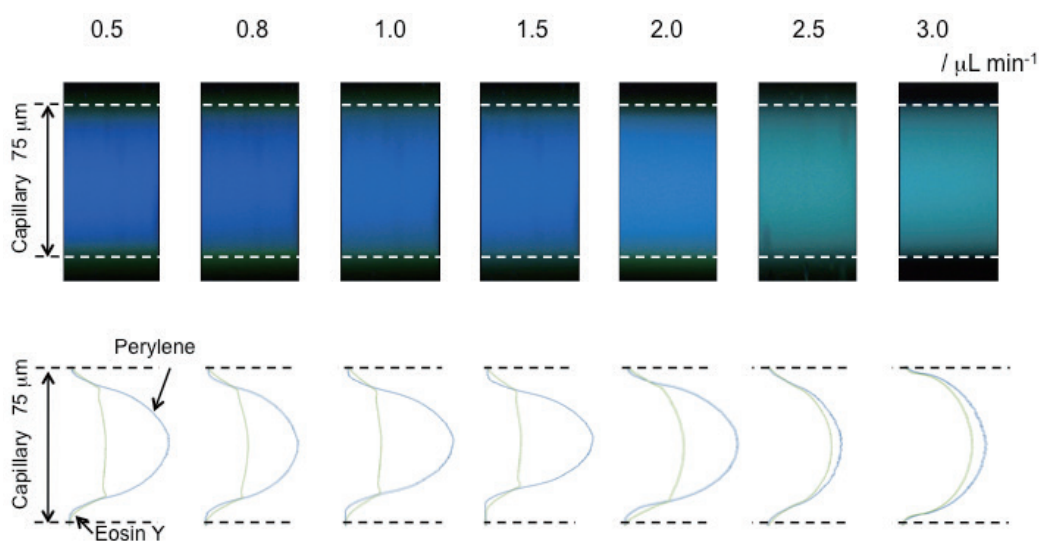


Figure 5. Fluorescence photographs and profiles of the fluorescent dyes dissolved in the aqueous-organic solvent mixture carrier solution at the various flow rates. Conditions: Capillary tube, 120 cm (effective length: 100 cm) of 75 μm i.d. fused-silica; carrier, water–acetonitrile–ethyl acetate (3:8:4, v/v/v) mixture, including 0.1 mM perylene and 1 mM Eosin Y; and flow rate, 0.5–3.0 $\mu\text{L min}^{-1}$.

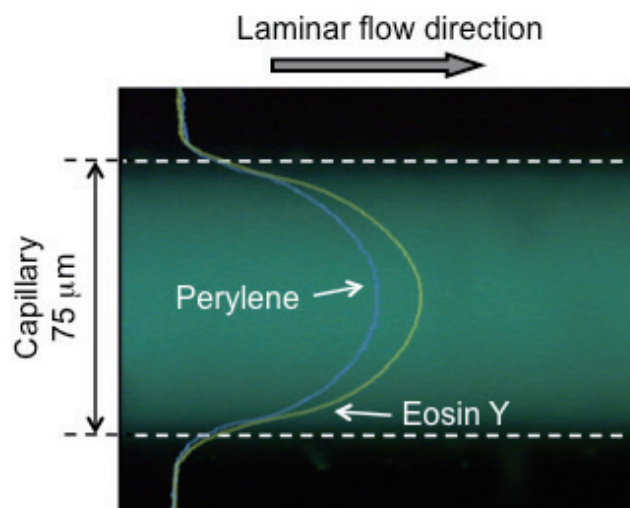
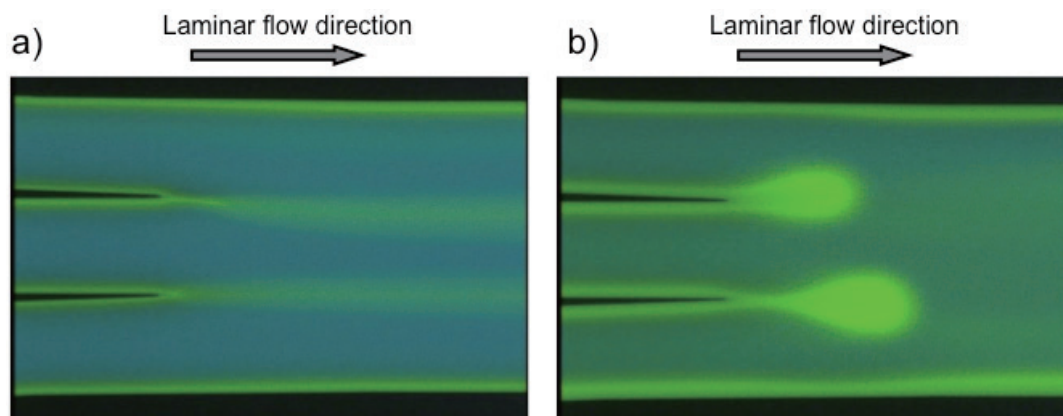


Figure 6. Fluorescence photographs and profiles of the fluorescent dyes dissolved in the aqueous-organic solvent mixture carrier solution without ethyl acetate. Conditions: Capillary tube, 120 cm (effective length: 100 cm) of 75 μm i.d. fused-silica; carrier, the water–acetonitrile (1:4, v/v) mixture, including 0.2 mM perylene and 1 mM Eosin Y; and flow rate 0.8 $\mu\text{L min}^{-1}$.



Blue (perylene) and green (Eosin Y)

Figure 7. Fluorescence photographs of the fluorescent dyes dissolved in the aqueous-organic solvent mixture carrier solution in a microchannel. Conditions: Microchannels, channels N1, N2, and N3 (100 μm -wide \times 40 μm -deep, each) and channel W (300 μm -wide \times 40 μm -deep) made of glass; carrier, water–acetonitrile–ethyl acetate (3:8:4, v/v/v) mixture, including 0.1 mM perylene and 1 mM Eosin Y; and flow rates (a) 5.0 and (b) 2.0 $\mu\text{L min}^{-1}$ for channels N1–N3.

2.2 Observation and characterization of TRDP with various flow rates and capillary tube lengths

When ternary mixed solutions of water-hydrophilic/hydrophobic organic solvents are fed into a microspace under laminar flow conditions, the solvent molecules are radially distributed in the microspace. The specific fluidic behavior of the solvents is termed tube radial distribution phenomenon (TRDP). Here, water–acetonitrile–ethyl acetate mixed solutions (3:8:4 volume ratio) containing fluorescent dyes, perylene (0.1 mM) and Eosin Y (1 mM), were fed into fused-silica capillary tubes (75 μm i.d.) for investigating the TRDP with a fluorescence microscope-CCD camera under various analytical conditions. The pressure at the observation point for the fluorescence on the tube was changed by altering the flow rates, capillary total lengths, and capillary effective lengths. The obtained fluorescence images showed that the TRDP in the capillary tube created the inner and outer phases, i.e., the organic solvent-rich major inner and the water-rich minor outer phases in this case, providing the kinetic liquid-liquid interface. The formation of the inner and outer phases in the capillary tube was observed at flow rates of 0.5–2.0 $\mu\text{L min}^{-1}$ under the present analytical conditions. We also discuss the specific formation locations of the major and minor solvents.

Introduction

Various types of aqueous–organic solvent mixed solutions are used in dissolution [9,10], cleaning [11], preservation [12], and as reaction solvents [13,14]. Such mixed solutions are also useful in separation science [15–17] as extraction solvents and in liquid chromatography. In liquid chromatography, hydrophilic and hydrophobic organic solvent mixtures are used as carrier solutions in normal phase chromatography, while water and hydrophilic organic solvent mixtures are used in reverse-phase chromatography. However, to date, ternary mixed solutions of water–hydrophilic/hydrophobic organic solvents have not been examined in detail for use as carrier solutions in liquid chromatography, or even for the other way around.

When ternary mixed solutions of water–hydrophilic/hydrophobic organic solvents are fed into a microspace, such as microchannels in a microchip or capillary tubes, under laminar flow conditions, the solvent molecules are radially distributed, regardless of the section shape and the inner wall material in the microspace. This is called the tube radial distribution phenomenon (TRDP). In the TRDP, with the organic solvent-rich solution, the organic solvent-rich major phase is generated around the middle of the microspace as an inner phase, while the water-rich minor phase is formed near the inner wall as an outer phase. On the other hand, with the water-rich solution the water-rich major phase is generated as an inner phase, while the organic solvent-rich minor phase is formed as an outer phase. The phenomenon has been supported by

fluorescence studies of dyes dissolved in ternary mixed solvents and the elution behavior of hydrophilic and hydrophobic solutes in capillary tubes under laminar flow conditions.

The phase diagrams for ternary mixed solvents of water, acetonitrile, and ethyl acetate were examined for TRDP and TRDC in our paper, and the results indicated that the pressure change in the capillary tube under laminar flow conditions might alter the carrier solution from homogeneous to heterogeneous, thus affecting the tube radial distribution of the solvents in the capillary tube. Therefore, here, we investigated the conditions needed for the formation of the inner and outer phases created through TRDP in the capillary tubes.

Experimental

Materials Fused-silica capillary tubes (75 μm i.d.), PTFE capillary tubes (100 μm i.d.), and a microchip made of glass with an incorporated microchannel line (100 μm wide \times 40 μm deep) were used.

Pressure applied in batch vessels Water–acetonitrile–ethyl acetate homogeneous solutions were prepared in different volume ratios (3:8:4, 3:8:3, and 3:8:2). Each homogeneous ternary mixed solution (3 mL) was put in a glass open batch vessel (5 mL volume), which was then placed in a pressure-resistant glass vessel (500 mL volume). Pressures of $1.1 - 1.4 \times 10^5$ Pa (cf. atmospheric pressure, 1.01×10^5 Pa) were applied to the solution with nitrogen gas.

Fluorescence images The fluorescence microscopy setup with either a fused-silica capillary tube, PTFE capillary tube, or a microchip incorporating a microchannel is shown in Fig. 1. The fluorescence in the capillary tubes or microchannels was monitored at various points using a fluorescence microscope equipped with an Hg lamp, a filter, and CCD camera. The effective capillary length, indicated in Fig. 1, is the distance from the fluorescence observation point to the capillary outlet. The ternary mixed solvent solutions were delivered into the capillary tube or the microchannel using a microsyringe pump.

Results and discussion

Dye fluorescence Our studies^{6,14)} showed that fluorescence from both dyes could be monitored in organic solvent-rich solutions of water–acetonitrile–ethyl acetate with a 3:8:4 volume ratio. However, in water-rich solutions of water–acetonitrile–ethyl acetate with a 15:3:2 volume ratio, only the fluorescence from Eosin Y (1 mM) was observed as the perylene was only slightly dissolved into the solution. Therefore, here, for both dyes to be dissolved in water–acetonitrile–ethyl acetate mixed solutions, the water-rich solution had an 80:20:9 volume ratio. The fluorescence photographs in a microchannel

for the organic solvent-rich solution (3:8:4 volume ratio) containing perylene (0.1 mM) and Eosin Y (1 mM), and the water-rich solution (80:20:9 volume ratio) containing perylene (0.1 mM) and Eosin Y (0.1 mM) are shown in Figs. 2a and 2b, respectively. The water-rich solution (80:20:9 volume ratio) with perylene (0.1 mM) and Eosin Y (0.5 mM) in a PTFE capillary tube is shown in Fig. 2c. In the water-rich solutions, the comparatively hydrophilic Eosin Y was distributed around the middle of the microspace of the microchannel and the capillary tube, and the hydrophobic perylene was distributed near the inner wall. The fluorescence photographs, in Figs. 2b and 2c, illustrate TRDP with two-colors in water-rich solutions in a microspace.

Effect of pressure in a batch vessel A phase diagram of the water–acetonitrile–ethyl acetate mixed solution is shown in Fig. 3. Solutions with volume ratios of 3:8:4, 3:8:3 and 3:8:2 are marked as solutions A, B, and C, respectively. It can be clearly seen that upon decreasing the ethyl acetate volume fraction in the solution, the distance between the homogeneous–heterogeneous solution boundaries increased. Under pressures of $1.1 - 1.4 \times 10^5$ Pa, the phase behaviors of the solutions in open batch vessels were observed; the results are summarized in Table 1. In solution A the homogeneous solution changed to a suspension solution in the pressure range of $1.1 - 1.15 \times 10^5$ Pa, and then changed to a heterogeneous solution between pressures of $1.2 - 1.4 \times 10^5$ Pa. In solution B, the homogenous solution changed to a suspension solution at pressures of $1.1 - 1.4 \times 10^5$ Pa, and solution C remained homogeneous. The suspension and homogeneous solutions in solutions B and C, respectively, under these pressures were stable for ca. 10 min. From these results, it is clear that pressures above atmospheric pressure greatly influence any ternary mixed solvent solutions that lie near the homogeneous–heterogeneous boundary curve in the phase diagram. As solution A changes from homogeneous to heterogeneous under the applied pressures in the bulk vessel, there is a possibility that pressure changes imposed on the solution in the capillary tube under laminar flow conditions might alter the carrier solution from homogeneous in a microsyringe to heterogeneous in a capillary tube; this is discussed in the following section.

Effects of flow rates in the capillary tube Fluorescence photographs and profiles, shown in Fig. 4, were observed for a capillary tube in which the organic solvent-rich carrier solution (volume ratio 3:8:4) containing perylene (0.1 mM) and Eosin Y (1.0 mM) was delivered at flow rates of $0.5 - 3.0 \mu\text{L min}^{-1}$. The hydrophobic perylene molecules (blue) were distributed around the middle of the tube, while the comparatively hydrophilic Eosin Y molecules (green) were distributed near the tube's inner wall at flow rates of $0.5 - 2.0 \mu\text{L min}^{-1}$ (the inflections were observed on the fluorescence profiles of Eosin Y). However, at flow rates of 2.5 and $3.0 \mu\text{L min}^{-1}$, the tube radial distributions of the dyes were not observed and the fluorescence profiles showed that

the dyes were homogeneously distributed in the ternary mixed solvent. Also, in the carrier solution at flow rates of 0.1 and 0.2 $\mu\text{L min}^{-1}$, we did not observe the tube radial distributions; also, the fluorescence photographs in Fig. 5 show that the dissolved dyes were distributed in the axial direction.

Relationships between the flow rates, pressures, and phase formation The data obtained in the previous section using an organic solvent-rich carrier solution (3:8:4, volume ratio) containing perylene (0.1 mM) and Eosin Y (1 mM) in a capillary tube are used to investigate the relationships between the flow rates, pressures, and phase formation. The pressure in the capillary tube under laminar flow conditions was calculated at each flow rate (0.1, 0.2, 0.5, 0.8, 1.0, 1.5, 2.0, 2.5, and 3.0 $\mu\text{L min}^{-1}$) using the following Hagen–Poiseuille equation:

$$Q = \frac{\pi a^4 \Delta p}{8\mu L},$$

where Q is the flow rate, a the inner radius, Δp the pressure (or pressure loss), μ the viscosity, and L the effective capillary length (the length from the observation point to the capillary outlet). The pressures in the capillary tube were calculated using Q , a , μ , and L values of 0.1 – 3.0 $\mu\text{L min}^{-1}$, 37.5 μm , $6.89 \times 10^{-4} \text{ kgm}^{-1}\text{s}^{-1}$, and $2.0 \times 10^{-1} \text{ m}$, respectively. The formation/non-formation of the inner and outer phases indicating TRDP creation and non-creation, respectively, are plotted in the pressure vs flow rate graph in Fig. 6. The capillary tube of length (110 cm) and the effective length (20 cm) is represented as (110-20) in Fig. 6. From the data, it can be seen that the flow rate and pressure in a capillary tube, as well as the component ratios of the mixed solvents play important roles in determining TRDP in the solvents.

Effects of flow rates and pressures in capillary tubes The relationships between the flow rates, pressures, and phase formation created through TRDP were examined under various conditions in capillary tubes. The pressures were changed by altering the flow rates as well as the effective capillary lengths. A 110 cm-long capillary tube was used, and the effective length was varied over 5 – 80 cm (Fig. 6). A capillary tube of length 110 cm with different effective lengths of 5 – 80 cm are represented as (110-effective length) in the figure. For flow rates of 0.5 – 2.0 $\mu\text{L min}^{-1}$, at all effective variable capillary lengths, the inner and outer phases formed in the capillary tube, even at very low pressures ($1.02 - 1.03 \times 10^5 \text{ Pa}$; effective length 5 cm). However, at low flow rates of 0.1 and 0.2 $\mu\text{L min}^{-1}$ and at high flow rates of 2.5 and 3.0 $\mu\text{L min}^{-1}$ there was no inner and outer phase formation. Different capillary tubes of total length, 290 cm (effective length, 200, 230, and 260 cm), 350 cm (effective length, 260, 290, and 320 cm), and 500 cm (effective length, 410, 440, and 470 cm) were also used. A longer effective capillary length than 470 cm could not be used because of the

limitation of the microsyringe pump capacity. due to the limitations in capacity of the the microsyringe pump. From these results in Fig. 7, TRDP was observed for flow rates of $0.5 - 1.5 \mu\text{L min}^{-1}$, and not at low flow rates of 0.1 and $0.2 \mu\text{L min}^{-1}$, or at high flow rates of 2.5 and $3.0 \mu\text{L min}^{-1}$. At a flow rate of $2.0 \mu\text{L min}^{-1}$, some capillary combinations of length-effective lengths of (290-230), (350-320), and (500-440) did not form the inner and outer phases. In addition, the capillary tube of length-effective length of (290-260) and that of (350-260) showed data quite similar to Fig. 7. That is, the same effective length that imposed the same pressure at the observation point in the capillary tube provided the same distribution behavior of the dyes in the tube, in spite of the different total capillary lengths. We summarise that the majority (with the exception of 3 results) of results with flow rates of $0.5 - 2.0 \mu\text{L min}^{-1}$ created the formation of the inner and outer phases in the capillary tube, i.e., the kinetic liquid-liquid interface through TRDP. Flow rates above and below this range did not provide phase formation through TRDP.

TRDP in a microspace under laminar flow conditions Fig. 8 shows the linear velocity and the shearing stress of the fluid in a capillary tube under laminar flow conditions at different phases (axial distribution, TRDP, and homogeneous distribution). At low flow rates (0.1 and $0.2 \mu\text{L min}^{-1}$), the axial distribution of the fluorescent dyes was observed. When the ternary mixed solvent solution is fed into the capillary tube, at flow rates greater than $0.5 \mu\text{L min}^{-1}$, the TRDP creates a kinetic liquid-liquid interface in the capillary tube. If the flow rates become lower than $0.5 \mu\text{L min}^{-1}$ or zero, the surface stress around the liquid-liquid interface, which naturally causes shrinking in the related interface area, changes the distribution pattern of the dyes and solvents from radial to axial. Although the lengths of colors, blue and green, in the axial direction in the axial distribution pattern, as shown in Fig. 5, were irregular, the length of the organic solvent-rich phase (blue) was much longer than that of the water-rich phase (green). At flow rates greater than $2.0 \mu\text{L min}^{-1}$, the kinetic liquid-liquid interface fluctuates and the shearing stress opposes the radial force. Consequently, the fluidic behavior at high flow rates leads to homogeneous solutions, where the molecular aggregates are dispersed homogeneously into the solvent. The pressure through the laminar flow in the capillary tube, induced by changes in the flow rate, trigger the phase change from homogeneous to heterogeneous in these ternary mixed solvents. However, with the experimental data we can show that the phase formation in the TRDP was controlled with the flow rates and not the pressures, at least under the present conditions. Although the reason has not been made clear yet, new information concerning the TRDP is interesting, and will lead the way to the next step in TRDP research. Briefly, we would like to discuss why the major solvents distribute around the middle of the tube and the minor solvents distribute near the inner wall, regardless of whether the

carrier solutions are organic solvent-rich or water-rich. Fig. 9 shows the linear velocity in the radial face section of the capillary tube (circle curves) under laminar flow conditions, based on the following equation:

$$u = -\frac{1}{4\mu} \frac{dP}{dx} (a^2 - r^2),$$

where u is the linear velocity, μ the viscosity, a the inner radius, r the radial length, and dP/dx the differential of pressure with the axial length. Each circle in the radial face expresses the same velocity, and the spaces between the circles have the same velocity interval. The spaces between the curves become smaller from the center to the inner wall, that is, the inside area has a lower gradient in velocity change than does the outside area. Strictly speaking, Fig. 9 represents an ideal velocity curve; the real velocity curve in an aqueous–organic solvent mixed solution may deviate from these, however. The possible distribution patterns of the phase formation in the radial profile in a capillary tube are schematically depicted in Fig. 9 as patterns I – III. The kinetic liquid–liquid interface created in TRDP form along one curve of a certain velocity; therefore, it must be generated along one of the circular curves. For TRDP, distribution patterns II or III are preferred over pattern I. Furthermore, the major solvents must occupy the inside area in the capillary tube, with consideration to fluidic stability based on the linear velocity gradients of the radial profile under laminar flow conditions. Therefore, the TRDP has distribution pattern III.

In conclusion, the TRDP creates a kinetic liquid–liquid interface in a microspace from homogeneous aqueous–organic mixed solutions under laminar flow conditions. The formation of the inner and outer phases in the capillary tube, examined using fluorescence microscopy, was observed at flow rates of 0.5 – 2.0 $\mu\text{L min}^{-1}$. The TRDP was controlled with the flow rates, not with pressures under the present conditions. This finding is both interesting and useful for proceeding to the next step in the TRDP research.

Table 1. Effects of pressures on the ternary mixed solvent solutions in a batch vessel.

Pressure / $\times 10^5$ Pa	Solution A	Solution B	Solution C
1.0	Homogeneous	Homogeneous	Homogeneous
1.1			
1.15			
1.2			
1.25			
1.3			
1.35			
1.4			

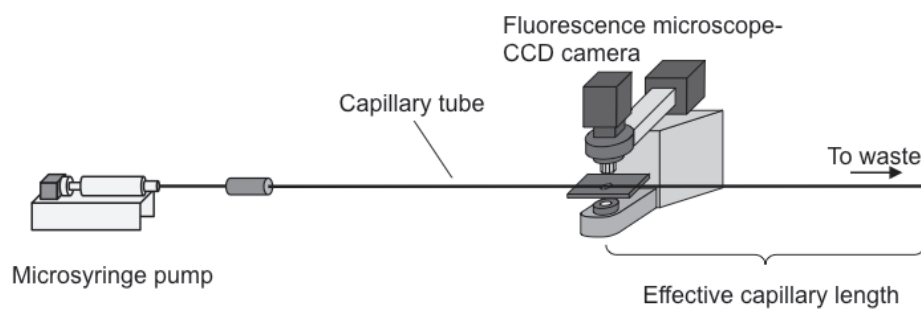


Figure 1. Schematic diagram of the TRDP system for fluorescence observations. The pressure in a capillary tube is estimated using the Hagen–Poiseuille equation with the effective capillary length (the length from the observation point to the capillary outlet).

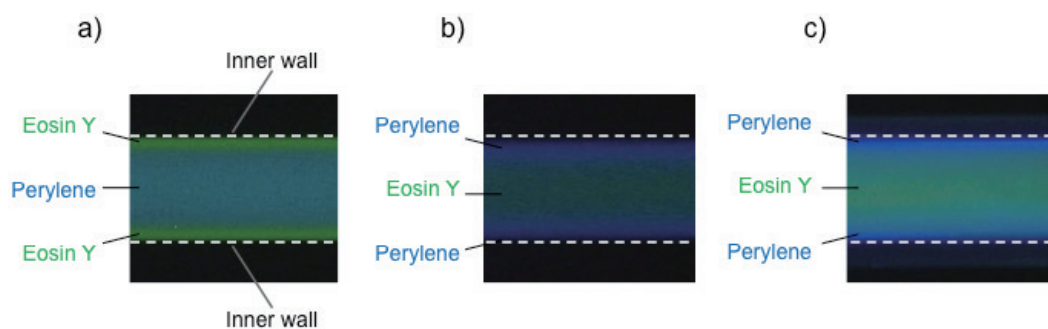


Figure 2. Fluorescence photographs of (a) perylene (0.1 mM) and Eosin Y (1.0 mM) dissolved in the water–acetonitrile–ethyl acetate mixture (3:8:4 volume ratio) in a microchannel, at a $1.0 \mu\text{L min}^{-1}$ flow rate. (b) Perylene (0.1 mM) and Eosin Y (0.1 mM) dissolved in the water–acetonitrile–ethyl acetate mixture (80:20:9 volume ratio) in a microchannel, at a $1.0 \mu\text{L min}^{-1}$ flow rate. (c) Perylene (0.1 mM) and Eosin Y (0.5 mM) dissolved in the water–acetonitrile–ethyl acetate mixture (80:20:9, volume ratio) in a PTFE capillary tube at a $3.0 \mu\text{L min}^{-1}$ flow rate.

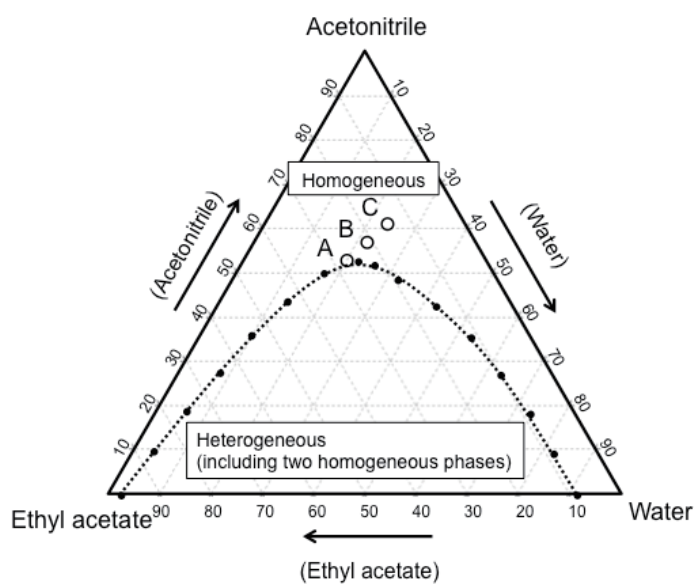


Figure 3. Phase diagram for the water–acetonitrile–ethyl acetate mixture. Solution volume ratios of (A) 3:8:4, (B) 3:8:3, and (C) 3:8:2 are marked and the homogeneous–heterogeneous solution boundary curve is represented by the dotted curve.

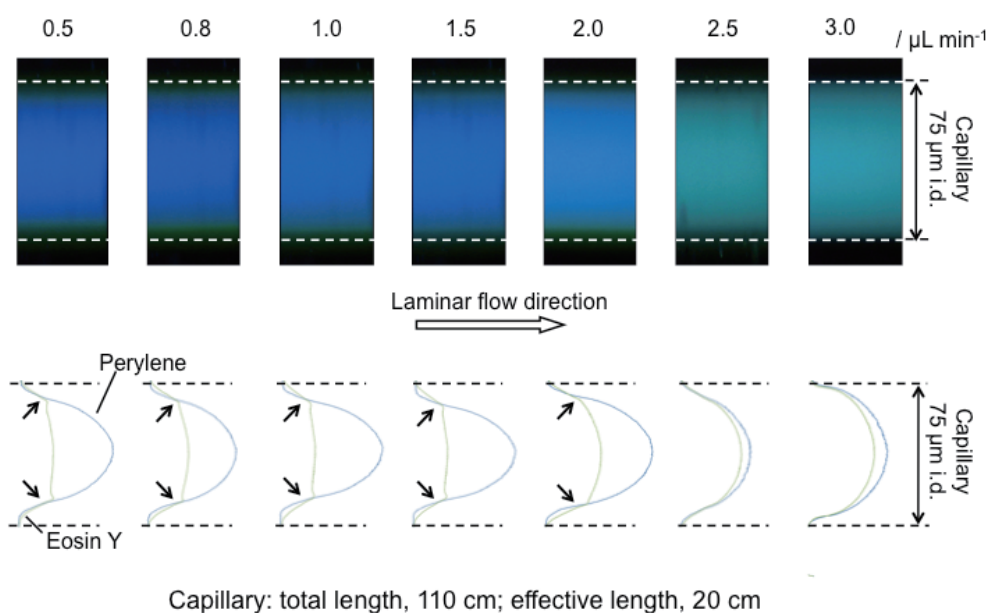


Figure 4. Fluorescence photographs and profiles of fluorescent dyes, perylene (0.1 mM) and Eosin Y (1.0 mM), dissolved in the water–acetonitrile–ethyl acetate mixture (3:8:4, volume ratio) at various flow rates in a capillary tube. The arrows point out the inflections on the fluorescence profiles of Eosin Y.

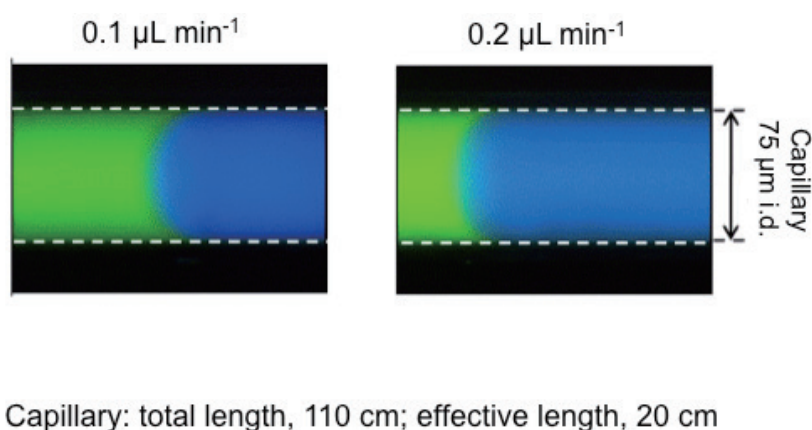


Figure 5. Fluorescence photographs of the fluorescent dyes perylene (0.1 mM) and Eosin Y (1.0 mM) dissolved in the water–acetonitrile–ethyl acetate mixture (3:8:4, volume ratio) at low flow rates in a capillary tube.

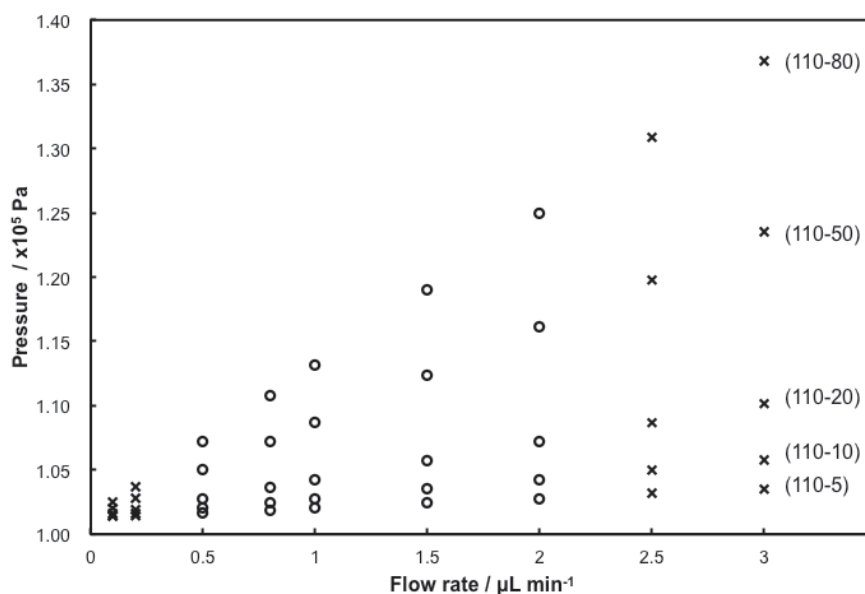


Figure 6. Phase formation of the inner and outer phases, formation (○) or non-formation (×), at different flow rates and pressures in a capillary tube of length 110 cm with different effective lengths of 5 – 80 cm, represented as (110-effective length) in the figure.

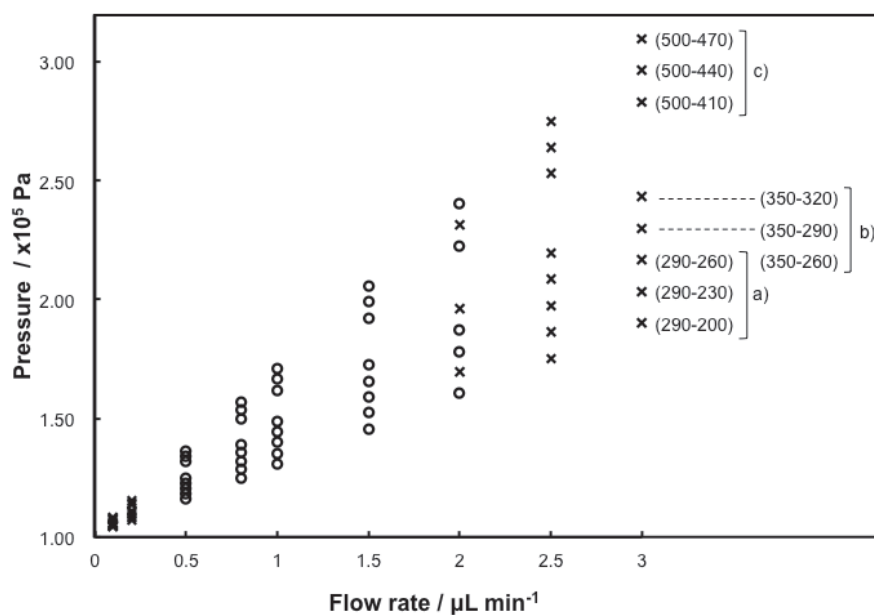


Figure 7. Phase formation of the inner and outer phases, formation (○) or non-formation (×), at different flow rates and pressures in various capillary tubes. a) capillary length 290 cm (effective length: 200, 230, and 260 cm), b) capillary length 350 cm (effective length: 260, 290, and 320 cm), and c) capillary length 500 cm (effective lengths: 410, 440, and 470 cm), represented as (capillary length-effective length) in the figures.

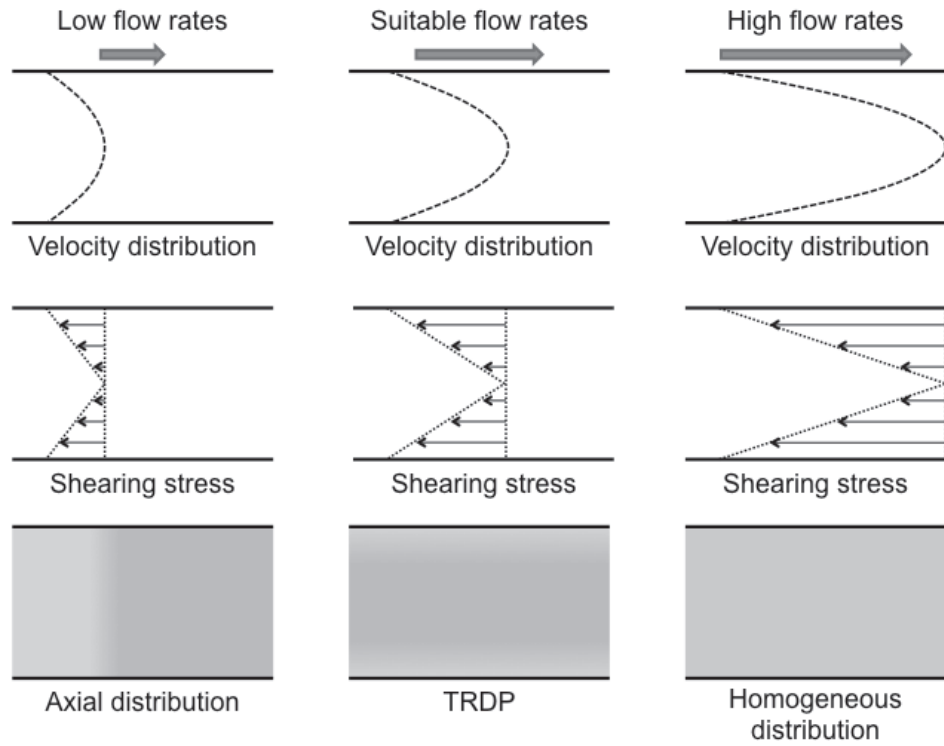


Figure 8. Illustration of the linear velocity and shearing stress of the fluid in the capillary tube under laminar flow conditions together with the fluorescence photographs.

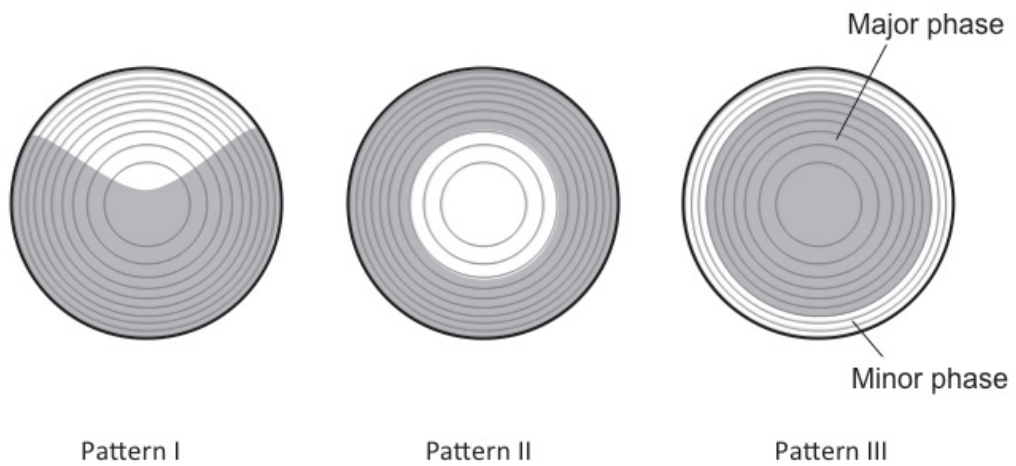


Figure 9. Schematic depictions of the possible distribution patterns in a capillary tube.

2.3 Observation and characterization of TRDP with various inner diameters of capillary tubes

We have developed a capillary chromatography system using an open-tubular capillary tube and a ternary water-hydrophilic/hydrophobic organic mixture carrier solution. We call the system tube radial distribution chromatography (TRDC). Here, fluorescence photographs of the dyes dissolved in the ternary mixed carrier solvents in the TRDC system were examined under various conditions concerning the inner diameters, tube temperatures, tube effective lengths, and flow rates (average linear velocities). The TRDC system used an untreated fused-silica capillary tube and a ternary water-acetonitrile-ethyl acetate mixture carrier solution (3:8:4 volume ratio; the organic solvent-rich solution). The tube radial distribution of the carrier solvents, which generated the organic solvent-rich major inner phase and the water-rich minor outer phase, could be observed in 50 – 700 μm inner diameter of the tubes at the average linear velocity of 11 cm min^{-1} through the fluorescence microscope-CCD camera. The model analyte solution of 1-naphthol, 1-naphthalenesulfonic acid, 2,6-naphthalenedisulfonic acid, and 1,3,6-naphthalenetrisulfonic acid was subjected to the TRDC system. They were separated and detected in this order with 50, 75, and 100 μm inner diameters of the open-tubular capillaries.

Introduction

Recently, our group reported on an interesting and useful microfluidic behavior of the solvents; tube radial distribution of ternary mixed solvents in a microspace, or the tube radial distribution phenomenon (TRDP) for short. When the ternary mixed homogeneous solution of water–hydrophilic/hydrophobic organic solvents is delivered into a microspace, such as a microchannel or a capillary tube, the carrier solvent molecules are radially distributed in the microspace, generating inner and outer phases. For example, when a homogeneous carrier solution of water–acetonitrile–ethyl acetate (3:8:4 volume ratio; the organic solvent-rich carrier solution) was fed into a fused-silica capillary tube, an organic solvent-rich major phase was generated around the middle of the tube as an inner phase far from the inner wall, while a water-rich minor phase formed near the inner wall as an outer phase, or capillary wall phase. A capillary chromatography system, where the outer phase functions as a pseudo-stationary phase under laminar flow conditions, has been developed based on the TRDP. We call this tube radial distribution chromatography (TRDC). Otherwise, we have investigated chemical reactions, extraction, and mixing procedures on the basis of the TRDP.

The TRDP, i.e., the creation of kinetic liquid-liquid interface in a microfluidic flow, while interesting, is an involved procedure by its very nature. The TRDP has left several subjects to be investigated in order to better clarify the microfluidic behavior.

Here the tube radial distribution of the carrier solvents was examined under various conditions through the fluorescence microscope-CCD camera system. Also, separation performance was examined for the model mixture analytes in the capillary chromatography; TRDC.

Experimental

Fluorescence photographs A capillary tube was set up for the fluorescence microscope-CCD camera system to confirm the tube radial distribution of the carrier solvents, i.e., TRDP. The water–acetonitrile-ethyl acetate mixture (3:8:4 volume ratio) including 0.1 mM perylene and 1 mM Eosin Y solutions was delivered into the capillary tube. The fluorescence in the capillary tube was monitored using a fluorescence microscope equipped with an Hg lamp, a filter, and a CCD camera.

Open-tubular capillary chromatography The present capillary chromatography system comprised of an open fused-silica capillary tube, microsyringe pump, and fluorescence detector. The tube temperature was controlled by dipping the capillary tube in water maintained at a fixed temperature in a beaker by stirring. Water-acetonitrile-ethyl acetate mixtures with volume ratios of 3:8:4 were used as carrier solutions. The homogeneous carrier solutions could be used independent from the left-time after the preparation. Analyte solutions were prepared along with the carrier solutions. The analyte solution was introduced directly into the capillary inlet side by the gravity method. After analyte injection, the capillary inlet was connected through a joint to a microsyringe. The syringe was set on the microsyringe pump. The carrier solution was fed into the capillary tube at a definite flow rate under laminar flow conditions. On-capillary fluorescence detection (ex. 495 nm and em. 520 nm) was performed with the detector.

Results and discussion

Phase diagram for water-acetonitrile-ethyl acetate mixture The phase diagrams that indicated the component ratios of the solvents in homogeneous and heterogeneous solutions are useful tools to explain the TRDP and examine the conditions for the TRDP and TRDC performance. A phase diagram for the ternary mixture solvents of water-acetonitrile (hydrophilic organic solvent)-ethyl acetate (hydrophobic organic solvent) was examined in a vessel at 0 and 20 °C under a constant pressure or atmospheric pressure (Fig. 1 a)) as well as at atmospheric pressure (1.0×10^5 Pa) and 1.3×10^5 Pa at a constant temperature of 20 °C (Fig. 1 b)). The obtained phase diagrams are shown in Fig. 1. The dotted curves in the diagrams indicate the boundary between homogeneous and heterogeneous phases. The phase diagram showed that each component ratio of the solvents made a homogeneous (one homogeneous phase) or a heterogeneous (two homogeneous phases) solution. As shown in Fig. 1, lower

temperatures and higher pressures expanded the boundary curves outwards in the phase diagrams.

TRDP created with an organic solvent-rich carrier solution We proposed a view of the inner and outer phase formation in the TRDP, based on the above experimental data. A specific homogeneous solution, whose component ratio was near the boundary between homogeneous and heterogeneous in the phase diagram, was cooled to lower than 20 °C (room temperature) or pressurized greater than atmospheric pressure in a batch vessel where it was under the control of gravity. In an organic solvent-rich solution (e.g., water-acetonitrile-ethyl-acetate mixture; 3:8:4 volume ratio), the homogeneous solution first became an emulsion or nontransparent solution that included minor solvent or water-rich tiny droplets and then changed to a heterogeneous solution that included an upper major organic solvent-rich solution and a lower minor water-rich solution due to the influence of gravity.

The phase formation of the ternary mixed solvents in a capillary tube under the change of temperature and pressure is estimated as follows, where it is under little control of gravity. A specific homogeneous solution with a component ratio near the boundary between homogeneous and heterogeneous in the phase diagram is delivered with a constant pressure to the radial face and at a lower temperature. In an organic solvent-rich solution, the homogeneous solution must first become an emulsion solution that includes minor solvent or water-rich tiny droplets. Although generation of emulsion was observed in a batch vessel as described above, it could not be observed in a capillary tube with the present fluorescence microscope-CCD camera system; because the present system was unable to catch either the emulsion formation or tiny droplets in the microfluidic flow in a capillary tube. The water-rich tiny droplets start to aggregate near the inner wall where the linear velocity is lowest under laminar flow conditions. Consequently, the ternary mixed solvent solution in a tube changes to a heterogeneous solution that includes a major inner organic solvent-rich solution and a minor outer water-rich solution, where it is under minimal gravitational control.

In order to create the TRDP, we have to take advantage of the phase separation from the homogeneous to the heterogeneous solution with changing pressure and temperature, referring to the phase diagrams (Fig. 1), although the volume ratios of the upper and lower phases in a vessel would not necessarily be equal to those of the inner and outer phases in a capillary tube. That is, a homogeneous solution is delivered into a capillary tube where it then changes into a heterogeneous solution, via emulsion solution, under higher pressure or lower temperature in the tube. The consideration of the TRDP process is illustrated in Fig. 2.

TRDP created with a water-rich carrier solution Similarly, in a water-rich solution, the homogeneous solution first became an emulsion solution that included minor

solvent or organic solvent-rich tiny droplets, and then changed to a heterogeneous solution that included an upper minor organic solvent-rich solution and a lower major water-rich solution in a batch vessel. The phase formation of the ternary mixed solvents in a capillary tube kept at a low temperature and under pressure due to laminar flow with minimal gravitational control is estimated as follows. In a water-rich solution, the homogeneous solution becomes an emulsion solution that includes minor solvent or organic solvent-rich tiny droplets. Under laminar flow conditions, the organic solvent-rich tiny droplets start to aggregate near the inner wall where the velocity is lowest under laminar flow conditions. The homogeneous solution had not changed before the delivery to the capillary tube. After introduction to the tube, the homogeneous solution shifted to a heterogeneous solution including inner and outer phases under higher pressure or lower temperature in the capillary tube, referring to the phase separation in the diagrams (Fig. 2). That is, the ternary-mixed solvent solution in a tube changes to a heterogeneous solution that includes a major inner water-rich solution and a minor outer organic solvent-rich solution where it is under minimal gravitational control.

Effects of flow rates in the capillary tube at tube temperature 20 °C Fluorescence photographs were observed for a capillary tube in which the organic solvent-rich carrier solution (3:8:4 volume ratio) containing perylene (0.1 mM) and Eosin Y (1.0 mM) was delivered at flow rates of 0.1 – 4.0 $\mu\text{L min}^{-1}$ with the inner diameter of 50, 75, and 100 μm at a tube temperature of 20 °C (the obtained data is shown in Fig. 4). The hydrophobic perylene molecules (blue) were distributed around the middle of the tube, while the relatively hydrophilic Eosin Y molecules (green) were distributed near the tube's inner wall at relatively intermediate flow rates of 0.5 – 2.5 $\mu\text{L min}^{-1}$ with 50 μm , 0.5 – 2.0 $\mu\text{L min}^{-1}$ with 75 μm , and 0.5 – 1.0 $\mu\text{L min}^{-1}$ with 100 μm , respectively. The inflections on the fluorescence profiles of Eosin Y in the outer phase were generated through the liquid-liquid interface created with TRDP. Inflections were observed in the above flow rate ranges for every inner diameter. Comparatively, at lower flow rates where surface tension might be predominant, we did not observe the tube radial distributions; the dissolved dyes were distributed in the axial direction, while, at higher flow rates where fluctuation at the liquid-liquid interface might become larger, the tube radial distributions of the dyes were not observed and the fluorescence profiles showed that the dyes were homogeneously distributed in the ternary mixed solvents. That is, fluidic behavior at high flow rates leads to homogeneous solutions, where the molecular aggregates are dispersed homogeneously in the solvent. The data obtained using the organic solvent-rich carrier solution in the capillary tubes were used to investigate the relationships between flow rates, pressures, and phase formation. The pressure in the capillary tube under laminar flow conditions was roughly calculated at each flow rate (0.1 – 4.0 $\mu\text{L min}^{-1}$) using the following Hagen–Poiseuille equation:

$$Q = \frac{\pi a^4 \Delta p}{8\mu L},$$

where Q is the flow rate, a the inner radius, Δp the pressure (or pressure loss), μ the viscosity, and L the effective capillary length (the length from the observation point to the capillary outlet). The pressures in the capillary tubes were calculated using Q , a , μ , and L values of 0.1 – 4.0 $\mu\text{L min}^{-1}$, 25.0, 37.5, or 50 μm , $6.89 \times 10^{-4} \text{ kgm}^{-1}\text{s}^{-1}$, and $2.0 \times 10^{-1} \text{ m}$, respectively.

The formation/non-formation of the inner and outer phases indicating TRDP creation/non-creation, respectively, is plotted in the pressure vs flow rate graph in Fig. 3. The TRDP creation/non-creation of the inner and outer phases is presented with symbol of \circ and \times , and partially TRDP observation is presented with symbol of Δ . From the data, it can be seen that the flow rate and pressure in a capillary tube play important roles in determining TRDP in the solvents. In addition, although we were unable to observe emulsion in the microfluidic flow in the capillary tubes with the present fluorescence microscope-CCD camera system, we may assume suitable flow rates for emulsion formation that leads to TRDP as another point of interest.

Effects of temperature and pressure on TRDP Fluorescence photographs were observed similarly to the above section, but at tube temperature of 0 °C instead of 20 °C. In contrast to the data shown in Fig. 3, the TRDP could be observed at up to 50 $\mu\text{L min}^{-1}$, with all capillary inner diameters, 50, 75, and 100 μm and 20, 50 and 80 cm effective lengths, where the limitation flow rates, 50 $\mu\text{L min}^{-1}$, were determined in the present microsyringe pump's capacity. Thinking of the phase diagrams shown in Fig. 1, the effects of both temperature and pressure must lead to stable TRDP in a large range of flow rates up to 50 $\mu\text{L min}^{-1}$. Relationships between the average linear velocities and pressure are shown in Fig. 5. The TRDP creation and non-creation are presented with the symbols of \circ and \times , respectively. It was discovered from the data that border average linear velocity in the TRDP between TRDP and non-TRDP was the same for all conditions of effective lengths and inner diameters. The energy generated by the average linear velocity, 1.13 cm min^{-1} , might be required to break the axial distribution of the solvents that was observed at lower velocities.

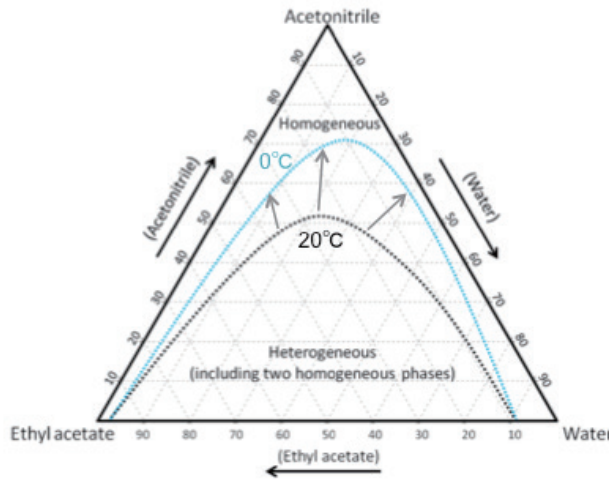
Effects of tube inner diameter on fluorescence photographs Although the inner diameter of the tube is one of the most important factors in the TRDP, there has not been enough data about it yet. Here we examined the effects of the tube inner diameter on fluorescence photographs in the TRDC system. We attempted to use commercially available fused-silica capillary tubes with various inner diameters; the capillary tubes with 50 – 700 μm inner diameters were used here. The obtained fluorescence photographs are shown in Fig. 5 together with the analytical conditions. The flow rates

for all the capillary tubes were adjusted to provide the same average linear velocity of ca. 11 cm min^{-1} . We observed the inner and outer phase formation, i.e., TRDP, in the fluorescence photographs in all the tubes.

Separation of mixture solution including four analytes We examined a mixture analyte solution of 1-naphthol, 1-naphthalenesulfonic acid, 2,6-naphthalenedisulfonic acid, and 1,3,6-naphthalenetrisulfonic acid using the present TRDC system with organic solvent-rich carrier solution. The obtained chromatograms are shown in Fig. 6 along with the analytical conditions. 1-Naphthol, 1-naphthalenesulfonic acid, 2,6-naphthalenedisulfonic acid, and 1,3,6-naphthalenetrisulfonic acid were eluted in this order, leading to good separation with the organic solvent-rich carrier solution in the inner diameters of 50, 75 and 100 μm (Fig. 6). The elution order seemed to be consistent with the hydrophilic character. In the 200, 250, and 320 μm inner diameter tubes, 2,6-naphthalenedisulfonic acid and 1,3,6-naphthalenetrisulfonic acid were not separated. With a 530 μm inner diameter, 1-Naphthol and 1-naphthalenesulfonic acid as well as 2,6-naphthalenedisulfonic acid and 1,3,6-naphthalenetrisulfonic acid were not separated on the chromatogram.

In conclusion, we investigated capillary chromatography on the basis of the TRDP. The tube radial distribution of the carrier solvents was examined by changing tube inner diameters, flow rates, effective lengths, and temperature through the fluorescence microscope-CCD camera system. Consequently, useful information was obtained to understand the TRDP and TRDC. Also, separation performance was examined for the model mixture analytes in the TRDC. The TRDC has potential as a separation tool that does not require using high voltage supply and/or any specific capillary columns, such as packed and monolithic.

a) Pressure constant (1.3×10^5 Pa)



b) Temperature constant (20°C)

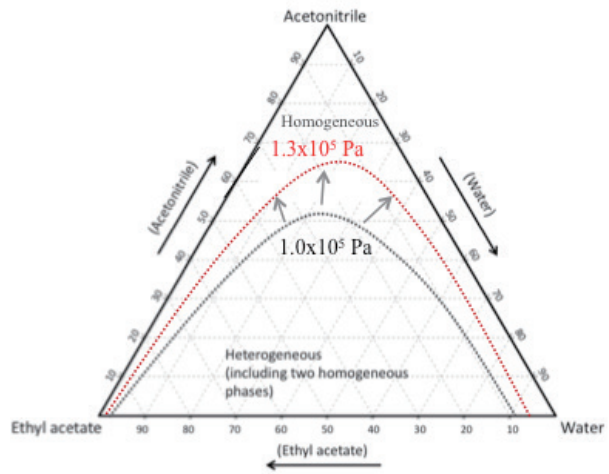


Figure 1. Phase diagram for the ternary water-acetonitrile-ethyl acetate mixture solution. a) Pressure constant (atmospheric pressure) and b) temperature constant (20°C).

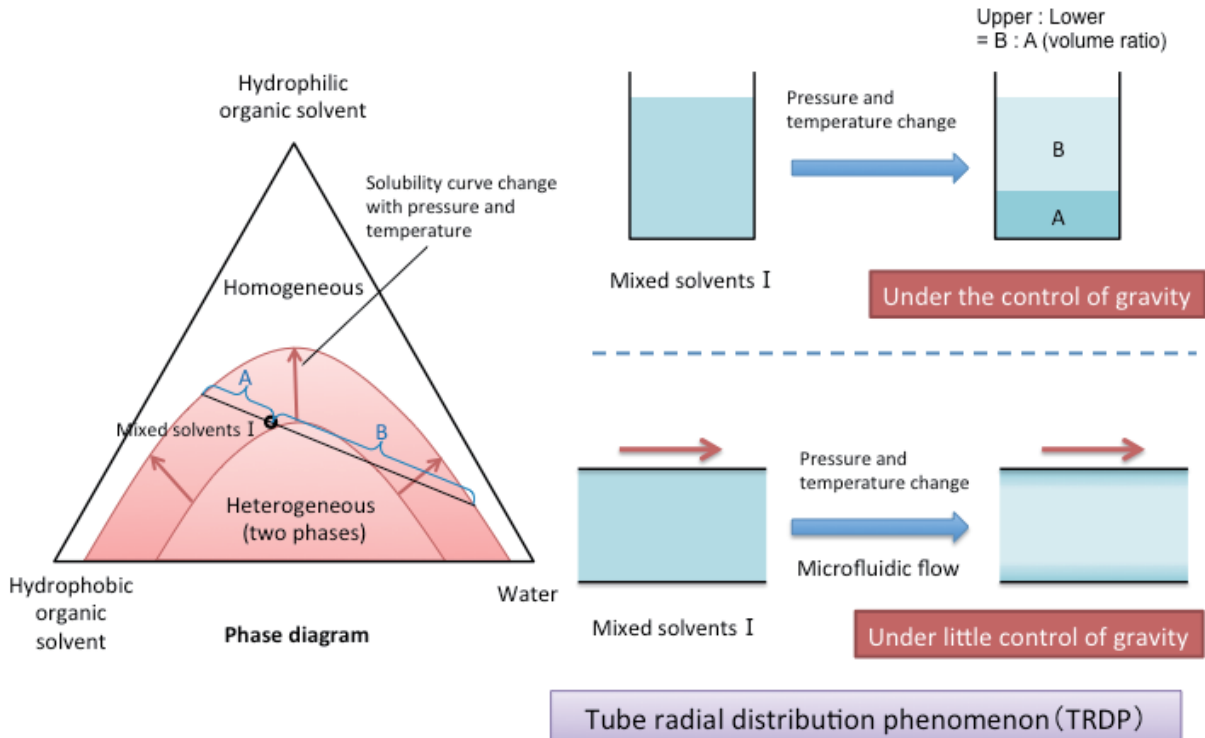


Figure 2. Illustration of tube radial distribution phenomenon (TRDP) appearance in a microfluidic flow.

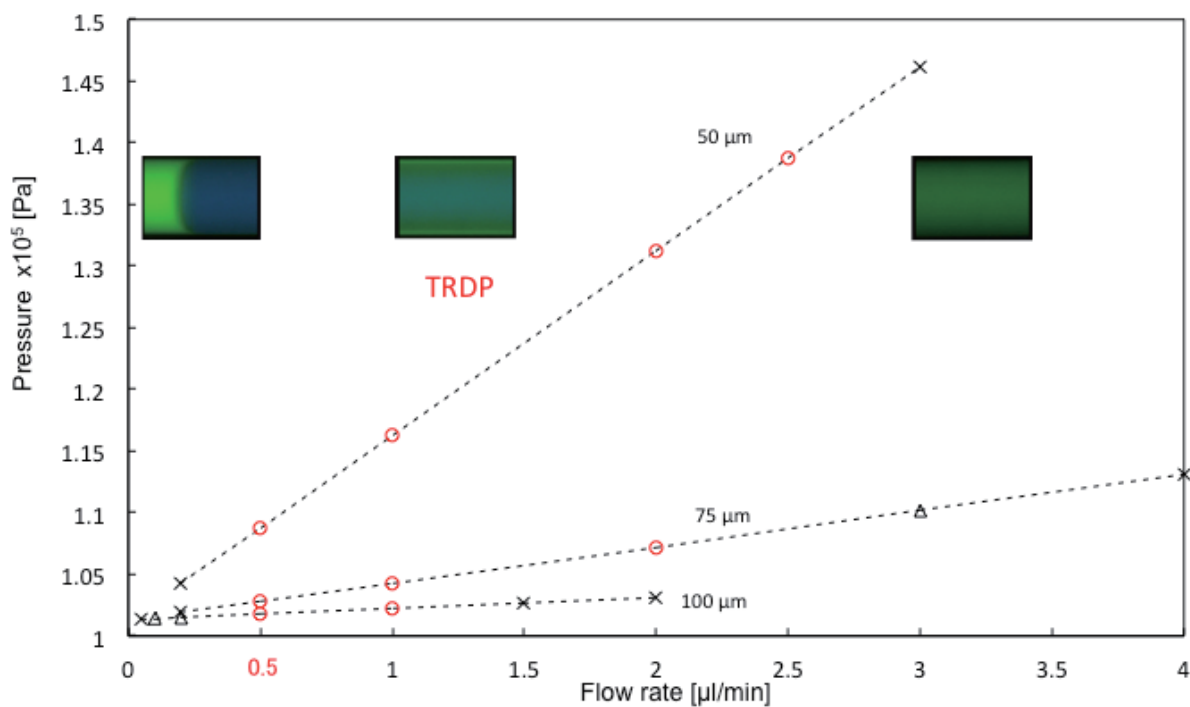


Figure 3. Relationships between flow rates and pressures in tube radial distribution phenomenon of the ternary mixed solvents at tube temperature of 20 °C, with capillary inner diameters of 50, 75, and 100 μm . The formation/non-formation of the inner and outer phases are presented with the symbols \circ and \times , and partially TRDP observation is presented with the symbol Δ . Conditions: Capillary, 110 cm total length and 20 cm effective length; carrier, water-acetonitrile-ethyl acetate (3:8:4 volume ratio) containing perylene (0.1 mM) and Eosin Y (1.0 mM).

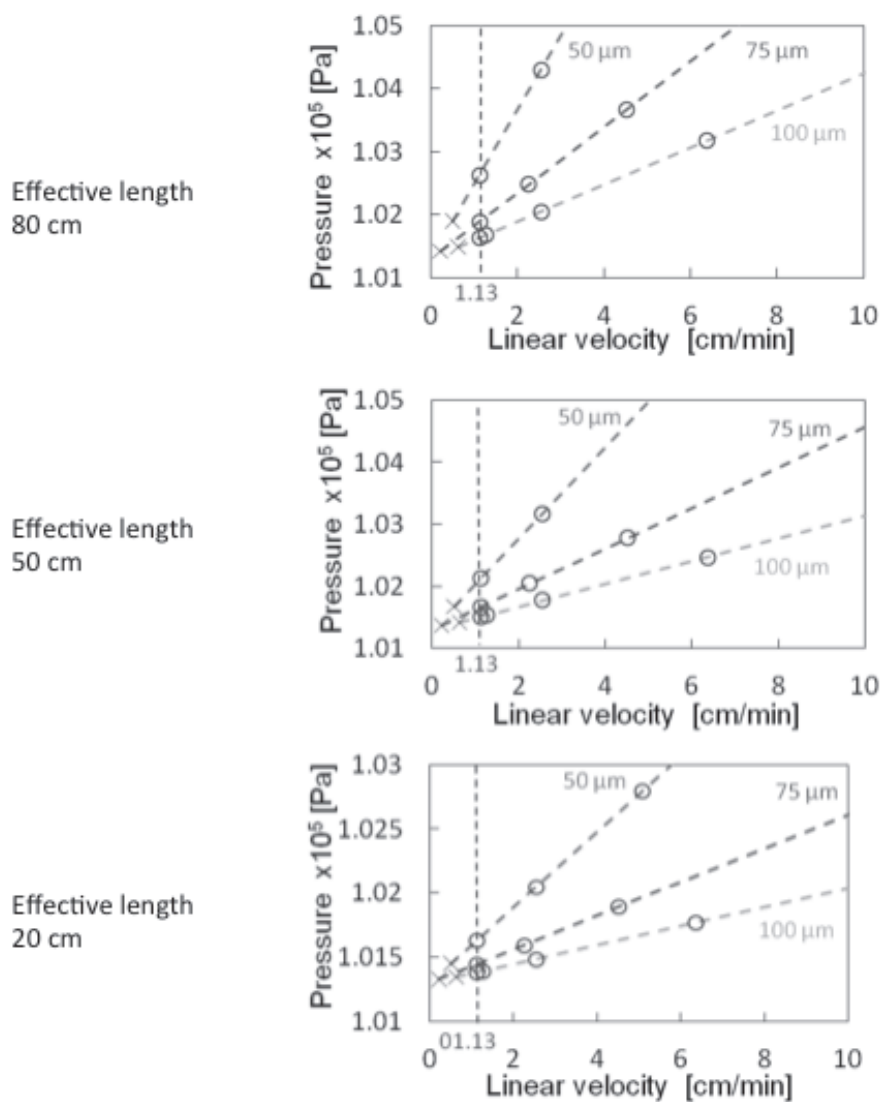


Figure 4. Relationships between average linear velocities and pressures in tube radial distribution phenomenon of the ternary mixed solvents at tube temperature of 0 °C. The formation/non-formation of the inner and outer phases are presented with symbol of \circ and \times . Conditions: Capillary, 110 cm total length and 20, 50, and 80 cm effective length; carrier, water-acetonitrile-ethyl acetate (3:8:4 volume ratio) containing perylene (0.1 mM) and Eosin Y (1.0 mM).

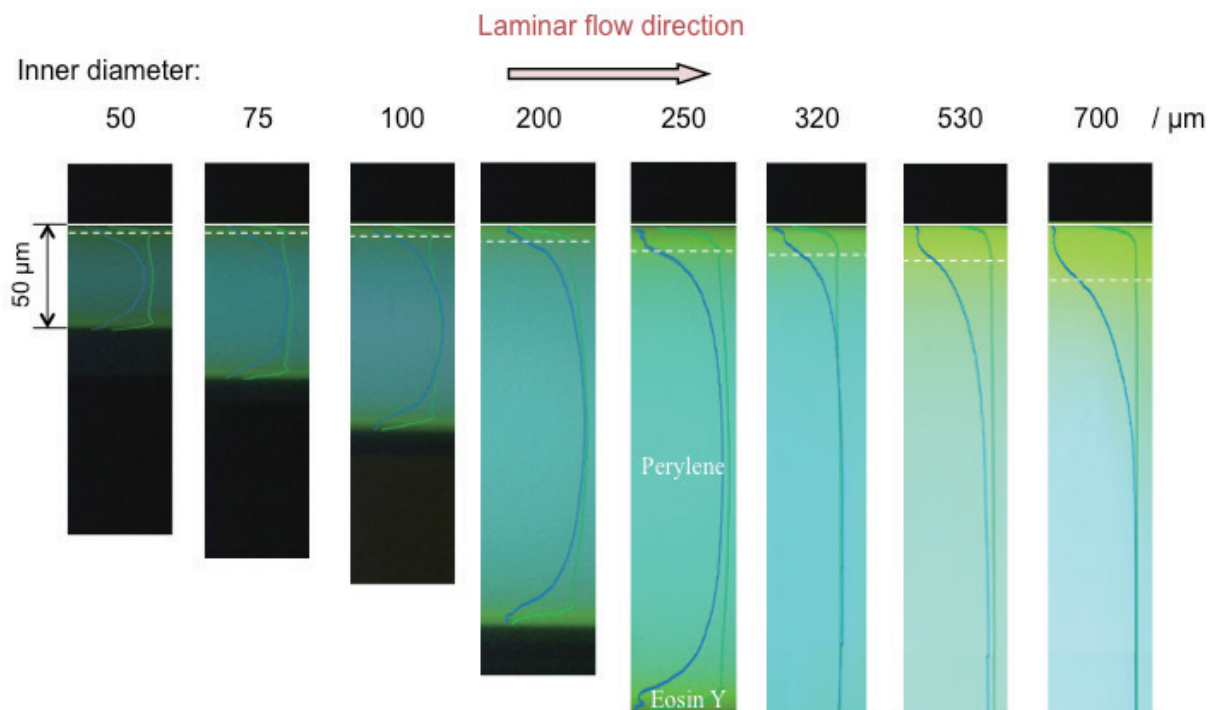


Figure 5. Fluorescence photographs in the capillary tubes having various inner diameters. Capillary inner diameter, 50, 75, 100, 200, 250, 320, 530, and 700 μm . Conditions: Capillary, 110 cm total length and 30 cm effective length fused-silica; carrier, water-acetonitrile-ethyl acetate (3:8:4 volume ratio) containing perylene (0.1 mM) and Eosin Y (1.0 mM); and average linear velocity of 11 cm min^{-1} for all tubes.

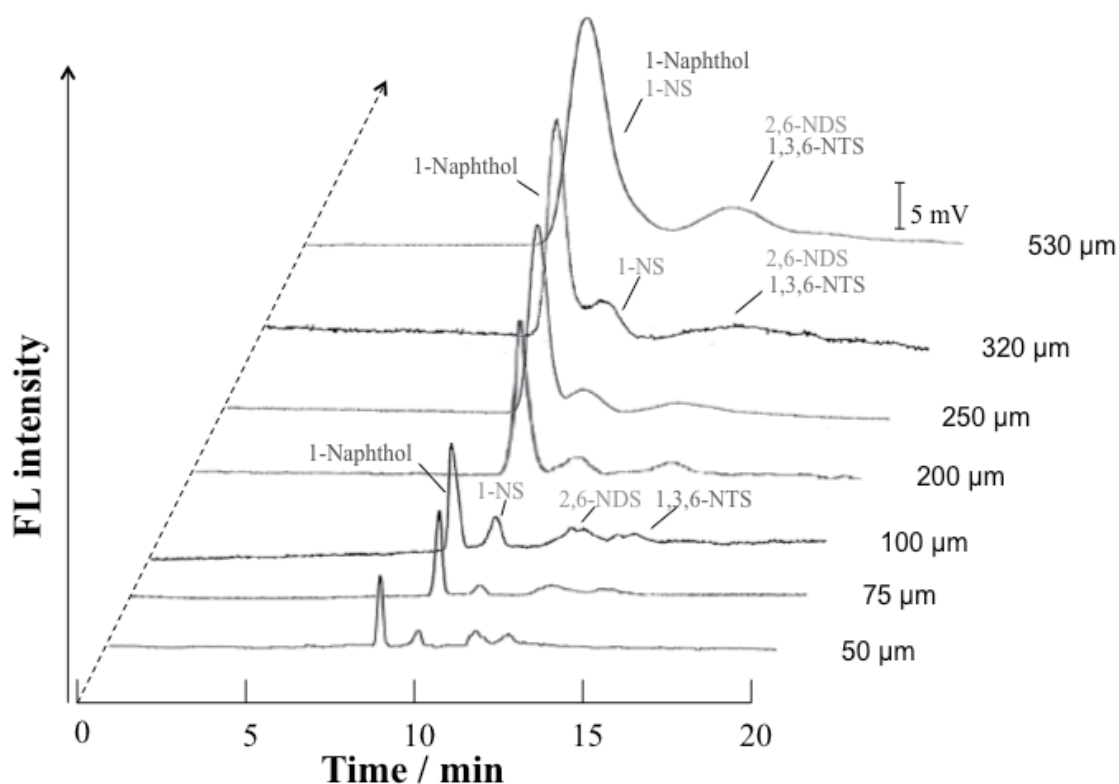


Figure 6. Chromatograms of a mixture analyte solution of 1-naphthol, 1-naphthalenesulfonic acid, 2,6-naphthalenedisulfonic acid, and 1,3,6-naphthalenetrisulfonic acid obtained by the present TRDC system. Capillary inner diameter, 50, 75, 100, 200, 250, 320, and 530 μm . Conditions: Capillary tube, 120 cm total length and 20 cm effective length fused-silica; carrier, water-acetonitrile-ethyl acetate (3:8:4 volume ratio) mixture solution; sample injection, gravity method from 20 cm height (5.4 mm sample length); average linear velocity, 11 cm min^{-1} ; temperature, 20 $^{\circ}\text{C}$; detection, fluorescence, ex. 290 nm and em. 355 nm; and 1-naphthol, 1-naphthalenesulfonic acid (1-NS), 2,6-naphthalenedisulfonic acid (2,6-NDS), 1 mM, 1,3,6-naphthalenetrisulfonic acid (1,3,6-NTS), 2.0 mM.

References

- [1] U. Pyell, *Electrophoresis*, **2010**, *31*, 814.
- [2] V. Cucinotta, A. Contino, A. Giuffrida, G. Maccarrone, and M. Messina, *J. Chromatogr., A*, **2010**, *1217*, 953.
- [3] N. W. Smith and Z. Jiang, *J. Chromatogr., A*, **2008**, *1184*, 416.
- [4] S. Terabe, *Annu. Rev. Anal. Chem.*, 2009, **2**, 99.
- [5] F. Carlucci and A. Tabucchi, *J. Chromatogr., B*, **2009**, *877*, 3347.
- [6] M. Chen, Y. Lu, Q. Ma, L. Guo, and Y.-Q. Feng, *Analyst*, **2009**, *134*, 2158.
- [7] T. Okada, M. Harada, and T. Kido, *Anal. Chem.*, **2005**, *77*, 6041.
- [8] T. Charoenraks, M. Tabata, and K. Fujii, *Anal. Sci.*, **2008**, *24*, 1239.
- [9] G. Heftner, *Pure Appl. Chem.*, **2005**, *77*, 605.
- [10] G. R. Castro and T. Knubovets, *Crit. Rev. Biotechnol.*, **2003**, *23*, 195.
- [11] J. Niu and B. E. Conway, *J. Electroanal. Chem.*, **2003**, *546*, 59.
- [12] D. M. Ruiz and R. E. De Castro, *J. Ind. Microbiol. Biotechnol.*, **2007**, *34*, 111.
- [13] H. Ogino, "Protein Adaptation in Extremophiles", ed. K. S. Siddiqui and T. Thomas, **2008**, Chap. 7, Nova Science Publishers, Inc., New York, 193.
- [14] M. Tjahjono, C. Huiheng, E. Widjaja, K. Sa-Ei, and M. Garland, *Talanta*, **2009**, *79*, 856.
- [15] M. K. Yeh, S. L. Lin, M. I. Leong, S. D. Huang, and M. R. Fuh, *Anal. Sci.*, **2011**, *27*, 49.
- [16] T. Maruyama, H. Matsushita, J. Uchida, F. Kubota, N. Kamiya, and M. Goto, *Anal. Chem.*, **2004**, *76*, 4495.
- [17] F. Torrens, *Chromatographia*, **2001**, *53*, S199.
- [18] F. F. Reuss, *Proceedings of the Imperial Society of Naturalists of Moscow*, **1809**, *2*, 327.
- [19] J. W. Jorgenson and K. D. Lukacs, *Anal. Chem.*, **1981**, *53*, 1298.
- [20] S. Terabe, K. Otsuka, K. Ichikawa, A. Tsuchiya, and T. Ando, *Anal. Chem.*, **1984**,

56, 111.

[21] T. Tsuda, *Anal. Chem.*, **1987**, *59*, 521.

[22] G. Hagen, *Ann. Phys. Chem.*, **1839**, *46*, 423.

[23] J. L. R. Poiseuille, *Comptes Rendus*, **1841**, *11*, 961.

[24] R. B. Bird, W. E. Stewart, and E. N. Lightfoot, *Transport Phenomena*, 2nd edn., Chap. 2, Wiley, Toronto, Canada, 2002.

[25] H. Small, *J. Colloid Interface Sci.*, **1974**, *48*, 147.

[26] Ch. -H. Fischer, M. Giersig, Analysis of Colloids, *J. Chromatogr., A*, **1994**, *688*, 97.

[27] J. C. Giddings, M. N. Myers, G. -C. Lin and M. Martin, *J. Chromatogr., A*, **1977**, *142*, 23.

Chapter 3 Consideration of tube radial distribution phenomenon (TRDP)

TRDP is specific fluidic behavior observed in a microspace under laminar flow conditions. The TRDP creation was considered through experimental data from various viewpoints, including chromatograms obtained with tube radial distribution chromatography (TRDC), phase diagram, tie lines, dimensionless numbers, and solution properties. The part of this chapter is reconstructed and rewritten based on the related manuscripts that have been published.^{27,35,39,51,52)}

3.1 Experimental consideration through the phase diagram in TRDC and TRDP

Capillary chromatography using an untreated open tubular capillary tube and a ternary solvent mixture consisting of water-hydrophilic/hydrophobic organic solvent as a carrier solution has been developed. The system is called tube radial distribution chromatography (TRDC). Separation performance of the TRDC system using a fused-silica capillary tube was examined through the phase diagram for the ternary water-acetonitrile-ethyl acetate solvent mixture. The TRDC system required homogeneous carrier solutions with solvent component ratios around the boundary curve between homogeneous and heterogeneous solution in the phase diagram. The data obtained using the fused-silica capillary tube were compared with those obtained using a polytetrafluoroethylene capillary tube in our study.

Introduction

Capillary tubes with inner diameters less than several hundred micrometers that provide micro-flow are known to exhibit interesting and useful physical or hydrodynamic phenomena, such as electro-osmotic flow and laminar flow. The electro-osmotic flow in a capillary tube promotes capillary electrophoresis [1,2] and capillary electrochromatography [3], while laminar flow conditions enable hydrodynamic chromatography [4,5]. Recently, our group reported the tube radial distribution phenomenon of carrier solvents in a micro-flow, which we call the tube radial distribution phenomenon (TRDP).

The TRDP can be phenomenologically described as follows. When the ternary mixed solvents of water-hydrophilic/hydrophobic organic solvent mixtures are delivered into a micro-space, such as a micro-channel or a capillary tube under laminar flow conditions, the solvent molecules are radially distributed in the micro-space, generating inner and

outer phases. The TRDP creates a phase interface or kinetic aqueous–organic interface in the micro-space. That is, in a water-rich solution we would observe a water-rich major inner phase and organic solvent-rich minor outer phase, while in an organic solvent-rich solution we would observe an organic solvent-rich major inner phase and water-rich minor outer phase in micro-flow under certain conditions.

An untreated open tubular capillary chromatography system where the outer phase functions as a pseudo-stationary phase under laminar flow conditions has been developed based on the TRDP, which we call tube radial distribution chromatography (TRDC). According to the inner and outer phase formation based on the TRDP, with a water-rich carrier solution, the hydrophilic analyte, which is dispersed in the water-rich major phase (around the middle of the capillary tube), is eluted with a nearly average linear velocity. The hydrophobic analyte, which is dispersed in the organic solvent-rich minor phase near the inner wall of the tube (pseudo-stationary phase), is eluted at a lower than average linear velocity. In contrast, with an organic solvent-rich carrier solution, the hydrophobic analyte dispersed in the organic solvent-rich major phase is eluted with a nearly average linear velocity. The hydrophilic analyte dispersed in the water-rich minor phase near the inner wall of the tube is eluted with a lower velocity. Therefore, the elution times of the analytes can be reversed by altering the component ratio of the solvents in the carrier solution.

Separation performance in the TRDC system was examined from the viewpoint of pressure in a capillary tube under laminar flow conditions and the phase diagram of the ternary mixed solvents of water-acetonitrile-ethyl acetate mixture. The component ratios of the solvents that were positioned near the boundary between homogeneous and heterogeneous solution in the diagram were required for TRDC separation. The data suggested that the phase transformation from homogeneous to heterogeneous solution in the capillary tube under pressure in micro-flow was important for TRDP and TRDC. That is, experiments and considerations based on the phase diagram are useful for the study of TRDP or TRDC.

In our study,¹⁵⁾ when using polytetrafluoroethylene (PTFE) capillary tubes, with water-rich carrier solution, hydrophilic 2,6-naphthalenedisulfonic acid and hydrophobic 1-naphthal as model analytes were separated in this order, while with the organic solvent-rich carrier solution, the reverse elution order was observed—i.e., 1-naphthol was first detected, followed by 2,6-naphthalenesulfonic acid—although they showed split-separation. Here, the separation performance of the analytes was examined by the TRDC in a similar way to the study through phase diagrams,¹⁵⁾ using a fused-silica capillary tube instead of a PTFE capillary tube.

Experimental

Fused-silica capillary tubes with an inner diameter of 50 μm were used. The present TRDC system comprised of a fused-silica capillary tube (120 cm total length and 100

cm effective length), micro-syringe pump, and absorption detector. The tube temperature was controlled by dipping the capillary tube (ca. 60 cm) in water maintained at a fixed temperature (0 °C or 20 °C) in a beaker by stirring. The ternary mixed solvents of water-hydrophilic/hydrophobic organic solvent mixture (water-acetonitrile-ethyl acetate) solutions with various volume ratios were used as carrier solutions. Analyte solutions containing 1-naphthol and 2,6-naphthalenedisulfonic acid (1 mM each) as models were prepared with the carrier solutions. The analyte solution was introduced directly into the capillary inlet side by the gravity method (20 cm height for 30 s). After analyte injection, the capillary inlet was connected through a joint to a micro-syringe. The syringe was placed on the micro-syringe pump. The carrier solution was fed into the capillary tube at 0.2 $\mu\text{L min}^{-1}$ flow rate under laminar flow conditions. On-capillary absorption detection (254 nm) was performed with the detector.

Results and discussion

Phase diagram for water-acetonitrile-ethyl acetate mixture The phase diagram for the ternary mixed solvents of water-acetonitrile (hydrophilic organic solvent)-ethyl acetate (hydrophobic organic solvent) in a vessel at a temperature of 20 °C was constructed. The obtained phase diagram is shown in Fig. 1. The dotted curve in the diagram indicates the boundary between homogeneous and heterogeneous phases. The phase diagram showed that each component ratio of the solvents formed a homogeneous (one homogeneous phase) or heterogeneous (two homogeneous phases) solution. The solutions with component ratios of a) – t) were used as carrier solutions in the TRDC system in the following sections. The component ratios of the solvents or the carrier solutions a) – t) are plotted in the diagram based on separation performance of analytes described below, where circles (\circ), triangles (Δ), and crosses (\times) indicated baseline-separation, split-separation (not baseline-separation), and non-separation for the analytes on the chromatograms, respectively.

Chromatograms obtained at various component ratios of water-acetonitrile-ethyl acetate mixture carrier solution Acetonitrile was added to a solution with a constant water-ethyl acetate volume ratio of 5:7 in a vessel at a temperature of 20 °C to prepare carrier solutions (organic solvent-rich carrier solutions) with the following compositions: a) water-acetonitrile-ethyl acetate 5:13:7 volume ratio; b) 5:15:7 volume ratio; c) 5:17:7 volume ratio; d) 5:19:7 volume ratio; and e) 5:20:7 volume ratio. The five carrier solutions a) – e) were all homogeneous solutions. The analyte mixtures of 1-naphthol and 2,6-naphthalenedisulfonic acid were examined with the present TRDC system using carrier solutions a) – e). The obtained chromatograms are shown in Fig. 2. Carrier solutions a) – c) could separate the analytes in the mixture. 1-Naphthol (hydrophobic) was eluted first with near the average linear velocity in the capillary tube

under laminar flow conditions and 2,6-naphthalenedisulfonic acid (hydrophilic) was eluted second at a lower than average linear velocity. The elution order was reasonable in the TRDC system with the organic solvent-rich carrier solution as mentioned in the Introduction. The other homogeneous carrier solutions, d) and e), of water-acetonitrile-ethyl acetate showed split-separation and non-separation of the analytes, respectively, under the present analytical conditions. The separation performances obtained with carrier solutions a) – e) are plotted with the following symbols: circles (○), triangles (Δ), and crosses (×) in the phase diagram in Fig. 1. The separation performance decreased from carrier solution a) to e) as shown in Fig. 2. However, even carrier solutions b) and c) in which the compositions were a little far from the boundary in the diagram also showed baseline-separation for the analytes. TRDP must occur with such allowance for the solvents compositions around the boundary in this area of the diagram. The chromatograms of the analytes, the mixture of 1-naphthol and 2,6-naphthalenedisulfonic acid, were examined with the homogeneous carrier solutions f) – t). The compositions for the solutions f) – t) were positioned near the boundary in the phase diagram; f) water-acetonitrile-ethyl acetate with a 0.25:0:10 volume ratio, g) 0.4:1:9 volume ratio, h) 0.55:2:8 volume ratio, i) 0.8:3:7 volume ratio, j) 1.1:4:6 volume ratio, k) 1.5:5:5 volume ratio, l) 2.05:6:4 volume ratio, m) 14:30:15 volume ratio, n) 4:6:2.4 volume ratio, o) 5:5:1.75 volume ratio, p) 6:4:1.3 volume ratio, q) 7:3:1.1 volume ratio, r) 8:2:0.95 volume ratio, s) 9:1:0.95 volume ratio, and t) 10:0:0.9 volume ratio. The carrier solutions f) – i) and p) – t) showed no separation behavior and presented just single peaks on the chromatograms with near the average linear velocity (data not shown). The carrier solutions j) – o) showed separation behavior as indicated in Fig. 3. The component ratios of the solvents for solutions f) – t) were plotted in the phase diagram in Fig. 1 with the symbols based on the chromatographic data. As shown in Fig. 1, the TRDC system was used with several homogeneous carrier solutions with component ratios of the solvents around the boundary curve in the phase diagram. Such specific carrier solutions caused a tube radial distribution of the carrier solvents in the capillary tube under laminar flow conditions, i.e., the TRDP. The pressure imposed on the carrier solution in the capillary tube under laminar flow conditions might alter the carrier solution from homogeneous in the batch vessel to heterogeneous in the tube, affecting the tube radial distribution of the solvents in the capillary tube.

Optimization of the component ratio of solvents for separation As shown in Fig. 3, high resolutions of the analytes in the TRDC system were observed around the carrier solutions of l) and m) in the phase diagram. The chromatograms were examined in more detail with carrier solutions u) – w) that had compositions between solutions l) and m) along the boundary curve in the phase diagram (Fig. 1). They were u) water-acetonitrile-ethyl acetate with a 5:14.5:8.5 volume ratio, v) 5:13:7 volume ratio,

and w) 6:13.5:6.5 volume ratio. The obtained chromatograms are shown in Fig. 4 together with their resolutions (R_s). Carrier solutions v) and w) showed the best resolutions, ca. 14, under the present analytical conditions.

Reversing of the elution order of the analytes As characteristic separation behavior of the TRDC system using the PTFE capillary tube, we reported that a water-rich carrier solution elutes the more hydrophilic analyte first and an organic solvent-rich carrier solution elutes the more hydrophobic analyte first.¹⁵⁾ However, the reverse elution behavior of the analytes was not observed in Fig. 3 under these analytical conditions. The analytical conditions, such as tube temperature, tube length, and flow rate, were significant and critical for separation performance in the TRDC system. Tentatively, the chromatograms were examined by the TRDC system using carrier solutions f) – t) where the capillary tube was dipped in the beaker controlled at 0 °C instead of 20 °C. The separation performance with solutions f) – t) were plotted with the symbols in the diagram in Fig. 5. The chromatograms obtained with carrier solutions l) – q) that show separation are presented in Fig. 6. Water-rich carrier solutions p) and q) gave the reverse elution order, 2,6-naphthalenedisulfonic acid first and then 1-naphthol second, although they showed split-separation. Furthermore, the analyte solutions were subjected to the TRDC system with the water-rich carrier solution of water-acetonitrile-ethyl acetate in a 15:3:2 volume ratio (water-rich carrier solution) under the analytical conditions of tube temperature 0 °C instead of 20 °C, a tube effective length of 200 cm instead of 100 cm, and a flow rate of 0.8 $\mu\text{L min}^{-1}$ instead of 0.2 $\mu\text{L min}^{-1}$. The obtained chromatogram is shown in Fig. 7. 2,6-Naphthalenedisulfonic acid and 1-naphthol were eluted in this order with baseline-separation. The individual peaks were identified with the chromatogram of each analyte.

Consideration of the influence of the tube materials on separation Almost the same elution behavior or elution order in the TRDC system with the fused-silica capillary tube was observed as that with the PTFE capillary tube reported in our work.¹⁵⁾ However, there were also differences in separation behavior between them. In the fused-silica capillary tube, the resolutions obtained with the organic solvent-rich carrier solution were better than those of the water-rich carrier solution. On the other hand, in the PTFE capillary tube, the resolutions obtained with the water-rich carrier solution were better than those of the organic solvent-rich carrier solutions as reported.¹⁵⁾ The interaction between the outer phase of water-rich and fused-silica inner wall as well as the outer phase of organic solvent-rich and PTFE (polymer material) inner wall may give prior conditions for making the outer phase (pseudo-stationary phase) in the capillary tube, while the interaction between the outer phase of water-rich and polymer material inner wall as well as the outer phase of organic solvent-rich and fused-silica inner wall may result in conditions inconvenient for forming the outer phase in the

capillary tube.

In conclusion, chromatograms of model analytes were examined by the TRDC system using a fused-silica capillary tube from the viewpoint of the phase diagram of ternary mixed solvents. The separation performances of the analytes were similar to those obtained with a PTFE capillary tube described in our work.¹⁵⁾ The organic solvent-rich carrier solution, model analytes, hydrophobic 1-naphthol and hydrophilic 2,6-naphthalenedisulfonic acid, were separated in this order, while they were eluted in the inverse order with the water-rich carrier solution, 2,6-naphthalenedisulfonic acid was detected first, followed by 1-naphthol detection. However, the fused-silica capillary tube resolutions obtained with the organic solvent-rich carrier solution were better than those of the water-rich carrier solution. The interaction between the outer phase of the water-rich and fused-silica surface may provide better conditions than that between the outer phase of organic solvent-rich and fused-silica surface for forming the outer phase in fused-silica capillary tubes.

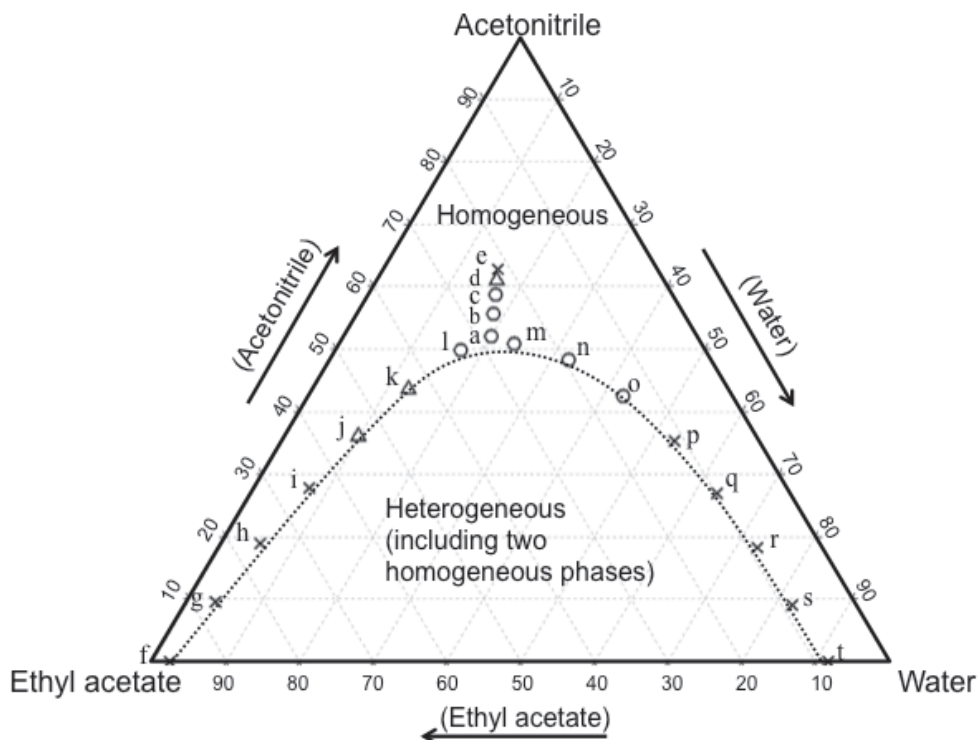


Figure 1. Phase diagram for water-acetonitrile-ethyl acetate mixture (20 °C) and the component ratios of the solvents for the chromatograms obtained by the TRDC system with tube temperature 20 °C. The component ratios of the carrier solutions a) – e) related to the experiments shown in Fig. 2 as well as the carrier solutions f) – t) related to the experiments in Fig. 3 are plotted in the diagram with the symbols ○, Δ, and ×, indicating baseline-separation, split-separation, and non-separation, respectively, for the analytes.

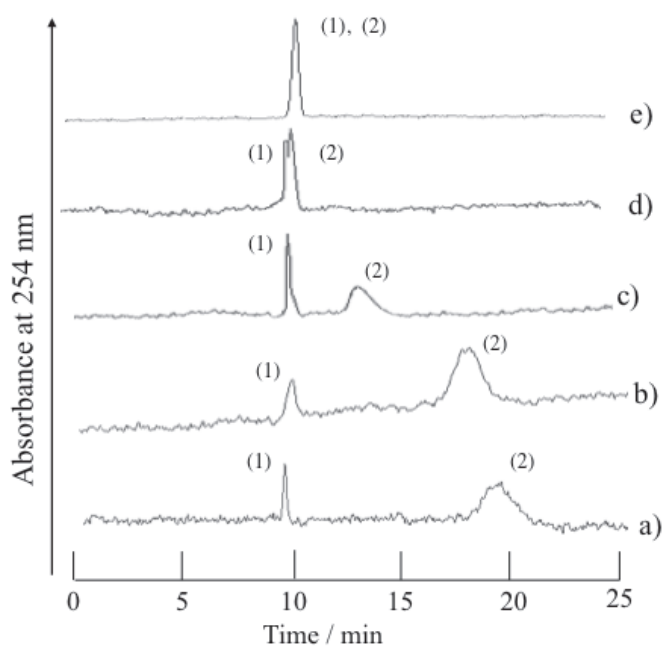


Figure 2. Chromatograms of a mixture of 1-naphthol and 2,6-naphthalenedisulfonic acid by the TRDC system using various component ratios of water-acetonitrile-ethyl acetate mixture as carrier solutions. Tube temperature 20 °C. (1) 1-Naphthol and (2) 2,6-naphthalenedisulfonic acid were eluted in this order with carrier solutions a) – d).

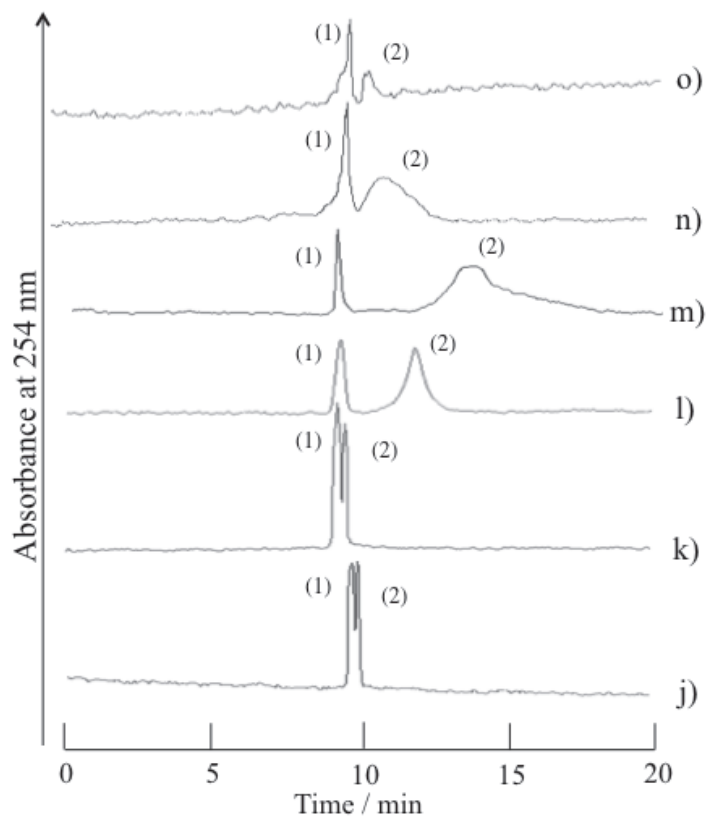


Figure 3. Chromatograms of a mixture of 1-naphthol and 2,6-naphthalenedisulfonic acid by the TRDC system using various component ratios of water-acetonitrile-ethyl acetate mixture as carrier solutions that were positioned near the boundary curve in the phase diagram. Tube temperature 20 °C. (1) 1-Naphthol and (2) 2,6-naphthalenedisulfonic acid were eluted in this order with the carrier solutions j) – o).

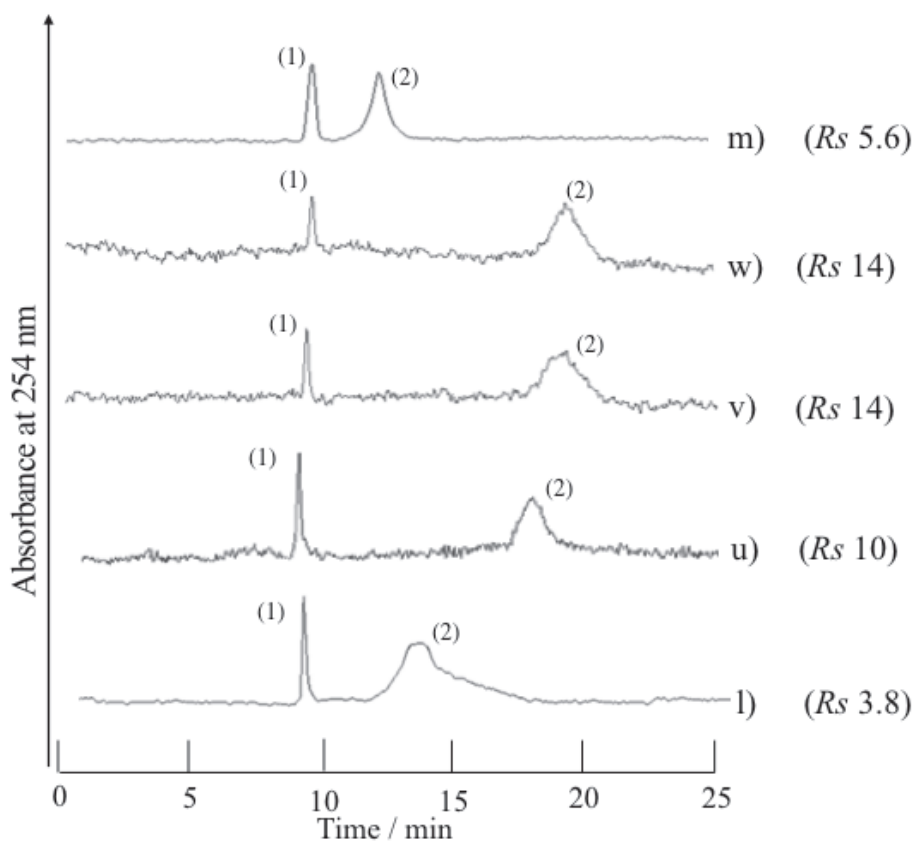


Figure 4. Chromatograms of a mixture of 1-naphthol and 2,6-naphthalenedisulfonic acid by the TRDC system using various component ratios of water-acetonitrile-ethyl acetate mixture as carrier solutions that were positioned between solutions l) and m) in Fig. 3 and the resolutions (R_s) for the analyte peaks. Tube temperature 20 °C. (1) 1-Naphthol and (2) 2,6-naphthalenedisulfonic acid were eluted in this order with carrier solutions l) – m).

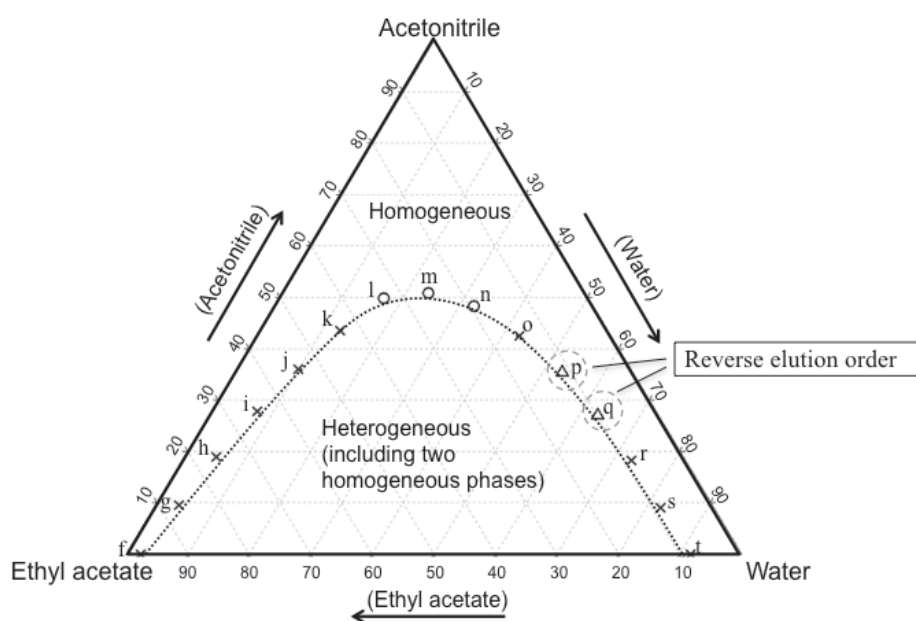


Figure 5. Phase diagram for water-acetonitrile-ethyl acetate mixture (20 °C) and the component ratios of the solvents for the chromatograms obtained by the TRDC system with tube temperature 0 °C. The component ratios of the carrier solvents f) – t) are plotted in the diagram with the symbols (○, Δ, and ×). 1-Naphthol and 2,6-naphthalenedisulfonic acid were eluted in this order with carrier solutions l) – n), while they were eluted in the reverse order with the carrier solutions p) and q).

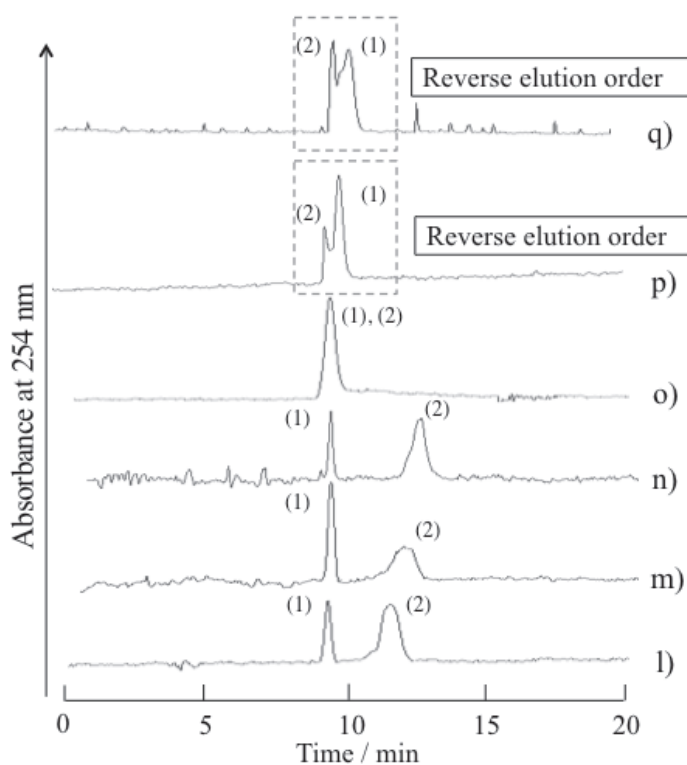


Figure 6. Chromatograms of a mixture of 1-naphthol and 2,6-naphthalenedisulfonic acid by the TRDC system using various component ratios of water-acetonitrile-ethyl acetate mixture as carrier solutions that were positioned near the boundary curve in the phase diagram. Tube temperature 0 °C. (1) 1-Naphthol and (2) 2,6-naphthalenedisulfonic acid were eluted in this order with carrier solutions l) – n), while they were eluted in the reverse order with carrier solutions p) and q). The component ratios of carrier solutions l) –p) used for the chromatograms are plotted in the phase diagram of Fig. 5.

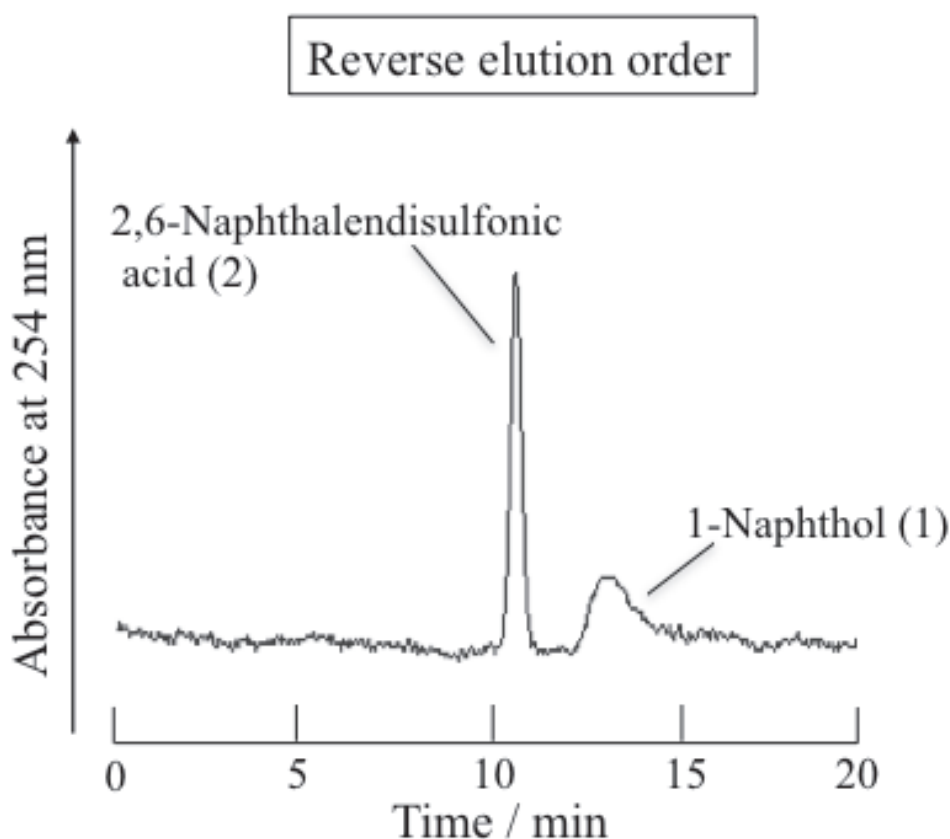


Figure 7. Chromatograms of a mixture of (1) 1-naphthol and (2) 2,6-naphthalenedisulfonic acid by the TRDC system. Capillary effective length, 200 cm (total length 220 cm); carrier, water-acetonitrile-ethyl acetate of 15:3:2 volume ratio; tube temperature, 0 °C; and flow rate, 0.8 $\mu\text{L min}^{-1}$.

3.2 Experimental consideration through the phase diagram including solubility curves at different temperatures in TRDC and TRDP

Open-tubular capillary chromatography using a ternary solvent mixture consisting of water–hydrophilic–hydrophobic organic solvent as a carrier solution has been developed. When the ternary carrier solution is fed into the capillary tube, the carrier solvents are radially distributed and generate inner and outer phases in the tube. The outer phase functions as a pseudo-stationary phase in chromatography. Here, investigations proceeded with reference to the solubility curves on the phase diagram of the ternary mixed solvents at 5 and 20 °C. Model analytes, 1-naphthol and 2,6-naphthalenedisulfonic acid (2,6-NDS), were examined with ternary water–acetonitrile–ethyl acetate solvent mixtures as carrier solutions and a fused-silica capillary tube (50 μm inner diameter). They were separated in this order with organic solvent-rich carrier solutions, while, in the reverse order with the water-rich carrier solutions at a tube temperature of 5 °C.

Introduction

Since the nineteenth century, microfluidic flow has been known to exhibit interesting and useful physical and hydrodynamic phenomena such as electroosmotic flow and laminar flow. Our group reported the tube radial distribution phenomenon of carrier solvents in 2009, which we call the tube radial distribution phenomenon (TRDP). When the ternary mixed solvents of water–hydrophilic/hydrophobic organic solvent mixtures are delivered into a microspace such as a microchannel or a capillary tube under laminar flow conditions, the solvent molecules are radially distributed in the microspace and generate inner and outer phases.

The TRDP creates a phase interface or a kinetic liquid-liquid interface in a microspace. We are currently investigating the TRDP from the viewpoint of chromatography,^{19,24)} extraction,¹⁶⁾ mixing,²⁶⁾ and chemical reaction space.²⁸⁾ A capillary chromatography system in which the outer phase acts as a pseudo-stationary phase under laminar flow conditions has been developed based on the TRDP. We call it tube radial distribution chromatography (TRDC).

The TRDP appears through phase separation from homogeneous solution to heterogeneous solution including two phases with pressure and temperature changes. The phase separation with associated changes forms an upper and lower phase in a batch vessel under the control of gravity. At the same time, the phase separation introduces TRDP, including inner and outer phases, in a micro-flow under laminar flow conditions with minimal control from gravity. During the TRDP and TRDC investigation, we considered that the solubility curves on the phase diagram must be useful tools for investigation. Here, various component ratios of the ternary mixed solvents on the phase diagram including solubility curves were used as carrier solutions

in the TRDC, and the obtained chromatograms are considered together along with the data provided through the solubility curves.

Experimental

Fused-silica capillary tubes (50 μm inner diameter) were used. A schematic diagram of the present capillary chromatography system (TRDC system) comprised an open-tubular fused-silica capillary tube having (120 cm total length and 100 cm effective length), microsyringe pump, and absorption detector. The tube temperature was controlled by dipping the capillary tube in water maintained at a definite temperature (5 or 20 $^{\circ}\text{C}$) in a beaker with stirring. Water–acetonitrile–ethyl acetate solvent mixtures were used as carrier solutions. Analyte solutions including 1-naphthol and 2,6-NDS (1 mM each) were prepared using the carrier solutions. The analyte solution was introduced directly into the capillary inlet using the gravity method (20 s \times 30 cm height). After analyte injection, the capillary inlet was connected through a joint to a microsyringe. The syringe was set on the microsyringe pump. The carrier solution was fed into the capillary tube at a definite flow rate (0.2 $\mu\text{L min}^{-1}$) under laminar flow conditions. On capillary absorption detection (254 nm) was performed using the detector.

Results and discussion

Phase diagram for ternary solvents A phase diagram for the ternary mixture of water–acetonitrile (hydrophilic organic solvent)–ethyl acetate (hydrophobic organic solvent) was examined in a batch vessel at temperatures of 5 and 20 $^{\circ}\text{C}$. The obtained phase diagram is shown in Fig. 1. The curves expressed in the diagram (\blacklozenge : 5 $^{\circ}\text{C}$ and \square : 20 $^{\circ}\text{C}$) indicate the solubility curves. The inside and outside of the curves represent heterogeneous and homogeneous solutions, respectively. The phase diagram shows that each component ratio of the solvents forms a homogeneous (one homogeneous phase) or heterogeneous (two homogeneous phases) solution. The heterogeneous solutions include the upper (organic solvent-rich solution) and lower (water-rich solution) phases in the batch vessel. The component ratios of the solvents in the solutions **1–10** are plotted in the diagram.

Chromatograms obtained with tube temperatures of 20 $^{\circ}\text{C}$ The model analytes, hydrophobic 1-naphthol and hydrophilic 2,6-NDS, were examined with the present TRDC system at a tube temperature of 20 $^{\circ}\text{C}$. The ternary mixture of water–acetonitrile–ethyl acetate homogeneous solution **1** (the volume ratio of 3:9:4) and **7** (60:13:7) were used as the organic solvent-rich and water-rich carrier solutions, respectively. The compositions of solvents **1** and **7** were positioned close to the solubility curve at 20 $^{\circ}\text{C}$ (Fig. 1). 1-Naphthol and 2,6-NDS were separated in this order with the organic solvent-rich carrier solution, but were not separated with the water-rich

carrier solution (Fig. 2).

Chromatograms obtained with tube temperatures of 5 °C The analytes were examined with the TRDC system at a tube temperature of 5 °C. The homogeneous carrier solutions **1–6** and **7–10** were used as the organic solvent-rich and water-rich carrier solutions, respectively. The obtained chromatograms are shown in Fig. 3. The solvent compositions are described in the figure captions. 1-Naphthol and 2,6-NDS were separated in this order with the organic solvent-rich carrier solution (**1–5**), but they were not separated with carrier solution **6**, for which the solvent composition was positioned outside the solubility curve at 5 °C (homogeneous region). With the water-rich carrier solution, 1-naphthol and 2,6-NDS were separated in the reverse elution order with carrier solutions **7** and **8**, but they were not separated with carrier solutions **9** and **10**, for which solvent compositions were placed outside the solubility curve at 5 °C (homogeneous region). The elution order of the analytes could be changed by altering the component ratios of the solvents, organic solvent-rich or water-rich, at a tube temperature of 5 °C. The experimental data were consistent with the TRDC separation performance and the principles, which were reported.^{2,14,17} With the organic solvent-rich solution, the organic solvent-rich major phase was generated around the middle of the capillary tube as an inner phase, whereas a water-rich minor phase was formed near the inner wall as an outer phase (pseudo-stationary phase). In contrast, with the water-rich solution, the water-rich major phase was generated as an inner phase, whereas the organic solvent-rich minor phase was formed as an outer phase. While undergoing chromatographic separation, the hydrophobic and hydrophilic model analytes were distributed in the inner and outer phases because of their nature.

Consideration through phase diagram and chromatogram The organic solvent-rich carrier solutions (**1–5**), for which solvent compositions existed in a large domain between the solubility curves of 5 and 20 °C as shown in Fig. 1, showed better resolution than the water-rich carrier solutions (**7** and **8**), for which solvent compositions existed in a more narrow domain. It was suggested that separation performance in the TRDC might be related to the data provided through the tie lines on the phase diagram.

In conclusion, a phase diagram including solubility curves at 5 and 20 °C was constructed and the component ratios of the solvents near the solubility curves were used as carrier solutions in the TRDC to expand our knowledge of the TRDP and TRDC. Model analytes, 1-naphthol and 2,6-NDS, were separated in this order with organic solvent-rich carrier solutions, and in the reverse order with the water-rich carrier solutions at a tube temperature of 5 °C. The organic solvent-rich carrier solutions, for which solvent compositions existed in a large domain between the solubility curves of 5

and 20 °C, showed better resolution than the water-rich carrier solutions, for which solvent compositions existed in a narrow domain. Introducing the phase diagram concept into the TRDC and TRDP will improve to ease and clarity of related investigations in the future.

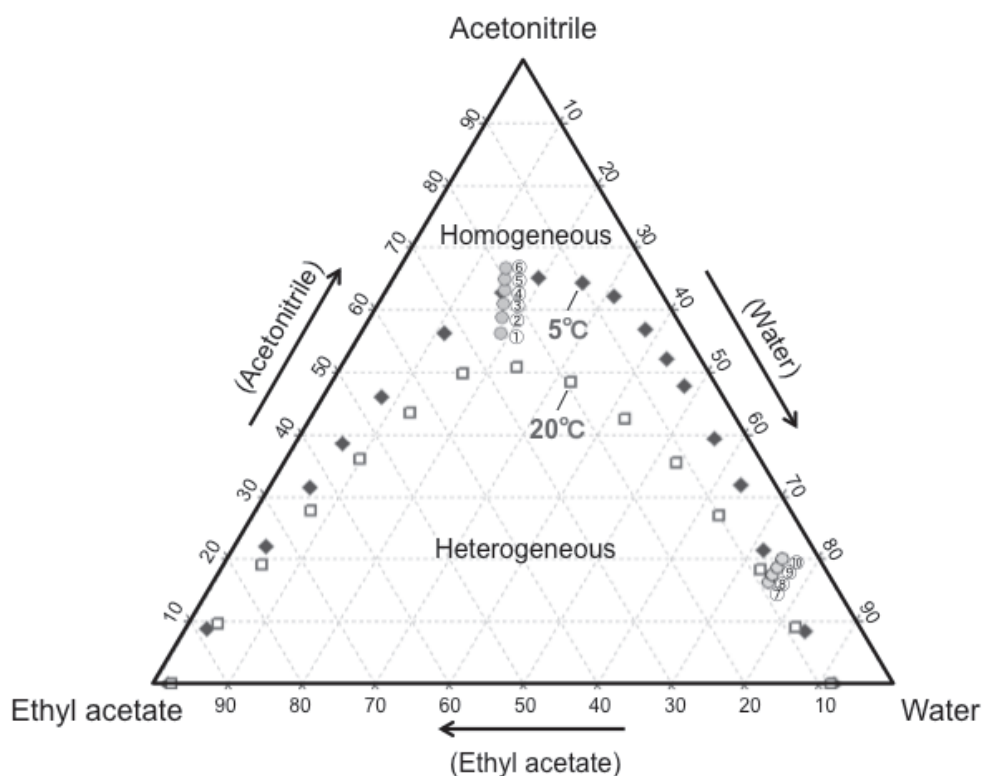


Figure 1. Phase diagram for water–acetonitrile–ethyl acetate mixture at 5 and 20 °C. The curves labeled with symbols ◆ and ◻ in the diagram indicate the solubility curves at 5 and 20 °C, respectively. The symbol ● shows the component ratios of solutions 1-10 that gave the chromatograms as shown in Fig. 3.

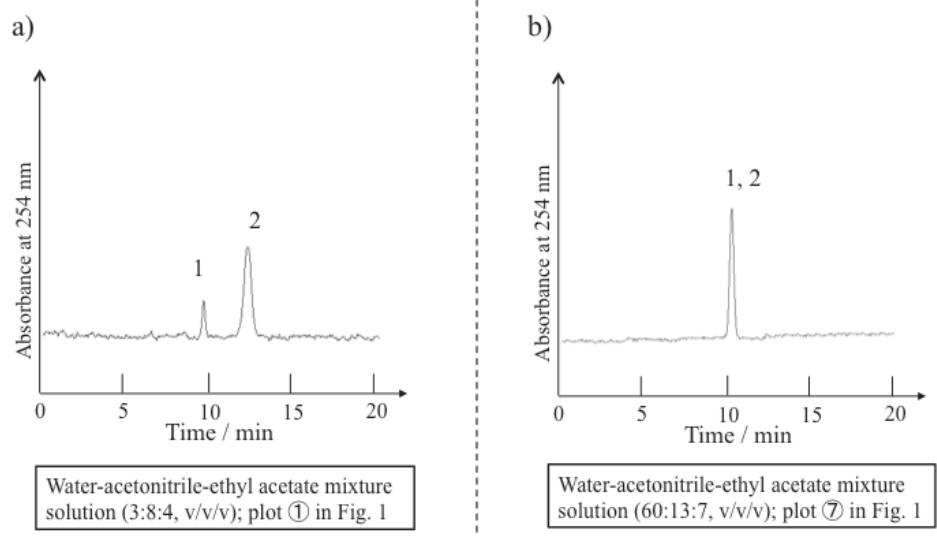


Figure 2. Chromatograms of 1-naphthol (peak 1) and 2,6-NDS (peak 2) by the TRDC system with tube temperature of 20 °C. a) Organic solvent-rich and b) water-rich carrier solution have water–acetonitrile–ethyl acetate mixture volume ratio of a) 3:8:4 and b) 60:13:7, respectively.

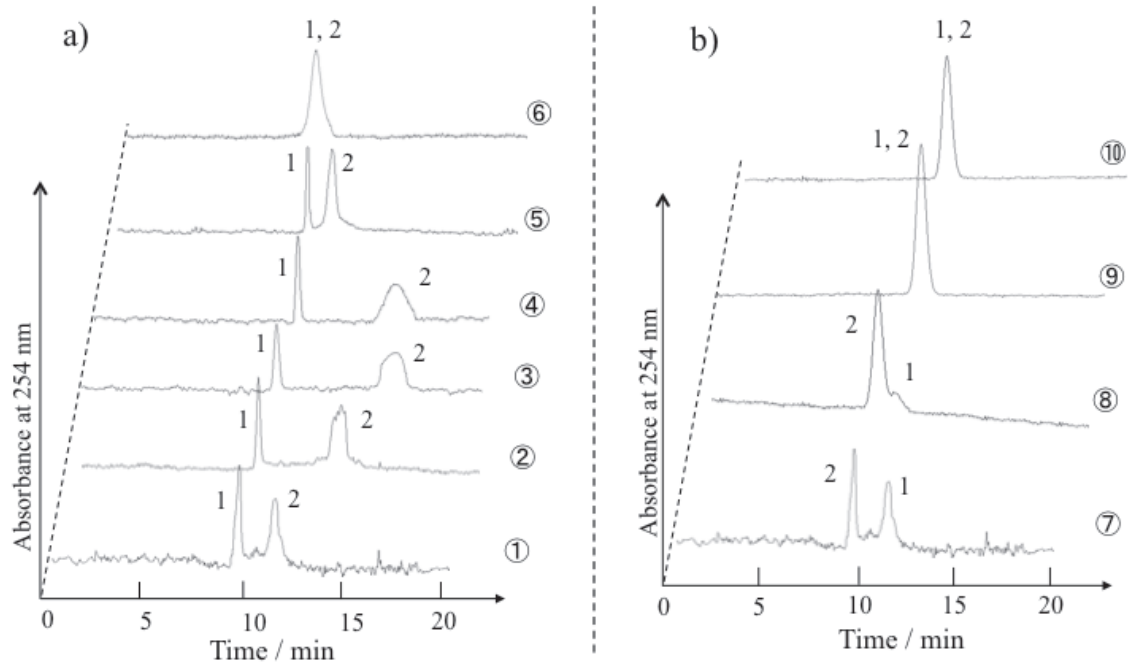


Figure 3. Chromatograms of 1-naphthol (peak 1) and 2,6-NDS (peak 2) by the TRDC system with tube temperature of 5°C. The water–acetonitrile–ethyl acetate mixture volume ratio of ① 3:9:4, ② 3:10:4, ③ 3:11:4, ④ 3:12:4, ⑤ 3:13:4, ⑥ 3:14:4 in a) organic solvent-rich carrier solutions and ⑦ 60:13:7, ⑧ 60:14:6, ⑨ 60:15:5, ⑩ 60:16:4 in b) water-rich carrier solutions.

3.3 Experimental consideration through the phase diagram including tie lines and solubility curves in TRDC and TRDP

Open-tubular capillary chromatography using a ternary solvent mixture consisting of a water–hydrophilic–hydrophobic organic solvent as a carrier solution has been developed. When the ternary carrier solution is fed into the capillary tube, the carrier solvents are radially distributed and generate inner and outer phases in the tube. The outer phase functions as a pseudo-stationary phase in chromatography. Here, investigations proceeded with reference to the tie lines and solubility curves on the phase diagram of the ternary mixed solvents. Model analytes, 1-naphthol and 2,6-naphthalenedisulfonic acid, were separated in this order with ternary water–acetonitrile–ethyl acetate solvent mixtures (organic solvent-rich solutions) that possessed various solvent compositions on the tie lines. In addition, fluorescence photographs of the dyes dissolved in the ternary solvents in the capillary tubes were observed with a fluorescence microscope-CCD camera system. It was found that the separation performance on the chromatograms and the phase formation observed in the fluorescence photographs were related to data provided through the tie lines and solubility curves on the phase diagram. The solvent compositions on the same tie line that gave different volume ratios of upper and lower phases in a vessel influenced the chromatographic separation, or the resolutions of the analytes, and also the inner and outer phase formation in the chromatography.

Introduction

The TRDP creates a phase interface or a kinetic liquid-liquid interface in a microspace. We are currently investigating the TRDP from the viewpoint of chromatography, extraction, mixing, and chemical reaction space. A capillary chromatography system in which the outer phase acts as a pseudo-stationary phase under laminar flow conditions has been developed based on the TRDP. We call it TRDC.

The TRDP appears through phase separation from a homogeneous solution to a heterogeneous solution including two phases with pressure and temperature changes. The phase separation with associated changes forms an upper and lower phase in a batch vessel under the influence of gravity. At the same time, the phase separation introduces TRDP, including inner and outer phases in a micro-flow under laminar flow conditions where gravity has no influence. During the TRDP and TRDC investigation, we considered that tie lines and the solubility curves on the phase diagram would be useful tools for investigation. Here, various component ratios of the ternary mixed solvents on the tie lines were used as carrier solutions in the TRDC, and the obtained chromatograms and fluorescence photographs were considered together along with data provided through the tie lines and solubility curves.

Experimental

TRDC system Fused-silica capillary tubes (50 μm inner diameter) were used. A schematic diagram of the present capillary chromatography system (TRDC system) comprised an open-tubular fused-silica capillary tube (120 cm total length and 100 cm effective length), a microsyringe pump, and an absorption detector (Fig. 1 A)). The tube temperature was controlled by dipping the capillary tube in water maintained at a steady temperature (5 $^{\circ}\text{C}$) in a beaker with stirring. Water–acetonitrile–ethyl acetate solvent mixtures were used as carrier solutions. Analyte solutions including 1-naphthol and 2,6-naphthalenedisulfonic acid (1 mM each) were prepared using the carrier solutions. The analyte solution was introduced directly into the capillary inlet using the gravity method (20 s \times 30 cm height). After analyte injection, the capillary inlet was connected through a joint to a microsyringe. The syringe was set on the microsyringe pump. The carrier solution was fed into the capillary tube at a definite flow rate (0.2 $\mu\text{L min}^{-1}$) under laminar flow conditions. Upon capillary absorption, detection (254 nm) was performed using the detector.

Fluorescence photographs We set up a capillary tube of the same size as that used in the TRDC system for the fluorescence microscope-CCD camera system (Fig. 1 B)). The fluorescence in the capillary tube was monitored at approximately 100 cm from the capillary inlet using a fluorescence microscope equipped with an Hg lamp, a filter, and a CCD camera. The carrier solution contained 0.1 mM perylene (blue) and 1 mM Eosin Y (green). The carrier solution was delivered into the capillary tube at a definite flow rate (0.2 $\mu\text{L min}^{-1}$) using a microsyringe pump.

Results and Discussion

Tie lines in the phase diagram Fig. 2 shows the tie lines at 5 $^{\circ}\text{C}$ on the phase diagram. The tie lines were constructed using the solvent composition of the homogeneous solution at 20 $^{\circ}\text{C}$, the water content of the lower phase (the water-rich phase) in a batch vessel at 5 $^{\circ}\text{C}$, and the solubility curve at 5 $^{\circ}\text{C}$. The plots of **i–vi** are on the same tie line, and the volume ratios of the upper and lower phases at 5 $^{\circ}\text{C}$ in the batch vessel change in accordance with the ratios of the line lengths, which are separated by the plots on the tie line (although the solvent compositions of the upper and lower phases are all the same for the plots of **i–vi**, water-acetonitrile-ethyl acetate volume ratios of upper and lower phases are 17:64:19 and 58:36:6, respectively). For example, the solvent composition of **i** changes from a homogeneous solution at 20 $^{\circ}\text{C}$ to a heterogeneous solution including upper (organic solvent-rich) and lower (water-rich) phases with the volume ratio of the upper and lower phases at 6:4 at 5 $^{\circ}\text{C}$ in a vessel. Similarly, the volume ratios of the upper and lower phase for plots **ii–vi** are 7:3, 8:2, 9:1, 9.5:0.5, and

9.8:0.2, respectively. In addition, the plots of **v** and **vii–ix** are on different tie lines on the phase diagram. However, the solutions of the plots of **v** and **vii–ix** at 20 °C are separated into a 9.5 (upper phase):0.5 (lower phase) volume ratio at 5 °C in the batch vessel (although the solvent compositions of the upper and lower phases are quite different for the plots of **v** and **vii–ix**).

Effects of volume ratios of the upper and lower phases in a batch vessel on separation performance in TRDC As described in the introduction, the phase separation with pressure and temperature changes forms between upper and lower phases in a batch vessel under the control of gravity. At the same time, the phase separation introduces TRDP, including inner and outer phases in a micro-flow where it is under laminar flow conditions and not controlled by gravity. The volume ratios of the upper and lower phases in a vessel that were estimated using the tie lines would not necessarily be equal to those of the inner and outer phases in TRDP. However, we believe that the volume ratios of the upper and lower phases in a vessel may be related to the formation of inner and outer phases in the TRDP. First, we attempted to examine the effects of the solvent compositions on the same tie line, or phase volume ratios in a vessel, on the separation performance in the TRDC. The solvent compositions provide different volume ratios of the upper and lower phases in a batch vessel (from 6:4 to 9.8:0.2), as described above. The analytes, 1-naphthol and 2,6-naphthalenedisulfonic acid, were examined with the TRDC system using carrier solutions **i–vi**. The obtained chromatograms are shown in Fig. 3 together with the resolutions (R_s), whereas the solvent compositions are described in the figure captions. 1-Naphthol and 2,6-naphthalenedisulfonic acid were separated in this order with carrier solutions **ii–vi**, but they were not separated with carrier solution **i**. Improved resolutions were observed around carrier solutions **iv** and **v**; R_s , 6.3–7.0. In addition, fluorescence photographs were observed with a fluorescence microscope-CCD camera system. The obtained results are shown in Fig. 4. The inner and outer phases in the capillary tube were formed with carrier solutions **ii–vi**, although the distribution patterns of the dyes differed from each other to some extent. However, the formation was not observed with carrier solution **i**. The observed TRDP was almost consistent with the chromatographic separation, as shown in Fig. 3. The solvent compositions on the same tie line that gave different volume ratios of upper and lower phases in the vessel, influenced the inner and outer phase formation in the TRDC, and also changed R_s on the chromatograms.

Effects of solvent compositions on the different tie lines on the separation performance in TRDC Next, the analytes, 1-naphthol and 2,6-naphthalenedisulfonic acid, were examined with the TRDC system using carrier solutions **v** and **vii–ix** on different tie lines. The solvent compositions of these systems provided the same volume ratios of the upper and lower phases (9.5:0.5) in the batch vessel, as described above. The obtained

chromatograms are shown in Fig. 5 together with R_s , whereas the solvent compositions are described in the figure captions. 1-Naphthol and 2,6-naphthalenedisulfonic acid were separated in this order with carrier solutions **v** and **vii–ix** at similar resolutions; R_s , 5.6–7.0. Furthermore, fluorescence photographs were observed with a fluorescence microscope-CCD camera system. The inner and outer phases in the capillary tube were formed with carrier solutions **v** and **vii–ix** with similar distribution patterns of the dyes (Fig. 6). The observed TRDP was consistent with the chromatographic separation shown in Fig. 5. The experimental data indicated that the TRDC proceeds through phase separation from a homogeneous solution to a heterogeneous solution, little influenced by the solvent compositions of the inner and outer phases in the capillary tube.

In conclusion, the component ratios of the solvents on the tie lines were used as carrier solutions in the TRDC to expand our knowledge of the TRDP and TRDC. The different solvent compositions on the same tie line that gave different volume ratios of the upper and lower phases in a vessel influenced the R_s of analytes on the chromatograms and the formation of inner and outer phases in the TRDC. Furthermore, if the different solvent compositions on the different tie lines provided the same volume ratio of the upper and lower phases in a vessel, then the obtained chromatograms and fluorescence photographs would be similar to each other in the TRDC. The experimental data supported that TRDC was performed through the phase separation from a homogeneous solution to a heterogeneous solution. Introducing the tie lines concept into the TRDC and TRDP will increase both the ease and clarity of related investigations in the future.

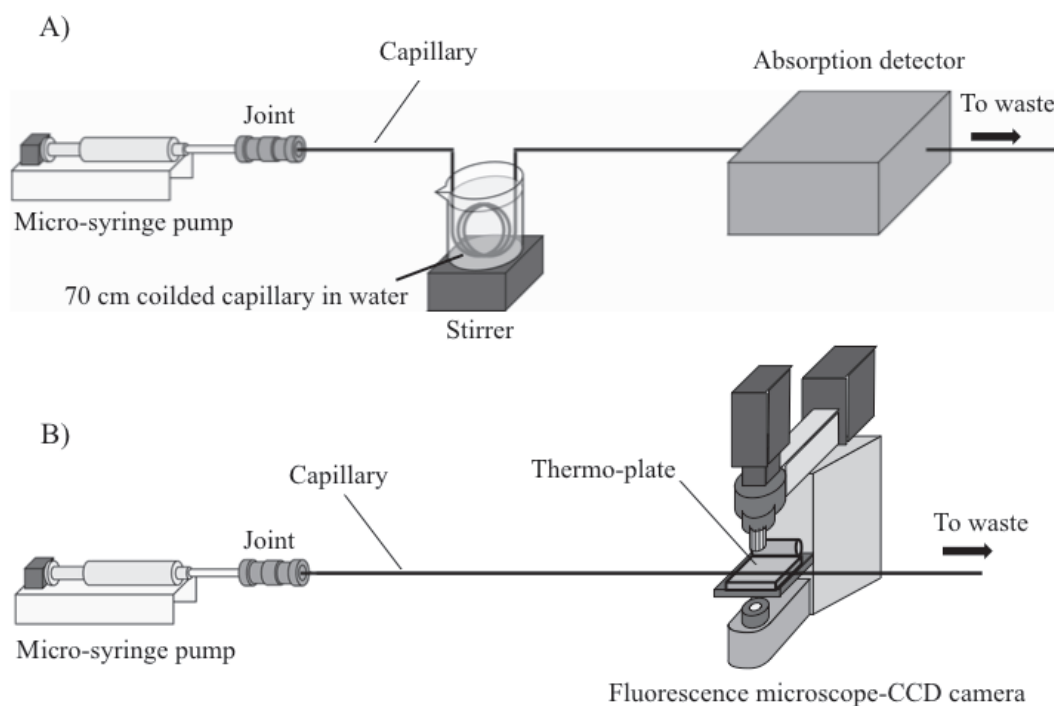


Figure 1. Schematic diagrams of A) open-tubular capillary chromatographic system (TRDC system) and B) fluorescence microscope-CCD camera.

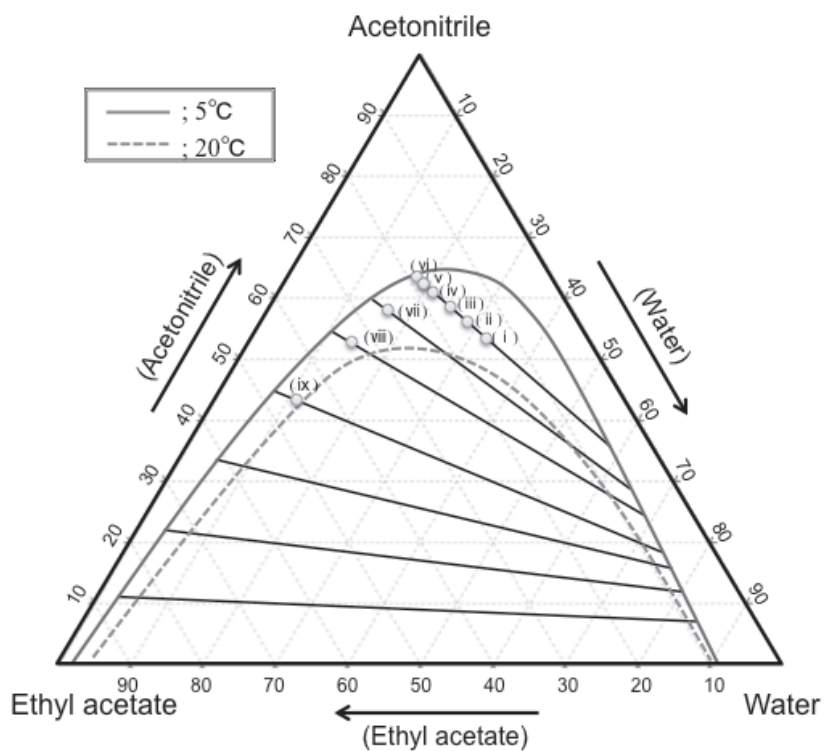


Figure 2. Tie lines in the phase diagram at 5 °C. The \circ s express the prepared component ratios of the solvents in the heterogeneous solutions at 20 °C.

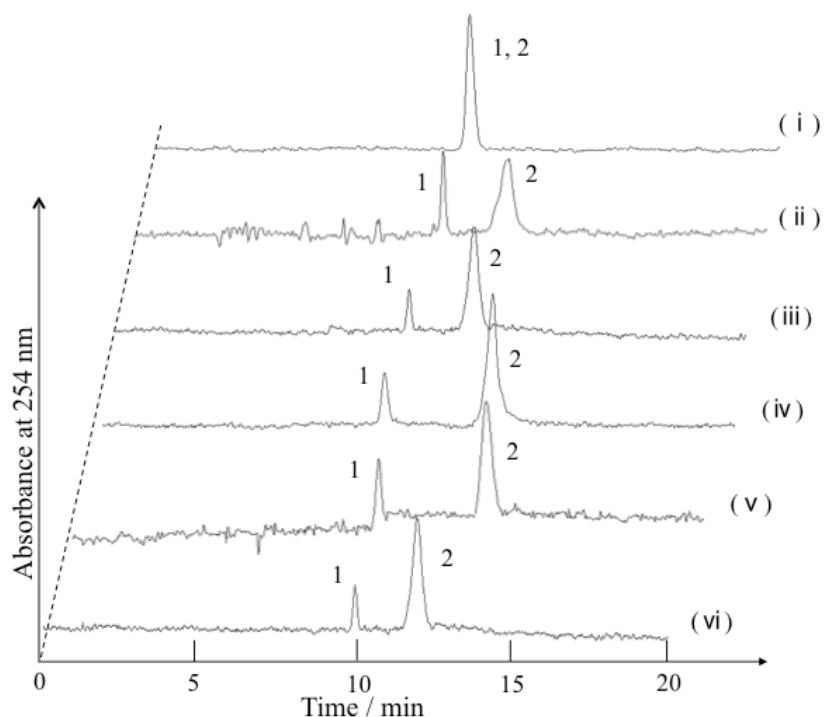


Figure 3. Chromatograms of 1-naphthol and 2,6-naphthalenedisulfonic acid by the TRDC system with tube temperature of 5 °C. 1; 1-Naphthol and 2; 2,6-naphthalenedisulfonic acid. Carrier, water–acetonitrile–ethyl acetate mixture volume ratio of (i) 34:53:13, (ii) 30:56:14, (iii) 26:58:16, (iv) 21:62:17, (v) 19:63:18, and (vi) 18:64:18.

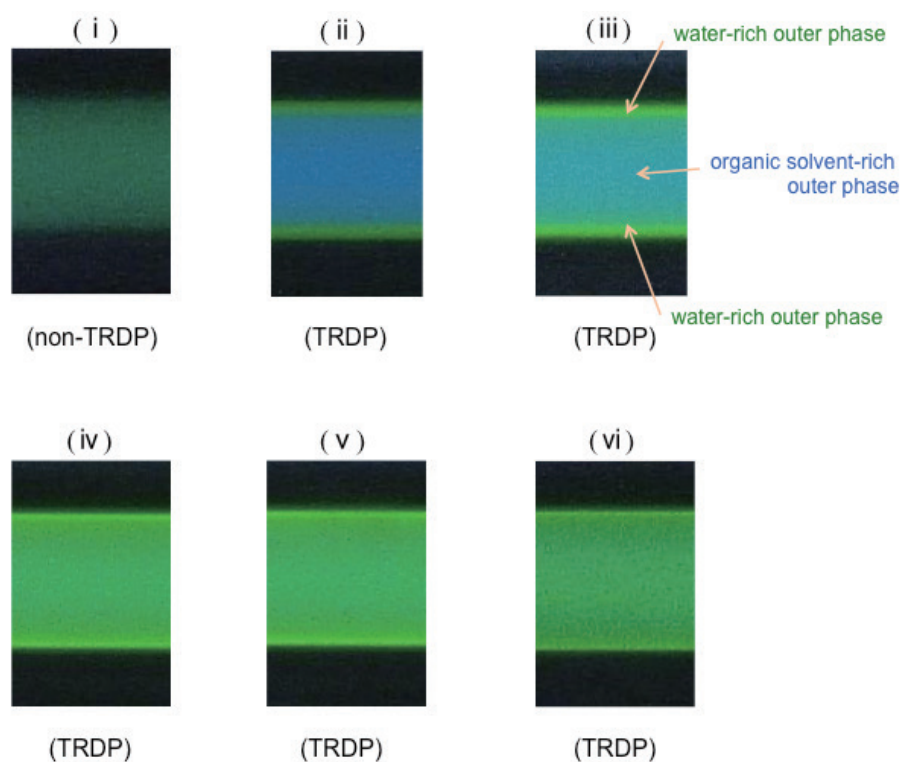


Figure 4. Fluorescence photographs of the fluorescent dyes dissolved in the ternary mixed carrier solvents. Carrier, water–acetonitrile–ethyl acetate mixture volume ratio of (i) 34:53:13, (ii) 30:56:14, (iii) 26:58:16, (iv) 21:62:17, (v) 19:63:18, and (vi) 18:64:18 including 0.1 mM perylene and 1.0 mM Eosin Y.

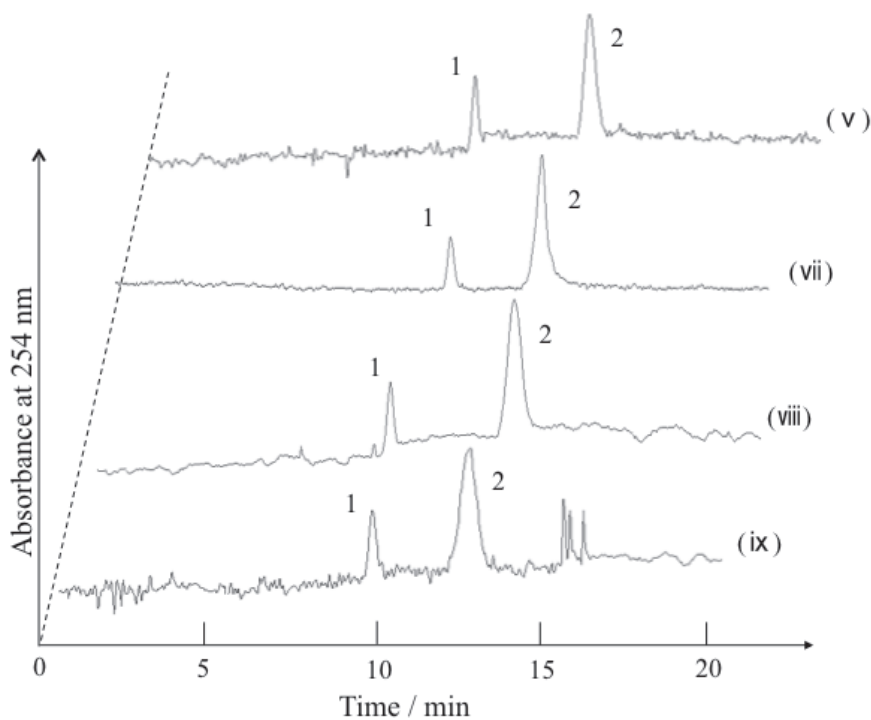


Figure 5. Chromatograms of 1-naphthol and 2,6-naphthalenedisulfonic acid by the TRDC system with tube temperature 5 °C. Carrier, water–acetonitrile–ethyl acetate mixture volume ratio of (v) 19:63:18, (vii) 16:59:25, (viii) 13:54:33, and (ix) 11:43:46.

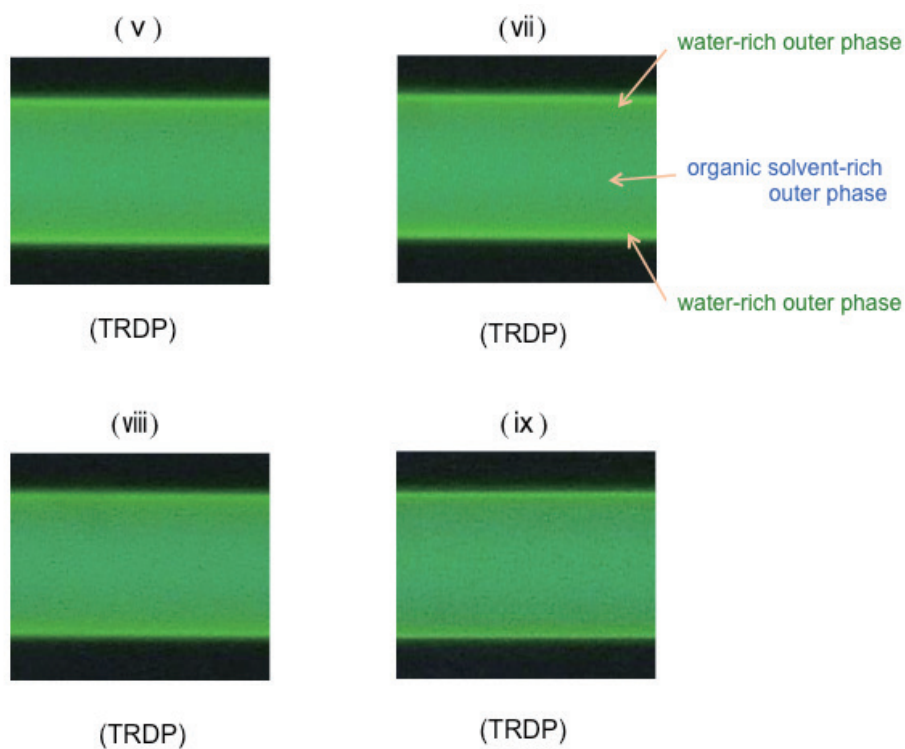


Figure 6. Fluorescence photographs of the fluorescent dyes dissolved in the ternary mixed carrier solvents. Carrier, water–acetonitrile–ethyl acetate mixture volume ratio of (v) 19:63:18, (vii) 16:59:25, (viii) 13:54:33, and (ix) 11:43:46; including 0.1 mM perylene and 1.0 mM Eosin Y.

3.4 Experimental consideration through the estimation of the dimensionless Weber number in TRDP

A ternary mixed solvents solution of water-hydrophilic/hydrophobic organic solvent is an example of a two-phase separation, mixed solvent solution system. Upon temperature change, the homogeneous solution (single-phase) changes to a heterogeneous solution (two-phases), generating upper (organic solvent-rich) and lower (water-rich) phases in a batch vessel. When the ternary mixed solution is fed into a microspace, the solvent molecules are radially distributed in the microspace under laminar flow conditions, generating inner and outer phases. This process is coined as tube radial distribution phenomenon (TRDP). Here, the dimensionless number, Weber number, of the inner and outer phases in the TRDP process was estimated for the water–acetonitrile–ethyl acetate and water–acetonitrile–chloroform systems. The relationship between the Weber number and TRDP formation was examined. TRDP was observed in both systems when the Weber numbers of the organic solvent-rich and water-rich phases were different. However, an either excessively large or small difference in the Weber numbers did not facilitate TRDP. TRDP formation was compared with an annular flow formation using the immiscible mixed solvent solutions.

Introduction

Phase separation of aqueous systems containing polymers, micelles, and ionic liquid solutions is well known and has been used in the many fields of analytical science since the last century [15,18,19]. However, a novel two-phase separation system involving ternary mixed solvents has been reported by our group.^{17,24)} Upon temperature and/or pressure changes, a ternary mixed solvents solution of water-hydrophilic/hydrophobic solvents changes from a homogeneous (single-phase) to a heterogeneous (two-phase) solution. Accordingly, we demonstrated that the two-phase separation system comprising a ternary mixed solvents solution in a batch vessel could be used for the extraction of metal ions.⁴¹⁾

Furthermore, interesting and unique fluidic behaviors of two-phase separation systems, such as water–hydrophilic/hydrophobic organic solvents, micelle aqueous solvent, and ionic liquid aqueous solvent solutions, in a microspace under laminar flow conditions were observed. When the homogeneous solutions of two-phase separation systems are delivered to a microspace, such as glass microchannels and capillary tubes (e.g., fused-silica, polyethylene, and polytetrafluoroethylene), the homogeneous solutions change to the heterogeneous solutions, generating a hydrodynamic liquid-liquid interface with inner and outer phases. We termed such a process as tube radial distribution phenomenon (TRDP).

Liquid–liquid flows have a wide range of applications in lab-on-a-chip devices and microreactors. Liquid–liquid flows using immiscible mixed solvents, oil and water, in conventional tubes and mixing procedures have been studied [14,16,17,20]. When the mixed solvents flows are successfully controlled, various types of flow patterns, such as droplet, slug, and annular flows, are observed in the tube. Flow patterns generated from immiscible mixed solvents were discussed in terms of dimensionless numbers, especially, the Weber number [14,16]. Here the dimensionless number, the Weber

number, was estimated for microfluidic flows in TRDP using a ternary mixed solvents solution of water-hydrophilic/hydrophobic organic solvent, and the relationship between the Weber number and TRDP formation was investigated.

Experimental

Phase diagrams Phase diagrams were constructed for the ternary mixed solvents of water-hydrophilic/hydrophobic organic solvents (water-acetonitrile-ethyl acetate and water-acetonitrile-chloroform systems) at 20 °C in a batch vessel. The phase diagram included the solubility curve that separates the component ratios of the solvents into homogeneous (single-phase) and heterogeneous (two-phase) areas.

Viscosity measurement The homogeneous solutions of all the mixed solvents changed to heterogeneous solutions that comprised two phases, the upper and lower phases, in a batch vessel by changing the temperature. The viscosities of the upper (organic solvent-rich) and lower (water-rich) solutions were measured with a viscometer (HAAKE RheoScope 1; Thermo Scientific, Sydney, NSW, Australia).

Interfacial tension calculation The surface tensions of the upper (organic solvent-rich) and lower (water-rich) solutions (upon conversion of the homogeneous solution into the heterogeneous solution) were measured with a surface tension balance. The interfacial tension (Σ) was calculated using the following equation [13] :

$$\Sigma = \frac{\sigma_o + \sigma_w - 2\sqrt{\sigma_o \sigma_w}}{1 - 0.015\sqrt{\sigma_o \sigma_w}},$$

where σ_o is the surface tension of the organic solvent-rich phase (O) and σ_w is the surface tension of the water-rich phase (W).

Fluorescence microscope-CCD camera system Fused-silica capillary tubes (inner diameter: 50 μm) were used. To monitor the TRDP, the capillary tube was set up accordingly and observed under a fluorescence microscope-CCD camera system. Ternary water-hydrophilic/hydrophobic organic solvent systems with various component ratios and comprising perylene (0.05–0.1 mM) and Eosin Y (0.1–1.0 mM) were used. The fluorescence in the capillary tube (total length: 120 cm) was monitored at 20 cm from the tube outlet using a fluorescence microscope equipped with an Hg lamp, a filter, and a CCD camera. Perylene and Eosin Y emit light at 470 and 550 nm, respectively. Accordingly, the resulting fluorescence observed was mainly blue and green.

Results and discussion

Estimation of weber number Various types of oil-water (immiscible solvents) flows in a tube were examined and discussed in terms of dimensionless numbers such as the Capillary, Reynolds, and Weber numbers [14,16,17,20]. More specifically, the Weber number has been used to examine the flow patterns of droplet, slug, and annular flows in a tube [14,16]. The Weber number, We , is expressed according to the following equation:

$$\text{We} = \frac{\rho_i V_i^2 D}{\Sigma}$$

where ρ_i is the density, V_i is the superficial velocity, D is the inner diameter, and Σ is the interfacial tension (subscript i refers to the organic solvent-rich solution (O) or water-rich solution (W)). The value of $\rho_i V_i^2 D$ corresponds to the inertial force. Hence, the Weber number is defined as the ratio of inertial force to the interfacial tension (interfacial force). The inertial force tends to extend the interface in the direction of the flow and maintain a continuous fluid. In contrast, the interfacial force tends to minimize the interfacial energy by reducing the oil–water interfacial area, leading to the formation of droplets and plugs. Fig. 1 shows illustrations of the flow systems, immiscible mixed solvent and TRDP, and their typical flow patterns in a tube. For typical immiscible mixed solvent solutions, the superficial velocities are obtained by dividing the flow rates in the individual delivery tubes, oil and water lines, by the cross-section of the tube, mixing single line (Fig. 1a) [14]. In contrast, in TRDP, the apparent flow rates of the organic solvent-rich and water-rich phases in the capillary single tube are obtained by dividing the flow rate in the capillary tube by the volume ratio of the upper (organic-solvent-rich) and lower (water-rich) phases in a batch vessel. The superficial velocities are then calculated by dividing the apparent flow rates by the cross-section of the capillary tube (Fig. 1b).

Flow patterns of ternary mixed solvents of water-hydrophilic/hydrophobic organic solvents Foroughi et al. reported the relationship between the flow patterns and associated Weber numbers for immiscible mixed solvents solutions [14]. Generally, when immiscible solutions (i.e., O and W) were fed into the mixing single tube with the two individual flow lines, as shown in Fig. 1a, and the flow rate of solution O was constant and that of solution W gradually increased, specific flow patterns in the single tube were generated. A droplet flow was observed when the flow rate and the Weber number of solution W were relatively small and the interfacial tension in the droplet of W was dominant relative to the inertial force. A slug flow was observed when the flow rate and the Weber number of solution W were at intermediate values and the inertial force and interfacial tension in the slug of W were comparable. An annular flow was observed when the flow rate and the Weber number of solution W were relatively large and the inertial force in the inner phase of W was dominant relative to the interfacial tension. When the ternary mixed solution of water–hydrophilic/hydrophobic organic solvent was introduced into a capillary tube, the solvents molecules were radially distributed in the tube under certain flow conditions, that is, TRDP. As shown in Fig. 1b, we examined flow patterns using varying component ratios of the ternary solvents in the TRDP flow system in a manner similar to that of the immiscible mixed solvents system. Specific flow patterns in the capillary tube were observed, as depicted in the phase diagrams in Fig. 2: TRDP (organic solvent-rich inner phase and water-rich outer phase (○)), and water-rich inner phase and organic solvent-rich outer phase (●)) and non-TRDP (axial distribution (△) and heterogeneous distribution (×)) for the water–acetonitrile–ethyl acetate and water–acetonitrile–chloroform systems. The relationship between the flow patterns and Weber numbers is discussed in the following section.

Relationship between the volume ratios, weber numbers, and flow patterns in the TRDP flow system The volume ratios of the generated upper (organic solvent-rich) and lower (water-rich) phases of the ternary mixed solvents at varying component ratios in a batch vessel at low temperatures were examined. Additionally, the Weber numbers of the inner (organic solvent-rich or water-rich) and outer (water-rich or organic solvent-rich) phases in the TRDP flow system were calculated. The flow patterns, TRDP and non-TRDP, in the capillary tube were determined on a fluorescence microscope-CDD camera system. The following two systems were studied: water-acetonitrile-ethyl acetate and water-acetonitrile-chloroform. The results are summarized in Fig. 3. The notation of the flow patterns, expressed with symbols, ○, ●, △, and ×, is similar to that employed in Fig. 2. As observed in Fig. 3, similar relationships between the volume ratios, Weber numbers, and flow patterns for both ternary mixed solvents systems studied (water–acetonitrile–ethyl acetate and water–acetonitrile–chloroform) were determined. At the water-rich (organic solvent-rich) phase volume ratio of ~50% vol where the Weber numbers of the two phases were comparable, TRDP was not observed; an axial distribution flow (△) was observed. In this case, the inertial force and interfacial tension in the phases were comparable. When the water-rich (organic solvent-rich) phase volume ratios were considerably small (<5% vol) or large (>95% vol), TRDP was not observed; a homogeneous flow (×) was observed. The significantly small Weber number or inertial force were unable maintain a continuous flow. In contrast, when the water-rich (organic solvent-rich) phase volume ratios were 5–30% vol and 60–95% vol, TRDP was clearly observed; an organic solvent-rich inner phase and water-rich outer phase (○) or a water-rich inner phase and organic solvent-rich outer phase (●) were formed. In this case, the inner phase that had a larger volume ratio possessed a relatively larger Weber number than that of the outer phase, leading to a dominant inertial force relative to the interfacial tension. Similar relationships between the Weber numbers (the ratio of the inertial force to the interfacial tension) in the larger volume phase and flow patterns (annular flow or TRDP flow) in immiscible mixed solvents solutions [14] and ternary mixed solvents solution of water–hydrophilic/hydrophobic organic solvent were observed.

In conclusion, the dimensionless number, the Weber number, was used to examine TRDP formation, including the inner and outer phases, in the water–acetonitrile–ethyl acetate and water–acetonitrile–chloroform systems. An interesting relationship between the Weber number and inner and outer phase formation in TRDP was determined. TRDP was clearly observed in the capillary tube when the Weber numbers of the organic solvent-rich and water-rich phases differed. The current findings are an extension of the application of the TRDP concept to investigate microfluidic behaviors, and thus present potential in developing new systems based on microfluidic technology relying on liquid–liquid interfacial processes such as chromatography and extraction.

Nomenclature; D = inner diameter [m], V = superficial velocity [m s^{-1}], We = Weber Number [-], Σ = interfacial tension (interfacial force) [mN m^{-1}], σ = surface tension [mN m^{-1}], and ρ = density [kg m^{-3}].

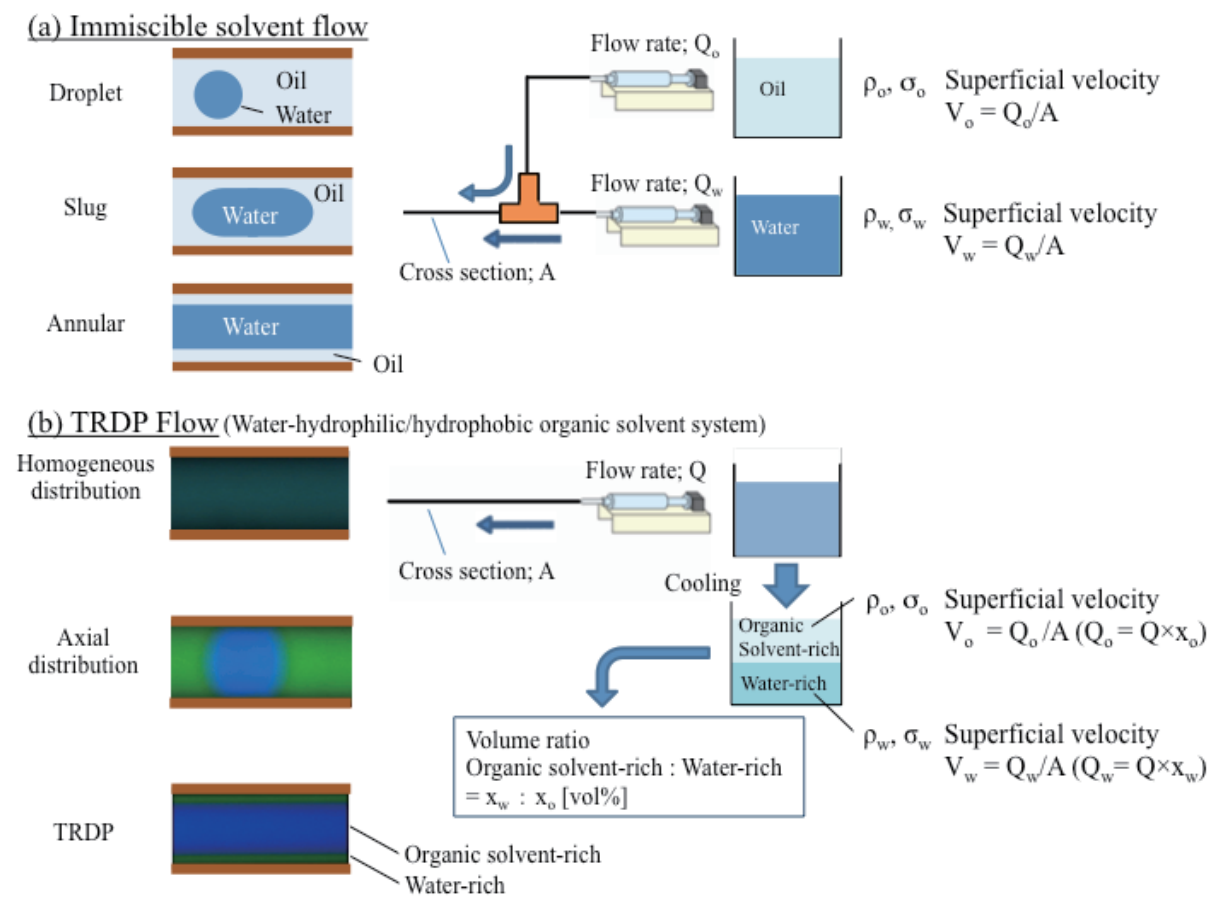


Figure 1. Illustration of the flow systems and typical flow patterns. (a) Immiscible mixed solvent flow and (b) TRDP flow systems.

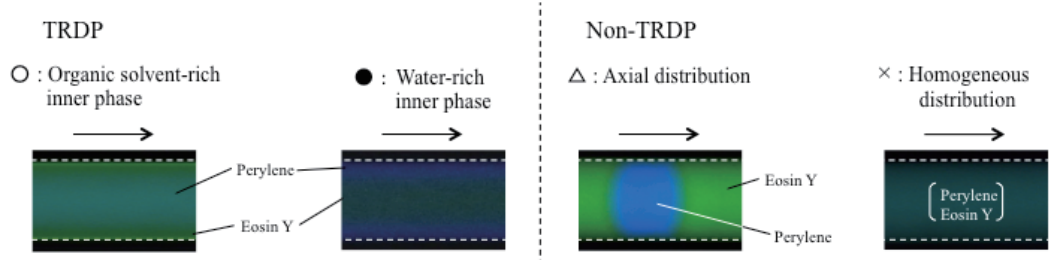
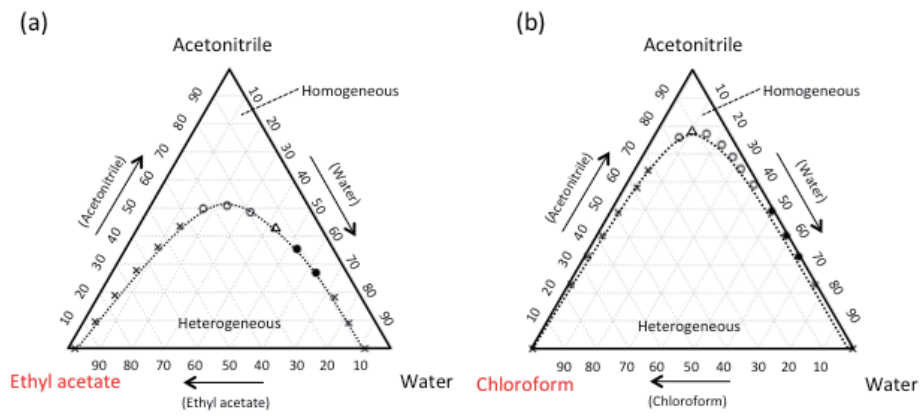


Figure 2. Phase diagram of (a) water–acetonitrile–ethyl acetate and (b) water–acetonitrile–chloroform systems determined at 20 °C. TRDP conditions: capillary tube, 50 μm inner diameter and 100 cm effective length; flow rate, 0.20 $\mu\text{L min}^{-1}$. The flow patterns are denoted as follows: TRDP, organic solvent-rich inner phase and water-rich outer phase (\circ), and water-rich inner phase and organic solvent-rich outer phase (\bullet); non-TRDP, axial distribution (\triangle) and homogeneous distribution (\times).

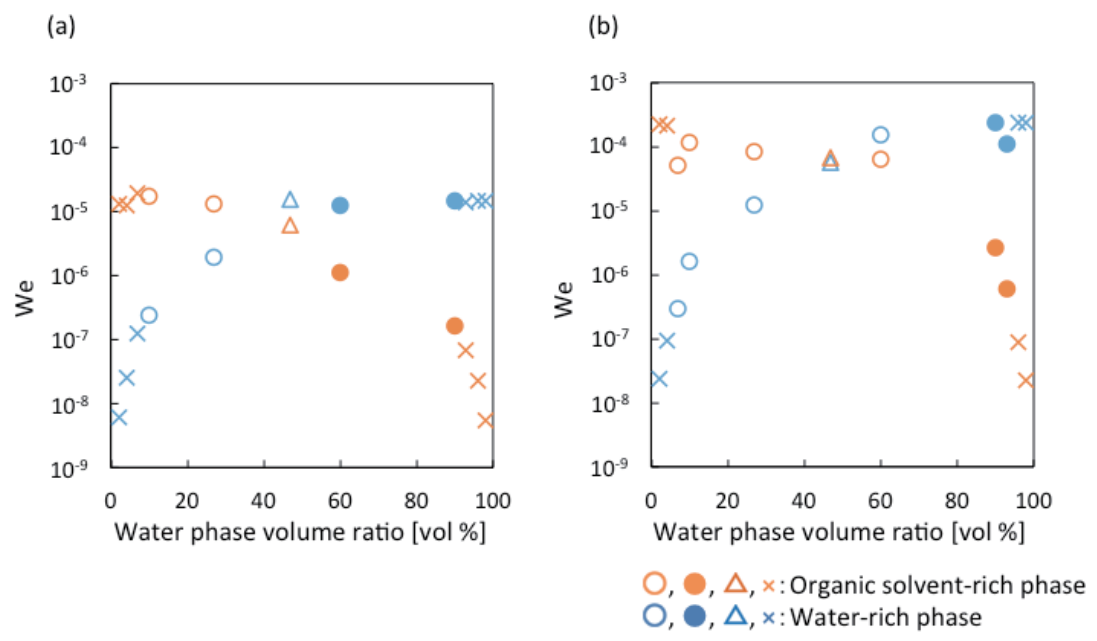


Figure 3. Relationship between the water phase volume ratio and Weber number for the following systems: (a) water–acetonitrile–ethyl acetate and (b) water–acetonitrile–chloroform. TRDP conditions: capillary tube, 50 μm inner diameter and 100 cm effective length; flow rate, 0.20 $\mu\text{L min}^{-1}$. The flow patterns are denoted as follows: TRDP, organic solvent-rich inner phase and water-rich outer phase (\circ) as well as water-rich inner phase and organic solvent-rich outer phase (\bullet) and non-TRDP, axial distribution (Δ) and homogeneous distribution (\times).

3.5 Experimental consideration through the inner and outer phase formation in TRDP using various types of mixed solvent solutions

When mixed solvent solutions, such as ternary water–hydrophilic/hydrophobic organic solvents, water–surfactant, water–ionic liquid, and fluoruous–organic solvents, are delivered into a microspace under laminar flow conditions, the solvent molecules are radially distributed in the microspace, generating inner and outer phases. This specific fluidic behavior is termed tube radial distribution phenomenon (TRDP). Here, the factors influencing the formation of inner and outer phases in the TRDP using the above-mentioned mixed solvent solutions were investigated. We examined phase diagrams, viscosities of the two phases (upper and lower phases in a batch vessel), volume ratios of the phases, and bright-light or fluorescence photographs of the TRDP. When the difference in viscosities between the two phases was large ($>$ ca. $0.73 \text{ mPa}\cdot\text{s}$), the phase with the larger viscosity formed an inner phase regardless of the volume ratios. Conversely, when the difference was small ($<$ ca. $0.42 \text{ mPa}\cdot\text{s}$), the phase with the larger volume formed an inner phase. The TRDP using a water–surfactant mixed solution was also investigated in capillary chromatography based on TRDP.

Introduction

The phase separation of aqueous systems containing polymers, micelles, and ionic liquids is well known, and has been used in the fields of analytical chemistry and separation science since the last century [15,18,21-23]. For example, aqueous micellar solutions of specific non-ionic surfactants separate into two distinct phases when heated above a certain temperature (cloud point), i.e., a temperature-induced phase separation occurs [24-28]. One phase behaves as an almost surfactant-free aqueous solution (aqueous phase), whereas the other phase is a concentrated surfactant solution (surfactant-rich phase). Hydrophobic compounds dissolved in the aqueous micellar solution flow into the surfactant-rich phase, whereas hydrophilic compounds remain in the aqueous phase.

Fluoruous or fluorocarbon chemistry, which involves phase separation processes, has also been investigated since the study reported by Horváth and Rábai in 1994 [29]. The phase separation of fluoruous (fluorocarbon)–organic (hydrocarbon) solvent mixed solutions has been applied in separation science [30,31]. Mixed solutions of fluoruous–organic solvents separate into two distinct phases when cooled below a certain temperature in a batch vessel [32]. In which the lower phase is comprised of a nearly pure fluoruous solvent and the upper phase consisting of an organic solvent. Based on this phase separation system, liquid–liquid and liquid–solid extractions have been reported using a variety of fluoruous solvents [33-35].

A novel phase separation system involving a ternary mixed solvent system has been reported by our group.^{14,17,38)} A ternary mixed solvent solution of

water–hydrophilic/hydrophobic solvents changes from a homogeneous (single-phase) to a heterogeneous (two-phase) system in a batch vessel according to temperature and/or pressure changes. Furthermore, when the ternary mixed solvent solution is introduced into a microspace, such as a microchannel on a microchip or a capillary tube, under laminar flow conditions, the solvent molecules are radially distributed in the microspace, generating inner and outer phases. This process is termed as tube radial distribution phenomenon (TRDP). The TRDP creates a kinetic liquid-liquid interface in a microspace. We developed new types of open-tubular capillary chromatography, i.e., tube radial distribution chromatography (TRDC) and microreactors based on the TRDP. More interestingly, such specific fluidic behavior, TRDP, could also be observed in a microspace, involving the other two-phase separation solutions such as water–surfactant, water–ionic liquid, and fluoruous-organic solvents.

However, comprehensive information about the factors influencing the formation of the inner and outer phases in the TRDP is still lacking for various types of mixed solutions. To this effect, the phase diagrams, viscosities of the two phases (upper and lower phases) in a batch vessel, volume ratios of the phases, and bright-light or fluorescence photograph of the TRDP were examined by using six kinds of phase separation solutions. General discussion for the TRDP creation has been done on the basis of the experimental data, and the TRDP with water–surfactant mixed solution was applied as an attempt to a capillary TRDC.

Experimental

Phase diagrams Phase diagrams were constructed for the six types of mixed solvent solutions: ternary water–hydrophilic/hydrophobic organic solvents (water–acetonitrile–ethyl acetate), water–surfactant (water–Triton X-100–KCl), water–ionic liquid where 1-butyl-3-methylimidazolium chloride ($[C_4mim]Cl$) and 1-ethyl-3-methylimidazolium methylphosphonate ($[C_2mim]MP$) were used (water– $[C_4mim]Cl$ –KOH, water– $[C_4mim]Cl$ – K_2HPO_4 , and water– $[C_2mim]MP$ – K_2HPO_4), and fluoruous-organic solvents (tetradecafluorohexane–hexane). All phase diagrams, regardless of the composition system, included solubility curves that separated the component ratio areas into homogeneous (single-phase) and heterogeneous (two-phase) areas in a batch vessel.

Viscosity measurement The homogeneous solutions of all the mixed solvent systems were converted to heterogeneous solution systems comprised of two phases, upper and lower, by changing the temperature. The viscosities of the upper and lower solutions were measured with a viscometer (HAAKE RheoScope 1; Thermo Scientific, Sydney, NSW, Australia).

Bright-field or fluorescence microscope–CCD camera system Fused-silica capillary

tubes (50 or 75 μm i.d.) were used. The bright-field or fluorescence microscope–CCD camera system was equipped with the fused-silica capillary tube. The fluorescent dye-containing mixed solvent solution that was introduced in the capillary tube was observed using a microscope and a CCD camera for bright-field and fluorescence imaging. For the latter imaging, the microscope was equipped with an Hg lamp and a filter (U-MWU2; excitation wavelength: 330–385 nm, emission wavelength: > 420 nm). The temperature of the capillary tube was maintained using a thermo-heater (Thermo Plate MATS-555RO; Tokai Hit Co., Shizuoka, Japan).

Capillary TRDC The open-tubular capillary chromatography, TRDC, was mainly comprised of a microsyringe pump, a fused-silica capillary tube (total length: 150 cm and effective length: 100 cm), a thermo-heater, and a fluorescence detector (excitation wavelength: 290 nm and emission wavelength: 355 nm). An aqueous solution containing 2% wt. Triton X-100 and 2.4 M KCl or 2% wt. Triton X-114 was used as a carrier solution. A model analyte solution comprising 1-naphthol (1 mM) and 2,6-naphthalenedisulfonic acid (1 mM) dissolved in the carrier solution was prepared. The analyte solution was injected into the capillary inlet using the gravity method (from 30 cm height and for 30 s), and then fed into the capillary tube at a flow rate of $1.0 \mu\text{L min}^{-1}$.

Results and discussion

Phase diagrams including solubility curves Phase diagrams were constructed for the following six types of mixed solvent systems studied; water–acetonitrile–ethyl acetate, water–Triton X-100–KCl, tetradecafluorohexane–hexane, water–[C₄mim]Cl–KOH, water–[C₄mim]Cl–K₂HPO₄, and water–[C₂mim]MP–K₂HPO₄ (Fig. 1). The compositions shown on the axes of the phase diagrams are different depending on the system studied. The phase diagram of water–acetonitrile–ethyl acetate was based on the solvent volume percentage of each component. The phase diagrams of water–Triton X-100–KCl and tetradecafluorohexane–hexane were constructed according to the relationship between the temperature and concentration of Triton X-100 (% wt.) or mole fraction of tetradecafluorohexane. The phase diagram of water–ionic liquid–salt was constructed based on the relationship between the concentrations of the salt and ionic liquid. All phase diagrams included solubility curves that separated the component ratio areas of the solvents into the two phases, i.e., homogeneous (single-phase) and heterogeneous (two-phases). In other words, the homogeneous solution changed to a heterogeneous solution or the heterogeneous solution changed to a homogeneous solution upon alteration of the temperature in the batch vessel. The solubility curves were constructed based on the experimental data. The homogeneous mixtures, at the associated component ratios, designated by the numbers in square brackets in the individual phase diagrams, separated into two phases (upper and lower) in the batch

vessel upon change in the temperature. The viscosities and volume ratios of the upper and lower phases were examined; furthermore, the homogeneous solutions were delivered into the capillary tube to observe the TRDP using either bright-field or fluorescence microscopy, as discussed in the following sections.

Viscosities of the upper and lower phases We examined the viscosities of the upper and lower solutions of the different mixed solvent systems following phase separation. The relationship between the designated solution mixture of a specific component's composition and the associated viscosity for each system is shown in Fig. 2. The differences in viscosities between the upper and lower solutions of the water–acetonitrile–ethyl acetate, water–Triton X-100–KCl, tetradecafluorohexane–hexane, water–[C₄mim]Cl–KOH, water–[C₄mim]Cl–K₂HPO₄, and water–[C₂mim]MP–K₂HPO₄ systems were roughly estimated to be respectively 0.42, 440, 0.36, 1.7, 0.22, and 0.73 mPa·s. The system may be tentatively classified according to the degree of difference in viscosities of the upper and lower phases for the following discussion: large (> ca. 0.73 mPa·s) and small (< ca. 0.42 mPa·s). A large viscosity difference between the upper and lower phases was observed for the water–Triton X-100–KCl, water–[C₄mim]Cl–KOH, and water–[C₂mim]MP–K₂HPO₄ systems, whereas a small viscosity difference was observed for the water–acetonitrile–ethyl acetate, tetradecafluorohexane–hexane, and water–[C₄mim]Cl–K₂HPO₄ systems.

Volume ratios of the upper and lower phases The volume ratios of the upper and lower phases of the solvent mixtures designated by the numbers in square brackets in the phase diagrams were evaluated. The upper/lower phase ratios for the mixed solvent systems: water–acetonitrile–ethyl acetate (20 → 0 °C), water–Triton X-100–KCl (20 → 34 °C), tetradecafluorohexane–hexane (20 → 10 °C), water–[C₄mim]Cl–KOH (20 → 15 °C), water–[C₄mim]Cl–K₂HPO₄ (20 → 15 °C), and water–[C₂mim]MP–K₂HPO₄ (20 → 15 °C) varied respectively as a function of the composition ratios from 90:10 to 4:96 (organic solvent-rich/water-rich), from 60:40 to 12:88 (surfactant-rich/water-rich), from 85:15 to 20:80 (organic solvent /fluorous solvent), from 80:20 to 20:80 (ionic liquid-rich/water-rich), from 95:5 to 20:80 (ionic liquid-rich/water-rich), and from 90:10 to 10:90 (ionic liquid-rich/water-rich). The volume ratios of the upper and lower phases are shown in Fig. 3.

Evaluation of the TRDP The homogeneous solutions were delivered to the capillary tube under laminar flow conditions. The solvents' behaviors, TRDP and non-TRDP, were assessed using bright-field or fluorescence microscopy. Typical photographs showing the development of TRDP are shown in Fig. 4. Interestingly, the solution mixtures of water–Triton X-100–KCl, water–[C₄mim]Cl–KOH, and

water-[C₂mim]MP-K₂HPO₄ generated the TRDP in the surfactant-rich inner phase and the ionic liquid-rich inner phase, regardless of the volume ratios of the two phases or component ratios of the solvents. In contrast, the solution mixtures of water-acetonitrile-ethyl acetate, tetradecafluorohexane-hexane, and water-[C₄min]Cl-K₂HPO₄ generated the TRDP in the major volume inner phase and minor volume outer phase. An inverse (reversible) distribution pattern was observed with a change in the volume ratios of the solvents. For example, when considering the water-acetonitrile-ethyl acetate system, introduction of the organic solvent-rich mixed solution to the capillary tube generated an organic solvent-rich major inner phase and a water-rich minor outer phase; in contrast, introduction of the water-rich mixed solution to the capillary tube produced a water-rich major inner phase and an organic solvent-rich minor outer phase. The TRDP processes in the different mixed solvent systems are denoted by the symbols ○, ●, and ×, and vary according to the lower and upper phases volume content (Fig. 3). The symbols ○ and ● denote the development of TRDP, whereas symbol × implies that TRDP was not observed in a given system at a particular upper/lower volume composition. The mixed solvent systems that include both symbols ○ and ● in the figures demonstrate the occurrence of a reversible distribution pattern of the inner and outer phases in accordance with the phase composition.

Investigation of the inner and outer phase formation The factors influencing the formation of the inner and outer phases, i.e., non-reversible TRDP or reversible TRDP, were evaluated based on the viscosities and volume ratios of the upper and lower phases, and TRDP observations. When the difference in the viscosities between the two phases was large (> ca. 0.73 mPa·s), the phase with the larger viscosity developed as the inner phase regardless of the volume ratios. Conversely, when the difference in the viscosities between the two phases was small (< ca. 0.42 mPa·s), the phase with the larger volume content formed as the inner phase. The flow characteristics of two immiscible liquids with different viscosities in a tube were investigated in the last century [36-39]. The experimental studies showed that low-viscosity fluids have a tendency to encapsulate high-viscosity fluids. This behavior is in accordance with the viscous-dissipation principle, which postulates that the degree of viscous dissipation is smaller for a given flow rate. Thus, the high-viscosity fluid is located at the core of the tube, away from the inner wall [36-27]. However, in 1984, Joseph et al. reported that if the low-viscosity fluid occupies an extremely large volume of space in a tube, the low-viscosity fluid is located at the core of the tube rather than near the wall of the tube, regardless of the viscosity values [40]. The discussions relating to the inner and outer flows in a tube in the previous papers [36-40] were consistent with the present experimental data. The flow characteristics of two immiscible liquids with different viscosities in a tube [36-40] strongly supported the existence of a correlation between the development of TRDP and

the viscosities of the two phases for the six types of mixed solvents systems examined herein.

Capillary TRDC A capillary TRDC system was tentatively developed using a fused-silica capillary tube as separation column and an aqueous micellar solution (2% wt. Triton X-100 and 2.4 M KCl or 2% wt. Triton X-114 solution) as a carrier solution. Triton X-114 is a well-known typical micelle aqueous two-phase separation system. Hydrophobic 1-naphthol and hydrophilic 2,6-naphthalenedisulfonic acid (2,6-NDS) as a model mixture was examined in the current TRDC system. The obtained chromatograms are shown in Fig. 5 as an initial result. 1-Naphthol and 2,6-NDS were separated and detected in this order; Triton X-114 system without salt gave better resolutions. The elution order was expected based on the distribution of the aqueous micellar solution that generated a surfactant-rich inner phase (hydrophobic) and a surfactant-poor outer phase (hydrophilic). The hydrophilic outer phase acted as a pseudo-stationary phase under laminar flow conditions. The two peaks were identified by analyzing individual analytes.

In conclusion, the TRDP generates a kinetic liquid–liquid interface in a microspace upon introduction of a homogeneous mixed solvent solution in a microspace under laminar flow conditions. The factors determining the formation of the inner and outer phases in the microspace were assessed by examining the phase diagrams incorporating solubility curves, viscosities of the upper and lower phases in a batch vessel, volume ratios of the phases, and development of the TRDP using microscopy imaging. When the difference in the viscosities between the two phases was large ($> \text{ca. } 0.73 \text{ mPa}\cdot\text{s}$), the phase with the higher viscosity formed the inner phase regardless of the volume ratios, whereas when the difference in viscosities was small ($< \text{ca. } 0.42 \text{ mPa}\cdot\text{s}$), the phase with the larger volume ratio formed the inner phase. This finding is a stepping stone to future work in the TRDP research area.

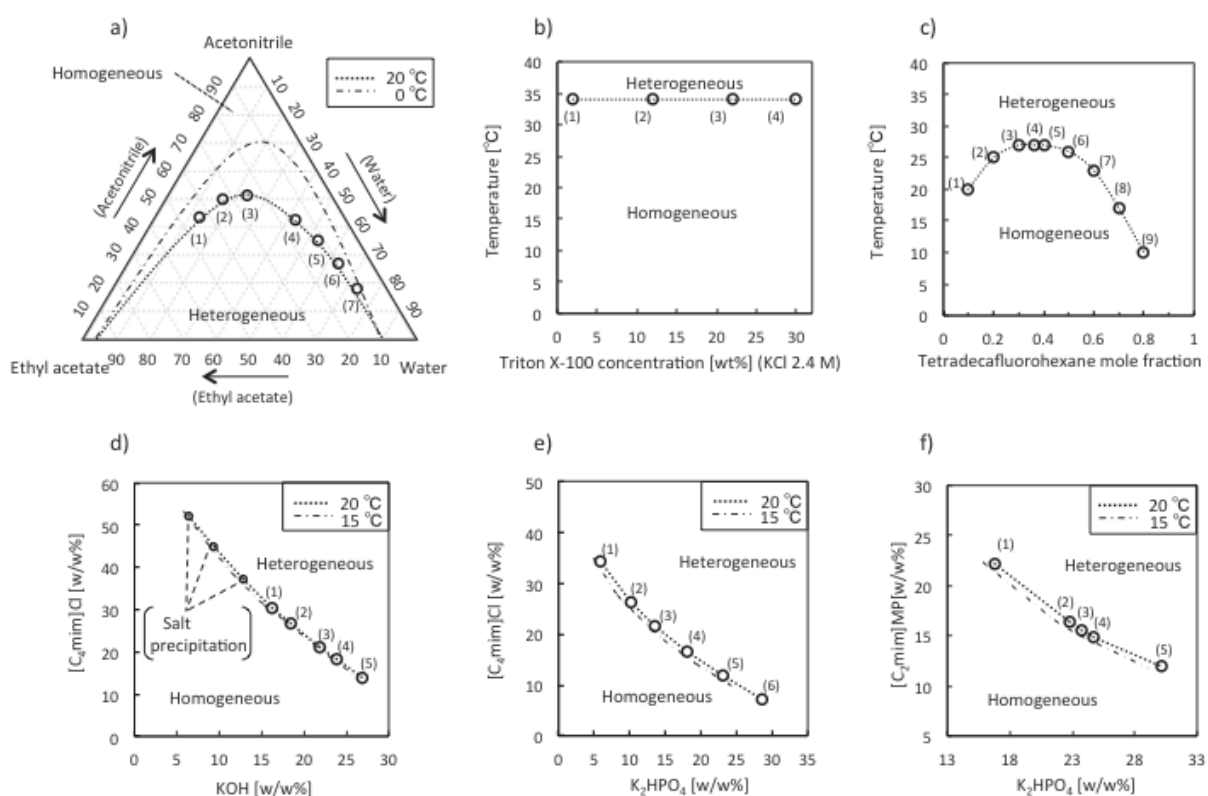


Figure 1. Phase diagrams incorporating solubility curves of a) water–acetonitrile–ethyl acetate, b) water–Triton X-100–KCl (2.4 M), c) tetradecafluorohexane–hexane, d) water–[C₄mim]Cl–KOH, e) water–[C₄mim]Cl–K₂HPO₄, and f) water–[C₂mim]MP–K₂HPO₄. The homogeneous solution mixtures, at the associated components composition, as denoted by the numbers in square brackets in the phase diagrams were used for subsequent experiments.

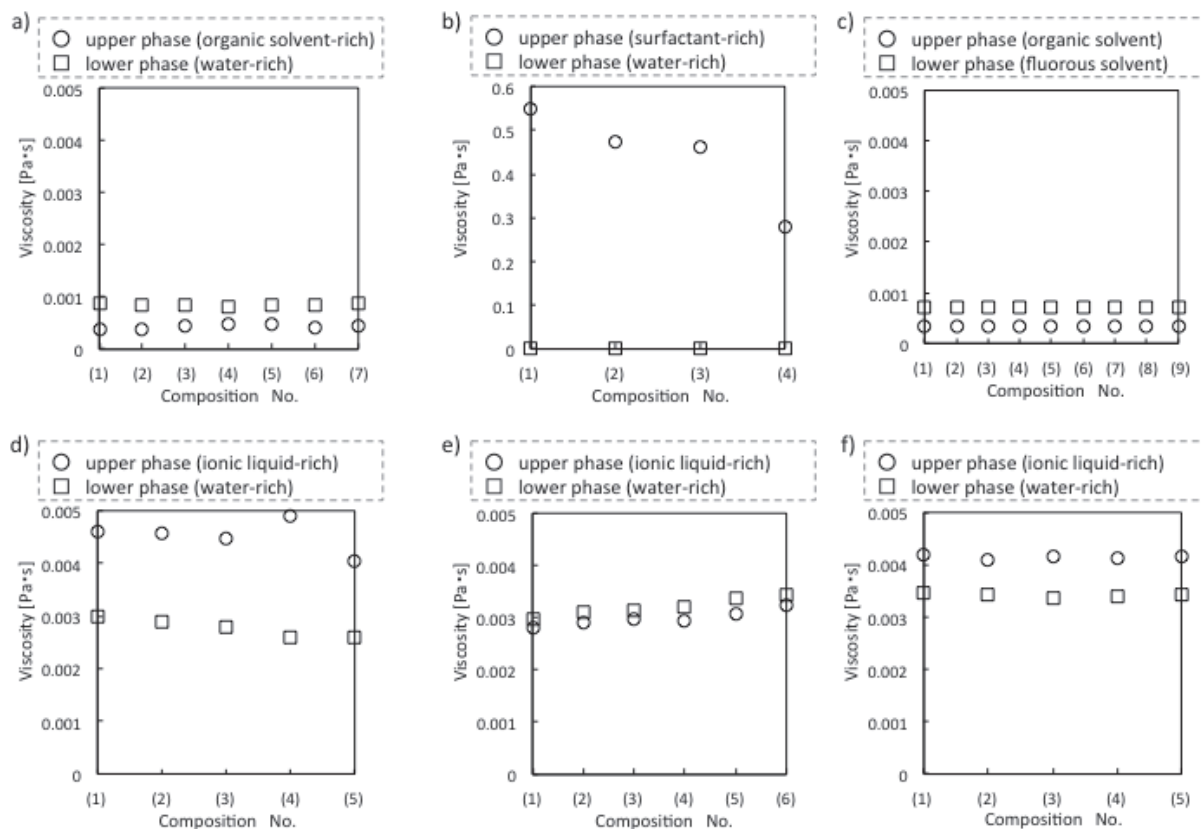


Figure 2. Viscosities of the (○) upper and (□) lower phases of the solvent mixtures, with different solvent compositions, denoted by the numbers in square brackets in Fig. 1: a) water–acetonitrile–ethyl acetate, b) water–Triton X-100–KCl (2.4 M), c) tetradecafluorohexane–hexane, d) water–[C₄mim]Cl–KOH, e) water–[C₄mim]Cl–K₂HPO₄, and f) water–[C₂mim]MP–K₂HPO₄.

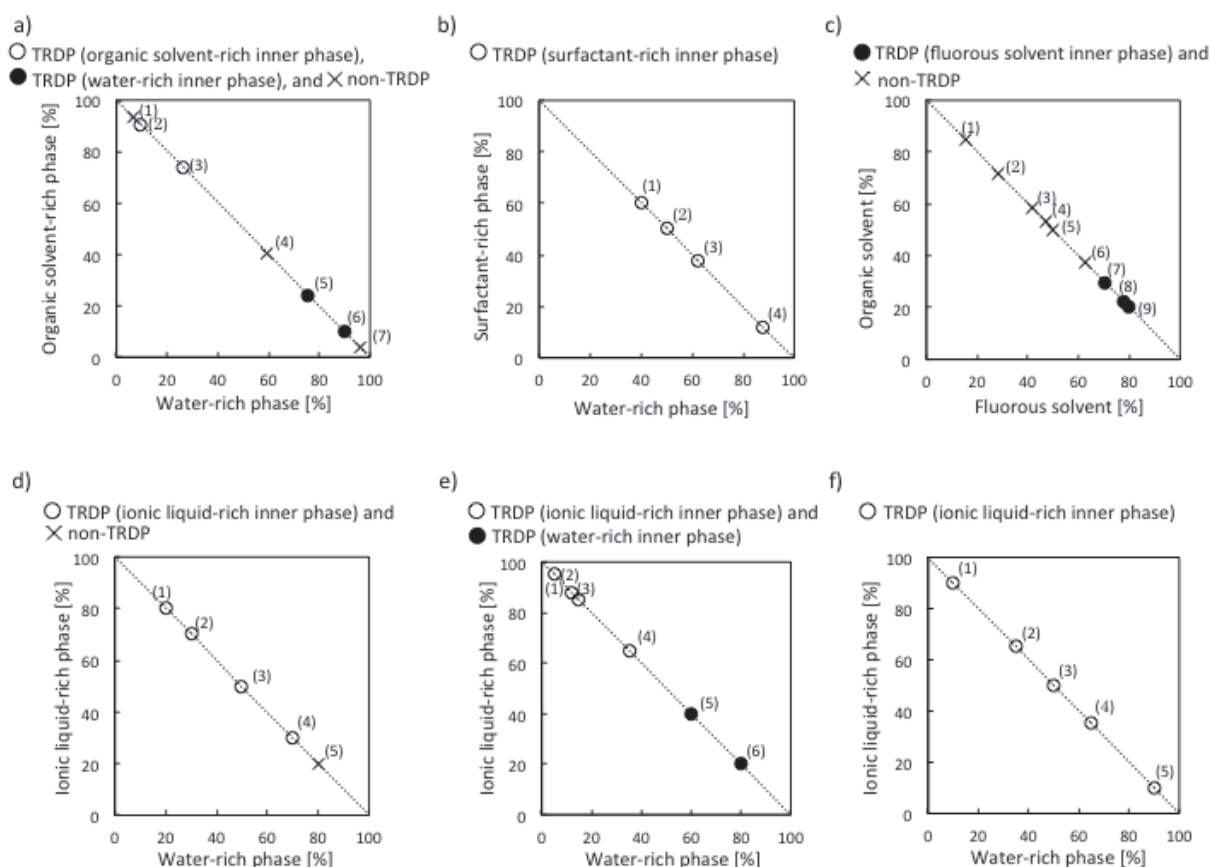


Figure 3. Relationship between the development of the TRDP and the volume contents of the lower and upper phases. Symbols ○ and ● denote the observation of the TRDP, whereas symbol × implies that the TRDP was not observed. Plots containing symbols ○ and ● show the reversible distribution patterns of the inner and outer phases. The different systems studied were: a) water–acetonitrile–ethyl acetate (flow rate: $0.2 \mu\text{L min}^{-1}$; temperature: $0 \text{ }^\circ\text{C}$); b) water–Triton X-100–KCl (2.4 M) (flow rate: $5.0 \mu\text{L min}^{-1}$; temperature: $34 \text{ }^\circ\text{C}$); c) tetradecafluorohexane–hexane (flow rate: $5.0 \mu\text{L min}^{-1}$; temperature: $10 \text{ }^\circ\text{C}$); d) water– $[\text{C}_4\text{mim}]\text{Cl}$ –KOH (flow rate: $1.0 \mu\text{L min}^{-1}$; temperature: $15 \text{ }^\circ\text{C}$); e) water– $[\text{C}_4\text{mim}]\text{Cl}$ – K_2HPO_4 (flow rate: $1.0 \mu\text{L min}^{-1}$; temperature: $15 \text{ }^\circ\text{C}$); and f) water– $[\text{C}_2\text{mim}]\text{MP}$ – K_2HPO_4 (flow rate: $1.0 \mu\text{L min}^{-1}$; temperature: $15 \text{ }^\circ\text{C}$). Capillary tube inner diameter: a) $50 \mu\text{m}$ and b)–f) $75 \mu\text{m}$.

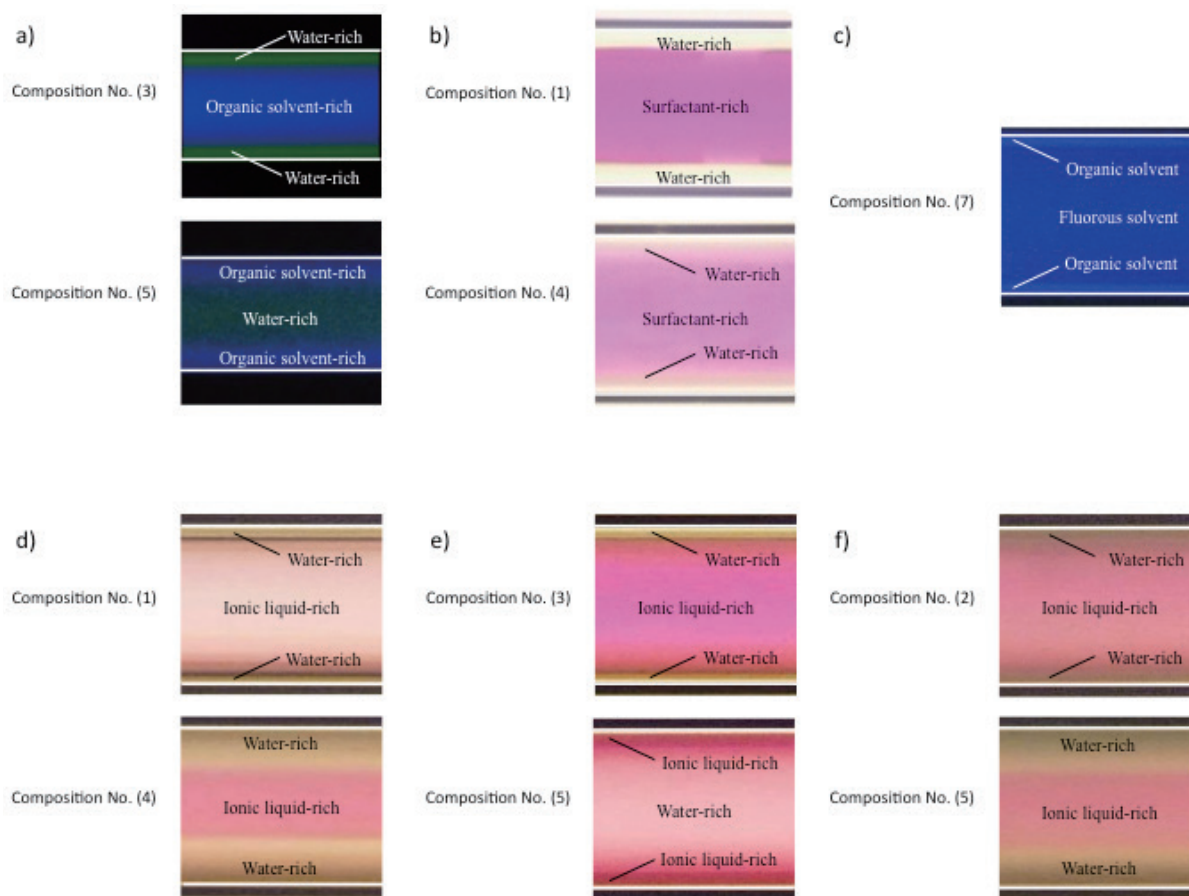


Figure 4. Bright-field and fluorescence photographs showing the development of the TRDP in the different systems: a) water–acetonitrile–ethyl acetate (flow rate: $0.2 \mu\text{L min}^{-1}$; temperature: $0 \text{ }^\circ\text{C}$; and 1 mM Eosin Y and 0.1 mM perylene); b) water–Triton X-100–KCl (2.4 M) (flow rate: $5.0 \mu\text{L min}^{-1}$; temperature: $34 \text{ }^\circ\text{C}$; and 5 mM Rhodamine B); c) tetradecafluorohexane–hexane (flow rate: $5.0 \mu\text{L min}^{-1}$; temperature: $10 \text{ }^\circ\text{C}$; and 0.1 mM perylene); d) water– $[\text{C}_4\text{mim}]\text{Cl}$ –KOH (flow rate: $1.0 \mu\text{L min}^{-1}$; temperature: $15 \text{ }^\circ\text{C}$; and 5 mM Rhodamine B); e) water– $[\text{C}_4\text{mim}]\text{Cl}$ – K_2HPO_4 (flow rate: $1.0 \mu\text{L min}^{-1}$; temperature: $15 \text{ }^\circ\text{C}$; and 2 mM Rhodamine B); and f) water– $[\text{C}_2\text{mim}]\text{MP}$ – K_2HPO_4 (flow rate: $1.0 \mu\text{L min}^{-1}$; temperature: $15 \text{ }^\circ\text{C}$; and 5 mM Rhodamine B). Capillary tube inner diameter: a) $50 \mu\text{m}$ and b)–f) $75 \mu\text{m}$.

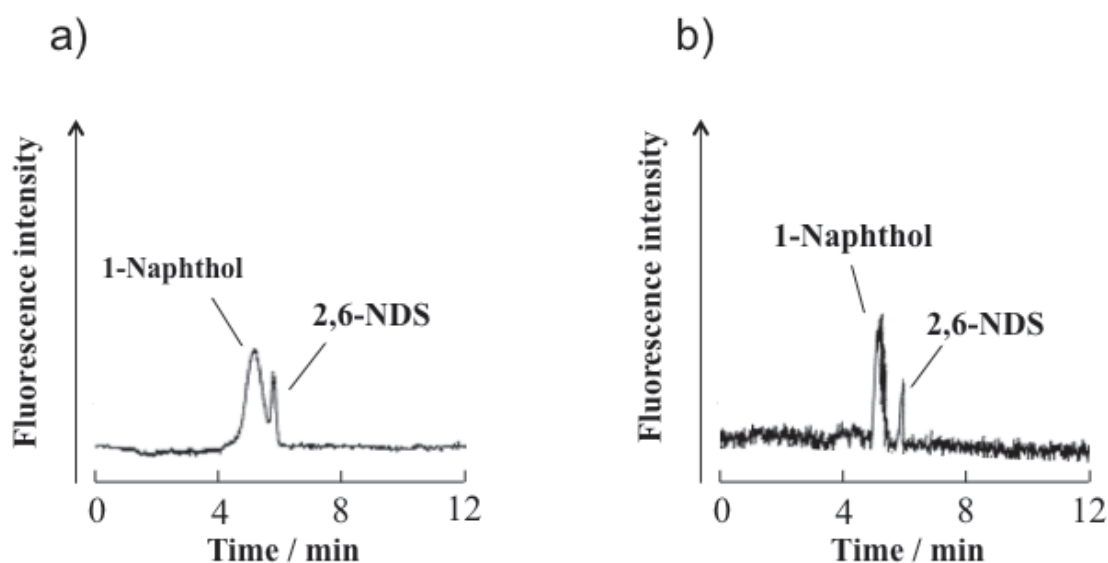


Figure 5. Chromatograms of the present capillary TRDC system: a) 2 wt.% Triton X-100 and 2.4 M KCl at 34 °C and b) 2 wt.% Triton X-114 at 23 °C. Capillary tube: inner diameter: 75 μm , total length: 150 cm, and effective length: 100 cm; flow rate: 1.0 $\mu\text{L min}^{-1}$; and analyte concentration: 1 mM.

References

- [1] S. Terabe, *Anal. Chem.*, **2004**, 76, 240.
- [2] C. A. Lucy, A. M. MacDonald, and M. D. Gulcev, *J. Chromatogr. A*, **2008**, 1184, 81.
- [3] K. Otsuka, *Chromatography*, **2007**, 28, 1.
- [4] H. Small, F. L. Saunders, and J. Solc, *Advances in Colloid and Interface Science*, **1976**, 6, 237.
- [5] R. Umehara, M. Harada, and T. Okada, *J. Sep. Sci.*, **2009**, 32, 472.
- [6] K. Hata, T. Kaneta, and T. Imasaka, *Anal. Chim. Acta.*, **2006**, 556, 178.
- [7] S. K. Poole and C. F. Poole, *J. Chromatogr. A*, **2008**, 1182, 1.
- [8] K. Sueyoshi, F. Kitagawa, and K. Otsuka, *Anal. Chem.*, **2008**, 80, 1255.
- [9] I. Miksik and P. Sedlakova, *J. Sep. Sci.*, **2007**, 30, 1686.
- [10] J. L. Chen, *Talanta*, **2011**, 85, 2330.
- [11] C. H. Fischer and M. Giersig, *J. Chromatogr. A*, **1994**, 688, 97.
- [12] M. T. Blom, E. Chmela, R. E. Oosterbroek, R. Tijssen, and A. Berg, *Anal. Chem.*, **2003**, 75, 6761.
- [13] T. Ami, K. Awata, H. Umekawa, and M. Ozawa, *Int. J. Multiphase Flow*, **2012**, 26, 302.
- [14] H. Foroughi and M. Kawaji, *Int. J. Multiphase Flow*, **2011**, 37, 1147.

- [15] K. E. Gutowski, G. A. Broker, H. D. Willauer, J. G. Huddleston, R. P. Swatloski, J. D. Holbrey, and R. D. Rogers, *J. Am. Chem. Soc.*, **2003**, *125*, 6632.
- [16] M. N. Kashid and L. K. Minsker, *Chem. Eng. Process*, **2012**, *50*, 972.
- [17] M. N. Kashid and D. W. Agar, *Chem. Eng. J.*, **2007**, *131*, 1.
- [18] Z. Li, Y. Pei, H. Wang, J. Fan, and J. Wang, *Trends Anal. Chem.*, **2010**, *29*, 1336.
- [19] C. Wu, J. Wang, H. Wang, Y. Pei, and Z. Li, *J. Chromatogr. A*, **2011**, *1218*, 8587.
- [20] A. L. Dessimoz, L. Cavin, A. Renken, and L. K. Minker, *Chem. Eng. Sci.*, **2008**, *63*, 4035.
- [21] Y. Lu, W. Lu, W. Wang, Q. Guo, and Y. Yang, *Talanta*, **2011**, *85*, 1621.
- [22] C. Wua, J. Wanga, H. Wanga, Y. Pei, and Z. Li, *J. Chromatogr. A*, **2011**, *1218*, 8587.
- [23] J. Han, Y. Wang, Y. Li, C. Yu, and Y. Yan, *J. Chem. Eng. Data*, **2011**, *56*, 3679.
- [24] H. Watanabe and H. Tanaka, *Talanta*, **1978**, *25*, 585.
- [25] K. Fujinaga, *Anal. Sci.*, **1993**, *9*, 479.
- [26] T. Saitoh, H. Tani, T. Kamidate, and H. Watanabe, *Trends Anal. Chem.*, **1995**, *14*, 213.
- [27] T. M. Z. Moattar and R. Sadeghi, *Fluid Phase Equilib.*, **2002**, *203*, 177.
- [28] P. L. Trindade, M. M. Diogo, D. M. F. Prazeres, and C. J. Marcos, *J. Chromatogr. A*, **2005**, *1082*, 176.
- [29] T. I. Horváth and J. Rábai, *J. Science*, **1994**, *266*, 72.
- [30] K. Nakashima, F. Kubota, M. Goto, and T. Maruyama, *Anal. Sci.*, **2009**, *25*, 77.
- [31] J. Lim and T. M. Swager, *Angew. Chem. Int. Ed.*, **2010**, *49*, 7486.
- [32] H. Matsuda, A. Kitabatake, M. Kosuge, K. Tochigi, and K. Ochi, *Fluid Phase Equilib.*, **2010**, *297*, 187.
- [33] C. Dennis and Z. R. Lee, *Green Chemistry*, **2001**, G3.
- [34] M. Masato, M. Hasegawa, D. Sadachika, S. Okamoto, M. Tomioka, Y. Ikeya, A. Masuhara, and Y. Mori, *Tetrahedron Lett.*, **2007**, *48*, 4147.
- [35] T. Maruyama, K. Nakashima, F. Kubota, and M. Goto, *Anal. Sci.*, **2007**, *23*, 763.
- [36] A. E. Everagae, *Trans. Soc. Rheol.*, **1973**, *17*, 629.
- [37] H. Sotjthernj and N. L. Ballmar, *Appl. Polymer Symp.*, **1973**, *20*, 175.
- [38] J. L. White and B. L. Lee, *Trans. SOC. Rheol.*, **1975**, *19*, 457.
- [39] D. L. Maclean, *Trans. Aoc. Rheol.*, **1973**, *17*, 385.
- [40] D. D. Joseph, Y. Renardy, and M. Renardy, *J. Fluid Mechanics*, **1984**, *141*, 309.

Chapter 4 Development of tube radial distribution chromatography (TRDC)

A TRDP-based capillary chromatography, referred to as tube radial distribution chromatography (TRDC), where the outer phase serves as a pseudo-stationary phase under laminar flow conditions, was developed as one of the applications of TRDP. The TRDC was examined in detail from various viewpoints of analytical conditions. The part of this chapter is reconstructed and rewritten based on the related manuscripts that have been published thus far.^{10,15,20,21,23,49)}

4.1 Analytical conditions and separation performance in TRDC

We have developed a capillary chromatography system using an open capillary tube made of fused-silica, polyethylene, or poly(tetrafluoroethylene), and a water-hydrophilic-hydrophobic organic mixture carrier solution. This tube radial distribution chromatography (TRDC) system works under laminar flow conditions. Here, the following analytical conditions in the TRDC system using a fused-silica capillary tube and a water-acetonitrile-ethyl acetate mixture carrier solution were examined: tube temperature, 5 – 25 °C; tube inner diameter, 50 - 250 μm; tube effective length, 100 – 200 cm; and flow rate, 0.2 – 1.5 μL min⁻¹. For example, the effects of temperature on separation performance in the TRDC system were observed with the organic solvent-rich carrier solution; 1-naphthol and 2,6-naphthalenedisulfonic acid in a model mixture were eluted with baseline separation over the temperature range of 5 – 23 °C. The resolution, theoretical plate number, and height equivalent to the theoretical plate were calculated from the experimental data obtained by examining the effects of tube length. The mixture of 1-naphthol, Eosin Y, 1-naphthalenesulfonic acid, 2,6-naphthalenedisulfonic acid, and 1,3,6-naphthalenetrisulfonic acid was subjected to the present TRDC system and the analytes in the mixture solution were eluted in the above order with the organic solvent-rich carrier solution, providing a good separation performance on the chromatogram.

Introduction

Miniaturization is one of the most active research directions in analytical chemistry. Valuable investigations with respect to miniaturization have also been done in the field of liquid chromatography: e.g., capillary liquid chromatography or capillary chromatography. Capillary chromatography is generally performed with fused-silica capillary tubes whose inner diameter (i.d.) is ca. 50 – 100 μm, because of their superior mechanical and optical properties compared to other materials. Various capillary chromatography techniques, including capillary electrochromatography [1,2], micellar electrokinetic capillary chromatography [3,4], and high-performance liquid capillary chromatography using packed and monolithic columns [5-7], have been investigated as powerful separation tools. However, they require specific treatments or procedures, such as applying a high voltage, additives (gels, surfactants, etc.), and packing agents.

Capillary chromatography using open fused-silica capillary tubes has also been investigated, and the results indicated interesting and unique characteristics. Most of these studies, however, used coated or modified capillary tubes. For example, one study coated the inner wall of the tube with silicone grease SE-30 [8] or modified it with a monolayer particle phase [9]. Porous silica structures were also introduced on the wall by dynamic or static coating techniques [10-12] and various polymeric siloxanes were immobilized on the walls [13,14]. We modified the inner walls with specific functional groups or molecules, such as phenylboronic acid, iminodiacetic acid, and antibodies for capillary chromatography to take advantage of specific interactions between the solutes and the modified walls [15-18]. Methods for the preparation of open capillary tubes coated with molecularly imprinted polymer [19] and cation exchange polymer [20] have also been reported for use in chromatography. Furthermore, such coating techniques have been applied to fused-silica capillary tubes less than 10 μm in i.d. to improve separation performance [21-23].

However, coating the inner walls in the manner required for separation in chromatography is both a time-consuming and laborious procedure, and it is made more difficult when trying to coat the inside of narrow-bored capillary tubes. Recently, capillary chromatography using open fused-silica capillary tubes that were not specially coated or modified were reported [24-28]. In one example, Tabata et al. developed an open tubular capillary chromatography method based on microphase separation of mixed solvents, even though narrow-bored tubes of 10 μm i.d. were used [27]. When an acetonitrile-water mixture with suitable salt concentration was pumped into a fused-silica capillary tube in which the inner wall was negatively charged due to the dissociation of its silanol groups, microphase separation occurred near the capillary wall, resulting in a water-enriched aqueous phase attached to the capillary inner wall. Furthermore, capillary chromatography using wide-bored tubes of 50 μm i.d. was carried out together with an ionic liquid and a gel [28].

We developed a capillary chromatography method using an open capillary tube and a water-hydrophilic-hydrophobic organic solvent mixture (homogeneous solution) as a carrier solution; the system worked under laminar flow conditions. We called this the tube radial distribution chromatography (TRDC) system. We have demonstrated the separation of a mixture of hydrophilic and hydrophobic molecules by capillary chromatography using open capillary tubes made of fused-silica, polyethylene, or poly(tetrafluoroethylene) (PTFE) (50, 200, or 100 μm i.d., respectively), and a water-acetonitrile-ethyl acetate mixture carrier solution (homogeneous solution). The elution times of the analytes in the system can be easily reversed by changing the component ratio of the carrier solvents (or by using an organic solvent-rich and a water-rich carrier solution) in all types of the capillary tubes. We proposed that separation in the capillary chromatography system was performed based on the tube radial distribution of the carrier solvents under laminar flow conditions, known here as a tube radial distribution chromatography (TRDC) system.

The tube radial distribution of the solvents in the TRDC system is illustrated in Fig. 1 and phenomenologically described as follows. Under laminar flow conditions, aqueous and organic solvents in the carrier solution of a water-hydrophilic-hydrophobic organic mixture are dispersed non-uniformly in a specific flow in the capillary tube generating

an organic solvent-rich phase and a water-rich phase. A major inner phase is formed around the center of the tube and away from the inner wall, while a minor outer or capillary wall phase is generated near the inner wall. An organic solvent-rich carrier solution generates an organic solvent-rich inner phase, while a water-rich carrier solution results in a water-rich inner phase as shown in Fig. 1. The analytes that are delivered through the capillary tube are distributed between inner and outer phases, undergoing chromatographic separation under laminar flow conditions. So far, the tube radial distribution in the TRDC system has been supported by experimental data using polymer particles as analytes and phenylboronic acid or iminodiacetic acid-modified fused-silica capillary tubes. The illustration of the tube radial distribution of the carrier solvents (Fig. 1) is also drawn based on the data of the fluorescence photographs and profiles obtained by the fluorescence microscope-CCD camera.

As investigation into the TRDC system has just begun, it is important to examine the elution behavior under various analytical conditions in the system to expand our knowledge regarding its separation performance. Here, we examined the analytical conditions of the TRDC system in detail, including tube temperature, tube inner diameter, tube length, and flow rate, using fused-silica capillary tubes and a water-acetonitrile-ethyl acetate mixture as a carrier solution. In contrast to polyethylene and PTFE capillary tubes, fused-silica capillary tubes with various inner diameters are commercially available for an economical rate. Using the present TRDC system we were able to demonstrate the separation and detection of a mixture sample solution that was comprised of five analytes.

Experimental

The present capillary chromatography system comprised of an open fused-silica capillary tube, microsyringe pump, and absorption detector. The tube temperature was controlled by dipping the capillary tube in water maintained at a fixed temperature in a beaker by stirring. Water-acetonitrile-ethyl acetate mixtures with volume ratios of 3:8:4 and 15:3:2 were used as carrier solutions. Analyte solutions were prepared with the carrier solutions. The analyte solution was introduced directly into the capillary inlet side using the gravity method. After an analyte injection, the capillary inlet was connected through a joint to a microsyringe. The syringe was set on the microsyringe pump. The carrier solution was fed into the capillary tube at a fixed flow rate under laminar flow conditions. On-capillary absorption detection (254 nm) was performed with the detector.

Results and discussion

Reversal of the elution times of the analytes in the TRDC system Model mixture solutions of 1-naphthol and 2,6-naphthalenedisulfonic acid as well as 1-naphthoic acid and 1,3,6-naphthalenetrisulfonic acid were analyzed using the present TRDC system. The obtained chromatograms are shown in Fig. 2; the analytical conditions are described in the figure caption. Using the organic solvent-rich carrier solution of water-acetonitrile-ethyl acetate with a volume ratio of 3:8:4, the mixtures of 1-naphthol and 2,6-naphthalenedisulfonic acid as well as 1-naphthoic acid and 1,3,6-naphthalenetrisulfonic acid were separated through the open capillary tube and

were detected in this order (Fig. 2 a)). On the other hand, using the water-rich carrier solution of water-acetonitrile-ethyl acetate with a volume ratio of 15:3:2, the two mixture solutions were separated and detected with the inverse elution times, i.e., 2,6-naphthalenedisulfonic and 1-naphthol as well as 1,3,6-naphthalenetrisulfonic acid and 1-naphthoic acid were detected in this order (Fig. 2 b)). The components of the analytes on the chromatograms were confirmed by their individual absorption signals. In both chromatograms, the first peaks were detected with elution times roughly corresponding to the average linear velocities under laminar flow conditions, and the second peaks were eluted with a velocity below the average linear velocity. When the organic solvent-rich carrier solutions were used, the comparatively hydrophobic analytes were first eluted, while when the water-rich carrier solutions were used as carrier solutions, the comparatively hydrophilic analytes were eluted first. That is, the chromatograms clearly indicated the reversibility of the elution times by changing the component ratio of the solvents in the carrier solution. The results shown in Fig. 2 are consistent with the tube radial distribution behavior of the carrier solvents in the TRDC system that was proposed in our studies.

Effects of tube temperature on separation We examined the effects of tube temperature on separation in the TRDC system with a mixture analyte solution of 1-naphthol and 2,6-naphthalenedisulfuric acid as a model. The following experiments were performed with the organic solvent-rich carrier solutions because the carrier solutions provided better resolution on the chromatograms than the water-rich carrier solutions as shown in Fig. 2. The obtained chromatograms are shown in Fig. 3 together with analytical conditions. As can be seen in Fig. 3, 1-naphthol and 2,6-naphthalenedisulfuric acid in the mixture solution were detected with baseline separation in the temperature range of 5 – 23 °C, while they were not separated at all at a temperature of 25 °C. In more detail, the resolutions were improved by increasing the temperature between 5 °C and 20 °C, but the resolution decreased suddenly at 23 °C. The data clearly indicated that the tube temperature had a significant and critical influence on separation performance in the TRDC system. From this we can claim that the formation of the inner and outer phases of the carrier solution in the tube due to the tube radial distribution of the solvents must change with temperature.

Effects of tube inner diameter on separation We examined the effects of the tube inner diameter on separation in the TRDC system with a mixture analyte solution of 1-naphthol and 2,6-naphthalenedisulfuric acid as a model. We attempted to use commercially available fused-silica capillary tubes with various inner diameters. However, as the tubes with an i.d. of more than 250 µm lacked flexibility, it was difficult to fix them in the present absorption detector. In addition, tubes of 25 µm i.d. generated severe backpressure, making a continuous delivery of the carrier solution difficult with the current microsyringe pump. Consequently, the capillary tubes with an i.d. of 50 – 250 µm were used here. The obtained chromatograms are shown in Fig. 4 together with the analytical conditions. The flow rates for all the capillary tubes were adjusted to provide almost the same average linear velocity of ca. 22 cm min⁻¹. We observed well-separated peaks on the chromatograms; the first peaks were eluted with

almost average linear velocity and the second peaks were eluted with a smaller than the average linear velocity. Also, the elution times of the second peaks appeared earlier with increasing inner diameter, although the elution times of the first peaks were almost constant. The formation of the inner and outer phases of the carrier solution in the tube due to the radial distribution of the solvents must change markedly in the wider tubes. Next, we will examine the TRDC system using the capillary tubes with wider inner diameters.

Effects of tube effective length on separation We also examined the effects of the tube effective length on separation in the TRDC system using the model mixture analyte solution. The obtained chromatograms are shown together with the analytical conditions in Fig. 5. The first peaks were eluted with almost average linear velocity and the second peaks were eluted with velocities smaller than the average linear velocity. The resolution, theoretical plate number, and height equivalent to the theoretical plate were calculated in the usual manner, and the obtained values are summarized in Table 1. As shown in Table 1, longer tubes showed a better resolution and theoretical plate number. On a different note, nearly the same height equivalent to a theoretical plate of 0.13 – 0.16 mm for 1-naphthol or 1.10 – 1.29 mm for 2,9-naphthalenedisulfonic acids was observed for all tube lengths. From the data, separation in the TRDC system seemed to be performed based on the usual chromatographic separation procedure, at least under the present analytical conditions.

Effects of flow rate on separation The effects of flow rate ($0.2 - 1.5 \mu\text{L min}^{-1}$) on separation were examined in the TRDC system. The obtained chromatograms are shown in Fig. 6 together with the analytical conditions. The first peaks were eluted with almost the average linear velocity and the second peaks were eluted with velocities smaller than the average linear velocity. Although the second peak showed broadening at lower flow rates, they showed almost Gaussian peaks with good separation. That is, Fig. 6 meant that the tube radial distribution of the solvents in the capillary tube was performed even at the minimum flow rate of $0.2 \mu\text{L min}^{-1}$ in the present system.

Separation of mixture solution including five analytes We examined a mixture analyte solution of 1-naphthol, Eosin Y, 1-naphthalenesulfonic acid, 2,6-naphthalenedisulfonic acid, and 1,3,6-naphthalenetrisulfonic acid using the present TRDC system with organic solvent-rich carrier solution and water-rich carrier solution. The obtained chromatograms are shown together with the analytical conditions in Fig. 7. The elution times of the analytes were reversed when using the organic solvent-rich and the water-rich carrier solutions in a similar way to other reported chromatograms in the TRDC system. 1-Naphthol, Eosin Y, 1-naphthalenesulfonic acid, 2,6-naphthalenedisulfonic acid, and 1,3,6-naphthalenetrisulfonic acid were eluted in this order, leading to a good separation from the organic solvent-rich carrier solution (Fig. 7 a)). The elution order seemed to be consistent with the hydrophilic character. With the water-rich carrier solution, the comparatively hydrophilic compounds 1-naphthalenesulfonic acid, 2,6-naphthalenedisulfonic acid, and 1,3,6-naphthalenetrisulfonic acid were not separated, but were eluted together with

almost average linear velocity, while the hydrophobic compounds Eosin Y and 1-naphthol were eluted in this order with velocities smaller than the average linear velocity (Fig. 7 b)), indicating the reverse elution order compared to that of the organic solvent-rich carrier solution.

In conclusion, the analytical conditions, such as temperature, tube inner diameter, tube length, and flow rate, were examined for the first time in the TRDC system. The resolution, theoretical plate number, and height equivalent to the theoretical plate were calculated based on the experimental data. The analytes that were delivered through the capillary tube were distributed between inner and outer phases, undergoing chromatographic separation under laminar flow conditions. Successful separation of a mixture solution including five analytes indicates that the TRDC system has potential that should be examined further in future studies.

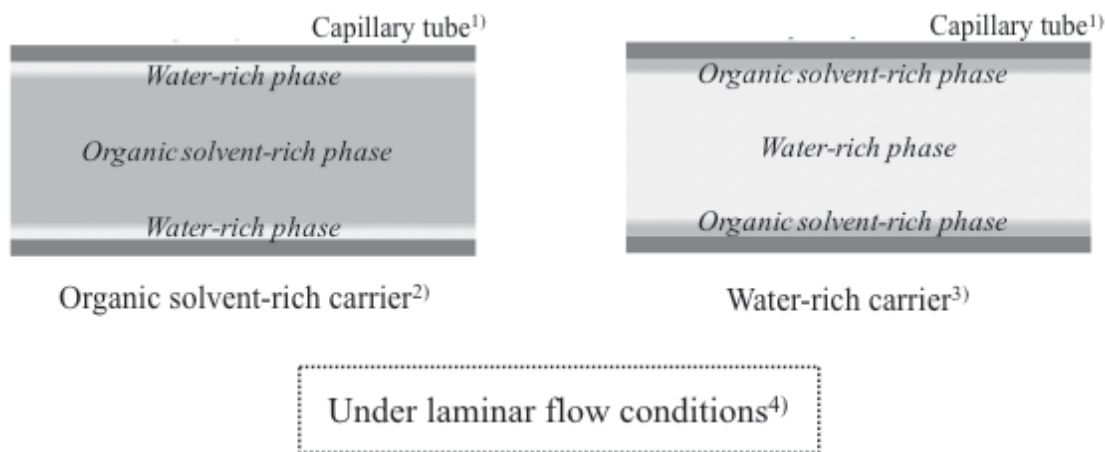
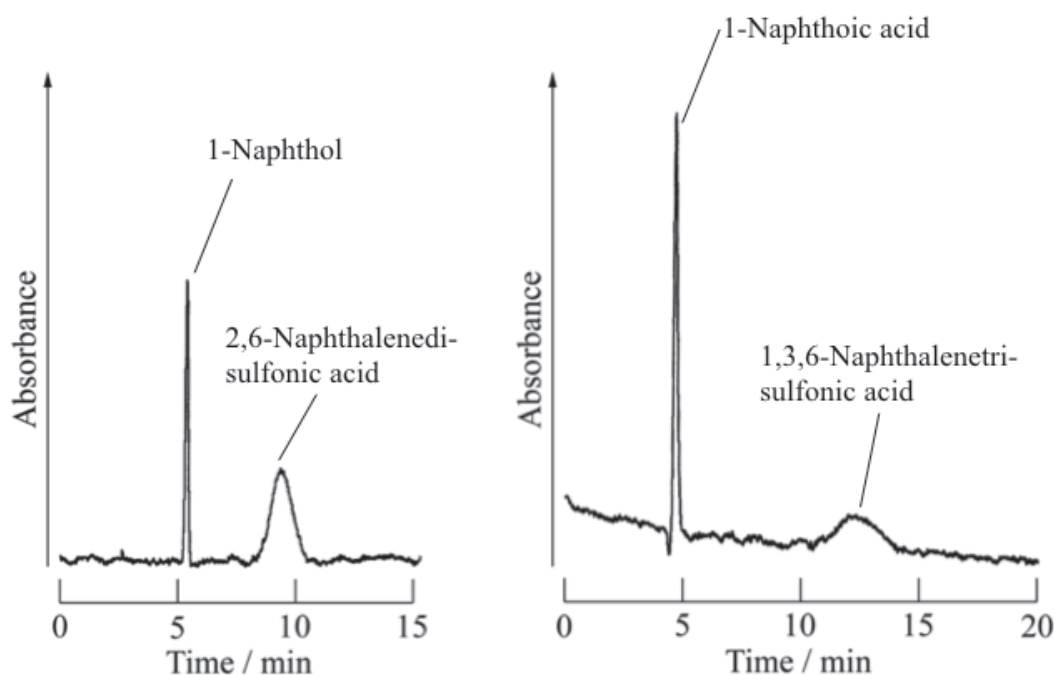


Figure 1. Illustration of a tube radial distribution of the carrier solvents in the TRDC system that is drawn based on the fluorescence photographs obtained by the fluorescence microscope-CCD camera. 1) Fused-silica (50 μm i.d.), polyethylene (200 μm i.d.), and PTFE (100 μm i.d.) capillary tubes were available. 2) For example, a water-acetonitrile-ethyl acetate (2:9:4 v/v/v) mixture solution was used as an organic solvent-rich carrier solution. 3) For example, a water-acetonitrile-ethyl acetate (15:3:2 v/v/v) mixture solution was used as a water-rich carrier solution. 4) The analytes that are delivered through the capillary tube are distributed between inner and outer phases, undergoing chromatographic separation under laminar flow conditions.

a)



b)

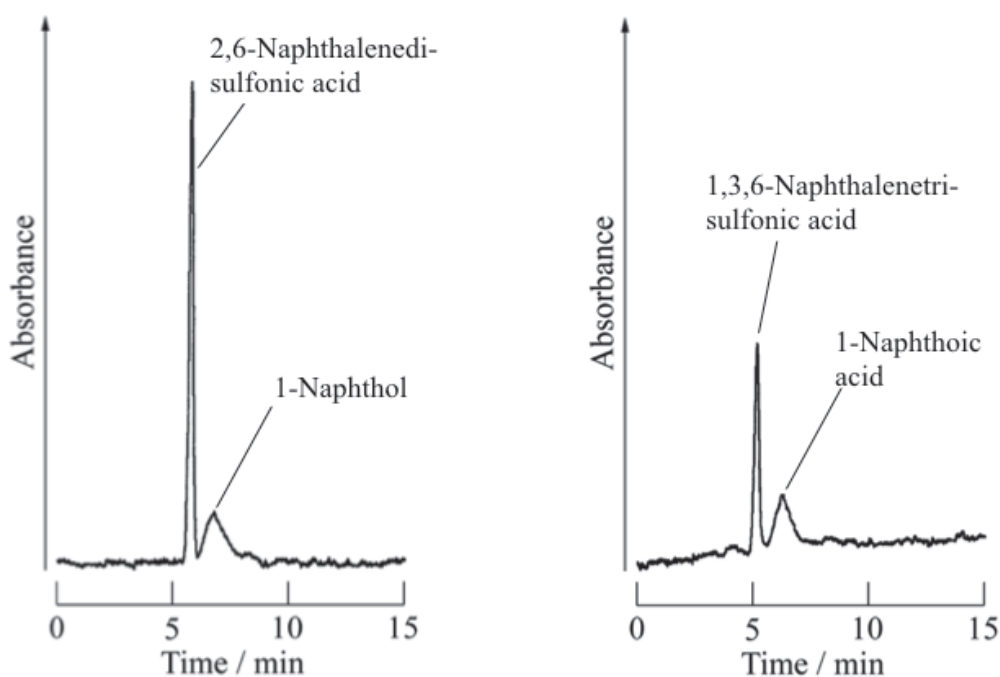


Figure 2. Chromatograms of a mixture of 1-naphthol and 2,6-naphthalenedisulfonic acid as well as 1-naphthoic acid and 1,3,6-naphthalenetrisulfonic acid obtained by the present system. Conditions: Capillary tube, 120 cm (effective length: 100 cm) of 75 μm i.d. fused-silica; carrier, a) water-acetonitrile-ethyl acetate (3:8:4 v/v/v) mixture solution and b) water-acetonitrile-ethyl acetate (15:3:2 v/v/v) mixture solution; sample injection, 20 cm height (gravity) \times 30 s; flow rate, 0.8 $\mu\text{L min}^{-1}$; tube temperature, 20 $^{\circ}\text{C}$; and 1-naphthoic acid, 2,6-naphthalenedisulfonic acid, and 1-naphthol, 1 mM each and 1,3,6-naphthalenetrisulfonic acid, 2 mM.

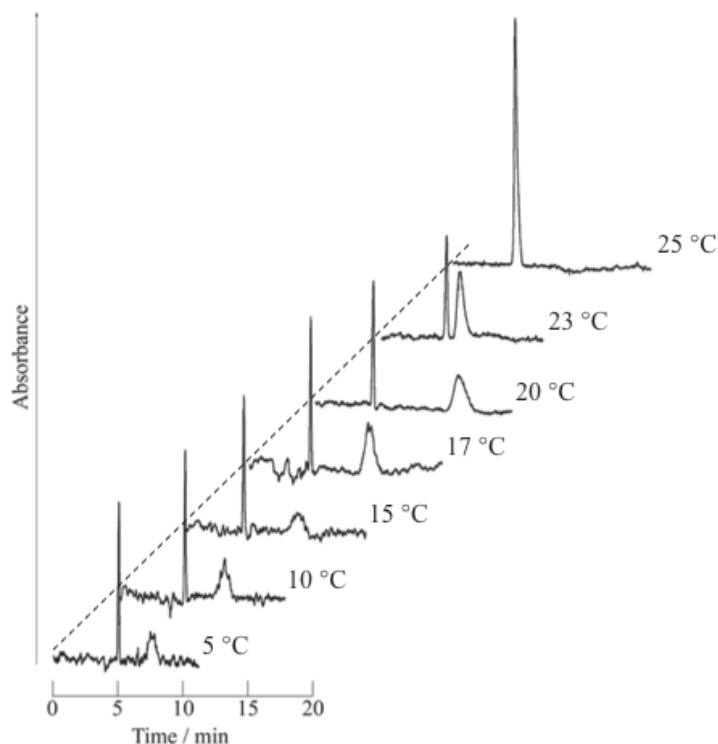


Figure 3. Effects of temperature on separation in the present system. Conditions: Capillary tube, 120 cm (effective length of 100 cm, where part of it (ca. 80 cm) was dipped in the temperature-controlled water) of 75 μm i.d. fused-silica; carrier, water-acetonitrile-ethyl acetate (3:8:4 v/v/v) mixture solution; sample injection, 20 cm height (gravity) \times 30 s; flow rate, 0.8 $\mu\text{L min}^{-1}$; tube temperature, 5 – 25 $^{\circ}\text{C}$; and 2,6-naphthalenedisulfonic acid and 1-naphthol, 1 mM each.

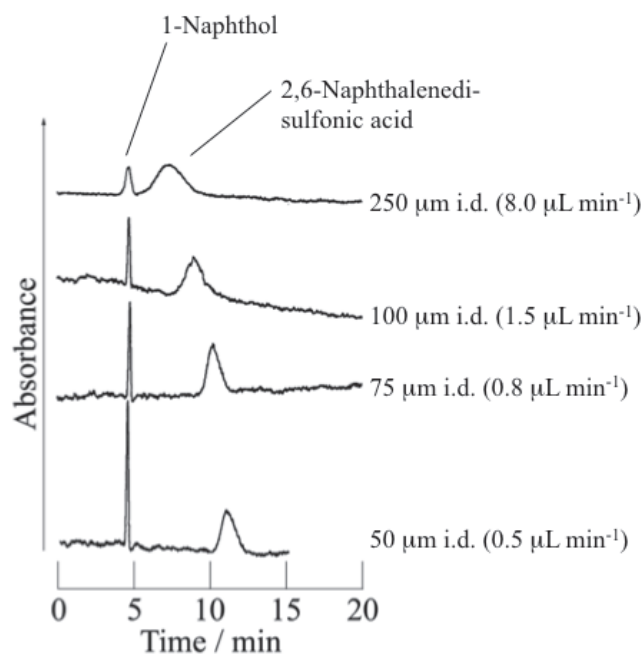


Figure 4. Effects of the inner diameter of the tube on separation in the present system. Conditions: Capillary tube, 120 cm (effective length: 100 cm) fused-silica; carrier, water-acetonitrile-ethyl acetate (3:8:4 v/v/v) mixture solution; sample injection, 20 cm height (gravity) \times 2 – 45 s; flow rate, 0.5 – 8.0 $\mu\text{L min}^{-1}$; tube temperature, 20 $^{\circ}\text{C}$; and 2,6-naphthalenedisulfonic acid and 1-naphthol, 1 mM.

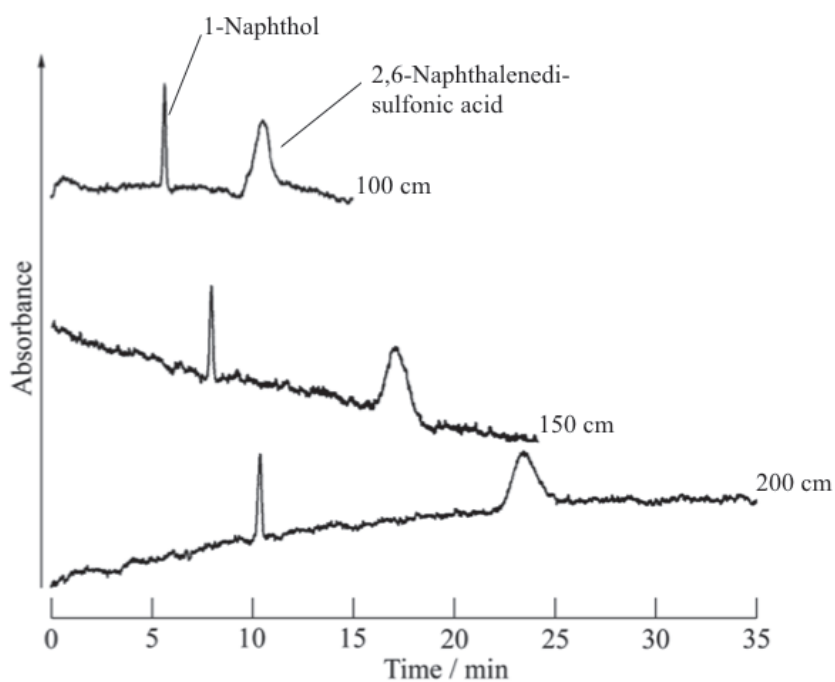


Figure 5. Effects of the effective length of the tube on separation in the present system. Conditions: Capillary tube, effective length (100 – 200 cm) of 75 μm i.d. fused-silica; carrier, water-acetonitrile-ethyl acetate (3:8:4 v/v/v) mixture solution; sample injection, 20 cm height (gravity) \times 30 s; flow rate, 0.8 $\mu\text{L min}^{-1}$; tube temperature, 20 $^{\circ}\text{C}$; and 2,6-naphthalenedisulfonic acid and 1-naphthol, 1 mM.

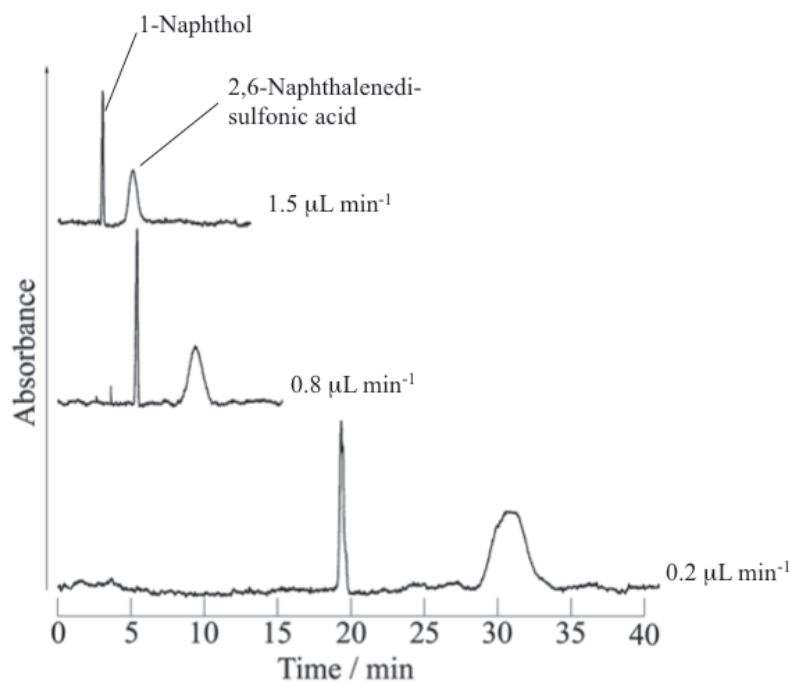
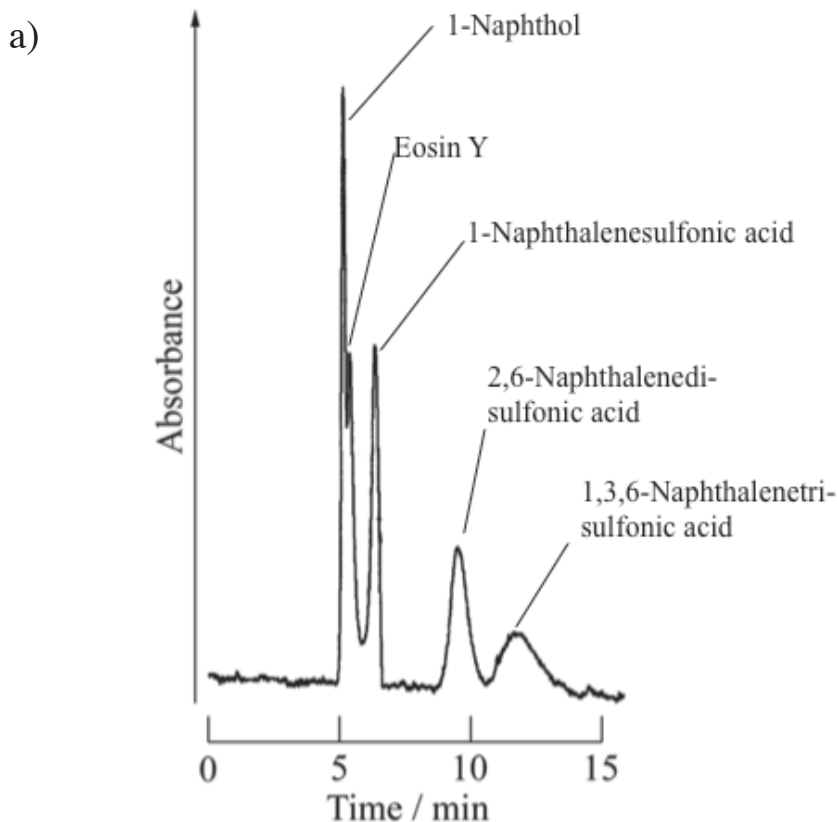


Figure 6. Effects of the flow rate of carrier solution on separation in the present system. Conditions: Capillary tube, 120 cm (effective length: 100 cm) of 75 μm i.d. fused-silica; carrier, water-acetonitrile-ethyl acetate (3:8:4 v/v/v) mixture solution; sample injection, 20 cm height (gravity) \times 30 s; flow rate, 0.2 – 1.5 $\mu\text{L min}^{-1}$; tube temperature, 20 $^{\circ}\text{C}$; and 2,6-naphthalenedisulfonic acid and 1-naphthol, 1 mM each.



b)

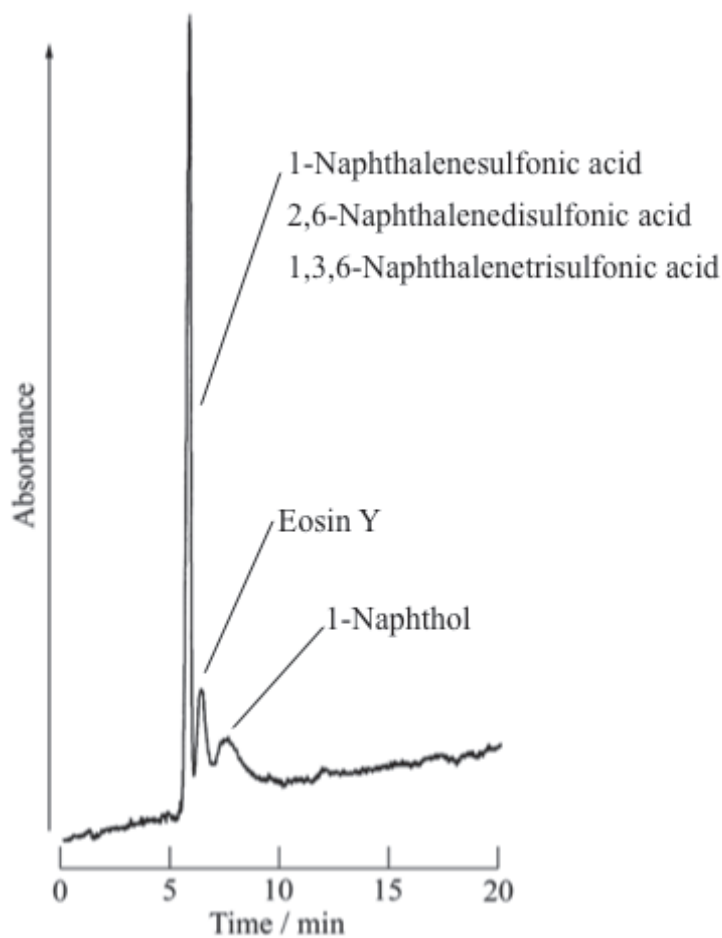


Figure 7. Chromatograms of the mixture analyte solution of 1-naphthol, Eosin Y, 1-naphthalenesulfonic acid, 2,6-naphthalenedisulfonic acid, and 1,3,6-naphthalenetrisulfonic acid obtained by the present method. Conditions: Capillary tube, 120 cm (effective length: 100 cm) of 75 μm i.d. fused-silica; carrier, a) water-acetonitrile-ethyl acetate (3:8:4 v/v/v) mixture solution and b) water-acetonitrile-ethyl acetate (15:3:2 v/v/v) mixture solution; sample injection, 20 cm height (gravity) \times 30 s; flow rate, 0.8 $\mu\text{L min}^{-1}$; temperature, 20 $^{\circ}\text{C}$; and 1-naphthol, 1-naphthalenesulfonic acid, and 2,6-naphthalenedisulfonic acid, 1 mM, 1,3,6-naphthalenetrisulfonic acid, 2.0 mM, and Eosin Y, 0.1 mM.

Table 1. Resolution (R_s), theoretical plate number (N), and height equivalent to the theoretical plate (H)

Effective length of capillary tube	R_s	N		H (mm)	
		1-Naphthol	2,6-Naphthalene-disulfonic acid	1-Naphthol	2,6-Naphthalene-disulfonic acid
100 cm	6.0	7800	900	0.13	1.10
150 cm	8.0	10800	1200	0.14	1.29
200 cm	9.7	12900	1600	0.16	1.24

4.2 Influences of analyte injection volumes and concentrations on the chromatograms in TRDC

We examined the effects of the analyte injection volume (injection time) and concentration on the chromatograms in the tube radial distribution chromatography (TRDC) system using a fused-silica capillary tube (50 μm i.d. and 100 cm effective length) and a water-acetonitrile-ethyl acetate mixture carrier solution (volume ratio, 3:8:4). Analyte solutions of 1-naphthol and 2,6-naphthalenedisulfonic acid (1 mM each) were injected into the system with various injection times of 10 – 1500 s from a height of 20 cm using gravity. They were separated and detected in this order with good reproducibility up to an injection time of 150 s. The analyte solutions (0.075 – 3.0 mM) were analyzed with the definite injection time of 30 s from a height of 20 cm using gravity. They were separated and detected with a baseline separation and their calibration curves showed linearity up to 1.5 mM. It was confirmed that the TRDC system was effective as a quantitative analysis.

Introduction

Analytical methods using capillary tubes have attracted a great deal of interest since the last century [29-31]. Well-known methods include capillary electrophoresis, capillary electrochromatography, micellar electrokinetic capillary chromatography, and high-performance liquid capillary chromatography using packed and monolithic columns. However, only a few new concepts concerning capillary chromatography have been reported in the last decade [25,28]. Related research has been discussed in detail in our papers.^{2,10)} We have developed a capillary chromatography system using an open capillary tube and a water-hydrophilic/hydrophobic organic mixture carrier solution. This system works under laminar flow conditions and does not require any packed reagents in the capillary tube or application of high voltage to the ends of the tube. It is called a tube radial distribution chromatography (TRDC) system.

To date, various mixtures of hydrophilic and hydrophobic analytes have been separated using the TRDC system. However, we have yet to examine the effects of the analyte injection volume or injection time and concentration on the chromatograms in the TRDC system in detail. The analyte injection volume and concentration are fundamental analytical factors in general chromatography separation and flow-injection analysis. Here, we examined separation performance with various analyte injection volumes and concentrations in the TRDC system to expand our knowledge regarding this new separation system.

Experimental

The TRDC system equipped with absorption on-line detection was comprised of an open fused-silica capillary tube (50 μm i.d., 120 cm length; 100 cm effective length), microsyringe pump, and absorption detector. The tube temperature was controlled by immersing the capillary tube in water maintained at a fixed temperature (0 $^{\circ}\text{C}$) in a beaker maintained by stirring. A water-acetonitrile-ethyl acetate mixture with a volume ratio of 3:8:4 was used as an organic solvent-rich carrier solution. An analyte solution including 1-naphthol and 2,6-naphthalenedisulfonic acid as a model was prepared with

the carrier solution. The analyte solution was introduced directly into the capillary inlet side by the gravity method (from a height of 20 cm). After analyte injection, the capillary inlet was connected through a joint to a microsyringe. The syringe was set on the microsyringe pump and the carrier solution was fed into the capillary tube at a fixed flow rate ($0.2 \mu\text{L min}^{-1}$) under laminar flow conditions (Reynolds number was calculated roughly to be 0.14 in the present system). On-capillary absorption detection (254 nm) was performed with the detector.

Results and discussion

Analyte injection times, volumes, and zone lengths An analyte solution consisting of 1-naphthol and 2,6-naphthalenedisulfonic acid was injected into the capillary tube using gravity from a height of 20 cm at various injection times of 10 – 1500 s (25 min) in the current TRDC system. In order to examine the analyte injection volumes and zone lengths in the capillary tube corresponding to the analyte injection times of 10 – 1500 s effectively, the rate of flow using gravity was estimated with the Hagen-Poiseuille equation. The flow rate in the capillary tube with gravity from a height of 20 cm was calculated using the Hagen-Poiseuille equation (Eq. 1), which is shown below: Q is the flow rate, a is the radius, Δp is loss of pressure, μ is viscosity, and L is total length.

$$Q = \frac{\pi a^4 \Delta P}{8\mu L} \quad \text{Eq. 1)}$$

The flow rate for the capillary $50 \mu\text{m}$ i.d. (a , 25×10^{-6} m) was calculated to be approximately $2.67 \times 10^{-13} \text{ m}^3 \text{ s}^{-1}$, where Δp , μ , and L were estimated to be $1.3 \times 10^3 \text{ kgm}^{-1} \text{ s}^{-2}$ (calculated from the difference in height or position between the capillary inlet and outlet, 20 cm), $6.2 \times 10^{-4} \text{ kgm}^{-1} \text{ s}^{-1}$ (measured by a viscosity measurement device for the carrier solution), and 1.2 m, respectively. In addition, the value of the flow rate, Q , was estimated experimentally by the experimental data from the gravity method. 1-Naphthol analyte (1 mM) was injected into the capillary tube in the usual way (from a height of 20 cm for 10 s) and then the analyte was delivered with the carrier solution into the tube by gravity (from a height of 20 cm) instead of the microsyringe pump. The flow rates for the capillary $50 \mu\text{m}$ i.d. were calculated with Eq. 2, where t is the elution time and L' is the effective length. The value of Q was calculated to be approximately $2.72 \times 10^{-13} \text{ m}^3 \text{ s}^{-1}$ (using t , L' , and a of 120 min, 1.0 m, and 25×10^{-6} m, respectively).

$$Q = \frac{a^2 \pi L'}{t} \quad \text{Eq. 2)}$$

There was good correspondence in the flow rate between the value calculated with the Hagen-Poiseuille equation and with that of the experimental data using gravity. The value of the flow rate, $2.7 \times 10^{-13} \text{ m}^3 \text{ s}^{-1}$, was used in the following estimations. The analyte injection volumes were calculated by multiplying the flow rates and the injection times, as well as the analyte zone lengths in the tube, were calculated by dividing the analyte injection volumes by the tube cross-section. That is, the injection times of 10 – 1500 s (25 min) corresponded to the analyte injection volumes of 2.7 – 400 nL and the zone lengths of 1.5 – 200 mm.

Effects of injection time on the chromatograms We examined the effects of analyte injection time on separation in the TRDC system with an analyte solution of 1-naphthol and 2,6-naphthalenedisulfuric acid as a model. The experiments were performed with the organic solvent-rich carrier solution because it provided better resolution than the water-rich carrier solution on the chromatograms when the fused-silica capillary tube was used in our studies [7,10]. The analyte solutions of 1-naphthol and 2,6-naphthalenedisulfonic acid (1 mM each) were analyzed with various injection times of 10 – 1500 s (25 min) by the TRDC system. The typical chromatograms obtained at injection times of 10, 40, 150, 600, 1320, and 1500 s are shown in Fig. 1. As shown in Fig. 1, 1-naphthol and 2,6-naphthalenedisulfonic acid were separated and detected in this order with the TRDC system using the organic solvent-rich carrier solution. These results offered good reproducibility for their peak shapes and elution times with the injection times of 10 – 150 s (2.7 – 40 nL injection volume or 1.5 – 20 mm zone length). The first peaks of 1-naphthol were eluted with nearly the average linear velocity in the present system, and the second peaks of 2,6-naphthalenedisulfonic acid were eluted lower at a lower than average linear velocity. The capacity factors of the second peaks, which were calculated using the first peaks as the dead (hold-up) times, at injection times of 10, 40, and 150 s were 0.57, 0.61, and 0.58, respectively. With injection times of 150 – 1350 s (22 min) (40 – 360 nL injection volume or 20 – 180 mm zone length), although they were separated on the chromatograms, the elution times of the second peaks started to come earlier. With injection times of more than 1400 s, even separation was not performed as shown in the typical chromatogram (injection time 1500 s (25 min) in Fig. 1. It is noted here that such experiments treated with such a wide range of injection volumes (2.7 – 400 nL) and zone lengths (1.5 – 200 mm) would not be carried out in the usual capillary chromatography using monolithic or packed columns combined with a sample injector. Large injection times or analyte injection volumes led to either non-Gaussian or trapezoidal peaks, as shown in Fig. 1. The relationships between the injection times and peak heights or peak areas for both analytes were examined for injection times of 10 – 150 s. The obtained relationships are shown in Fig. 2. The relationships between the injection times and peak areas for both analytes indicated good linearity, while those between injection times and peak heights indicated linearity up to ca. 40 s for 1-naphthol and up to ca. 60 s for 2,6-naphthalendisulfonic acid. The inflection point (ca. 40 s) of 1-naphthol appeared earlier than that of 2,6-naphthalendisulfonic acid (ca. 60 s). The difference in inflection points may have been caused by the differences in elution time or diffusion time between 1-naphthol and 2,6-naphthalenedisulfonic acid.

Effects of analyte concentrations on the chromatogram We examined the effects of the analyte concentrations (0.075 – 3.0 mM) on separation in the TRDC system with an analyte solution of 1-naphthol and 2,6-naphthalenedisulfuric acid as a model. The analyte solution was injected into the capillary tube using gravity from a height of 20 cm for 30 s. The typical chromatograms obtained with concentrations of 0.1, 0.5, 1.5, 2.0, and 3.0 mM are shown in Fig. 3. 1-naphthol and 2,6-naphthalenedisulfuric acid were separated with a base-line separation and detected up to 1.5 mM. The capacity factors at concentrations of 0.1, 0.5, and 1.5 mM were 0.54, 0.59, and 0.57, respectively.

At concentrations higher than 1.5 mM, the resolutions gradually decreased until they could no longer be separated on the chromatogram at all at about 3.0 mM, as shown in Fig. 3. The calibration curves were examined up to 1.5 mM for both analytes with peak heights and peak areas. The obtained calibration curves are shown in Fig. 4. Good linearity was observed in the curves shown in Fig. 4. Correlation coefficients were 0.996 – 0.998 for all calibration curves. Relative standard deviations of 1-naphthol were 2.5 % (n=8) for both peak heights and areas, while those of 2,6-naphthalenedisulfuric acid were 3.2 % (n=8) for peak heights and 5.4 % (n=8) for peak areas. It was confirmed from the obtained data in Fig. 4 that the TRDC system was effective as a quantitative analysis.

In conclusion, we examined the effects of analyte injection volume and concentration on the chromatograms in the TRDC system. The injection volumes and concentrations are fundamental analytical factors in chromatographic research. The analyte solution of 1-naphthol and 2,6-naphthalenedisulfuric acid was used as a model to first be separated and then detected to varying injection times up to 150 s (injection volume 40 nL or zone length 20 mm), they were also analyzed up to 1.5 mM with good reproducibility. Separation in the present TRDC system became difficult at analyte injection times of more than 150 s or analyte concentrations of more than 1.5 mM. The difficulty may be due to instability or the collapse of the inner and outer phase formations based on the tube radial distribution of the carrier solvents in the capillary tube with extremely large analyte injection volumes or concentrations. Additionally, the ranges of analyte injection volume and concentration that provide quantitative analysis might be influenced by analytical conditions, such as capillary inner diameter, flow rates, and component ratios of the carrier solvents.

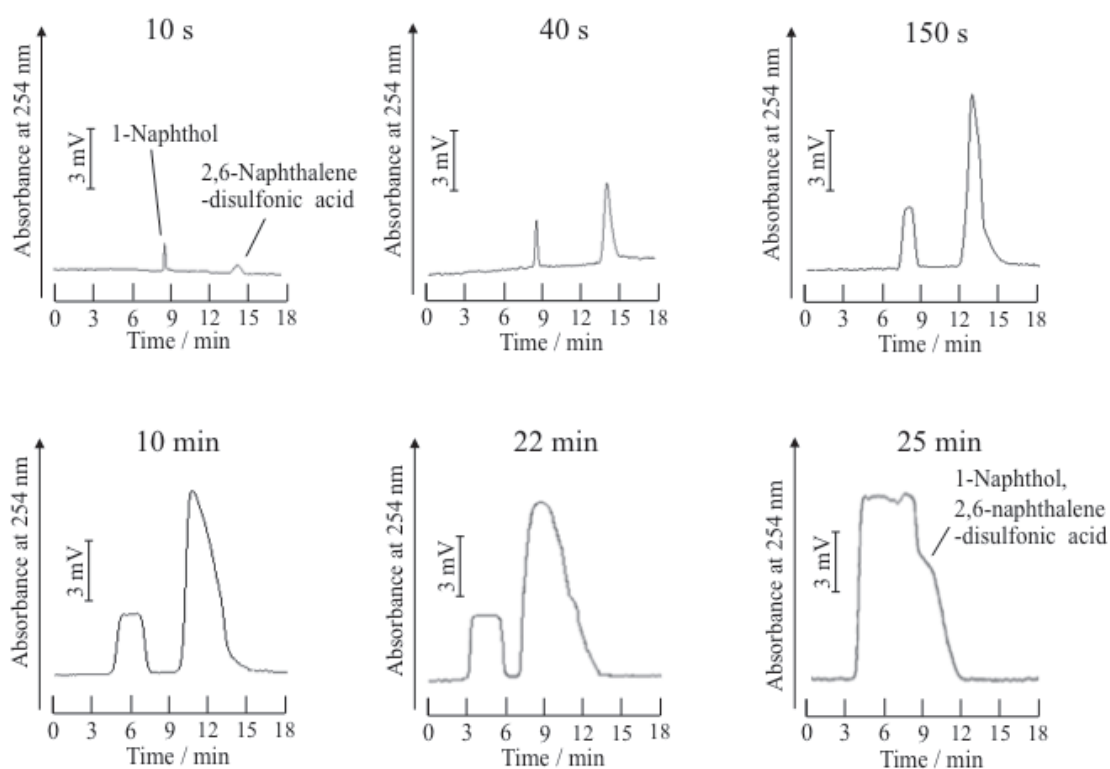


Figure 1. Chromatograms of a mixture of 1-naphthol and 2,6-naphthalenedisulfonic acid obtained by the TRDC system with various injection times. Conditions: Capillary tube, 120 cm (effective length: 100 cm) of 50 μm i.d. fused-silica; carrier, water-acetonitrile-ethyl acetate (3:8:4 v/v/v) mixture solution; sample injection, 20 cm height (gravity) \times 10, 40, 150, 600, 1320, and 1500 s; flow rate, 0.2 $\mu\text{L min}^{-1}$; tube temperature, 0 $^{\circ}\text{C}$; and analyte concentration, 1 mM.

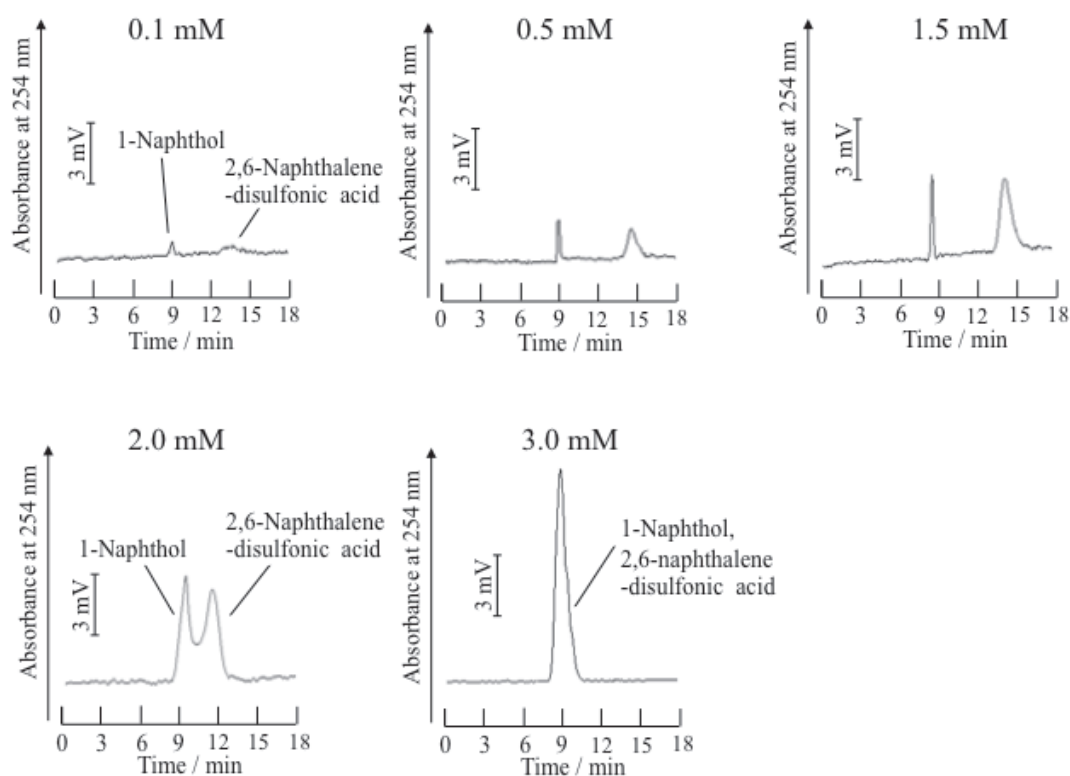


Figure 2. Relationships between injection times and peak heights or peak areas for 1-naphthol and 2,6-naphthalenedisulfonic acid in the TRDC system. Conditions: Capillary tube, 120 cm (effective length: 100 cm) of 50 μm i.d. fused-silica; carrier, water-acetonitrile-ethyl acetate (3:8:4 v/v/v) mixture solution; sample injection, 20 cm height (gravity) \times 10 – 150 s; flow rate, 0.2 $\mu\text{L min}^{-1}$; tube temperature, 0 $^{\circ}\text{C}$; and analyte concentration, 1 mM.

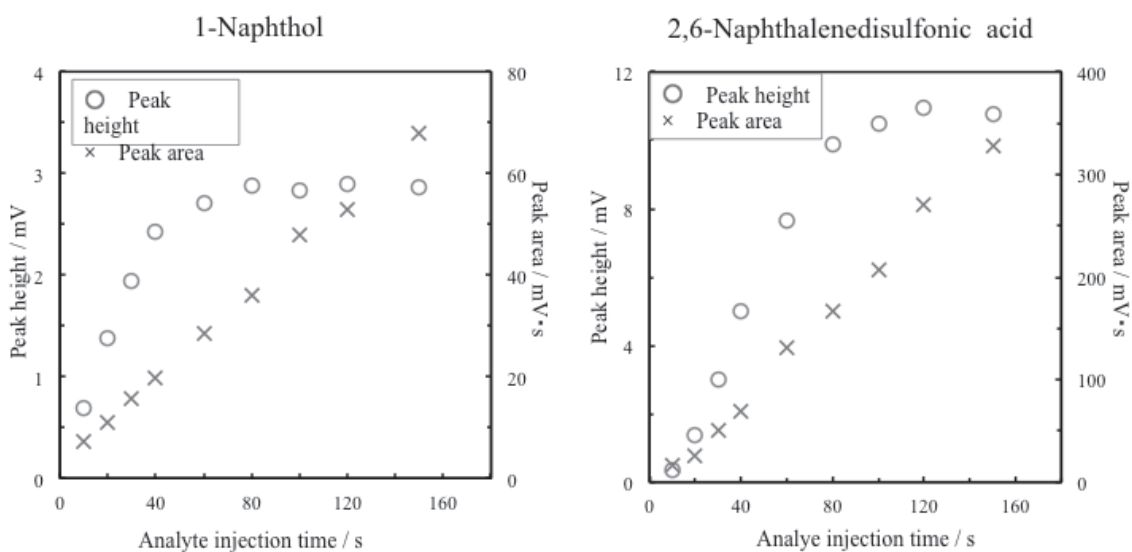


Figure 3. Chromatograms of a mixture of 1-naphthol and 2,6-naphthalenedisulfonic acid obtained by the TRDC system with various analyte concentrations. Conditions: Capillary tube, 120 cm (effective length: 100 cm) of 50 μm i.d. fused-silica; carrier, water-acetonitrile-ethyl acetate (3:8:4 v/v/v) mixture solution; sample injection, 20 cm height (gravity) \times 30 s; flow rate, 0.2 $\mu\text{L min}^{-1}$; tube temperature, 0 $^{\circ}\text{C}$; and analyte concentration, 0.1, 0.5, 1.5, 2.0, and 3.0 mM.

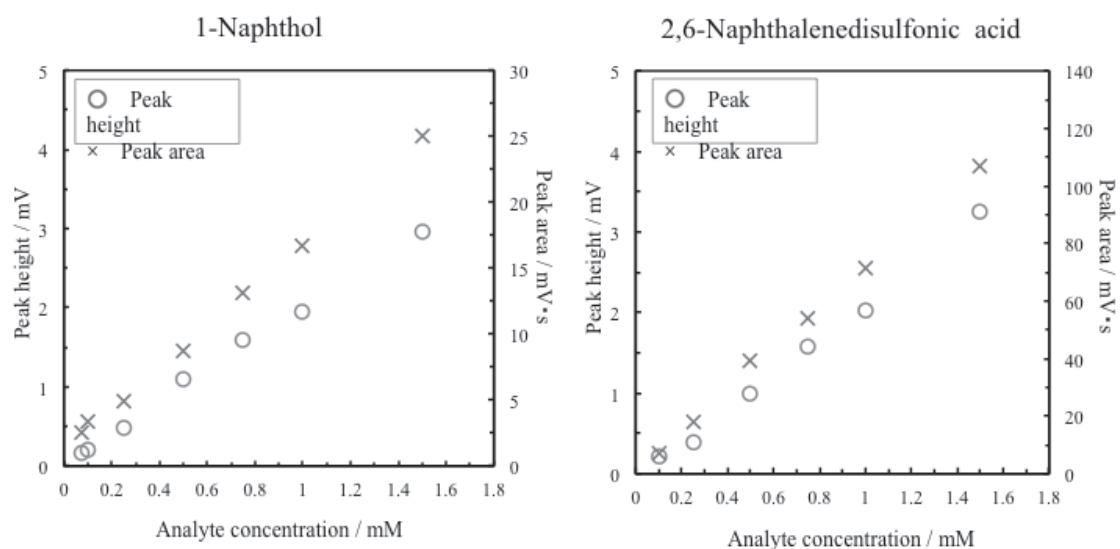


Figure 4. Calibration curves of 1-naphthol and 2,6-naphthalenedisulfonic acid obtained by the TRDC system. Conditions: Capillary tube, 120 cm (effective length: 100 cm) of 50 μm i.d. fused-silica; carrier, water-acetonitrile-ethyl acetate (3:8:4 v/v/v) mixture solution; sample injection, 20 cm height (gravity) \times 30 s; flow rate, 0.2 $\mu\text{L min}^{-1}$; tube temperature, 0 $^{\circ}\text{C}$; and analyte concentration, 0.1 – 1.5 mM.

4.3 Investigation of the composition for a ternary mixed solvent system in TRDC using PTFE capillary tube

The tube radial distribution chromatography (TRDC) system works under laminar flow conditions. Here, a phase diagram for the ternary mixture carrier solvents of water, acetonitrile, and ethyl acetate was constructed. The phase diagram that included a boundary curve between homogeneous and heterogeneous solutions was considered to be together with the component ratios of the solvents in the homogeneous carrier solutions required for the TRDC system where a poly(tetrafluoroethylene) (PTFE) capillary tube was used. It was found that the TRDC system performed well with homogeneous solutions having component ratios of the solvents that were positioned near the homogeneous-heterogeneous solution boundary of the phase diagram. For preparing the carrier solutions of water-hydrophilic/hydrophobic organic solvents for the TRDC system, we used methanol, ethanol, 1,4-dioxane, and 1-propanol instead of acetonitrile (hydrophilic organic solvent), as well as chloroform and 1-butanol, instead of ethyl acetate (hydrophobic organic solvent). The homogeneous ternary mixture carrier solutions were prepared near the homogeneous-heterogeneous solution boundary. Analyte mixtures of 2,6-naphthalenedisulfonic acid and 1-naphthol were separated with the TRDC system using these homogeneous ternary mixture carrier solutions. The pressure change in the capillary tube under laminar flow conditions might alter the carrier solution from homogeneous to heterogeneous in the batch vessel, thus affecting the tube radial distribution of the solvents in the capillary tube.

Introduction

Capillary tubes, e.g., fused-silica and PTFE, that feature inner diameters less than several hundred micrometers are found to have uniform bores, inert inner surfaces, and good flexibility. Capillary tubes with these characteristics play an important role in several unique micro-flow analyses [27, 32-36]. The capillary tubes are also known to exhibit interesting and useful physical or hydrodynamic phenomena, such as electro-osmotic flow and laminar flow. The electro-osmotic flow in a capillary tube has capillary electrophoresis [37-39] and capillary electrochromatography [40-42] properties while laminar flow conditions enable hydrodynamic chromatography [43-45].

The tube radial distribution of the solvents, or the TRDP, was also observed in a microchannel in a microchip under laminar flow conditions.⁶⁾ A carrier solution containing fluorescent dyes was introduced into a microchannel (100 μm width by 40 μm depth) and the tube radial distribution of the dyes was monitored using a fluorescence microscope. For example, when an organic solvent-rich carrier solution (water-acetonitrile-ethyl acetate; 3:8:4 volume ratio) containing perylene and Eosin Y was fed into the channel, perylene (hydrophobic) and Eosin Y (comparatively hydrophilic) were distributed around the center and near the inner wall of the microchannel, respectively. A capillary chromatography system has been developed based on the tube radial distribution of the carrier solution in the capillary tube under laminar flow conditions. The chromatography system is called a tube radial distribution chromatography (TRDC) system.

However, further information on the TRDC system or the TRDP is required for various applications, such as in analytical chemistry, physical chemistry, and chemical engineering laboratories. Here, a phase diagram for the ternary mixture carrier solvents of water, acetonitrile, and ethyl acetate was constructed and is considered to be congruent with the component ratios of the solvents required for the TRDC system where the PTFE capillary tube was used. Subsequently, various kinds of water-hydrophilic/hydrophobic organic solvent mixture solutions, other than the usual water-acetonitrile-ethyl acetate mixture solution, were prepared and examined as carrier solutions in the TRDC system.

Experimental

Figure 1 shows a schematic diagram of the present capillary chromatography system, comprised of an open PTFE capillary tube [$100 \pm 25 \mu\text{m}$ i.d., 120 cm length (effective length, 100 cm)], a micro-syringe pump, and an absorption detector. The tube temperature was controlled by dipping the capillary tube (ca. 80 cm) in water maintained at a fixed temperature (0 or 15 °C) in a beaker by stirring. Water-hydrophilic/hydrophobic organic solvent mixture solutions with the various volume ratios were used as carrier solutions. Analyte solutions were prepared with the carrier solutions. The analyte solution was introduced directly into the capillary inlet side by the gravity method (20 cm height for 30 s). After analyte injection, the capillary inlet was connected through a joint to a micro-syringe. The syringe was placed on the microsyringe pump. The carrier solution was fed into the capillary tube at $2.0 \mu\text{L min}^{-1}$ flow rate under laminar flow conditions. On-capillary absorption detection (320 nm) was performed using the detector.

Results and Discussion

Preliminary experiments at various component ratios of water-acetonitrile-ethyl acetate mixture carrier solution The solution having a constant component ratio of water-acetonitrile (hydrophilic) of 100:20 volume ratio was added ethyl acetate (hydrophobic) in a vessel at a temperature of 22 °C to prepare carrier solutions with the following compositions: a) water-acetonitrile-ethyl acetate of 100:20:0 volume ratio; b) 100:20:4 volume ratio; c) 100:20:9 volume ratio; d) 100:20:10 volume ratio; and e) 100:20:11 volume ratio. The first four carrier solutions, a) – d), were homogeneous, but the last carrier solution, e), was heterogeneous (including two homogeneous phases). The carrier solution d), the water-acetonitrile-ethyl acetate of the 100:20:10 volume ratio, was the specific homogeneous solution that possessed the component ratio of the solvents near the homogeneous-heterogeneous solution boundary region of the phase diagram. The analyte mixtures of 2,6-naphthalenedisulfonic acid and 1-naphthol were examined with the capillary chromatography system with the first four homogeneous carrier solutions a) – d). The obtained chromatograms are shown in Fig. 2. Only the specific homogeneous carrier solution d), the water-acetonitrile-ethyl acetate of 100:20:10 volume ratio, could separate the analytes in the mixture. 2,6-Naphthalenedisulfonic acid (comparatively hydrophilic) was eluted first with near the average linear velocity in the capillary tube under laminar flow conditions and 1-naphthol (comparatively hydrophobic) was eluted second with lower at a lower than average linear velocity. The elution order was reasonable in the TRDC system. As

shown in Fig. 1, a major inner phase was formed with the water-rich solvent and a minor outer phase, or capillary wall phase, was formed with the organic-rich solvent in a capillary with a water-rich carrier solution. The analytes that were delivered through the capillary tube were distributed between the inner and outer phases, undergoing chromatographic separation under laminar flow conditions. The other homogeneous carrier solutions a) – c) of water-acetonitrile-ethyl acetate did not show any separation behavior for the analytes under the current analytical conditions (Fig. 2).

Phase diagram for water-acetonitrile-ethyl acetate mixture and the component ratios required for TRDC

A phase diagram for the ternary mixture solvents of water-acetonitrile (hydrophilic organic solvent)-ethyl acetate (hydrophobic organic solvent) was examined in a vessel at a temperature of 22 °C. The obtained phase diagram is shown in Fig. 3. The dotted curve in the diagram indicates the boundary between homogeneous and heterogeneous phases. The phase diagram showed that each component ratio of the solvents made a homogeneous (one homogeneous phase) or a heterogeneous (two homogeneous phases) solution. The component ratios of the solvents in the carrier solutions a) – d) that gave the chromatograms shown in Fig. 2 were plotted in the diagram. Circles (○) and crosses (×) indicate baseline-separation and non-separation for the analytes, respectively. The chromatograms obtained with the homogeneous carrier solutions that had solvent component ratios positioned near the homogeneous-heterogeneous solution boundary curve in the phase diagram are shown in Fig. 4. The carrier solution component ratios were as follows: f) water-acetonitrile-ethyl acetate of 100:0:9 volume ratio; g) 80:20:9 volume ratio; h) 60:40:12.5 volume ratio; i) 50:50:17 volume ratio; j) 30:70:33 volume ratio; and k) 14.5:50:50 volume ratio. The component ratios of the solvents for the chromatograms in Fig. 4 were also plotted in the phase diagram with circles and crosses together with triangles (Δ) which indicate split-separation (not baseline-separation). As is clearly shown in Figs. 2–4, the TRDC system performed with the specific homogeneous carrier solutions having the component ratios of the solvents that were positioned almost directly on the homogeneous-heterogeneous solution boundary curve in the phase diagram. Specific carrier solutions such as these caused tube radial distribution of the carrier solvents in the capillary tube under laminar flow conditions, i.e., the TRDP. The pressure imposed on the carrier solution in the capillary tube under laminar flow conditions might alter the carrier solution from homogeneous in the batch vessel to heterogeneous (although not necessarily with two clear homogeneous phases), affecting the tube radial distribution of the solvents in the capillary tube. We reported that, characteristically, a water-rich carrier solution elutes the more hydrophilic analyte first and an organic solvent-rich carrier solution elutes the more hydrophobic analyte first in a TRDP system [16-18]. That is, in the case of a water-rich carrier solution, the hydrophilic analyte, which is dispersed in the water-rich major phase (around the middle of the capillary tube), is eluted with nearly average linear velocity. The hydrophobic analyte, which is dispersed in the organic solvent-rich minor phase near the inner wall of the tube (pseudo-stationary phase), is eluted at a lower than average linear velocity. In the case of an organic solvent-rich carrier solution, the hydrophobic analyte dispersed in the organic solvent-rich major phase is eluted with nearly average linear velocity. The hydrophilic analyte dispersed in the water-rich minor phase near the

inner wall of the tube (pseudo-stationary phase) is eluted at a lower than average linear velocity. Therefore, the elution times of the analytes can be easily reversed by altering the component ratio of the solvents in the carrier solution. In fact, in Fig. 4, the water-rich carrier solutions, such as f) water-acetonitrile-ethyl acetate of 100:0:9 volume ratio, g) 80:20:9 volume ratio, h) 60:40:12.5 volume ratio, and i) 50:50:17 volume ratio, separated 2,6-naphthalenedisulfonic acid and 1-naphthol in this order, while the organic solvent-rich carrier solution, j) 30:70:33 volume ratio, separated them in the reverse order, i.e., 1-naphthol was first eluted and secondly 2,6-naphthalenedisulfonic acid was detected, although baseline separation could not be provided under the present analytical conditions.

Chromatograms obtained with the carrier solutions using various hydrophilic organic solvents instead of acetonitrile The ternary mixture carrier solutions consisting of water-hydrophilic/hydrophobic organic solvent were prepared by using the water-acetonitrile-ethyl acetate mixture, as indicated in our reports. Here, instead of acetonitrile (hydrophilic organic solvent), methanol, ethanol, 1,4-dioxane, and 1-propanol were used to prepare the homogeneous ternary mixed carrier solutions that had the specific component ratios of the solvents near the homogeneous-heterogeneous solution boundary region. The component ratios of the solvents in the prepared carrier solutions were as follows: water-methanol-ethyl acetate (100:20:15 volume ratio), water-ethanol-ethyl acetate (100:20:15 volume ratio), water-1,4-dioxane-ethyl acetate (100:5:10 volume ratio), and water-1-propanol-ethyl acetate (100:10:11 volume ratio). The chromatograms obtained with the homogeneous carrier solutions are shown in Fig. 5, together with that obtained with the water-acetonitrile-ethyl acetate mixture (100:20:10 volume ratio). It was confirmed from the chromatograms that 2,6-naphthalenedisulfonic acid and 1-naphthol were separated and detected in this order with the TRDC system using the water-rich carrier solutions prepared with various hydrophilic organic solvents.

Chromatograms obtained with the carrier solutions using various hydrophobic organic solvents instead of ethyl acetate Here, instead of including ethyl acetate (hydrophobic organic solvent) in the ternary mixture carrier solution of water-acetonitrile-ethyl acetate, chloroform, hexane, and 1-butanol were used to prepare the homogeneous ternary mixed carrier solutions that had the specific component ratios of the solvents near the homogeneous-heterogeneous solution boundary region. The component ratios of the carrier solutions were as follows: water-acetonitrile-hexane (100:30:1 volume ratio), water-acetonitrile-chloroform (100:30:1 volume ratio), and water-acetonitrile-1-butanol (100:15:20 volume ratio). The chromatograms obtained with the carrier solutions are shown in Fig. 6, along with those obtained with the water-acetonitrile-ethyl acetate mixture as well. It was also confirmed that under the present analytical conditions, 2,6-naphthalenedisulfonic acid and 1-naphthol were separated in this order with the TRDC system using the water-rich carrier solutions that were prepared with chloroform, 1-butanol, and ethyl acetate as hydrophobic organic solvents, but not hexane.

Separation of mixture solution including three analytes We next examined a mixture analyte solution of 1-naphthalenesulfonic acid, 1-naphthoic acid, and 1-naphthol using the present TRDC system with PTFE capillary tube and several types of homogeneous water-rich carrier solutions. The carrier solutions were water-acetonitrile-ethyl acetate (100:20:10 volume ratio), water-ethanol-ethyl acetate (100:20:15 volume ratio), and water-acetonitrile-chloroform (100:30:1 volume ratio). These carrier solutions were prepared based on the concept that the homogeneous carrier solutions were nearly on the homogeneous-heterogeneous solution boundary region. The obtained chromatograms are shown in Fig. 7, together with the analytical conditions. 1-Naphthalenesulfonic acid (pKa, 0.57), 1-naphthoic acid (pKa, 3.70), and 1-naphthol (pKa, 9.34) were eluted in this order, leading to separation with the water-rich carrier solution. 1-Naphthalenesulfonic acid was eluted at nearly the average linear velocity under laminar flow conditions, while the other compounds, 1-naphthoic acid and 1-naphthol, were eluted in this order at lower than average linear velocities. The elution order of 1-naphthalenesulfonic acid, 1-naphthoic acid, and 1-naphthol was reasonable if one considers the hydrophilicity, or hydrophobicity, based on their molecular structures or pKa values.

In conclusion, the phase diagram for the water, acetonitrile, and ethyl acetate mixture was examined and considered to be congruent with the component ratios of the solvents required for the TRDC system. The TRDC system was performed with homogeneous solutions having the component ratios of the solvents that were positioned almost on the homogeneous-heterogeneous solution boundary curve of the phase diagram. Various types of water-hydrophilic/hydrophobic organic solvents, other than the usual water-acetonitrile-ethyl acetate mixture, were prepared for the TRDC system. Thus-prepared carrier solutions were found to be usable for chromatographic separation in the TRDC system.

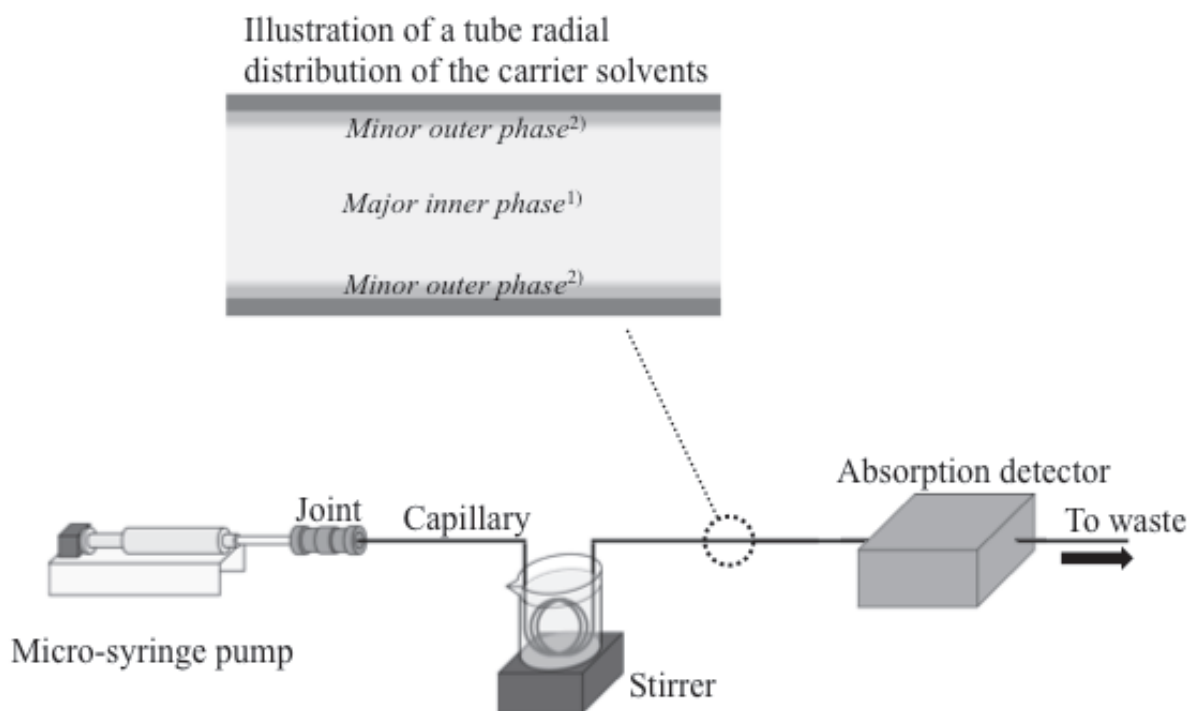


Figure 1. Schematic diagram of the present capillary chromatography system. With a water-rich carrier solution, 1) a major inner phase is formed with a water-rich solvent, and 2) a minor outer phase is formed with an organic-rich solvent.

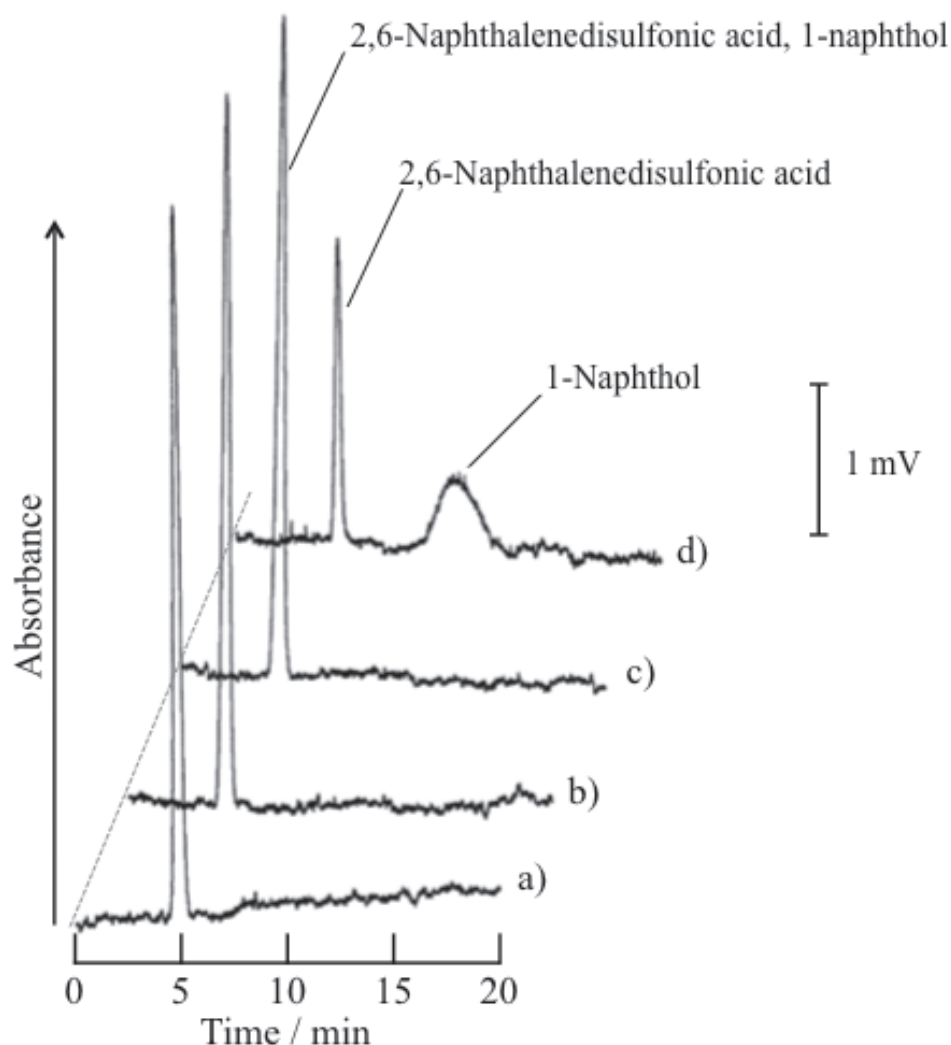


Figure 2. Chromatograms of a mixture of 2,6-naphthalenedisulfonic acid and 1-naphthol with the capillary chromatography system using various component ratios of water-acetonitrile-ethyl acetate mixture as carrier solutions. Conditions: Capillary tube, 120 cm (effective length: 100 cm) of 100 μm i.d. PTFE; carrier, a) water-acetonitrile-ethyl acetate of 100:20:0 volume ratio, b) 100:20:4 volume ratio, c) 100:20:9 volume ratio, and d) 100:20:10 volume ratio; sample injection, 20 cm height (gravity) \times 30 s; flow rate, 2.0 $\mu\text{L min}^{-1}$; tube temperature, 15 $^{\circ}\text{C}$; and 2,6-naphthalenedisulfonic acid and 1-naphthol, 2 mM each. The component ratios of the carrier solutions a) - d) used for the chromatograms are plotted in the phase diagram of Fig. 3.

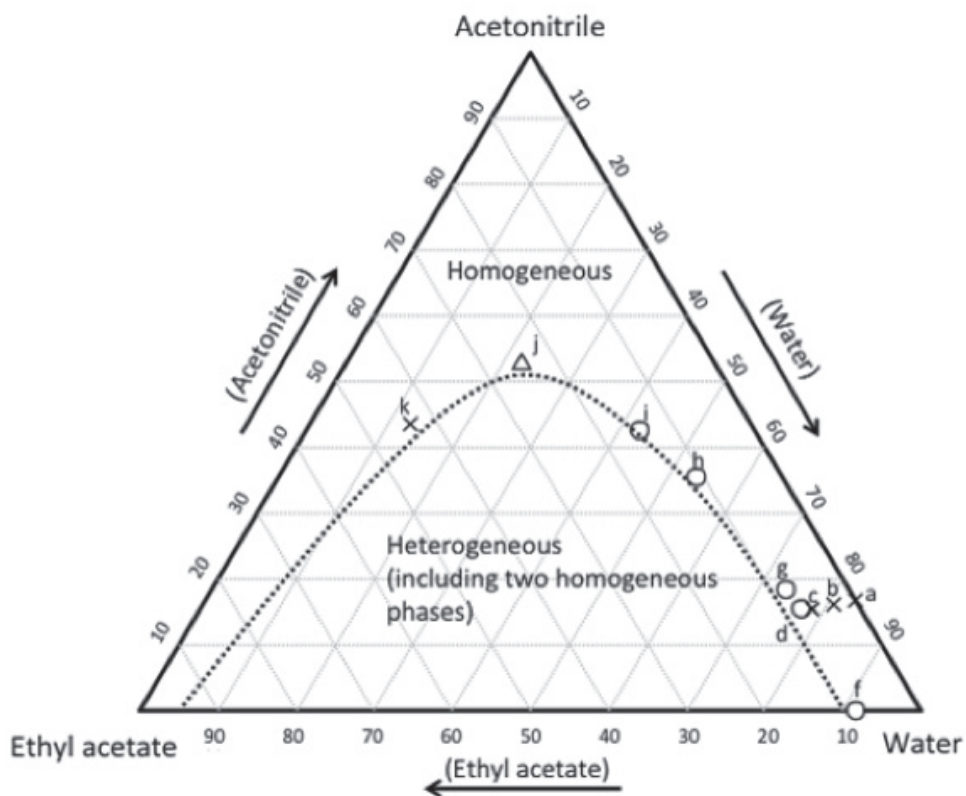


Figure 3. Phase diagram for water-acetonitrile-ethyl acetate mixture and the component ratios of the solvents for the chromatograms obtained with the TRDC system. The dotted curve in the diagram indicates the homogeneous-heterogeneous solution boundary curve. The component ratios of the carrier solvents, a) – d) and f) – k), for the chromatograms in Figs. 2 and 4 are plotted in the diagram with the symbols \circ , Δ , and \times , to express baseline-separation, split-separation, and non-separation, respectively, for the analytes. The chromatograms obtained with a) water-acetonitrile-ethyl acetate of 100:20:0 (or 83:17:0 as a percentage) volume ratio, b) 100:20:4 (or 81:16:3) volume ratio, c) 100:20:9 (or 78:16:7) volume ratio, and d) 100:20:10 (or 77:15:8) volume ratio are shown in Fig. 2 and the chromatograms obtained with f) water-acetonitrile-ethyl acetate of 100:0:9 (or 92:0:8) volume ratio, g) 80:20:9 (or 73:18:8) volume ratio, h) 60:40:12.5 (or 53:36:11) volume ratio, i) 50:50:17 (or 43:43:15) volume ratio, j) 30:70:33 (or 23:53:25) volume ratio, and k) 14.5:50:50 (or 13:44:44) volume ratio are shown in Fig. 4.

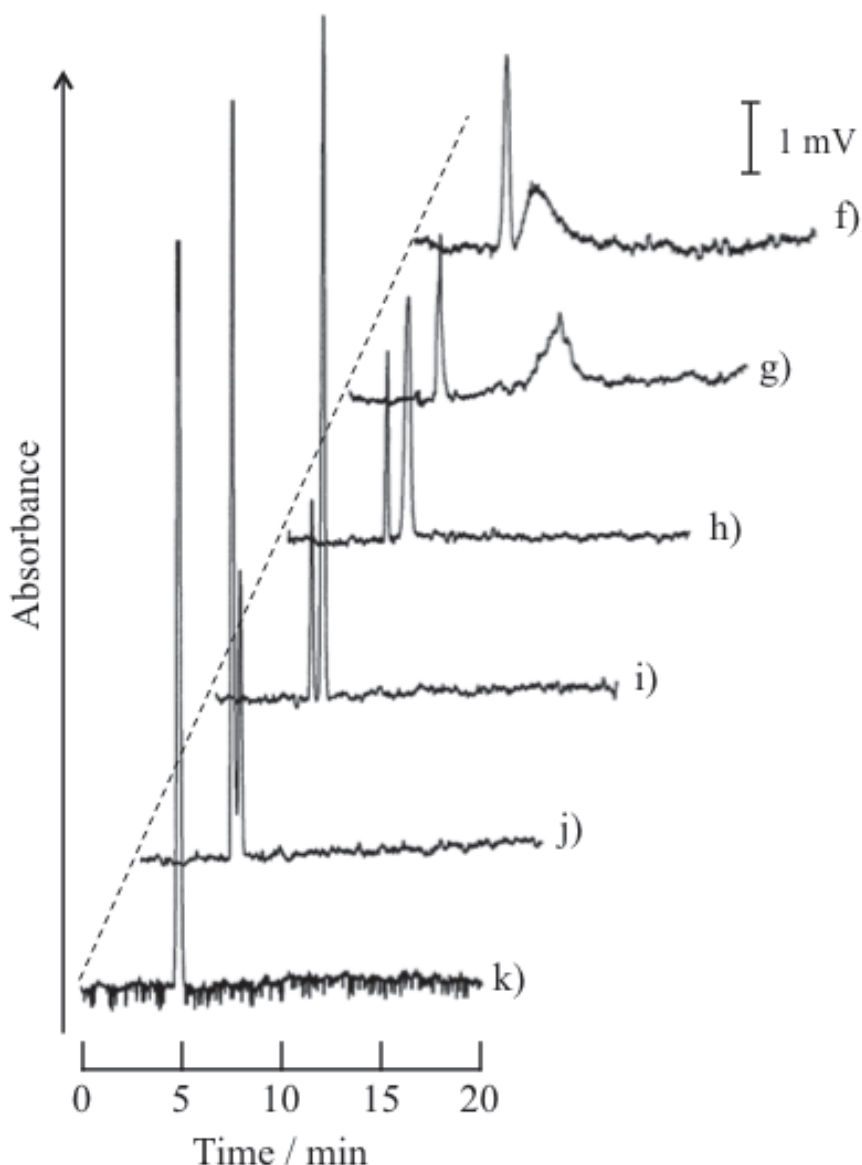


Figure 4. Chromatograms of a mixture of 2,6-naphthalenedisulfonic acid and 1-naphthol with the capillary chromatography system using various component ratios of water-acetonitrile-ethyl acetate mixture as carrier solutions that were positioned almost on the homogeneous-heterogeneous solution boundary curve of the phase diagram. 2,6-Naphthalenedisulfonic acid and 1-naphthol were eluted in this order with the carrier solutions of f) – i), while they were eluted in the reverse order with the carrier solution of j). Conditions: Capillary tube, 120 cm (effective length: 100 cm) of 100 μm i.d. PTFE; carrier, f) water-acetonitrile-ethyl acetate of 100:0:9 volume ratio, g) 80:20:9 volume ratio, h) 60:40:12.5 volume ratio, i) 50:50:17 volume ratio, j) 30:70:33 volume ratio, and k) 14.5:50:50 volume ratio; sample injection, 20 cm height (gravity) \times 30 s; flow rate, 2.0 $\mu\text{L min}^{-1}$; tube temperature, 0 $^{\circ}\text{C}$; and 2,6-naphthalenedisulfonic acid and 1-naphthol, 2 mM each. The component ratios of the carrier solutions f) – k) used for the chromatograms are plotted in the phase diagram of Fig. 3.

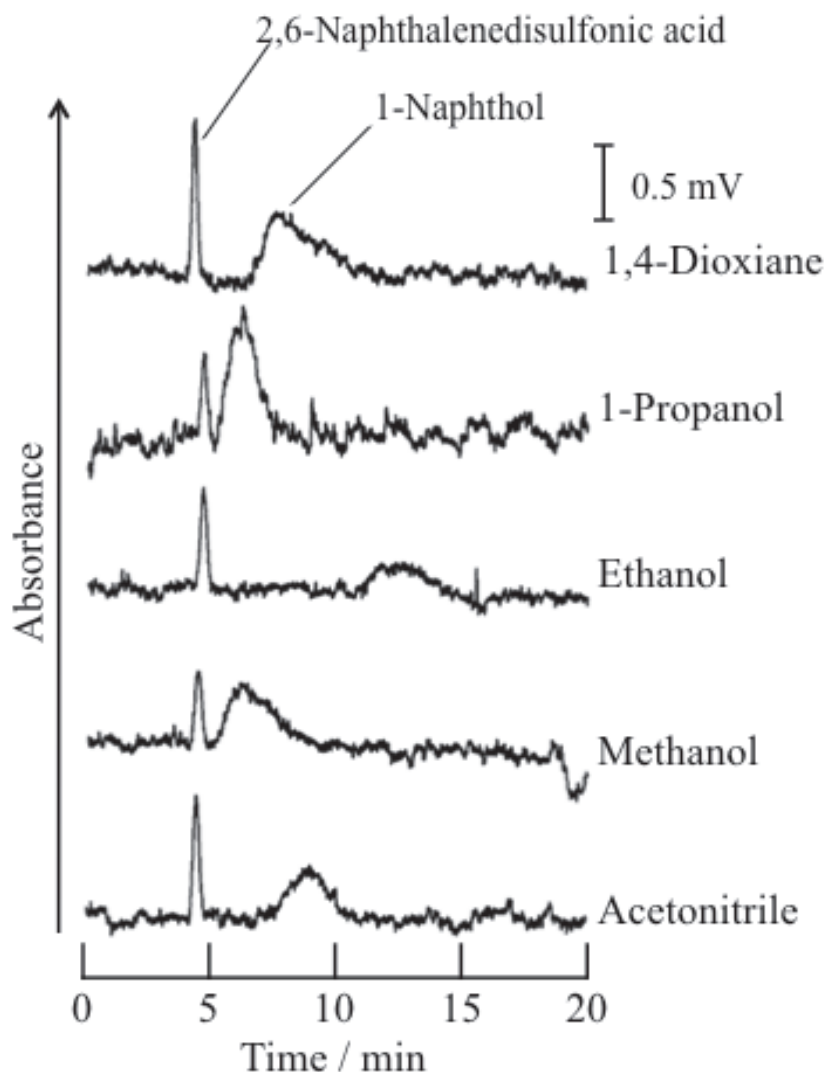


Figure 5. Chromatograms of a mixture of 2,6-naphthalenedisulfonic acid and 1-naphthol obtained by the TRDC system using various hydrophilic organic solvents instead of acetonitrile. Conditions: Capillary tube, 120 cm (effective length: 100 cm) of 100 μ m i.d. PTFE; carrier, water-methanol-ethyl acetate (100:20:15 volume ratio), water-ethanol-ethyl acetate (100:20:15 volume ratio), water-1,4-dioxane-ethyl acetate (100:5:10 volume ratio), water-1-propanol-ethyl acetate (100:10:11 volume ratio), and water-acetonitrile-ethyl acetate (100:20:10 volume ratio); sample injection, 20 cm height (gravity) \times 30 s; flow rate, 2.0 μ L min^{-1} ; tube temperature, 15 $^{\circ}\text{C}$; and 2,6-naphthalenedisulfonic acid and 1-naphthol, 2 mM each.

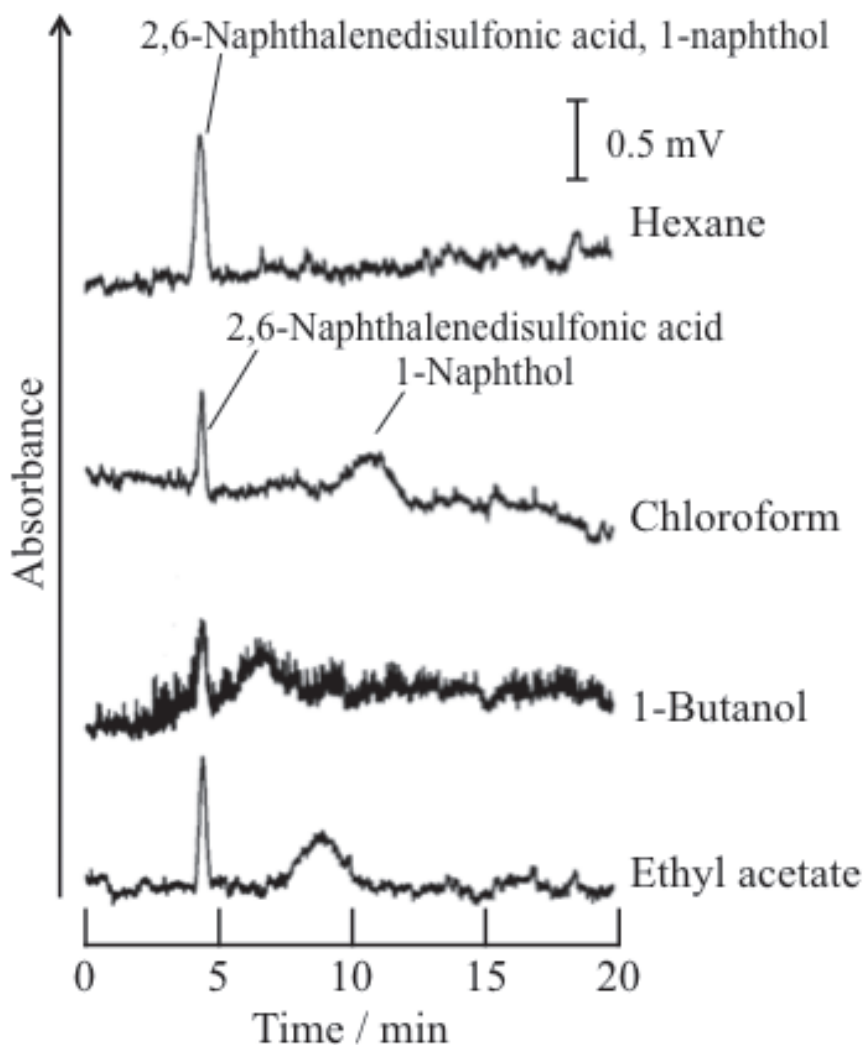


Figure 6. Chromatograms of a mixture of 1-naphthol and 2,6-naphthalenedisulfonic acid obtained by the TRDC system using various hydrophobic organic solvents instead of ethyl acetate. Conditions: Capillary tube, 120 cm (effective length: 100 cm) of 100 μm i.d. PTFE; carrier, water-acetonitrile-chloroform (100:30:1 volume ratio), water-acetonitrile-hexane (100:30:1 volume ratio), water-acetonitrile-1-butanol (100:15:20 volume ratio), and water-acetonitrile-ethyl acetate (100:20:10 volume ratio); sample injection, 20 cm height (gravity) \times 30 s; flow rate, 2.0 $\mu\text{L min}^{-1}$; tube temperature, 15 $^{\circ}\text{C}$; and 2,6-naphthalenedisulfonic acid and 1-naphthol, 2 mM each.

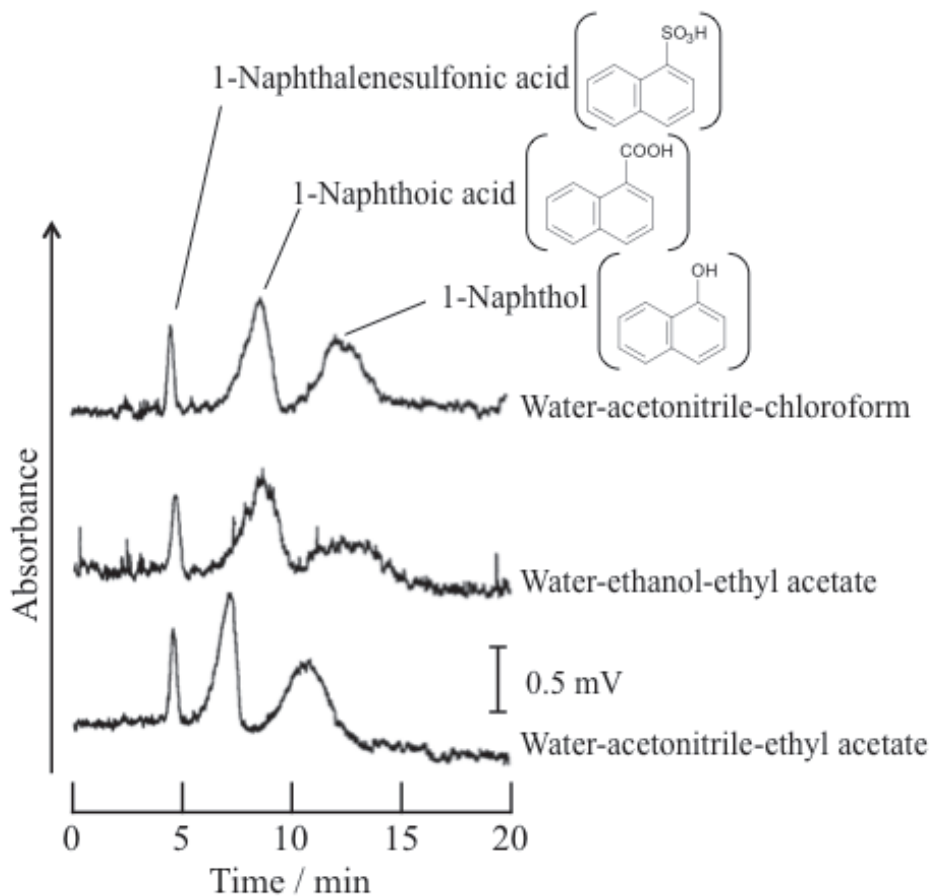


Figure 7. Chromatograms of the mixture analyte solution of 1-naphthalenesulfonic acid, 1-naphthoic acid, and 1-naphthol obtained by the TRDC system. Conditions: Capillary tube, 120 cm (effective length: 100 cm) of 100 μm i.d. PTFE; carrier, water-acetonitrile-ethyl acetate (100:20:10 volume ratio), water-ethanol-ethyl acetate (100:20:15 volume ratio), and water-acetonitrile-chloroform (100:30:1 volume ratio); sample injection, 20 cm height (gravity) \times 30 s; flow rate, 2.0 $\mu\text{L min}^{-1}$; tube temperature, 15 $^{\circ}\text{C}$; and 1-naphthalenesulfonic acid, 1-naphthoic acid, and 1-naphthol, 2 mM each.

4.4 Investigation of the composition for a ternary mixed solvent system in TRDC using fused-silica capillary tube

The composition for the water–hydrophilic organic solvent–hydrophobic organic solvent in tube radial distribution chromatography (TRDC) using fused-silica capillary tubes was investigated using phase diagrams, chromatograms, and fluorescence photographs. Mixtures of a hydrophilic organic solvent (acetonitrile, ethanol, methanol, 1-propanol, or 1,4-dioxane) and a hydrophobic solvent (ethyl acetate, hexane, 1-butanol, or chloroform) were examined as the ternary solvent system, which was the carrier solution in TRDC. Water–acetonitrile–chloroform and water–acetonitrile–ethyl acetate systems performed well in TRDC. A model analyte solution of 1-naphthol and 2,6-naphthalenedisulfonic acid was separated by TRDC using the chloroform solvent system with a range of volume ratios for the solvent components. The elution order of these two compounds could be reversed by changing the system from an organic solvent-rich solvent to water-rich one. A mixture of five analytes, 1-naphthol, Eosin Y, 1-naphthalenesulfonic acid, 2,6-naphthalenedisulfonic acid, and 1,3,6-naphthalenetrisulfonic acid, was also separated using the water–acetonitrile–chloroform solvent system (32:65:3 volume ratio). These compounds eluted in the order given above.

Introduction

Micro-flow analyses using microfluidics have been carried out in microspaces such as capillary tubes (e.g., fused-silica and poly(tetrafluoroethylene)) and microchannels in a microchip [27,32-36]. In microfluidics, various types of fluidic behavior are observed for solvents in a microspace based on electro-osmotic and laminar flow [46-48]. The fluidic behavior of solvents in the microspace is related to the mixing, separation, diffusion, and reaction of solutes. These properties are important and useful in the design of micro-reactors or micro-total analysis systems [49-51].

Several groups have reported that water and oil flow separately in a tube with a liquid-liquid radial interface under specific fluidic conditions [52-54]. Our group has published the reports on the tube radial distribution phenomenon (TRDP) of different solvent systems since 2009. TRDP has been observed in many mixed solutions, including ternary water–hydrophilic solvent–hydrophobic solvent, water–surfactant, water–ionic liquid, and fluoruous/organic solvents. For example, when a ternary solvent of water–acetonitrile–ethyl acetate is introduced into a microspace under laminar flow conditions, inner and outer phases are generated as the solvent molecules are radially distributed in the microspace. Based on TRDP, we have investigated capillary chromatography (tube radial distribution chromatography, TRDC), extraction, reaction spaces, and mixing processes.

Here, the types of solvents and their volume ratios in a ternary solvent mixture of water–hydrophilic organic solvent–hydrophobic organic solvent were investigated for TRDC. The optimum solvent mixture was determined using phase diagrams, chromatograms, and fluorescence photographs. A hydrophilic organic solvent (acetonitrile, ethanol, methanol, 1-propanol, or 1,4-dioxane) and hydrophobic organic solvent (ethyl acetate, hexane, 1-butanol, or chloroform) were mixed with water to

produce a ternary water–hydrophilic organic solvent–hydrophobic organic solvent system. The water–acetonitrile–chloroform solvent system was examined in detail and compared with a water–acetonitrile–ethyl acetate solvent system, which is commonly used in the TRDC.

Experimental

Open-tubular capillary chromatography Fused-silica capillary tubes (internal diameter 50 μm) were used. The TRDC system included an open fused-silica capillary tube (total length 120 cm and effective length 100 cm), microsyringe pump, and absorption detector. The tube temperature was controlled by dipping the capillary tube in water maintained at a fixed temperature in a beaker by stirring. Various water–hydrophilic organic solvent–hydrophobic organic solvent systems were used as the carrier solution. Analyte solutions were prepared with the carrier solutions. The analyte solution was introduced directly into the capillary inlet by the gravity method (from a height of 20 cm and for 30 s). After analyte injection, the capillary inlet was connected to a microsyringe attached to a pump. The carrier solution was fed into the capillary tube at a set flow rate under laminar flow conditions. On-capillary absorption detection (254 nm) was performed.

Fluorescence microscope-charge coupled device (CCD) camera system To monitor TRDP with the solvent system, the capillary tube was set up with a fluorescence microscope-CCD camera system. Ternary water–hydrophilic organic solvent–hydrophobic organic solvent systems, with various volume ratios and containing perylene and Eosin Y, were used. The fluorescence in the capillary tube was monitored using a fluorescence microscope equipped with an Hg lamp, a filter, and a CCD camera. Perylene and Eosin Y emit light at 470 and 550 nm, respectively, and because of this the resulting fluorescence was mostly blue and green.

Results and discussion

Preliminary experiments with water–hydrophilic organic solvent–ethyl acetate solvent mixtures The hydrophilic organic solvent was either acetonitrile, methanol, ethanol, 1-propanol, or 1,4-dioxane. Phase diagrams of water–hydrophilic organic solvent–ethyl acetate ternary solutions were examined at 0 and 20 $^{\circ}\text{C}$ (Fig. 1). The curves in the phase diagram show the boundary or solubility curves between homogeneous (single phase) and heterogeneous (two phases) solutions. The separation performance for a model analyte mixture of NA and NDS in TRDC was examined. The volume ratios of the components in the homogeneous ternary solvent solutions were positioned near the boundary curve at 20 $^{\circ}\text{C}$, with an organic solvent-rich solution, NA eluted before NDS, and a water-rich solution, NDS eluted before NA. This reversal of the elution order for the analytes was only observed in the water–acetonitrile–ethyl acetate system. With the other ternary mixtures investigated, NA eluted before NDS with organic solvent-rich solutions and no separation occurred with water-rich solutions.

Preliminary experiments with water–acetonitrile–hydrophobic solvent mixtures The hydrophobic organic solvent was ethyl acetate, chloroform, 1-butanol, or hexane. Phase diagrams of the water–acetonitrile–hydrophobic organic solvent mixtures were

examined at 0 and 20 °C (Fig. 2). The separation performance for a model analyte mixture of NA and NDS was investigated. The volume ratios of the components in the homogeneous ternary solvent systems were positioned near the boundary curve at 20 °C. The separation order of the analytes in TRDC was reversible using different volume ratios with water–acetonitrile–chloroform and water–acetonitrile–ethyl acetate. With water–acetonitrile–1-butanol, NA was eluted before NDS when the mixture was an organic solvent-rich mixture. With the water–acetonitrile–hexane mixture, NA and NDS were not separated.

Phase diagrams, chromatograms, and fluorescence photographs with water–acetonitrile–chloroform Seeing how water–acetonitrile–chloroform performed in a similar manner to water–acetonitrile–ethyl acetate, we examined the water–acetonitrile–chloroform system in more detail using phase diagrams, chromatograms, and fluorescence photographs. Figure 3 shows the phase diagrams of the water–acetonitrile–chloroform system. At a constant pressure (1 atm), as the temperature decreased from 20 to 0 °C, the boundary curve expanded (Fig. 3 a)). The curve also expanded as the pressure was increased from 1.0 to 1.3 atm at a constant temperature (20 °C) (Fig. 3 b)). These changes in the boundary curves are similar to those observed in our study for water–acetonitrile–ethyl acetate. Separation information of the NA and NDS mixture with the water–acetonitrile–chloroform system is shown in the phase diagram with the symbols (Fig. 4). With an organic-solvent rich carrier solution (solutions (f)–(k) in Fig. 4), NA was eluted before NDS, contrary to the water-rich carrier solutions (solutions (c)–(e)) where NDS eluted before NA. With solutions (a), (b), and (l)–(r), NDS and NA were not separated under the present conditions. Typical chromatograms are shown in Fig. 4. Typical fluorescence photographs are also shown in Fig. 4. TRDP was observed in the mixtures (f)–(k), which had an organic solvent-rich major inner phase and water-rich minor outer phase, and (c)–(e), which had a water-rich major inner phase and organic solvent-rich minor outer phase. TRDP was not observed in mixtures (a), (b), or (l)–(r). In other words, when organic solvent-rich solutions ((f)–(k)) were delivered into the capillary tube, the major phase that formed in the tube was an organic solvent-rich mixture. In contrast, when water-rich solutions ((c)–(e)) were delivered into the capillary tube, the major phase that formed in the tube was water-rich. Separation of compounds by TRDC is based on the distribution of the hydrophilic compounds (e.g. NDS) in the water-rich phase and hydrophobic compounds (e.g. NA) in the organic solvent-rich phase. The outer phase acts as a pseudo-stationary phase under laminar flow conditions. In the present study, the elution order in the chromatograms was consistent with this separation mechanism. With an organic solvent-rich inner phase, NA eluted before NDS, but in a water-rich inner phase, NDS eluted before NA. The mixtures that did not show TRDP did not provide any chromatographic separation in the TRDC. The TRDP and TRDC results with the water–acetonitrile–chloroform system were the same as those observed for the water–acetonitrile–ethyl acetate system.

Separation of an analyte mixture We examined separation of an analyte mixture (NA, Eosin Y, NS, NDS, and NTS) using the TRDC system with organic solvent-rich and water-rich carrier solutions prepared using the water–acetonitrile–chloroform system.

The obtained chromatograms are shown in Fig. 5. The elution orders of the analytes were different with the organic solvent-rich than they were with the water-rich carrier solutions, as was reported for other TRDC systems. With the organic-solvent rich carrier solution, the elution order was NA, Eosin Y, NS, NDS, and finally NTS (Fig. 5 a)). This elution order is consistent with the increasingly hydrophilic character of the compounds. In contrast, with the water-rich carrier solution, the comparatively hydrophilic compound, NTS, was eluted first, followed by co-elution of NS and NDS, and then the hydrophobic compounds Eosin Y and 1-naphthol (Fig. 6 b)). This elution order was the reverse of that observed with the organic solvent-rich carrier solution.

Comparison of water–acetonitrile–ethyl acetate and water–acetonitrile–chloroform solvent systems Figure 6 shows the phase diagrams (20 °C) and separation performance for the water–acetonitrile–ethyl acetate and water–acetonitrile–chloroform solvent systems. The water–acetonitrile–ethyl acetate and the water–acetonitrile–chloroform solvent systems have quite different boundaries in the phase diagrams. Therefore, we were unable to draw any relevant comparisons of their separation performance with similar ratios for the ternary components of the solvent system. We, tentatively, investigated the TRDC separation performance through carrier solutions with same volume ratios for the two phases, organic solvent-rich and water-rich, at a lower temperature in a batch vessel. The composition positions in the phase diagram, (1)–(5) in Fig. 6, showed the same volume ratios of the two phases both for the water–acetonitrile–ethyl acetate and the water–acetonitrile–chloroform solution systems, and these ratios are also given in the figure captions. The separation performance for NA and NDS was dependent on the ratio of the organic solvent-rich and water-rich phases (Fig. 6). With the ethyl acetate system, the upper and lower phases were organic solvent-rich and water-rich solutions, respectively, while with the chloroform system, the upper and lower phases were water-rich and organic solvent-rich solutions, respectively. Compared to the ethyl acetate system, TRDC separation was achieved with the chloroform system with a wider range of organic solvent-rich and water-rich volume ratios. The reason for this difference in performance has not been made clear yet. Chloroform is more hydrophobic ($\log P$, 1.97) than ethyl acetate ($\log P$, 0.73), and this may generate a more stable liquid-liquid interface between water-rich and organic solvent-rich phases through TRDP. Table 1 shows the resolutions for the model analytes, NA and NDS, obtained with the ethyl acetate and the chloroform solvent systems. The ethyl acetate system provided better resolution than the chloroform system, although TRDP was observed over a wider range of volume ratios for the chloroform system than for the ethyl acetate system. We examined the distribution ratios, D , in the two solvent systems with various compositions ((1)–(5) in Figs. 6 and 7) at a low temperature, generating upper and lower phases in a batch vessel. D is given by the ratio of analyte concentration in the organic-solvent rich phase to analyte concentration in the water-rich phase. If $D > 1$, most of the analyte dissolves in the organic solvent-rich phase, and if $D < 1$, most of the analyte is dissolved in the water-rich phase. The concentrations of the analytes in the two phases were determined using capillary electrophoresis with a calibration curve. For NA, all the D values (solutions (1)–(5)) were greater than one, which indicates it was easier for NA to dissolve in an organic solvent-rich solution than a water-rich solution. The D values of the ethyl

acetate system (4.2–14.5) were larger than those of the chloroform system (1.5–3.0). For NDS, all the *D* values (solutions (1)–(5)) were less than one, indicating that it is easier for NDS to dissolve in a water-rich solution than an organic solvent-rich solution. The *D* values of the ethyl acetate system (0.5–0.25) were smaller than those of the chloroform system (0.30–0.65). Consequently, NA dissolves in the organic solvent-rich phase and NDS in the water-rich phase with the ethyl acetate system more effectively than the chloroform system. That is, the trends observed with the *D* values are consistent with the better resolution for NA and NDS observed with the ethyl acetate system compared with the chloroform system.

In conclusion, we examined various water–hydrophilic organic solvent–hydrophobic organic solvent systems for TDRP and TRDC. Phase diagrams, fluorescence photographs, and chromatograms for a water–acetonitrile–chloroform solvent system showed particular TRDP and TRDC. The performance of this solvent system in TRDC was comparable to that of a water–acetonitrile–ethyl acetate system. The results of this study provide basic data on the microfluidic behavior, TRDP, and the separation technology, TRDC, with the studied solvent systems.

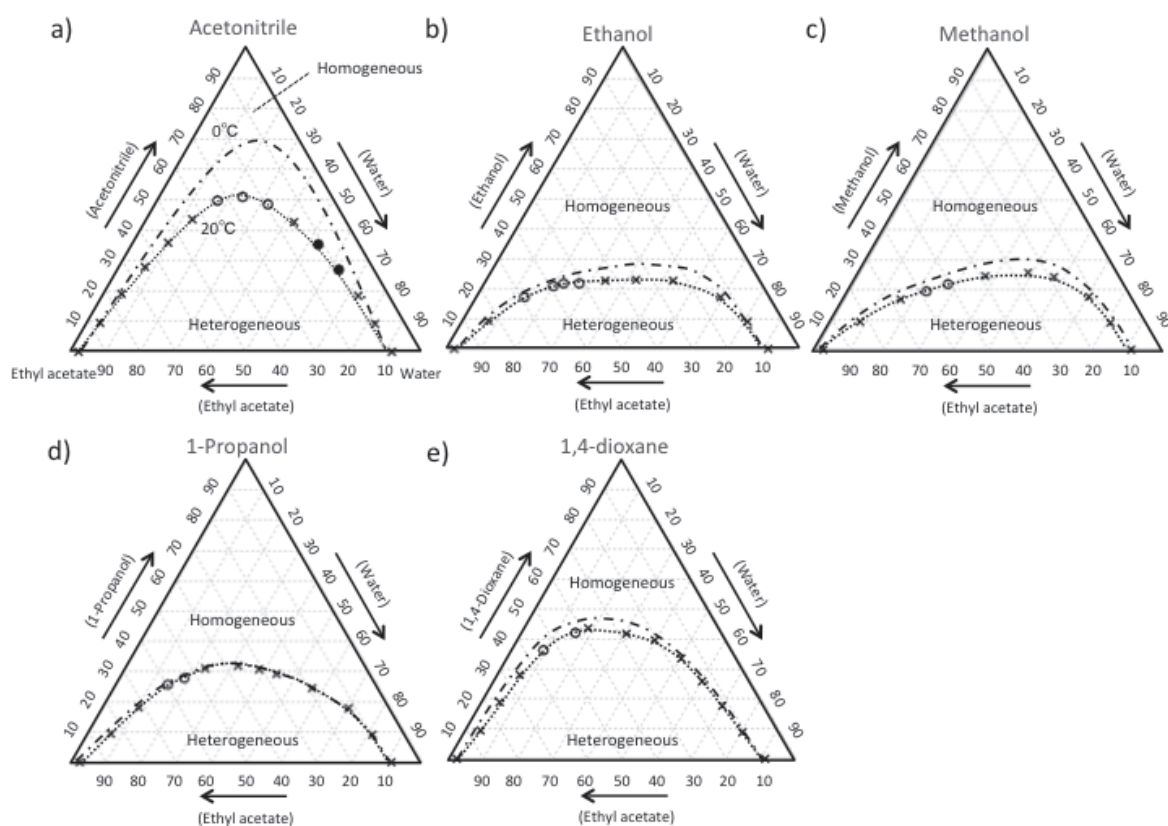


Figure 1. Phase diagrams for water–hydrophilic organic solvent–ethyl acetate solvent systems, and separation performance of a NA and NDS mixture on chromatograms. a) Acetonitrile, b) methanol, c) ethanol, d) 1-propanol, and e) 1,4-dioxane. The dotted-dashed and dotted curves show the boundaries between homogeneous and heterogeneous solutions at 0 and 20 °C. The symbols ○, ●, and × show separation with NA eluted before NDS, separation with NDS eluted before NA, and no separation, respectively. Chromatography conditions: capillary tube, 120 cm (effective length, 100 cm) of 50 μm i.d. fused-silica; carrier, water–hydrophilic organic solvent–ethyl acetate; sample injection, 20 cm height (gravity) \times 30 s; flow rate, 0.2 $\mu\text{L min}^{-1}$; tube temperature, 3 °C; and NA and NDS concentrations, 2 mmol L^{-1} each.

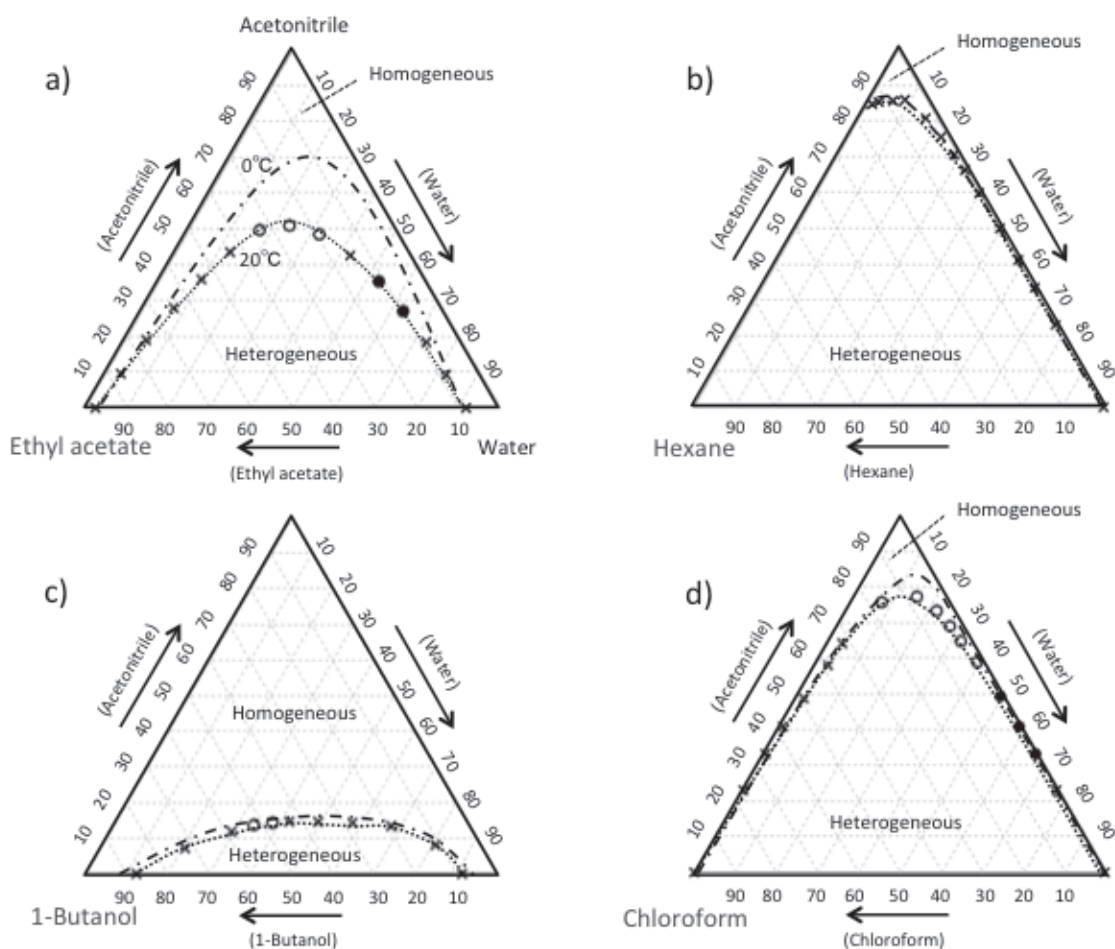


Figure 2. Phase diagrams for water–acetonitrile–hydrophobic organic solvent systems, and separation performance of an NA and NDS mixture on chromatograms. a) Ethyl acetate, b) hexane, c) 1-butanol, and d) chloroform. The dotted-dashed and dotted curves show the boundaries between homogeneous and heterogeneous solutions at 0 and 20 °C. The symbols ○, ●, and × show separation with NA eluted before NDS, separation with NDS eluted before NA, and no separation. The chromatography conditions are the same as those in Fig. 1.

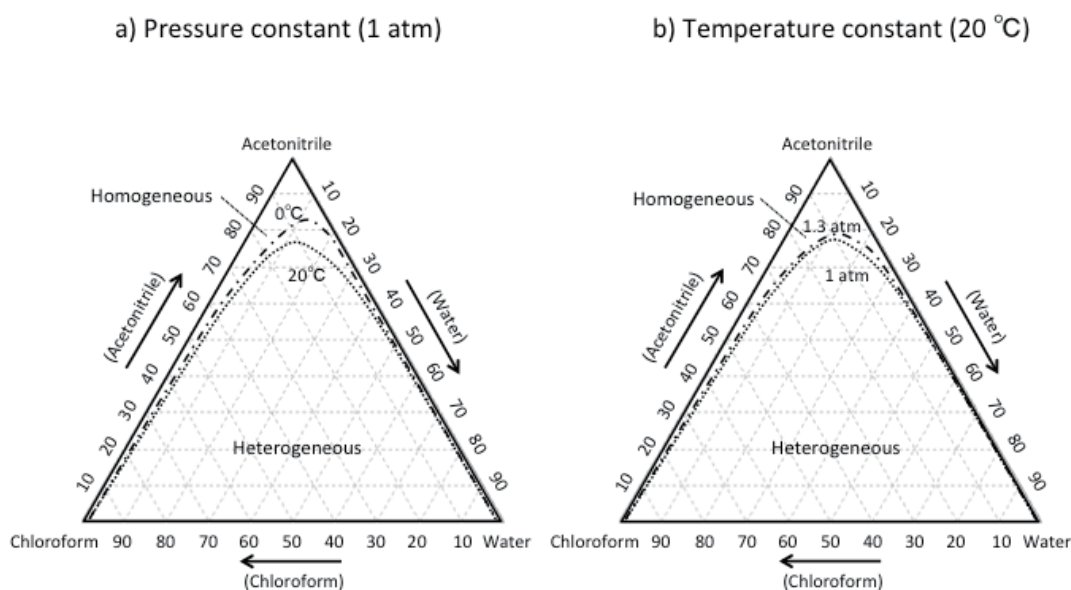


Figure 3. Phase diagrams for the water–acetonitrile–chloroform solvent system. a) Constant pressure (1 atm) and b) constant temperature (20 °C).

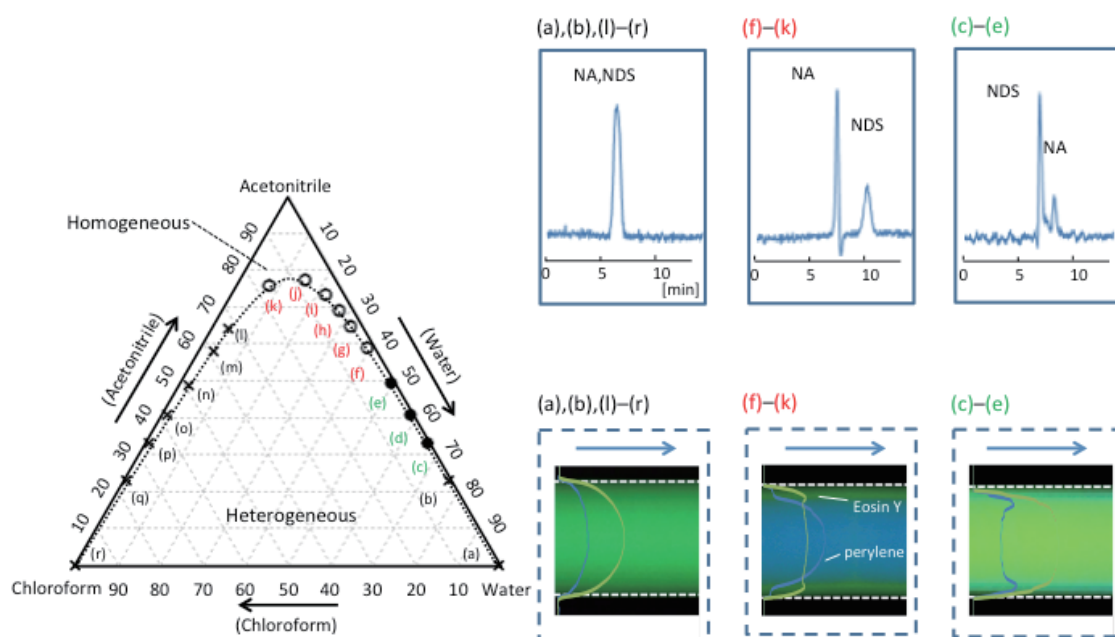


Figure 4. Phase diagrams, chromatograms, and fluorescence photographs for the water–acetonitrile–chloroform solvent system. Water–acetonitrile–chloroform volume ratios were as follows: (a) 99.5:0:0.5, (b) 76.2:23:0.8, (c) 66:33:1, (d) 58:41:1, (e) 49.5:49.5:1, (f) 39:59:2, (g) 32:65:3, (h) 27:69:4, (i) 22:73:5, (j) 15:77:8, (k) 8:76:16, (l) 4:64:32, (m) 4:58:38, (n) 2:49:49, (o) 1:41:58, (p) 0.7:33:66.3, (q) 0.5:23:76.5, and (r) 0.1:0:99.9, containing perylene ($\sim 0.1 \text{ mmol L}^{-1}$) and Eosin Y ($\sim 1.0 \text{ mmol L}^{-1}$). The symbols \circ , \bullet , and \times show separation with NA eluted before NDS, separation with NDS eluted before NA, and no separation. Chromatography conditions are the same as those in Fig. 1.

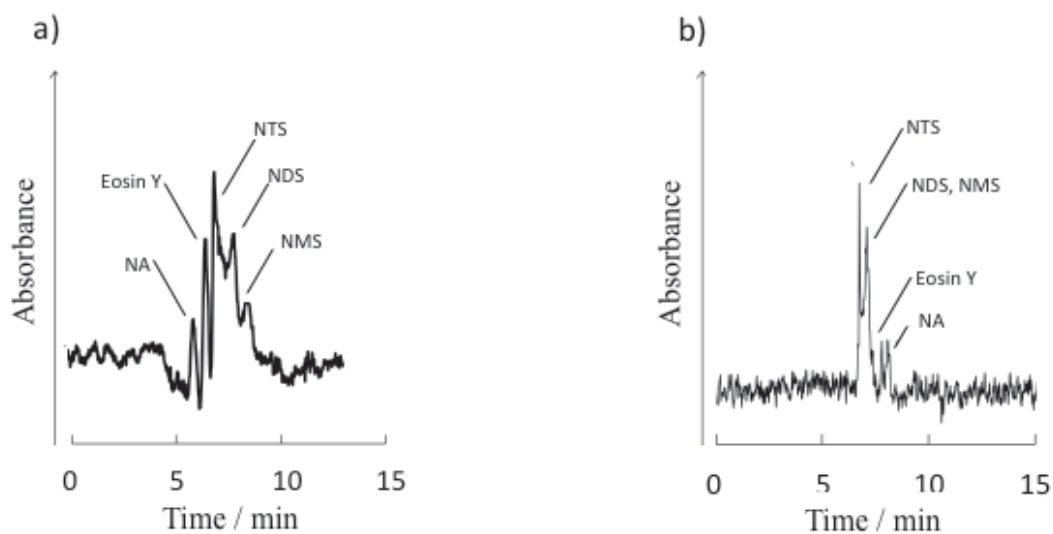


Figure 5. Chromatograms of the analyte mixture of NA, Eosin Y, NS, NDS, and NTS obtained by TRDC with the water–acetonitrile–chloroform solvent system. Chromatography conditions: capillary tube, 120 cm (effective length, 100 cm) of 50 μm i.d. fused-silica; carrier, water–acetonitrile–chloroform a) organic solvent-rich (20:53:27 volume ratio) and b) water-rich (75:15:10 volume ratio); sample injection, 20 cm height (gravity) \times 30 s; flow rate, 0.2 $\mu\text{L min}^{-1}$; tube temperature, 3 $^{\circ}\text{C}$; and analyte concentrations, NA, NS, NDS and NTS 1 mmol L^{-1} each and Eosin Y 0.5 mmol L^{-1} .

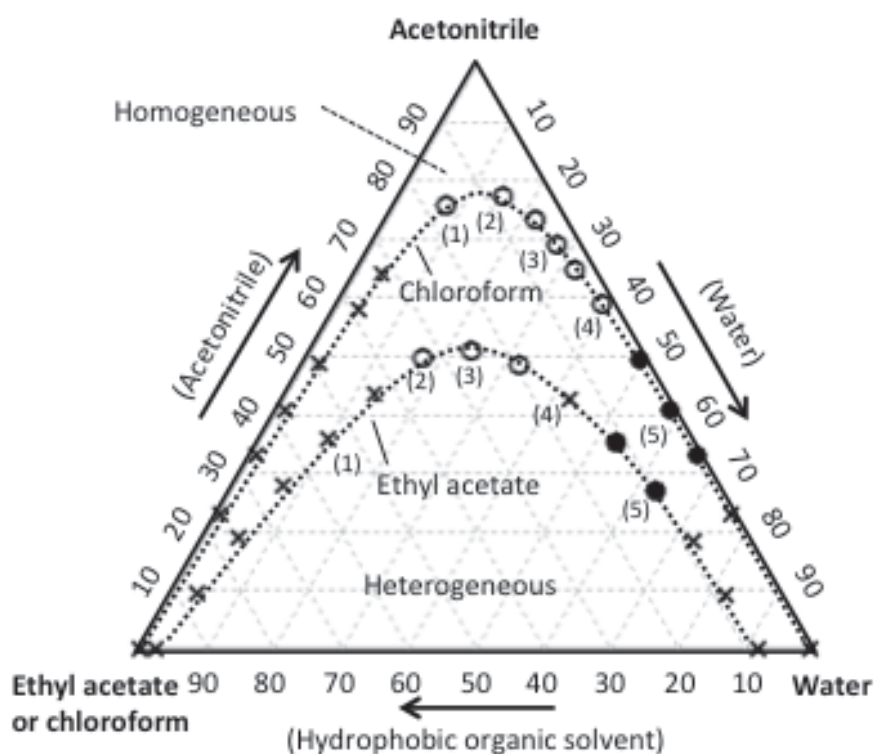


Figure 6. Comparison of phase diagrams and TRDC separation performance with water–acetonitrile–ethyl acetate and water–acetonitrile–chloroform solvent systems. The volume ratios of the upper and lower phases in a batch vessel are as follows: Water-rich:organic solvent-rich; (1) 2:98, (2) 10:90, (3) 28:72, (4) 60:40, and (5) 90:10 in the two systems. The symbols \circ , \bullet , and \times show separation with NA eluted before NDS, separation with NDS eluted before NA, and no separation.

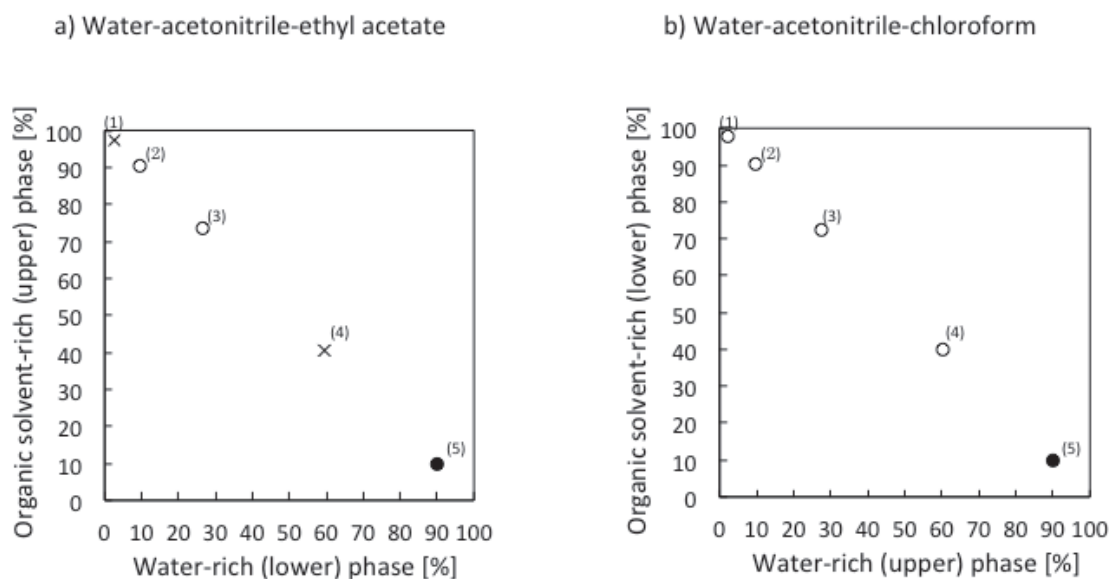


Figure 7. The separation performance with various volume ratios of upper and lower phases in a) water–acetonitrile–ethyl acetate and b) water–acetonitrile–chloroform solvent systems. The volume ratios of the upper and lower phases in a batch vessel are as follows: Water-rich:organic solvent-rich; (1) 2:98, (2) 10:90, (3) 28:72, (4) 60:40, and (5) 90:10 in the two systems. The symbols of \circ , \bullet , and \times mean show separation with NA eluted before NDS, separation with NDS eluted before NA, and no separation, respectively.

Table 1 Comparison of separation performance with TRDC and chromatographic resolutions for water–acetonitrile–ethyl acetate and water–acetonitrile–chloroform solvent systems. The composition number means the mixed solvent solution in Fig. 6. The symbols \circ , \bullet , and \times show separation with NA eluted before NDS, separation with NDS eluted before NA, and no separation, respectively. The resolutions are calculated based on the chromatograms of NA and NDS separation.

Composition number	Volume ratio (water-rich : organic solvent-rich)	TRDC		Resolutions	
		Ethyl acetate system	Chloroform system	Ethyl acetate system	Chloroform system
(1)	2 : 98	\times	\circ	-	0.58
(2)	10 : 90	\circ	\circ	3.8	0.77
(3)	28 : 72	\circ	\circ	5.6	0.88
(4)	60 : 40	\times	\circ	-	2.0
(5)	90 : 10	\bullet	\bullet	0.75	2.0

4.5 Fundamental experiments for tentative comparison of TRDC and capillary zone electrophoresis

A capillary chromatography using an untreated open tubular capillary tube and ternary mixed solvents of a water-hydrophilic/hydrophobic organic solvent as a carrier solution has been developed; the system is called tube radical distribution chromatography (TRDC). A model mixture analyte solution, including 1-naphthol, 1-naphthoic acid, 1-naphthalenesulfonic acid, 2,6-naphthalenedisulfonic acid, 1,3,6-naphthalenetrisulfonic acid, was examined by the TRDC and capillary zone electrophoretic (CZE) systems that comprised mainly a capillary tube and a detector. In the TRDC system the elution order of analytes could be changed by altering the component ratios of the solvents, as in the CZE system the elution order was changed by altering the electro-osmotic flow direction. The experimental data obtained here gave a clue for thinking of the features and utility of the TRDC as a new separation method.

Introduction

Capillary tubes with inner diameters less than several hundred micrometers that provide a micro-flow are known to exhibit interesting and useful physical or hydrodynamic phenomena, such as electro-osmotic flow and laminar flow. The electro-osmotic flow in a capillary tube promotes capillary electrophoresis [38,39,55], and capillary electrochromatography [42,56,57], while laminar flow conditions enable hydrodynamic chromatography [44,45]. Recently, our group reported the tube radial distribution phenomenon of carrier solvents, which we call the tube radial distribution phenomenon (TRDP).

When the ternary mixed solvents of water-hydrophilic/hydrophobic organic solvent mixtures are delivered into a microspace, such as a microchannel or a capillary tube under laminar flow conditions, the solvent molecules are distributed radially within the microspace, generating inner and outer phases. The TRDP creates a phase interface or kinetic aqueous–organic interface in a microspace. A capillary chromatography system where the outer phase functions as a pseudo-stationary phase under laminar flow conditions has been developed based on the TRDP. We call it tube radial distribution chromatography (TRDC). In the TRDC system the analytes are distributed between the inner and outer phases due to their hydrophobic or hydrophilic nature, undergoing chromatographic separation. The TRDC system does not require any specific columns, such as packed and monolithic, or application of high voltage to the ends of the capillary tube.

As the investigation of TRDP and TRDC has just begun, we have to examine anything we can imagine in order to expand our knowledge about TRDP and TRDC. The TRDC and capillary zone electrophoresis (CZE) systems have quite simple instruments comprising mainly a capillary tube and a detector, although they have different separation mechanisms. After the analyte solution was injected in the inlet capillary side, the carrier solution was delivered with a microsyringe pump in the TRDC system, while the running buffer was fed by applying high voltage in the CZE system. We are interested in examining separation performance of these open-tubular capillary analyses. The model analyte solution was subjected to the TRDC and CZE systems. The

obtained chromatograms and electropherograms were compared and discussed each other through the fundamental experiments.

Experimental

TRDC system Fused-silica (75 μm inner diameter) and poly(tetrafluoroethylene) (PTFE) (100 μm inner diameter) capillary tubes were used. A schematic diagram of the present TRDC system comprised the fused-silica or PTFE capillary tube (120 cm length, effective length 100 cm), a microsyringe pump, and an absorption detector. The tube temperature was controlled by dipping the capillary tube (ca. 60 cm) in water maintained at a specific temperature (0 or 20 $^{\circ}\text{C}$) in a beaker maintained by stirring. Water-acetonitrile-ethyl acetate mixture solutions (3:8:4 or 15:3:2 volume ratio) were used as carrier solutions. The component ratios of the solvents were recommended as an organic solvent-rich and water-rich carrier solution in our works. Analyte solutions were prepared with the carrier solutions. The analyte solution was introduced directly into the capillary inlet side by the gravity method (30 cm height for 20 s). After analyte injection, the capillary inlet was connected through a joint to a micro-syringe. The syringe was placed on the microsyringe pump. The carrier solution was fed into the capillary tube at 0.8 $\mu\text{L min}^{-1}$ for fused-silica tube and 2.0 $\mu\text{L min}^{-1}$ for PTFE tube under laminar flow conditions. On-capillary absorption detection (254 nm for fused-silica tube or 320 nm for PTFE tube²⁾) was performed with the detector.

CZE system A schematic diagram of the present CZE system comprised the fused-silica or PTFE capillary tube (120 cm length, effective length 100 cm), a DC power supplier (Model HCZE-30PNO.25, Matsusada Precision Devices Co., LTD.), and an absorption detector. 10 mM Phosphate buffer (pH 7.0) was used as a running buffer solution. Analyte solutions were prepared with the running buffer solution. The analyte solution was introduced directly into the capillary inlet side by the gravity method (30 cm height for 20 s). After analyte injection, a high voltage of 12 kV was applied to the electrodes. On-capillary absorption detection (254 nm for fused-silica tube or 320 nm for PTFE tube²⁾) was performed with the detector.

Results and discussion

Separation performance in the TRDC system The molecular structures of five model analytes are shown in Fig. 1; 1-naphthol, 1-naphthoic acid, 1-NS, 2,6-NDS, and 1,3,6-NTS. The hydrophobicity of the analytes decreases from 1-naphthol to 1,3,6-NTS. The solution including the five model analytes was subjected to the TRDC system with the organic solvent-rich carrier solution (water-acetonitrile-ethyl acetate, 3:8:4 volume ratio) and the water-rich carrier solution (15:3:2 volume ratio). The TRDC system with the organic solvent-rich carrier solution showed the best resolutions at around a 20 $^{\circ}\text{C}$ tube temperature using the fused-silica tube, while the system with the water-rich carrier solution showed the best resolutions at around a 0 $^{\circ}\text{C}$ tube temperature using the PTFE tube.^{11,10,14)} The chromatograms obtained under the recommended analytical conditions are shown in Fig. 2. With the organic solvent-rich carrier solution 1-naphthol and 1-naphthoic acid, 1-NS, 2,6-NDS, and 1,3,6-NTS were eluted in this order due to their hydrophobic or hydrophilic nature, although 1-naphthol and 1-naphthoic acid were not

separated (Fig. 2 a)). On the other hand, the water-rich carrier solution 1-NS, 2,6-NDS, and 1,3,6-NTS were not separated; however, after that, 1-naphthoic acid and 1-naphthol were eluted in this order due to their nature (Fig. 2b)). Roughly speaking, the reverse elution orders were observed in the TRDC system between the organic solvent-rich and water-rich carrier solutions. The separations were performed on the chromatograms within ca. 15 min.

Separation performance in the CZE system using the fused-silica capillary tube The solution including the five model analytes was subjected to the CZE system using the fused-silica capillary tube with the normal electro-osmotic flow direction where the cathode was set to the capillary outlet and the reverse electro-osmotic flow direction where the cathode was set to the capillary inlet. The obtained electropherograms are shown in Fig. 3. With the normal electro-osmotic flow direction (Fig. 3 a)), 1-naphthol, 1-naphthoic acid, and 1-NS were eluted in this order on the electropherogram within ca. 60 min, but 2,6-NDS and 1,3,6-NTS were not detected within 120 min due to their negative charge using the present analytical conditions. 2,6-NDS and 1,3,6-NTS must require a large electrophoretic flow to the capillary inlet. However, when electro-osmotic flow direction was reversed, none of the analytes were detected within 120 min (Fig. 3 b)). Electro-osmotic flow was larger than electrophoretic flow for the analytes under the conditions.

Separation performance in the CZE system with the PTFE capillary tube It is well known that a PTFE capillary tube shows a much smaller electro-osmotic flow than a fused-silica capillary tube. Similarly, the solution including the five model analytes was subjected to the CZE system using the PTFE capillary tube with the normal and reverse electro-osmotic flow directions. The obtained electropherograms are shown in Fig. 4. With the normal electro-osmotic flow direction (Fig. 4 a)), 1-naphthol, 1-naphthoic acid, and 1-NS were eluted in this order on the electropherogram within ca. 110 min due to the small electro-osmotic flow in the PTFE tube. 2,6-NDS and 1,3,6-NTS were not detected within 120 min due to their negative charge under the analytical conditions. On the other hand, with the reverse electro-osmotic flow direction (Fig. 4 b)), 1,3,6-NTS and 2,6-NDS were eluted in this order within ca. 65 min due to their negative charge. However, 1-naphthol, 1-naphthoic acid, and 1-NS were not detected within at least 120 min. Even in the PTFE capillary tube electro-osmotic flow was larger than electrophoretic flow for the three analytes under the conditions.

In conclusion, the elution behavior of the model five analytes was examined through the chromatogram obtained by the TRDC system and the electropherogram obtained by the CZE system. In the TRDC system, the elution order of analytes could be changed by altering the component ratios of the solvents, the organic solvent-rich and the water-rich carrier solutions, within ca. 15 min, while in the CZE system, as is well known, the elution order was changing by altering the electro-osmotic flow direction to within ca. 60 or 120 min. The TRDC system can easily reverse the elution order of analytes without applying high voltage within short analytical time. The experimental data may show the feature of the TRDC system through the fundamental experiments with the CZE data.

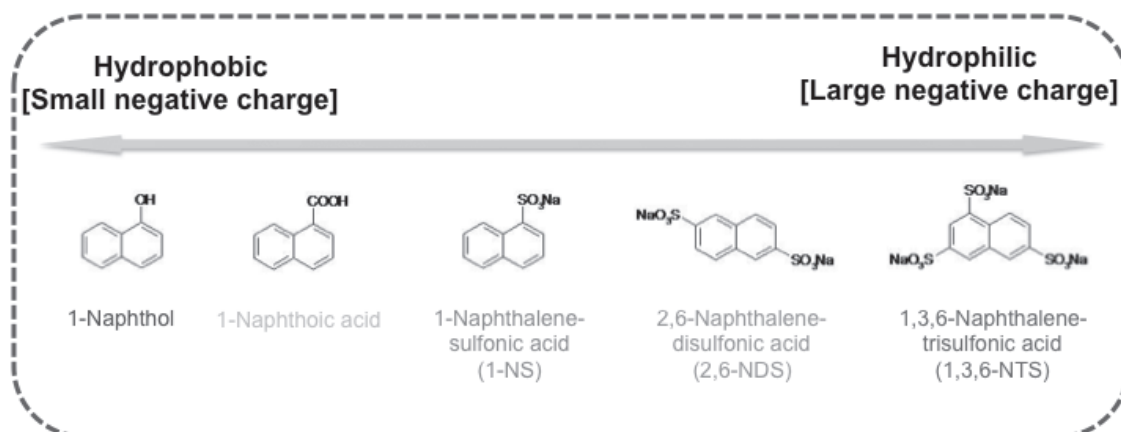


Figure 1. Molecular structures of analytes and their hydrophobic and hydrophilic nature.

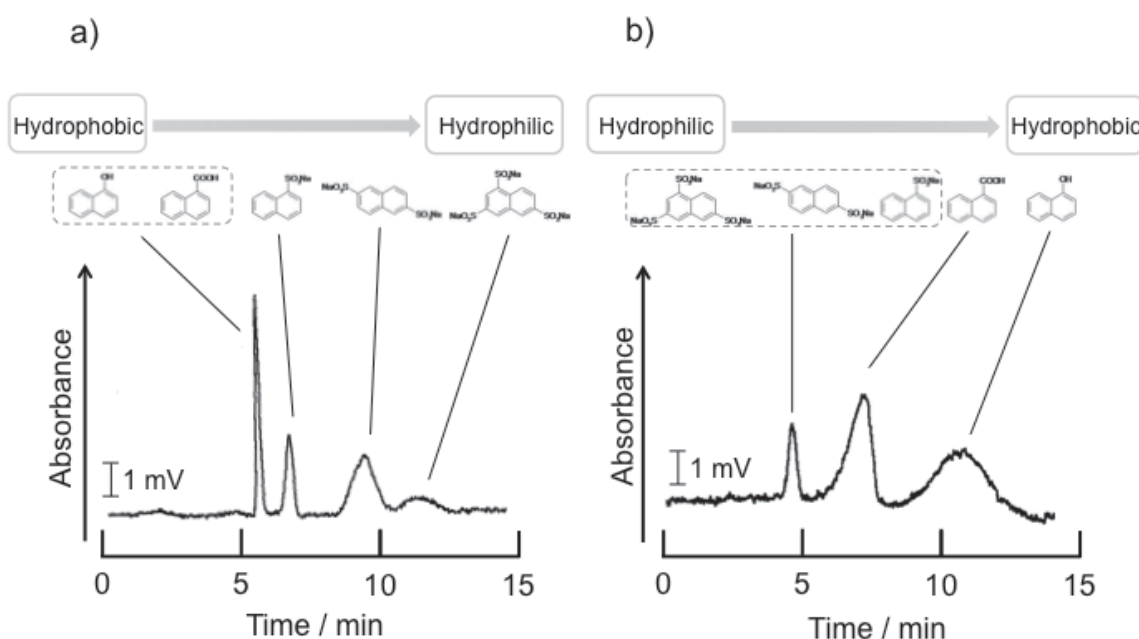


Figure 2. Chromatograms of the analyte mixture with the TRDC system using a) the organic solvent-rich and b) water-rich carrier solutions. Conditions: Capillary tube, 120 cm (effective length: 100 cm), a) fused-silica and b) PTFE; carrier, a) organic solvent-rich (water-acetonitrile-ethyl acetate of 3:8:4 volume ratio) and b) water-rich (15:3:2 volume ratio); sample injection, 30 cm height (gravity) \times 20 s; flow rate, a) $0.8 \mu\text{L min}^{-1}$ and b) $2.0 \mu\text{L min}^{-1}$; tube temperature, a) $20 \text{ }^\circ\text{C}$ and b) $0 \text{ }^\circ\text{C}$; detection wavelength, a) 254 nm and b) 320 nm; and analyte concentration, 2 mM each.

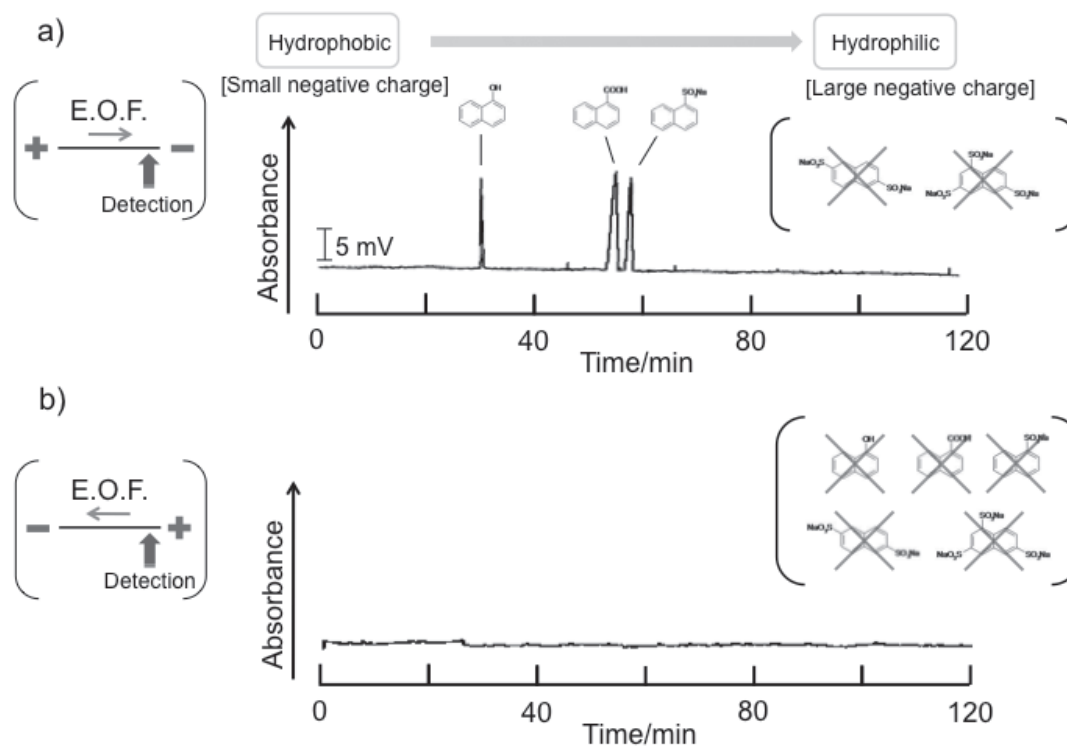


Figure 3. Electropherograms of analyte mixture with the CZE system using the fused-silica capillary tube. Electro-osmotic flow direction a) from the capillary inlet to the outlet and b) from capillary outlet to inlet. Conditions: Capillary tube, 120 cm (effective length: 100 cm) of fused-silica; running buffer, 10 mM phosphate buffer (pH 7.0); sample injection, 30 cm height (gravity) \times 20 s; applied voltage, 12 kV; detection wavelength, 254 nm; and analyte concentration, 2 mM each.

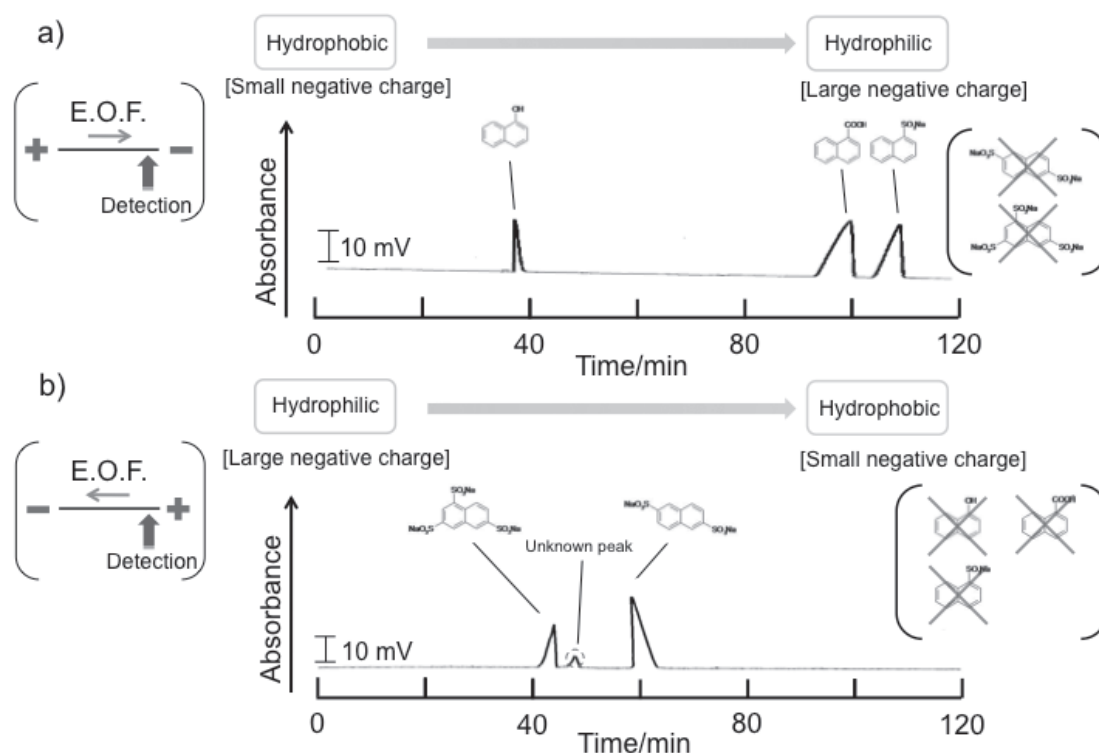


Figure 4. Electropherograms of analyte mixture with the CZE system using the PTFE capillary tube. Electro-osmotic flow direction a) from capillary inlet to outlet and b) from capillary outlet to inlet. Conditions: Capillary tube, 120 cm (effective length: 100 cm) of PTFE; running buffer, 10 mM phosphate buffer (pH 7.0); sample injection, 30 cm height (gravity) \times 20 s; applied voltage, 12 kV; detection wavelength, 320 nm; and analyte concentration, 2 mM each.

References

- [1] H. J. Issaq, K. C. Chan, J. Blonder, X. Ye, and T. D. Veenstra, *J. Chromatogr., A*, **2009**, *1216*, 1825.
- [2] I. Miksik and P. Sedlakova, *J. Sep. Sci.*, **2007**, *30*, 1686.
- [3] M. Silva, *Electrophoresis*, **2007**, *28*, 174.
- [4] S. K. Poole and C. F. Poole, *J. Chromatogr., A*, **2008**, *1182*, 1.
- [5] A. P. Navaza, J. R. Encinar, A. Ballesteros, J. M. Gonzalez, and A. Sanz-Medel, *Anal. Chem.*, **2009**, *81*, 5390.
- [6] Q. Ma, M. Chen, Z.-G. Shi, and Y.-Q. Feng, *J. Sep. Sci.*, **2009**, *32*, 2592.
- [7] Y. Watanabe, T. Ikegami, K. Horie, T. Hara, J. Jaafar, and N. Tanaka, *J. Chromatogr., A*, **2009**, *1216*, 7394.
- [8] K. Hibi, D. Ishii, I. Fujishima, T. Takeuchi, and T. Nakanishi, *J. High Resolution Chromatogr. & Chromatogr. Communications*, **1978**, *1*, 21.
- [9] K. Vainikka, J. Chen, J. Metso, M. Jauhiainen, and M.-L. Riekkola, *Electrophoresis*, **2007**, *28*, 2267.

- [10] P. P. H. Tock, G. Stegeman, R. Peerboom, H. Poppe, J. C. Kraak, and K. K. Unger, *Chromatographia*, **1987**, *24*, 617.
- [11] A. L. Crego, J. C. Diez-Masa, and M. V. Dabrio, *Anal. Chem.*, **1993**, *65*, 1615.
- [12] Y. Guo and L. A. Colon, *Anal. Chem.*, **1995**, *67* 2511.
- [13] S. Folestad, B. Josefsson, and M. Larsson, *J. Chromatogr., A*, **1987**, *391*, 347.
- [14] K. Gohlin, A. Buskhe, and M. Larsson, *Chromatographia*, **1994**, *39*, 729.
- [15] K. Tsukagoshi, M. Hashimoto, K. Ichien, S. Gen, and R. Nakajima, *Anal. Sci.*, **1997**, *13*, 485.
- [16] K. Tsukagoshi, M. Hashimoto, M. Otsuka, R. Nakajima, and K. Kondo, *Bull. Chem. Soc. Jpn.*, **1998**, *71*, 2831.
- [17] K. Tsukagoshi, Y. Shimadzu, T. Yamane, and R. Nakajima, *J. Chromatogr., A*, **2004**, *1040*, 151.
- [18] K. Tsukagoshi, H. Indou, K. Sawanoi, T. Oguni, and R. Nakajima, *Bull. Chem. Soc. Jpn.*, **2004**, *77*, 1353.
- [19] S. A. Zaidi and W. J. Cheong, *J. Sep. Sci.*, **2008**, *31*, 2962.
- [20] P. Kuban, P. Pelcova, V. Kuban, L. Klakurkova, and P. K. Dasgupta, *J. Sep. Sci.*, **2008**, *31*, 2745.
- [21] R. Swart, J. C. Kraak, and H. Poppe, *Trends Anal. Chem.*, **1997**, *16*, 332.
- [22] Q. Luo, T. Rejtar, S.-L. Wu, and B. L. Karger, *J. Chromatogr., A*, **2009**, *1216*, 1223.
- [23] X. Wang, J. Kang, S. Wang, J. J. Lu, and S. Liu, *J. Chromatogr., A*, **2008**, *1200*, 108.
- [24] M. Harada, T. Kido, T. Masudo, and T. Okada, *Anal. Sci.*, **2005**, *21*, 491.
- [25] T. Okada, M. Harada, and T. Kido, *Anal. Chem.*, **2005**, *77*, 6041.
- [26] K. Tsukagoshi, S. Ishida, and R. Nakajima, *J. Chem. Eng. Jpn.*, **2008**, *41*, 130.
- [27] M. Tabata, Y. G. Wu, T. Charoenraks, and S. S. Samaratunga, *Bull. Chem. Soc. Jpn.*, **2006**, *79*, 1742.
- [28] T. Charoenraks and M. Tabata, K. Fujii, *Anal. Sci.*, **2008**, *24*, 1239.
- [29] R. Koike, F. Kitagawa, and K. Otsuka, *J. Sep. Sci.*, **2009**, *32*, 399.
- [30] U. Pyell, *Electrophoresis*, **2010**, *31*, 814-831.
- [31] V. Cucinotta, A. Contino, A. Giuffrida, G. Maccarrone, and M. Messina, *J. Chromatogr. A*, **2010**, *1217*, 953.
- [32] A. Zlatkis, R. P. J. Ranatunga, and B. S. Middleditch, *Anal. Chem.*, **1990**, *62*, 2471.
- [33] D. Ishii, *Bunseki Kagaku*, **2000**, *49*, 929.
- [34] Z.-L. Fang, H.-W. Chen, Q. Fang, and Q.-S. Pu, *Anal. Sci.*, **2000**, *16*, 197.
- [35] M. T. Galceran and L. Puignou, *Trends Anal. Chem.*, **2005**, *24*, 743.
- [36] T. Takeuchi, A. Sedyohutomo, and L. W. Lim, *Anal. Sci.*, **2009**, *25*, 851.
- [37] J. W. Jorgenson and K. D. Lukacs, *Science*, **1983**, *222*, 266.
- [38] S. Terabe, *Anal. Chem.*, **2004**, *76*, 240A.
- [39] C. A. Lucy, A. M. MacDonald, and M. D. Gulcev, *J. Chromatogr., A*, **2008**, *1184*, 81.
- [40] M. G. Cikalo, K. D. Bartle, M. M. Robson, P. Myers, and M. R. Euerby, *Analyst*, **1998**, *123*, 87R.
- [41] R. Nakashima, S. Kitagawa, T. Yoshida, and T. Tsuda, *J. Chromatogr., A*, **2004**, *1044*, 305.
- [42] K. Otsuka, *Chromatography*, **2007**, *28*, 1.

- [43] T. Takahashi and W. N. Gill, *Chem. Eng. Commun.*, **1980**, *5*, 367.
- [44] H. Small, F. L. Saunders, and J. Solc, *Adv. Colloid Interface Sci.*, **1976**, *6*, 237.
- [45] R. Umehara, M. Harada, and T. Okada, *J. Sep. Sci.*, **2009**, *32*, 472.
- [46] N. Kaji, Y. Okamoto, M. Tokeshi, and Y. Baba, *Chem. Soc. Rev.*, **2010**, *39*, 948.
- [47] P. Mondal, S. Ghosh, G. Das, and S. Ray, *Chem. Engi. Process.: Process Intensification*, **2010**, *49*, 1051.
- [48] T. Kaneta, D. Yamamoto, and T. Imasaka, *Electrophoresis*, **2009**, *30*, 3780.
- [49] A. Hibara, M. Tokeshi, K. Uchiyama, H. Hisamoto, and T. Kitamori, *Anal. Sci.*, **2001**, *17*, 89.
- [50] H. Nakamura, Y. Yamaguchi, M. Miyazaki, H. Maeda, and M. Uehara, *Chem. Commun.*, **2002**, *23*, 2844.
- [51] H. Kawazumi, A. Tashiro, K. Ogino, and H. Maeda, *Lab Chip*, **2002**, *2*, 8.
- [52] T. Ami, K. Awata, H. Umekawa, and M. Ozawa, *Int. J. Multiphase Flow*, **2012**, *26*, 302.
- [53] J. Jovanovic, E. V. Rebrov, T. A. X. Nijhuis, M. T. Kreutzer, V. Hessel, and J. C. Schouten, *Ind. Eng. Chem. Res.*, **2012**, *51*, 1015.
- [54] M. Kashid and L. K. Minsker, *Chem. Eng. Process.*, **2011**, *50*, 972.
- [55] C. W. Huck, G. Stecher, R. Bakry, and G. K. Bonn, *Electrophoresis*, **2003**, *24*, 3977.
- [56] Y. Wang, Q. L. Deng, G. Z. Fang, M. F. Pan, Y. Yu, and W. S. Shuo, *Anal. Chim. Acta*, **2012**, *712*, 1.
- [57] J. L. Chen , *Talanta*, **2011**, *8*, 2330.

Chapter 5 Effects of inner wall characteristics of capillary tubes on tube radial distribution chromatography (TRDC)

TRDP is basically caused through phase transformation of the two-phase separation solution systems, not through interaction between an inner wall of the capillary tubes and solvent molecules. However, the stability of TRDP formation, especially outer phase formation, seemed to be influenced by the materials of the inner wall. The effects of the inner wall characteristics of capillary tubes on TRDC performance were examined. The part of this chapter is reconstructed and rewritten based on the related manuscripts that have been published.^{4,5,22)}

5.1 Effects of the inner-wall characteristics of the fused-silica capillary tube on TRDC

A capillary chromatography system was developed using an open capillary tube and a water–acetonitrile (hydrophilic)–ethyl acetate (hydrophobic) mixture carrier solution. Here, we examine the effects of the inner–wall characteristics of a fused-silica capillary tube on the separation performance in this system. Untreated (silanol group-intact) and inactivated (silanol group-end-blocked) fused-silica capillary tubes were used. The mixture analyte of 1-naphthol and 2,6-naphthalenedisulfonic acid was injected into two types of capillary tubes. They were eluted from both tubes in this order with water–acetonitrile–ethyl acetate (volume ratio 2:7:4) mixture carrier solution, and eluted in reverse order with water–acetonitrile–ethyl acetate (volume ratio 15:3:2). The peak shapes observed here were analyzed while considering the inner–wall characteristics of the capillary tubes from the viewpoint of the tube radial distribution of the carrier solvents in the tubes.

Introduction

We developed a capillary chromatography system using an open capillary tube and an aqueous–organic mixture carrier solution that worked under laminar flow conditions. Unlike conventional capillary electrochromatography [1,2], capillary electrophoresis [3,4] and capillary liquid chromatography [5,6], separation in this system was performed without the use of any specific materials, such as packed capillary tubes, additives, such as gels, surfactants, host molecules or salts, or high-voltage supply devices.

Based on our results, we proposed that separation in the capillary chromatography system was performed based on the tube radial distribution of the aqueous–organic mixture solvents in the capillary tubes under laminar flow conditions. We call this a tube radial distribution chromatography (TRDC) system. Here, to expand our knowledge regarding the TRDC system, we examined the effects of the inner-wall characteristics of a fused-silica capillary tube on the separation performance in the system. Untreated (silanol group-intact) and inactivated (silanol group-end-blocked)

fused-silica capillary tubes were used. Aside from the altered inner-wall characteristics of the fused-silica capillary tubes, the following experiments were carried out under the same analytical conditions used previously. The data obtained here were considered from the viewpoint of the tube radial distribution of the carrier solvents in the tubes under laminar flow conditions.

Experimental

Fused-silica capillary tubes (50 μm i.d., 150 μm o.d.), untreated (silanol group-intact) and inactivated (silanol group-end-blocked), were used; they were commercially available. The capillary chromatography system consisted of a fused-silica capillary tube (80 cm in length; effective length, 60 cm), a microsyringe pump, and an absorption detector. Aqueous–organic solvent mixture carrier solutions of the water–acetonitrile–ethyl acetate mixture with volume ratios of 2:7:4 and 15:3:2 were used. A mixture analyte solution of 1-naphthol and 2,6-naphthalenedisulfonic acid was prepared with the carrier solutions. The analyte solution was introduced directly into the capillary inlet for 20 s from a height of 20 cm by a gravity method. After analyte injection, the capillary inlet was connected through a joint to a microsyringe. The syringe was set on a microsyringe pump. The carrier solution was fed into the capillary tube at a specified flow rate under laminar flow conditions (setting flow rate of the pump; $0.3 \mu\text{L min}^{-1}$). On-capillary absorption detection (254 nm) was performed with a detector.

Results and discussion

The TRDC systems were performed using fused-silica, polyethylene, and poly(tetrafluoroethylene) capillary tubes in our previous work. However, because they had quite different inner diameters of 50, 200, and 100 μm , respectively, it was hard to strictly evaluate the influence of the inner-wall of the capillary tube. Here, we tried to examine the effects of the inner-wall characteristic on the separation performance in the TRDC system by using fused-silica capillaries under quite the same analytical conditions, except for the inner-wall characteristics.

First, we examined an untreated (silanol group-intact) fused-silica capillary tube with aqueous–organic solvent mixture carrier solutions, an organic solvent-rich carrier solution (water–acetonitrile–ethyl acetate (volume ratio 2:7:4)) and a water-rich carrier solution (the water–acetonitrile–ethyl acetate (volume ratio 15:3:2)). The obtained chromatograms are shown in Fig. 1. 1-Naphthol and 2,6-naphthalenedisulfonic acid were eluted from the capillary in this order with the organic solvent-rich carrier solution (Fig. 1a)). 1-Naphthol was eluted at ca. 4.2 min with a near average linear velocity (average linear velocity under the laminar flow conditions was confirmed through an experiment using a normal carrier solution not including organic solvents), and 2,6-naphthalenedisulfonic acid was eluted at a lower than average linear velocity. A water-rich phase (minor solvent phase) was formed near the inner wall as a pseudo-stationary phase, due to the tube radial distribution of the carrier solvents in which phase 2,6-naphthalenedisulfonic acid was dispersed and eluted with a lower than average linear velocity. 1-Naphthol and 2,6-naphthalenedisulfonic acid were eluted in reverse order when the carrier solution was water-rich (Fig. 1b)). An organic solvent-rich phase (the minor solvent phase) generated near the inner wall due to the

tube radial distribution of the carrier solvents in which phase 1-naphthol was dispersed and eluted at a lower than average linear velocity. The elution times and the peak shapes of the chromatograms shown in Fig. 1 were partly different from those reported in our work using the same untreated fused-silica capillary tube. The difference between them must have been caused by the different analytical conditions, such as the capillary length and the flow rate.

Next, we examined an inactivated (silanol group-end-blocked) fused-silica capillary tube with an aqueous–organic solvent carrier solution, an organic solvent-rich carrier solution and a water-rich carrier solution. The obtained chromatograms are shown in Fig. 2; an elution behavior similar to that of the untreated capillary tube was observed. 1-Naphthol and 2,6-naphthalenedisulfonic acid were eluted from the capillary in this order with an organic solvent-rich carrier solution (Fig. 2a)), and were eluted in reverse order in the water-rich carrier solution (Fig. 2b)). The inner-wall characteristics of the fused-silica capillary tubes did not change the elution orders of the model analytes in the present TRCD system. However, it should be noted that the second peak of 1-naphthol, obtained through an inactivated tube with the water-rich carrier in Fig. 2b), indicated broadening on the peak shape, compared with the other peaks observed in Figs. 1 and 2. The component of the second peak was dispersed in the minor solvent phase generated near the inner wall of the capillary tube as a pseudo-stationary phase. When using the inactivated (comparatively hydrophobic) fused-silica capillary with the water-rich carrier solution, 1-naphthol (hydrophobic) was eluted as a second peak along the inner wall surface, as shown in Fig. 2b). In this case, the hydrophobic interaction between the analyte (1-naphthol) and the inner wall of the inactivated fused-silica must have led to a peak broadening of 1-naphthol. That is, the specific broadening of the second peak in Fig. 2b) consists of the separation performance based on the tube radial distribution of the carrier solvents in the TRDC system.

In addition, in the case of no interaction between the analyte and the inner wall, it was observed for both analytes, 1-naphthol and 2,6-naphthalenedisulfonic acid, in Figs. 1 and 2 that the peak area of the anylyte as a second peak was smaller than it was as the first peak. Although such a phenomenon may have been caused by the light-path lengths of the major and minor solvent phases in the capillary tube as well as reflection and refraction of the entrance and transmittance light at the outer and inner wall surfaces of the capillary tube; the reason has yet to be clarified.

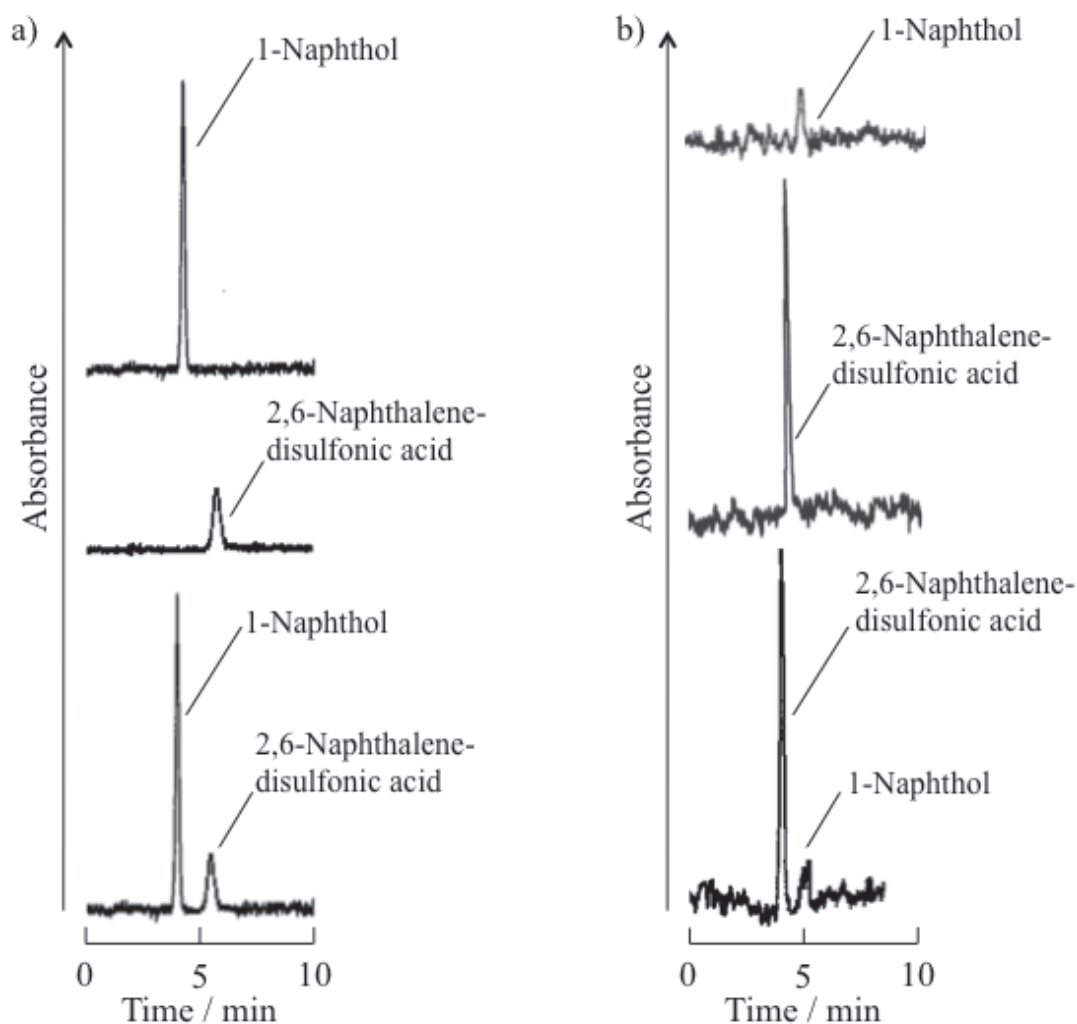


Figure 1. Obtained chromatograms of a mixture analyte of 1-naphthol and 2,6-naphthalenedisulfonic acid by the present TRDC system using an untreated fused-silica capillary tube. a) Water-acetonitrile-ethyl acetate mixture (2:7:4) carrier and b) water-acetonitrile-ethyl acetate mixture (15:3:2) carrier. Conditions: capillary tube, 80 cm (effective length: 60 cm) of 50 μm i.d. fused-silica capillary; sample injection, 20 cm height (gravity) \times 20 s; and analyte concentration, 2 mM each.

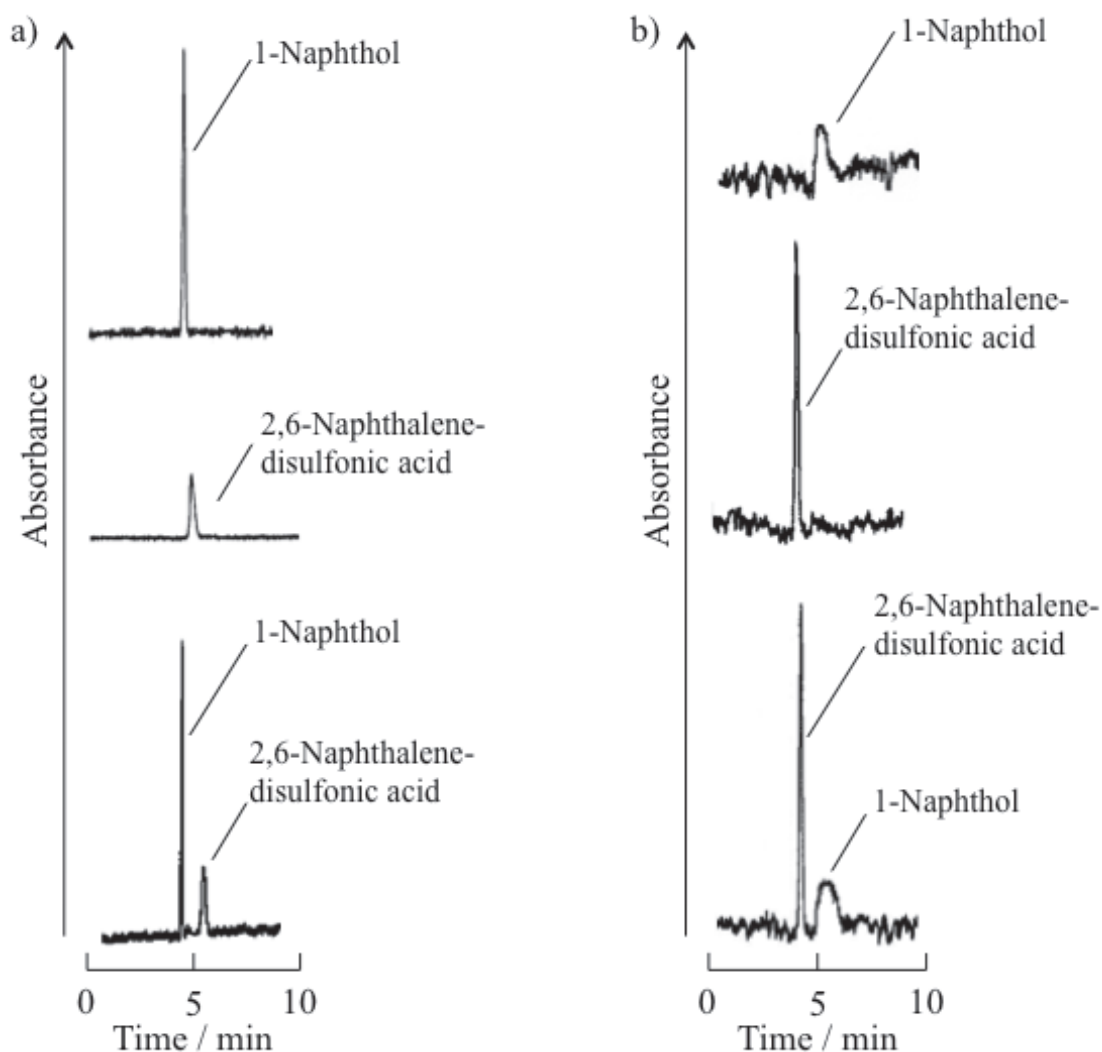


Figure 2. Obtained chromatograms of a mixture of 1-naphthol and 2,6-naphthalenedisulfonic acid by the present TRDC system using an inactivated fused-silica capillary tube. a) Water–acetonitrile–ethyl acetate mixture (2:7:4) carrier and b) water–acetonitrile–ethyl acetate mixture (15:3:2) carrier. Conditions: capillary tube, 80 cm (effective length: 60 cm) of 50 μm i.d. fused-silica capillary; sample injection, 20 cm height (gravity) \times 20 s; and analyte concentration, 2 mM each.

5.2 Effects of inner-wall-modified capillary tubes on TRDC

We tried to introduce inner-wall-modified (e.g., phenylboronic-acid- and iminodiacetic-acid-modified) fused-silica capillary tubes to the tube radial distribution chromatography (TRDC) system to separate model mixture analytes. The phenylboronic-acid-modified capillary tube was combined with absorption detection to analyze a mixture of adenosine and deoxyadenosine. The iminodiacetic-acid-modified capillary tube was combined with chemiluminescence detection using a luminol reaction to analyze a mixture of copper(II) and hematin. A water (carbonate buffer)-acetonitrile-ethyl acetate (2:7:4 v/v/v) and a water (carbonate buffer)-acetonitrile-ethyl acetate (15:3:2 v/v/v) mixture solution were used as carrier solutions in the TRDC system, and typical carbonate buffer solutions not containing any organic solvents were also used as carrier solutions as reference solutions. In both modified capillary tubes, the organic-solvent-rich carrier solution successfully improved the separation of the mixture analytes in the system, and the water-rich carrier solution greatly depressed their separation, when compared with chromatography using carbonate buffer carrier solutions containing no organic solvents. Such observed phenomena were discussed with consideration given to the separation mechanism of the TRDC system.

Introduction

Miniaturization generally has a number of merits, so it has been one of best-recognized research directions in analytical chemistry. Interesting investigations with respect to miniaturization have also been done in the field of liquid chromatography; e.g., they are called open tubular liquid chromatography and capillary liquid chromatography. Open tubular liquid chromatography is generally identified with tube inner diameters less than several decades μm [7-9]. Knox et al. reported in their theoretical study that the optimum inner diameter of the open tubular column was approximately one-fifth of the diameter of the particles in the optimum packed column [9]. Recently, hydrophilic-interaction chromatography using 10 μm i.d. porous layer open tubular column was developed for ultra-trace glycan analysis [10]. However, open tubular liquid chromatography naturally has some difficulties in the construction and operation of such very narrowly bored tubes.

Capillary liquid chromatography is performed with wide-bored capillary tubes that are usually applied up to several hundreds μm i. d. Various capillary chromatography techniques, including capillary electrochromatography [1,4], micellar electrokinetic capillary chromatography [11,12], and high-performance liquid capillary chromatography using packed and monolithic columns [6,13], have been investigated as powerful separation tools. We proposed a novel capillary chromatography using an open capillary tube (50 – 200 μm i.d.) and a water-hydrophilic/hydrophobic organic solvent mixture (homogeneous solution) as a carrier solution; the system worked based on the radial distribution of carrier solvents in the capillary tube under laminar flow conditions. We called this system of capillary chromatography; a tube radial distribution chromatography (TRDC) system.

Data obtained in the TRDC system so far indicates that the properties of the materials used in the capillary tube, such as fused-silica, polyethylene, and poly(tetrafluoroethylene), have little influence on separation performance. However, what we are interested in is if the inner wall characteristics of a capillary tube affects or improves separation performance in the TRDC system. Here, we prepared two types of inner-wall-modified open fused-silica capillary tubes, phenylboronic-acid- and iminodiacetic-acid-modified, according to the preparation procedures described in our previous works [14-15], and tried to introduce the modified tubes into the TRDC system using an aqueous-organic solvent mixture carrier solution. The fused-silica, polyethylene, and poly(tetrafluoroethylene) capillary tubes used so far in the TRDC system were relatively inert, although they have quite different chemical characteristics on their inner walls. In contrast, the modified capillary tubes have specific interaction affinity to certain specific analytes. The phenylboronic acid moieties on the inner wall of the capillary tube have specific interactions with compounds having *cis*-diol groups in the molecules, such as nucleosides and saccharides [14,15]. The iminodiacetic acid moieties on the inner wall have another specific affinity to metal ions through complex formation [16].

We examined the interaction between the function moieties, phenylboronic acid and iminodiacetic acid, on the inner walls and the model analytes using the modified capillary tubes, as reflected in the separation performance in the TRDC system. The TRDC system with the organic-solvent-rich carrier solution improved separation performance and the system with the water-rich carrier solution did not show any separation performance under the present analytical conditions. Also, the findings in the TRDC system using the modified capillary tubes provided us important information that strongly supported our proposed separation mechanism in the TRDC system.

Experimental

A fused-silica capillary tube (75 μm i.d. and 150 μm o.d.) was used. Phenylboronic-acid- and iminodiacetic-acid-modified fused-silica capillary tubes were prepared as described in our previous papers [13–15]. TRDC systems equipped with absorption detection (System 1) and chemiluminescence (CL) detection (System 2) are shown in Fig. 1 a and b, respectively. System 1 in Fig. 1 a was used with the phenylboronic-acid-modified capillary tube (60 cm length, 40 cm effective length) for nucleoside analysis. System 2 in Fig. 1 b, taking advantage of the luminol reaction, was used with the iminodiacetic-acid-modified capillary tube (70 cm length) for metal catalyst analysis. A batch-type CL detection cell equipped with an optical fiber [17] was used in System 2. The CL reagent solution [10 mM carbonate buffer solution (pH 10.8), including 5 μM luminol and 50 mM hydrogen peroxide] was delivered to the capillary outlet, where the analytes having catalytic activity for the luminol reaction and the CL reagent were mixed to generate CL light. The aqueous-organic solvent mixture carrier solutions were prepared with a water (10 mM carbonate buffer, pH 9.5 or 10.8)-acetonitrile-ethyl acetate mixture (2:7:4 v/v/v) and a water (10 mM carbonate buffer, pH 9.5 or 10.8)-acetonitrile-ethyl acetate mixture (15:3:2 v/v/v) mixture. Ten mM carbonate buffer solutions of pH 9.5 and 10.8, not including any organic solvents, were used as reference carrier solutions to the aqueous-organic solvent carrier solution for Systems 1 and 2, respectively. A mixture of adenosine and deoxyadenosine, as well

as a mixture of Cu(II) and hematin, were prepared as model analytes by dissolving them into the carrier solution. The metal catalyst solution included potassium sodium tartrate with a concentration 20 times higher than that of the catalyst. The analyte solutions were injected into the capillary tube inlet using the gravity method (from a 30 cm height for 15 s for System 1 and from a 35 cm height for 5 s for System 2). The analytes were further delivered in the capillary tubes with the carrier solution by micro-syringe pumps at a flow rate of $0.13 \mu\text{L min}^{-1}$ for System 1 and $0.33 \mu\text{L min}^{-1}$ for System 2. Analytes of nucleosides in System 1 were detected by adsorption (267 nm), and analytes of metal compounds in System 2 were detected by CL detection.

Results and discussion

Phenylboronic-acid-modified capillary tube Boronic acids and boronic acid compounds are known to interact with *cis*-diol groups included in saccharide and nucleoside molecules through ester formation, leading to separation and molecular recognition of such biomolecules [18]. We reported capillary liquid chromatography and capillary electrophoresis using phenylboronic-acid-modified capillary tubes [14,15]. Mixtures of a nucleoside and deoxynucleoside, for example, adenosine and deoxyadenosine, were successfully separated in the modified capillary tube; their resolution in capillary electrophoresis was better than in capillary liquid chromatography, where the analytes were delivered in the capillary tube by the gravity method. The mixture of adenosine and deoxyadenosine as a model was examined by the present TRDC system using the phenylboronic-acid-modified capillary tube with a water (10 mM carbonate buffer, pH 9.5)-acetonitrile-ethyl acetate mixture (2:7:4 v/v/v) and a water (10 mM carbonate buffer, pH 9.5)-acetonitrile-ethyl acetate mixture (15:3:2 v/v/v). The obtained chromatograms are shown in Fig. 2, together with the chromatogram obtained using a carbonate buffer carrier solution which didn't include any organic solvents as a reference. The mixture of adenosine and deoxyadenosine was separated through the modified capillary tube with the carbonate buffer carrier solution (Fig. 2 a). Deoxyadenosine has no *cis*-diol group in its molecules but adenosine has one. Consequently, the former moved first in the capillary tube without any interaction with the inner wall of the phenylboronic-acid-modified capillary, but the latter moved slowly in the tube because of the interaction of the *cis*-diol groups with the phenylboronic acid moiety on the inner wall, causing a prolonged elution time. Interesting separation performance was observed in the TRDC system with the organic-solvent-rich (Fig. 2 b) and water-rich (Fig. 2 c) carrier solutions. The resolution of the nucleosides was improved with the organic-solvent-rich carrier solution. The obtained chromatogram in Fig. 2 b provided a complete baseline separation. In contrast, the resolution was extremely depressed with the water-rich carrier solution; no separation was observed on the chromatogram in Fig. 2 c.

Iminodiacetic-acid-modified capillary tube Capillary liquid chromatography using the iminodiacetic-acid-modified capillary tube was reported; a mixture of Cu(II) or Co(II) and hematin was separated through the tube and detected with CL detection where the mixture was delivered in the tube by the gravity method [16]. The experiment using the iminodiacetic-acid-modified capillary tube in the TRDC system was carried out similar to the capillary liquid chromatography experiment. The mixture of Cu(II)

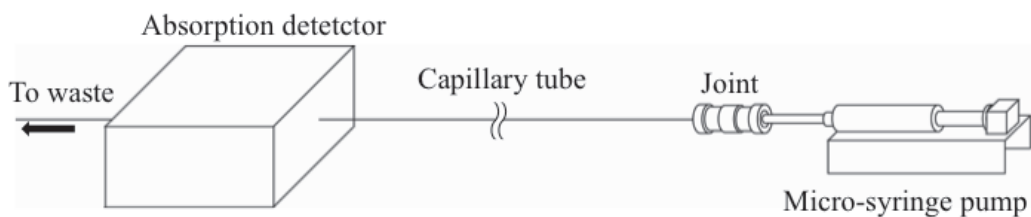
and hematin was examined by the TRDC system using the iminodiacetic-acid-modified capillary tube with water (10 mM carbonate buffer, pH 10.8)-acetonitrile-ethyl acetate mixture (2:7:4 v/v/v) and water (10 mM carbonate buffer, pH 10.8)-acetonitrile-ethyl acetate mixture (15:3:2 v/v/v) carrier solutions. The obtained chromatograms are shown in Fig. 3, along with the chromatogram obtained with a carbonate buffer solution (pH 10.8) as a reference. The mixture was separated with the carbonate buffer solution; hematin and Cu(II) were hence eluted in this order (Fig. 3 a). The metal complexation interaction between Cu(II) and the iminodiacetic acid moiety on the inner wall must cause the separation of Cu(II) and hematin. Hematin [Fe(III)-porphyrin complex] undergoes little complex formation with the iminodiacetic acid moiety. An interesting separation performance was again observed in the TRDC system with the organic-solvent-rich and water-rich carrier solutions, as shown in Fig. 3 b and c, respectively. The TRDC system with the organic-solvent-rich carrier solution showed a better resolution (Fig. 3 b) than capillary chromatography using the modified capillary tube and the normal carbonate buffer without organic solvents (Fig. 3a). In contrast, the TRDC system with the water-rich carrier solution showed no separation on the chromatogram (Fig. 3 c).

Consideration of separation performance Until now, the TRDC system was operated with open capillary tubes, such as a fused-silica capillary, polyethylene, and poly(tetrafluoroethylene) capillary tube, whose inner wall of them were unmodified and untreated. The two types of modified capillary tubes, phenylboronic-acid- and iminodiacetic-acid-modified, were introduced into the TRDC system with a water-acetonitrile-ethyl acetate mixture carrier solution. In both capillary tubes, the TRDC system with the organic-solvent-rich carrier solution showed improved separation performance compared to capillary chromatography using the modified tubes and carbonate buffer carrier solutions with no organic solvents. In contrast, both capillary tubes in the TRDC system with the water-rich carrier solution showed no separation performance despite being modified. As nucleosides are comparatively hydrophilic, they are dispersed in the water-rich phase. When using the organic-solvent-rich carrier solution, the minor solvent phase or the water-rich phase forms near the inner wall of the capillary. Therefore, nucleosides that were dispersed in the water-rich phase could easily interact with phenylboronic acid moieties, showing better resolution (Fig. 2 b) than in the chromatogram obtained with the normal carbonate buffer carrier solution (Fig. 2 a). When using the water-rich carrier solution, the major solvent phase or the water-rich phase forms around the middle of the tube. Therefore, nucleosides dispersed in the water-rich phase might exist far from the inner wall, leading to a lower probability of interaction with phenylboronic acid moieties; no separation was observed on the chromatogram (Fig. 2 c). Similarly, we could explain the separation performance in the TRDC system using the iminodiacetic-acid-modified capillary tube. Cu(II) is completely dispersed in the water-rich phase. When using the organic-solvent-rich carrier solution, the Cu(II) dispersed in the water-rich phase or minor solvent phase must exist near the inner wall of the capillary, providing better complex formation with the iminodiacetic acid moieties on the wall, as compared to the chromatography separation mode using a carbonate buffer carrier solution with no organic solvents. When using the water-rich carrier solution, the Cu(II) in the major

solvent phase or the water-rich phase that formed around the center of the tube interacted little with the iminodiacetic acid moieties on the inner wall, leading to no separation from hematin, which had little ability to form complexes with the iminodiacetic acid moieties.

In conclusion, for the first time, we tried to introduce inner-wall-modified (phenylboronic-acid- and iminodiacetic-acid-modified) fused-silica capillary tubes into the TRDC system with an aqueous-organic solvent carrier solution. We examined the interaction between the functional moieties on the inner walls and the analytes using the modified capillary tubes, as reflected in the separation performance of the TRDC system. TRDC with an organic-solvent-rich carrier solution was found to successfully improve the separation performance, although the system with a water-rich carrier solution did not show any separation performance under the present conditions. Also, the findings in the TRDC system using the modified capillary tubes gave us important information that supported our proposed separation mechanism in the TRDC system.

a)



b)

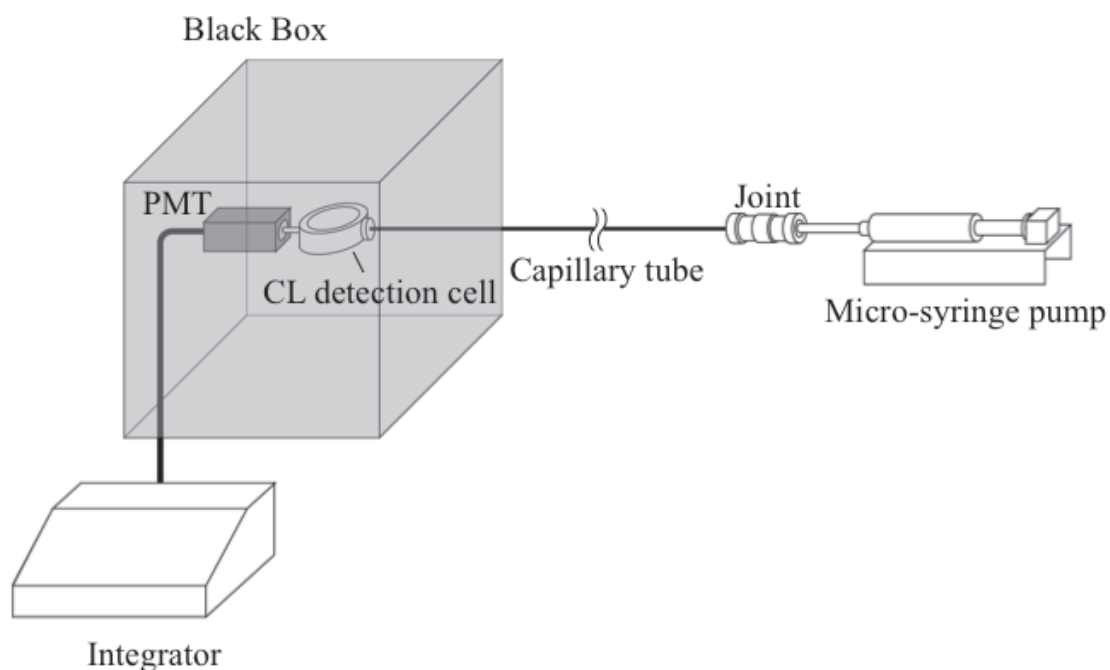


Figure 1. Schematic diagrams of the TRDC system. a) System 1, equipped with absorption detection and b) System 2, equipped with CL detection.

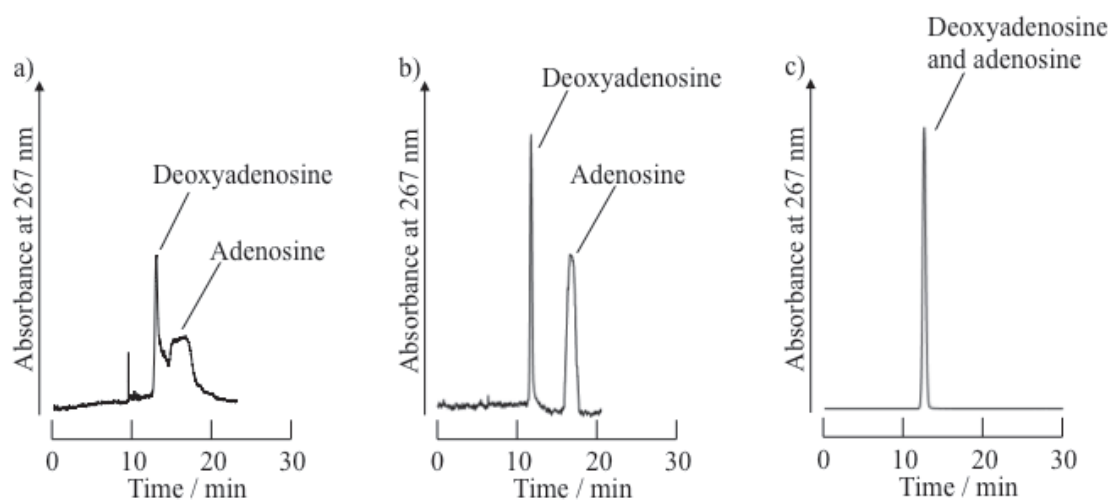


Figure 2. The chromatograms obtained using the phenylboronic-acid-modified capillary tube. a) Capillary chromatography with the 10 mM carbonate buffer solution (pH 9.5), b) TRDC system with the organic-solvent-rich carrier solution [water (10 mM carbonate buffer, pH 9.5)-acetonitrile-ethyl acetate; 2:7:4 v/v/v], and c) TRDC system with the water-rich carrier solution [water (10 mM carbonate buffer, pH 9.5)-acetonitrile-ethyl acetate; 15:3:2 v/v/v]. Conditions: Capillary tube, 60 cm length (effective length 40 cm) of 75 μm i.d.; sample injection, 30 cm height (gravity) \times 15 s; flow rate, 0.13 $\mu\text{L min}^{-1}$; detection, 267 nm absorption; and analyte concentration, 19 mM each.

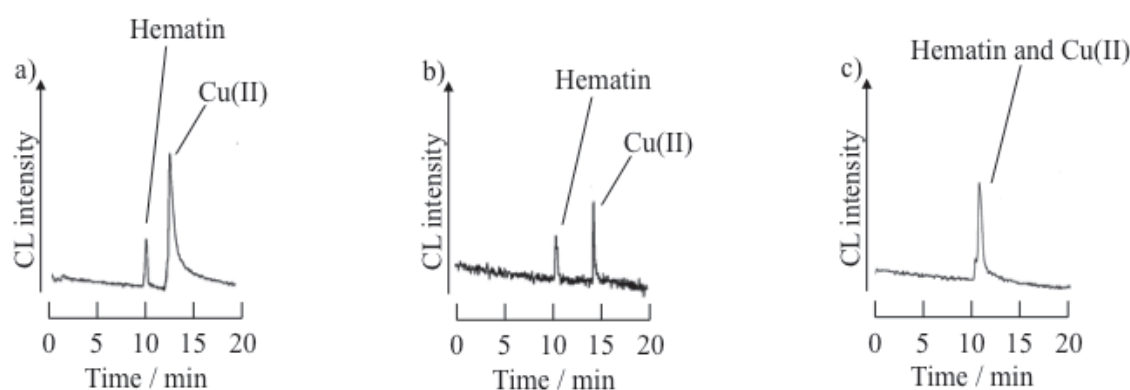


Figure 3. The chromatograms obtained using the iminodiacetic-acid-modified capillary tube. a) Capillary chromatography with the 10 mM carbonate buffer solution (pH 10.8), b) TRDC system with the organic-solvent-rich carrier solution [water (10 mM carbonate buffer, pH 10.8)-acetonitrile-ethyl acetate; 2:7:4 v/v/v], and c) TRDC system with the water-rich carrier solution [water (10 mM carbonate buffer pH, 10.8)-acetonitrile-ethyl acetate; 15:3:2 v/v/v]. Conditions: Capillary tube, 70 cm of 75 μm i.d.; sample injection, 35 cm height (gravity) \times 5 s; flow rate, 0.33 $\mu\text{L min}^{-1}$; detection, luminol CL detection; and analyte concentration, 1 mM Cu(II) and 10 μM hematin.

5.3 Effects of the inner wall materials of capillary tubes on TRDC

The effects of tube materials on separation performance were examined within the tube radial distribution chromatography (TRDC) system, by using poly(tetrafluoroethylene) (PTFE; 100–400 μm inner diameter), polyethylene (PE; 200 μm inner diameter), and a copolymer of (tetrafluoroethylene-perfluoroalcoxyethylene) (PTFE-PFAE; 100 μm inner diameter) capillary tubes. An analyte solution of 2,6-naphthalenedisulfonic acid and 1-naphthol as a model was subjected to the system with a water-acetonitrile-ethyl acetate carrier solution; a volume ratio of 5:3:2 (water-rich carrier) and a volume ratio of 3:8:4 (organic solvent-rich carrier). The flow rates were set to 0.5 $\mu\text{L min}^{-1}$ for PTFE and PTFE-PFAE tubes as well as 2.0 $\mu\text{L min}^{-1}$ for PE tubes under laminar flow conditions. The analytes in the solution were separated in this order using the water-rich carrier solution with baseline separation occurring in the three capillary tubes, while they were eluted in the reverse order or not separated at all with the organic solvent-rich carrier solution. The effects of tube temperature on separation performance were also examined in the water-rich carrier solution; the best resolutions were observed at a tube temperature of 0 $^{\circ}\text{C}$. The obtained results were compared with those for the case of the fused-silica capillary tube and discussed.

Introduction

Capillary chromatography and CE have received a lot of attention as powerful separation methods, where fused-silica capillaries are mainly used for separation tubes [19–21]. A fused-silica capillary tube was found to have uniform narrow bore and good flexibility for micro-analysis. A poly(tetrafluoroethylene) (PTFE) capillary tube that possesses similar properties to those of the fused-silica capillary tube is also widely used not only in analytical chemistry but also in fields including pharmaceutical chemistry and medicine [22–25], though the nature of the inner wall surface of the PTFE is different from that of fused-silica. We have developed a novel capillary chromatography system using an open capillary tube and a ternary mixed solvent of water-hydrophilic/hydrophobic organic mixture solution. This system works under laminar flow conditions and does not require any packed reagents in the capillary tube or the application of high voltage to the ends of the tube. It is called a tube radial distribution chromatography (TRDC) system. To date, fused-silica capillary tubes have been mainly examined in the TRDC system. Here, the effects of polymer tube materials, such as PTFE, polyethylene (PE), and a copolymer of (tetrafluoroethylene-perfluoroalcoxyethylene) (PTFE-PFAE), on the separation performance of the TRDC system were examined.

Experimental

PTFE capillary tubes (100 μm i.d., 200 μm o.d.; 150 μm i.d., 300 μm o.d.; 200 μm i.d., 350 μm o.d.; and 250 μm i.d., 400 μm o.d.), PE (200 μm i.d., 500 μm o.d.) capillary tubes, and PTFE-PFAE (100 μm i.d., 300 μm o.d.) capillary tubes were used. The present capillary chromatography system was comprised of an open capillary tube, micro-syringe pump, and absorption detector. A capillary tube, 110 cm in length

(effective length: 90 cm), was also placed in the system. The tube temperature was controlled by immersing the capillary tube in water maintained at a specific temperature in a beaker by stirring. Water-acetonitrile-ethyl acetate mixtures with volume ratios of 15:3:2 and 3:8:4 were used as water-rich and organic solvent-rich carrier solutions. Analyte solutions were prepared with the carrier solutions. The analyte solution was introduced directly into the capillary inlet side for 10 s from a height of 25 cm for the capillary tube. After analyte injection, the capillary inlet was connected through a joint to a micro-syringe which was set on the micro-syringe pump. The carrier solution was fed into the capillary tube at a flow rate of 0.5 $\mu\text{L min}^{-1}$ for PTFE and PTFE-PFAE, as well as at 2.0 $\mu\text{L min}^{-1}$ for PE. On-capillary absorption detection (254 nm) was performed by the detector.

Results and discussion

Effects of tube inner diameter on separation We examined the effects of the tube inner diameter on separation in the TRDC system with a mixture analyte solution of 2,6-naphthalenedisulfuric acid and 1-naphthol as a model. We used commercially available PTFE capillary tubes with various inner diameters of 100–250 μm i.d. The obtained chromatograms are shown in Fig. 1 together with analytical conditions. The flow rates for all the capillary tubes were adjusted to provide almost the same average linear velocity of ca. 6.4 cm min^{-1} . We observed well-separated peaks on the chromatograms; 2,6-naphthalenedisulfuric acid and 1-naphthol were separated in this order with the water-rich carrier solution. The first peaks were eluted with an almost average linear velocity and the second peaks were eluted at a slower than average linear velocity. Also, the elution times of the second peaks appeared earlier with increasing inner diameter, although the elution times of the first peaks were nearly constant. Additionally, the second peak of 1-naphthol showed broadening on the chromatograms. The outer phase (the organic solvent-rich solution) worked as a pseudo-stationary phase that had a larger diffusion coefficient in the TRDC system than that in a usual stationary phase in liquid chromatography. Hydrophobic 1-naphthol distributed in a specific stationary phase, which lead to the peak broadening.

Effects of tube temperature on separation using polymer capillary tubes The effects of tube temperature on separation in the TRDC system using PTFE, PE, and PTFE-PFAE capillary tubes were examined with the water-rich and the organic solvent-rich carrier solutions. First, the chromatograms obtained using PTFE are shown in Fig. 2 together with those obtained using other capillary tubes. As can be seen in Fig. 2, with the water-rich carrier solution, 2,6-naphthalenedisulfuric acid and 1-naphthol were detected in the mixture solution with baseline separation in the temperature range of 0–30 $^{\circ}\text{C}$, but the resolutions decreased gradually between 30 $^{\circ}\text{C}$ and 45 $^{\circ}\text{C}$ and finally they were not separated on the chromatogram at 50 $^{\circ}\text{C}$ (Fig. 2 a)). On the other hand, with the organic solvent-rich carrier solution they were eluted in reverse order, but not separated with baseline separation at 0 and 10 $^{\circ}\text{C}$ (Fig. 2 d)). The data clearly indicated that the tube temperature had a crucially significant influence on separation performance in the TRDC system. The formation of the inner and outer phases in a tube based on TRDP must change with temperature. Also, an analyte solution of

2,6-naphthalenedisulfuric acid and 1-naphthol was examined with the TRDC system using PE and PTFE-PFAE with the water-rich and organic solvent-rich carrier solutions at the tube temperature of 0 °C. They were eluted with baseline separation in this order with the water-rich carrier solution in both of the tubes, while, with the organic solvent-rich carrier solution, they were eluted in the reverse order without baseline separation in PE and they were not separated in PTFE-PFAE. We examined the effects of tube temperature on separation in the TRDC system using PE and PTFE-PFAE capillary tubes with water-rich carrier solutions. The obtained chromatograms are also shown in Fig. 2 along with the analytical conditions. As can be seen in the figure, through PE capillary tubes 2,6-naphthalenedisulfuric acid and 1-naphthol in the mixture solution were separated and detected within the temperature range of 0–10 °C, but the resolutions decreased gradually between 15 °C and 25 °C and finally they were not separated on the chromatogram at 30 °C (Fig. 2 b)). In a similar way 2,6-naphthalenedisulfuric acid and 1-naphthol in the mixture solution were eluted with the water-rich carrier solution through PTFE-PFAE capillary tube (Fig. 2 c))

Separation of mixture solution including three analytes We examined a mixture analyte solution of 2,6-naphthalenedisulfonic acid, Eosin Y, and 1-naphthol using the present TRDC system with a water-rich carrier solution. The obtained chromatograms are shown in Fig. 3. 2,6-Naphthalenedisulfonic acid, Eosin Y, and 1-naphthol were eluted in this order, leading to good separation with the water-rich carrier solution. The elution order seemed to be consistent with the substances' hydrophilic characters. With the water-rich carrier solution, the hydrophilic compounds 2,6-naphthalenedisulfonic acid were eluted with almost average linear velocity, while the relatively hydrophobic compounds Eosin Y and 1-naphthol were eluted in this order at a lower than average linear velocity..

Consideration of the influence of the tube materials on separation Since separation in the TRDC system is performed based on the tube radial distribution of the carrier solvents as described in the introduction, 2,6-naphthalendisulfonic acid and 1-naphthol were separated in this order with the water-rich carrier solution, while they were eluted in reverse order with the organic solvent-rich carrier solution under the present analytical conditions using polymer capillary tubes, such as PTFE, PE, and PTFE-PFAE, except for when using PTFE-PFAE with the organic solvent-rich carrier solution. The same elution behavior was observed in the TRDC system using the fused-silica capillary tube as shown in Fig. 4. However, there was a difference in the separation behavior between the polymer capillary tubes and fused-silica capillary tubes. First, in polymer capillary tubes resolutions obtained with the water-rich carrier solution were much better than those with the organic solvent-rich carrier solution. However, as was previously reported in fused-silica capillary tubes,¹⁰⁾ the resolutions obtained with the organic solvent-rich carrier solution were better than those of the water-rich carrier solutions. The interaction between the outer phase of the organic solvent-rich solution and the polymer surface as well as the outer phase of the water-rich solution and silanol surface might give prior conditions for creating the inner and outer phases in the capillary tube, while, the interaction between the outer phase of the water-rich solution and polymer surface as well as the outer phase of the organic solvent-rich solution and

silanol surface might create inconvenient conditions for the generation of the inner and outer phases in the capillary tube. Secondly, in polymer tube materials, the resolutions decreased with the increase of the tube temperature, while, in fused-silica tubes, the resolutions increased with increasing of the tube temperature until up to 20 °C (Fig. 2 e)).¹⁰⁾ The tendency concerning the effect of tube temperature, tube materials, and the component ratio of the carrier solvents on separation performance is interesting, where energy or enthalpy for separation must be complexly influenced by various types of heat, such as dissolution, adsorption, desorption and solvation at the liquid-liquid interface.

In conclusion, the polymer tube materials, such as PTFE, PE, and PTFE-PFAE, were examined in the TRDC system and the obtained results were discussed together with those concerning the fused-silica capillary tube that we reported previously. Although there is a difference in the nature of the wall's inner-surface between polymer and fused-silica capillary tube, the fundamental elution behavior in the TRDC system is the same in all capillary tubes. However, the resolutions provided by the water-rich carrier are better than organic solvent-rich carrier in polymer capillary tubes, conversely, the resolutions provided by the organic solvent-rich carrier solution are better than those water-rich carrier solution in fused-silica capillary tubes.

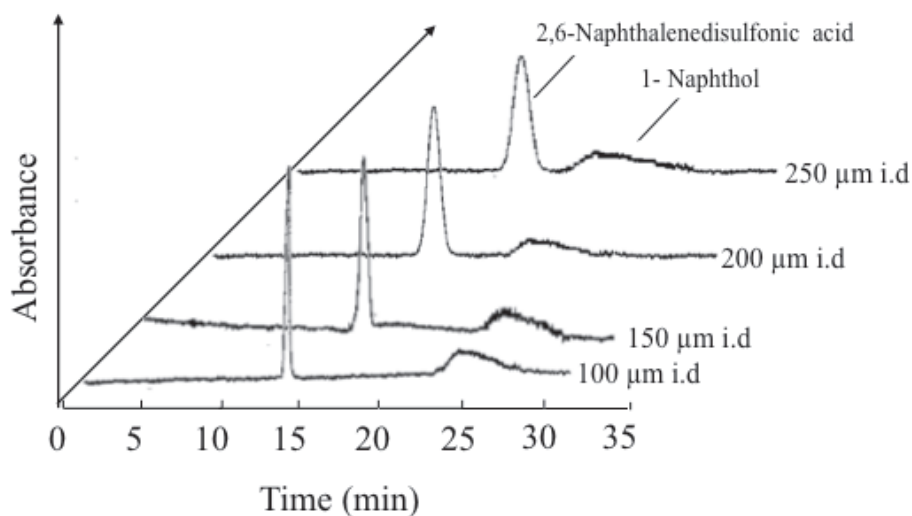


Figure 1. Effects of the inner diameter of the tube on separation in the TRDC system using PTFE capillary tube. Conditions: Capillary tube, 110 cm (effective length: 90 cm) PTFE of 100, 150, 200, and 250 μm i.d.; carrier, water-acetonitrile-ethyl acetate (15:3:2 v/v/v) mixture solution; sample injection, 25 cm height (gravity) \times 10 s; flow rate, 0.5–3.0 $\mu\text{L min}^{-1}$; tube temperature, 0 $^{\circ}\text{C}$; and 2,6-naphthalenedisulfonic acid and 1-naphthol, 1 mM.

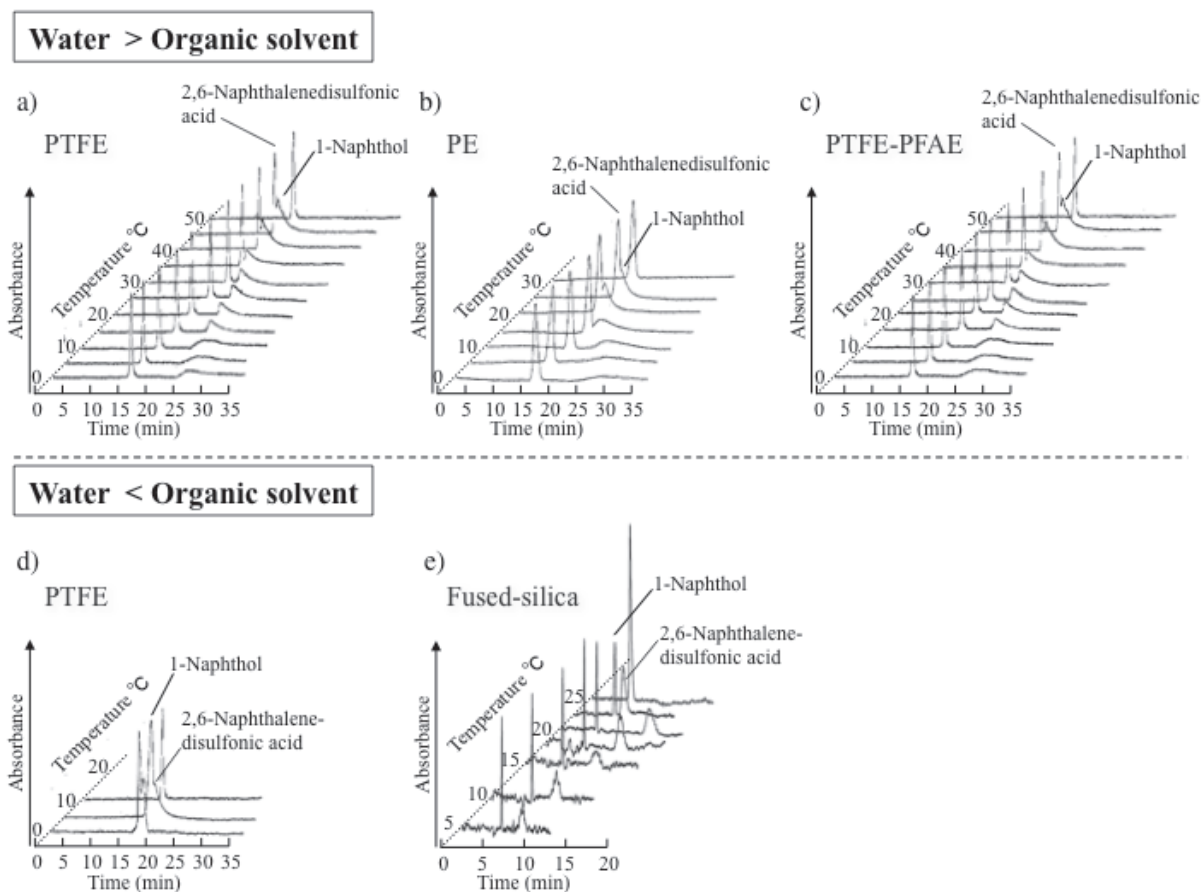


Figure 2. Effects of tube temperature on separation in the TRDC system using various types of capillary tube. Conditions for a) and d): Capillary tube, 110 cm (effective length of 90 cm, the part of it (ca. 60 cm) was dipped in the temperature-controlled water) of 100 μm i.d. PTFE; carrier, water-acetonitrile-ethyl acetate (15:3:2 v/v/v) mixture solution; sample injection, 25 cm height (gravity) \times 10 s; flow rate, 0.5 $\mu\text{L min}^{-1}$; and tube temperature, 0–50 $^{\circ}\text{C}$. Conditions for b) and c): Capillary tube, 110 cm (effective length of 90 cm, the part of it (ca. 60 cm) was dipped in the temperature-controlled water) of 200 μm i.d. PE and 100 μm i.d. PTFE-PFAE; carrier, water-acetonitrile-ethyl acetate (15:3:2 v/v/v) mixture solution; sample injection, 20 cm height (gravity) \times 10 s; flow rate, 2.0 $\mu\text{L min}^{-1}$ for PE and 0.5 $\mu\text{L min}^{-1}$ for PTFE-PFAE; and tube temperature, 0–30 or 50 $^{\circ}\text{C}$. Conditions for e): Capillary tube, 120 cm (effective length of 100 cm, the part of it (ca. 80 cm) was dipped in the temperature-controlled water) of 75 μm i.d. fused-silica; carrier, water-acetonitrile-ethyl acetate (3:8:4 v/v/v) mixture solution; sample injection, 20 cm height (gravity) \times 30 s; flow rate, 0.8 $\mu\text{L min}^{-1}$; and tube temperature, 5–25 $^{\circ}\text{C}$. Analyte concentrations for a) – e): 2,6-Naphthalenedisulfonic acid and 1-naphthol, 1 mM each.

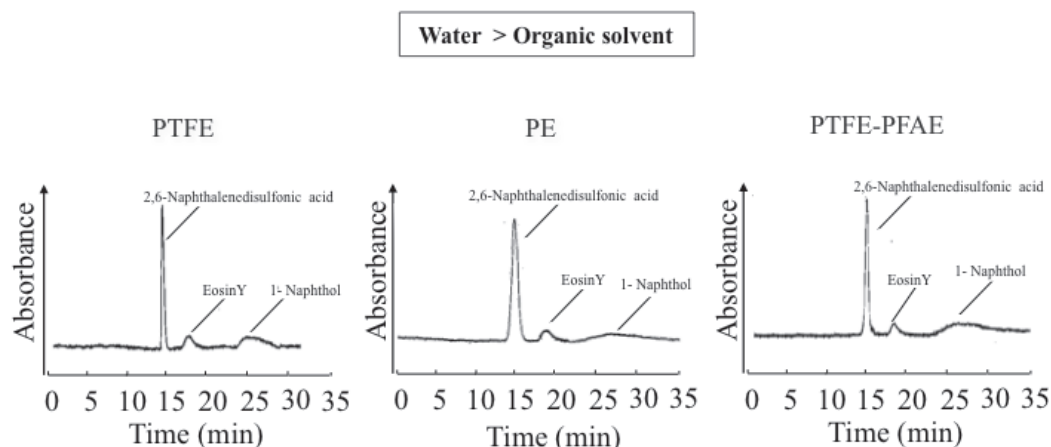


Figure 3. Chromatograms of the mixture analyte solution of 2,6-naphthalenedisulfonic acid, Eosin Y, and 1-naphthol obtained by the TRDC system. Conditions: Capillary tube, 110 cm (effective length: 90 cm) of 100 μm i.d. PTFE, 200 μm i.d. PE, and 100 μm i.d. PTFE-PFAE; carrier, water-acetonitrile-ethyl acetate (15:3:2 v/v/v) mixture solution; sample injection, 20 cm height (gravity) \times 10 s; flow rate, 0.5 $\mu\text{L min}^{-1}$ for PTFE and PTFE-PFAE, and 2.0 $\mu\text{L min}^{-1}$ for PE; temperature, 0 $^{\circ}\text{C}$; and 1-naphthol, 2,6-naphthalenedisulfonic acid, 1 mM, and Eosin Y, 3 mM.

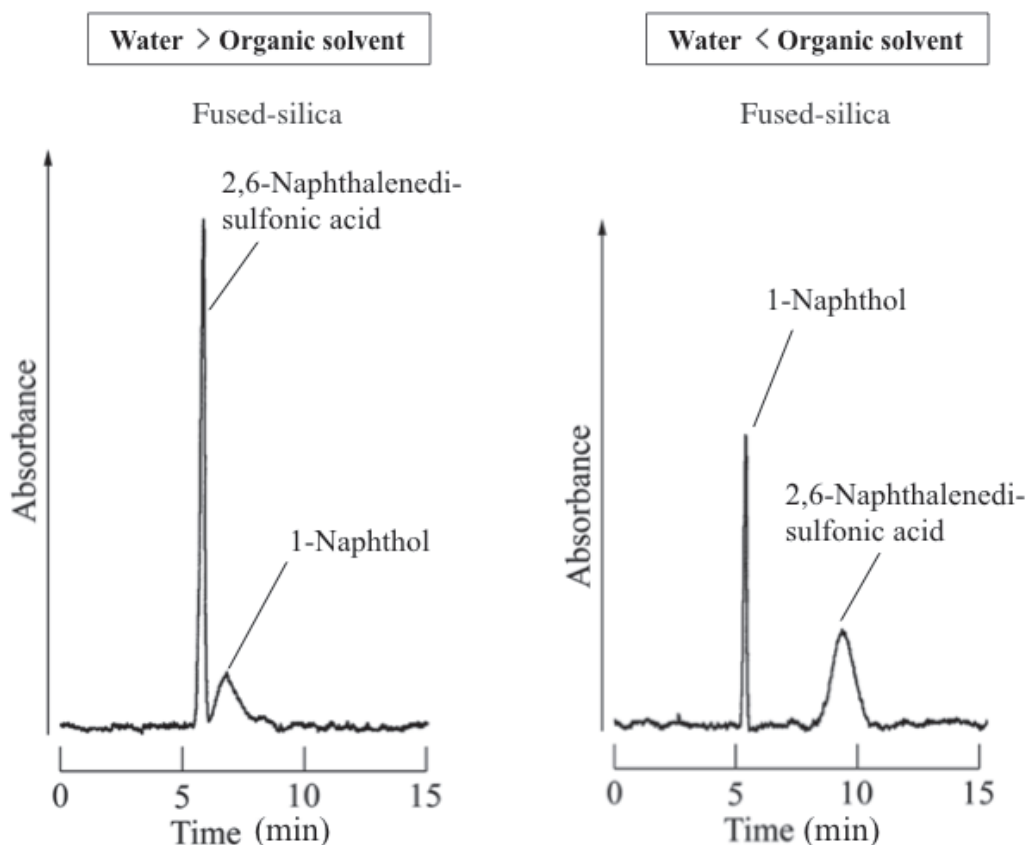


Figure 4. Chromatograms of the mixture analyte solution of 2,6-naphthalenedisulfonic acid and 1-naphthol obtained by the TRDC system using a fused-silica capillary tube. Conditions: Capillary tube, 120 cm (effective length: 90 cm) of 75 μm i.d. fused-silica; carrier, water-acetonitrile-ethyl acetate (15:3:2 and 3:8:4 v/v/v) mixture solution; sample injection, 20 cm height (gravity) \times 30 s; flow rate, 0.8 $\mu\text{L min}^{-1}$; temperature, 20 $^{\circ}\text{C}$; and 1-naphthol and 2,6-naphthalenedisulfonic acid, 1 mM.

References

- [1] H. J. Issaq, K. C. Chan, J. Blonder, X. Ye, and T. D. Veenstra, *J. Chromatogr., A*, **2009**, *1216*, 1825.
- [2] A. C. Otieno and S. M. Mwangela, *Anal. Chim. Acta*, **2008**, *624*, 163.
- [3] K. Tsukagoshi, N. Jinno, and R. Nakajima, *Anal. Chem.*, **2005**, *77*, 1684.
- [4] M. C. Breadmore, J. R. E. Thabano, M. Dawod, A. A. Kazarian, J. P. Quirino, and R. M. Guijt, *Electrophoresis*, **2009**, *30*, 230.
- [5] R. Wu, L. Hu, F. Wang, M. Ye, and H. Zou, *J. Chromatogr., A*, **2008**, *1184*, 369.
- [6] J. Urban and P. Jandera, *J. Sep. Sci.*, **2008**, *31*, 2521.
- [7] K. Slais, M. Horka, and K. Kleparnik, *J. Chromatogr.*, **1992**, *605*, 167.
- [8] R. Swart, J. C. Kraak, and H. Poppe, *Trends Anal. Chem.*, **1997**, *16*, 332.
- [9] J. H. Knox and M. T. Gilbert, *J. Chromatogr.*, 1979, *186*, 405.
- [10] Q. Luo, T. Rejtar, S.-L. Wu, and B. L. Karger, *J. Chromatogr. A*, **2009**, *1216*, 1223.

- [11] K. Otsuka and S. Terabe, *Trends Anal. Chem.*, **1993**, *12*, 125.
- [12] R. Koike, F. Kitagawa, and K. Otsuka, *J. Sep. Sci.*, **2009**, *32*, 399.
- [13] N. W. Smith and Z. Jiang, *J. Chromatogr. A*, **2008**, *1184*, 416.
- [14] K. Tsukagoshi, M. Hashimoto, K. Ichien, S. Gen, and R. Nakajima, *Anal. Sci.*, **1997**, *13*, 485.
- [15] K. Tsukagoshi, M. Hashimoto, M. Otsuka, R. Nakajima, and K. Kondo, *Bull. Chem. Soc. Jpn.*, **1998**, *71*, 2831.
- [16] K. Tsukagoshi, Y. Shimadzu, T. Yamane, and R. Nakajima, *J. Chromatogr. A*, **2004**, *1040*, 151.
- [17] K. Tsukagoshi, K. Nakahama, and R. Nakajima, *Anal. Chem.*, **2004**, *76*, 4410.
- [18] K. Tsukagoshi and S. Shinkai, *J. Org. Chem.*, **1991**, *56*, 4089.
- [19] C. W. Huck and L. Bittner, *Chromatographia*, **2011**, *73*, 29.
- [20] P. L. Garcia, F. P. Gomes, M. I. R. M. Santoro, E. R. M. Kedor-Hackmann, J. L. V. Quero, A. N. Monton, G. C. Montoya, and M. A. Cabrera, *Chromatographia*, **2011**, *73*, 799.
- [21] T. O. Ajimura, K. B. Borges, A. F. Ferreira, F. A. De Castro, and C. M. De Gaitani, *Electrophoresis*, **2011**, *32*, 1885.
- [22] J. Kawase, *Anal. Chem.*, 1980, *52*, 2124.
- [23] T. Hara, K. Tsukagoshi, A. Arai, and T. Iharada, *Bull. Chem. Soc. Jpn.*, **1988**, *61*, 301.
- [24] M. Macka, W. C. Yang, P. Zakaria, A. Shitangkoon, E. F. Hilder, P. Andersson, P. Nesterenko, and P. R. Haddad, *J. Chromatogr. A*, **2004**, *1039*, 193.
- [25] K. Tsukagoshi, S. Ishida, Y. Oda, K. Noda, and K. Nakajima, *J. Chromatogr. A*, **2006**, *1125*, 144.

Chapter 6 Detection methods in tube radial distribution chromatography (TRDC)

In order to expand a range of detectable analytes, fluorescence and chemiluminescence detection was introduced into the TRDC systems in addition to absorption detection. The part of this chapter is reconstructed and rewritten based on a related, published manuscript.¹¹⁾

6.1 Introduction of fluorescence and chemiluminescence detection to TRDC

Fluorescence and chemiluminescence detection were introduced into a tube radial distribution chromatography (TRDC) system using an open fused-silica capillary tube and a water-acetonitrile-ethyl acetate mixture carrier solution. Model analyte mixture solutions, such as Eosin Y and perylene as well as dansyl methionine and perylene, were injected into the capillary tube through the utilization of a gravity method. The analyte solution was subsequently delivered through the capillary tube with the carrier solution by a microsyringe pump; the system worked under laminar flow conditions. The analytes were separated through the tube and detected by on-capillary with fluorescence detection or by end-capillary with chemiluminescence detection by taking advantage of a peroxyoxalate chemiluminescence reaction. Eosin Y and perylene as well as dansyl methionine and perylene were detected in this order with a carrier solution of water-acetonitrile-ethyl acetate (15:3:2 volume ratio), while they were detected in the reverse order with a carrier solution of water-acetonitrile-ethyl acetate (3:8:4 or 2:7:4 volume ratio) with fluorescence or chemiluminescence detection. The elution times of the analytes were reversed by changing the component ratio of the solvents in the carrier solution. A fluorescein isothiocyanate-labeled bovine serum albumin was also analyzed and separated from the coexisting labeling reagent using the present system.

Introduction

Capillary chromatography and related separation technology, including capillary electrochromatography [1,2], capillary electrophoresis [3,4], capillary liquid chromatography [5-7], and hydrodynamic chromatography [8], are among the most active areas of research in chemical engineering, analytical technology, and separation science. A novel capillary chromatography method using an open capillary tube and the use of a water-hydrophilic-hydrophobic organic mixture as a carrier solution was developed. This is called a tube radial distribution chromatography (TRDC) system, which is based on the tube radial distribution of carrier solvents in the capillary tube under laminar flow conditions.

Fluorescence and chemiluminescence detection, as well as absorption detection, have been widely used in many flow analyses, including flow-injection analysis, high-performance liquid chromatography, and capillary electrophoresis, in order to

improve the analytical performance with regards to sensitivity and analytical subjects [9-13]. Here, we have attempted to introduce fluorescence and chemiluminescence detection into the TRDC system.

Experimental

Fused-silica capillary tubes (50 or 75 μm i.d., 150 μm o.d.) were used. Schematic diagrams of the TRDC systems comprised of an open capillary tube and a microsyringe pump equipped with a fluorescence detector and a chemiluminescence detector, as shown in Fig. 1 a) and b), respectively. Fused-silica capillary tubes, 80 cm in length (effective length: 60 cm) and 75 μm i.d. for fluorescence detection, and 90 cm in length and 50 μm i.d. for chemiluminescence detection, were installed in the systems. Mixtures of water-acetonitrile-ethyl acetate at different volume ratios (15:3:2, 2:7:4, and 3:8:4) were used as the carrier solution. Analyte mixture solutions, Eosin Y and perylene mixture as well as dansyl methionine and perylene mixture, were prepared along with the carrier solutions. The analyte solution was introduced directly into the capillary inlet for 10 s from a height of 25 cm for fluorescence detection, or for 10 s from a height of 30 cm for chemiluminescence detection by the gravity method. After analyte injection, the capillary inlet was connected through a joint to a microsyringe which was set on the microsyringe pump. The carrier solution was fed into the capillary tube at a flow rate of $0.2 \mu\text{L min}^{-1}$ for fluorescence and chemiluminescence detection under laminar flow conditions. On-capillary fluorescence detection was carried out for Eosin Y and perylene mixture with ex. 430 nm and em. 520 nm as well as with ex. 360 nm and em. 515 nm for dansyl methionine and perylene mixture. End-capillary chemiluminescence detection was performed through making use of peroxyoxalate chemiluminescence reactions as follows. A flow-type chemiluminescence detection cell (0.5 mm i.d. poly(tetrafluoroethylene) tube) was used (Fig. 1 b)). The chemiluminescence reagent consisting of acetonitrile solution (2 mM bis[2-(3,6,9-trioxadecyloxycarbonyl)-4-nitrophenyl] oxalate (TDPO) and 200 mM hydrogen peroxide) was delivered at the flow rate of $20 \mu\text{L min}^{-1}$ to the capillary outlet in the detection cell where the chemiluminescence reagent and the analytes were mixed to induce chemiluminescence.

Results and discussion

Fluorescence detection The analyte mixture solution of Eosin Y and perylene was examined with the present TRDC system which was outfitted with a fluorescence detector using an open fused-silica capillary and water-acetonitrile-ethyl acetate mixture carrier solution. Eosin Y and perylene were eluted through the capillary tube in this order with the water-acetonitrile-ethyl acetate carrier solution (15:3:2 volume ratio). In addition, they were eluted in the reverse order with the water-acetonitrile-ethyl acetate carrier solution (2:7:4 volume ratio). The chromatograms obtained with the water-rich and organic solvent-rich carrier solutions are shown in Fig. 2 a) and b), respectively. The analyte mixture solution of dansyl methionine and perylene was analyzed in a similar way using the system equipped with a fluorescence detector. Dansyl methionine and perylene were separated and detected in this order with the water-rich carrier

solution and they were detected in the reverse order with the organic solvent-rich carrier solution. The chromatograms thus obtained are shown in Fig. 3 a) and b), respectively.

Chemiluminescence detection The peroxyoxalate chemiluminescence reaction [14] is one of the most important reactions used in various flow systems. Oxalate reagents, such as bis(2,4,6-trichlorophenyl) oxalate (TCPO) and TDPO, react with hydrogen peroxide to give a dioxetane compound as an immediate, which interacts with fluorescent compounds. Energy transfer occurs from the dioxetane compound to the fluorescent compound through a complex formation, and the excited fluorescent compound drops to the ground state, emitting chemiluminescence. These fluorescent compounds can be detected with a high level of sensitivity through chemiluminescence by taking advantage of the peroxyoxalate chemiluminescence reaction. The analyte mixture solution of Eosin Y and perylene was subjected to the present TRDC system equipped with a chemiluminescence detector. They were eluted with the water-acetonitrile-ethyl acetate carrier solution (15:3:2 volume ratio) in this order and in the reverse order with the water-acetonitrile-ethyl acetate carrier solution (3:8:4 volume ratio). The chromatograms obtained with the water-rich carrier solution and the organic solvent-rich carrier solution are shown in Figs. 4 a) and b), respectively. The analyte mixture of dansyl methionine and perylene was examined in a similar way using this system with the chemiluminescence detector. The chromatograms obtained with the water-rich and organic solvent-rich carrier solutions are shown in Fig. 5 a) and b), respectively. Dansyl methionine and perylene were eluted in this order with the water-rich carrier solution and in the reverse order with the organic solvent-rich carrier solution. The detection limits of the fluorescent compounds for fluorescence detection were 10–100 μM order ($S/N=3$), and those for chemiluminescence detection were 1–10 μM order ($S/N=3$), respectively. Chemiluminescence detection provided greater detection sensitivity than fluorescence detection under the present analytical conditions. The data obtained here through fluorescence and chemiluminescence detection suggested that the TRDC system could be applied successfully to the separation and determination of fluorescence-labeled compounds, such as amino acids, peptides, proteins, saccharides, and nucleic acids.

Consideration of the elution order Various mixtures consisting of hydrophilic and hydrophobic molecules as analytes have been examined using the TRDC system with fused-silica, polyethylene, or poly(tetrafluoroethylene) capillary tubes and a water-acetonitrile-ethyl acetate mixture carrier solution. The separation performance in the TRDC system is explained as follows. 1) Water and organic solvents in the carrier solution are not dispersed uniformly in the capillary tube based on the tube radial distribution of the solvents under laminar flow conditions. A major solvent phase (water-rich or organic solvent-rich) forms around the middle of the tube far from the inner wall, while a minor solvent phase (organic solvent-rich or water-rich) is generated near the inner wall of the capillary tube as a pseudo-stationary phase. 2) Hydrophilic molecules in the analyte mixture are subsequently dispersed in the water-rich phase, and hydrophobic molecules are dissolved in the organic solvent-rich phase. 3) The analyte dispersed in the major solvent phase around the middle of the capillary tube is eluted

with near average linear velocity, while the analyte dispersed in the minor solvent phase near the inner wall of the tube is eluted with smaller than average linear velocity; the separation is chromatographically performed through distribution between inner and outer phases. The elution times of the analytes can be easily reversed by changing the component ratio of the solvents in the carrier solution. Eosin Y and dansyl methionine are comparatively hydrophilic compounds and perylene is a hydrophobic compound. The elution orders observed on the chromatograms in Fig. 2–5 were consistent with separation performance based on the tube radial distribution of the carrier solvents in the TRDC system. For example, Eosin Y (hydrophilic) and perylene (hydrophobic) were eluted in this order with the water-rich carrier solution (Fig. 2 a) and Fig. 4 a)) and in the reverse order with the organic solvent-rich carrier solution (Fig. 2 b) and Fig. 4 b)).

Analysis of fluorescence labeled protein Bovine serum albumin as a model protein was labeled with fluorescein isothiocyanate (FITC) which is one of the most useful labeling reagents for biomolecules. Bovine serum albumin (0.5 μmol) and FITC (1.0 μmol) were dissolved in a solution of water-triethylamine (95:5 volume ratio) (100 μL). The mixture was stirred for 1 min and left in the dark for 20 min. After the evaporation of the solvent, the residue was redissolved in the carrier solution (1 mL) to give the analyte solution including an excess (or free)-FITC and FITC-labeled bovine serum albumin (BSA). The mixture of FITC and FITC-labeled BSA was subjected to the TRDC with fluorescence detection. FITC and FITC-labeled BSA were separated and detected in this order with the organic solvent-rich carrier solution, while they were detected in the reverse order with the water-rich carrier solution. Clearly, the elution times of the analytes were changed by altering the component ratios of the carrier solvents. The elution orders obtained from the mixture of FITC and FITC-labeled BSA were reasonable considering the free-FITC more hydrophobic than the FITC-labeled protein. The chromatograms obtained for the mixture of FITC and FITC-labeled BSA as well as the mixture of FITC, FITC-labeled BSA, and perylene that was added to the solution after the labeling procedure are shown in Fig. 6, together with the analytical conditions in the captions. As shown in Fig. 6 b), perylene, FITC, and FITC-labeled BSA were separated and detected in this order with the organic solvent-rich carrier solution. The first peak of perylene on the chromatograms roughly appeared with the average linear velocity and the others, FITC and FITC-labeled BSA peak, were eluted with lower velocity under laminar flow conditions. The average linear velocity was confirmed by the experiment with a normal aqueous carrier solution not including any organic solvents. The elution order of perylene, FITC, and FITC-labeled BSA on the chromatogram was consistent with the nature of hydrophilicity or hydrophobicity of these analytes including the labeled protein. Separation was performed using an untreated open fused silica capillary tube and a water-acetonitrile-ethyl acetate mixture carrier solution without any additives, such as gels, or applying a high voltage. To date, the TRDC has mostly been applied to the analysis of organic compounds with low molecular weights. The results obtained for biopolymer analysis here provide insight to expand the TRDC system to future research.

In conclusion, we attempted to introduce fluorescence and chemiluminescence detection into the TRDC system to extend its analytical performance with regards to both analyte subjects and sensitivity. The model analyte solutions of Eosin Y and perylene mixture as well as dansyl methionine and perylene mixture were separated and detected with fluorescence or chemiluminescence detection in the TRDC system. Chemiluminescence detection was about 10–100 times more sensitive than fluorescence detection in the present TRDC system. The elution times of the analytes of the mixture solution could be easily changed by altering the component ratio of the carrier solvents. The data obtained here suggested that the present TRDC system would be useful for the separation and determination of fluorescence-labeled compounds.

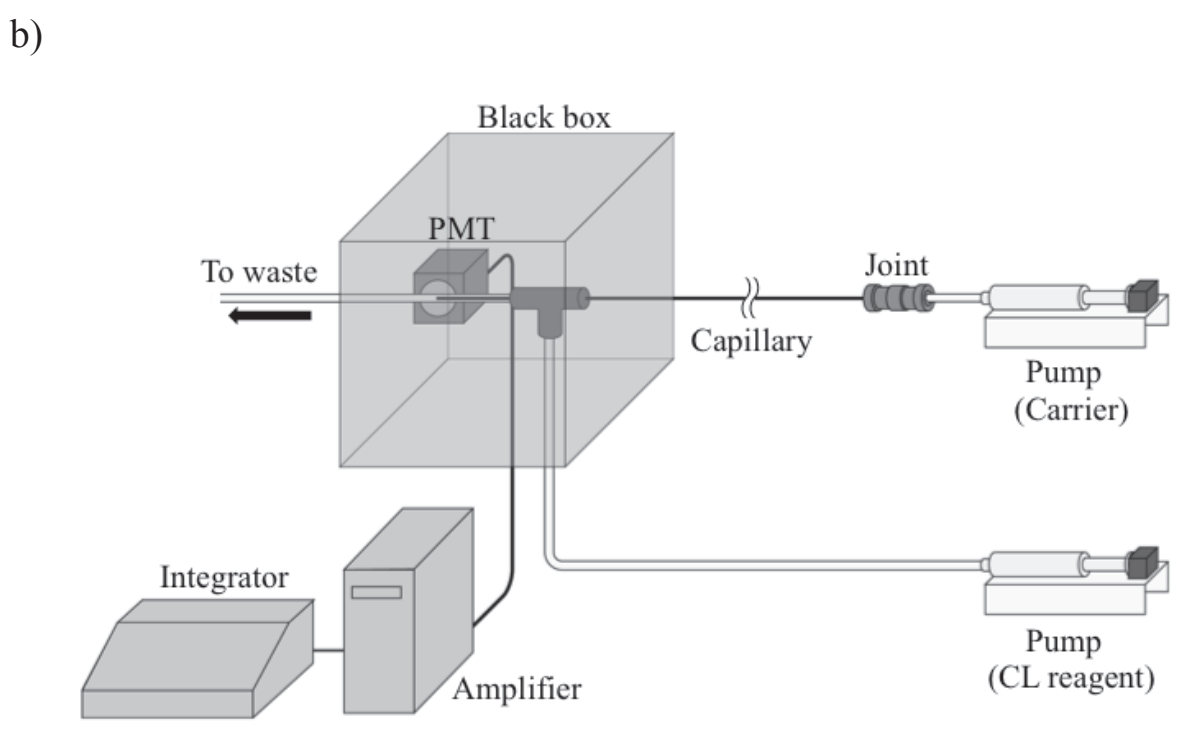
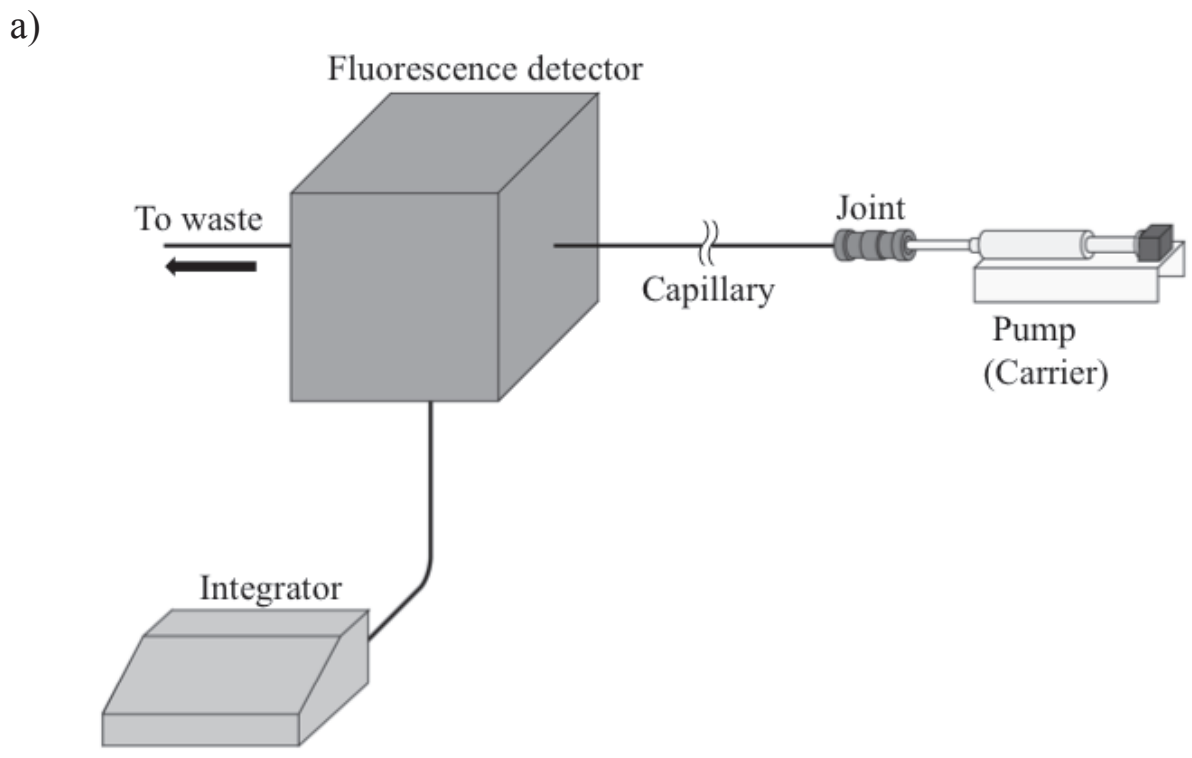


Figure 1. Schematic diagrams of the present TRDC systems with a) fluorescence detection and b) chemiluminescence detection.

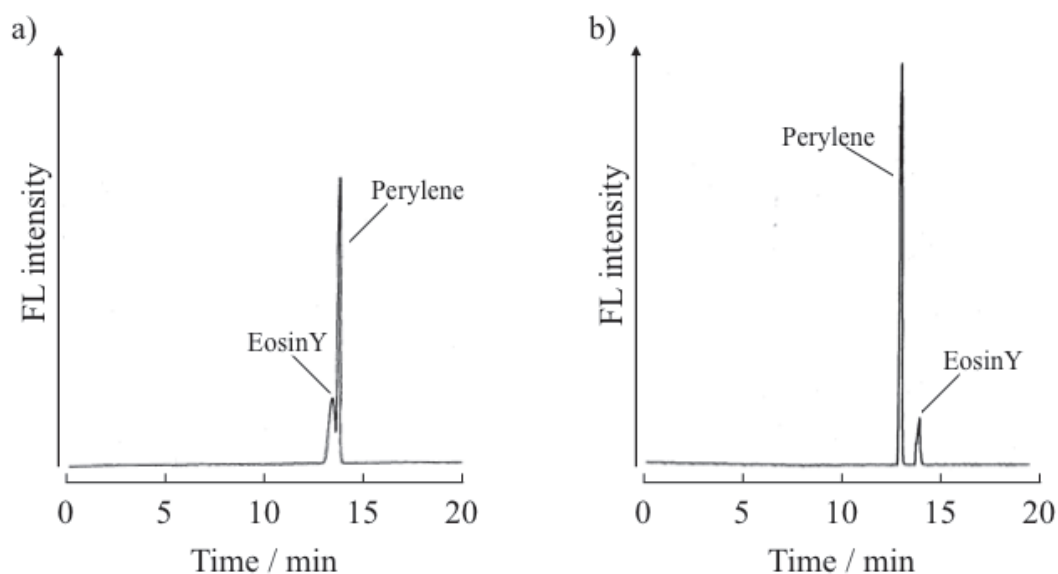


Figure 2. Chromatograms of a mixture of Eosin Y and perylene by the present TRDC system with fluorescence detection. Conditions: Capillary tube, 80 cm (effective length: 60 cm) of 75 μm i.d. fused-silica; carrier, a) water-acetonitrile-ethyl acetate (15:3:2 volume ratio) mixture solution and b) water-acetonitrile-ethyl acetate (2:7:4 volume ratio) mixture solution; sample injection, 25 cm height (gravity) $\times 10$ s; flow rate, 0.2 $\mu\text{L min}^{-1}$; analyte concentration, 1 mM each.

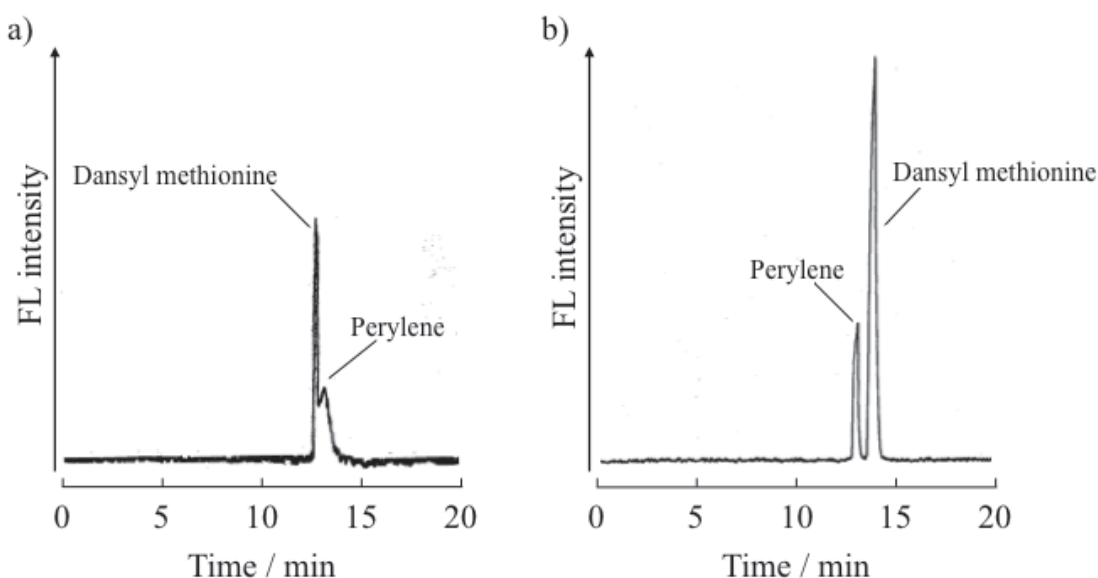


Figure 3. Chromatograms of a mixture of dansyl methionine and perylene by the present TRDC system with fluorescence detection. Conditions: Capillary tube, 80 cm (effective length: 60 cm) of 75 μm i.d. fused-silica; carrier, a) water-acetonitrile-ethyl acetate (15:3:2 volume ratio) mixture solution and b) water-acetonitrile-ethyl acetate (2:7:4 volume ratio) mixture solution; sample injection, 25 cm height (gravity) $\times 10$ s; flow rate, 0.2 $\mu\text{L min}^{-1}$; analyte concentration, 1 mM each.

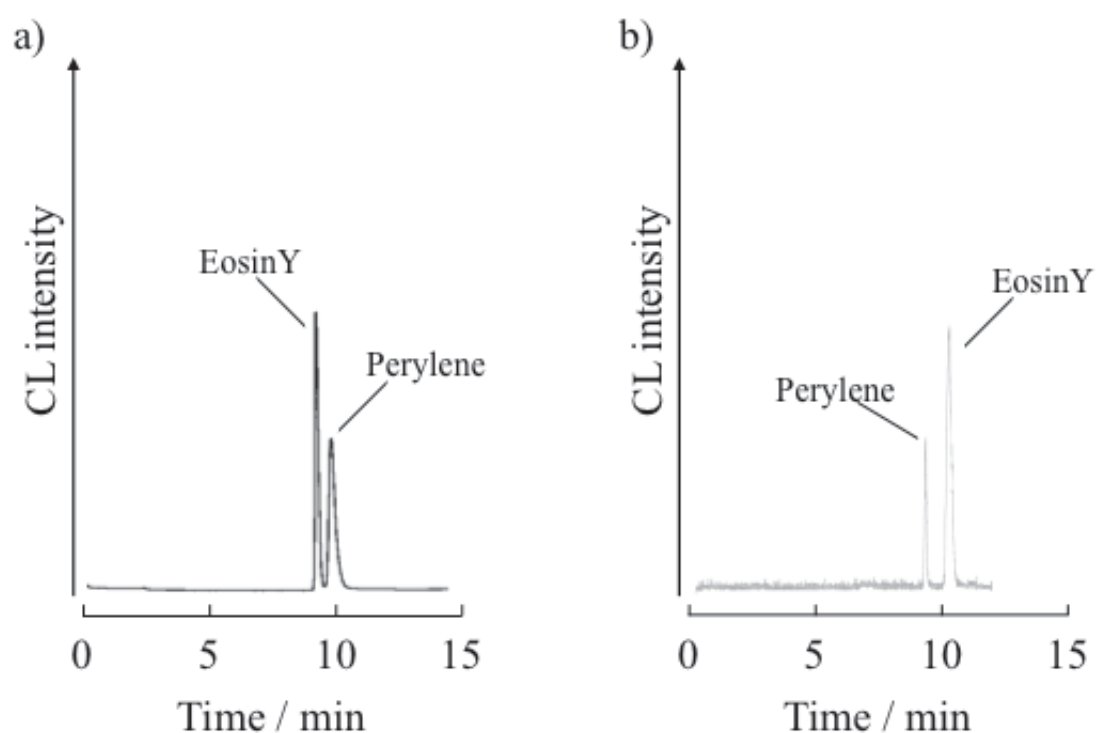


Figure 4. Chromatograms of a mixture of Eosin Y and perylene by the present TRDC system with chemiluminescence detection. Conditions: Capillary tube, 90 cm of 50 μm i.d. fused-silica; carrier, a) water-acetonitrile-ethyl acetate (15:3:2 volume ratio) mixture solution and b) water-acetonitrile-ethyl acetate (3:8:4 volume ratio) mixture solution; sample injection, 30 cm height (gravity) $\times 10$ s; flow rate, 0.2 $\mu\text{L min}^{-1}$; analyte concentration, 50 μM each.

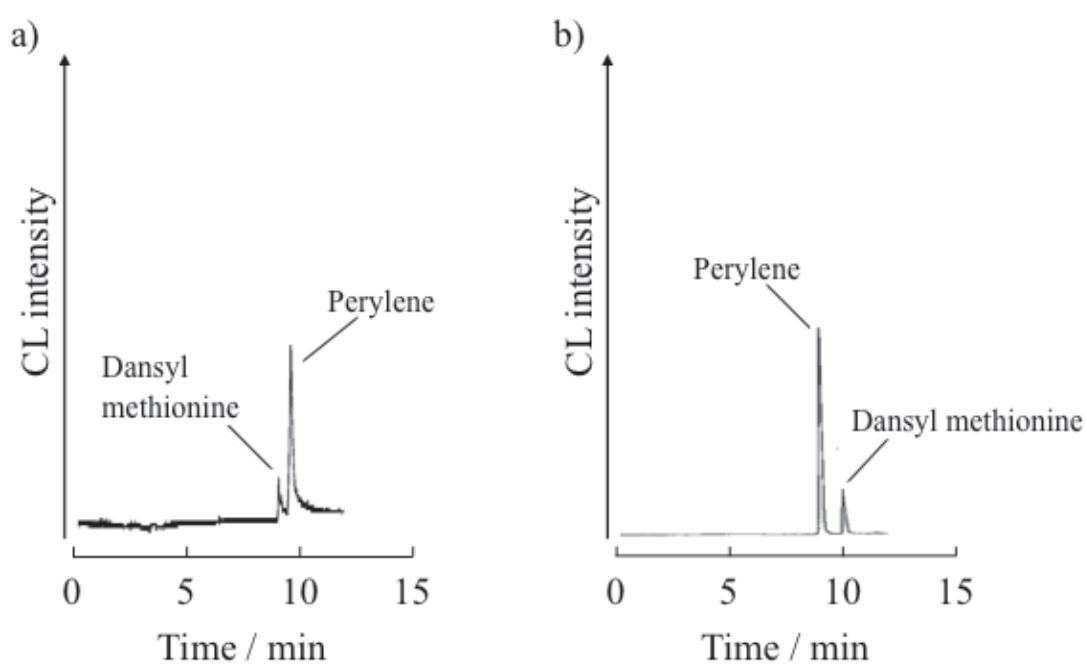


Figure 5. Chromatograms of a mixture of dansyl methionine and perylene by the present TRDC system with chemiluminescence detection. Conditions: Capillary tube, 90 cm of 50 μm i.d. fused-silica; carrier, a) water-acetonitrile-ethyl acetate (15:3:2 volume ratio) mixture solution and b) water-acetonitrile-ethyl acetate (3:8:4 volume ratio) mixture solution; sample injection, 30 cm height (gravity) \times 10 s; flow rate, 0.2 $\mu\text{L min}^{-1}$; analyte concentration, 50 μM each.

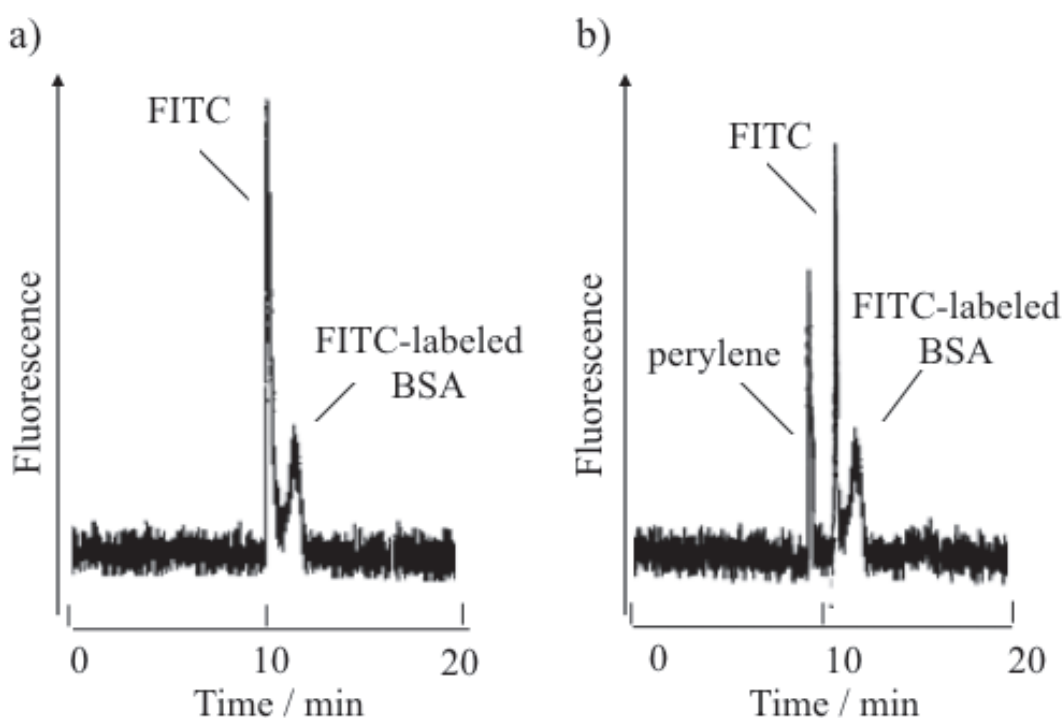


Figure 6. Chromatograms of a) a mixture of FITC and FITC-labeled BSA as well as b) a mixture of perylene, FITC, and FITC-labeled BSA by the present TRDC system with fluorescence detection. Conditions: Capillary tube, 120 cm (effective length: 100 cm) of 50 μm i.d. fused-silica; carrier, water-acetonitrile-ethyl acetate (3:8:4 volume ratio) mixture solution; sample injection, 30 cm height (gravity) \times 30 s; flow rate, 0.2 $\mu\text{L min}^{-1}$; fluorescence detection, ex. 495 nm and em. 520 nm; analyte concentration, 1 mM perylene and 0.5 mM FITC-labeled BSA.

References

- [1] H. J. Issaq, K. C. Chan, J. Blonder, X. Ye, and T. D. Veenstra, *J. Chromatogr. A*, **2009**, *1216*, 1825.
- [2] A. C. Otieno, and S. M. Mwangela, *Anal. Chim. Acta*, **2008**, *624*, 163.
- [3] K. Tsukagoshi, N. Jinno, and R. Nakajima, *Anal. Chem.*, **2005**, *77*, 1684.

- [4] M. C. Breadmore, J. R. E. Thabano, M. Dawod, A. A. Kazarian, J. P. Quirino, and R. M. Guijt, *Electrophoresis*, **2009**, *30*, 230.
- [5] M. C. Jung, N. Munro, G. Shi, A. C. Michael, and S. G. Weber, *Anal. Chem.*, **2006**, *78*, 1761.
- [6] J. Urban and P. Jandera, *J. Sep. Sci.*, **2008**, *31*, 2521.
- [7] T. Charoenraks, M. Tabata, and K. Fujii, *Anal. Sci.*, **2008**, *24*, 1239.
- [8] T. Okada, M. Harada, and T. Kido, *Anal. Chem.*, **2005**, *77*, 6041.
- [9] L. Gámiz-Gracia, A. M. García-Campaña, J. F. Huertas-Pérez, and F. J. Lara, *Anal. Chim. Acta*, **2009**, *640*, 7.
- [10] K. Tsukagoshi, M. Tahira, and R. Nakajima, *Anal. Sci.*, **2003**, *19*, 1019.
- [11] K. Tsukagoshi, K. Matsumoto, F. Ueno, K. Noda, R. Nakajima, and K. Araki, *J. Chromatogr. A*, **2006**, *1123*, 106.
- [12] G. Rammouz, M. Lacroix, J. C. Garrigues, V. Poinso, and F. Couderc, *Biomed. Chromatogr.*, **2007**, *21*, 1223.
- [13] Z. Yang, X. Wang, W. Qin, and H. Zhao, *Anal. Chim. Acta*, **2008**, *623*, 231.
- [14] "Chem- and Bioluminescence", ed. J. G. Burr, 1985, Chap. 5, Marcel Dekker, Inc.

Chapter 7 Development of microchip-tube radial distribution chromatography (microchip-TRDC)

We tried to apply the TRDC to a microchip device. The TRDC system was well matched to the concept of micro-total analysis system (μ -TAS) or lab on a microchip. The microchip-TRDC with chemiluminescence detection was developed. The part of this chapter is reconstructed and rewritten based on related, published manuscripts.^{36,40)}

7.1 Microchip-TRDC with chemiluminescence detection

A capillary chromatography system has been developed using a ternary mixed solvents solution, i.e., water-hydrophilic/hydrophobic organic solvent mixture as a carrier solution. Here, we tried to carry out the chromatographic system on a microchip incorporating the open-tubular microchannels. A model analyte solution of isoluminol isothiocyanate (ILITC) and ILITC-labeled biomolecule was injected to the double T-junction part on the microchip. The analyte solution was delivered in the separation microchannel (40 μm deep \times 100 μm wide \times 22 cm long) with the ternary water-acetonitrile-ethyl acetate mixture carrier solution (3:8:4 volume ratio; the organic solvent-rich or 15:3:2 volume ratio; the water-rich). The analyte, free-ILITC and labeled bovine serum albumin (BSA) mixture, was separated through the microchannel, where the carrier solvents were radially distributed in the separation channel generating inner and outer phases. The outer phase acts as a pseudo-stationary phase under laminar flow conditions in the system. The ILITC and the labeled BSA were eluted and detected through a chemiluminescence reaction.

Introduction

Our group reported the tube radial distribution phenomenon (TRDP) of carrier solvents under microfluidic flow conditions in 2009. When the ternary mixed solvents of water-hydrophilic/hydrophobic organic solvent mixture are delivered into a microspace, such as a microchannel or a capillary tube, the solvent molecules are radially distributed in the microspace generating inner and outer phases. A capillary chromatography system based on the TRDP in which the outer phase acts as a pseudo-stationary phase under laminar flow conditions has been developed. We call the separation method tube radial distribution chromatography (TRDC). All of TRDC systems have been performed by using various types of capillary tubes. Miniaturization on a microchip incorporating the microchannels has not been applied to the TRDC system.

Microchip devices are among the most active areas of research in chemical engineering, analytical technology, and separation science. Such research areas were well known as micro-total analysis systems (μ -TAS) or Lab on a Chip [1]. As one of these, microchip-electrophoresis is widely investigated as a small and rapid separation method. However, the microchip-electrophoresis necessarily needs a voltage supplier device and electrodes. Also, capillary chromatography as a microfluidic analysis requires specific separation columns, such as monolithic or packed channels or tubes.

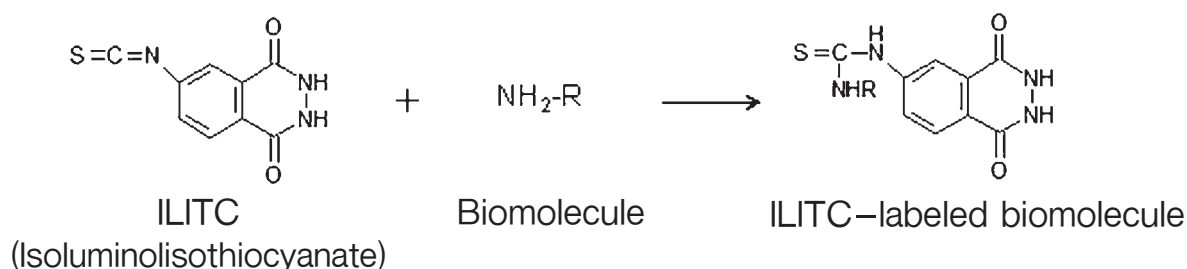
Although they might improve the separation performance, such as resolutions, they are time-consuming and boring for the preparation and cost the users a great deal.

Here we tried to carry out the TRDC system on a microchip, i.e., microchip-TRDC system. Furthermore, detection on the microchip was performed with chemiluminescence (CL) reactions. The ILITC and ILITC-labeled biomolecule mixtures were used as model analytes, referring to the previous paper.²⁵⁾ Biomolecule analysis, such as protein and enzyme are interesting and useful in bioscience, however it has some problems in μ -TAS such as adsorption onto a microspace wall. The microchip-TRDC system with CL detection will bring out new research area in the TRDP and TRDC.

Experimental

Microchip-TRDC system with CL detection A microchip made of glass was manufactured with Microchemical Technology (Kanagawa, Japan). Fig. 1 illustrates the microchip and microchip-holder used herein. The microchannels were 100 μm wide and 40 μm deep, except the microchannel line (400 μm wide and 100 μm deep) for the hydrogen peroxide solution. The microchip-TRDC system comprised a microchip, a microsyringe pumps, and a CL detector. A water-acetonitrile-ethyl acetate mixture (3:8:4 volume ratio; the organic solvent-rich solution or 15:3:2 volume ratio; the water-rich solution) was used as the carrier solution for chromatography, where the water component was 10 mM carbonate buffer at pH 11.8 including 4 μM microperoxidase.

Labeling procedure Bio-macromolecules, such as BSA (Mw; 66000) and alcohol dehydrogenase from yeast (ADH) (Mw; 148000), were labeled with ILITC as follows: biomolecules (0.5 μmol) and ILITC (1.0 μmol) were dissolved in a solution of water-triethylamine (95:5 volume ratio) (100 μL). The mixture was stirred for 1 min and left in the dark for 20 min. After evaporation of the solvent, the residue was redissolved into the carrier solution (1000 μL) to produce an analyte solution, including excess (or free)-ILITC and ILITC-labeled biomolecules.



Hydrophobic-modified microchannel preparation First, 1.0 vol% trichloro (octadecyl) silane toluene solution was fed into the microchannel from the point C at a flow rate of 10 $\mu\text{L min}^{-1}$ for 10 min. Next, toluene solution was fed at a flow rate of 100 $\mu\text{L min}^{-1}$ for 100 min. Then, chloroform solution was fed at a flow rate of 100 $\mu\text{L min}^{-1}$

for 10 min. Finally, the microchannel was heated by thermo-controller at 150 °C for 30 min.

Fluorescence microscope-CCD camera system The microchip was set up so that the fluorescence microscope-CCD camera system could confirm the tube radial distribution of the carrier solvents, i.e., TRDP. The carrier solution, water–acetonitrile–ethyl acetate mixture including perylene (em. 470 nm; blue) and Eosin Y (em. 550 nm; green), was delivered into the separation channel in the same way as the preparation procedure mentioned above. The fluorescence at the four points in the microchannel was monitored using a fluorescence microscope equipped with an Hg lamp, a filter, and a CCD camera.

Analytical procedure in the TRDC The analytical procedure was carried out by the following three steps; 1) preparation, 2) sample load, and 3) analysis. The schematic illustration is shown in Fig. 2. The analyte (sample) and carrier solutions were delivered into the microchannels from points S and C with the microsyringe pumps, pumps A and B, respectively. In 1) preparation, the microchannel from point S to double T-junction was first filled with the analyte solution with pump A. The carrier solution was then fed into the separation channel (from double T-junction to detection point) and the waste channel (from detection point to point W) at the flow rate 10 $\mu\text{L min}^{-1}$ with pump B, where the organic solvent-rich carrier solution divided into the two channels, the separation and waste channels, with 1:24 ratio due to their back pressures as well as where the water-rich carrier solution divided into the two channels with 1:9 ratio due to their back pressures that might be larger in the hydrophobic-modified channel than in the bare microchannel. In 2) sample load, the analyte solution was fed by pump A with 5 $\mu\text{L min}^{-1}$ for 10 s, while, pump B did not feed the carrier solution. After that, in 3) analysis, the carrier solution was fed into the separation and waste channels again as mentioned in the above-preparation procedure, while, the pump A did not feed the analyte solution. 50 mM hydrogen peroxide (10 mM carbonate buffer; pH 10.8) was delivered to the microchannel from points H to HW at the flow rate of 5 $\mu\text{L min}^{-1}$ with pump X. The analytes were mixed with the hydrogen peroxide solution in the detection point to induce CL. The CL was detected with a photomultiplier tube (PMT). Microchannels were cooled with ice through the experiments to keep the TRDP well.

Results and discussion

The TRDP and the microchip design The TRDP appears through phase separation from homogeneous solution to heterogeneous solution including two phases with pressure and temperature changes. The phase separation with associated changes forms an upper and lower phase in a batch vessel under the control of gravity. At the same time, the phase separation introduces TRDP, including inner and outer phases in a micro-flow where it is under laminar flow conditions with minimal control by gravity. When the ternary mixed solvent mixture, i.e., water–hydrophilic/hydrophobic organic solvent mixture, is delivered into a microspace, the solvent molecules are radially distributed in the microspace regardless of the material (fused silica, polyethylene, and

PTFE). In the microspace, with an organic-solvent-rich solution, an organic-solvent-rich major phase is generated around the middle of the microspace as an inner phase, while a water-rich minor phase is formed near the inner wall as an outer phase. In contrast, with a water-rich solution, the water-rich major phase is generated as an inner phase, while the organic-solvent-rich minor phase is formed as an outer phase. The microchip incorporating the microchannels used in this study was designed with reference to our previous papers and other groups' papers regarding microchip-electrophoresis [2-6]. The injection protocol was also introduced on the microchip system with reference to our previous paper where the sample introduction into the capillary was made hydrodynamically by pressure, caused by the flow of the sample solution [7].

Fluorescence photographs and chromatogram with the organic solvent-rich carrier solution The obtained fluorescence photographs with the organic solvent-rich carrier solution are shown in Fig. 3 together with the conditions. The carrier solution containing fluorescence dyes was fed into the separation channel and the waste channel. The organic solvent-rich major phase including perylene (blue) generated in the middle of the center of the microchannel as an inner phase. While, the water-rich minor phase including relatively hydrophilic Eosin Y (green) was formed near the inner wall of the channel as an outer phase. A bare or untreated microchannel in glass-microchip was used because the water-rich outer phase was reported to be more stable on the inner wall of a fused-silica tube than that of a polymer tube in our paper.²²⁾ The TRDP with the organic solvent-rich carrier solution, generating inner organic solvent-rich and outer water-rich phases, were consistent and reasonable with our previously recorded data and the TRDP concept.^{14,15,17)} The obtained chromatogram with the organic solvent-rich carrier solution is shown in Fig. 4. The experimental conditions described in the experimental session were determined, referring to analytical conditions previously reported by our group.^{19,24,25)} With the organic solvent-rich carrier solution the water-rich minor outer phase worked as a pseudo-stationary phase under laminar flow conditions in the TRDC. Relatively hydrophobic free- or excess-ILITC that distributed in the organic solvent-rich major inner phase was eluted first and relatively hydrophilic ILITC-labeled BSA that distributed in the water-rich minor outer phase was detected on the chromatogram afterwards. The outer phase constructed with the alkaline water-rich solution (pH of the water component is 11.8) may minimize adsorption of ILITC-labeled BSA onto the inner wall. The peaks were identified with the individual analyte solutions. The elution behavior of the analytes was quite similar to that obtained with the TRDC system using a fused-silica capillary tube in our previous paper.²⁵⁾ ILITC-labeled BSA could be determined in the range of 2.5 – 50 mM with the detection limit of 2.5 mM (S/N=3). The resolutions (R_s) and the theoretical plate numbers (N) were calculated to be 4.4 and 7800, respectively, for ILITC-labeled BSA analysis. CL detection in a microchip relatively shows poor sensitivity due to a small sample volume [20]. But we will try to improve the sensitivity in the present system through the detailed examination of the analytical conditions.

Fluorescence photograph and chromatogram with the water-rich carrier solution The obtained fluorescence photographs with the water-rich carrier solution are shown in Fig. 5 together with the conditions. A hydrophobic-modified microchannel was used for

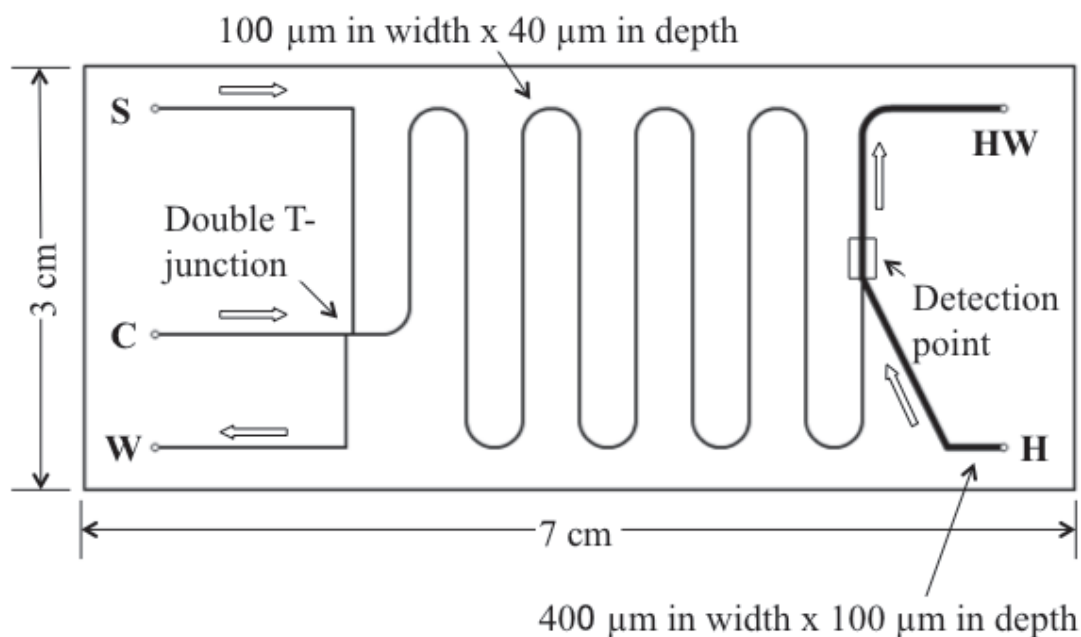
the water-rich carrier solution because the organic solvent-rich outer phase was more stable on the inner-wall of a polymer tube than that of a fused-silica tube.²²⁾ The carrier solution containing fluorescence dyes was fed into the separation and waste channels. In this case, the water-rich major phase including Eosin Y (green) generated in the middle of the center of the microchannel as an inner phase. While, the organic solvent-rich minor phase including perylene (blue) was formed near the inner wall of the channel as an outer phase. The TRDP with the water-rich carrier solution, in contrast to the organic solvent-rich carrier solution, generating inner water-rich and outer organic solvent-rich phases, were consistent and reasonable with our previous data and the TRDP concept.^{14,15,17)} The obtained chromatogram with the water-rich carrier solution is shown in Fig. 6. A hydrophobic-modified microchannel was used for the water-rich carrier solution. In contrast to the chromatogram obtained with the organic solvent-rich carrier solution, relatively hydrophilic ILITC-labeled BSA was first detected, followed by relatively hydrophobic free-ILITC detection. But baseline separation was not obtained between the two peaks under the present analytical conditions. The outer phase constructed with the organic solvent-rich solution may lead to adsorption of free-ILITC onto the inner wall and thus peak broadening. The peaks were identified with the individual analyte solutions.

Chromatogram of ADH We also analyzed a mixture of free-ILITC and ILITC-labeled ADH. We are interested in bio-macromolecules that are generally difficult to determine with capillary zone electrophoresis comprising an open-tubular capillary tube and no additive-containing carrier solution. ADH is a much larger biomolecule than BSA and is easily labeled with ILITC. The obtained chromatogram of ADH with the organic solvent-rich carrier solution and untreated fused-silica capillary tube is shown in Fig. 7. Free-ILITC was first eluted and secondly ILITC-labeled ADH was detected on the chromatogram. As the organic solvent-rich solution was used as a carrier solution, relatively hydrophobic free-ILITC was first detected, followed by relatively hydrophilic ILITC-labeled ADH detection. The outer phase constructed with the alkaline water-rich solution (pH of the water component is 11.8) may also minimize adsorption of ILITC-labeled ADH onto the inner wall. The peaks were identified with individual analyte solutions. The elution behavior of the analytes was similar to that obtained with the TRDC system using a fused-silica capillary tube in our paper. ADH was more insoluble than BSA in water maybe due to the larger molecular weight. ADH may aggregate partially through the labeling procedure and make larger hydrophobic macromolecules to give unknown peaks. Then, the unknown peaks appeared in earlier elution time than ILITC and lacked reproducibility. It was confirmed that the ILITC-labeling technique was useful for analyzing biomolecules having an amino group, such as amino acid, peptide, protein, and enzyme, in the TRDC system. We plan to examine a specific protein, such as a cancer marker, in the simple and economical separation system, that is, the microchip-TRDC.

In conclusion, the TRDC based on the TRDP was successfully developed on the microchip, leading to the microchip-TRDC system. The model analyte mixture of free-ILITC and ILITC-labeled BSA as well as free-ILITC and ILITC-labeled ADH were analyzed with the microchip-TRDC system. The system worked without applying

a voltage supplier device like a microchip-electrophoresis and specific columns, such as packed and monolithic, like normal capillary chromatography. In addition, the analytes were detected with CL reaction. The CL detection did not require any light source or wavelength discrimination. Consequently, the present microchip-TRDC system with CL detection was simple and matched to the concept of μ -TAS or Lab on a Chip. We reported unique extraction and mixing methods based on TRDP on a microchip. If we combine these techniques of separation, extraction, and mixing based on the TRDP, on a microchip, we will be able to develop a novel type of Lab on a Chip system based on TRDP.

a)



b)

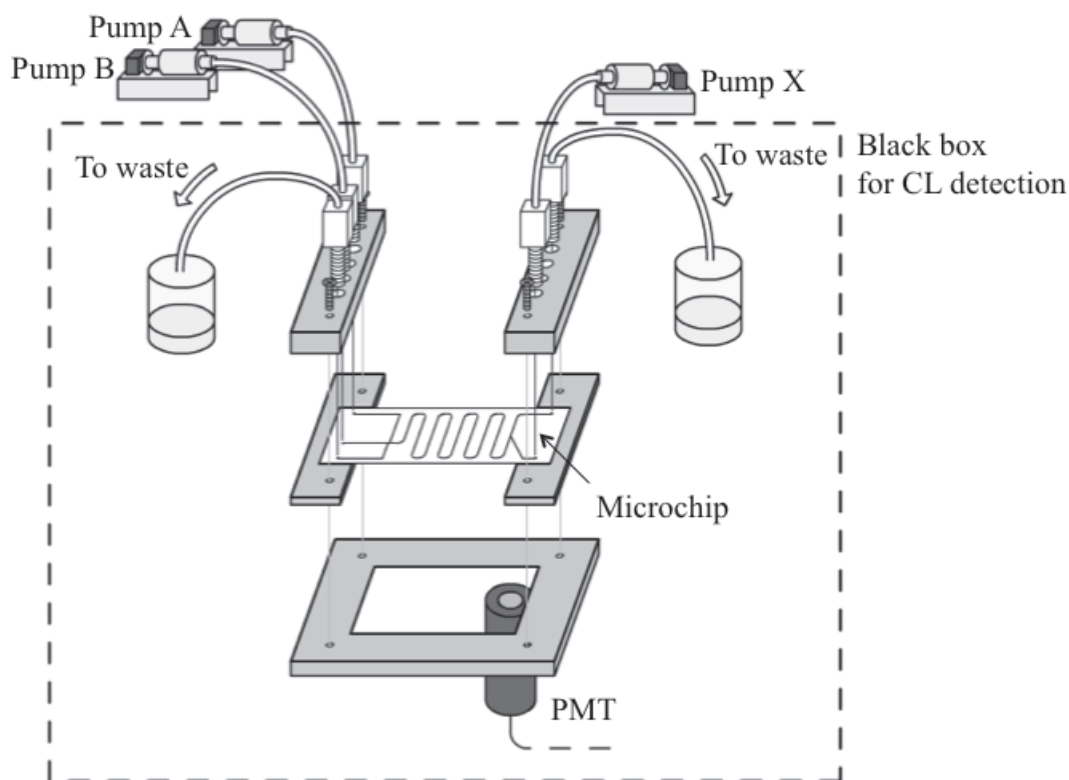


Figure 1. Schematic diagram of a) microchip incorporating the microchannels and b) microchip-holder. S, sample (analyte) solution delivery point; C, carrier solution delivery point; W, analyte or carrier solution waste point; H, hydrogen peroxide solution delivery point; and HW, hydrogen peroxide solution waste point.

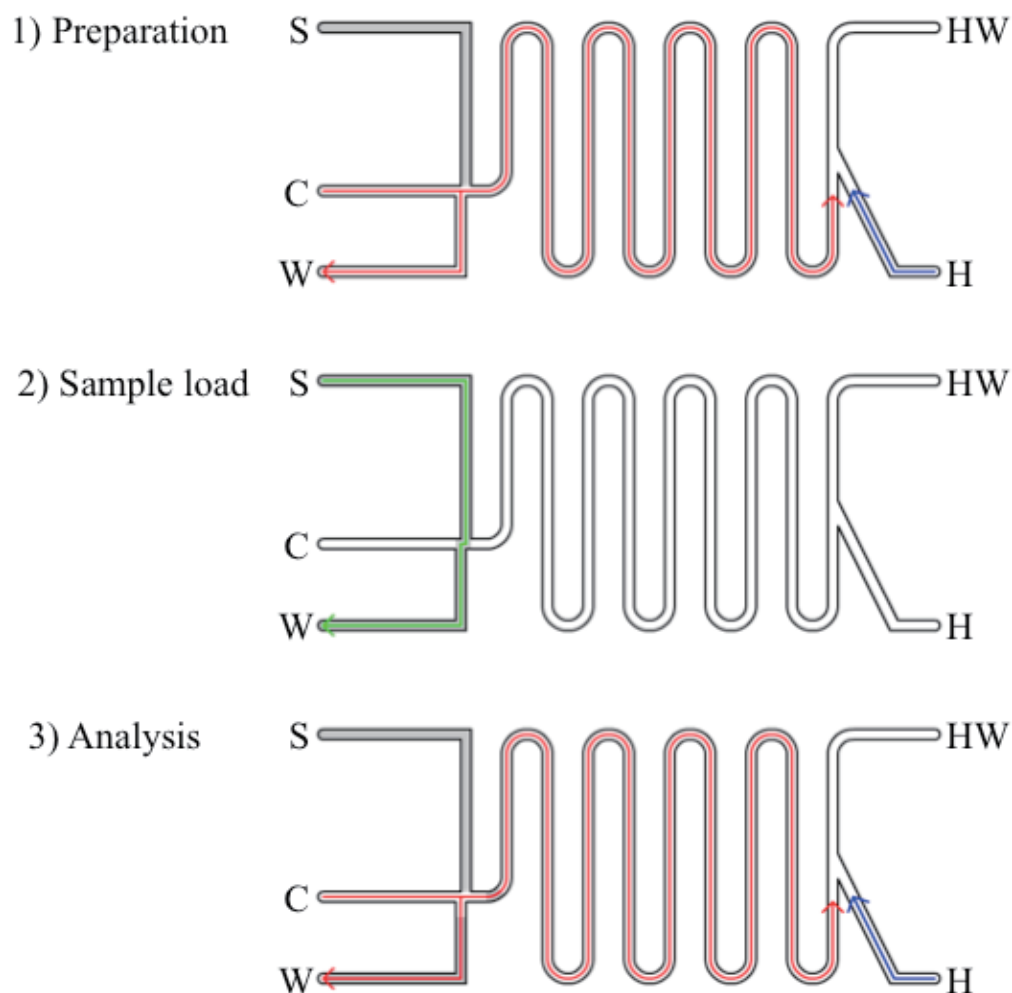


Figure 2. Schematic illustration of analytical procedures, 1) preparation, 2) sample load, and 3) analysis. S, sample (analyte) solution delivery point; C, carrier solution delivery point; W, analyte or carrier solution waste point; H, hydrogen peroxide solution delivery point; and HW, hydrogen peroxide solution waste point.

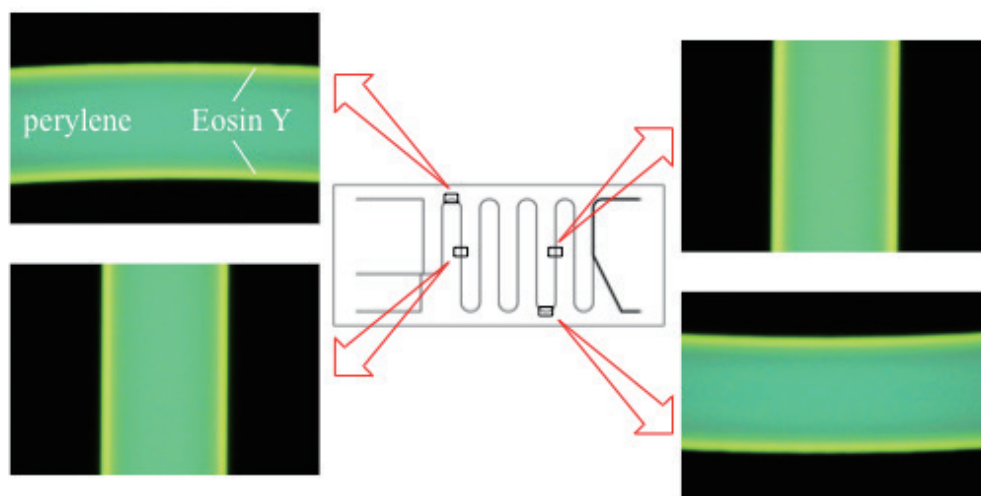


Figure 3. Fluorescence photographs of the organic solvent-rich carrier solution including perylene and Eosin Y fed into the separation microchannel. Carrier, water-acetonitrile-ethyl acetate (3:8:4 volume ratio) containing 0.1 mM perylene and 1 mM Eosin Y.

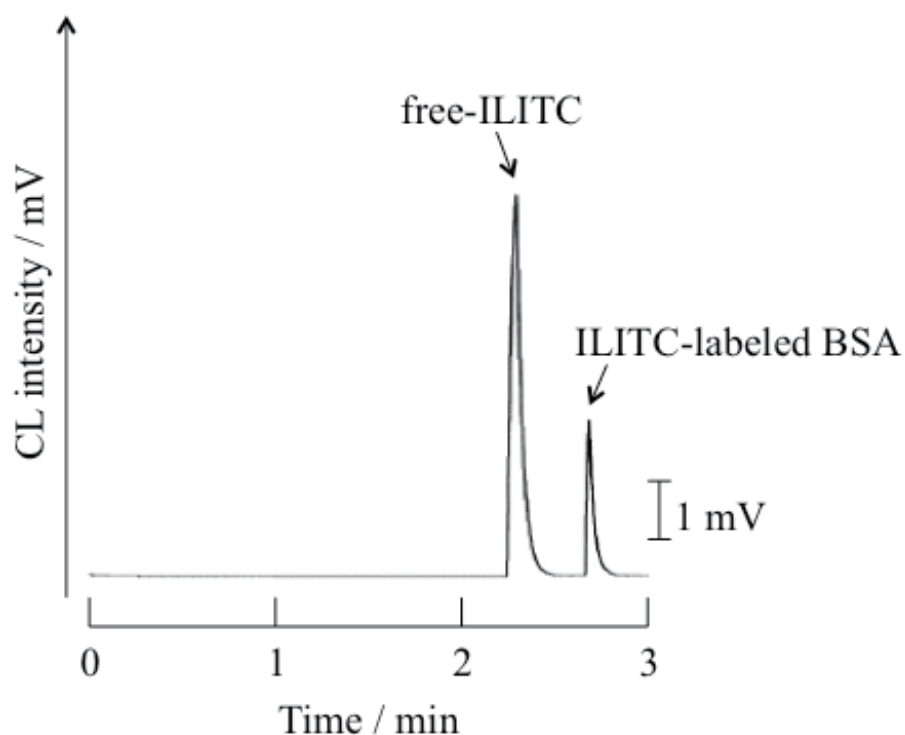


Figure 4. Chromatogram of free-ILITC and ILITC-labeled BSA mixture obtained with the microchip-TRDC system using the organic solvent-rich carrier solution. Carrier, water-acetonitrile-ethyl acetate (3:8:4 volume ratio) and analyte, 50 μ M ILITC-labeled BSA.

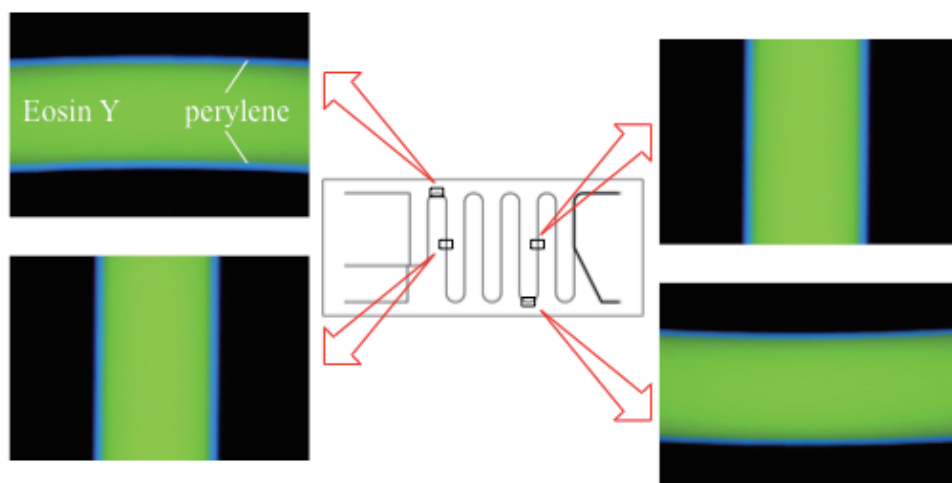


Figure 5. Fluorescence photographs of the water-rich carrier solution including perylene and Eosin Y fed into the separation microchannel. Carrier, water-acetonitrile-ethyl acetate (80:20:9 volume ratio) containing 0.1 mM perylene and 0.5 mM Eosin Y.

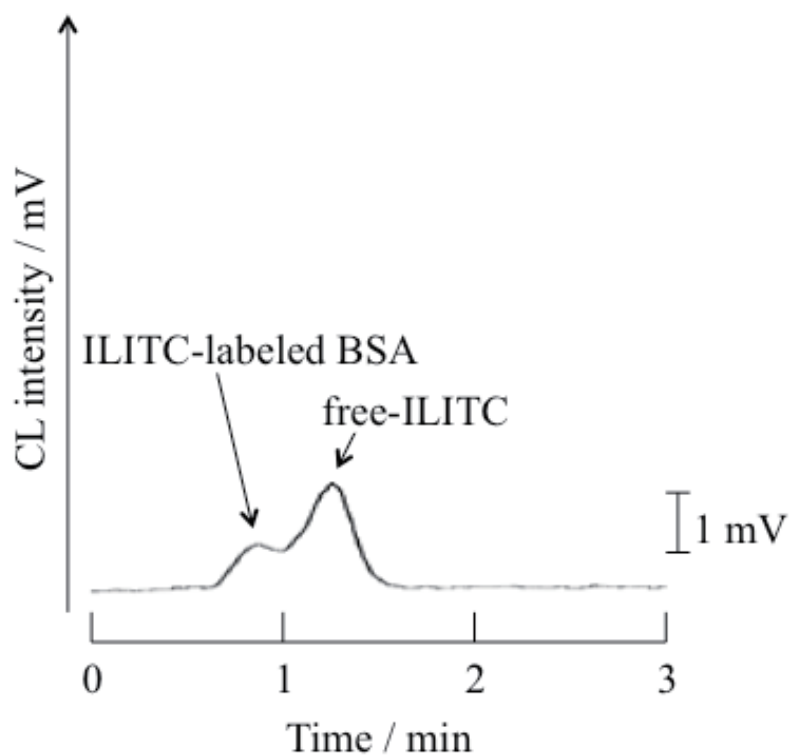


Figure 6. Chromatogram of free-ILITC and ILITC-labeled BSA mixture obtained with the microchip-TRDC system using the water-rich carrier solution. Carrier, water-acetonitrile-ethyl acetate (15:3:2 volume ratio) and analyte, 50 μ M ILITC-labeled BSA.

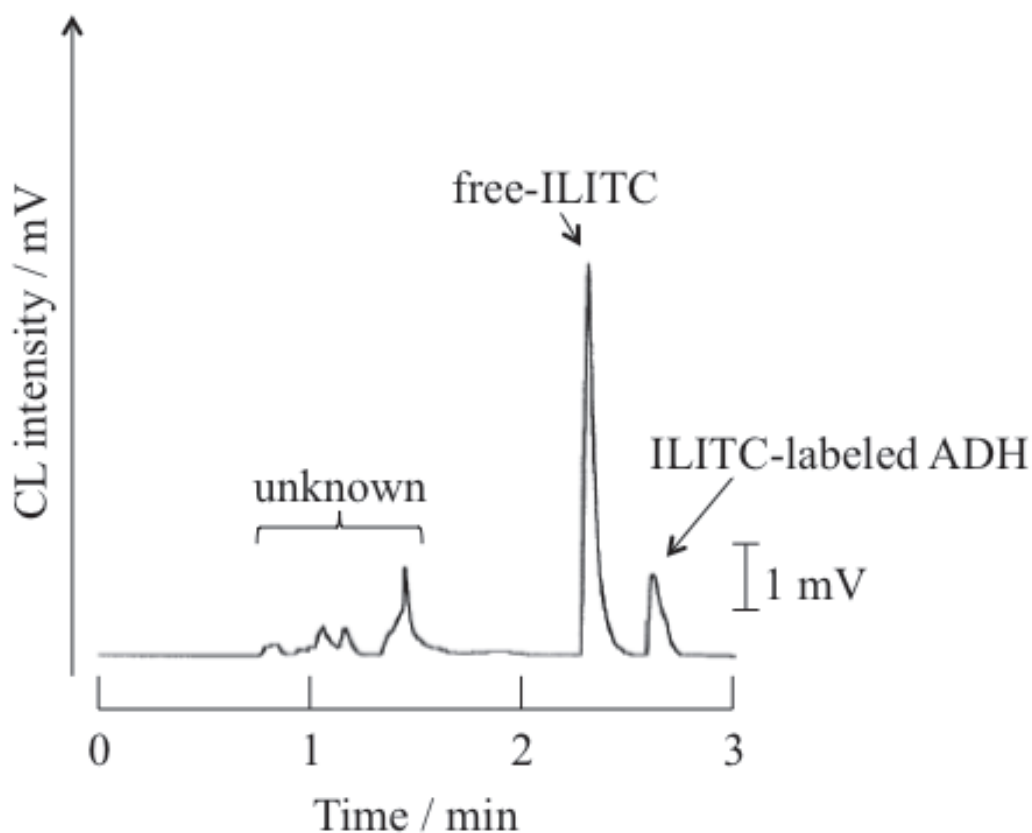


Figure 7. Chromatogram of free-ILITC and ILITC-labeled ADH mixture obtained with the microchip-TRDC system using the organic solvent-rich carrier solution. Carrier, water-acetonitrile-ethyl acetate (3:8:4 volume ratio) and analyte, 50 μ M ILITC-labeled ADH.

References

- [1] Y. Fujii, T. G. Henares, K. Kawamura, T. Endo, H. and Hisamoto, *Lab. Chip*, **2012**, *12*, 1522.
- [2] M. Hashimoto, K. Tsukagoshi, R. Nakajima, K. Kondo, and A. Arai, *J.Chromatogr. A*, **2000**, *867*, 271.
- [3] K. Tsukagoshi, N. Jinno, and R. Nakajima, *Anal. Chem.*, **2005**, *77*, 1684.
- [4] K. Tsukagoshi, T. Saito, and R. Nakajima, *Talanta*, **2008**, *77*, 514.
- [5] B.-F. Liu, M. Ozaki, Y. Utsumi, T. Hattori, and S. Terabe, *Anal. Chem.*, **2003**, *75*, 36.
- [6] R. Su, J.-M. Lin, , K. Uchiyama, and M. Yamada, *Talanta*, **2004**, *64*, 1024.
- [7] K. Tsukagoshi, K. Nakahama, and R. Nakajima, *Anal. Sci.*, *b*, **20**, 379.

Chapter 8 Examination of various types of analytes with tube radial distribution chromatography (TRDC)

Various types of analytes, such as organic compounds, amino acids, peptides, proteins, nucleosides, metal ions, metal complexes, fluorescent compounds, lambda-DNA, polymer compounds, and optical isomers were analyzed using the TRDC system.^{3,8,9,13,19,24,25,30,33)}

8.1 Examination of carboxylated polymer particles as analytes with TRDC using a polyethylene capillary tube

A tube radial distribution chromatography (TRDC) system has been developed using an open capillary tube and an aqueous–organic solvent mixture as a carrier solution under laminar flow conditions. Here, we examine the elution behavior of carboxylated polymer particles (1.0 μm diameter) together with fluorescein isothiocyanate in the TRDC system using a polyethylene capillary tube in order to extend our knowledge regarding the separation performance of the system. The model analyte solution of fluorescein isothiocyanate and carboxylated polymer particles was injected into the open polyethylene capillary tube utilizing the gravity method, and subsequently delivered through the capillary tube with the carrier solution of the water–acetonitrile–ethyl acetate mixture (15:3:2 volume ratio) using a microsyringe pump. On-capillary detection was performed for the analytes using an absorption detector, which indicated individual elution times and peak shapes on the chromatograms. We discuss the observed phenomena considering the separation mechanism of the TRDC system.

Introduction

It is important to examine the elution behavior of various types of analytes in the TRDC system for expanding our knowledge regarding the separation performance. Here, we examined a nondiffusive analyte of carboxylated polymer particles with 1.0 μm diameter together with fluorescein isothiocyanate (FITC) in the TRDC system. The mixture solution of FITC and carboxylated polymer particles was used as an analyte solution in our previous study [1] concerning wide-bore hydrodynamic chromatography in which we used a carrier solution which didn't include any organic solvents. These analytes were comparatively hydrophilic, but were quite different with respect to their sizes and diffusion properties. We compared the data obtained by the present TRDC system with that obtained by the wide-bore hydrodynamic chromatography system in our previous study [1]. The separation performance of the carboxylated polymer particles in the TRDC system gave us important information that supported the explanation of the separation mechanism of the TRDC system that we proposed.

Experimental

Carboxylated polymer particles (1.0 μm diameter) prepared from polystyrene matrix, FluoSpheres (1.0 μm), were provided as suspension (2% solids, 4×10^{10} particles mL^{-1}) and diluted with a carrier solution as necessary. A high-density polyethylene capillary

tube (200 μm i.d., 500 μm o.d.) was used. The present TRDC system was comprised of an open polyethylene capillary tube (70 cm length, effective length 50 cm), microsyringe pump, and absorption detector. The solution mixture of water–acetonitrile–ethyl acetate (15:3:2 volume ratio) was used as the carrier solution. We prepared the analyte solutions, FITC, FluoSpheres (1.0 μm), and their mixture with the carrier solution. The solutions were introduced directly into the capillary inlet side for 5 s from a height of 20 cm by the gravity method. After the analyte injection, the capillary inlet was connected through the joint to the microsyringe, and the syringe was set on the microsyringe pump. The carrier solution was fed into the capillary tube at a flow rate of 4.0 $\mu\text{L min}^{-1}$ under laminar flow conditions. On-capillary detection was performed for the absorption (254 nm) by the detector.

Results and discussion

We examined FITC, FluoSpheres (1.0 μm), and the mixture of the two in the present TRDC system using an open polyethylene capillary tube and a water–acetonitrile–ethyl acetate carrier solution. The Reynolds number was roughly estimated to be < 1 under the present analytical conditions, confirming that the present system worked under laminar flow conditions. As shown in Figs. 1 (a) and (b), FITC and FluoSpheres (1.0 μm) were detected at ca. 3.9 min with a Gaussian peak and ca. 1.9 min with a non-Gaussian peak, respectively. The elution times of 1.9 and 3.9 min almost corresponded to the maximum and average linear velocities, respectively, in the capillary tube under laminar flow conditions. The maximum and average linear velocities were tentatively calculated with the ordinary equations [1] concerning linear velocity under laminar flow conditions, although the linear velocity of a water-organic solvent mixture carrier solution in the capillary tube may deviate from an ideal parabolic curve under laminar flow conditions. When the mixture of FITC and FluoSpheres (1.0 μm) was subjected to the present TRDC system, they separated through the polyethylene capillary tube, as shown in Fig. 1 (c). Although some overlapping was observed in Fig. 1 (c), the separation performance was much better than that reported in our previous study [1], as outlined below.

In our previous study [1], we also examined FITC and FluoSpheres (1.0 μm) by means of wide-bore hydrodynamic chromatography, in which we used an aqueous carrier solution that did not include any organic solvents. Previously, researchers have noted that under laminar flow conditions, compounds and particles with diffusion indexes greater than 1, such as FITC, fed into a capillary tube can be delivered with average linear velocities and show Gaussian peaks. In contrast, those with diffusion indexes less than 0.1, such as FluoSpheres (1.0 μm), can be delivered with maximum linear velocities and show non-Gaussian peaks, while analytes with diffusion indexes between 0.1 and 1 are better characterized by intermediate behavior. The chromatograms of FITC and FluoSpheres (1.0 μm) reported in the previous study were consistent with the estimated chromatograms based on their calculated diffusion indexes. FluoSpheres (1.0 μm) and FITC were eluted in this order with the maximum linear velocity and showed non-Gaussian peaks and with the average linear velocity with Gaussian peaks, respectively. We should emphasize that, in principle, these peaks are never separated by wide-bore hydrodynamic chromatography; a Gaussian peak necessarily appears on the slope of a non-Gaussian peak.

The data of FITC and FluoSpheres (1.0 μm) obtained with the present TRDC system were different from those obtained by wide-bore hydrodynamic chromatography. Although the peak of the FluoSpheres (1.0 μm) appeared with the apex of the maximum linear velocity in the capillary tube, the slope of the non-Gaussian peak did not last longer than the elution time at the average linear velocity in the tube (see Fig. 1 (b)), leading to the separation of FITC and the FluoSpheres (1.0 μm) in the mixture (see Fig. 1 (c)). The data obtained here were considered in the TRDC system as follows: no solvent (composed of aqueous and organic components) in the carrier solution was dispersed fully uniformly inside the capillary tube. A major solvent phase or a water-rich phase formed around the middle of the tube far from the inner wall, while a minor solvent phase or an organic solvent-rich phase occurred near the inner wall of the capillary tube. FITC and FluoSpheres (1.0 μm) were comparatively hydrophilic and dispersed in the water-rich phase around the middle of the tube.

For further consideration of the obtained chromatograms, we calculated the diffusion coefficients and indexes. The Einstein–Stokes equation (see Eq. (1)) and the diffusion index equation (see Eq. (2)) are shown below, where D is the diffusion coefficient, τ the diffusion index, k the Boltzmann constant, T the absolute temperature, μ the viscosity, d the particle diameter, L the length, a the radius, and u_{av} the average linear velocity.

$$D = \frac{kT}{3\pi\mu d} \quad (1)$$

$$\tau = \frac{DL}{a^2 \mu_{\text{av}}} \quad (2)$$

Table 1 summarizes the roughly calculated results concerning the diffusion coefficients, D , and diffusion indexes, τ , for FITC and FluoSpheres (1.0 μm) under the present analytical conditions. FITC, diffusive solute, and FluoSpheres (1.0 μm), non-diffusive solute, were delivered with the average linear velocity in the capillary tube with Gaussian peak and with the maximum linear velocity with non-Gaussian peak, respectively. However, the carboxylated FluoSpheres (1.0 μm) were mainly dispersed in the water phase (around the middle of the tube) and not in the organic phase (near the inner wall of the tube), providing the disappearance of the non-Gaussian peak around the elution time at the average linear velocity in the tube.

In conclusion, the chromatogram of the mixture of FITC and FluoSpheres (1.0 μm) obtained using the TRDC system had a much better resolution than that obtained by wide-bore hydrodynamic chromatography. They were almost completely separated in the TRDC. The peak of FluoSpheres (1.0 μm) appeared with the apex at the maximum linear velocity in the capillary tube, but the slope of the non-Gaussian peak did not last longer than the elution time at the average linear velocity in the tube. The observed phenomena was explained by means of the tube radial distribution of the carrier solvents in the tube within the TRDC system.

Nomenclature; a = inner diameter [m], D = diffusion coefficient [m^2s^{-1}], d = particle diameter [m], k = Boltzmann constant [NK^{-1}], L = length [m], T = absolute temperature [K], u_{av} = average linear velocity [ms^{-1}], μ = viscosity, [$\text{kgm}^{-1}\text{s}^{-1}$], and τ = diffusion index [-]

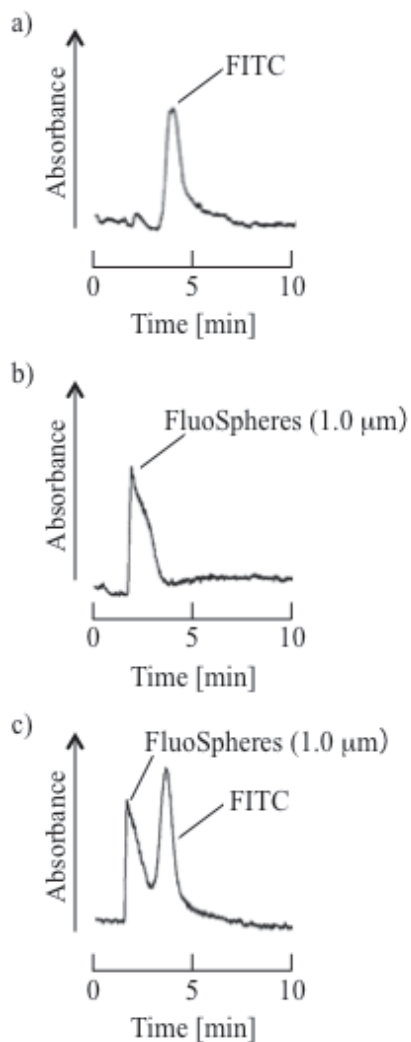
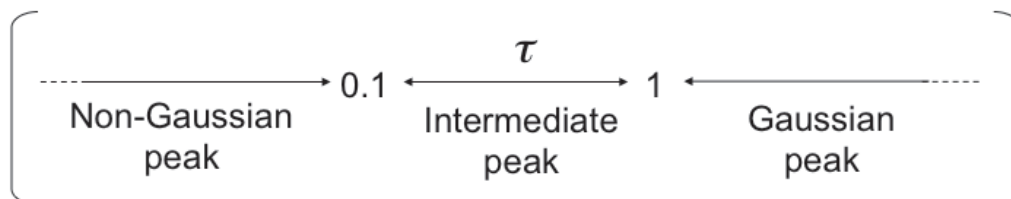


Figure 1. Chromatograms of FITC, FluoSpheres (1.0 μm), and their mixture as obtained by the present TRDC system. (a) 0.5 mM FITC, (b) 200 times dilution of FluoSpheres, and (c) the mixture of 0.5 mM FITC and 200 times dilution of FluoSpheres. Conditions: Capillary, 70 cm (effective length 50 cm) with 200 μm i.d. polyethylene capillary; carrier, water–acetonitrile–ethyl acetate mixture (15:3:2 volume ratio); sample injection, 20 cm height (gravity) \times 5 s; and flow rate, 4.0 $\mu\text{L min}^{-1}$.

Table 1. Diffusion coefficients and diffusion indexes.

Sample	D [m^2s^{-1}]	τ
FITC	$1 \times 10^{-9} - 3 \times 10^{-9}$	20 – 60
FluoSphere (1.0 μm)	$5 \times 10^{-13} - 1 \times 10^{-12}$	0.01 – 0.03



8.2 Examination of polymer compounds as analytes with TRDC using a fused-silica capillary tube

Fluidic behavior of the polymer compounds, FluoSpheres (1.0 μm diameter), was examined by tube radial distribution chromatography (TRDC) system. The ternary mixture of water-acetonitrile-ethyl acetate, 15:3:2 (water-rich) or 3:8:4 (organic solvent-rich) volume ratio, as a carrier solution was fed into the fused-silica capillary tube under laminar flow conditions. The peak of the FluoSpheres appeared with the apex at the maximum linear velocity and the slope of the non-Gaussian peak did not last longer than the elution time at the average linear velocity with the water-rich carrier solution. With the organic solvent-rich carrier solution FluoSpheres was eluted at near the average linear velocity.

Introduction

Although various types of analyte were analyzed using the TRDC system, we have not had enough information about fluidic behavior of the polymer compounds in the TRDP. Here, we examined the fluidic behavior of the polymer compounds, FluoSpheres (1.0 μm diameter), through the TRDP in fused-silica capillary tubes by use of the TRDC system.

Experimental

Lambda-DNA (48502 bp, 32,300,000 molecular weight) was used. Carboxylated polymer particles prepared from polystyrene matrix, FluoSpheres (1.0 μm diameter), from Molecular Probes Inc., were provided as suspension (2% solids, 4×10^{10} particles mL^{-1}) and diluted with a carrier solution as necessary. The present chromatography system comprised of an open fused-silica capillary tube (50 μm inner diameter), microsyringe pump, and absorption detector. The tube temperature was controlled by dipping the capillary tube in water maintained at a specific temperature of 20 $^{\circ}\text{C}$ in a vessel. Water-acetonitrile-ethyl acetate mixtures with volume ratios of 15:3:2 and 3:8:4 were used as water-rich and organic solvent-rich carrier solutions in the TRDC system. The component ratios of 15:3:2 and 3:8:4 were recommended in our reports.^{15,17,19} Analyte solutions were prepared with the carrier solutions. Here, 200 times-diluted FluoSpheres and 0.8 nM lambda-DNA (MW 32,300,000; 48502bp) were used as analyte solutions. The analyte solution was introduced directly into the capillary inlet side by the gravity method. After analyte injection, the capillary inlet was connected through a joint to a microsyringe which was then set on the microsyringe pump. The carrier solution was fed into the capillary tube at a definite flow rate under laminar flow conditions. On-capillary absorption detection (260 nm) was performed with the detector.

Results and discussion

When the present capillary chromatography is carried out with a water carrier solution, the chromatographic system inevitably works as a wide-bore hydrodynamic chromatography for polymer compounds. The wide-bore hydrodynamic chromatography works by a different mechanism originating from the solute distribution coupled with the laminar flow conditions [2-4]. A diffusive solute gives an elution curve with an apex at the time required for the average linear velocity to the detector (i.e., such a curve is characterized by a Gaussian peak), whereas a non-diffusive solute yields an asymmetric elution curve with the apex at the maximum

linear velocity in a capillary (i.e., such a curve is characterized by a non-Gaussian peak).

As preliminary experiments, FluoSpheres as artificial polymer particles and lambda-DNA as a natural biopolymer, were examined by the wide-bore hydrodynamic chromatography mode using a water carrier solution (not containing any chemicals or additives). The obtained chromatogram is shown in Fig. 1 together with analytical conditions. FluoSpheres were eluted first at the maximum flow rate under the laminar flow conditions with non-Gaussian peak and then lambda-DNA was eluted with almost average linear velocity with Gaussian peak. They showed typical elution patterns on the chromatograms by the wide-bore hydrodynamic chromatography as described above. FluoSphere was non-diffusive and lambda-DNA was diffusive solutes in the water carrier.

Lambda DNA that is rather large molecular weight features hydrophilic and partially hydrophobic character, although it depends on the conditions such as temperature, solvent, and added additives. The solubility of lambda-DNA was examined in the carrier solutions for the TRDC system. Lambda-DNA was dissolved with the water-rich carrier solution but could not be dissolved with the organic solvent-rich carrier solution due to its hydrophilic nature. In addition the absorption spectra of lambda-DNA gradually changed in the water-rich carrier solution. Lambda-DNA would change from double helix conformation to single coil one with ethyl acetate. Such a change was not observed with a water-acetonitrile mixture solution. Only FluoSpheres were examined by the present system with a water carrier solution (wide-bore hydrodynamic chromatography mode), a water-acetonitrile-ethyl acetate mixture solution (15:3:2; volume ratio) (TRDC mode using the water-rich carrier solution), and a water-acetonitrile-ethyl acetate mixture solution (3:8:4; volume ratio) (TRDC mode using the organic solvent-rich carrier solution). The obtained chromatograms are shown in Fig. 2 along with analytical conditions. With the water carrier solution, FluoSpheres showed a typical chromatogram of non-diffusive solute in a wide-bore hydrodynamic chromatography (Fig. 2 a)). The data of FluoSpheres obtained with the TRDC system (Fig. 2 b) and c)) were different from those obtained by the wide-bore hydrodynamic chromatography (Fig. 2 a)). In the TRDC system using the water-rich carrier solution, although the peak of the FluoSpheres appeared with the apex at the maximum linear velocity in the capillary tube, the tailing slope of the non-Gaussian peak did not last longer than the elution time at the average linear velocity in the tube (Fig. 1 b)). FluoSpheres were comparatively hydrophilic and dispersed largely around the middle of the tube in the water-rich phase with only a little in the organic solvent-rich outer phase. On the other hand, with the organic solvent-rich carrier solution FluoSpheres were eluted at near the average linear velocity with nearly Gaussian peaks. It might be attributed to few dissociated carboxyl groups of FluoSpheres in the organic solvent-rich solution and higher diffusion coefficient of organic solvents (acetonitrile and ethyl acetate) to the solutes than that of water. We will try to consider the chromatographic data together with computer simulation and fluorescence microscopy observation in the future.

In conclusion, we tried to examine the fluidic behavior of the polymer compounds, FluoSpheres (1.0 μm diameter), with the TRDC system based on the TRDP. FluoSpheres showed specific fluidic behavior with the TRDC system compared to the chromatogram obtained by the wide-bore hydrodynamic chromatography. The data also meant that the

TRDC system had potential to deal with various types of analyte, from low molecular weight ones to polymer compounds, with the same system and a similar procedure. Information about the fluidic behavior of the polymer compounds obtained here is interesting in the TRDP or TRDC study, and will be useful to design a microreactor or micro total analysis systems related with polymer compounds.

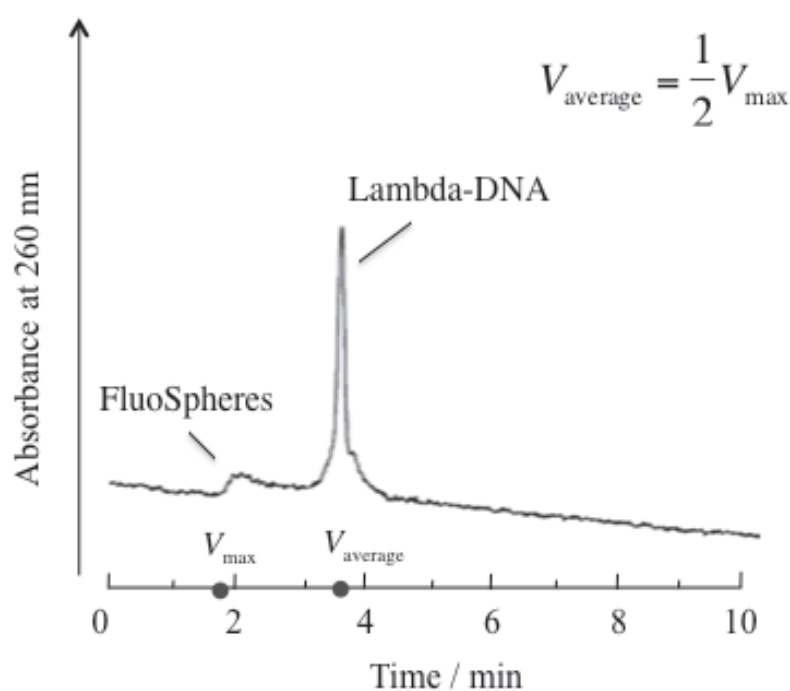


Figure 1. Chromatograms of Fluospheres and lambda-DNA obtained by wide-bore hydrodynamic chromatography. Conditions: Capillary tube, 110 cm (effective length: 90 cm) of 50 μm i.d. fused-silica; carrier, water; sample injection, 50 cm height (gravity) \times 20 s; flow rate, 0.5 $\mu\text{L min}^{-1}$; tube temperature, 20 $^{\circ}\text{C}$; and 200 times-diluted FluoSpheres and 0.8 nM lambda-DNA. V_{max} and V_{average} mean the maximum linear velocity and the average linear velocity under the present laminar flow conditions, respectively. The plots on the horizontal line mean the estimated elution times with V_{max} and V_{average} .

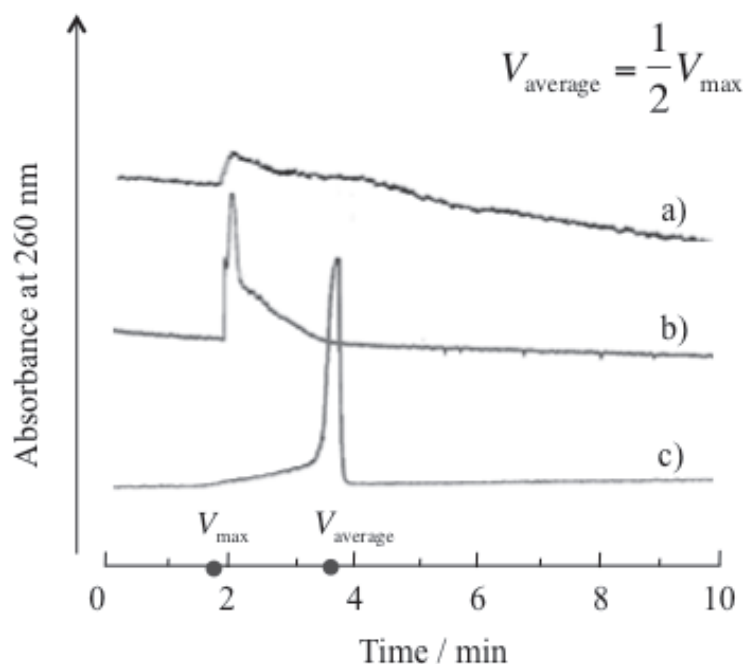


Figure 2. Chromatograms of FluoSpheres obtained by the present chromatographic system. a) Wide-bore hydrodynamic chromatography mode, b) TRDC mode with the water-rich carrier solution, and c) TRDC mode with the organic solvent-rich carrier solution. Conditions: Capillary tube, 110 cm (effective length: 90 cm) of 50 μm i.d. fused-silica; carrier, a) water, b) water-rich carrier solution (water-acetonitrile-ethyl acetate, 15:3:2 volume ratio), c) organic solvent-rich carrier solution (water-acetonitrile-ethyl acetate, 3:8:4 volume ratio); sample injection, 50 cm height (gravity) \times 20 s; flow rate, 0.5 $\mu\text{L min}^{-1}$; tube temperature, 20 $^{\circ}\text{C}$; and 200 times-diluted FluoSpheres. V_{max} and V_{average} mean the maximum linear velocity and the average linear velocity under the present laminar flow conditions, respectively. The plots on the horizontal line mean the estimated elution times with V_{max} and V_{average} .

8.3 Examination of metal compounds as analytes with TRDC

We examined metal compounds such as copper(II) sulfate, hematin, and hemoglobin using tube radial distribution chromatography (TRDC) system equipped with a chemiluminescence detector. The model mixture solutions of hematin–copper(II) and hemoglobin–copper(II) were injected into a fused-silica capillary tube using a gravity method and subsequently delivered with the carrier solutions of water–acetonitrile–ethyl acetate (2:7:4 volume ratio) and water–acetonitrile–ethyl acetate (15:2:1 volume ratio), respectively, using a microsyringe pump. The mixture of hematin–copper(II) as well as hemoglobin–copper(II) was well separated and eluted with the organic solvent-rich carrier solution based on the tube radial distribution and detected by chemiluminescence in the present TRDC system.

Introduction

We have just begun a series of investigations of the TRDC system in order to broaden our knowledge about its capabilities. In our studies, model mixtures of hydrophilic and hydrophobic molecules were mainly analyzed using the TRDC system. Here, we have attempted to examine the separation characteristics of metal compounds, such as Cu(II), hematin, and hemoglobin, in the TRDC system with an untreated open capillary tube and also the effects of pH value of the aqueous component in the carrier solution on the separation performance of the TRDC system.

Experimental

A fused-silica capillary tube (75 μm i.d. and 150 μm o.d.) was used. The present TRDC system consists of a fused-silica capillary tube (70 cm in length), a microsyringe pump, and a chemiluminescence (CL) detector that takes advantage of the luminol reaction. The flow-type CL detection cell (0.5 mm i.d. poly(tetrafluoroethylene) tube) [5] was used in the system. Three water-hydrophilic-hydrophobic organic solvent mixture carrier solutions were prepared. In the first solution (the organic solvent-rich carrier solution), the water or aqueous component was 10 mM carbonate buffer at pH 10.8, containing 25 μM luminol; the water–acetonitrile–ethyl acetate mixture was in a volume ratio of 2:7:4. In the second solution (the water-rich carrier solution, containing pH 10.8 carbonate buffer), the aqueous component was the same as in the first, but the water–acetonitrile–ethyl acetate mixture volume ratio was 15:2:1. In the third solution (the water-rich carrier solution, containing pH 7.0 phosphate buffer), the aqueous component was 10 mM phosphate buffer at pH 7.0, containing 25 μM luminol; the volume ratio of the water–acetonitrile–ethyl acetate mixture was 15:2:1. The mixture of hematin and copper(II) sulfate (Cu(II)), as well as the mixture of hemoglobin and Cu(II), as models were dissolved in the carrier solutions. The metal catalyst solution included potassium sodium tartrate at a concentration 20 times higher than that of the catalyst. The analyte solutions were injected into the capillary tube inlet by the gravity method (from a 25 cm height for 10 s). The analytes were then delivered in the capillary tube with the carrier solution using a microsyringe pump at a flow rate of 0.5 $\mu\text{L min}^{-1}$. The oxidant reagent solution of 50 mM hydrogen peroxide (10 mM carbonate buffer, pH 10.8) was delivered at a flow rate of 10 $\mu\text{L min}^{-1}$ to the capillary outlet where the analyte having catalytic activities for luminol reaction, the luminol, and the oxidant reagent were mixed to generate CL light.

Results and discussion

The TRDC system with the organic solvent-rich carrier solution First, we examined the mixture analytes of hematin–Cu(II) or hemoglobin–Cu(II) using the present TRDC system with the organic solvent-rich carrier solution, where the aqueous component was 10 mM carbonate buffer at pH 10.8, containing 25 μ M luminol, and the water–acetonitrile–ethyl acetate was in a 2:7:4 ratio. Cu(II) is hydrophilic, and hematin and hemoglobin were comparatively hydrophobic. The mixture of hematin and Cu(II) was eluted in this order at ca. 6.5 min and 7.8 min, respectively (Fig. 1a). They were delivered at near the average linear velocity and a slower than the average velocity, respectively, under laminar flow conditions. Similarly, the mixture of hemoglobin and Cu(II) was eluted in this order (Fig. 1b). The chromatogram of the mixture of hematin or hemoglobin (hydrophobic) and Cu(II) (hydrophilic) in Fig. 1a or b was consistent with the separation principle of the TRDC system with the organic solvent-rich carrier solution.

The TRDC system with the water-rich carrier solution We examined the mixture analytes of hematin–Cu(II) or hemoglobin–Cu(II) with the present TRDC system using the water-rich carrier solution. The aqueous component was 10 mM carbonate buffer at pH 10.8, containing 25 μ M luminol; the water–acetonitrile–ethyl acetate volume ratio was 15:2:1. The obtained chromatograms showed no separation; all peaks appeared at about 6.5 min with near average linear velocity. Despite the slight hydrophobicity of hematin and hemoglobin in comparison to Cu(II), they should be also dissolved due to the presence of carboxylate anion groups or protonated amino groups with the water-rich phase or the major solvent phase under the present analytical conditions. We tried to increase the hydrophobicity of hematin and hemoglobin by reducing the pH value of the aqueous component from pH 10.8 to 7.0 in the carrier solution; the mixture analytes were dissolved with the carrier solution prepared with 10 mM phosphate buffer (see the water-rich carrier solution, containing pH 7.0 phosphate buffer, above). Hematin was soluble in this carrier solution at 0.5 μ M, but hemoglobin, with an isoelectric point of 6.8–7.0, did not dissolve in the carrier solution. The obtained chromatogram of the mixture of hematin and Cu(II) with the carrier solution is shown in Fig. 2. They were eluted in the reverse order, although the hematin peak featured a little broadening. Cu(II) was eluted with near average linear velocity and hematin with a velocity slower than the average linear velocity. The carboxyl groups of the hematin molecular structure might become protonated in such an aqueous–organic mixture solvent because of the lower pH value, leading to an increase in the hydrophobicity of hematin. Such hematin was easily dissolved in the organic solvent-rich phase or the minor solvent phase in the water-rich carrier solution, and delivered with the velocity slower than the average linear velocity. In consideration of the separation behavior of Cu(II) and hematin, the chromatogram shown in Fig. 2 was consistent with the separation principle of the TRDC system with the water-rich carrier solution described previously.

In conclusion, metal compounds, such as Cu(II), hematin, and hemoglobin, which are of great interest as biocompounds, were analyzed through the TRDC system with a chemiluminescence detector based on a luminal reaction. Cu(II) is hydrophilic, and hematin and hemoglobin are comparatively hydrophobic. The mixtures were separated through a capillary tube with the help of the tube radial distribution of carrier solvents in

the TRDC system and detected through their catalytic activity for the luminol chemiluminescence reaction. The data obtained herein suggest the possibility to extend the application of the TRDC system to other analytes.

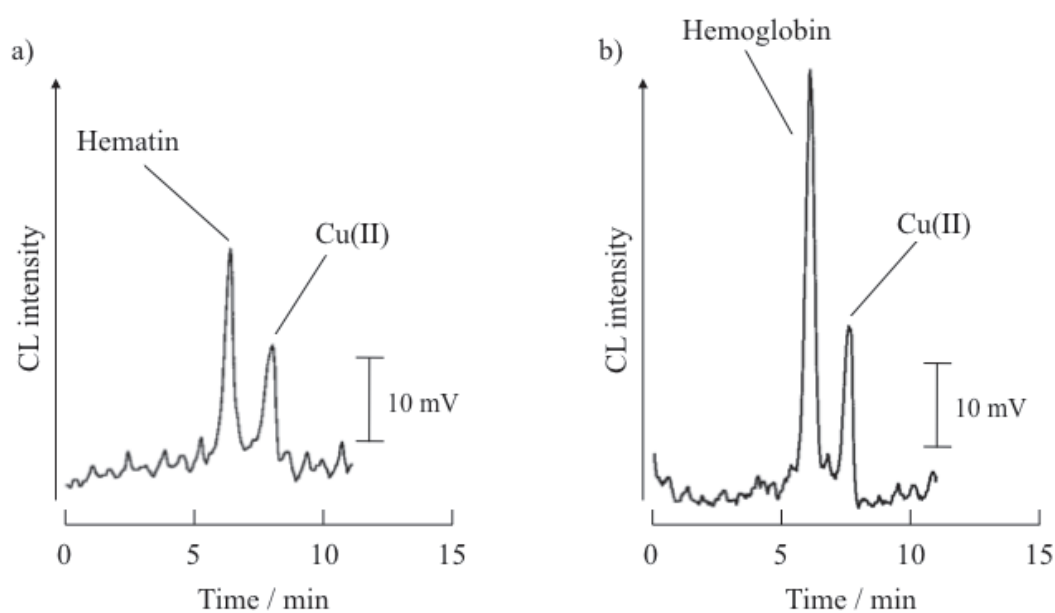


Figure 1. Chromatograms of mixtures of a) hematin and Cu(II) and b) hemoglobin and Cu(II) obtained using the present TRDC system with the organic solvent-rich carrier solution (with 10 mM carbonate buffer, pH 10.8). Conditions: capillary tube, 70 cm of 75 μm i.d. fused-silica; carrier, water (10 mM carbonate buffer, pH 10.8, containing 25 mM luminol)–acetonitrile–ethyl acetate (2:7:4 volume ratio) mixture solution; sample injection, 25 cm height (gravity) \times 10 s; carrier flow rate, 0.5 $\mu\text{L min}^{-1}$; oxidant reagent flow rate, 10 $\mu\text{L min}^{-1}$; analyte concentration, 0.1 μM hematin, 0.05 μM hemoglobin, and 2 mM Cu(II).

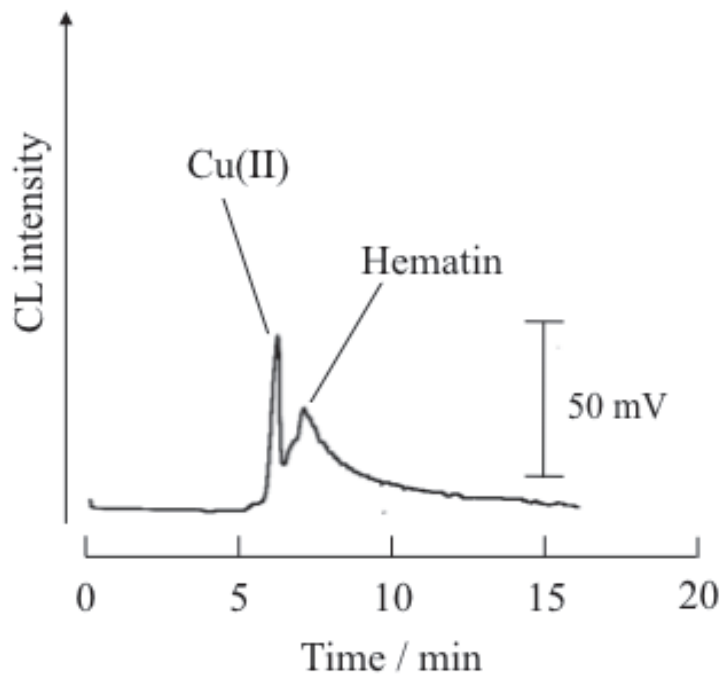


Figure 2. Chromatogram of a mixture of hematin and Cu(II) obtained using the present TRDC system with a chemiluminescence detector (with 10 mM phosphate buffer, pH 7.0). Conditions: capillary tube, 70 cm of 75 μm i.d. fused-silica; carrier, water (10 mM phosphate buffer, pH 7.0, containing 25 mM luminol)-acetonitrile-ethyl acetate (15:2:1 volume ratio) mixture solution; sample injection, 25 cm height (gravity) \times 10 s; carrier flow rate, 0.5 $\mu\text{L min}^{-1}$; oxidant reagent flow rate, 10 $\mu\text{L min}^{-1}$; analyte concentration, 0.5 μM hematin and 1 mM Cu(II).

8.4 Examination of biomolecules as analytes with TRDC

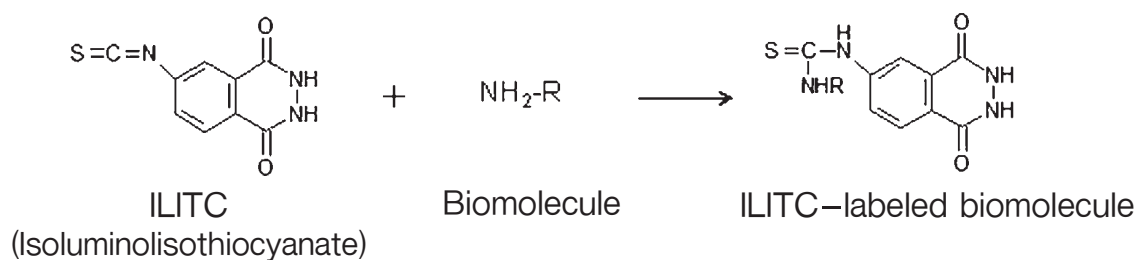
We examined the elution behavior of isoluminol isothiocyanate (ILITC)-labeled biomolecules (α -amino acids, peptides, and proteins) in an open-tubular capillary chromatography system using an untreated fused-silica capillary tube and a water-acetonitrile-ethyl acetate mixture carrier solution. Such an open-tubular capillary chromatography is called tube radial distribution chromatography (TRDC). A mixture of ILITC and ILITC-labeled biomolecules was analyzed using TRDC with chemiluminescence detection that provided simple instrument without a light source and complex optical devices. The ILITC and the twenty labeled α -amino acids were separated, in this order or the reverse order, or not separated with an organic solvent-rich and water-rich carrier solution. Their elution behavior was considered to be of a hydrophilic or hydrophobic nature of ILITC and the labeled α -amino acids. The ILITC and the labeled protein, alcohol dehydrogenase and bovine serum albumin, were separated in this order with an organic solvent-rich carrier solution, while they were eluted in reverse order given a water-rich carrier solution, based on the TRDC separation performance. The TRDC system worked with the untreated open-tubular capillary tube not using any specific capillary tubes, such as coated, packed, or monolithic.

Introduction

To date, various mixtures of hydrophilic and hydrophobic analytes have been separated using the TRDC system. However, most of these have been organic compounds with low molecular weights: 1-naphthol and 2,6-naphthalenedisulfonic acid are typical model analytes. Here, we examined the elution behavior of biomolecule analytes, isoluminol isothiocyanate (ILITC)-labeled α -amino acids, peptides, and proteins, in the TRDC system with chemiluminescence (CL) detection. We briefly described the preliminary results of this investigation in a previous communication.⁹⁾

Experimental

A fused-silica capillary tube (untreated or silanol group-intact; 75 μm i.d. and 150 μm o.d.) was used. A schematic representation of the present TRDC system with CL detection is shown in Fig. 1. The system consists of a fused-silica capillary tube (70 cm in length), a microsyringe pump, and a CL detector that takes advantage of the luminol reaction. A flow CL detection cell (0.5 μm i.d. polytetrafluoroethylene (PTFE) tube) [6] was used in this system. A water-acetonitrile-ethyl acetate mixture was prepared in a volume ratio of 3:8:4 as an organic solvent-rich carrier solution or in a volume ratio of 15:3:2 as a water-rich carrier solution, where the water component was 10 mM phosphate buffer at pH 7.0 or 10 mM carbonate buffer at pH 10.8 or pH 11.8, including 4 μM microperoxidase. α -Amino acids, peptides, and proteins were labeled with isoluminol isothiocyanate (ILITC) as follows. Biomolecule (0.5 μmol) and ILITC (1.0 μmol) were dissolved in a solution of water-triethylamine (95:5 volume ratio) (100 μL). The mixture was stirred for 1 min and left in the dark for 20 min. After the evaporation of the solvent, the residue was redissolved in the carrier solution (1 mL) to give an analyte solution, including excess (or free)-ILITC and ILITC-labeled biomolecules.



The analyte solution was injected into the capillary tube inlet by gravity from a height of 25 cm for 10 s. The analytes were then delivered into the capillary tube with the carrier solution using a microsyringe pump at a flow rate of $0.5 \mu\text{L min}^{-1}$. An oxidant reagent solution of 50 mM hydrogen peroxide (10 mM carbonate buffer, pH 10.8 or 11.8) was delivered at a flow rate of $10 \mu\text{L min}^{-1}$ to the capillary outlet where the analytes were mixed with the reagents to generate CL. The analytes of the mixture were confirmed with the individual peaks on the chromatograms.

Results and discussion

Preliminary experiments In the TRDP an organic solvent-rich carrier solution generates an organic solvent-rich inner phase and a water-rich outer phase, while a water-rich carrier solution results in a water-rich inner phase and an organic solvent-rich outer phase. That is, a major inner phase is formed around the center of the tube away from the inner wall and a minor outer or capillary wall phase is generated near the inner wall. In the TRDC separation system, the analytes that are delivered through the capillary tube are distributed between the inner and outer phases created by the TRDP, undergoing chromatographic separation where the outer phase works as a pseudo-stationary phase in chromatography. The analytes distributed in the outer phase would also interact with an inner-wall surface of the capillary tube. As preliminary experiments, an excess (or free)-ILITC and ILITC-labeled aspartic acid mixture was examined by the present TRDC system with CL detection. The CL detection features a simple instrument without a light source and complex optical devices, and is useful for analytes possessing a low absorption properties. The carrier solutions, the organic solvent-rich and the water-rich solutions, were prepared by using three different aqueous solutions: 10 mM phosphate buffer (pH 7.0) and 10 mM carbonate buffer (pH 10.8 and 11.8). ILITC and ILITC-labeled aspartic acid were not separated with both carrier solutions using the 10 mM phosphate buffer (pH 7.0). Although, ILITC and ILITC-labeled aspartic acid were separated with the organic solvent-rich solution in this order, they were not separated with the water-rich carrier solution using a 10 mM carbonate buffer (pH 10.8 and 11.8). From the data, ILITC-labeled aspartic acid was found to be more hydrophilic than ILITC in the TRDC system with the organic solvent-rich solution using a 10 mM carbonate buffer (pH 10.8 and 11.8). A labeling reaction between ILITC and biomolecules possessing an amino group, such as amino acids, peptides, and proteins, is performed; the isothiocyanate group of ILITC reacts with the amino group to produce the labeled molecules under the conditions described in the experimental sections. The pH value influences the hydrophilic and hydrophobic natures of the analytes, ILITC and ILITC-labeled biomolecules, through dissociation and protonation of the functional groups of the molecules. However, the pH in an aqueous-organic solvent solution cannot be treated in a similar way as the one in an aqueous solution. In the following experiments, ternary mixed carrier solutions were

prepared using a 10 mM carbonate buffer (pH 11.8), which might effect dissociation of the carboxyl groups of biomolecules.

Typical chromatograms obtained for α -amino acids Twenty α -amino acids were labeled with ILITC. The mixtures including free-ILITC and ILITC-labeled α -amino acid were subjected to the present TRDC system. Typical chromatograms obtained for cysteine, aspartic acid, phenylalanine, and tyrosine are shown in Fig. 2. ILITC and ILITC-labeled cysteine were eluted with the organic solvent-rich carrier solution in this order, while they were separated in the reverse order with the water-rich carrier solution. Also, ILITC and ILITC-labeled aspartic acids were eluted with the organic solvent-rich carrier solution in this order, while they were not separated with the water-rich carrier solution. From the results and the TRDC separation performance, ILITC-labeled cysteine and aspartic acid could be more hydrophilic than ILITC under the present TRDC conditions. On the other hand, ILITC and ILITC-labeled phenylalanine were eluted with the organic solvent-rich carrier solution in the reverse order, while they were separated in this order with the water-rich carrier solution. Also, ILITC and ILITC-labeled tyrosine were separated with the organic solvent-rich carrier solution in the reverse order, while they were not separated with the water-rich carrier solution. From the results and the TRDC separation performance, ILITC-labeled phenylalanine and tyrosine could be more hydrophobic than ILITC under the present TRDC conditions.

Separation performance of α -amino acids From the obtained chromatograms, the twenty ILITC-labeled α -amino acids were classified according to their nature into the three types: more hydrophilic than ILITC, like ILITC-labeled cysteine and aspartic acid; more hydrophobic than ILITC, like ILITC-labeled phenylalanine and tyrosine; and almost equal hydrophilic or hydrophobic nature to ILITC, which showed no separation between ILITC and ILITC-labeled α -amino acid on the chromatograms. The three types were denoted as “hydrophilic”, “hydrophobic”, and “neutral” were compared to ILITC nature for convenience. The classification of ILITC-labeled α -amino acids nature is summarized in Table 1. Here, excess ILITC was estimated to almost react with active function groups of α -amino acids through a labeling reaction. α -Amino acids other than alanine, leucine, and asparagine that were expressed by “neutral” were separated by the TRDC system with the organic solvent-rich carrier solution. Also, α -amino acids other than alanine, isoleucine, leucine, asparagine, serine, methionine, tyrosine, aspartic acid, glutamic acid, lysine, and arginine, which were “neutral”, were separated by the system with the water-rich carrier solution. As a rough estimation for the labeled α -amino acids separation performance in the present TRDC system, shown in the table, neutral amino acids, such as aliphatic amino acids, aromatic amino acids, and heterocyclic compound amino acids were labeled “hydrophobic”. However, neutral amino acids, such as oxy amino acid and sulfur-containing amino acid, as well as, acidic amino acid and basic amino acids were labeled “hydrophilic”. The classification of the data in Table 1 was reasonable and consistent with the molecular structures of ILITC-labeled α -amino acids.

Separation of peptides Glycine, glycylglycine, glycylglycylglycine, and glycylglycylglycylglycine were reacted with ILITC, and the obtained mixture solutions

were examined by the TRDC system. The chromatograms are shown in Fig. 3. With the organic solvent-rich carrier solution, ILITC-labeled glycine and peptides were first eluted; secondly, ILITC was detected. However, in the water-rich carrier solution they were eluted in the reverse order, but mixtures of ILITC and ILITC-labeled glycyglycyglycyglycine were not separated. From the results, roughly speaking, ILITC was more hydrophobic than the ILITC-labeled glycine and peptides. Tentatively, the mixture including ILITC, the labeled glycine, and the three labeled-peptides was subjected to the TRDC system with the organic solvent-rich carrier solution. The obtained chromatogram is shown in Fig. 4. The elution order was as follows: first, ILITC-labeled glycyglycyglycyglycine, secondly ILITC-labeled glycine, ILITC-labeled glycyglycine, and ILITC-labeled glycyglycyglycine (these three analytes were not separated), thirdly ILITC; the order was consistent with the elution behavior observed in Fig. 3.

Separation of protein The chromatograms of the mixture of ILITC and ILITC-labeled bovine serum albumin (BSA) (M_w 66000) were examined by TRDC with the organic solvent-rich and water-rich carrier solutions. ILITC and ILITC-labeled BSA were separated and detected in this order with the organic solvent-rich carrier solution, while they were detected in the reverse order with the water-rich carrier solution.⁹⁾ Clearly, the elution times of the analytes were changed by altering the component ratios of the carrier solvents. The mixture of ILITC and ILITC-labeled alcohol dehydrogenase from yeast (ADH) (M_w 140000) was also analyzed with the TRDC system; these components showed similar elution behaviors to the labeled BSA on the chromatograms. The elution orders obtained for the mixture of ILITC and ILITC-labeled BSA or ADH were reasonable, considering the free-ILITC to be more hydrophobic than the ILITC-labeled protein.

Separation of biomolecules mixture We examined the mixture of ILITC, ILITC-labeled ADH, and ILITC-labeled BSA with the present TRDC system. The obtained chromatograms are shown in Fig. 5a). ILITC, ILITC-labeled ADH, and ILITC-labeled BSA were detected in this order with the organic solvent-rich carrier solution, while they were eluted in the reverse order with the water-rich carrier solution. The orders of analyte elution on the chromatograms indicated that the hydrophilicity of the ILITC-labeled BSA must be larger than that of the ILITC-labeled ADH. The isoelectric points of BSA and ADH are 4.8 and 5.8, respectively [7]. It is difficult to describe the dissociation and protonation of carboxyl groups and amino groups on labeled proteins in an aqueous-organic solvent mixture. However, for the moment, the difference in the gaps between the isoelectric points (4.8 for BSA and 5.8 for ADH) and pH 11.8 of the water component in the carrier solution seemed consistent with the nature of the hydrophilicity or hydrophobicity of the labeled proteins observed on the chromatograms. The mixture of ILITC, ILITC-labeled glutamic acid, ILITC-labeled ADH, and ILITC-labeled BSA was also examined with the TRDC system with luminol CL detection. The obtained chromatograms are shown in Fig. 5b). ILITC, ILITC-labeled glutamic acid, ILITC-labeled ADH, and ILITC-labeled BSA were detected in this order with the organic solvent-rich carrier solution, while they were eluted in the reverse order with the water-rich carrier solution. The elution orders obtained for the mixture of ILITC and ILITC-labeled biomolecules were reasonable, considering the

free-ILITC to be more hydrophobic than the ILITC-labeled biomolecules. The elution orders for ILITC-labeled glutamic acid, ILITC-labeled ADH, and ILITC-labeled BSA on the chromatograms could indicate the hydrophilicity or hydrophobicity of these ILITC-labeled biomolecules.

In conclusion, biomolecules, α -amino acids, peptides, and proteins, were labeled with ILITC for analysis using the TRDC with the CL detection system. Separation was carried out using an untreated open-tubular fused-silica capillary tube and a water-acetonitrile-ethyl acetate mixture carrier solution without any additives, such as gels; specific columns, such as packed and monolithic; or applying a high voltage. Detection was also simply performed using CL detection without a light source and complex optical devices. The separation performance of free-ILITC and ILITC-labeled biomolecules gave interesting information about the hydrophilic or hydrophobic nature in the labeling biomolecules. ILITC, ILITC-labeled α -amino acid, ILITC-labeled protein in the mixture solution were separated and confirmed by the individual peaks on the chromatograms. TRDC has mostly been applied to the analysis of organic compounds with low molecular weights. The results obtained for biomolecules, especially, biopolymer analysis considered here provide insight to expand the TRDC system to future research.

Table 1 Classification of ILITC-labeled α -amino acids nature compared to the ILITC one from the view point of hydrophilicity or hydrophobicity in the TRDC system

			Organic solvent – rich	Water - rich	
Neutral amino acid	Aliphatic amino acid	Gly	Hydrophobic	Hydrophobic	
		Ala	Neutral	Neutral	
		Val	Hydrophobic	Hydrophobic	
		Leu	Neutral	Neutral	
		Ile	Hydrophobic	Neutral	
		Asn	Neutral	Neutral	
		Gln	Hydrophobic	Hydrophobic	
	Oxy amino acid	Ser	Hydrophilic	Neutral	
		Thr	Hydrophilic	Hydrophilic	
		Sulfur-containing amino acid	Sys	Hydrophilic	Hydrophilic
	Met		Hydrophilic	Neutral	
	Aromatic amino acid		Phe	Hydrophobic	Hydrophobic
			Tyr	Hydrophobic	Neutral
	Heterocyclic compound amino acid	Trp	Hydrophobic	Hydrophobic	
Pro		Hydrophobic	Hydrophobic		
Acidic amino acid	Asp	Hydrophilic	Neutral		
	Glu	Hydrophilic	Neutral		
Basic amino acid	Aliphatic amino acid	Lys	Hydrophilic	Neutral	
		Arg	Hydrophilic	Neutral	
	Heterocyclic compound amino acid	His	Hydrophilic	Hydrophilic	

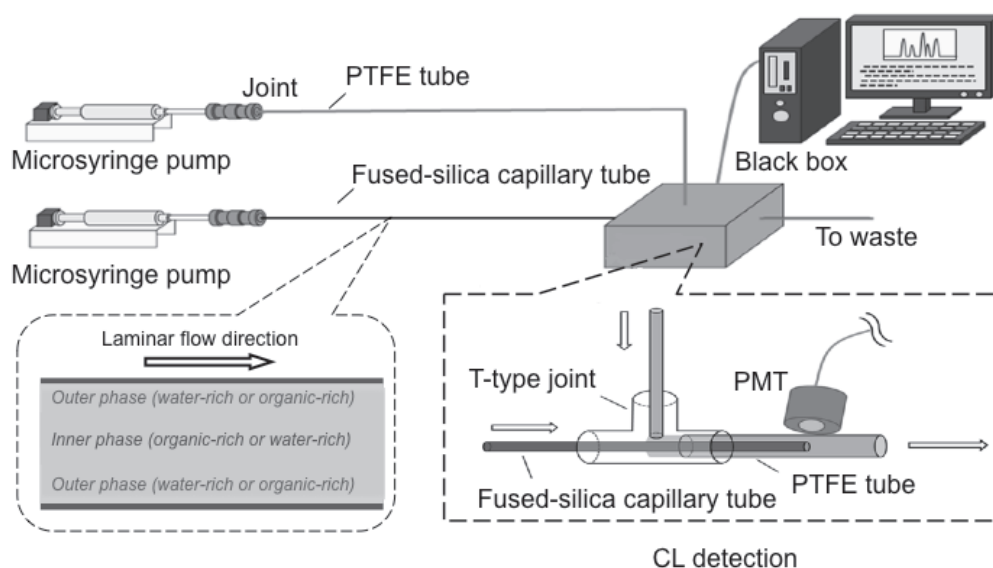


Figure 1. Schematic diagram of the present TRDC system with CL detection.

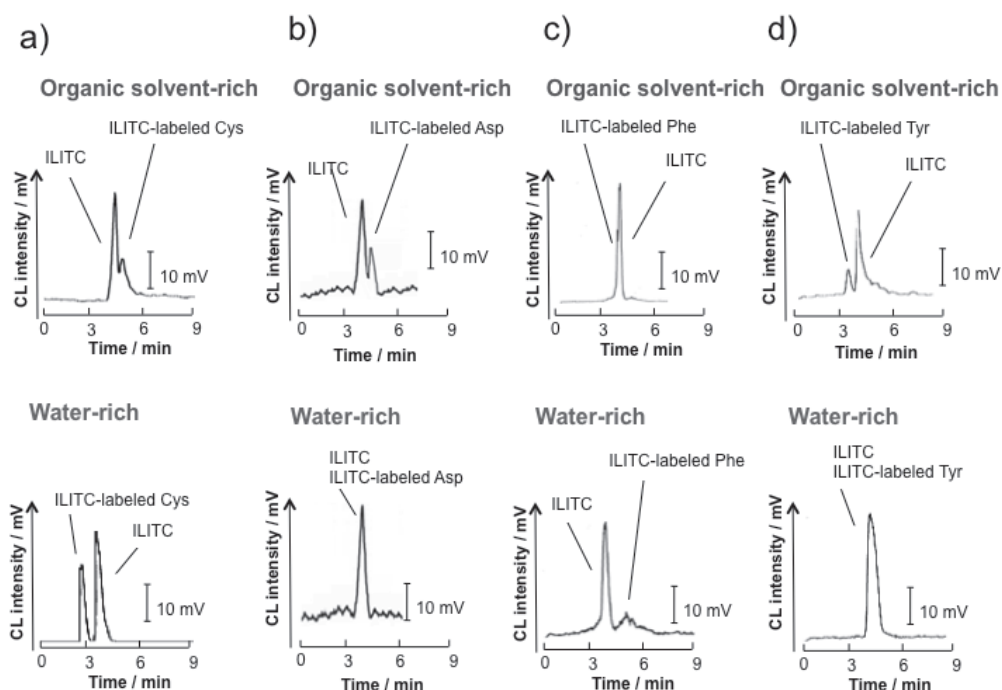


Figure 2. Chromatograms of a mixture of ILITC and ILITC-labeled a) cysteine, b) aspartic acid, c) phenylalanine, and d) tyrosine obtained by the present TRDC system. Conditions: Capillary tube, 70 cm length of 75 μm i.d. fused-silica; carrier, water-acetonitrile-ethyl acetate (3:8:4 v/v/v) mixture solution (organic solvent-rich) and water-acetonitrile-ethyl acetate (15:3:2 v/v/v) mixture solution (water-rich); sample injection, 25 cm height (gravity) \times 10 s; flow rate of the carrier solution, 0.5 $\mu\text{L min}^{-1}$; and ILITC-labeled α -amino acid concentration, 50 mM.

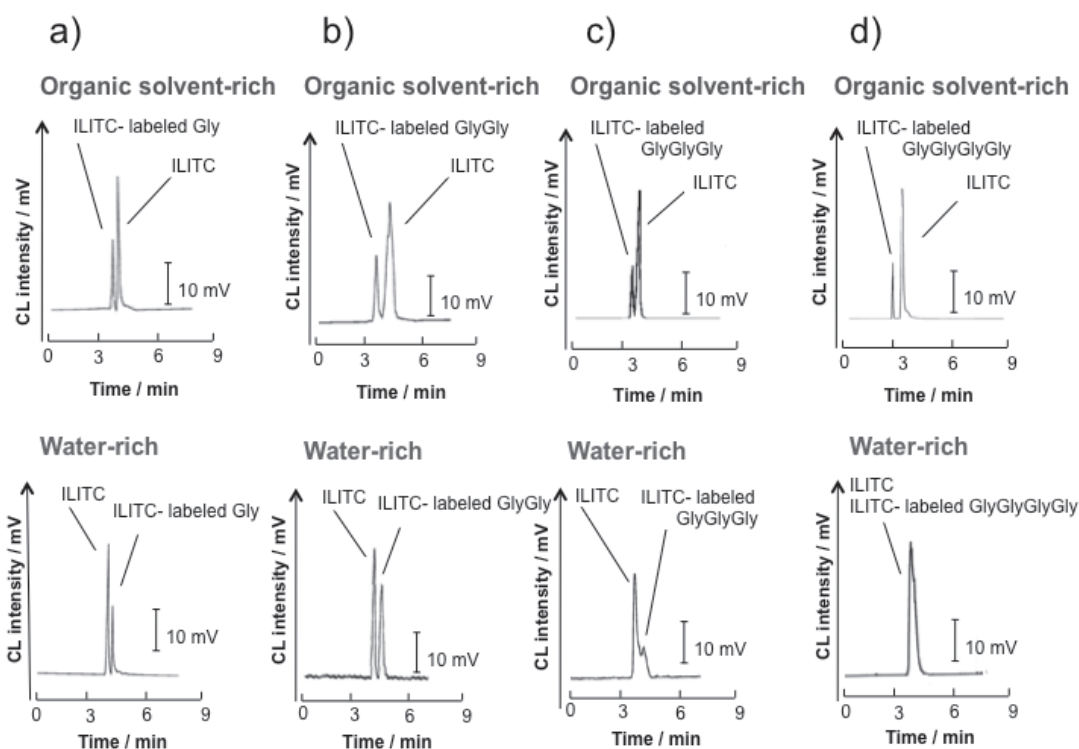


Figure 3. Chromatograms of a mixture of ILITC and ILITC-labeled glycine or peptides obtained by the present TRDC system. ILITC-labeled glycine and peptides concentration, 50 mM. Other conditions are the same as in Fig. 2.

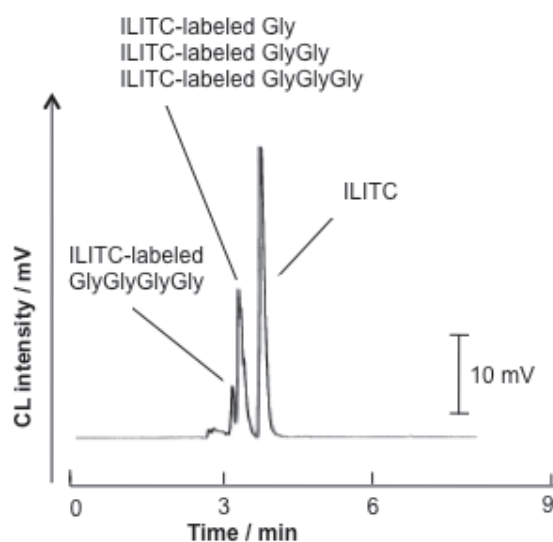


Figure 4. Chromatograms of a mixture of ILITC, ILITC-labeled glycine, and three kinds of peptides obtained by the present TRDC system. Carrier, water-acetonitrile-ethyl acetate (3:8:4 v/v/v) mixture solution (organic solvent-rich). Other conditions are the same as in Fig. 2.

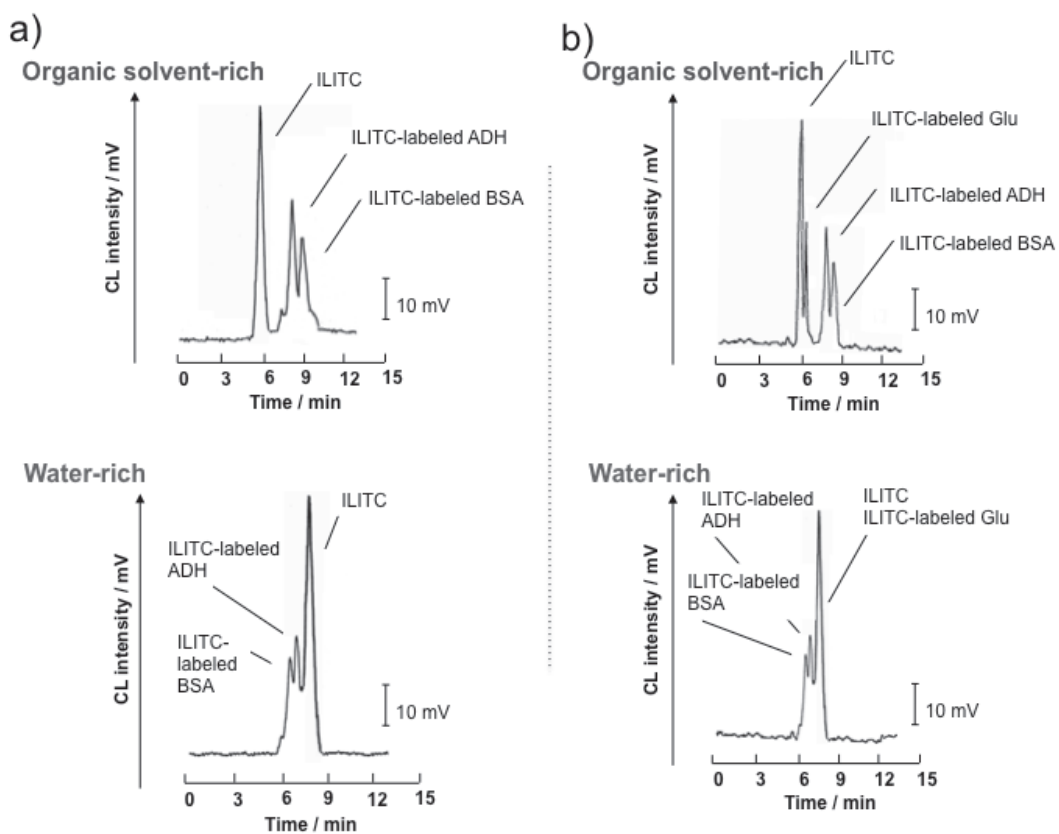


Figure 5. Chromatograms of mixtures of a) ILITC, ILITC-labeled ADH, and ILITC-labeled BSA as well as b) ILITC, ILITC-labeled glutamic acid, ILITC-labeled ADH, and ILITC-labeled BSA obtained by the present TRDC system. ILITC-labeled analytes concentration, 50 mM. Other conditions are the same as in Fig. 2.

8.5 Examination of lambda-DNA molecules as analytes with TRDC

The elution behavior of lambda-DNA (48502 bp) as a biopolymer was examined by the tube radial distribution chromatography TRDC system. The ternary mixture of water-acetonitrile-ethyl acetate, 15:3:2 or 3:8:4 volume ratio, as a carrier solution was fed into the capillary tube made of PTFE or fused-silica. The mixture of hydrophobic 1-naphthol and hydrophilic lambda-DNA was subjected to the TRDC system using the water-rich carrier solution. Lambda-DNA and 1-naphthol were distributed between the inner and outer phases due to their hydrophilic and hydrophobic nature, and then eluted in this order, undergoing chromatographic separation. The mixture of hydrophilic 2,6-naphthalenedisulfonic acid and hydrophobic lambda-DNA that was treated with surfactants was also examined with the organic solvent-rich carrier solution. The modified hydrophobic DNA and 2,6-naphthalenedisulfonic acid were distributed and eluted in this order due to their nature.

Introduction

The TRDP is a new phase-interface concept and can be applied in various technological, engineering, and other scientific fields. We are currently investigating the TRDP from the viewpoints of chromatography, extraction, and chemical reaction space. In the open-tubular capillary chromatography called tube radial distribution chromatography (TRDC), the outer phase created based on the TRDP in a capillary tube acts as a pseudo-stationary phase. The TRDC system works without applying high voltages or using specific columns, e.g., monolithic or packed. Although various types of analytes have been analyzed using the TRDC system, there has not been enough information about the elution behavior of polymer compounds in the TRDC system or the TRDP. We were interested in the elution behavior of such large biomolecules, such as lambda-DNA, and here we tentatively examined such behavior by the TRDC system.

Experimental

Polytetrafluoroethylene (PTFE) capillary tubes with 100 μm inner diameter and fused-silica capillary tubes with 50 μm inner diameter were used. A schematic diagram of the present capillary chromatography system comprises an open-tubular capillary tube, microsyringe pump (55-1111, Harvard Apparatus; Bioanalytical Systems, Inc., West Lafayette, IN), and absorption detector (Fig. 1). The tube temperature was controlled by dipping the capillary tube in water that was maintained at a constant temperature in a vessel. Water-acetonitrile-ethyl acetate mixtures with volume ratios of 15:3:2 and 3:8:4 were used as carrier solutions. The component ratios of 15:3:2 and 3:8:4 were recommended as water-rich and an organic solvent-rich carrier solutions in our previous reports [5,6,12]. Analyte solutions were prepared with the carrier solutions. The analyte solution was introduced directly into the capillary inlet side through the gravity method. After analyte injection, the capillary inlet was connected through a joint to a microsyringe. The syringe was set on the microsyringe pump. The carrier solution was fed into the capillary tube at a definite flow rate under laminar flow conditions. On-capillary absorption detection (254 or 260 nm) was performed by using the detector.

Results and discussion

Preliminary experiments concerning lambda-DNA Lambda-DNA (M_w 32300000; 48502 bp) that has a relatively large molecular weight features hydrophilic and partially hydrophobic characters, although the details depend on circumstances and conditions, such as temperature, the dissolved solvent, and which additives were added. We tried to examine the elution behavior of lambda DNA with the TRDC system with the water-rich and organic solvent-rich carrier solutions. First, the solubility of lambda-DNA was examined in the carrier solutions for the TRDC system. Lambda-DNA was dissolved by the water-rich carrier solution but was not dissolved by the organic solvent-rich carrier solution due to its hydrophilic nature. The absorption spectra of lambda-DNA were examined in the water-rich carrier solution. The spectra changed gradually up until 48 h (the absorbance at 260 nm increased) and after that, it did not change, maintaining its shape. As far as we know, there have been no reports regarding the absorbance change of lambda-DNA in water-hydrophilic/hydrophobic organic solvent mixture solutions. The absorbance change of lambda-DNA must be attributed to the change from a double helix conformation to a single coil one with ethyl acetate or water-acetonitrile-ethyl acetate mixture. That type of change was not observed with a water-acetonitrile (15:3 volume ratio) mixture solution. We will continue investigating further details in the future.

Chromatograms of lambda-DNA obtained by the TRDC system with the water-rich carrier solution The carrier temperature is critical to the performance of TRDC separation. The PTFE capillary tube showed overall better resolutions than the fused-silica ones in the TRDC system with the water-rich carrier solution.¹⁵⁾ Typical model analytes for the TRDC separation, hydrophobic 1-naphthol and hydrophilic 2,6-naphthalenedisulfonic acid, were subjected to the TRDC system with the water-rich carrier solution and a PTFE capillary tube at a tube temperature of 0 - 50 °C (Fig. 2). The TRDC system with the water-rich carrier solution creates the water-rich major inner phase and organic solvent-rich minor outer phase (pseudo-stationary phase), as described in the Introduction. Hydrophilic 2,6-naphthalenedisulfonic acid, which was dispersed in the inner phase, and hydrophobic 1-naphthol, which was dispersed in the outer phase, were eluted in this order, undergoing chromatographic separation. The resolutions were improved at lower temperatures and showed the best resolution at 0 °C. In the TRDC system using the water-rich carrier solution, the peaks of lambda-DNA on the chromatogram gradually changed up until 48 h and after that ceased to change, as shown in Fig. 3. The times in Fig. 3 mean the standing-times of the analyte solution before injection into the system. The change-tendency on chromatograms was similar to that on the absorption spectra mentioned above. Then, the mixture of hydrophobic 1-naphthol and hydrophilic lambda-DNA that was left for 48 h in the carrier solution was examined with the TRDC system with the water-rich carrier solution at a tube temperature of 0 °C. Other analytical conditions, such as flow rate, an analyte injection volume, and a capillary length were recommended through our reports. The obtained chromatograms are shown in Fig. 4. Lambda-DNA and 1-naphthol were completely separated on the chromatogram. They were distributed between the inner and outer phases due to their hydrophilic and hydrophobic nature, and then eluted in this order,

Chromatograms of lambda-DNA obtained by the TRDC system with the organic solvent-rich carrier solution When the organic solvent-rich carrier solution was used in the TRDC system, the fused-silica capillary tube showed better resolutions than the

PTFE tube.¹⁰⁾ Then, the model analytes for the TRDC, hydrophobic 1-naphthol and hydrophilic 2,6-naphthalenedisulfonic acid, were subjected to the TRDC system with the organic solvent-rich carrier solution and a fused-silica capillary tube at tube temperatures 0 - 65 °C (Fig. 5). The TRDC system with the organic solvent-rich carrier solution creates an organic solvent-rich major inner phase and a water-rich minor outer phase. Hydrophobic 1-naphthol dispersed in the inner phase and hydrophilic 2,6-naphthalenedisulfonic acid dispersed in the outer phase were eluted in this order, undergoing chromatographic separation. The resolutions changed with the tube temperatures and showed their best resolutions at 20 °C. As lambda-DNA was not directly dissolved by the organic solvent-rich carrier solution as mentioned above, lambda-DNA was dissolved in 20 mM sodium dodecylsulfonate (SDS) solutions to prepare the lambda-DNA analyte solution. The treatments that surrounded lambda-DNA with surfactants made lambda-DNA stable hydrophobically. The mixture of hydrophilic 2,6-naphthalenedisulfonic acid and surfactant-modified hydrophobic lambda-DNA was examined through the TRDC system with the organic solvent-rich carrier solution at a tube temperature of 20 °C. The other analytical conditions were recommended through our papers. The obtained chromatograms are shown in Fig. 6. Surfactant-modified lambda-DNA and 2,6-naphthalenedisulfonic acid were completed and separated on the chromatogram. They were distributed between the inner and outer phases due to their hydrophobic and hydrophilic natures, and then eluted in this order.

In conclusion, the elution behavior of lambda-DNA was examined with the TRDC based on the TRDP. 1-Naphthol and bare lambda-DNA mixture as well as 2,6-naphthalenesulfonic acid and surfactant-modified lambda-DNA were separated with the TRDC system, due to their hydrophilic and hydrophobic natures. The elution behavior of lambda-DNA was consistent with the separation performance of the TRDC system. The elution behavior observed for lambda-DNA, a rather large biomolecule, is interesting and will be important in future applications of the TRDP or TRDC.

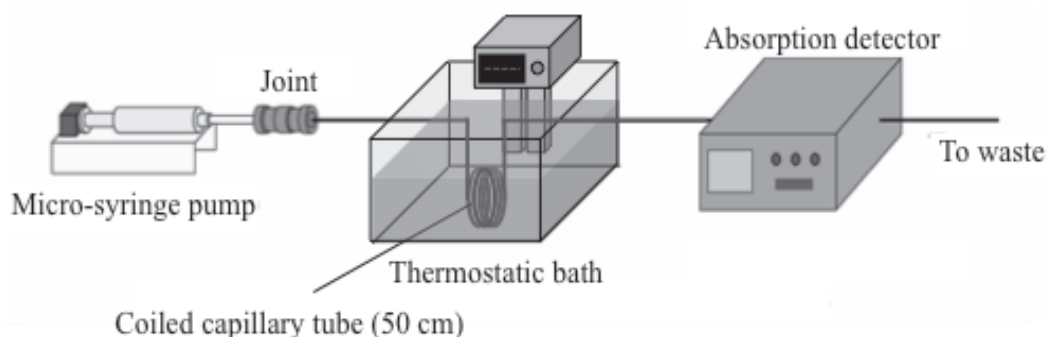


Figure 1. Schematic diagram of the present TRDC system.

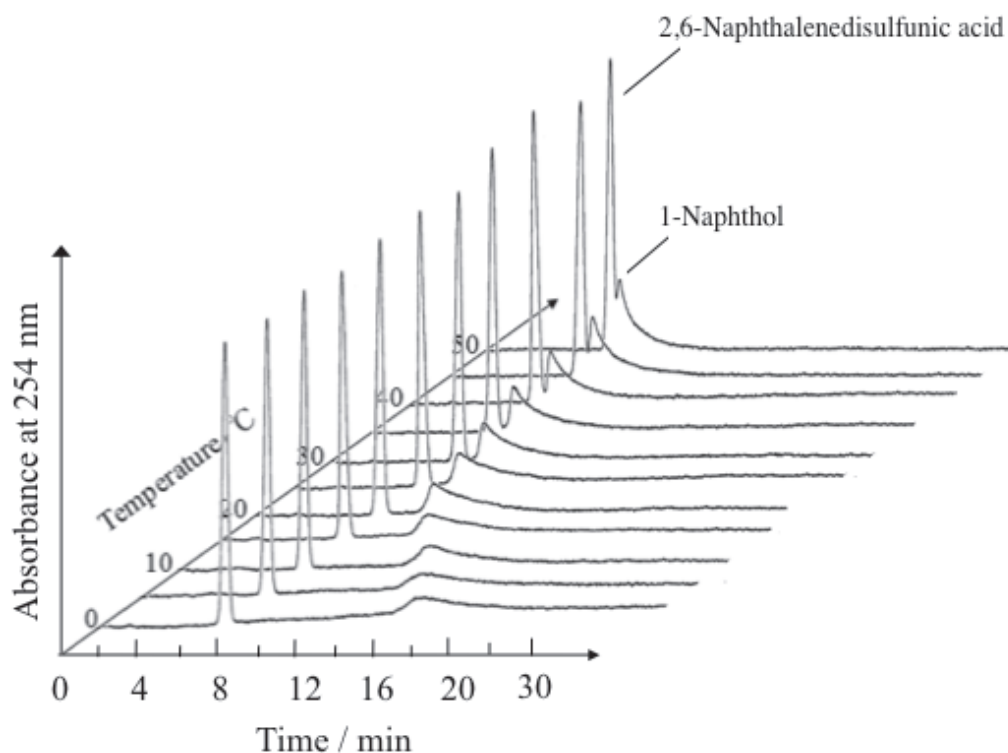


Figure 2. Chromatograms of 1-naphthol and 2,6-naphthalenedisulfonic acid obtained by the TRDC system using the water-rich carrier solution. Conditions: Capillary tube, 110 cm (effective length: 90 cm) of 100 μm i.d. PTFE; carrier, the water-rich solution (water-acetonitrile-ethyl acetate, 15:3:2 volume ratio); sample injection, 50 cm height (gravity) \times 20 s; flow rate, 1.3 $\mu\text{L min}^{-1}$; tube temperature, 0 - 50 $^{\circ}\text{C}$; absorption detection, 254 nm; and 1 mM 1-naphthol and 2,6-naphthalenedisulfonic acid.

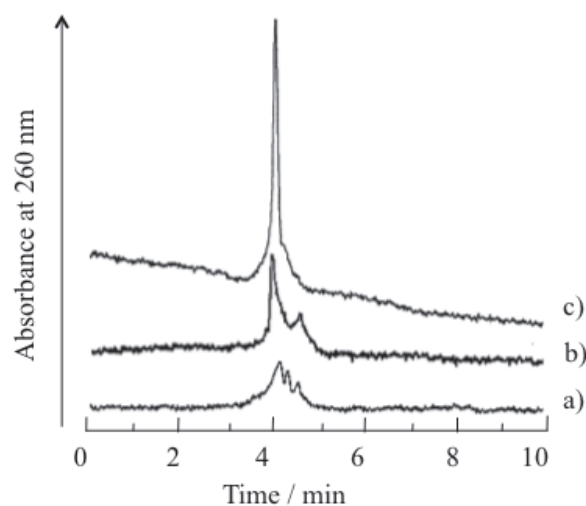


Figure 3. Chromatograms of lambda-DNA obtained by the TRDC system using the water-rich carrier solution. a) 0 h, b) 24 h and c) 48 h after analytes preparation. Conditions: Capillary tube, 110 cm (effective length, 90 cm) of 50 μm i.d. fused-silica; carrier, the water-rich carrier solution (15:3:2, volume ratio); sample injection, 50 cm height (gravity) \times 20 s; flow rate, 0.5 $\mu\text{L min}^{-1}$; tube temperature, 20 $^{\circ}\text{C}$; absorption detection, 260 nm; and lambda-DNA, 0.8 nM.

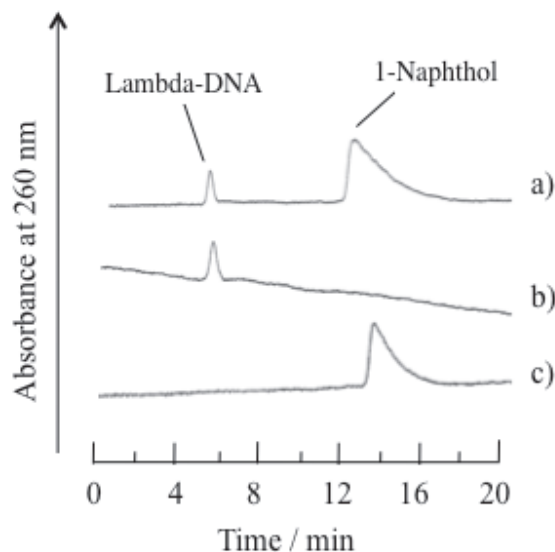


Figure 4. Chromatograms of 1-naphthol and lambda-DNA obtained by the TRDC system using the water-rich carrier solution. a) 0.8 nM lambda-DNA and 1 mM 1-naphthol, b) 0.8 nM lambda-DNA, c) 1 mM 1-naphthol. Conditions: Capillary tube, 110 cm (effective length, 90 cm) of 100 μm i.d. PTFE; carrier, the water-rich solution (water-acetonitrile-ethyl acetate, 15:3:2 volume ratio); sample injection, 50 cm height (gravity) \times 20 s; flow rate, 1.3 $\mu\text{L min}^{-1}$; tube temperature, 0 $^{\circ}\text{C}$; absorption detection, 260 nm.

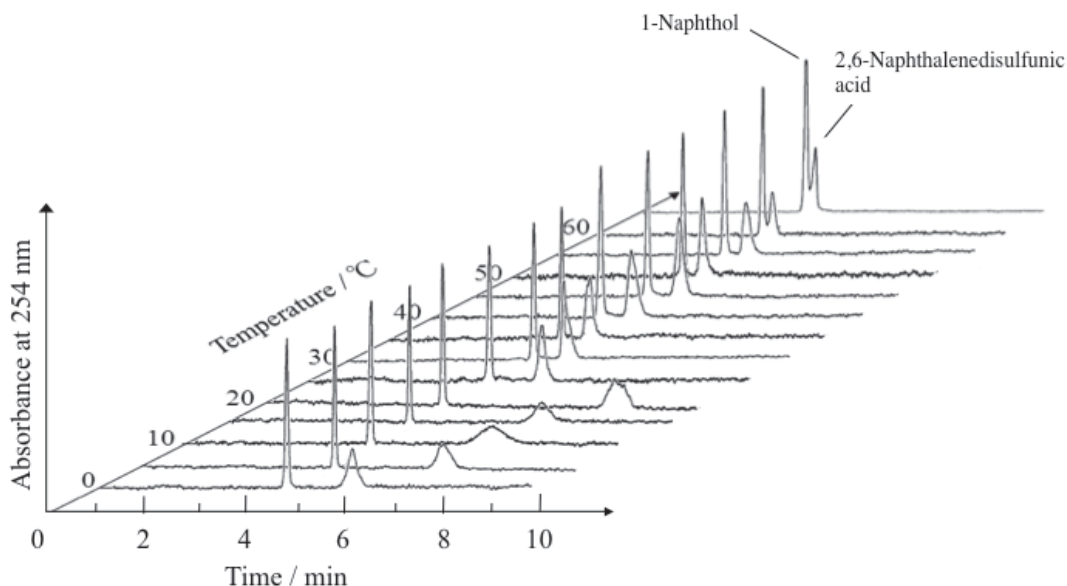


Figure 5. Chromatograms of 1-naphthol and 2,6-naphthalenedisulfonic acid obtained by the TRDC system using the organic solvent-rich carrier solution. Conditions: Capillary tube, 110 cm (effective length: 90 cm) of 50 μm i.d. fused-silica; carrier, the organic solvent-rich solution (water-acetonitrile-ethyl acetate, 3:8:4 volume ratio); sample injection, 50 cm height (gravity) \times 20 s; flow rate, 0.5 $\mu\text{L min}^{-1}$; temperature, 0 - 65 $^{\circ}\text{C}$; absorption detection, 254 nm; and 1 mM 1-naphthol and 2,6-naphthalenedisulfonic acid.

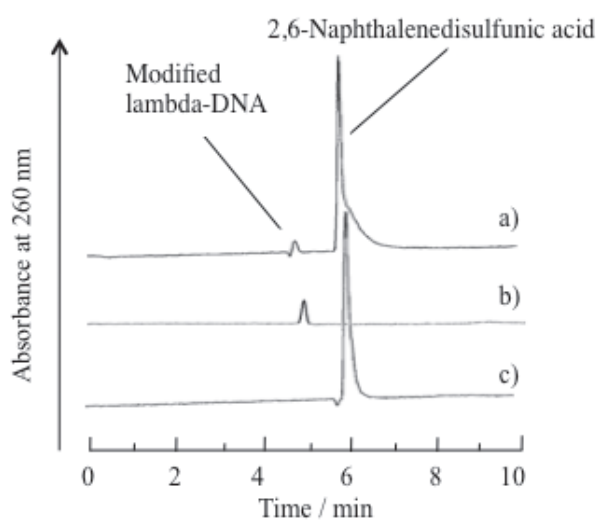


Figure 6. Chromatograms of 2,6-naphthalenedisulfonic acid and SDS-modified lambda-DNA obtained by the TRDC system using the organic solvent-rich carrier solution. a) 0.8 nM lambda-DNA and 1 mM 2,6-naphthalenedisulfonic acid, b) 0.8 nM lambda-DNA, c) 1 mM 2,6-naphthalenedisulfonic acid. Conditions: Capillary tube, 110 cm (effective length, 90 cm) of 50 μm i.d. fused-silica; carrier, the organic solvent-rich solution (water-acetonitrile-ethyl acetate, 3:8:4 volume ratio); sample injection, 50 cm height (gravity) \times 20 s; flow rate, 0.5 $\mu\text{L min}^{-1}$; tube temperature, 20 $^{\circ}\text{C}$; absorption detection, 260 nm; and analyte solution includes 20 mM SDS.

8.6 Examination of metal ions as analytes with TRDC using absorption reagent

Chrome Azurol S as an absorption reagent was introduced into the tube radial distribution chromatography (TRDC) system for metal ion separation and on-line detection. The fused-silica capillary tube (75 μm i.d. and 110 cm length) and a water-acetonitrile-ethyl acetate mixture (3:8:4 volume ratio) including 20 mM Chrome Azurol S as a carrier solution were used. Metal ions, i.e., Co(II), Cu(II), Ni(II), Al(III), and Fe(III), as models were injected into the present TRDC system. Characteristic individual absorption characteristics and elution times were obtained as a result of complex formation between the metal ions and Chrome Azurol S in the water-acetonitrile-ethyl acetate mixture solution. The elution times of the metal ions were examined based on their absorption behavior; Co(II), Ni(II), Al(III), Fe(III), and Cu(II) were eluted in this order over elution times of 4.7 - 6.8 min. The elution orders were determined from the molar ratios of the metal ions to Chrome Azurol S and Irving-Williams series for bivalent metal ions.

Introduction

Various types of analytes, such as organic compounds, amino acids, proteins, nucleosides, metal ions, metal complexes, fluorescent compounds, and optical isomers, were analyzed using the TRDC system. However, metal ions and metal complexes were separated and detected by our TRDC system which was equipped with chemiluminescence detection. The metal ions and metal complexes show catalytic activity for luminol-hydrogen peroxide chemiluminescence reactions. Although chemiluminescence detection has several advantages, including no requirement for a light source and high sensitivity, it requires a hydrogen peroxide delivery line and pump, mixing device, and flow detection cell to perform chemiluminescence analysis in the system.

Here, Chrome Azurol S was introduced as an absorption reagent into the TRDC system for metal ion separation and on-line detection. Metal ions, i.e., Co(II), Cu(II), Ni(II), Al(III), and Fe(III), as models were examined by the TRDC system. Characteristic individual absorption characteristics and elution times were obtained as the results of complex formations between the metal ions and Chrome Azurol S even in the water-acetonitrile-ethyl acetate mixture solution. The successful use of the absorption reagent in the TRDC system with the water-hydrophilic/hydrophobic organic solvent mixture for on-line metal ion analysis indicated that the TRDC system and TRDP are attractive and applicable in separation science.

Experimental

Fused-silica capillary tubes (75 μm i.d. and 150 μm o.d.) were utilized. A fused-silica capillary tube (75 μm i.d., 110 cm length; 90 cm effective length), a microsyringe pump, and an absorption detector made up the TRDC system with absorption detection. Tube temperature was controlled by immersing the capillary tube (40 cm) in water maintained at 20 $^{\circ}\text{C}$ in a beaker by stirring. A water-acetonitrile-ethyl acetate mixture in volume ratios of 3:8:4 including 20 mM Chrome Azurol S was used as carrier solution. Analyte solutions, including 1-naphthol, 2,6-naphthalenedisulfonic acid, and the metal ions (Co(II), Cu(II), Ni(II),

Cu(II), Al(III), and Fe(III) (chloride salts) as well as Ni(II) (nitrate salt), were prepared along with the carrier solution. The analyte solution was introduced directly into the capillary inlet side via the gravity method (30 cm height for 20 s), then, the capillary inlet was connected through a joint to a microsyringe. The syringe was set on the microsyringe pump. The carrier solution was fed into the capillary tube at a definite flow rate (ca. $0.8 \mu\text{L min}^{-1}$) under laminar flow conditions. On-capillary absorption detection was performed with the detector; 254 nm for 1-naphthol and 2,6-naphthalenedisulfonic acid or 600 nm for metal ions.

Results and discussion

Absorption spectra for metal ion-Chrome Azurol S complexes The molecular structure of Chrome Azurol S is shown in Fig. 1. Chrome Azurol S is used as an absorption reagent for metal ion detection through a complex formation reaction with metal ions in aqueous solution [8-10]. First, whether Chrome Azurol S reacts with metal ions to produce a complex in the ternary mixed solvents of water-acetonitrile-ethyl acetate (3:8:4 volume ratio) as well as whether the complex shows characteristic absorption in the ternary mixed solvent solution were examined. Absorption spectra based on metal ion-Chrome Azurol S complex formation in the ternary mixed solvents of water-acetonitrile-ethyl acetate (3:8:4 volume ratio) are shown in Fig. 2 together with analytical conditions. It was clearly shown that the metal ions, Co(II), Cu(II), Ni(II), Al(III), and Fe(III), had specific absorption spectra through complex formation with Chrome Azurol S in the ternary mixed solvent solution, compared to the absorption spectrum of Chrome Azurol S itself, in the absence of any metal ions. A wavelength of 600 nm was used for on-line metal detection in the TRDC system equipped with absorption detection in the following experiments.

Phase diagram of the ternary mixed solvents including Chrome Azurol S A phase diagram for the ternary mixture solvents of water-acetonitrile (hydrophilic organic solvent)-ethyl acetate (hydrophobic organic solvent) including 20 mM Chrome Azurol S was examined in a vessel at a temperature of 22 °C. The obtained phase diagram is shown in Fig. 3. As shown in the diagram, 20 mM Chrome Azurol S was not dissolved in the ternary mixed solvent solutions with a water component ratio of less than ca. 12 volume %. The phase diagram showed that each component ratio of the solvents made a homogeneous (one homogeneous phase) or heterogeneous (two homogeneous phases) solution. The curve in the diagram indicates the boundary between the homogeneous and heterogeneous phases. The TRDC system was used with certain homogeneous carrier solutions with component ratios of solvents that were positioned near the homogeneous-heterogeneous solution boundary curve in the phase diagram. Such specific carrier solutions caused a tube radial distribution of the carrier solvents in the capillary tube under laminar flow conditions, i.e., the TRDP. In addition, in the TRDC system using the fused-silica capillary tube, the organic solvent-rich carrier solution had better resolution than the water-rich carrier solution.¹⁰⁾ Here, the homogeneous solution of water-acetonitrile-ethyl acetate mixture (3:8:4 volume ratio) including 20 mM Chrome Azurol S, the component ratio of which was near the boundary curve in the phase diagram (Fig. 3), was used as a carrier solution in the present TRDC system using the fused-silica capillary tube.

Separation and detection of 1-naphthol and 2,6-naphthalenedisulfonic acid The TRDP leads to the formation of inner and outer phases, i.e., a kinetic liquid-liquid interface, in a capillary tube under laminar flow conditions. In this case using the water-acetonitrile-ethyl acetate mixture (3:8:4 volume ratio) including 20 mM Chrome Azurol S carrier solution (organic solvent-rich carrier solution), the organic solvent-rich major inner phase was generated around the middle of the tube, while the water-rich minor outer phase was formed near the inner wall. In the TRDC system, the outer phase that moved relatively little under laminar flow conditions acted as a pseudo-stationary phase. Analytes were distributed between the inner and outer phases due to their nature, undergoing chromatographic separation. To confirm that the TRDP occurred in the capillary tube under the present analytical conditions, a mixture of 1-naphthol and 2,6-naphthalenedisulfonic acid was injected into the present TRDC system which was designed for the separation and detection of metal ions through complex formations between a metal ion and Chrome Azurol S. The mixture of them has been used as a model analyte for the TRDC system. The obtained chromatogram is shown in Fig. 4. 1-Naphthol (hydrophobic) and 2,6-naphthalenedisulfonic acid (hydrophilic) were separated and detected (254 nm) in this order. The first peak of 1-naphthol was eluted near the average linear velocity under laminar flow conditions. The elution behavior observed on the chromatogram supported the occurrence of TRDP in the present TRDC system.

Chromatograms of metal ions The metal ions Co(II), Cu(II), Ni(II), Al(III), and Fe(III) were examined in the present TRDC system. The obtained individual chromatograms are shown in Fig. 6 together with analytical conditions. The elution times and peak areas of the metal ions are summarized in Table 1 with those of 1-naphthol and 2,6-naphthalenedisulfonic acid shown in Fig. 5. As shown in the table, the elution times of Co(II), Ni(II), Al(III), Fe(III), and Cu(II) metal ions increased in this order. Elution order will be discussed later. Tentatively, the Al(III) and Cu(II) mixture as well as the Co(II) and Cu(II) mixture were analyzed in the present TRDC system. The obtained chromatograms are shown in Fig. 7. As shown in the figures, they were completely separated and detected on the chromatograms. To obtain quantitative information, the calibration curves of Al(III) and Cu(II) were examined by the TRDC system. Al(III) and Cu(II) were linearly determined over the range of 0.2 – 5 mM (coefficient of correlation 0.997) and 0.2 – 4 mM (coefficient of correlation 0.994), respectively.

Molar ratios of metal ions to Chrome Azurol S on complex formation The molar ratios of the metal ions to Chrome Azurol S at the point of complex formation in the ternary mixed solvents of water-acetonitrile-ethyl acetate mixture were examined using a standard molar ratio method. To each, 1.0 mM metal ion solution (0.5 mL) was added to various concentrations of Chrome Azurol S solution (4.5 mL) to obtain a metal ion-Chrome Azurol S mixture solution including 0.1 mM metal ions and 0.025-0.400 mM Chrome Azurol S, where all solutions were prepared with the ternary mixed solvents of the water-acetonitrile-ethyl acetate mixture (3:8:4 volume ratio). Fig. 7 shows the relationship between the molar ratio of Chrome Azurol S to Fe(III) and the absorption due to complex formation. From the figure, it was clearly shown that the molar ratio of Fe(III) to Chrome Azurol S was 1:2. In a similar way, the molar ratios of

the other metal ions, Co(II), Ni(II), Cu(II), and Al(III), to Chrome Azurol S were examined, and respective values were 1:1, 1:1, 1:2, and 1:1.

Elution order and separation mechanism The TRDP in the present TRDC system created an organic solvent-rich major inner phase and a water-rich minor outer phase in the capillary tube. Hydrophilic Chrome Azurol S was distributed in the water-rich minor outer phase and acted as a pseudo-stationary phase on chromatography. Complex formation between the metal ion and Chrome Azurol S must make the complex more hydrophobic through charge counteraction concerning the positive charge of the metal ion, negative charge of Chrome Azurol S, or the counteranion (chloride ion). That is, the complexes would be effectively distributed in the organic solvent-rich major inner phase that acts as a mobile phase, leading to earlier elution times in the TRDC system. However, due to the naturally hydrophilic nature of Chrome Azurol S, the complexes with lower stabilities instead showed earlier elution times. Furthermore, the molar ratio of metal ions to Chrome Azurol S of 1:1 would elute earlier than that of 1:2. With regard to bivalent metal ions, the elution order of Co(II), Ni(II), and Cu(II) was consistent with the Irving-Williams series (Co(II) < Ni(II) < Cu(II)) and the molar ratios calculated above (the ratio of metal ion to Chrome Azurol S; 1:1 for Co(II) and Ni(II) as well as 1:2 for Cu(II)). For trivalent metal ions, the elution order of Al(III) and Fe(III) was also consistent with the molar ratios calculated above (1:1 for Al(III) and 1:2 for Fe(III)).

Different elution behavior between nickel (II) chloride and nickel (II) nitrate In the experiments performed in the present study, the nickel (II) nitrate solution as an analyte showed a later elution time (7.5 min) than the nickel (II) chloride (5.2 min). The difference in elution times between nickel (II) chloride and nickel (II) nitrate exhibited excellent reproducibility. Although the reason has not yet been clarified, the electron density and the ion diameter of the counteranion, chloride or nitrate anion, may influence hydrophobicity of the complexes. By taking advantage of the elution behavior of nickel (II) nitrate, we attempted to separate a metal ion mixture solution including Co(II), Cu(II), and Al(III) (chloride salts) as well as Ni(II) (nitrate salt) using the present TRDC system. The obtained chromatogram is shown in Fig. 8. Co(II), Al(III), Cu(II), and Ni(II) were completely separated and detected with good reproducibility by the present TRDC system.

In conclusion, metal ions and metal complexes were separated and detected by a TRDC system equipped with chemiluminescence detection. Although chemiluminescence detection has several advantages, such as lack of light source requirements and high sensitivity, it requires an oxidant delivery line and pump, a solution mixing device, and a flow detection cell for performing chemiluminescence flow analysis. Here, Chrome Azurol S as an absorption reagent was introduced into the TRDC system for metal ion separation and on-line absorption detection. Characteristic individual absorption characteristics and elution times were obtained as a result of complex formation between the metal ions and Chrome Azurol S in the water-acetonitrile-ethyl acetate mixture solution. Co(II), Al(III), Cu(II), and Ni(II) were completely separated and detected in this order on-line by the TRDC system with absorption detection. The system worked without requiring the application of a high voltage and without the use of any specific columns. Metal separation was performed

using an untreated open tubular fused-silica capillary. The successful utilization of the absorption reagent in the TRDC system with the water-hydrophilic/hydrophobic organic solvent mixture for on-line metal ion analysis has great potential to expand the use of TRDP in further research.

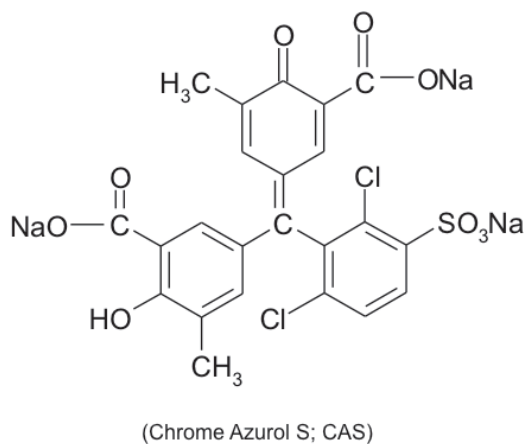


Figure 1. The molecular structure of Chrome Azurol S as an absorption reagent.

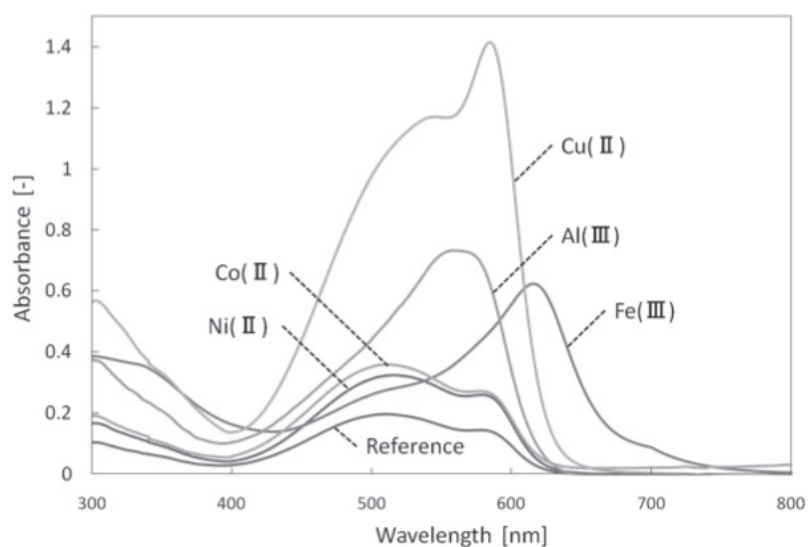


Figure 2. Absorption spectra of the metal ion-Chrome Azurol S complex in the ternary mixed solvents of water-acetonitrile-ethyl acetate (3:8:4 volume ratio). Conditions: 0.1 mM Chrome Azurol S and 0.1 mM metal ion (Co (II), Cu (II), Ni (II), Al (III), and Fe (III); chloride salts).

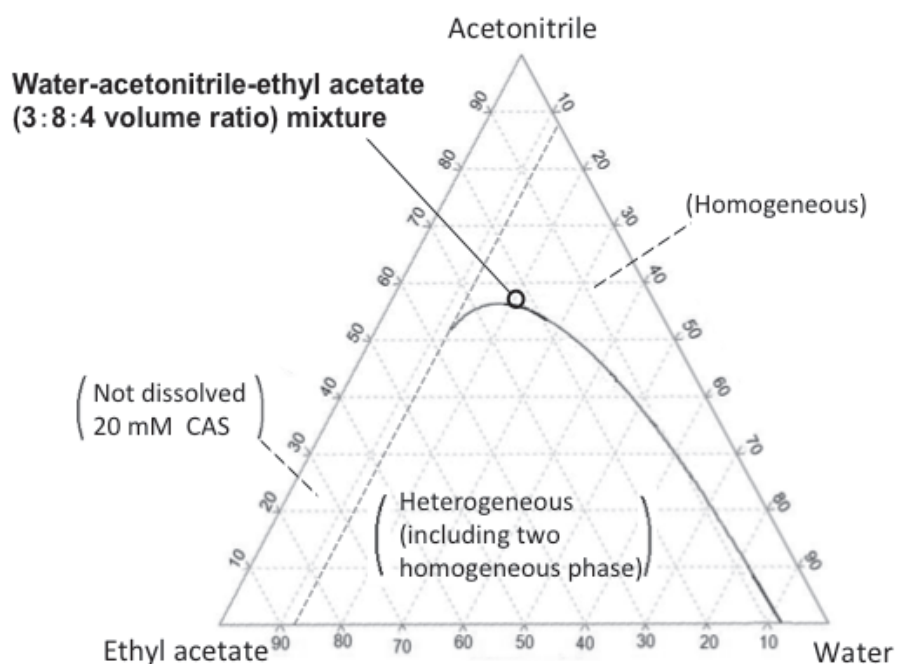


Figure 3. A phase diagram for the ternary mixture solvents of water-acetonitrile-ethyl acetate mixture including 20 mM Chrome Azurol S. Chrome Azurol S (20 mM) was not dissolved in ternary mixed solutions with water component ratios of less than ca.12 volume %. The curve in the diagram indicates the boundary between the homogeneous and heterogeneous phases.

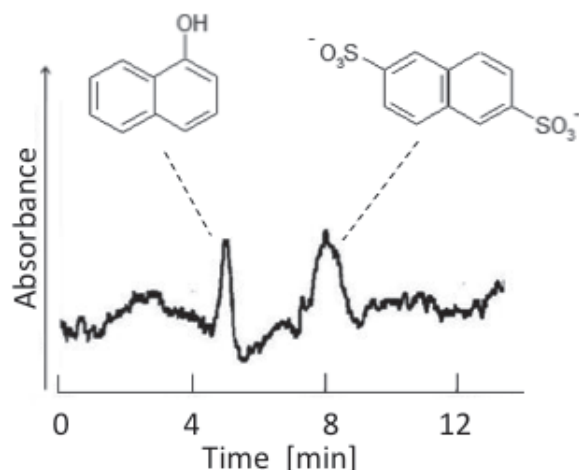


Figure 4. Chromatograms of the mixture analyte solution of 1-naphthol and 2,6-naphthalenedisulfonic acid obtained by the TRDC system. Conditions: Capillary tube, 110 cm (effective length: 90 cm) of 75 μm i.d. fused-silica; carrier, water-acetonitrile-ethyl acetate (3:8:4 volume ratio) including 20 mM Chrome Azurol S; sample injection, 30 cm height (gravity) \times 20 s; flow rate, 0.8 $\mu\text{L min}^{-1}$; and 1-naphthol and 2,6-naphthalenedisulfonic acid, 1 mM each.

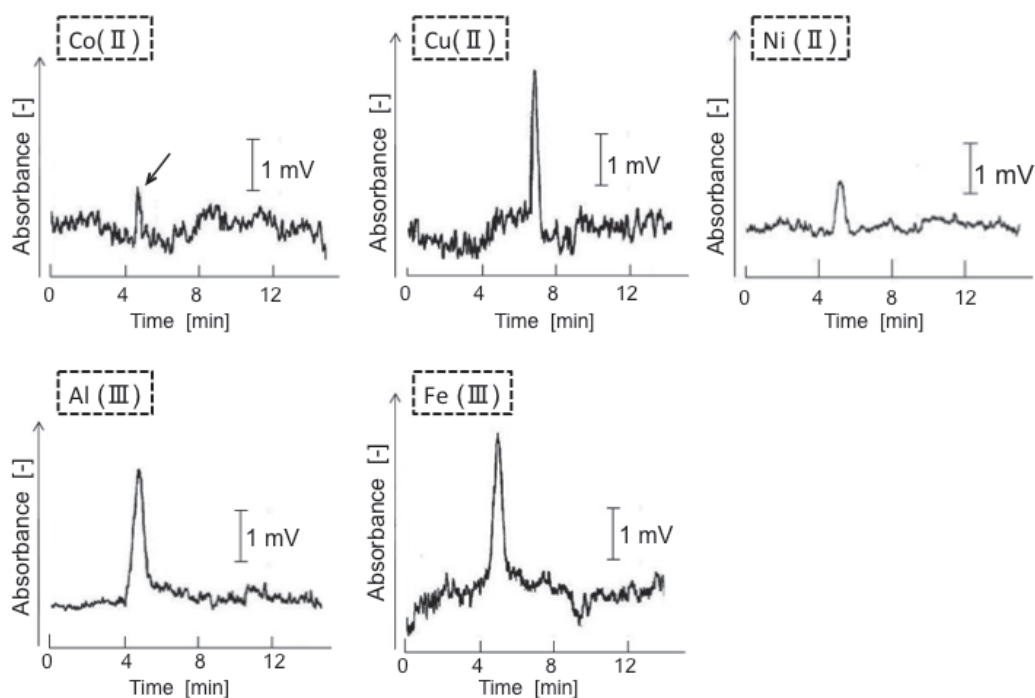


Figure 5. Chromatograms of the metal ions obtained by the TRDC system. Conditions: Capillary tube, 110 cm (effective length: 90 cm) of 75 μm i.d. fused-silica; carrier, water-acetonitrile-ethyl acetate (3:8:4 volume ratio) including 20 mM Chrome Azurol S; sample injection, 30 cm height (gravity) \times 20 s; flow rate, 0.8 $\mu\text{L min}^{-1}$; and metal ions, 1 mM each.

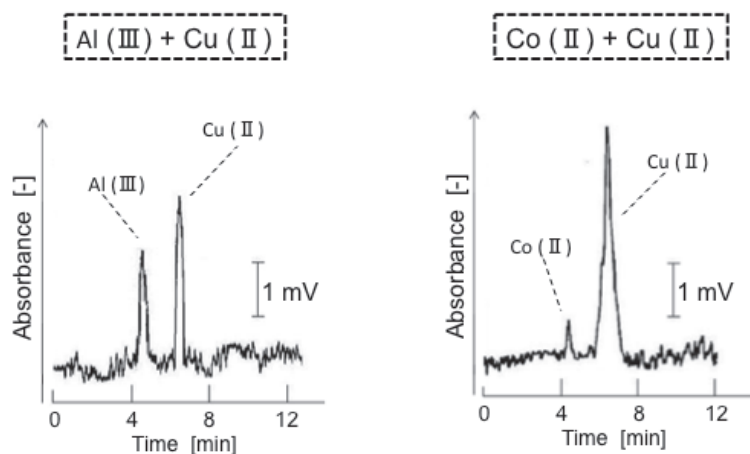


Figure 6. Chromatograms of the mixtures of metal ions, Al(III) and Cu(II) mixture as well as Co(II) and Cu(II) mixture obtained by the TRDC system. Conditions: Capillary tube, 110 cm (effective length: 90 cm) of 75 μm i.d. fused-silica; carrier, water-acetonitrile-ethyl acetate (3:8:4 volume ratio) including 20 mM Chrome Azurol S; sample injection, 30 cm height (gravity) \times 20 s; flow rate, 0.8 $\mu\text{L min}^{-1}$; and Co(II), Cu(II), and Al(III), 1 mM each.

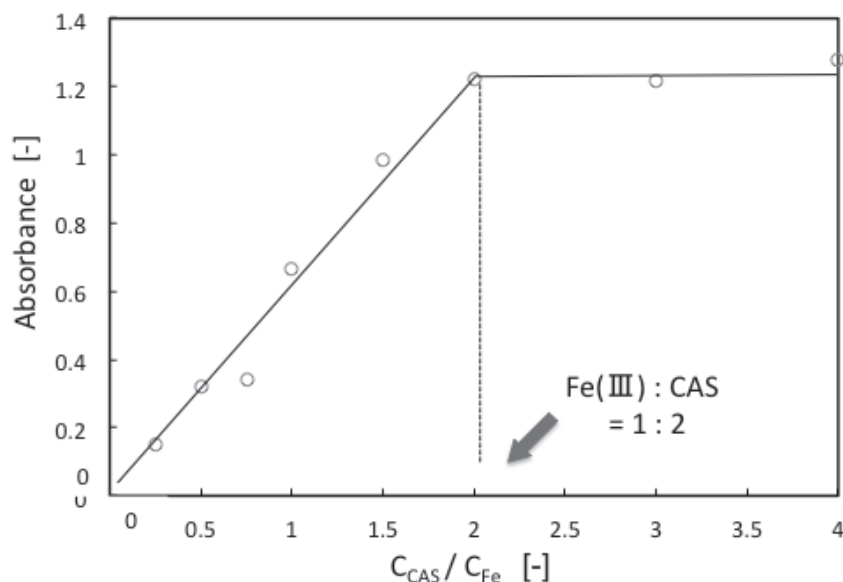


Figure 7. The relationship between the molar ratio of Chrome Azurol S to Fe(III) and absorption due to complex formation. To each 1.0 mM of metal ion solution (0.5 mL) various concentrations of Chrome Azurol S solution (4.5 mL) were added in order to produce a metal ion-Chrome Azurol S mixture solution including 0.1 mM metal ions and 0.025-0.400 mM Chrome Azurol S; all solutions were prepared with the ternary mixed solvents of water-acetonitrile-ethyl acetate mixture (3:8:4 volume ratio).

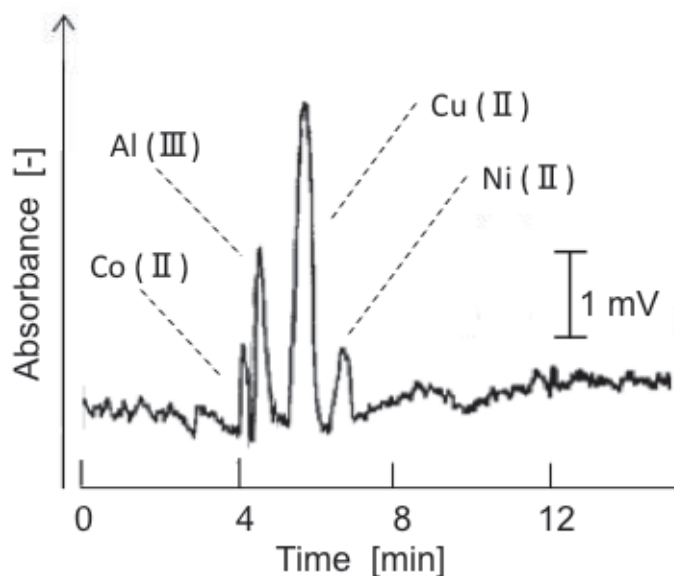


Figure 8. Chromatograms of the mixtures of metal ions, Co(II), Cu(II), and Al(III) (chloride salts) as well as Ni(II) (nitrate salt). Conditions: Capillary tube, 110 cm (effective length: 90 cm) of 75 μm i.d. fused-silica; carrier, water-acetonitrile-ethyl acetate (3:8:4 volume ratio) including 20 mM Chrome Azurol S; sample injection, 30 cm height (gravity) \times 20 s; flow rate, 0.8 $\mu\text{L min}^{-1}$; and metal ions, 1 mM each.

Table 1 Elution times and peak areas of analytes

Analyte	Elution time [min]	Peak area [mV \cdot s]
1-Naphtol	5.0	11.6
2,6-NDS	8.1	20.9
Cu(II)	6.8	25.5
Co(II)	4.7	8.3
Ni(II)	5.2	13.1
Al(III)	5.4	50.9
Fe(III)	6.3	46.5

Analyte concentration, 1.0 mM.

2,6-NDS means 2,6-naphthalenedisulfonic acid.

8.7 Examination of dansyl-DL-amino acids as analytes with TRDC using cyclodextrin

The separation of enantiomers, dansyl-DL-amino acids, was carried out through open-tubular capillary chromatography based on the tube radial distribution of the carrier solvents. An untreated poly(tetrafluoroethylene) capillary tube (100 μm inner diameter and 90 cm effective length) was used as a separation column and a water–acetonitrile–ethyl acetate mixture containing cyclodextrin used as a carrier solution were utilized for the chromatography. An analyte solution of dansyl-DL-amino acids, such as dansyl-DL-methionine, was injected into the capillary tube using a gravity method, and then the analyte solution was subsequently delivered through the capillary tube with the carrier solution using a microsyringe pump. The ternary mixed carrier solution (water-rich carrier solution) was radially distributed in the capillary tube based on the tube radial distribution phenomenon, causing the formation of inner (water-rich) and outer (organic-solvent-rich) phases. The outer or capillary wall phase acted as a pseudo-stationary phase in the chromatography. The analytes were separated through the capillary tube with on-capillary detection by an absorption or a fluorescence detector. D-Enantiomer and L-enantiomer were eluted in this order through a baseline separation. The separation mechanism of the enantiomers in the open-tubular capillary using cyclodextrin was discussed.

Introduction

Various types of aqueous-organic solvent mixture solutions are used for the processes of dissolution [11, 12], cleaning [13], and preservation [14] and as reaction solvents [15,16]. Such mixtures are also useful in processes involved in separation science [17-19], such as solvent extraction and liquid chromatography. In liquid chromatography, a hydrophilic and hydrophobic organic solvent mixture is delivered into a separation column as a carrier solution in a normal-phase chromatography, while a water and hydrophilic organic solvent mixture is delivered into the column as a carrier solution in a reverse-phase chromatography. Wang et al. examined sorption isomers of ternary eluents of water–methanol–acetonitrile in reverse-phase liquid chromatography [20]. Bhushan et al. reported direct enantiomeric TLC resolution with the ternary solvent system of water–methanol–ethyl acetate mixture [21]. However, to the best of our knowledge, the use of ternary mixed solvents consisting of water–hydrophilic/hydrophobic organic solvent mixture solutions, such as water–acetonitrile–ethyl acetate mixture, being used as carrier solutions in liquid chromatography has not yet been examined in great detail.

In addition, with the progress of microfabrication technology, fluid flow in a microspace, such as in a microchannel in a microchip or capillary tube, has received much attention. Capillary tubes are known to exhibit interesting and useful physical and hydrodynamic phenomena, such as electro-osmotic and laminar flows. Electro-osmotic flow in a capillary tube has established capillary electrophoresis [22-24] and capillary electrochromatography [24-26] properties, while laminar flow conditions enable hydrodynamic chromatography [27-29]. Recently, we investigated the specific fluid behavior of a ternary mixed solvent solution in a microspace under laminar flow conditions.

In contrast to other capillary separation techniques, such as capillary electrophoresis or capillary electrochromatography, the TRDC system performs without requiring the application of high voltages or the use specific columns, e.g., monolithic or packed. Enantiomer separation is one of the most interesting and attractive aspects of analytical chemistry and separation science [30-33]. Here, we attempted to apply the system to enantiomer separation for the first time, although we have briefly described the preliminary results of this investigation in a previous communication.⁸⁾ A combination of cyclodextrin as host molecule (chiral selector) and dansyl-DL-amino acids as guest molecules (enantiomers) was adopted as a model for enantiomer separation with reference to previous reports [32,33].

Experimental

PTFE capillary tubes (100 μm inner diameter, 200 μm outer diameter) were used. The capillary chromatography system consisted of an open-tubular PTFE capillary tube (110 cm length, 90 cm effective length), a microsyringe pump, and an absorption or a fluorescence detector. A mixture of water–acetonitrile–ethyl acetate containing cyclodextrin was used as a carrier solution. The tube temperature was controlled by dipping the tube (ca. 40 cm) in a beaker filled with water maintained at a specific temperature (0 $^{\circ}\text{C}$) and stirring. The analyte solution was prepared with the carrier solution. The analyte solution was introduced directly into the capillary inlet side for 10 s from a height of 25 cm by a gravity method. After analyte injection, the capillary inlet was connected through a joint to the microsyringe, which was set on a microsyringe pump. The carrier solution was fed into the capillary tube at a flow rate of 0.8 $\mu\text{L min}^{-1}$ under laminar flow conditions. Using this apparatus, on-capillary absorption detection (254 nm) or fluorescence detection (ex. 335 nm and em. 520 nm) was performed.

Results and discussion

Preliminary experiments In preliminary experiments, a solution of 2,6-naphthalenedisulfonic acid (1 mM) and dansyl-DL-methionine (500 μM) was analyzed using a normal TRDC system with a water–acetonitrile–ethyl acetate carrier solution with a volume ratio of 75:15:10 (15:3:2 volume ratio) and not containing cyclodextrin. 2,6-Naphthalenedisulfonic acid and dansyl-DL-methionine were eluted with baseline separation in this order, although enantiomer separation of dansyl-DL-methionine was not performed. With the water-rich carrier solution, 2,6-naphthalenedisulfonic acid (hydrophilic) was eluted with a velocity near the average linear velocity and dansyl-DL-methionine (relatively hydrophobic) was eluted at a lower than average linear velocity under the laminar flow conditions.

Phase diagram for ternary mixed solvents including cyclodextrin Phase diagrams for the ternary mixed solvents of water–acetonitrile (hydrophilic organic solvent)–ethyl acetate (hydrophobic organic solvent) containing 1 or 2 mM β -cyclodextrin, 10 mM α -cyclodextrin, and 10 mM γ -cyclodextrin in a vessel were examined at a temperature of 22 $^{\circ}\text{C}$. It was difficult to construct the phase diagrams for the ternary mixed solvents with cyclodextrin at higher concentrations because of their solubility. For example, the phase diagrams for mixed solvents including 1 and 2 mM β -cyclodextrin are shown in Fig. 1. In the diagrams, 1 and 2 mM β -cyclodextrin were not dissolved in ternary mixed solvents solutions with a water component ratio of less than ca. 32 and 52 volume %, respectively.

respectively. The phase diagram shows that each component ratio of the solvents comprised a homogeneous (one homogeneous phase) or a heterogeneous (two homogeneous phases) solution. The curves in the diagrams indicate the boundary between homogeneous and heterogeneous phases. In the phase diagram of the mixed solvents including 1 mM β -cyclodextrin, the component ratios of the solvents that were positioned extremely close to the boundary curve in the homogeneous phase are plotted as I–VIII in Fig. 1 a. In the phase diagram of the mixed solvents containing 2 mM β -cyclodextrin, the component ratios of the solvents positioned close to the boundary curve in the homogeneous phase are also plotted in I–VI in Fig. 1 b. The ternary mixed solvents of water–acetonitrile–ethyl acetate including 10 mM α -cyclodextrin and 10 mM γ -cyclodextrin showed phase diagrams similar to those of the mixed solvents including 1 and 2 mM β -cyclodextrin shown in Figs. 1 a) and b), although 10 mM α -cyclodextrin and 10 mM γ -cyclodextrin were not dissolved in ternary mixed solvent solutions with water component ratios of less than ca. 42 or 52 volume %, respectively (data not shown). In the phase diagram of the mixed solvents including 10 mM α -cyclodextrin, the component ratios of the solvents positioned close to the boundary curve in the homogeneous phase are plotted as I–VII. In addition, in the diagram of the mixed solvents including 10 mM γ -cyclodextrin, the component ratios of the solvents positioned close to the boundary curve in the homogeneous phase are plotted as I–VI. Similar boundary curves between homogeneous and heterogeneous phases were observed along the plots in all phase diagrams, except for the component ratio of water that indicated the limitation of the dissolution of cyclodextrin. In our study, the TRDC system used specific homogeneous carrier solutions with component ratios of solvents positioned near the homogeneous–heterogeneous solution boundary curve in the phase diagram. Such specific carrier solutions caused a tube radial distribution of the carrier solvents in the capillary tube under laminar flow conditions, i.e., the TRDP. In addition, in the TRDC system using the PTFE capillary tube, the water-rich carrier solution had better resolution than the organic-solvent-rich carrier solution. Here, the homogeneous solution of water–acetonitrile–ethyl acetate mixture including cyclodextrin, with a component ratio near the boundary curve (plots I–VIII for 1 mM β -cyclodextrin, plots I–VI for 2 mM β -cyclodextrin, plots I–VII for 10 mM α -cyclodextrin, and plots I–VI for 10 mM γ -cyclodextrin), was used as a carrier solution.

Separation of 1-naphthol and 2,6-naphthalenedisulfonic acid with the ternary mixed solvents including cyclodextrin The TRDP leads to the formation of inner and outer phases, i.e., a kinetic liquid–liquid interface, in a capillary tube under laminar flow conditions. In this case, using the water–acetonitrile–ethyl acetate mixture including cyclodextrin as a carrier solution (water-rich), an organic-solvent-rich major inner phase was generated around the middle of the tube, while a water-rich minor outer phase was formed near the inner wall. In the TRDC system, the outer phase, which had negligible movement under laminar flow conditions, acted as a pseudo-stationary phase. Analytes were distributed between the inner and outer phases because of their natures, and they underwent chromatographic separation. First of all, we confirmed that adding cyclodextrin as an additive molecule in the ternary mixed solvents carrier solution did not influence the TRDP or TRDC performance as follows. A solution of 2,6-naphthalenedisulfonic acid (1 mM) and 1-naphthol (1 mM), typical analytes for the TRDC system, was analyzed using the water–acetonitrile–ethyl acetate carrier solution

containing cyclodextrin in order to examine the influence of cyclodextrin in the carrier solution on TRDP performance. The component ratios of the solvents were positioned near the boundary curves in every phase diagram. The obtained chromatograms for carrier solutions including α , β , and γ -cyclodextrin are shown in Fig. 2. For example, in the ternary mixed solvents including 1 mM β -cyclodextrin (Fig. 2 a)), 2,6-naphthalenedisulfonic acid (hydrophilic) and 1-naphthol (hydrophobic) were separated and detected in this order based on their TRDC separation performance with carrier solutions containing 1 mM β -cyclodextrin. The component ratio of the solvents plotted in I, II, and VII exhibited split separation. The component ratios of the solvents showed baseline separation at III, IV, V, and VI and non-separation at VIII. In the separation cases, 2,6-naphthalenedisulfonic acid and 1-naphthol were separated and detected in this order. The first peak of 2,6-naphthalenedisulfonic acid was eluted with a velocity near the average linear velocity under laminar flow conditions. Similar elution behaviors in 2,6-naphthalenedisulfonic acid and 1-naphthol were observed using ternary mixed solvents containing 2 mM β -, 10 mM α -, and 10 mM γ -cyclodextrin as shown in Fig. 2 b) – 2 d). Reasonable elution behavior observed on the chromatogram supported the occurrence of TRDP in the present TRDC system containing cyclodextrin. Fig. 3 shows the chromatograms of 2,6-naphthalenedisulfonic acid (1 mM) and 1-naphthol (1 mM) obtained by the TRDC system using carrier solutions with and without 1 mM β -cyclodextrin. Under the present analytical conditions, cyclodextrin (additive molecule) appears to exert very little influence on the chromatograms or the TRDC system.

Separation of dansyl-DL-methionine with ternary mixed solvents including 1 mM β -cyclodextrin⁸⁾ The solutions of 500 μ M dansyl-DL-methionine, 250 μ M dansyl-L-methionine, and 500 μ M dansyl-DL-methionine plus 250 μ M dansyl-L-methionine were subjected to the present TRDC system utilizing a water–acetonitrile–ethyl acetate (15:3:2 volume ratio) carrier solution containing 1 mM β -cyclodextrin. The chromatograms obtained for the above three analyte solutions are shown in Fig. 4. The elution times and the peak shapes clearly show that the D-enantiomer and L-enantiomer in dansyl-DL-methionine were separated and detected in this order. As shown in Fig. 4, the D-enantiomer was eluted with a near average linear velocity and the L-enantiomer was eluted with a lower than average linear velocity. As shown in preliminary experiments, dansyl-DL-methionine was eluted with a lower than average linear velocity based on the nature of hydrophobicity with a carrier solution that did not contain β -cyclodextrin; that is, dansyl-DL-methionine was relatively hydrophobic. In the water-rich carrier solution containing 1 mM β -cyclodextrin, β -cyclodextrin was primarily distributed in the major inner phase or the water-rich phase. Dansyl-D-methionine has a stronger interaction with β -cyclodextrin as a chiral selector than with dansyl-L-methionine [33]. The interaction between dansyl-D-methionine and β -cyclodextrin must alter the distribution of the D-enantiomer from the outer phase to the inner phase, leading to an earlier elution time of the D-enantiomer than the L-enantiomer for separation. Separation performance for the enantiomers in the TRDC system is illustrated in Fig. 5.

Separation of dansyl-DL-methionine with the ternary mixed solvents including various cyclodextrins Dansyl-DL-methionine was examined using the ternary mixed solvents

containing α , β , and γ -cyclodextrin. The carrier solutions were specified by the component ratios of the solvents that showed separation performance for the mixture of 2,6-naphthalenedisulfonic acid and 1-naphthol, as shown in Fig. 2. The obtained chromatograms are shown in Fig. 6. Enantiomer separation was observed in ternary mixed solvents including cyclodextrin in a manner similar to that of the chromatograms shown in Fig. 4 and the illustration in Fig. 5. D-Enantiomer and L-enantiomer were separated and detected in this order. In carrier solvents with 1 mM β -cyclodextrin, the component ratio of the solvents, plot III, showed enantiomer separation (Fig. 6 a). In carrier solvents with 2 mM β -cyclodextrin, plots III–V, showed separation (Fig. 6 b). In carrier solvents with 10 mM α -cyclodextrin, plots III–VI, showed separation (Fig. 6 c). Finally, in carrier solvents with 10 mM γ -cyclodextrin, plots III–V, showed separation (Fig. 6 d). Resolutions (R_s) were calculated in the usual manner in chromatograms exhibiting enantiomer separation. The relationships between the component ratios of the solvents and the R_s are shown in Fig. 7. The resolutions decreased as the component ratios of the organic solvents in the carrier solutions increased, which might affect the formation of inner and outer phases in the capillary tube. Furthermore, α -cyclodextrin showed better resolutions than the other cyclodextrin chromatograms.

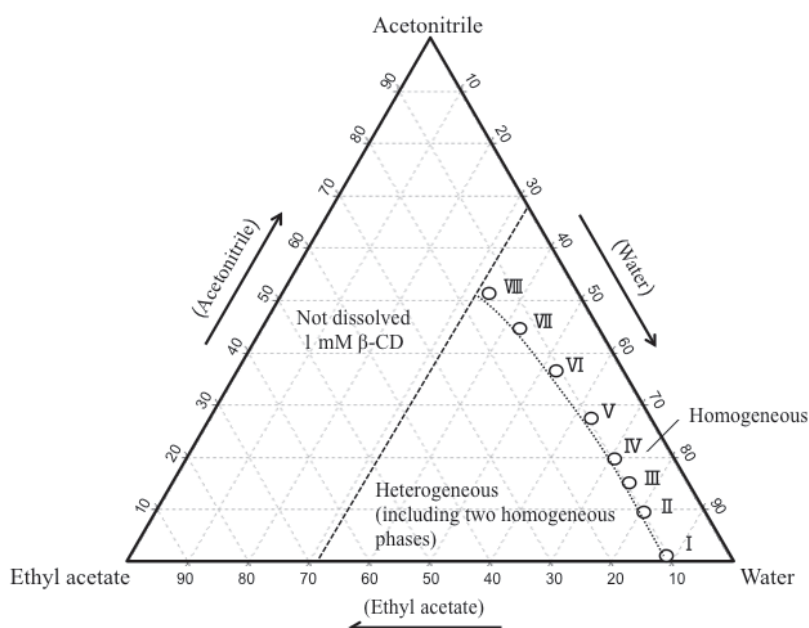
Comparison of absorption and fluorescence detection Enantiomer separation of dansyl-DL-methionine was examined using the ternary mixed solvents containing α , β , and γ -cyclodextrin under the same conditions as in Fig. 6, except that fluorescence detection was used instead of absorption detection. As an example, the chromatograms obtained with 10 mM α -cyclodextrin are shown in Fig. 8. The chromatograms obtained with 2 mM α - and 10 mM γ -cyclodextrin showed similar elution behavior (data not shown). D-enantiomer and L-enantiomer were separated and detected in this order. Peak areas of D-enantiomer and L-enantiomer in absorption and fluorescence detection are summarized in Table 1. Clearly, the peak area ratios of D-enantiomer to L-enantiomer with fluorescence detection were larger than those with absorption detection for the data obtained with α , β , and γ -cyclodextrin. D-enantiomers that were effectively included in cyclodextrin might indicate larger fluorescence yields than L-enantiomers in fluorescence detection.

Separation of the mixture of dansyl amino acids with ternary mixed solvents including cyclodextrin Dansyl amino acids other than dansyl-DL-methionine, such as dansyl-DL-aspartic acid and dansyl-DL-phenylalanine, were examined using 10 mM α -cyclodextrin, 2 mM β -cyclodextrin, and 10 mM γ -cyclodextrin. Dansyl-DL-aspartic acid showed optical separation with the elution order of D-enantiomer and L-enantiomer, but dansyl-DL-phenylalanine did not show any separation (data not shown). The experimental data were consistent with the interaction abilities between dansyl amino acids and cyclodextrin [33]. Fig. 9 shows the chromatograms of the mixtures of dansyl-DL-aspartic acid and dansyl-DL-phenylalanine obtained with absorption detection. The four isomers were separated on the chromatograms.

In conclusion, enantiomer separation of dansyl-DL-amino acids, such as dansyl-DL-methionine and dansyl-DL-aspartic acid, was performed by the TRDC system with a water-rich carrier solution containing cyclodextrin. Cyclodextrin was not immobilized on the inner wall surface but simply included in the carrier solution. The

observed elution order of D-enantiomer and L-enantiomer was explained based on the tube radial distribution of the carrier solvents, providing the major water-rich and minor organic solvent-rich phases. The results obtained here regarding enantiomer separation provide important insights that indicate directions for future research to expand the TRDC system.

a)



b)

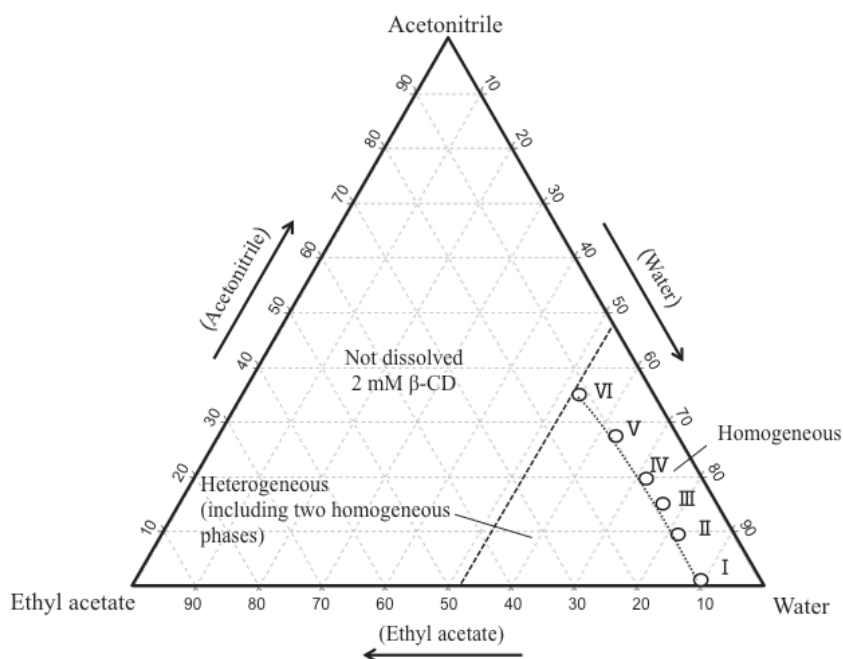
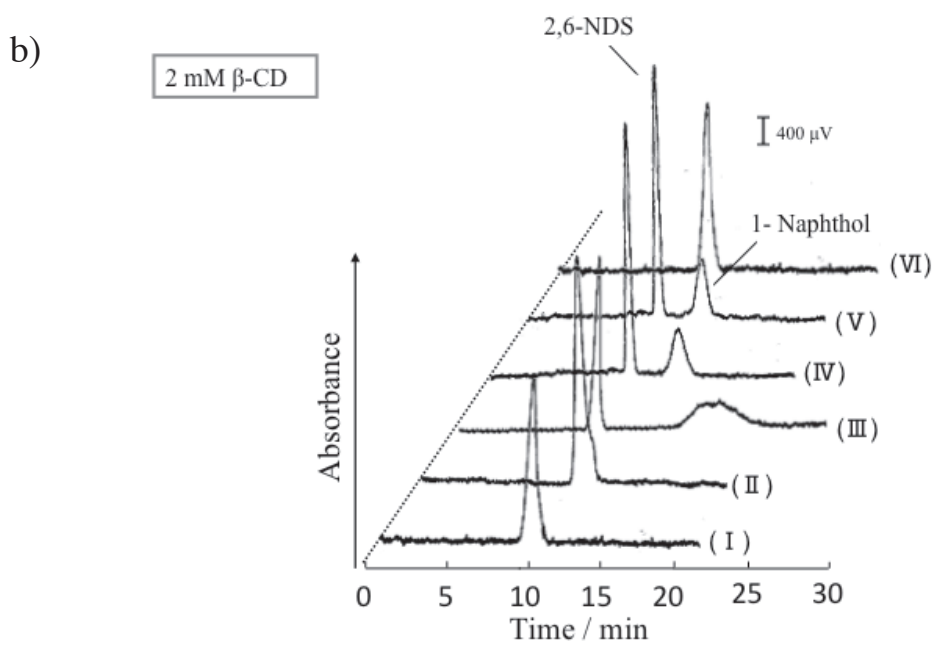
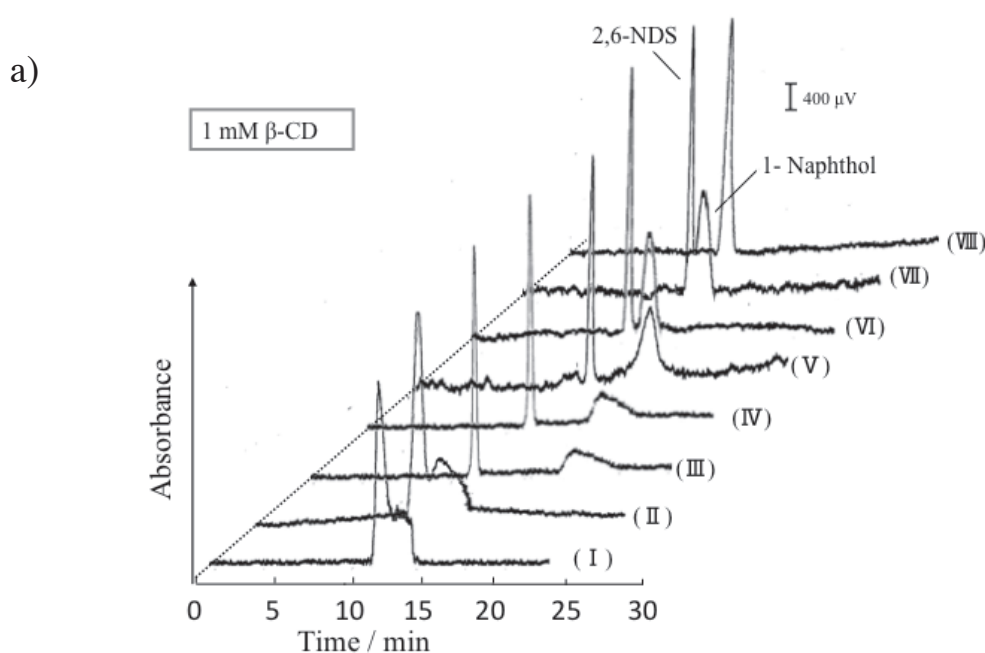


Figure 1. Phase diagrams for the ternary mixture solvents of water–acetonitrile–ethyl acetate including a) 1 mM and b) 2 mM β -cyclodextrin. 1 and 2 mM β -cyclodextrin were not dissolved in ternary mixture solutions with water component ratios of less than ca. 32 and 52 volume %, respectively. The curves in the diagrams indicate the boundary between the homogeneous and heterogeneous phases. The component ratios of the solvents for plots (I–VIII) that provide homogeneous solutions were positioned almost on the homogeneous–heterogeneous solution boundary curves of the phase diagrams. The component ratios for the plots (I–VIII) in the diagrams are I) water–acetonitrile–ethyl acetate of 100:0:10.5 volume ratio, II) 90:10:10.5 volume ratio, III) 75:15:10 volume ratio (15:3:2 volume ratio), IV) 80:20:10.5 volume ratio, V) 70:30:11.5 volume ratio, VI) 60:40:13.5 volume ratio, VII) 50:50:17.5 volume ratio, and VIII) 40:60:23.5 volume ratio.



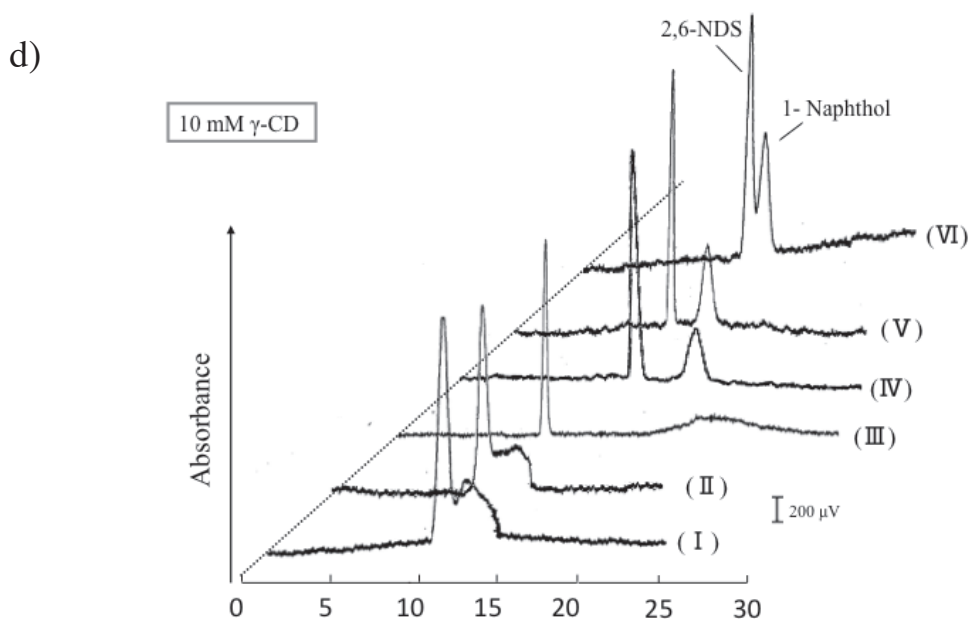
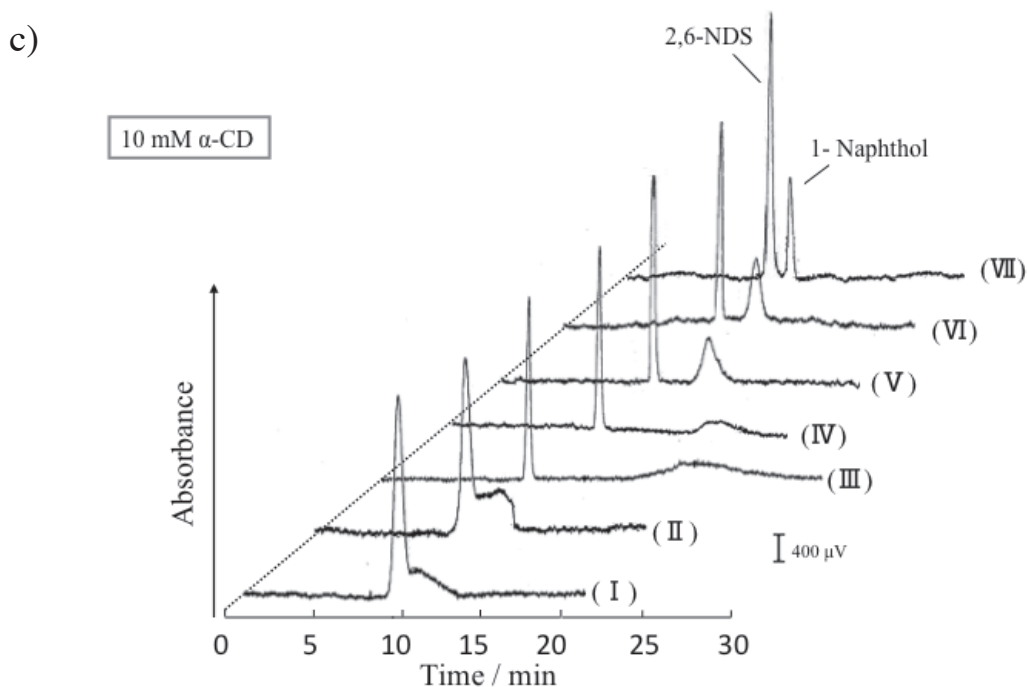


Figure 2. Chromatograms of a mixture of 2,6-naphthalenedisulfonic acid and 1-naphthol with the capillary chromatography system using various component ratios of water–acetonitrile–ethyl acetate mixture including a) 1 mM and b) 2 mM β -cyclodextrin, c) 10 mM α -cyclodextrin, and d) 10 mM γ -cyclodextrin as carrier solutions. The component ratios of the solvents for the plots (I–VIII) are described in Fig. 1. 2,6-Naphthalenedisulfonic acid and 1-naphthol were eluted in this order with certain carrier solutions. Conditions: Capillary tube, 110 cm (90 cm effective length) of 100 μ m i.d. PTFE; carrier, water–acetonitrile–ethyl acetate mixture solution containing cyclodextrin; sample injection, 20 cm height (gravity) \times 5 s; flow rate, 0.8 μ L min^{-1} and analyte concentration, 1 mM.

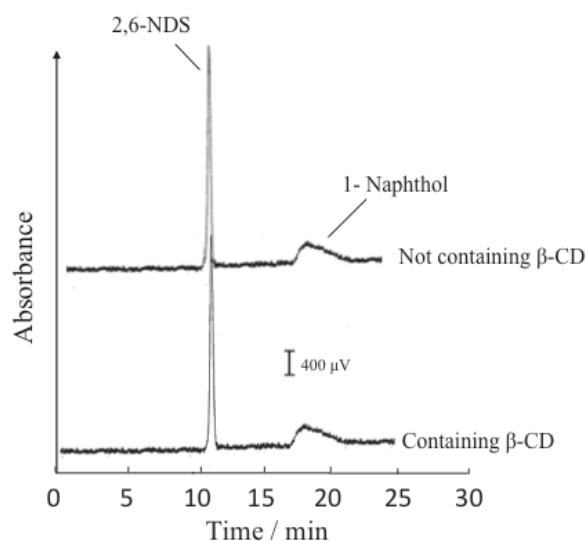


Figure 3. Chromatograms of a mixture of 2,6-naphthalenedisulfonic acid and 1-naphthol with a capillary chromatography system using water–acetonitrile–ethyl acetate mixture carrier solution with 1 mM β -cyclodextrin and one without β -cyclodextrin. Conditions: Capillary tube, 110 cm (90 cm effective length) of 100 μ m i.d. PTFE; carrier, water–acetonitrile–ethyl acetate (15:3:2 volume ratio) mixture solution containing 1 mM β -cyclodextrin and not containing β -cyclodextrin; sample injection, 20 cm height (gravity) \times 5 s; flow rate, 0.8 μ L min^{-1} ; and analyte concentration, 1 mM.

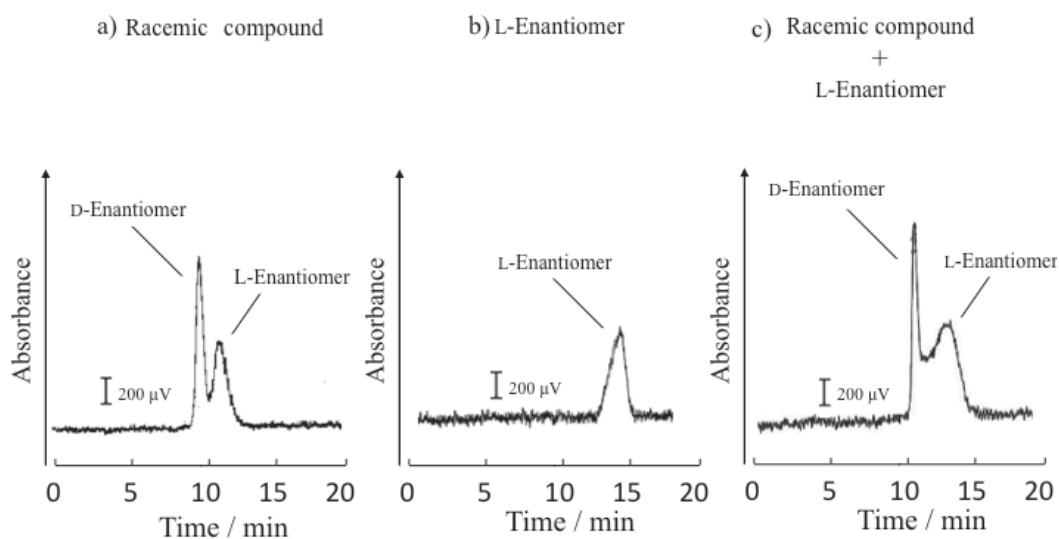


Figure 4. Chromatograms of the mixture of a) 500 μ M dansyl-DL-methionine, b) 250 μ M dansyl-L-methionine, and c) 500 μ M dansyl-DL-methionine plus 250 μ M dansyl-L-methionine mixture. Conditions: Capillary tube, 110 cm (90 cm effective length) of 100 μ m i.d. PTFE; carrier, water–acetonitrile–ethyl acetate (15:3:2 volume ratio) mixture solution containing 1 mM β -cyclodextrin; sample injection, 20 cm height (gravity) \times 5 s; and flow rate, 0.8 μ L min^{-1} .

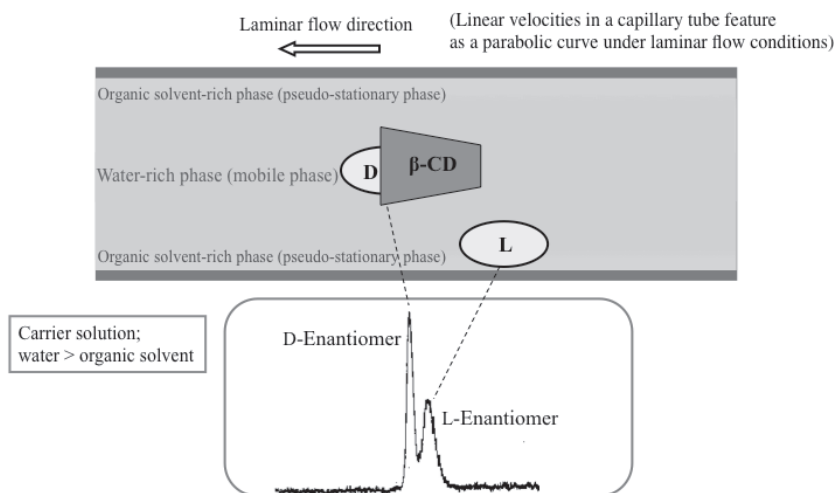
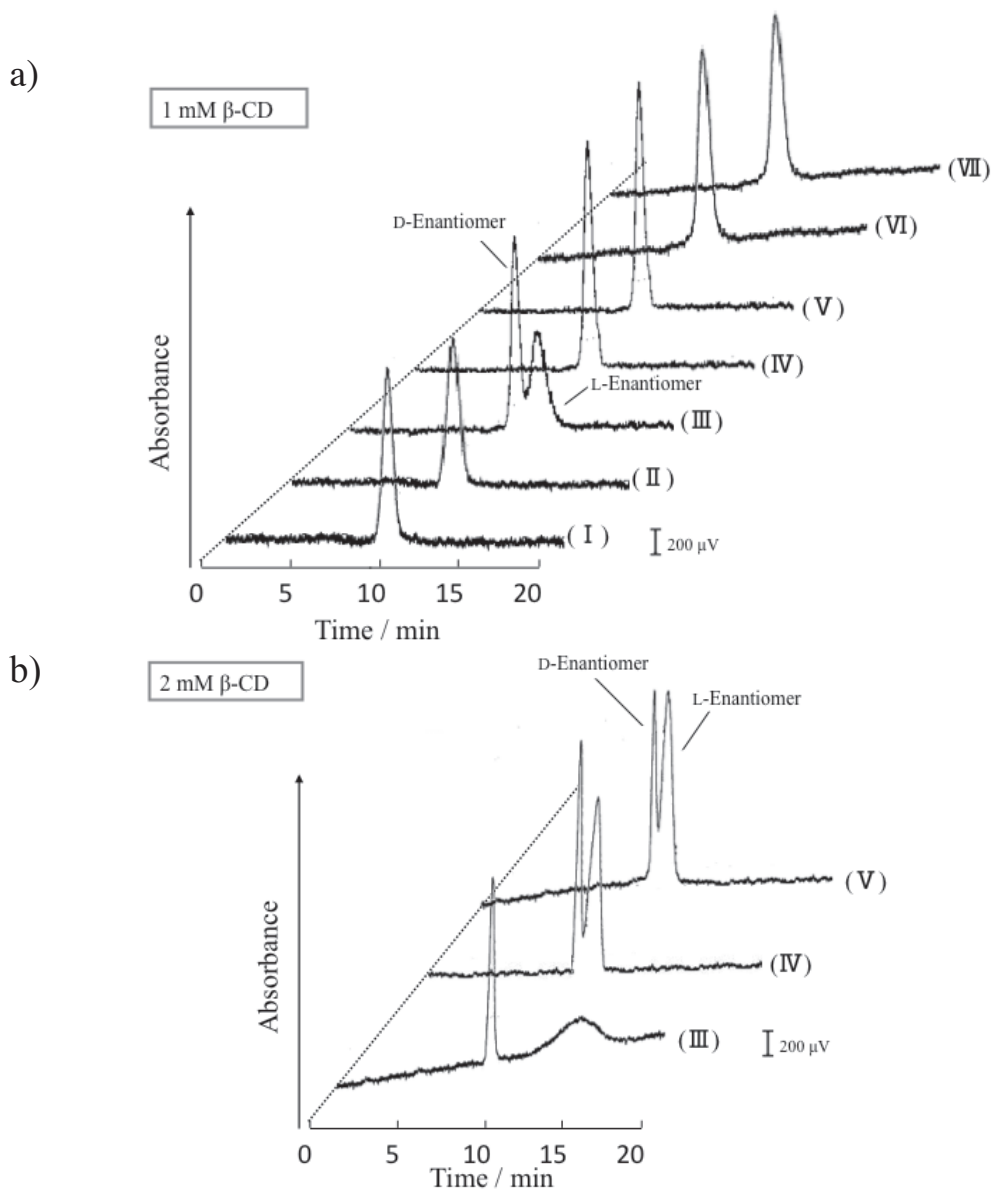


Figure 5. Illustration of separation performance in the capillary chromatography system using water–acetonitrile–ethyl acetate mixture carrier solution including cyclodextrin.



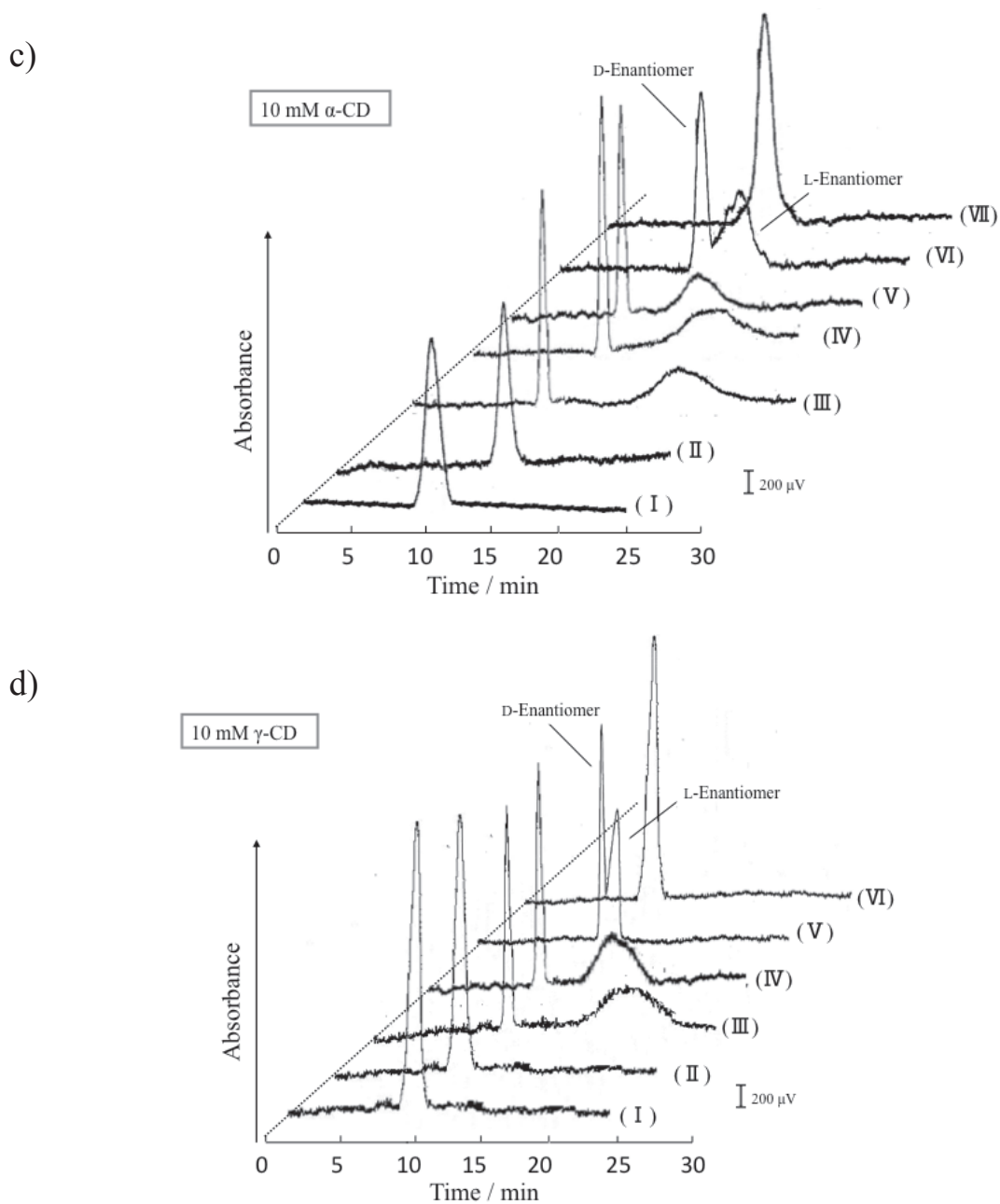


Figure 6. Chromatograms of dansyl-DL-methionine obtained using various component ratios of water–acetonitrile–ethyl acetate mixture including a) 1 mM and b) 2 mM β -cyclodextrin, c) 10 mM α -cyclodextrin, and d) 10 mM γ -cyclodextrin as carrier solutions. The component ratios of the solvents for plots (I–VII) are described in Fig. 1. D-Enantiomer and L-enantiomer were eluted in this order with the certain carrier solutions. Conditions: Capillary tube, 110 cm (90 cm effective length) of 100 μ m i.d. PTFE; carrier, water–acetonitrile–ethyl acetate mixture solution containing cyclodextrin; sample injection, 20 cm height (gravity) \times 5 s; flow rate, 0.8 μ L min^{-1} ; and analyte concentration, 500 μ M.

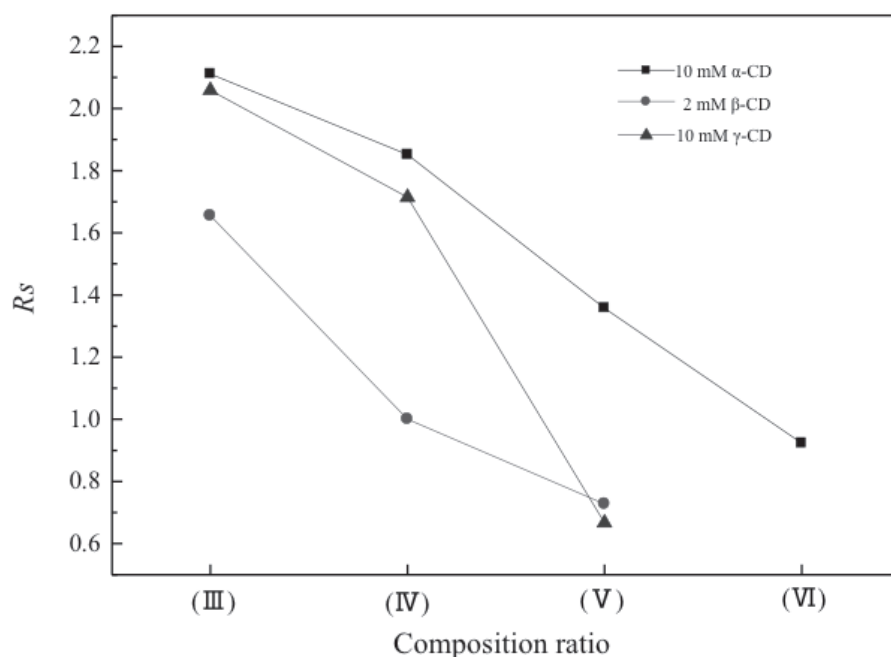


Figure 7. Relationships between component ratios of the carrier solvents and resolutions (R_s) for the data calculated in Fig. 6.

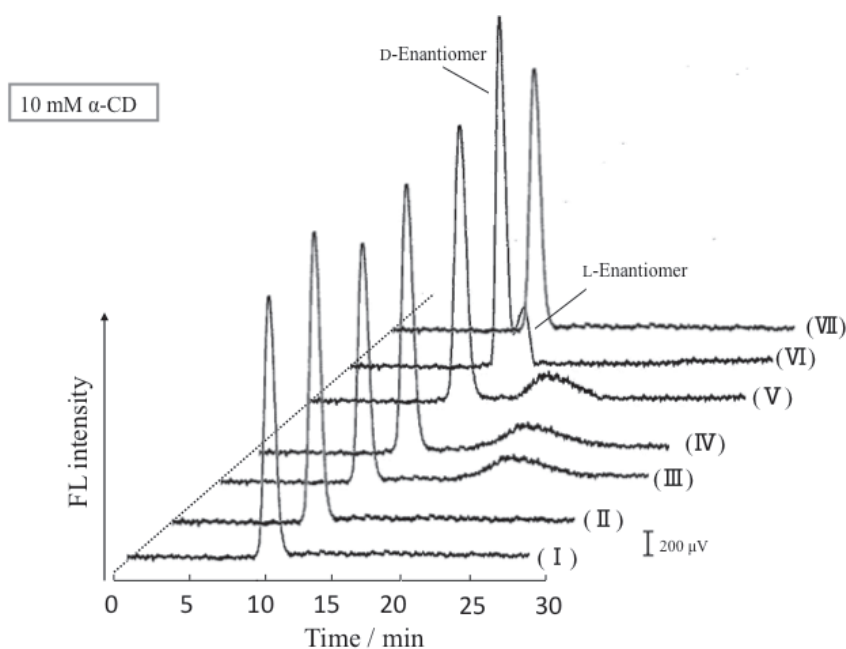


Figure 8. Chromatograms of dansyl-DL-methionine obtained using various component ratios of water–acetonitrile–ethyl acetate mixture including 10 mM α -cyclodextrin as carrier solutions with fluorescence detection. The component ratios of the solvents for the plots (I–VII) are described in Fig. 1. Conditions: Capillary tube, 110 cm (90 cm effective length) of 100 μm i.d. PTFE; carrier, water–acetonitrile–ethyl acetate mixture solution containing cyclodextrin; sample injection, 20 cm height (gravity) \times 5 s; flow rate, 0.8 $\mu\text{L min}^{-1}$; and analyte concentration, 500 μM .

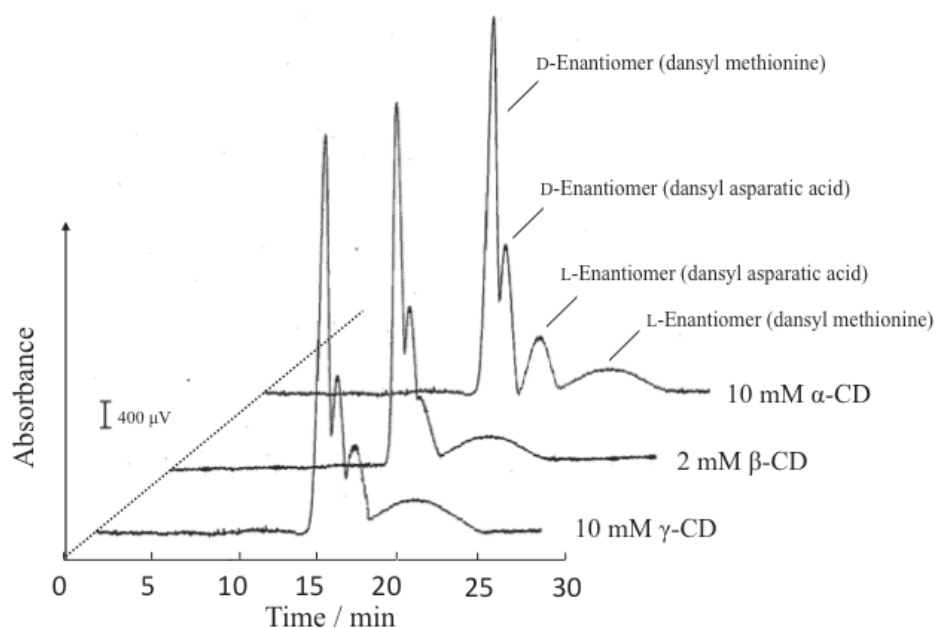


Figure 9. Chromatograms of mixtures of dansyl-DL-amino acids obtained using water–acetonitrile–ethyl acetate mixture including 10 mM α -cyclodextrin, 2 mM β -cyclodextrin, and 10 mM γ -cyclodextrin as carrier solutions with absorption detection. Conditions: Capillary tube, 110 cm (90 cm effective length) of 100 μ m i.d. PTFE; carrier, water–acetonitrile–ethyl acetate (15:3:2 volume ratio) mixture solution containing cyclodextrin; sample injection, 20 cm height (gravity) \times 5 s; flow rate, 0.8 μ L min^{-1} ; and analyte concentration, 500 μ M.

Table 1 Peak areas of D- and L-enantiomers for dansyl DL-methionine that were obtained with absorption and fluorescence detections.

Cyclodextrin	Carrier solvents	Absorption detection /mV s			Fluorescence detection /mV s		
		Peak area of D-enantiomer	Peak area of L-enantiomer	Peak ratio of D- / L-enantiomer	Peak area of D-enantiomer	Peak area of L-enantiomer	Peak ratio of D- / L-enantiomer
10 mM α -CD	(III)	270	280	0.96	380	180	2.11
	(IV)	275	280	0.98	385	170	2.26
	(V)	270	285	0.95	390	185	2.11
	(VI)	280	290	0.97	420	190	2.21
2 mM β -CD	(III)	180	370	0.49	250	150	1.67
	(IV)	210	350	0.60	260	160	1.63
	(V)	190	320	0.59	245	165	1.48
10 mM γ -CD	(III)	260	280	0.93	510	180	2.83
	(IV)	265	280	0.95	520	190	2.74
	(V)	270	300	0.90	535	200	2.68

References

- [1] K. Tsukagoshi, S. Ishida, and R. Nakajima, *J. Chem. Eng. Japan*, **2008**, *41*, 130.
- [2] T. Okada, M. Harada, and T. Kido, *Anal. Chem.*, **2005**, *77*, 6041.
- [3] T. Masudo and T. Okada, *J. Chromatogr. A.*, **2006**, *196*, 1106.
- [4] M. Harada, T. Kido, T. Masudo, and T. Okada, *Anal. Sci.*, **2005**, *21*, 491.
- [5] K. Tsukagoshi, K. Sawanoi, and R. Nakajima, *J. Chromatogr. A*, **2007**, *1143*, 288.
- [6] K. Tsukagoshi, K. Matsumoto, F. Ueno, K. Noda, R. Nakajima, and K. Araki, *J. Chromatogr., A*, **2006**, *1123*, 106.
- [7] “*A Data Book of Biochemistry P*”, ed. The Japanese Biochemical Society, Chap. 1, **1976**, Tokyo Kagaku-Dojin, Tokyo.
- [8] W. J. Bernhard, F. P. C. Blamey, J. V. Hanna, P. M. Kopittke, G. L. Kerven, N. W. Menzies, *J. Agric. Food. Chem.*, **2010**, *58*, 5553.
- [9] Z. Marczenko, H. Kalowska, *Anal. Chimica. Acta*, **1981**, *123*, 279.
- [10] P. Pakalns, *Anal. Chimica. Acta*, **1965**, *32*, 57.
- [11] G. Hefter, *Pure Appl. Chem.*, **2005**, *77*, 605.
- [12] G. R. Castro and T. Knubovets, *Crit. Rev. Biotechnol.*, **2003**, *23*, 195.
- [13] J. Niu and B.E. Conway, *J. Electroanal. Chem.*, **2003**, *546*, 59.
- [14] D. M. Ruiz and R. E. De Castro, *J. Ind. Microbiol. Biotechnol.*, **2007**, *34*, 111.
- [15] H. Ogino, in K. S. Siddiqui, T. Thomas (Eds.), *Protein Adaptation in Extremophiles*, Nova Science Publishers, Inc., New York, 2008, pp.193.
- [16] M. Tjahjono, C. Huiheng, E. Widjaja, K. Sa-Ei, and M. Garland, *Talanta*, **2009**, *79*, 856.
- [17] M. K. Yeh, S. L. Lin, M. I. Leong, S. D. Huang, and M.R. Fuh, *Anal. Sci.*, **2011**, *27*, 49.
- [18] T. Maruyama, H. Matsushita, J. Uchida, F. Kubota, N. Kamiya, and M. Goto, *Anal. Chem.*, **2004**, *76*, 4495.
- [19] F. Torrens, *Chromatographia*, **2001**, *53*, S199.
- [20] M. Wang, J. Mallette, and J. F. Parcher, *Anal. Chem.*, **2009**, *81*, 984.
- [21] R. Bhushan and C. Agarwal, *Biochem. Chromatogr.*, **2008**, *22*, 1237.
- [22] J. W. Jorgenson and K. D. Lukacs, *Science*, **1983**, *222*, 266.
- [23] S. Terabe, *Anal. Chem.*, **2004**, *76*, 240A.
- [24] C. A. Lucy, A. M. MacDonald, and M. D. Gulcev, *J. Chromatogr. A*, **2008**, *1184*, 81.
- [25] M. G. Cikalo, K. D. Bartle, M. M. Robson, P. Myers, and M. R. Euerby, *Analyst*, **1998**, *123*, 87R.
- [26] R. Nakashima, S. Kitagawa, T. Yoshida, and T. Tsuda, *J. Chromatogr. A*, **2004**, *1044*, 305.
- [27] K. Otsuka, *Chromatography*, **2007**, *28*, 1.
- [28] T. Takahashi and W.N. Gill, *Chem. Eng. Commun.*, **1980**, *5*, 367.
- [29] H. Small, F.L. Saunders, and J. Solc, *Adv. Colloid Interface Sci.*, **1976**, *6*, 237.
- [30] L. Bluhm, J. Huang, and T. Li, *Anal. Bioanal. Chem.*, **2005**, *82*, 592.
- [31] T. J. Ward and B. A. Baker, *Anal. Chem.*, **2006**, *78*, 3947.
- [32] K. Kano and R. Nishiyabu, *Adv. Supramol. Chem.*, **2009**, *9*, 39.
- [33] I. E. Valko, H. Siren, and M. L. Riekkola, *Electrophoresis*, **1997**, *18*, 919.

Chapter 9 Consideration of tube radial distribution chromatography (TRDC)

TRDC was developed based on TRDP. The TRDC separation was considered from various viewpoints, including temperature, outer phase formation, adding surfactant, and computer simulation. The part of this chapter is reconstructed and rewritten based on related, published manuscripts.^{12,29,31,34)}

9.1 Experiments and consideration through temperature effect in TRDC

We have developed a capillary chromatography system using an open capillary tube made of fused-silica, polyethylene, or poly(tetrafluoroethylene), and a water-hydrophilic/hydrophobic organic mixture carrier solution. This so-called tube radial distribution chromatography (TRDC) system works under laminar flow conditions. Previously, the effects of capillary temperature on separation performance in the TRDC system had been examined using a fused-silica capillary tube and a water-acetonitrile-ethyl acetate mixture carrier solution; 1-naphthol and 2,6-naphthalenedisulfonic acid in a model mixture were eluted with baseline separation over a temperature range of 5–23 °C with the organic solvent-rich carrier solution. Here, based on the special assumption that the phase distribution of inner and outer phases in the capillary tube induced by the tube radial distribution of the carrier solvents did not change with temperature over a limited range, we attempted to apply the van't Hoff equation to the chromatographic data obtained at various capillary temperatures.

Introduction

Since the investigation of the TRDC system is still at the preliminary stage, it is important to examine elution behavior under various analytical conditions in the system to expand our knowledge regarding its separation performance. In our study,¹⁰⁾ we examined the analytical conditions of the TRDC system in detail, including tube temperature, tube inner diameter, tube length, and flow rate, using fused-silica capillary tubes and water-acetonitrile-ethyl acetate mixture as the carrier solution. Here, we tried to examine the effects of capillary temperature on separation performance in the TRDC system through the van't Hoff equation on the assumption that the phase distribution of the inner and outer phases did not change under a certain condition.

Experimental

The present capillary chromatography system comprised an open fused-silica capillary tube, 120 cm (effective length of 100 cm) of 75 μm i.d., microsyringe pump, and

absorption detector. The tube temperature was controlled by dipping the capillary tube in water preset at a definite temperature in a beaker while stirring. A water-acetonitrile-ethyl acetate mixture with volume ratio of 3:8:4 was used as the carrier solution. Analyte solutions were prepared with the carrier solutions. The analyte solution was introduced directly into the capillary inlet by the gravity method (20 cm height \times 30 s). After the analyte injection, the capillary inlet was connected through a joint to a microsyringe. The syringe was set on the microsyringe pump. The carrier solution was fed into the capillary tube at a flow rate ($0.8 \mu\text{L min}^{-1}$) under laminar flow conditions. On-capillary absorption detection (254 nm) was performed with the detector.

Results and discussion

We previously examined the effects of tube temperature on separation in the TRDC system with a mixture analyte solution of 1-naphthol and 2,6-naphthalenedisulfuric acid as a model. The experiments were performed with the organic solvent-rich carrier solution (water-acetonitrile-ethyl acetate; 3:8:4 v/v/v) because the carrier solution provided better resolution on the chromatograms than the water-rich carrier solution (water-acetonitrile-ethyl acetate; 15:3:2 v/v/v). The obtained chromatograms in our work are shown in Fig. 1 together with analytical conditions as a reference. As can be seen in Fig. 1, 1-naphthol and 2,6-naphthalenedisulfuric acid in the mixture solution were detected with baseline separation within the temperature range of 5–23 °C, while they were not separated at all at a temperature of 25 °C. More specifically, the resolution was improved with an increase in temperature from 5 °C to 20 °C but suddenly decreased at 23 °C. The data clearly indicated that the tube temperature had a significant, critical influence on the separation performance of the TRDC system.

In our chromatographic investigation, enthalpy (ΔH) is often calculated by using the van't Hoff equation as a standard method, leading to thermodynamical discussion, such as exothermic ($\Delta H < 0$) or endothermic ($\Delta H > 0$) in the separation system. We attempted to apply the van't Hoff equation to the chromatographic data of TRDC system (Fig. 1), for the first time. The equation is shown below, where ΔH , ΔS , T , R , and Φ are enthalpy, entropy, absolute temperature, gas constant, and phase ratio, respectively.

$$\ln k' = -\frac{\Delta H}{RT} + \frac{\Delta S}{R} + \ln \Phi$$

Here the capacity factor (k') was calculated using the first peak as dead (hold-up) time. In addition, we assumed that the phase distribution of the inner and outer phases of the carrier solution in the tube due to the tube radial distribution of the solvents did not change with temperature over the range of 5–20 °C.

The values of $\ln k'$ were plotted against $1/T$ for the data obtained with the organic solvent-rich carrier solutions (Fig. 2). Obviously, Fig. 2 does not show a simple linear plot based on the separation performance observed on the chromatograms in Fig. 1. Tentatively, we examined the value of enthalpy (ΔH) from the line over the temperature

range of 10–20 °C where separation was observed with increasing resolution. The value of enthalpy was roughly estimated to be 37.1 kJ mol⁻¹. The enthalpy is generally influenced by various types of heat, such as dissolution, adsorption, desorption, and solvation. At the present it is difficult to discuss interactions between the fused-silica inner-wall surface and the analytes that may contribute to separation performance in the TRDC system. However, the obtained data for the fused-silica capillary tube would give a clue to further account for the separation performance (including the contribution of the activity on the inner-wall surface) of the TRDC system from the viewpoint of thermodynamics, comparing the theory with the data for polyethylene or poly(tetrafluoroethylene) capillary tube.

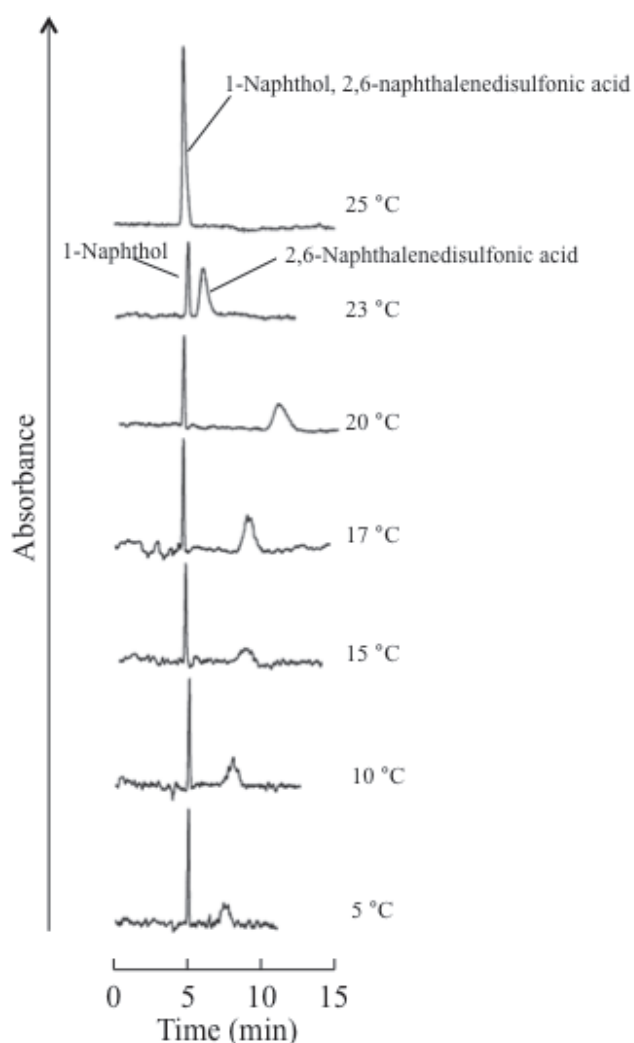


Figure 1. Chromatograms obtained at various capillary temperatures in the TRDC system.¹⁰⁾ Conditions: Capillary tube, 120 cm (effective length of 100 cm, the part of it (ca. 80 cm) was dipped in the temperature-controlled water) of 75 μ m i.d. fused-silica; carrier, water-acetonitrile-ethyl acetate (3:8:4 v/v/v) mixture solution; sample injection, 20 cm height (gravity) \times 30 s; flow rate, 0.8 μ L min⁻¹; tube temperature, 5–25 °C; and 2,6-naphthalenedisulfonic acid and 1-naphthol, 1 mM each.

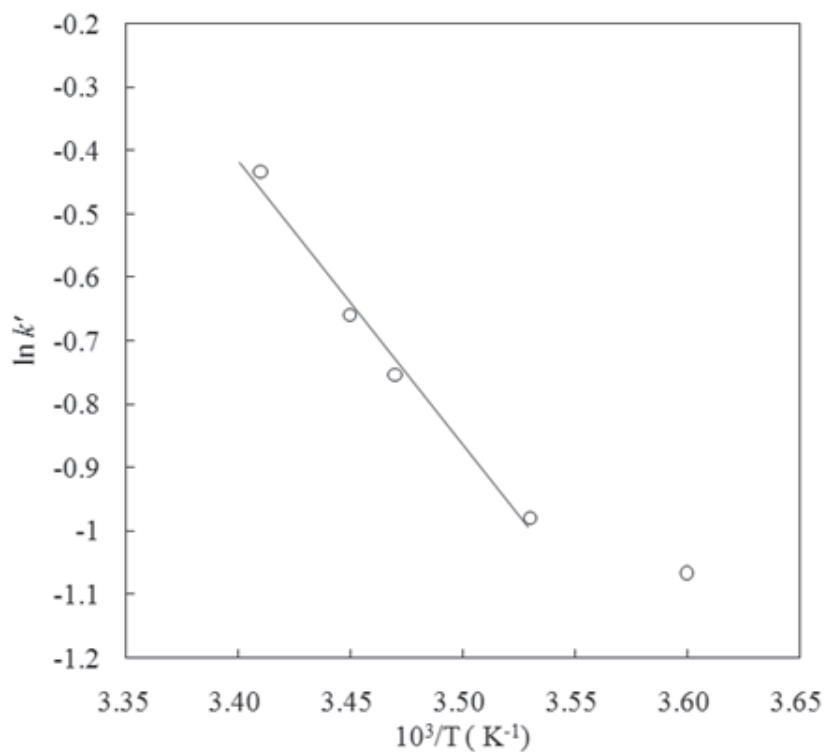


Figure 2. The van't Hoff plots obtained in the TRDC system. Conditions: Capillary tube, 120 cm (effective length: 100 cm) of 75 μm i.d. fused-silica; carrier, water-acetonitrile-ethyl acetate (3:8:4 v/v/v) mixture solution; sample injection, 20 cm height (gravity) \times 30 s; flow rate, 0.8 $\mu\text{L min}^{-1}$; tube temperature, 5–23 $^{\circ}\text{C}$; and 2,6-naphthalenedisulfonic acid and 1-naphthol, 1 mM each.

9.2 Experiments and consideration through adding surfactants to an analyte solution in TRDC

The influences on separation performance of adding surfactants to an analyte solution was examined in a chromatographic system, tube radial distribution chromatography (TRDC), using a fused-silica capillary tube (75 μm inner diameter and 100 cm effective length) and a ternary mixture of water–acetonitrile–ethyl acetate (3:8:4 volume ratio) carrier solution. Sodium dodecyl sulfate (anionic), ethylhexadecyldimethylammonium bromide (cationic), and Triton X-100 (nonionic) were used as surfactants. Model analytes, 1-naphthol and 2,6-naphthalenesulfonic acid, were separated in this order by adding the anionic and nonionic surfactants. These surfactants in the analyte solution extremely improved the separation performance (theoretical plate numbers for 2,6-naphthalenesulfonic acid; >10,000) compared with the same separation performed in the absence of surfactants. On the other hand, the analytes were not separated at all using a cationic surfactant.

Introduction

Various types of analytes, such as miscellaneous organic compounds, amino acids, peptides, proteins, nucleosides, lambda-DNA, metal ions, metal complexes, fluorescent compounds, polymer compounds, and optical isomers, were analyzed using the TRDC system. Through all experimental data, we can notice a tendency for the analytes distributed in the outer phase or pseudo-stationary phase to possess lower elution velocity and a consequential broadening of their peak shapes. Here, we tried to improve the separation performance for the later peaks by adding surfactants to the analyte solution. It was observed that the addition of anionic and nonionic surfactants could improve the resolution and theoretical plate numbers for the model analytes.

Experimental

Fused-silica capillary tubes (75 μm inner diameter) were used. The TRDC system comprised a fused-silica capillary tube (120 cm total length and 100 cm effective length), a microsyringe pump, and a fluorescence detector. The tube temperature was controlled by immersing the capillary tube (40 cm) in water maintained at 15 °C in a beaker while stirring. A water–acetonitrile–ethyl acetate mixture (3:8:4 volume ratio) was used as the carrier solution. Analyte solutions of 1-naphthol and 2,6-naphthalenedisulfonic acid (1 mM each) were prepared using the carrier solution either with or without surfactants. The analyte solution was introduced directly into the capillary inlet side by the gravity method (30 cm height for 25 s). After analyte injection, the capillary inlet was connected through a joint to a microsyringe. The syringe was set on the microsyringe pump. The carrier solution was fed into the capillary tube at a constant flow rate (0.5 $\mu\text{L min}^{-1}$) under laminar flow conditions. On-capillary fluorescence detection of the analytes was performed with the detector; ex. 290 nm and em. 355 nm.

Results and discussion

Figure 1 shows the chromatograms obtained through the use of the present TRDC system, where the analytes were prepared with the carrier solution containing the surfactants, 20 mM sodium dodecyl sulfate (SDS) (anionic), 10 mM ethylhexadecyldimethylammonium bromide (EHDAB) (cationic), and 2.0 wt% Triton X-100 (nonionic). On the other hand, the analytes prepared with a surfactant-free carrier solution were used as a reference. Hydrophobic 1-naphthol and hydrophilic 2,6-naphthalenedisulfonic acid were separated in this order in the absence and presence of surfactants (SDS and Triton X-100). The first peak (1-naphthol) was eluted with an average linear velocity, while the second peak (2,6-naphthalenedisulfonic acid) was detected with a velocity lower than the average linear velocity under the laminar flow conditions. The elution behavior of the analytes was reasonable because of their hydrophobic and hydrophilic natures and also because of the TRDP created by the organic solvent-rich carrier solution generating major organic solvent-rich inner phase and minor water-rich outer phase. However, the analytes were not separated with the carrier solution containing EHDAB.

Furthermore, as is clearly shown in Fig. 1, the addition of SDS and Triton X-100 to the analyte solutions improved the separation of the analytes significantly. The resolution and theoretical plate numbers are calculated in the usual manner and summarized in Table 1 together with other experimental data. The theoretical plate numbers for 2,6-naphthalenedisulfonic acid with added SDS and Triton X-100 were 10,100 and 22,800, respectively. These data are generally competitive with those obtained using capillary electrophoresis. However, it is significant that the present TRDC system featured such superior separation performance without the necessity of applying high voltages or using any specific columns, such as those of the monolithic or packed varieties.

The reason why the addition of surfactants to the analyte solutions provided such high resolution has not yet been determined. However, we tentatively suggest the following explanation of our findings. The tentative suggestion is illustrated in Fig. 2. First, the broadening of the second peak in the general system without surfactant might be caused by the greater thickness of the micrometer order of the outer phase that functions as a pseudo-stationary phase. The analyte having an anionic nature, 2,6-naphthalenedisulfonic acid, is easily surrounded by the surfactants, SDS (anionic) and Triton X-100 (nonionic), to generate a micellar assembly. The formation of hydrophilic micelles might reduce adsorption on the inner wall resulting in very sharp peaks. On the other hand, the anionic analyte was strictly surrounded with the cationic surfactant, EHDAB, generating reverse micellar assemblies. The hydrophobic micelle containing the analyte must behave similarly to the hydrophobic analyte, 1-naphthol, in the capillary tube leading to no separation. As another suggestion, there is some turbulence nearby the interface between the two phases moving downward in the capillary tube, since a shear stress is generated due to differences in physical properties of these phases. The addition of surfactants may suppress the influence of the turbulence by the decrease in the friction coefficient between the two phases, leading to decrease in peak broadening or solute diffusion.

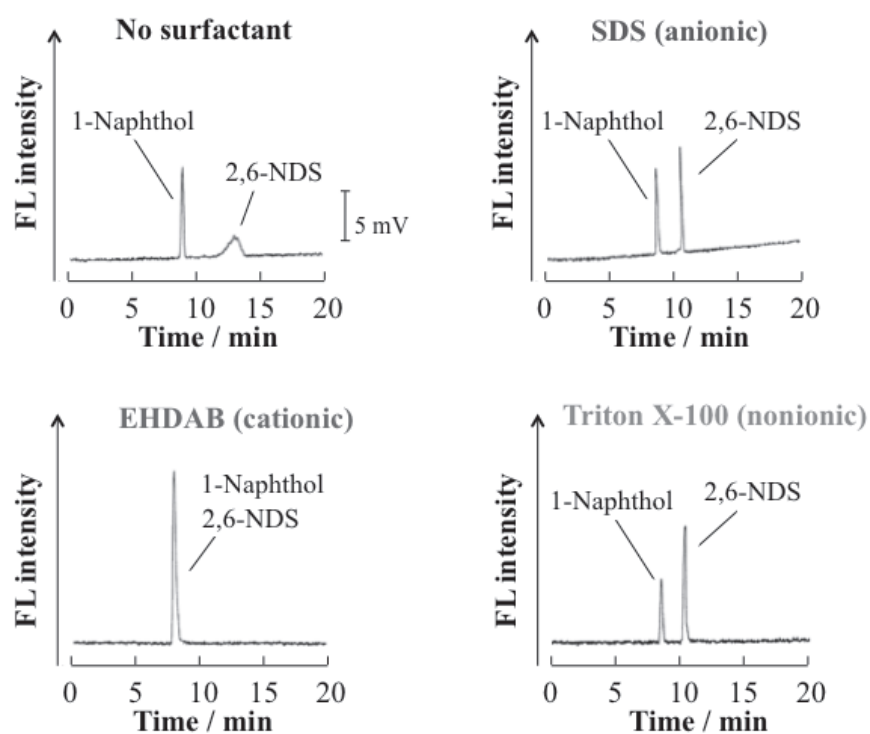


Figure 1. Chromatograms of 1-naphthol and 2,6-naphthalenedisulfonic acid (2,6-NDS) obtained with the present TRDC system using analyte solutions with or without surfactants.

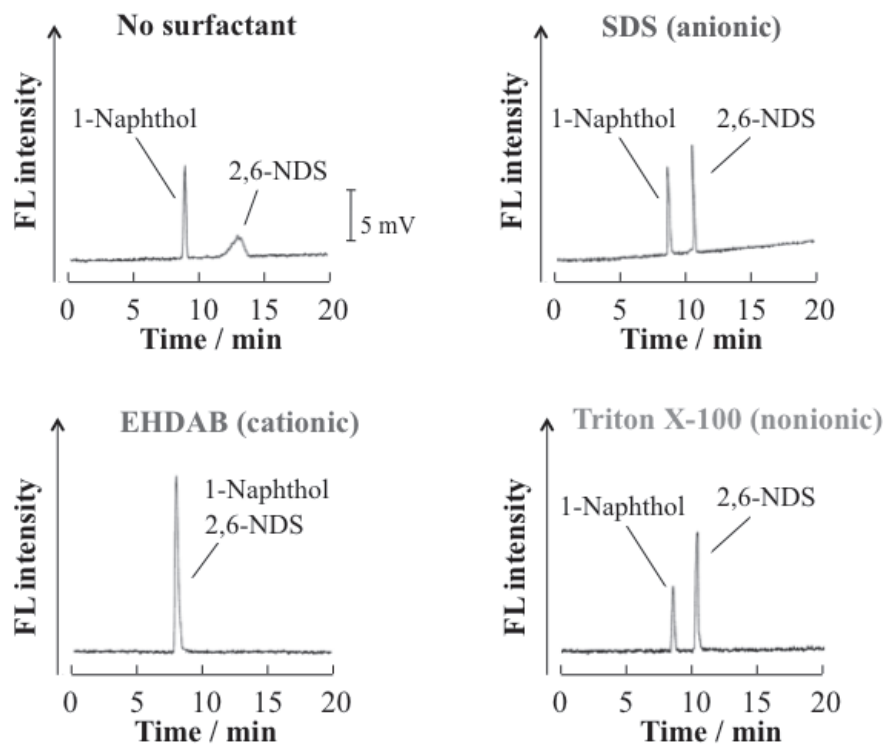


Figure 2. Illustration of the analyte distribution between the inner and outer phases with or without surfactants.

Table 1. Experimental data of the elution times (t_1 and t_2), the peak widths (W_1 and W_2), the capacity factors (k'), the resolutions (R_s), the theoretical plate numbers (N), and the height of equivalent theoretical plate (H) in the present TRDC system. The subscript 1 and 2 are for 1-naphthol and 2,6-naphthalenedisulfonic acid, respectively.

Surfactant	t_1 /min	t_2 /min	W_1 /min	W_2 /min	k'	R_s	N	H /mm
None	8.85	13.00	0.42	2.08	0.47	3.32	625	1.60
SDS	8.65	10.58	0.38	0.28	0.22	5.84	22800	0.04
EHDAB	8.80	—	0.60	—	—	—	—	—
Triton X-100	8.50	10.29	0.41	0.41	0.21	4.37	10100	0.10

9.3 Theoretical consideration through outer phase formation in TRDC

A capillary chromatography system that consists of an open capillary tube composed of fused silica, polyethylene, and poly(tetrafluoroethylene), and a water–hydrophilic/hydrophobic organic mixture carrier solution has been developed. We call this system the tube radial distribution chromatography (TRDC) system. Here, variance, theoretical plate number, and height equivalents to a theoretical plate for a solute peak in the chromatogram were expressed using theoretical equations derived from the differential equation for the secondary moment of a solute. The relationship between the thickness and diffusion coefficient in the outer phase in the capillary tube in the TRDC system was calculated from theoretical equations using numerical values for analytical conditions and experimental data. The outer phase that featured the TRDC system had a larger diffusion coefficient and a larger thickness than those of the stationary phase in standard liquid chromatography. We confirmed the separation performance obtained on the basis of the tube radial distribution of the carrier solvents under laminar flow conditions in the TRDC system by considering the inner and outer phase generation in the capillary tube.

Introduction

It is important to experimentally and theoretically examine separation performances in the TRDC system. Here, for a solute peak in a capillary chromatogram, variance, theoretical plate number, and height equivalent to a theoretical plate were successfully expressed using theoretical equations derived from the differential equation for the secondary moment of a solute reported by Aris [1]. The relationship between the thickness and the diffusion coefficient in the outer phase in the capillary tube in the TRDC system was estimated from the theoretical equations using the numerical values for the analytical conditions and experimental data. We discuss the TRDC feature that as a stationary phase, the outer phase consists of carrier solvents and has a larger diffusion coefficient and thickness than those in standard liquid chromatography systems.

Experimental

TRDC system with absorption detection The TRDC system with UV absorption spectrometer consisted of an open fused-silica capillary tube (75 μm i.d., 120 cm length; 100 cm effective length), a microsyringe pump, and an absorption detector. The tube temperature was controlled by immersing the capillary tube in water maintained at a temperature of 15 $^{\circ}\text{C}$ in a beaker while stirring. Water–acetonitrile–ethyl acetate mixtures with volume ratios of 3:8:4 and 15:3:2 were used as carrier solutions, and analyte solutions including 1-naphthol and 2,6-naphthalenedisulfonic acid were prepared with them. The analyte solution was directly introduced into the capillary inlet side using the gravity method (20 cm height for 30 s). Then, the capillary inlet was connected through a joint to a microsyringe. The joint (PEEK-tough-connector) was

purchased from GL Science. It was used for the connection between the capillary tube and from the PTFE tube to the microsyringe. The syringe was set on a microsyringe pump. The carrier solution was fed into the capillary tube at a flow rate of $0.8 \mu\text{L min}^{-1}$ under laminar flow conditions. On-capillary absorption detection (254 nm) was performed using a detector.

Fluorescence microscope–charge coupled device (CCD) camera system A fused-silica capillary tube of the same size as that used in the TRDC system with absorption detection (75 μm i.d., 120 cm length) was set up for a fluorescence microscope–CCD camera system. The fluorescence in the capillary tube was monitored using a fluorescence microscope equipped with an Hg lamp, a filter, and a CCD camera. The organic solvent-rich carrier solution (water–acetonitrile–ethyl acetate; 3:8:4 volume ratio) contained 0.1 mM perylene and 1 mM Eosin Y, and the water-rich carrier solution (water–acetonitrile–ethyl acetate; 15:3:2 volume ratio) contained 1 mM Eosin Y (perylene was only slightly dissolved in the solution). The carrier solution was introduced into the capillary tube at a specific flow rate using a microsyringe pump.

Results and discussion

Differential equation of the secondary moment of a solute in a capillary tube Aris theoretically studied the dispersion in capillary chromatography and expressed it as a differential equation that represents the secondary moment of a solute; the secondary moment of a solute $m^{(2)}$ represents the variance of the solute [1]. The model conditions for a fluid in a capillary tube are determined by considering the dispersion of the solute dissolved in the fluid, which is introduced into the capillary tube under laminar flow conditions. The inner and outer phases (corresponding to phases 1 and 2, respectively) flow in the annular space between two coaxial cylinders of radii r_0 and r_2 in the capillary tube, the interface being a cylinder of equal axis and radius r_1 ($0 \leq r_0 < r_1 < r_2$). A schematic diagram of the inner and outer phases in a capillary tube is shown in Fig. 1.

We suppose that both phases move with a linear velocity that is a function of the radial distance from the axis, r , and the solute diffuses in both phases with a diffusion coefficient that may also be a function of r (average the diffusion coefficient are used in the following equations, though). At equilibrium, the solute concentration in phase 2, c_2 , is a constant multiple of that in phase 1, i.e., $c_2 = \alpha c_1$, and at any instant, the transfer rate across the interface is proportional to the distance from the equilibrium at that point, i.e., $c_2 - \alpha c_1$. Dispersion of the solute arises from three processes: (i) the combined effects of diffusion and convection in phase 1; (ii) the finite transfer rate at the interface; and (iii) the combined effects of diffusion and convection in phase 2.

The standard equations (I) for diffusion and flow under the above mentioned boundary conditions are derived as follows.

$$\left. \begin{aligned}
D_1\psi_1(r)\frac{\partial c_1}{\partial r} &= 0 \quad (r = r_0) \quad (a) \\
\frac{\partial c_1}{\partial t} &= D_1 \frac{1}{r} \frac{\partial}{\partial r} \left(r\psi_1(r) \frac{\partial c_1}{\partial r} \right) + D_1\psi_1(r) \frac{\partial^2 c_1}{\partial x^2} - U_1\phi_1(r) \frac{\partial c_1}{\partial x} \quad (r_0 < r < r_1) \quad (b) \\
D_1\psi_1(r)\frac{\partial c_1}{\partial r} &= D_2\psi_2(r)\frac{\partial c_2}{\partial r} = k(c_2 - \alpha c_1) \quad (r = r_1) \quad (c) \\
\frac{\partial c_2}{\partial t} &= D_2 \frac{1}{r} \frac{\partial}{\partial r} \left(r\psi_2(r) \frac{\partial c_2}{\partial r} \right) + D_2\psi_2(r) \frac{\partial^2 c_2}{\partial x^2} - U_2\phi_2(r) \frac{\partial c_2}{\partial x} \quad (r_1 < r < r_2) \quad (d) \\
D_2\psi_2(r)\frac{\partial c_2}{\partial r} &= 0 \quad (r = r_2) \quad (e)
\end{aligned} \right\} (I)$$

The standard equations (I) are a set of five equations labeled (a), (b), (c), (d), and (e). The differential equations expressing the three processes (i), (ii), and (iii) are (b), (c), and (d), respectively. Equations (a) and (e) represent the condition where there is no flow over the boundaries at $r = r_0$ and $r = r_2$.

The following notations are used, and unless otherwise stated, the suffixes 1 and 2 refer to quantities in the inner and outer phases, respectively: c_i , solute concentration; U_i , average linear velocity; $U_i\phi_i(r)$, linear velocity at radius r ; D_i , average diffusion coefficient; $D_i\psi_i(r)$, diffusion coefficient at radius r ; x , the coordinate along the common axis; r , radial coordinate; and t , time. Furthermore, for simplicity, the variable of length is changed along the axis so that its origin moves with constant speed V . The quantity V is later chosen to move at the speed of the center of gravity of the solute ($y = x - Vt$).

Finally, the following differential equation for the secondary moment of a solute was introduced in the paper by Aris [1].

$$\frac{1}{2} \frac{dm^{(2)}}{dt} = \beta \left\{ D_1 + \kappa_1 \frac{U_1^2 (r_1^2 - r_0^2)}{D_1} \right\} + (1 - \beta) \left\{ D_2 + \kappa_2 \frac{U_2^2 (r_2^2 - r_1^2)}{D_2} \right\} + \frac{\{\beta(1 - \beta)\}(U_1 - U_2)^2}{2k\alpha r_1} \quad (1)$$

Here,

$$\kappa_1 = \int_{r_0}^{r_1} \frac{dr}{2r\psi_1(r)} \left\{ \Phi_1(r) - \frac{R}{\gamma} \frac{r^2 - r_0^2}{r_1^2 - r_0^2} \right\}^2$$

$$\kappa_2 = \int_{r_1}^{r_2} \frac{dr}{2r\psi_2(r)} \left\{ \Phi_2(r) - \frac{R}{\gamma - 1} \frac{r_2^2 - r^2}{r_2^2 - r_1^2} \right\}^2$$

$$\Phi_1(r) = \frac{\int_{r_0}^r 2r'\phi_1(r')dr'}{r_1^2 - r_0^2}$$

$$\Phi_2(r) = \frac{\int_r^{r_2} 2r'\phi_1(r')dr'}{r_2^2 - r_1^2}$$

$$\beta = \frac{r_1^2 - r_0^2}{s^2} : \text{fraction of the solute in the inner phase at equilibrium}$$

$$\gamma = \frac{U_1}{U_1 - U_2} : \text{ratio of the inner phase velocity to the relative velocity}$$

$$s^2 = (r_1^2 - r_0^2) + \alpha (r_2^2 - r_1^2)$$

Variance of solute in capillary chromatography The equation expressing the variance of a solute in capillary chromatography is derived from the differential equation (Eq. 1) for the secondary moment of a solute under the following conditions: (i) the diffusion coefficient are constant in the phases, (ii) the inner phase (mobile phase) moves under laminar flow conditions, (iii) there is no flow in the outer phase (stationary phase), and (iv) $r_0 = 0$.

As the mobile phase moves under laminar flow conditions, the distribution of the flow rate is expressed as a parabolic curve. Then, the following equation is obtained.

$$U_1 \phi_1(r) = C(r_1^2 - r^2)$$

Here, U_1 is the average linear velocity; therefore,

$$U_1 = \frac{\int_0^{r_1} U_1 \phi_1(r) \cdot 2\pi r dr}{\pi r_1^2} = \frac{2C \int_0^{r_1} (r_1^2 - r^2) dr}{r_1^2} = \frac{1}{2} C r_1^2.$$

Accordingly,

$$U_1 \phi_1(r) = \frac{1}{2} C r_1^2 \phi_1(r) = C(r_1^2 - r^2)$$

$$\phi_1(r) = 2 \left(1 - \frac{r^2}{r_1^2} \right).$$

From the above equation, the following equation is obtained for κ_1 .

$$\kappa_1 = \int_0^{r_1} \frac{dr}{2r\psi_1(r)} \left\{ \Phi_1(r) - R \frac{r^2}{r_1^2} \right\}^2$$

$$= \int_0^{r_1} \frac{dr}{2r\psi_1(r)} \Phi_1(r)^2 - \int_0^{r_1} \frac{dr}{r\psi_1(r)} \Phi_1(r) \frac{r^2}{r_1^2} R + \int_0^{r_1} \frac{dr}{2r\psi_1(r)} \frac{r^4}{r_1^4} R^2$$

The first term in the above equation is calculated as follows.

$$\int_0^{r_1} \frac{dr}{2r\psi_1(r)} \Phi_1(r)^2 = \int_0^{r_1} \frac{dr}{2r\psi_1(r)} \left\{ \frac{\int_0^r 2r' 2 \left(1 - r'^2/r_1^2 \right) dr'}{r_1^2} \right\}^2 = \frac{11}{48}$$

The second term is written as follows.

$$- \int_0^{r_1} \frac{dr}{r\psi_1(r)} \Phi_1(r) \frac{r^2}{r_1^2} R = - \int_0^{r_1} \frac{dr}{r\psi_1(r)} \left\{ \frac{\int_0^r 2r' 2 \left(1 - r'^2/r_1^2 \right) dr'}{r_1^2} \right\} \frac{r^2}{r_1^2} R = -\frac{1}{3} R$$

The third term is written as follows.

$$\int_0^{r_1} \frac{dr}{2r\psi_1(r)} \frac{r^4}{r_1^4} R^2 = \left[\frac{1}{8} \frac{r^4}{r_1^4} \right]_0^{r_1} R^2 = \frac{1}{8} R^2$$

Finally, the following equation is obtained.

$$\kappa_1 = \frac{11}{48} - \frac{1}{3}R + \frac{1}{8}R^2 = \frac{1}{48}(11 - 16R + 6R^2)$$

The condition of no flow in the stationary phase provides the equation $U_2 = 0$. Then,

$$\gamma = \frac{U_1}{U_1 - U_2} = \frac{U_1}{U_1} = 1$$

$$\frac{U_1}{\gamma} = \frac{U_2}{\gamma - 1}$$

$$\therefore U_1 = \lim_{\gamma \rightarrow 1} \frac{U_2}{\gamma - 1}$$

As $\Phi_2(r)$ expresses the flow from r to r_2 , it is clear that $\Phi_2(r) = 0$ for $U_2 = 0$. Then,

$$\begin{aligned} \kappa_2 &= \int_{r_1}^{r_2} \frac{dr}{2r\psi_2(r)} \left(-\frac{R}{\gamma - 1} \frac{r_2^2 - r^2}{r_2^2 - r_1^2} \right)^2 \\ &= \left(\frac{R}{\gamma - 1} \right)^2 \int_{r_1}^{r_2} \frac{dr}{2r\psi_2(r)} \left(\frac{r_2^2 - r^2}{r_2^2 - r_1^2} \right)^2 \end{aligned}$$

In the second term of Eq. 1, the component in the parentheses is rewritten as

$$\begin{aligned} \kappa_2 \frac{U_2^2 (r_2^2 - r_1^2)}{D_2} &= \left(\frac{R}{\gamma - 1} \right)^2 \int_{r_1}^{r_2} \frac{dr}{2r\psi_2(r)} \left(\frac{r_2^2 - r^2}{r_2^2 - r_1^2} \right)^2 \cdot \frac{U_2^2 (r_2^2 - r_1^2)}{D_2} \\ &= R^2 \frac{U_2^2}{(\gamma - 1)^2} \frac{r_2^2 - r_1^2}{D_2} \int_{r_1}^{r_2} \frac{dr}{2r\psi_2(r)} \left(\frac{r_2^2 - r^2}{r_2^2 - r_1^2} \right)^2 \end{aligned}$$

From $\gamma \rightarrow 1$, the following equation is obtained.

$$\kappa_2 \frac{U_2^2 (r_2^2 - r_1^2)}{D_2} = R^2 \frac{U_1^2 (r_2^2 - r_1^2)}{D_2} \int_{r_1}^{r_2} \frac{dr}{2r\psi_2(r)} \left(\frac{r_2^2 - r^2}{r_2^2 - r_1^2} \right)^2$$

Then,

$$\begin{aligned}
 \kappa_2 &= \int_{r_1}^{r_2} \frac{dr}{2r\psi_2(r)} \left(\frac{r_2^2 - r^2}{r_2^2 - r_1^2} \right)^2 R^2 \\
 &= \frac{1}{(r_2^2 - r_1^2)^2} \int_{r_1}^{r_2} \frac{dr}{\psi_2(r)} \left(\frac{r_2^4}{2r} - r_2^2 r^2 + \frac{r^3}{2} \right) R^2 \\
 &= \frac{1}{8(r_2^2/r_1^2 - 1)} \left\{ 2 \frac{r_2^4/r_1^4}{r_2^2/r_1^2 - 1} \ln \left(\frac{r_2}{r_1} \right)^2 - \left(3 \frac{r_2^2}{r_1^2} - 1 \right) \right\} R^2.
 \end{aligned}$$

By substituting $\rho = \frac{r_2}{r_1}$, $P = \frac{\rho^2 - 1}{\ln \rho^2}$, the following equation is obtained.

$$\begin{aligned}
 \kappa_2 &= \frac{1}{8(\rho^2 - 1)} \left\{ 2 \frac{\rho^4}{\rho^2 - 1} \ln \rho^2 - (3\rho^2 - 1) \right\} R^2 \\
 &= \frac{2\rho^4 P^{-1} - (3\rho^2 - 1)}{8(\rho^2 - 1)} R^2
 \end{aligned}$$

From the above, Eq. 1 is rewritten as follows.

$$\begin{aligned}
 \frac{1}{2} \frac{dm^{(2)}}{dt} &= R \left\{ D_1 + \frac{U_1^2 r_1^2}{48D_1} (11 - 16 + 6R^2) \right\} + (1 - R) \left\{ D_2 + \frac{U_1^2 (r_2^2 - r_1^2) 2\rho^4 P^{-1} - (3\rho^2 - 1)}{D_2 8(\rho^2 - 1)} R^2 \right\} \\
 &\quad + \frac{\{R(1 - R)kU_1\}^2}{2k\alpha r_1}
 \end{aligned}$$

By integrating the above equation with t , the following equation is obtained.

$$\begin{aligned}
 m^{(2)} &= t \left\{ 2RD_1 + \frac{U_1^2 r_1^2}{24D_1} R(11 - 16 + 6R^2) + 2(1 - R)D_2 + 2 \frac{U_1^2 (r_2^2 - r_1^2) 2\rho^4 P^{-1} - (3\rho^2 - 1)}{D_2 8(\rho^2 - 1)} (1 - R)R^2 \right. \\
 &\quad \left. + \frac{\{R(1 - R)kU_1\}^2}{k\alpha r_1} \right\}
 \end{aligned}$$

The secondary moment of a solute expresses the variance (σ^2) of the solute on t .

When the capillary length is L , the time (t_R) required to reach the outlet is given by

$$t_R = \frac{L}{V} = \frac{L}{U_1 R}.$$

The variance $\sigma^2(L)$ of a solute at the outlet is then expressed as follows.

$$\begin{aligned}
 \sigma^2(L) &= \frac{L}{U_1 R} \left\{ 2RD_1 + \frac{U_1^2 r_1^2}{24D_1} R(11 - 16 + 6R^2) + 2(1 - R)D_2 + 2 \frac{U_1^2 (r_2^2 - r_1^2) 2\rho^4 P^{-1} - (3\rho^2 - 1)}{D_2 8(\rho^2 - 1)} (1 - R)R^2 \right. \\
 &\quad \left. + \frac{\{R(1 - R)kU_1\}^2}{k\alpha r_1} \right\}
 \end{aligned}$$

This equation represents the variance $\sigma^2(L)$ of solute distribution in a real capillary column.

Variance, theoretical plate number, and the height equivalent to a theoretical plate for a solute peak in a chromatogram The variance $\sigma^2(t_R)$ for a solute peak eluted in the chromatogram is expressed by changing the variable as follows.

$$\sigma^2(t_R) = \sigma^2\left(\frac{L}{V}\right) = \frac{1}{V^2} \sigma^2(L) = \frac{1}{U_1^2 R^2} \sigma^2(L)$$

Accordingly, the variance $\sigma^2(t_R)$ is expressed by the following equation.

$$\sigma^2(t_R) = \frac{L}{U_1^3 R^3} \left\{ 2RD_1 + \frac{U_1^2 r_1^2}{24D_1} R(11-16+6R^2) + 2(1-R)D_2 + 2 \frac{U_1^2 (r_2^2 - r_1^2)}{D_2} \frac{2\rho^4 P^{-1} - (3\rho^2 - 1)}{8(\rho^2 - 1)} (1-R)R^2 + \frac{\{R(1-R)\{U_1\}^2\}}{k\alpha r_1} \right\}$$

The theoretical plate number and the height equivalent to a theoretical plate, respectively, are expressed as follows.

$$N = 16 \left(\frac{t_R}{W} \right)^2 = 16 \left(\frac{t_R}{4\sigma} \right)^2 = \left(\frac{t_R}{\sigma} \right)^2$$

$$H = \frac{L}{N} = \frac{L}{\left(\frac{t_R}{\sigma} \right)^2} = \sigma^2 \frac{L}{t_R^2} = \sigma^2 \frac{L}{(L/U_1 R)^2} = \sigma^2 \frac{U_1^2 R^2}{L}$$

When $\sigma^2(t_R)$ is introduced in the above equation, we get

$$H = 2 \frac{D_1}{U_1} + \frac{U_1 r_1^2}{24D_1} (11-16+6R^2) + 2 \frac{(1-R)D_2}{R U_1} + 2 \frac{U_1 (r_2^2 - r_1^2)}{D_2} \frac{2\rho^4 P^{-1} - (3\rho^2 - 1)}{8(\rho^2 - 1)} (1-R)R + \frac{RU_1(1-R)^2 s^2}{k\alpha r_1}$$

Using the capacity factor k' , where

$$R = \frac{1}{1+k'}$$

the height equivalent to a theoretical plate H is expressed as follows.

$$H = 2 \frac{D_1}{U_1} + \frac{U_1 r_1^2}{24D_1} \frac{1+6k'+11k'^2}{(1+k')^2} + 2k' \frac{D_2}{U_1} + 2 \frac{U_1 (r_2^2 - r_1^2)}{D_2} \frac{2\rho^4 P^{-1} - (3\rho^2 - 1)}{8(\rho^2 - 1)} \frac{k'}{(1+k')^2} + \frac{U_1 s^2}{k\alpha r_1} \frac{k'^2}{(1+k')^3} \quad (2)$$

The above equation represents the height equivalent to a theoretical plate for capillary chromatography with an inner phase (mobile phase) and an outer phase (stationary phase); D_1 is the inner phase diffusion coefficient; D_2 is the outer phase diffusion coefficient; r_1 is the inner radius of the capillary tube (from the axis to the inner-outer phase surface); r_2 is the outer radius of the capillary tube (from the axis to the capillary wall surface); U_1 is the average linear velocity, and k' is the capacity factor.

Basic experimental data for the TRDC system Basic experimental data for the TRDC system, i.e., chromatograms and fluorescence images, were examined in our studies. These data must again be used to examine the relationship between the thickness and

diffusion coefficient in the outer phase obtained from the theoretical equations in this study. The data are summarized in Fig. 2.

A model mixture solution of 1-naphthol and 2,6-naphthalenedisulfonic acid was analyzed using the TRDC system with absorption detection. The obtained chromatograms are shown in Fig. 2A. Using an organic solvent-rich carrier solution of water–acetonitrile–ethyl acetate with a volume ratio of 3:8:4, the mixture of 1-naphthol and 2,6-naphthalenedisulfonic acid was separated through an open capillary tube and the order of detection was 1-naphthol and 2,6-naphthalenedisulfonic acid (Fig. 2A-1). In contrast, using a water-rich carrier solution of water–acetonitrile–ethyl acetate with a volume ratio of 15:3:2, the mixture solution was separated and detected with inverse elution times, i.e., the order of detection was 2,6-naphthalenedisulfonic and 1-naphthol (Fig. 2A-2). In both chromatograms, the first peaks were detected with elution times roughly corresponding to average linear velocities, and the second peaks were detected with elution times roughly corresponding to below average linear velocities. The chromatograms clearly indicated the reversibility of the elution times by changing the solvent ratio in the carrier solution.

In addition, we examined the fluorescence images and profiles of the fused-silica capillary tube. The experiment with the fluorescence–CCD camera system and the fused-silica capillary tube was performed under almost the same analytical conditions (capillary tube length, tube inner diameter, and flow rate) as those used for the TRDC system with absorption detection (i.e., the chromatograms shown in Fig. 2A). Fig. 2B shows the fluorescence images and profiles obtained for a fused-silica capillary tube into which dye-containing mixed aqueous–organic solvent carrier solutions were introduced.

The fluorescence images and profiles for the organic solvent-rich carrier solution showed that the hydrophobic perylene molecule (blue) was distributed around the tube center, whereas the hydrophilic Eosin Y molecule (green) was distributed near the tube inner wall (Fig. 2B-1). In contrast, the fluorescence images and profiles showed that Eosin Y was distributed around the capillary tube center for the water-rich carrier solution (Fig. 2B-2). The tube radial distribution of perylene and Eosin Y present in the carrier solutions in the capillary tube confirmed a partition reversal between the organic solvent-rich and water-rich carrier solutions (Fig. 2B).

The distributions of perylene and Eosin Y at the capillary tube center and near its inner wall, respectively, supported the idea of nonuniform dispersion of the aqueous and organic components of the carrier solutions in the capillary tube in the TRDC system. They generated a major inner phase (organic solvent-rich or water-rich) and a minor outer phase or capillary wall phase (water-rich or organic solvent-rich) in the capillary tube. As a result, the analytes were also distributed between the inner and outer phases depending on their nature and were separated by chromatography (i.e., corresponding to the chromatograms shown in Fig. 2A).

Relationship between the thickness and diffusion coefficient in the outer phase As

described in the previous sections, the elution behaviors of the analytes and the distributions of the dyes dissolved in the carrier solvents in the capillary tube, illustrated by the chromatograms, supported the separation performance obtained on the basis of the tube radial distribution of the carrier solvents in the TRDC system, as proposed in our papers. Here, we examined the relationship between the thickness and the diffusion coefficient in the outer phase from theoretical equations using experimental data obtained from the chromatogram (Fig. 2A) and the fluorescence image and profile (Fig. 2B) obtained for the organic solvent-rich carrier solution. These data were used because for the fused-silica capillary tube in the TRDC system, the chromatographic resolution with the organic solvent-rich carrier solution was better than that using the water-rich carrier solution. In addition, the organic solvent-rich carrier solution gave clear fluorescence images and profiles with perylene and Eosin Y.

As shown in Fig. 2A-1, the baseline separation of the analytes 1-naphthol and 2,6-naphthalenedisulfonic acid was achieved completely with the organic solvent-rich carrier solution. The chromatogram shown in Fig. 2A-1 provided the following separation performance for the second peak of 2,6-naphthalenedisulfonic acid under the analytical conditions of a tube inner diameter of 75 μm and an average linear velocity of $3.0 \times 10^{-3} \text{ ms}^{-1}$: resolution, 6.0; theoretical plate number, 900; height equivalent to a theoretical plate, 1.1 mm; and capacity factor, 0.87. By fluorescent dyes observation, formation of inner and outer phases due to the distribution of the carrier solvents was similarly observed as in a capillary tube with an effective length of 20–100 cm. Although a capillary tube with an effective length of less than ca. 20 cm could not be set on the fluorescence microscope stage for fluorescence observations, the radial distribution of fluorescent dyes in the microchannels (effective lengths 0.5–3 cm) of a microchip were clearly observed. With reference to the experimental data, the height equivalent to a theoretical plate was estimated using the capillary effective length of 100 cm.

Using Eq. 2 along with the above-mentioned numerical values such as the theoretical plate number, height equivalent to a theoretical plate, capacity factor, tube inner diameter, and average linear velocity, we attempted to calculate the relationship between the thickness and diffusion coefficient in the outer phase, or capillary wall phase. We used a diffusion coefficient of $2.0 \times 10^{-9} \text{ m}^2 \text{ s}^{-1}$ of a solute in ethyl acetate for the inner phase (although we also used this in acetonitrile, $2.5 \times 10^{-9} \text{ m}^2 \text{ s}^{-1}$, for the inner phase, there was little difference in the calculated results; the diffusion coefficient of the inner (mobile) phase generally has little influence on the separation performance). Furthermore, it was assumed that in the TRDC system, the outer phase moved slightly and its movement could be neglected under laminar flow conditions. The relationship between the thickness and diffusion coefficient in the outer phase is shown in Fig. 3.

The outer phase, in the TRDC system, functions similarly to the stationary phase in standard liquid chromatography. However, the outer phase in TRDC is a very specific stationary phase. It comprises the carrier solvents and the organic solvent-rich or water-rich solution. Therefore, the outer phase in the system has a larger diffusion

coefficient and a larger thickness (in the order of microns) than those of the stationary phase in standard chromatography. In fact, the large diffusion coefficient and thickness of the outer phase, which acts as the stationary phase in the TRDC system, might result in broadening of the second peaks shown in Fig. 2A.

At present, it is impossible to directly measure the diffusion coefficient and thickness in the outer phase in the TRDC system. However, if the process used to derive the related equations is accurate, the diffusion coefficient and thickness values in the outer phase should theoretically exist on the relationship curve in Fig. 3. We attempted to obtain the values by assuming that the relationship (Fig. 3) is valid and using the following numerical values of the diffusion coefficient and thickness. First, the diffusion coefficient of poly(dimethylsiloxane), a high viscosity liquid which has also been used as a stationary phase in coated-capillary chromatography [2], is $8.9 \times 10^{-13} \text{ m}^2 \text{ s}^{-1}$. The real diffusion coefficient in the present TRDC system must be larger than that of poly(dimethylsiloxane). Second, the fluorescence image and profile shown in Fig. 2B-1 obtained with the organic rich-solvent carrier solution clearly indicated formation of inner and outer phases in the capillary tube. We estimated the thickness of the outer phase from the inflection of the fluorescence profiles in Fig. 2B-1 and found to be $< \text{ca. } 8 \text{ }\mu\text{m}$.

These two numerical values, i.e., the diffusion coefficient of poly(dimethylsiloxane) ($8.9 \times 10^{-13} \text{ m}^2 \text{ s}^{-1}$) and the estimated thickness ($8 \text{ }\mu\text{m}$), are clearly shown on the curve in Fig. 3. If the process used to plot the relationship curve in Fig. 3 is inaccurate, such a specific part of the curve between the two values would not appear. The diffusion coefficient and thickness in the relevant part of the curve were both larger than those for a stationary phase in standard chromatography. In conclusion, the relationship between the thickness and the diffusion coefficient in the outer phase estimated from Eq. 2 using the present analytical conditions and experimental data was consistent with the features of the outer phase in the TRDC system, i.e., a large diffusion coefficient and a large thickness of the order of microns. Therefore, in the TRDC system, the relationship between the thickness and the diffusion coefficient in the outer phase theoretically supports the chromatographic separation performance obtained on the basis of the tube radial distribution of the carrier solvents in the capillary tube.

In conclusion, using experimental data, inner and outer phase formation due to the tube radial distribution of the carrier solvents was considered from the elution behaviors of the analytes in chromatograms, the distributions of dyes dissolved in aqueous–organic solvent mixture carrier solutions in the capillary tube, and theoretical estimations of the thickness and diffusion coefficient in the outer phase. The data obtained both experimentally and theoretically were consistent with our proposed separation performance explained on the basis of tube radial distribution of the carrier solvents.

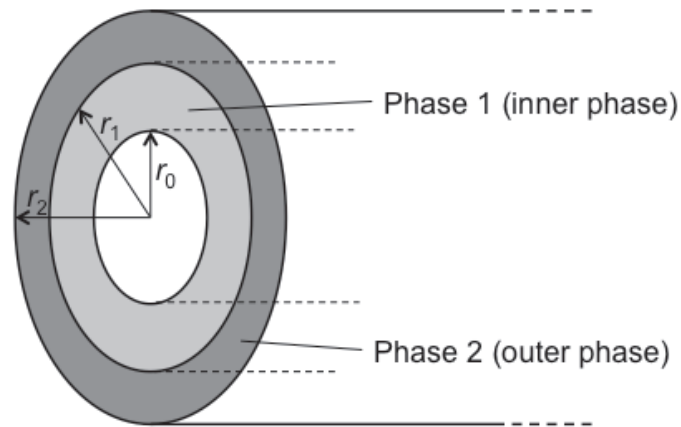


Figure 1. Schematic diagram of the inner and outer phases in a capillary tube. The inner and outer phases, phase 1 and phase 2, respectively, flow in the annular space between two coaxial cylinders of radii r_0 and r_2 in the capillary tube, the interface being a cylinder of equal axis and radius r_1 ($0 \leq r_0 < r_1 < r_2$). The standard equations (I) are derived based on this model conditions for a fluid in a capillary tube (the details are described in the text).

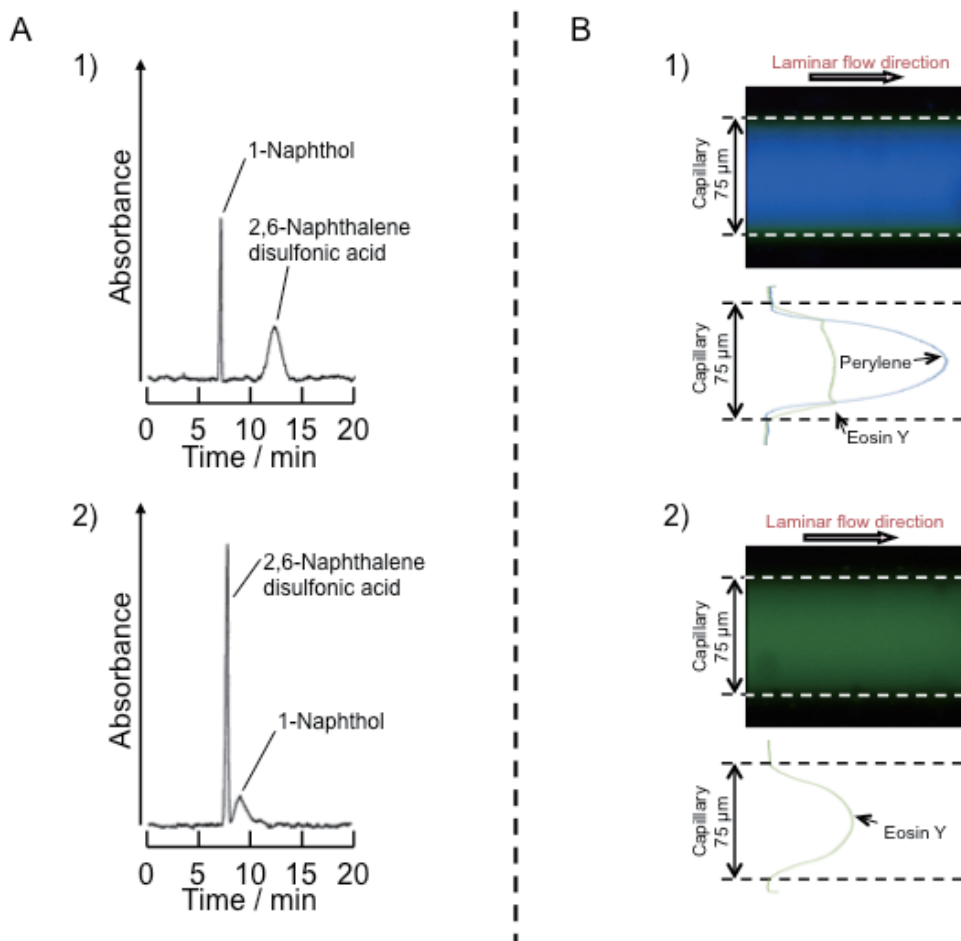


Figure 2. A) Chromatograms of a mixture of 1-naphthol and 2,6-naphthalenedisulfonic acid obtained by the TRDC system with absorption detection; B) fluorescence images and profiles of fluorescent dyes dissolved in ternary mixed carrier solutions observed by a fluorescence microscope–CCD camera system. Conditions A: Capillary tube, 120 cm (effective length: 100 cm), i.d. 75 μm, fused silica; carrier 1) water–acetonitrile–ethyl acetate (3:8:4 v/v/v) solution, and 2) water–acetonitrile–ethyl acetate (15:3:2 v/v/v) solution; sample injection, 20 cm height (gravity) × 30 s; flow rate, 0.8 μL min⁻¹; tube temperature, 15 °C; and analyte concentration, 1 mM. Conditions B: Capillary tube, 120 cm (effective length: 100 cm), 75 μm i. d., fused silica; carrier, 1) water–acetonitrile–ethyl acetate (3:8:4 v/v/v) mixture containing 0.1 mM perylene and 1 mM Eosin Y, and 2) water–acetonitrile–ethyl acetate (15:3:2 v/v/v) mixture containing 1 mM Eosin Y; and flow rate, 0.8 μL min⁻¹.

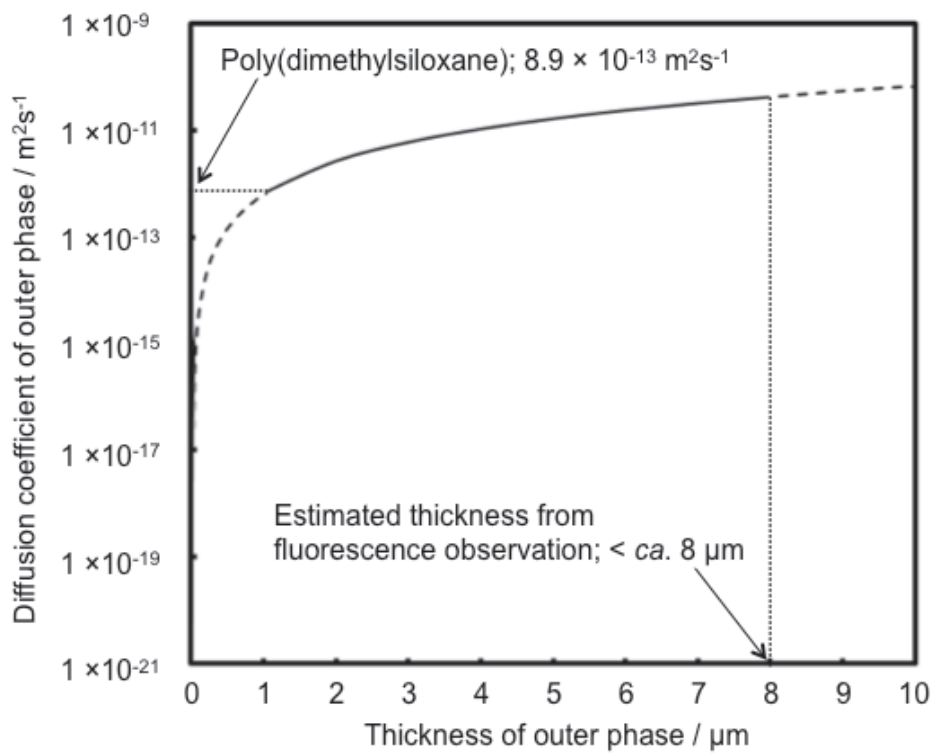


Figure 3. Relationship between the thickness and diffusion coefficient in the outer phase.

9.4 Consideration through computer simulation in TRDC

When the ternary mixed solvents of a water-hydrophilic/hydrophobic organic solvent mixture are delivered under microspace under laminar flow conditions, the solvent molecules are radially distributed in the microspace, and generate a major inner phase and a minor outer phase. We call this fluidic phenomenon as the tube radial distribution phenomenon (TRDP). Here, phase formation in the TRDP was collectively considered based on experimental data, such as the inner and outer phase formation in a microchannel under laminar flow conditions, the phase diagram for the ternary mixed solvents, the solvent-component ratios required for the TRDP, and the phase transformation in a batch vessel above atmospheric pressure, which were mainly reported in our papers. Furthermore, the formation of inner and outer phases in a capillary tube was simulated with the two-component solvents mixture model of water and ethyl acetate. Phase formations in capillary tubes were expressed through computer simulations.

Introduction

The TRDP creates a liquid–liquid (aqueous–organic) interface in a microflow from a homogeneous aqueous–organic mixture solution in a batch vessel. The phase interface is specific; it is kinetic, not static. That is, the TRDP is a new phase interface concept, and can be applied to various technological, engineering, and scientific fields. We are currently investigating the TRDP from the viewpoints of chromatography, extraction, and chemical reaction space. Here, the formation of inner and outer phases in the TRDP is considered based on experimental data that were reported in our papers. Also, the results of computer simulations agree well with the phase formation observed through the TRDP.

Experimental

A microchip made of glass incorporating a microchannel line (100 μm wide \times 40 μm deep) was used. The fluorescence in the microchannel was monitored using a fluorescence microscope equipped with an Hg lamp, a filter, and a CCD camera. The ternary mixed solvent solutions were delivered into the microchannel using a microsyringe pump. Fluorescence photographs, which contained mainly blue and green color because perylene and Eosin Y emit light at 470 and 550 nm, respectively, were transformed into line drawings to assess the color depth (red, green, and blue (RGB)). The line drawings were then digitized, and the numbers were standardized to the line-drawing data to give the fluorescence profiles. The phase formation in a capillary tube was computer-simulated with the volume of the fluid method (VOF) (Fluent program; ANSYS, Inc., Canonsburg, USA). The simulation conditions were as follows. The carrier solution was a water-ethyl acetate mixture with a 3:7 volume ratio (organic solvent-rich) and a water-ethyl acetate mixture with a 7:3 volume ratio

(water-rich). The capillary length was 1,000 μm , the capillary inner diameter was 50 μm , the contact angles of 30° and 150° of water (water-rich outer phase) on the inner wall expressed the hydrophilic and hydrophobic nature of the inner wall against the outer phase, respectively; as well as contact angles of 30° and 150° of the organic solvent (organic solvent-rich outer phase) on the inner wall expressed the hydrophobic and hydrophilic nature of the inner wall against the outer phase, respectively. The linear velocity was 3.7 mm s^{-1} , the outlet pressure was atmospheric pressure ($1.0 \times 10^5 \text{ Pa}$), the total mesh number was 807,500 (radial size length, 1.1 μm ; axial size length, 20 μm), and the capillary was filled with the carrier solution in advance.

Results and discussion

Under specific microflow conditions of the ternary carrier solvents of a water-hydrophilic/hydrophobic organic solvent, an organic solvent-rich major inner phase and a water-rich minor outer phase were generated by the TRDP in an organic solvent-rich carrier solution. In contrast, with a water-rich carrier solution, a water-rich major inner phase and an organic solvent-rich minor outer phase were generated, regardless of the inner wall material in a microspace. However, specific homogeneous solutions which of the compositions of the ternary solvents are positioned near to the homogeneous-heterogeneous boundary in the phase diagram are required for the TRDP. It is possible that pressure changes imposed on the solution in a microspace under laminar flow conditions might alter the carrier solution from a homogeneous one in a batch vessel to a heterogeneous one in a microspace.

In our previous paper [9], microchannel fluorescence photographs for the organic solvent-rich solution (water-acetonitrile-ethyl acetate; 3:8:4 volume ratio) containing perylene (0.1 mM) and Eosin Y (1 mM) and the water-rich solution (80:20:9 volume ratio) containing perylene (0.1 mM) and Eosin Y (0.1 mM) were examined with a fluorescence microscope-CCD camera (Figs. 1(a) and 1(b), respectively). A phase diagram of the ternary mixed solvents is also shown in Fig. 2, and the component ratios of the above-mentioned solutions are plotted in the diagram. For an organic solvent-rich solution, hydrophobic perylene was distributed around the middle of the microspace in the microchannel, and the relatively hydrophilic Eosin Y was distributed near the inner wall (Fig. 2(a)). In the water-rich solution, Eosin Y was distributed around the middle of the channel and perylene was distributed near the inner wall (Fig. 2(b)).

We considered why major solvents are distributed around the middle of the tube, whereas minor solvents are distributed close to the inner wall, irrespective of whether the carrier solutions are organic solvent-rich or water-rich [9]. The linear velocity in the radial face section of the capillary tube (circle curves) under laminar flow conditions indicates that the inside area of a tube has a lower velocity-change gradient than the outside area. The real velocity curve in an aqueous-organic solvent mixed solution may deviate from an ideal velocity curve. Considerations of fluidic stability based on the

linear velocity gradients in the radial profile under laminar flow conditions imply that the major solvents must occupy the inside area instead of the outside area in the capillary tube (Fig. 3).

Here, we tentatively tried to propose another view of the inner and outer phase formation in the TRDP, based on the above and below experimental data. A specific homogeneous solution, whose component ratio was near the boundary between homogeneous and heterogeneous in the phase diagram, was pressurized greater than atmospheric pressure with nitrogen gas in a batch vessel where it was under the control of gravity. In an organic solvent-rich solution (e.g., water-acetonitrile-ethyl-acetate mixture; 3:8:4 volume ratio), the homogeneous solution first became an emulsion or nontransparent solution that included minor solvent or water-rich tiny droplets and then changes to a heterogeneous solution that included an upper major organic solvent-rich solution and a lower minor water-rich solution under the control of gravity. In a similar way, in a water-rich solution (e.g., water-acetonitrile-ethyl-acetate mixture; 80:20:9 volume ratio), the homogeneous solution first became an emulsion solution that included minor solvent or organic solvent-rich tiny droplets, and then changed to a heterogeneous solution that included an upper minor organic solvent-rich solution and a lower major water-rich solution (Fig. 4).

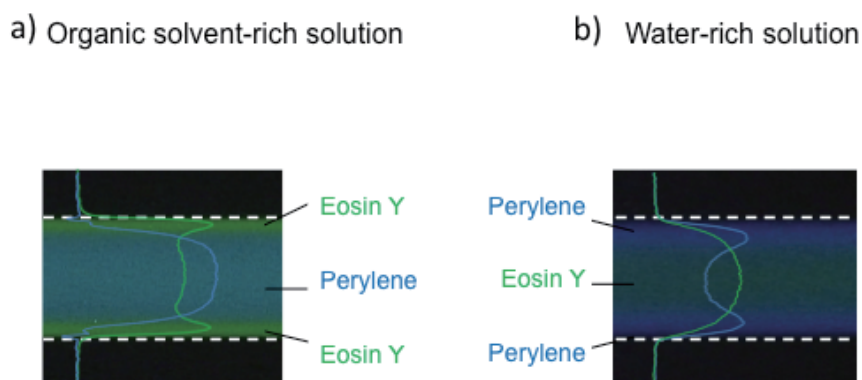
The phase formation of the ternary mixed solvents in a capillary tube under pressure due to laminar flow is estimated as follows, where it is not under the control of gravity. A specific homogeneous solution with a component ratio near the boundary between homogeneous and heterogeneous in the phase diagram is delivered under laminar flow conditions that produce a constant pressure to the radial face. In an organic solvent-rich solution, the homogeneous solution first becomes an emulsion solution that includes minor solvent or water-rich tiny droplets. The water-rich tiny droplets start to aggregate near the inner wall where the linear velocity is lowest under laminar flow conditions. Consequently, the ternary mixed solvent solution in a tube changes to a heterogeneous solution that includes a major inner organic solvent-rich solution and a minor outer water-rich solution, where it is not under the control of gravity. Similarly, in a water-rich solution, the homogeneous solution becomes an emulsion solution that includes minor solvent or organic solvent-rich tiny droplets. The organic solvent-rich tiny droplets start to aggregate near the inner wall where the velocity is lowest under laminar flow conditions. The ternary mixed solvent solution in a tube changes to a heterogeneous solution that includes a major inner water-rich solution and a minor outer organic solvent-rich solution where it is not under the control of gravity (Fig. 5).

In order to better understand the tube radial distribution of the solvents in a capillary tube, the formation of inner and outer phases in a capillary tube was simulated with a mixture of the two-component solvents, a water and ethyl acetate mixture, which were not homogeneously mixed. As the volume of fluid method (VOF) (Fluent program) functions for multi-phase flow model and actual fluid in the capillary tube generates the two phases, the above mixture of the two-component solvents was adopted as a model in this simulation. Phase-formation images in the organic solvent-rich and water-rich

carrier solutions were obtained with the simulation program under the conditions described in the Experimental section. They are shown in Figs. 6 and 7, respectively. These images are generated at 0.25, 0.50, 1.00, 2.00, and 3.00 s from the start of the flow. The blue color is composed of 100% volume ratio water per a mesh and the red color is 100% volume ratio ethyl acetate per a mesh. The volume ratios between 100% water (blue) and 100% ethyl acetate (red) per a mesh are expressed with 18 color gradients from blue to red. The color gradient bars are also shown in Figs. 6 and 7.

As shown in Fig. 6, with the organic solvent-rich carrier solution, a minor water-rich thin layer (blue) is first generated very close to the inner wall, following which the aqueous–organic mixed solvents become a heterogeneous solution that includes minor water-rich outer (blue) and major organic solvent-rich inner (from red to yellow green) phases. Such distributions are observed in the simulation images, regardless of whether the inner-wall characteristics were hydrophilic (contact angle 30°) or hydrophobic (contact angle 150°). With the water-rich carrier solution (Fig. 7), regardless of whether the inner wall is hydrophilic or hydrophobic, a minor organic solvent-rich thin layer (red) is first generated near the inner wall, following which the aqueous–organic mixed solvents become a heterogeneous solution that includes minor organic solvent-rich outer (red) and major water-rich inner (from blue to yellow) phases. The simulation images for phase formation in a capillary tube are consistent with the phase formation observed experimentally through the TRDP. From experimental data reported in our previous papers, the TRDP must be constructed under rather complicated conditions, including the composition ratios of solvents, flow rates, the inner diameter of the tubes, and pressure. The results obtained here imply that the computer simulation is useful for our investigation of the TRDP, such as setting the conditions and designing the microfluidic device.

In conclusion, the phase formation in the TRDP was explained in one point of view based on the experimental data as follows. The ternary mixed homogeneous solution in a microflow first becomes an emulsion solution that includes minor tiny solvent droplets. The tiny droplets then start to aggregate near the inner wall where the linear velocity is lowest under laminar flow conditions, leading to a heterogeneous solution that includes a phase interface in a microflow. Also, the results of our computer simulation were consistent with the concept of TRDP, i.e., inner and outer phase formations in microspaces.



(a microchannel (100 μm wide \times 40 μm deep) in a microchip made of quartz)

Figure 1. Fluorescence photographs of a) organic solvent-rich and b) water-rich solutions in the microchannel. Conditions: Carrier, a) perylene (0.1 mM) and Eosin Y (1.0 mM) dissolved in water-acetonitrile-ethyl acetate mixture (3:8:4 volume ratio) and b) perylene (0.1 mM) and Eosin Y (0.1 mM) dissolved in water-acetonitrile-ethyl acetate mixture (80:20:9 volume ratio) and flow rate, 1.0 $\mu\text{L min}^{-1}$.

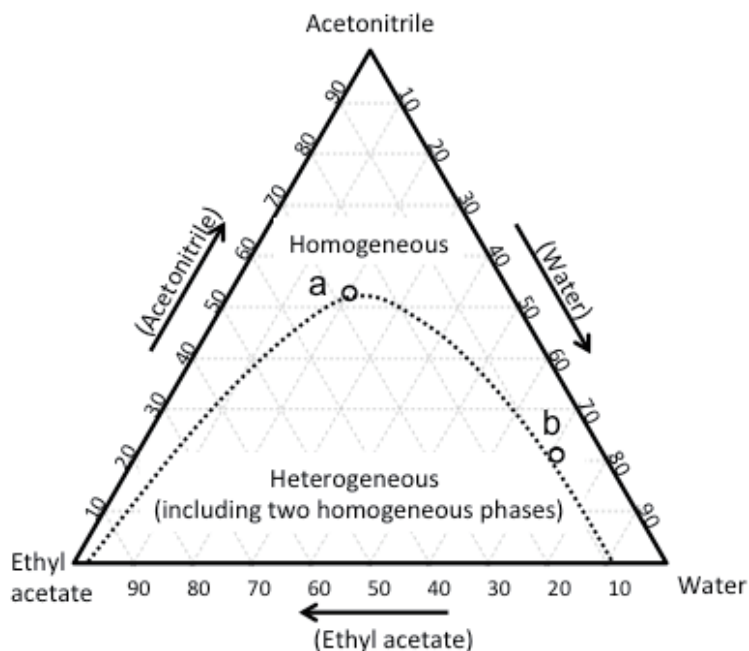


Figure 2. Phase diagram for a water-acetonitrile-ethyl acetate mixture and the component ratios of the solvents. Water-acetonitrile-ethyl acetate volume ratio (a) 3:8:4 and (b) 80:20:9. The homogeneous-heterogeneous solution boundary curve is represented by the dotted curve.

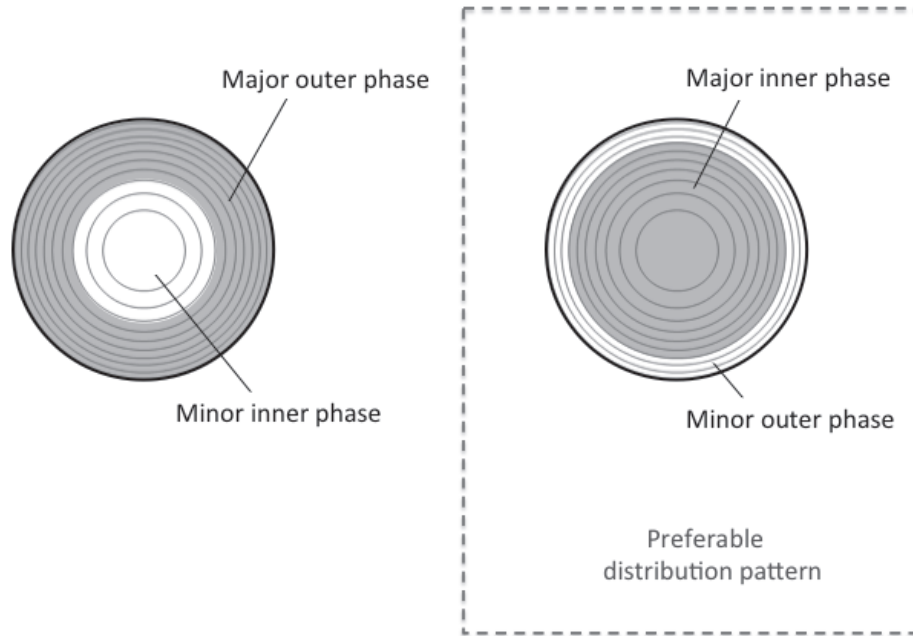


Figure 3. Schematic depictions of the possible distribution patterns of major and minor phases in a capillary tube.⁹

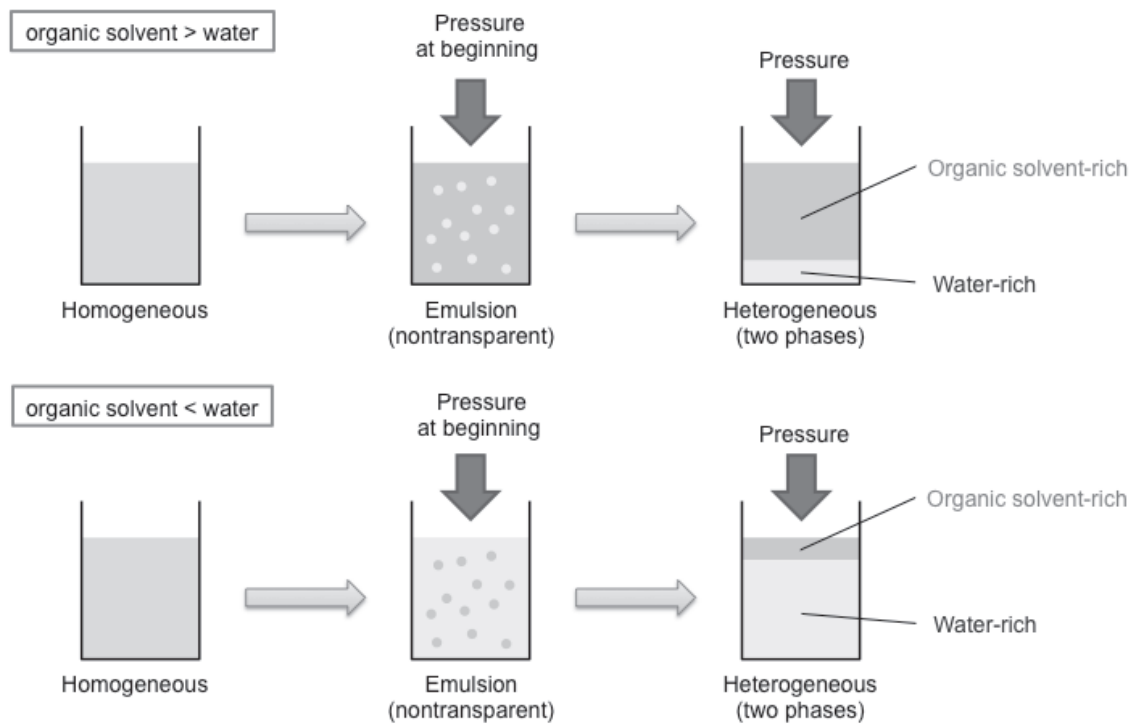


Figure 4. Illustration of phase formation in ternary mixed solvents in a batch vessel under pressure with nitrogen gas where it is under the control of gravity.

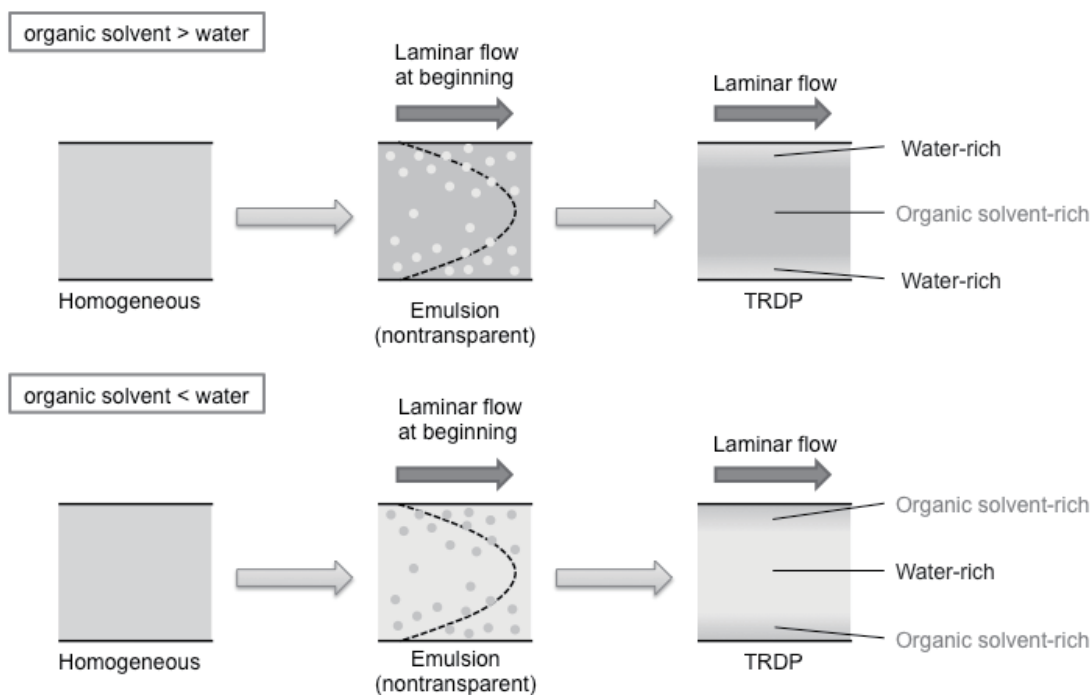


Figure 5. Illustration of phase formation of ternary mixed solvents in a capillary tube under pressure due to laminar flow where it is not under the control of gravity.

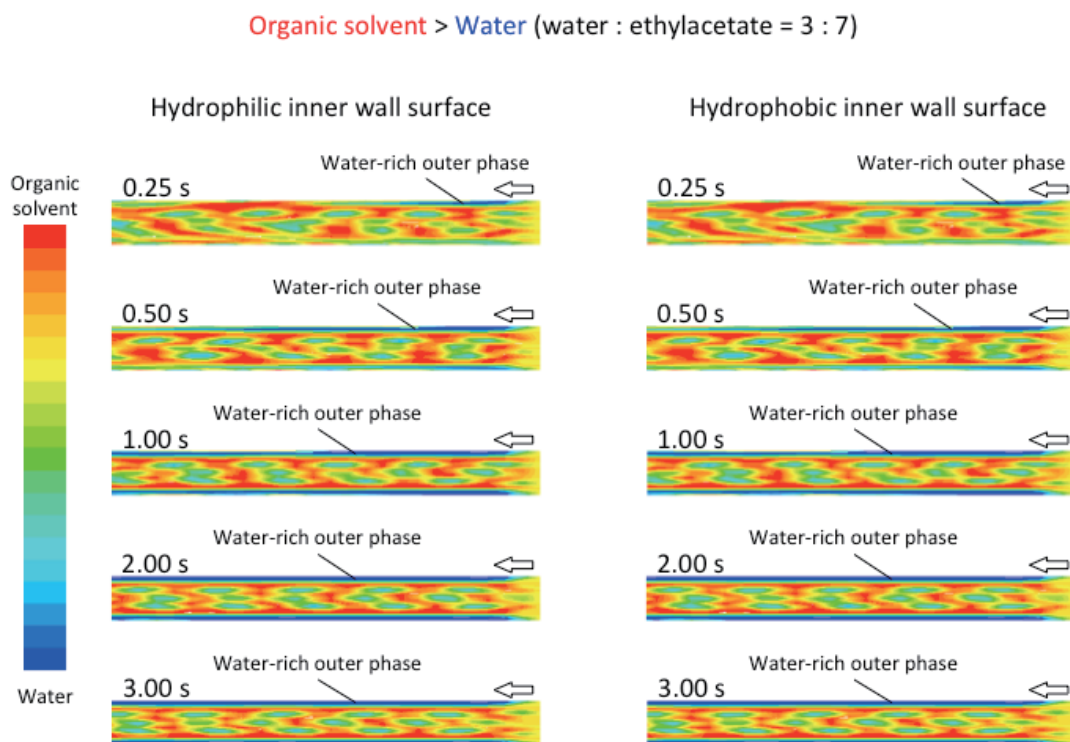


Figure 6. Phase formation in capillary tubes obtained by a computer simulation. Organic solvent-rich carrier solution.

Organic solvent < Water (water : ethyl acetate = 7 : 3)

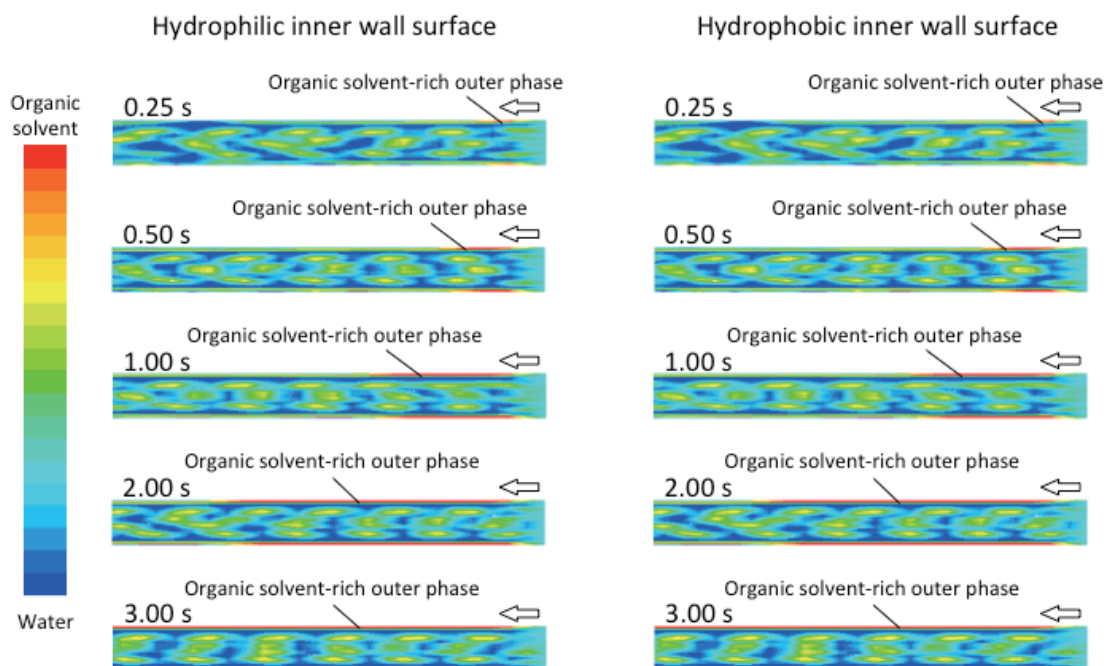


Figure 7. Phase formation in capillary tubes obtained by a computer simulation. Water-rich carrier solution.

References

- [1] R. Aris, Proc. R. Soc. London, Ser. A, **1959**, 252, 538.
- [2] K. Hibi, D. Ishii, I. Fujishima, T. Takeuchi, T. Nakanishi, *J. High Resolut. Chromatogr., Chromatogr. Commun.*, **1978**, 1, 21.

Chapter 10 Development of tube radial distribution extraction (TRDE)

A TRDP-based extraction in a microspace, referred to as tube radial distribution extraction (TRDE), has been performed as one of the applications of TRDP. The TRDE was developed using a microchip having a triple-branched microchannel and using a device having double tubes of different inner diameters. The part of this chapter is constructed rewritten based on related, published manuscripts.^{16,32,50)}

10.1 TRDE using a microchip that has triple-branched microchannels

Microfluidic behavior of ternary mixed carrier solvents of water–acetonitrile–ethyl acetate (2:3:1 volume ratio) was examined by use of a microchip incorporating microchannels in which one wide channel was separated into three narrow channels, i.e., triple-branched microchannels. When the ternary carrier solution containing the fluorescent dyes, hydrophobic perylene (blue) and relatively hydrophilic Eosin Y (green), was fed into the wide channel under laminar flow conditions, the carrier solvent molecules or fluorescence dyes were radially distributed in the channel, forming inner (organic solvent-rich major; blue) and outer (water-rich minor; green) phases in the wide channel. And then, in the narrow channels, perylene molecules mostly appeared to flow through the center narrow channel and Eosin Y, which is distributed in the outer phases in the wide channel, flowed through the both side narrow channels. A metal ion, Cu(II) as a model, dissolved in the ternary mixed carrier solution was also examined. The Cu(II) showed fluidic behavior, transferring from the homogeneous carrier solution to the water-rich solution in the side narrow channels through the triple-branched microchannels.

Introduction

The development of micro total analysis systems that include a microchip or microfluidic device technology is an interesting aspect of analytical chemistry [1,2]. Microfluidics exhibit various types of fluidic behavior in solvents in a microchannel. The microfluidic behavior has been examined by varying the channel configuration and flow rate of the solvents, by using aqueous–organic solvent mixtures, and by introducing specific obstacles into the microchannel [3-5]. The fluidic behavior of the solvents in the microchannel is related to the mixing, separation, diffusion, and reaction of the solutes. Information regarding the flow pattern of the solvents is important and useful to design microreactors or micro total analysis systems [6,7].

We reported that when ternary mixed solvents of water–hydrophilic/hydrophobic organic solvents are fed into a microspace, such as microchannels in a microchip or capillary tubes, the solvent molecules are radially distributed under laminar flow

conditions. This is called the tube radial distribution phenomenon (TRDP). In TRDP, in an organic solvent-rich carrier solution, the organic solvent-rich major phase is formed around the center of the microspace as an inner phase, while the water-rich minor phase is formed near the inner wall as an outer phase. On the other hand, in the water-rich carrier solution, the water-rich major phase is formed as an inner phase and the organic solvent-rich minor phase as an outer phase. TRDP forms a specific liquid–liquid interface, which is not static but kinetic, in a microspace.

Until now, TRDP has been investigated by the use of mainly capillary tubes and straight single line microchannels. The triple-branched microchannels in which one wide channel was separated into three narrow channels in a microchip was designed and manufactured in our study to conform TRDP, where the ternary mixed carrier solution was fed from the three narrow channels to the one wide channels.¹⁴⁾ Here microfluidic behavior of the ternary mixed carrier solution in the triple-branched microchannels was examined with the reverse flow direction against the previous paper,¹⁴⁾ i. e., the flow direction from the one wide channel to the three narrow channels. By these experiments, we could observe unique fluidic behavior of the solvents and solutes in the microchannels based on TRDP. The preliminary results were reported in a communication previously.¹⁶⁾

Experimental

Materials Figure 1 illustrates the setup of the microchip in the microchip holder (Fig. 1 a)) and the enlarged view of the microchip incorporating the triple-branched microchannels (Fig. 1 b)). As shown in Fig. 1 b), one wide channel (300 μm wide \times 40 μm deep) denoted as channel W was separated into three narrow channels (each 100 μm wide \times 40 μm deep) designated as channels N1–N3.

Fluorescence microscope equipped with a CCD camera system A microchip incorporating the microchannels was set up for the fluorescence microscope–CCD camera system. Fluorescence in the microchannel was monitored using a fluorescence microscope equipped with an Hg lamp, a filter, and a CCD camera. The ternary mixed solvents of the water–acetonitrile–ethyl acetate mixture (3:8:4 volume ratio) contained 0.1 mM perylene and 1 mM Eosin Y. The carrier solution was fed into the microchannels using a microsyringe pump.

Cu(II) analysis The homogenous carrier solution of the water–acetonitrile–ethyl acetate mixture (2:3:1 volume ratio) including 2.0 mM Cu(II) was fed into channel W at a definite flow rate. 100 μL of the solution in channels N1–N3 was collected through polytetrafluoroethylene (PTFE) tubes into the corresponding vessel. The solution was dried under a vacuum, and 0.5 M ammonia solution (100 μL) was added to the residue for flow absorption measurement at 600 nm (modified SPD-6AV spectrophotometric detector, Shimadzu Co., Kyoto, Japan).

Results and discussion

Fundamental experiments for TRDP in a microchannel Microchips with single-branched microchannels having widths of 100, 200, 300, and 400 μm and identical channel depths of 40 μm were also manufactured. The influences of channel width on TRDP in the microchannels were examined with fluorescent dyes, perylene and Eosin Y, dissolved in an organic solvent-rich carrier solution (water–acetonitrile–ethyl acetate; 3:8:4 volume ratio). The fluorescence images of the dyes in the solution fed into the microchannels were observed with the fluorescence microscope–CCD camera system (Fig. 2). The flow rates in all microchannels (100–400 μm width) were adjusted to achieve the same average linear velocity of 25 cm min^{-1} . It is evident from Fig. 2 that TRDP was observed in all microchannels regardless of the channel width. Hydrophobic perylene molecule (blue) was distributed around the center of the channel away from the side inner walls of the channel, while relatively hydrophilic Eosin Y molecule (green) was distributed near the side inner walls of the channel. That is, the major inner phase (organic solvent-rich phase) and the minor outer phase (water-rich phase) were formed in the microchannels of 100–400 μm width.

Effects of flow rates on TRDP in triple-branched microchannels The effects of flow rate on TRDP in the triple-branched microchannels was examined with an organic solvent-rich carrier solution (water–acetonitrile–ethyl acetate, 3:8:4 volume ratio) containing Orange G by using the bright-field microscope–CCD camera system. The Orange G-containing carrier solution was fed at the flow rates of 2.0–50.0 $\mu\text{L min}^{-1}$. The images are shown in Fig. 3. The hydrophilic Orange G molecule was distributed near the channel side inner walls, and the interface between the water-rich outer phase and the organic solvent-rich inner phase was distinguished because of the color of Orange G (Fig. 3). The TRDP was observed for the first time with a bright-field microscope–CCD camera system in our TRDP investigation. The system was confirmed to be useful for TRDP observation in a similar way to the fluorescence system. At the low flow rates of 2.0 and 5.0 $\mu\text{L min}^{-1}$, the liquid–liquid interface was unstable, considerably changed, or appeared to instantaneously disappear, however, stability was observed at the flow rates higher than 5 $\mu\text{L min}^{-1}$. Thus, flow rates higher than 5 $\mu\text{L min}^{-1}$ created a stable liquid–liquid interface in the triple-branched microchannels under the present conditions.

Fluorescence images of the dyes based on TRDP in triple-branched microchannels

The microchip incorporating triple-branched microchannels was shown in Fig. 1 b) with their respective measurements. The organic solvent-rich carrier solution (water–acetonitrile–ethyl acetate, 3:8:4 volume ratio) containing Eosin Y and perylene was fed into channel W of the microchip at the flow rate of 6.3 $\mu\text{L min}^{-1}$. The mixture carrier solution excluding ethyl acetate (water–acetonitrile, 1:4 volume ratio) but containing the dyes was also fed into the channel as a reference. Fig. 4 shows the

fluorescence images of the dyes in the triple-branched microchannels of the microchip. Figs. 4 a) and b) were obtained with the water–acetonitrile mixture as a reference and the water–acetonitrile–ethyl acetate mixture as ternary mixed solvents, respectively. The distribution behavior of the dyes, i.e., TRDP, was not observed in the image of Fig. 4 a) with the water–acetonitrile mixture. Conversely, the image of Fig. 4 b) with the ternary solvent mixture shows TRDP, in which the hydrophobic perylene molecule (blue) was distributed around the center of channel W away from the channel side inner walls, while relatively hydrophilic Eosin Y molecule (green) was distributed near the channel side inner walls. The distribution phenomena of the ternary mixed carrier solvents fed into the microchannels was evident in the wide channel. And then, perylene molecules mostly appeared to flow through the center channel (channel N2) and Eosin Y, which is distributed in the outer phases in channel W, flowed through channels N1 and N3, as shown in Fig. 4 b).

Distribution of Eosin Y based on TRDP in triple-branched microchannels The homogenous carrier solution of the water–acetonitrile–ethyl acetate mixture (3:8:4 volume ratio) including 0.5 mM Eosin Y was fed into channel W at a flow rate of $10 \mu\text{L min}^{-1}$. 100 μL of the solution in channels N1–N3 was collected through PTFE tubes into the corresponding vessel. The solution was subjected to flow absorption measurement at 517 nm. Eosin Y concentrations in the center channel (channel N2) and the two side channels (channels N1 and N3) were 0.36, 0.59, and 0.58 mM, respectively (Fig. 4). The concentrations were averages for five measurements. The experimental data indicated that relatively hydrophilic Eosin Y was distributed from the homogeneous carrier solution to the water-rich solution in the side narrow channels rather than the organic solvent-rich solution in the central narrow channel. The distribution of the fluorescent dyes in the triple-branched microchannels might suggest the possibility of extraction or separation for some solutes by utilizing the phase interface formed by TRDP in these channels.

Distribution of Cu(II) based on TRDP in triple-branched microchannels Distribution of Cu(II) was examined in the triple-branched microchannels by utilizing the kinetic liquid–liquid or aqueous–organic interface formed by TRDP. First, the calibration curve of Cu(II) was examined in a manner similar to that described in the experimental section. Cu(II) was determined over the concentration range of 0.5–10 mM with good linearity ($R^2 = 0.999$). The homogenous carrier solution of the water–acetonitrile–ethyl acetate mixture (2:3:1 volume ratio) including 2.0 mM Cu(II) was fed into channel W at the flow rate of $40 \mu\text{L min}^{-1}$. 100 μL of the solution in channels N1–N3 was collected with PTFE tubes into the corresponding vessel. Cu(II) concentrations in the center wide channel (channel N2) and the two side channels (channels N1 and N3) were 0.8, 2.5, and 2.7 mM, respectively (Fig. 6 a)). The concentrations were averages for five measurements. As a reference, Cu(II) concentrations were examined with the water–acetonitrile (2:3 volume ratio) carrier solution in a similar manner. Cu(II)

concentrations in channels N1–N3 were 2.1, 2.1, and 2.0 mM, respectively (Fig. 6 b)). The experimental data indicated that Cu(II) was extracted to the water-rich solution in the side narrow channels from the homogeneous solution by the formation of a phase interface in the microchannel; we refer to this process as tube radial distribution extraction (TRDE). Moreover, we examined the Cu(II) distribution by TRDE at other flow rates of 32 and 63 $\mu\text{L min}^{-1}$ in channel W. At 32 $\mu\text{L min}^{-1}$, Cu(II) concentrations in the center channel (channel N2) and the two side channels (channels N1 and N3) were 0.8, 3.0, and 2.9 mM, whereas, at 63 $\mu\text{L min}^{-1}$, those were 1.1, 2.9, and 2.7 mM, respectively. Comparing with the Cu(II) concentration, 2.0 mM, in the homogeneous carrier solution, the Cu(II) concentration in the solution collected from the center channel (channel N2) decreased, while that from the two side channels (channels N1 and N3) increased at every flow rates. The obtained data showed that TRDE occurred in the triple-branched microchannels of the microchip.

In conclusion, TRDP has been investigated by the use of mainly capillary tubes and straight single line microchannels. The TRDP of the ternary mixed carrier solution in the triple-branched microchannels was observed with a fluorescence microscope-CDD camera system. Consequently, perylene molecules mostly appeared to flow through the center narrow channel and Eosin Y flowed through channels in the side narrow channels. The TRDP was also observed through bright-light microscope-CCD camera system. We tried to apply the phase interface formed by TRDP, i.e., inner and outer phases, to the distribution or extraction procedure of Cu(II) in the triple-branched microchannels. This process will be helpful for investigating separation and extraction in a microfluidic device.

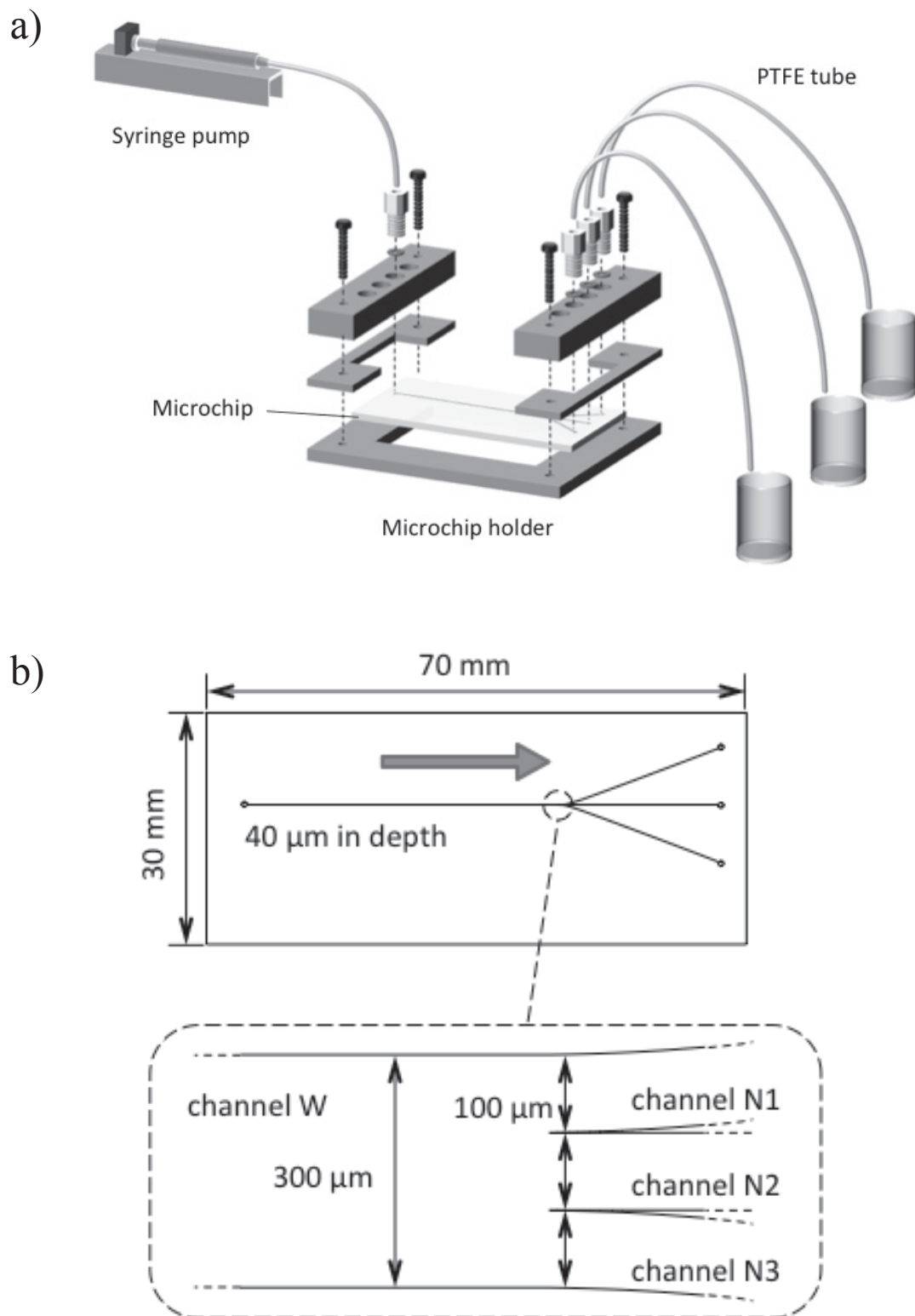


Figure 1. Schematic representation of a) setup of the microchip in the microchip holder and b) the enlarged view of the microchip incorporating triple-branched microchannels.

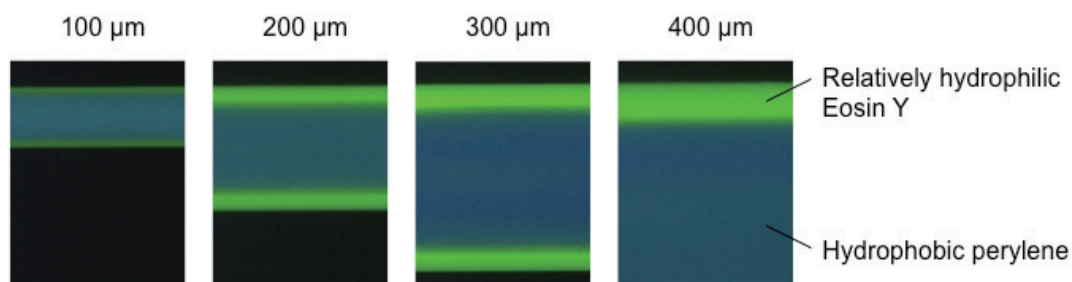


Figure 2. Fluorescence images of fluorescent dyes dissolved in a ternary mixed carrier solvent in microchannels with channel widths of 100, 200, 300, and 400 μm and identical channel depth of 40 μm . Conditions: Carrier, water–acetonitrile–ethyl acetate (3:8:4 v/v/v) mixture including 0.1 mM perylene and 1 mM Eosin Y; and flow rates, 1, 2, 3, and 4 $\mu\text{L min}^{-1}$ for microchannel widths of 100, 200, 300, and 400 μm , respectively.

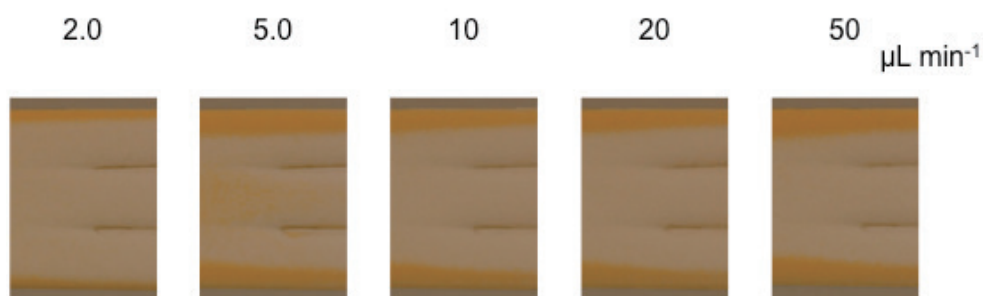


Figure 3. Effects of flow rates of the carrier solution on TRDP. Conditions: Carrier, water–acetonitrile–ethyl acetate (3:8:4 v/v/v) mixture containing 2 mM Orange G and flow rate, 2.0–50 $\mu\text{L min}^{-1}$ for channel W.

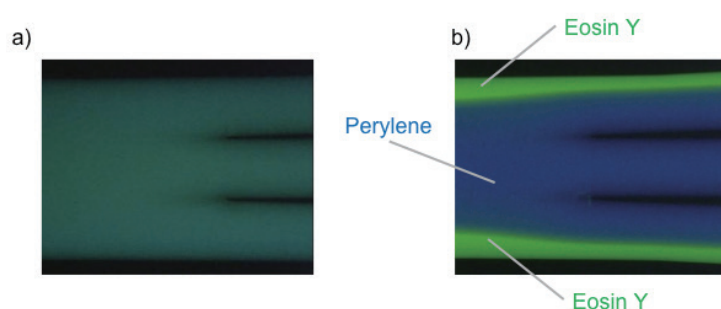


Figure 4. Fluorescence images of fluorescent dyes dissolved in a mixed carrier solvent in triple-branched microchannels. a) Water–acetonitrile (1:4 v/v) and b) water–acetonitrile–ethyl acetate (3:8:4 v/v/v) mixtures. Conditions: Carrier, aqueous–organic mixtures including 0.1 mM perylene and 1 mM Eosin Y; and flow rate, 6.3 $\mu\text{L min}^{-1}$ for channel W.

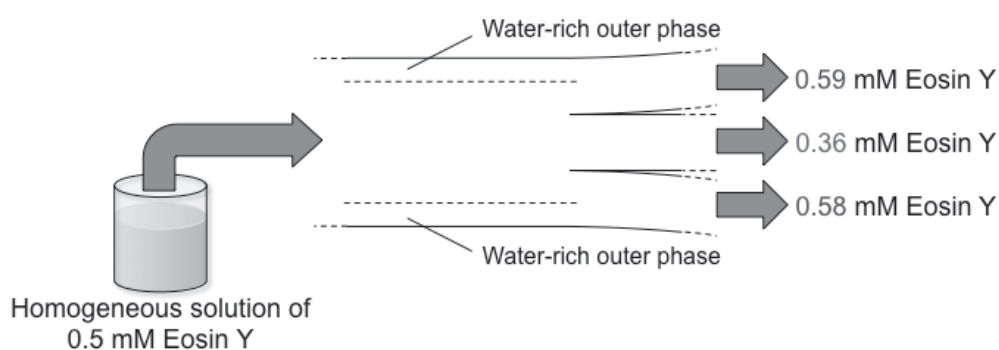


Figure 5. Distribution of Eosin Y from the homogeneous ternary mixed solution into the outer phases in the side narrow channels by TRDP. Conditions: Carrier, water–acetonitrile–ethyl acetate (3:8:4 v/v/v) mixture; flow rate, $10 \mu\text{L min}^{-1}$ for channel W; Eosin Y concentration in the homogeneous solution, 0.50 mM.

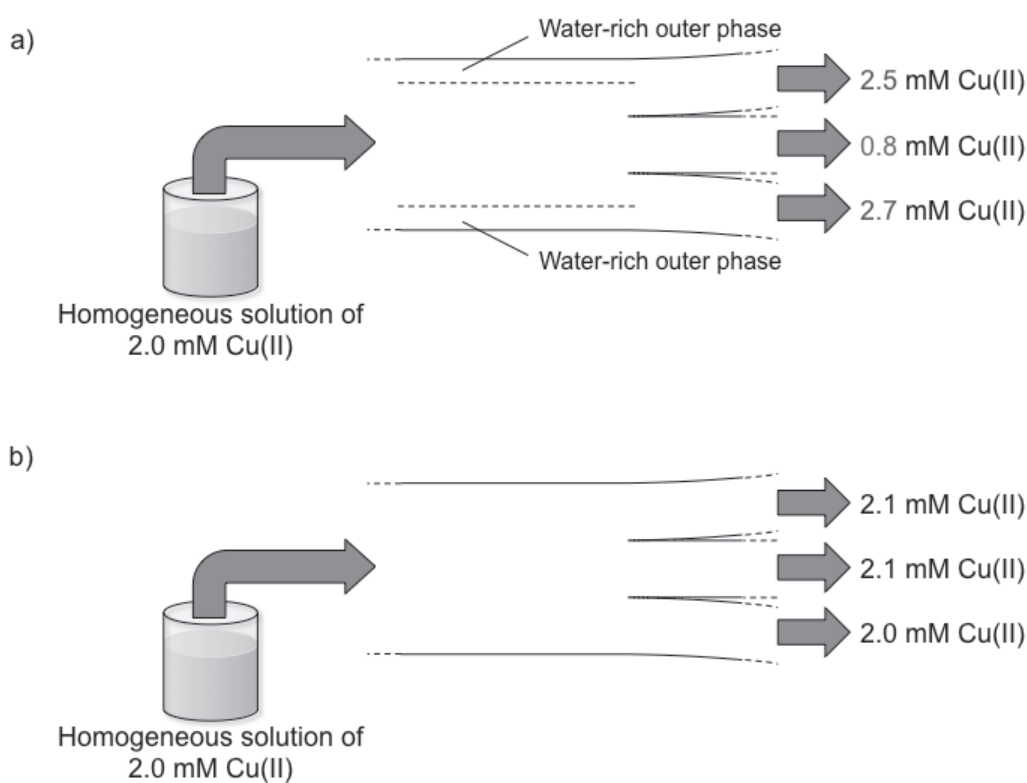


Figure 6. Distribution of Cu(II) in triple-branched microchannels. a) Water–acetonitrile–ethyl acetate (2:3:1 v/v/v) mixture and b) water–acetonitrile (2:3 v/v) mixture carrier solution. Conditions: Flow rate, $40 \mu\text{L min}^{-1}$ for channel W and Cu(II) concentration in the homogeneous solution, 2.0 mM.

10.2 TRDE using a device having double tubes of different inner diameters

A novel microflow-extraction system was proposed using double capillary tubes having different inner diameters in tube radial distribution phenomenon (TRDP). The tubes were fused-silica capillary tubes with 75 and 250 μm inner diameters; the smaller tube was inserted into the larger one through a T-type joint. A homogeneous aqueous solution containing 12 wt% Triton X-100 as a non-ionic surfactant and 2.4 M potassium chloride was fed into the larger tube at a flow rate of 20 $\mu\text{L min}^{-1}$, where the tube was maintained at a temperature of 34 $^{\circ}\text{C}$. The homogeneous aqueous solution changed to a heterogeneous solution with two phases in the tube; the surfactant-rich phase was generated in the middle of the tube as an inner phase, while the aqueous phase containing little of the surfactant was formed near the tube wall as an outer phase. In the TRDP Rhodamine B dissolved in the homogeneous solution was distributed into the inner surfactant-rich phase. The distributed Rhodamine B (red color) was observed with a bright-field microscope-CCD camera system. In the present microflow-extraction system, taking advantage of the TRDP, the inner phase containing Rhodamine B flowed inside the smaller tube, while the outer phase flowed outside the tip of the smaller tube into the larger tube, which was made using double tubes having inner diameters. This observation showed that Rhodamine B dissolved in the homogeneous solution was separated or extracted into the inner surfactant-rich phase through the double capillary tubes based on the specific microfluidic behavior of TRDP.

Introduction

The fluidic behavior of the solvents in the microspace is related to the mixing, separation, diffusion, and reaction of the solutes. Extraction is, generally, one of the most useful and effective separation methods; however, recently, microflow solvent extraction systems have been investigated by a liquid-liquid interface between an aqueous and organic solvent solution in a microspace [8-10]. The microflow solvent extraction has several advantages over conventional macroscale solvent extraction. For example, the microflow system has a larger surface/interface area per unit volume than that of the conventional macroscale system and the increase in the interface area provides enhancement of extraction efficiency [8].

We reported that when homogeneous solutions that feature a two-phase separation property, such as a water-acetonitrile-ethyl acetate mixed solvent solution and non-ionic surfactant aqueous solution, are fed into a microspace, such as microchannels in a microchip or capillary tubes, the solvent molecules are radially distributed in the microspace under laminar flow conditions. This is called the tube radial distribution phenomenon (TRDP). For example, in the TRDP with a non-ionic surfactant aqueous solution, through the two-phase separation property, the surfactant-rich phase is formed around the center of the microspace as an inner phase, while the aqueous, or almost surfactant-free, phase is formed near the inner wall as an outer phase.⁴⁴⁾ The TRDP

creates a specific liquid–liquid interface that is not static but kinetic in a microspace, providing an inner and outer phase.

Here, a novel microflow-extraction system was proposed using double capillary tubes having different inner diameters: smaller and larger ones.⁴⁵⁾ A homogeneous aqueous solution containing a non-ionic surfactant was fed into the larger tube, leading to the TRDP that created the inner surfactant-rich phase and the outer almost surfactant-free aqueous phase. At the tip of the smaller tube in the larger one, the inner phase flowed inside the smaller tube, while, the outer phase flowed outside the smaller tube. The specific flow showed the possibility that a certain substance dissolved in the homogeneous solution was extracted into the inner phase, or surfactant-rich phase, through the double capillary tubes, based on the TRDP.

Experimental

Fused-silica capillary tubes (75 μm inner diameter and 150 μm outer diameter; 250 μm inner diameter and 350 μm outer diameter) were used. A schematic diagram of the present microflow extraction system using double capillary tubes, having different inner diameters, is shown in Fig. 1. The smaller tube (75 μm i.d.) was inserted into the larger one (250 μm i.d., 120 cm length) through a T-type joint. A homogeneous aqueous solution containing 12 wt% Triton X-100 and 2.4 M KCl was fed into the larger tube at a flow rate of 20 $\mu\text{L min}^{-1}$, where the tube was maintained at a temperature of 34 $^{\circ}\text{C}$ with a thermo-heater (Thermo Plate MATS-555RO; Tokai Hit Co., Shizuoka, Japan). The homogeneous aqueous solution changed to a heterogeneous solution with two phases in the capillary tube. The radial distribution of the surfactant was observed through Rhodamine B dissolved in the homogeneous aqueous solution with a bright-field microscope-CCD camera system that was comprised of a microscope and a CCD camera.

Results and discussion

Two-phase separation in a batch vessel Homogeneous aqueous solutions of specific non-ionic surfactants separate into two distinct phases in a batch vessel when heated above a certain temperature (i.e., cloud point); a temperature-induced phase separation occurs. One phase behaves as a concentrated surfactant solution containing considerable amounts of water (surfactant-rich phase), whereas the other phase is an almost surfactant-free aqueous solution. The hydrogen bond between an oxygen atom of an ether bond in a non-ionic surfactant and water molecule leads to good solubility of the surfactant in water. However, a high temperature above the cloud point attempts to cut the hydrogen bond, leading to separation of surfactant-rich and aqueous phases. In addition, the cutting or dihydration increases in the presence of salts. Hydrophobic compounds dissolved in the homogeneous aqueous solution are extracted into the surfactant-rich phase, whereas hydrophilic compounds remain in the aqueous phase. Clouding points of an aqueous solution containing 2 wt% Triton X-100 as a non-ionic surfactant were examined through inspection with various concentrations of KCl, 0–3.0

M. The obtained data, or phase diagram, is shown in Fig. 2. The homogeneous and transparent solution at 25 °C changed through a clouding point into the heterogeneous solution including two phases: the upper surfactant-rich suspension phase and the aqueous lower phase. The clouding points gradually decreased from 65 °C to 30 °C with an increasing KCl concentration from 0 to 3.0 M as shown in Fig. 2. Also, clouding points of an aqueous solution containing 2.4 M KCl were examined with various concentrations of Triton X-100, 0–30 wt%. The homogeneous solution at 25 °C changed through a clouding point to the heterogeneous solution including two phases, the surfactant-rich phase and the aqueous phase, at 34 °C for all concentrations of Triton X-100 (data not shown).

TRDP observation Homogeneous aqueous solutions containing Triton X-100 (2, 12, 22, and 30 wt%) and 2.4 M KCl possessed a clouding point at 34 °C, as described above. The homogeneous solutions that included 5 mM Rhodamine B were fed into the capillary tube (250 μm i. d.) at a flow rate of 20 $\mu\text{L min}^{-1}$ under laminar flow conditions, where the tube was maintained at temperatures of 25 °C or 34 °C. The bright-field photographs of the aqueous solution were examined with the microscope-CCD camera system. Non-TRDP (homogeneous) was observed at 25 °C and TRDP was created at 34 °C for all aqueous solutions. Typical photographs obtained from the aqueous solution containing 12 wt% Triton X-100 and 2.4 M KCl are shown in Fig. 3. The homogeneous red solution as a result of Rhodamine B was observed at a temperature of 25 °C, which was under the clouding point. That is, the distribution of the surfactant in the tube did not occur at a temperature of 25 °C (non-TRDP). At a temperature of 34 °C, the solution phase containing the surfactant was generated in the middle of the tube as an inner phase (the surfactant-rich phase) and the solution phase containing little of the surfactant was formed near the inner wall as an outer phase (the aqueous phase). Rhodamine B dissolved into the solution was distributed in the surfactant-rich phase (red color). The homogeneous aqueous solution containing 12 wt% Triton X-100 and 2.4 M KCl with a clouding point of 34 °C clearly brought about phase transformation to the heterogeneous solution with the surfactant-rich phase and the aqueous phase through the tube, the temperature of which was controlled at 34 °C (TRDP).

Microflow extraction with TRDP The homogeneous aqueous solution containing 12 wt% Triton X-100, 2.4 M KCl, and 5 mM Rhodamine B was fed at a flow rate of 20 $\mu\text{L min}^{-1}$ into the larger capillary tube. The aqueous solution containing 12 wt% Triton X-100 was selected mainly because of the volume ratio of the two phases and because the viscosity of the solution could be easily delivered into the capillary tube. The photographs obtained at the tip of the smaller tube within the larger one at 25 °C and 34 °C are shown in Fig. 4. At 25 °C, the homogeneous red solution resulting from Rhodamine B was fed without any specific fluidic behavior. On the other hand, notable and specific fluidic behavior was observed on the tip of the smaller tube at 34 °C. The inner phase (red color) containing Rhodamine B flowed inside the smaller tube, while

the outer phase flowed outside the small tube, as shown in Fig. 4. This observation implies that Rhodamine B dissolved into the homogeneous solution was separated or extracted into the inner phase (surfactant-rich phase) through the double capillary tubes based on specific microfluidic behavior, TRDP.

In conclusion, a novel microflow extraction was demonstrated through double capillary tubes having different inner diameters, a smaller and larger tube, in the specific microfluidic behavior of TRDP. A homogeneous aqueous solution containing Triton X-100 as a non-ionic surfactant and KCl was fed into the larger tube, where the tube was maintained at the temperature of the clouding point. The homogeneous aqueous solution changed to a heterogeneous solution through two phases in the tube: the surfactant-rich inner phase and nearly surfactant-free outer phase (TRDP). Rhodamine B dissolved into the homogeneous solution was distributed into the surfactant-rich inner phase in the TRDP. Rhodamine B was extracted into the surfactant-rich phase through the double capillary tubes based on the specific microfluidic behavior of TRDP.

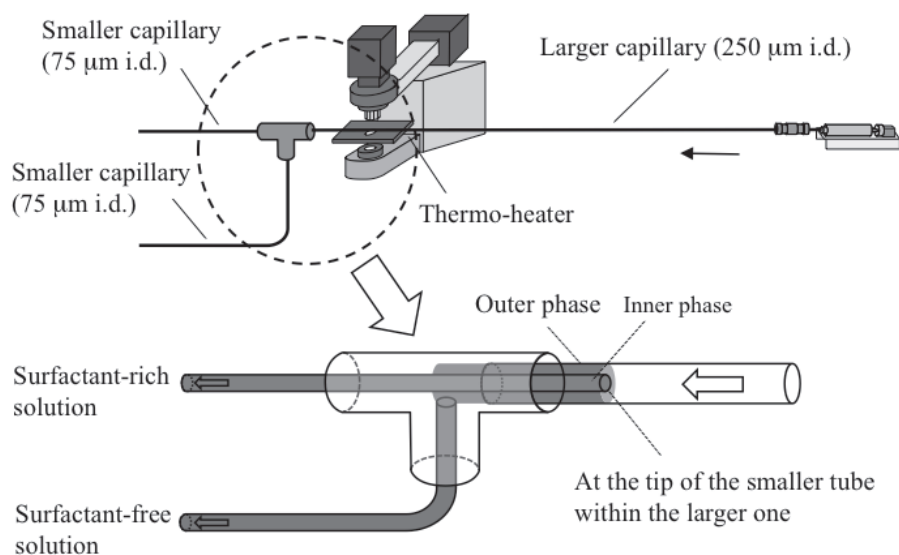


Figure 1. Schematic diagram of microflow extraction system using double capillary tubes having different inner diameters.

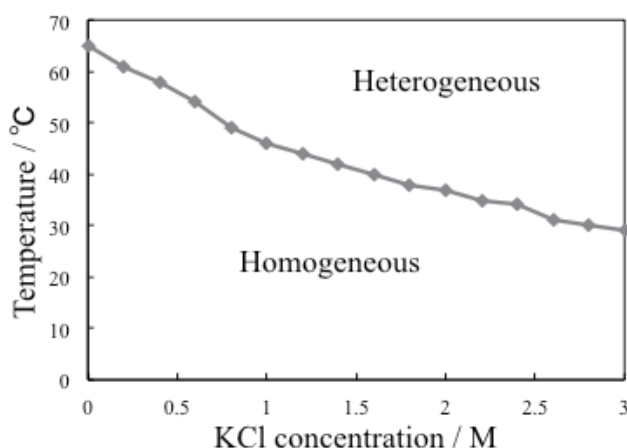


Figure 2. Phase diagram of aqueous solution containing Triton X-100 and KCl. 2 wt% Triton X-100 and various concentrations of KCl. The solubility curve between homogeneous and heterogeneous solutions is depicted with the clouding points.

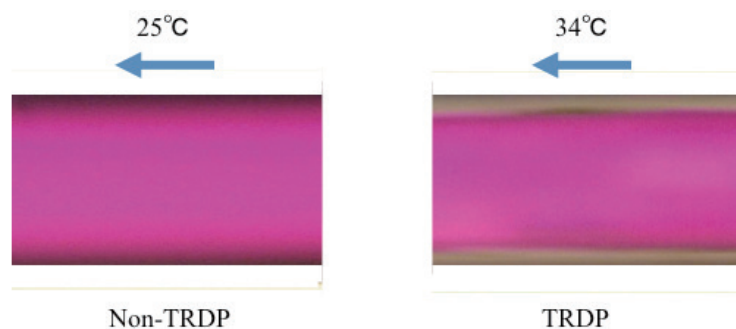


Figure 3. Bright-field photographs in the larger capillary tube (250 μm i.d.) at 25 $^{\circ}\text{C}$ and 34 $^{\circ}\text{C}$. The homogeneous aqueous solution containing 12 wt% Triton X-100, 2.4 M KCl, and 5 mM Rhodamine B was fed at a flow rate of 20 $\mu\text{L min}^{-1}$ into the larger capillary tube.

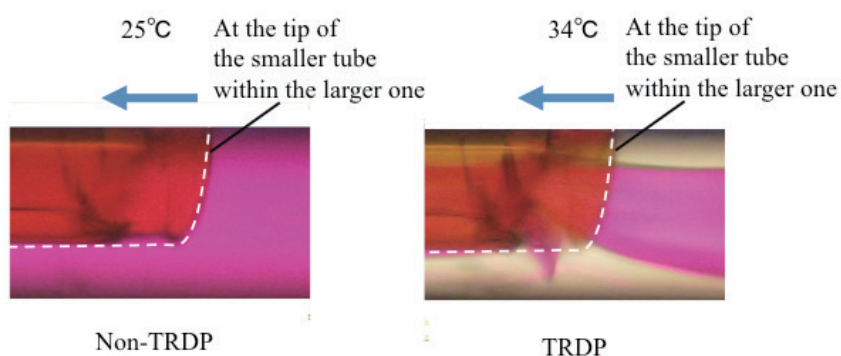


Figure 4. Bright-field photographs at the tip of the smaller capillary tube (75 μm i.d.) within the larger tube (250 μm i.d.) at 25 $^{\circ}\text{C}$ and 34 $^{\circ}\text{C}$. The homogeneous aqueous solution containing 12 wt% Triton X-100, 2.4 M KCl, and 5 mM Rhodamine B was fed at a flow rate of 20 $\mu\text{L min}^{-1}$ into the larger capillary tube.

References

- [1] K. Ueno, F. Kitagawa, and N. Kitamura, *Bull. Chem. Soc. Jpn.*, 2011, **77**, 1331.
- [2] D. R. Reyes, D. Iossifidis, P. A. Auroux, and A. Manz, *Anal. Chem.*, 2002, **74**, 2623.
- [3] Y. Kikutani, H. Hisamoto, M. Tokeshi, and T. Kitamori, *Lab. Chip*, 2004, **4**, 328.
- [4] A. Hibara, M. Tokeshi, K. Uchiyama, H. Hisamoto, and T. Kitamori, *Anal. Sci.*, 2001, **17**, 89.
- [5] N. Kaji, Y. Okamoto, M. Tokeshi, and Y. Baba, *Chem. Soc. Rev.*, 2010, **39**, 948.
- [6] H. Nakamura, Y. Yamaguchi, M. Miyazaki, H. Maeda, and M. Uehara, *Chem. Commun.*, 2002, **23**, 2844.
- [7] H. Kawazumi, A. Tashiro, K. Ogino, and H. Maeda, *Lab. Chip*, 2002, **2**, 8.
- [8] M. Maeki, Y. Hatanaka, K. Yamashita, M. Miyazaki, and K. Ohto, *Solent. Extr. Res. Dev., Jpn.*, 2014, **21**, 77.
- [9] Z. X. Cai, Q. Fang, H. W. Chen, and Z. I. Fang, *Anal. Chem. Acta*, 2006, **556**, 151.
- [10] A. Aota, M. Nonaka, A. Hibara, T. Kitamori, *Angew. Chem. Int. Ed*, 2007, **46**, 878.
- [11] K. Fujinaga, *Anal. Sci.*, 1993, **9**, 479.
- [12] T. Saitoh, H. Tani, T. Kamidate, H. Watanabe, *Trends Anal. Chem.*, 1995, **14**, 213.
- [13] P. I. Trindade, M. M. Diogo, D. M. F. Prazeres, C. J. Marcos, *J. Chromatogr. A*, 2005, **1082**, 176.

Chapter 11 Development of tube radial distribution mixing (TRDM)

A TRDP-based specific mixing of solvents in a microspace, referred to as tube radial distribution mixing (TRDM), has been developed as an application of TRDP. The TRDM was developed using a microchip on which three narrow channels were combined to form one wide channel. The part of this chapter is constructed and rewritten based on the related manuscript that has been published.²⁶⁾

11.1 TRDM using a microchip having three-to-one line microchannels

The mixing process of ternary solvents (water–hydrophilic/hydrophobic organic mixture) prepared in microchannels in a microchip was examined by fluorescence observation of the dyes dissolved in the solvents under laminar flow conditions. A microchip incorporating microchannels was used. In it, three narrow channels were combined to form one wide channel. Water–acetonitrile (hydrophilic) mixture containing relatively hydrophilic Eosin Y (green) was fed into the narrow center channel and an acetonitrile–ethyl acetate (hydrophobic) mixture containing hydrophobic perylene (blue) was fed into the two narrow side channels in the microchip. The mixtures in the narrow channels combined in the wide channel to prepare the ternary solvents of water–acetonitrile–ethyl acetate, causing the tube radial distribution of the solvents. We observed the mixing process of the ternary solvents in the wide channel through fluorescence of the green and blue dyes, including an aqueous–organic interface. For example, the green dye that was fed into the center channel was distributed near the inner side walls and the blue dye that was fed into the two side channels was distributed around the center area in the wide channel. Such specific mixing behavior was not observed for two-component solvents in the wide channel, such as water–acetonitrile mixture and water–ethyl acetate mixture.

Introduction

The development of micro total analysis systems that include a microchip or microfluidic device technology is an interesting aspect of analytical science [1,2]. Microfluidics exhibits various types of fluidic mixing processes of solvents in a microchannel. Solvent mixing has been examined by varying the channel configuration and flow rate of the solvents, by using aqueous–organic solvent mixtures, and by introducing specific obstacles into the microchannel [3-5]. Fluidic mixture of the solvents in the microchannel is related to the separation, diffusion, and reaction of the solutes. Information regarding the mixing process of the solvents is important and useful to design microreactors or micro total analysis systems [6,7].

Various types of aqueous-organic solvent mixture solutions are used in dissolution

[8,9], cleaning [10], preservation [11], and as reaction solvents [12,13]. Such mixtures are also useful in separation science [14-16]. However, to our knowledge, the use of ternary mixed solvents of water–hydrophilic/hydrophobic organic solvent mixture solutions has not been examined in detail. When ternary mixed solvents of water–hydrophilic/hydrophobic organic solvents were fed into a microspace, such as microchannels in a microchip or capillary tubes, under laminar flow conditions, the solvent molecules were radially distributed in a microspace regardless of the section shape and the inner wall material; we call it the “tube radial distribution phenomenon” (TRDP). To be concrete, with an organic solvent-rich solution, the organic solvent-rich major phase was generated around the center of the microspace as an inner phase, while the water-rich minor phase was formed near the inner wall as an outer phase. On the other hand, with a water-rich solution, water-rich major inner and organic solvent-rich minor outer phases were formed, respectively.

Here, fluidic mixing of the ternary solvents (water–acetonitrile–ethyl acetate mixture) was examined through fluorescence observation of the dyes in a microchannel. A microchip was designed with three narrow channels that combine to form one wide channel. The water–acetonitrile mixture and acetonitrile–ethyl acetate mixture solutions were fed into the narrow channels to prepare the ternary solvent solution of the water–acetonitrile–ethyl acetate mixture in the wide channel. The ternary solvents solutions caused specific fluidic mixing process of the solvents in the wide channel, based on the tube radial distribution of the ternary solvents, i.e., the TRDP.

Experimental

Figure 1 illustrates the design and setup of the microchip in the microchip holder used herein. The three narrow channels (each 100 μm wide \times 40 μm deep) denoted as channels N1 – N3 combine to form one wide channel (300 μm wide \times 40 μm deep), which is denoted as channel W in the microchip.

A microchip incorporating the microchannels was set up for the fluorescence microscope–CCD camera system. The water–acetonitrile mixture (3:2 volume ratio) containing 3.0 mM Eosin Y and acetonitrile–ethyl acetate mixture (3:2 volume ratio) containing 0.15 mM perylene were fed into channel N2 and channels N1 and N3, respectively, using microsyringe pumps. The fluorescence in the microchannel was monitored around the combining point and 3 cm from the combining point in channel W using a fluorescence microscope equipped with an Hg lamp, a filter, and a CCD camera.

Results and discussion

Mixing process of ternary solvents prepared in microchannels The water–acetonitrile mixture (3:2 volume ratio) containing 3.0 mM Eosin Y and the acetonitrile–ethyl acetate mixture (3:2 volume ratio) containing 0.15 mM perylene were fed into channel N2 and channels N1 and N3, respectively, to prepare the ternary solvents of water–acetonitrile–ethyl acetate in channel W. The mixture solutions were

fed into channels N1 – N3 at a flow rate of $2.0 \mu\text{L min}^{-1}$. The volume ratio of the water–acetonitrile–ethyl acetate mixed solution in channel W was 3:8:4 (the organic solvent-rich solution). Fig. 2 shows the fluorescence photographs of the solvents at the combining point and 3 cm from the combining point in channel W. The specific mixing process was observed clearly in the microchannel in Fig. 2, based on the TRDP with the organic solvent-rich solution. That is, the photographs indicate that the hydrophobic perylene (blue) fed from the side channels N1 and N3 was distributed around the center of channel W away from the side inner walls of the channel. On the other hand, hydrophilic Eosin Y (green) fed from the center channel N2 was distributed near the side inner walls. The TRDP of the water–acetonitrile–ethyl acetate mixture solution (the organic solvent-rich solution) occurred in the wide channel W by feeding the water–acetonitrile mixture and acetonitrile–ethyl acetate mixture solutions from the narrow channels.

Mixing process of ternary solvents prepared in microchannels through various mixing procedures The fluorescence photographs and profiles of the solvents were examined at a distance of 3 cm from the combining point in channel W through various mixing procedures (Fig. 3). The water–acetonitrile mixture (3:2 volume ratio) containing 3.0 mM Eosin Y and the acetonitrile–ethyl acetate mixture (3:2 volume ratio) containing 0.15 mM perylene were fed into channel N2 and channels N1 and N3, respectively. The mixture solutions were fed into channels N1 – N3 by varying mixing flow rates ranging from 2.0 to $50 \mu\text{L min}^{-1}$. The details of the combined flow rates are shown in Fig. 3. Lines a - f indicate flow rates of channel N2 (ranging from 2.0 to $50 \mu\text{L min}^{-1}$), and rows 1 – 6 indicate flow rates of channels N1 and N3 (ranging from 2.0 to $50 \mu\text{L min}^{-1}$). All of the fluorescence photographs in Fig. 3 were named using line letters and row numbers. For example, the fluorescence photograph positioned at Line a and Row 2, which was denoted “photograph a-2,” was obtained from water-acetonitrile mixture containing Eosin Y delivered in channel N2 at $2.0 \mu\text{L min}^{-1}$ and acetonitrile-ethyl acetate mixture containing perylene delivered in channels N1 and N3 at $5.0 \mu\text{L min}^{-1}$. It was confirmed that the fluorescence photographs in Fig. 3 did not change for at least 20 min. Specific microfluidic mixing process of the solvents was performed based on the TRDP in the microchannels. For example, photographs a-1, b-1, c-2, d-1, e-1, and f-1 show photographs of the mixture solutions fed into channels N1 and N3 at a flow rate of $2.0 \mu\text{L min}^{-1}$ and in channel N2 at flow rates ranging from 2.0 to $50 \mu\text{L min}^{-1}$. The volume ratios of the water–acetonitrile–ethyl acetate mixed solution in channel W were changed from 3:8:4 (the organic solvent-rich solution) to 56:41:3 (the water-rich solution). With the TRDP, the mixing process of the solvents changed from the patterns of the organic solvent-rich major inner phase (blue) and the water-rich minor outer phase (green) to the patterns of the water-rich major inner phase (green) and the organic solvent-rich minor outer phase (blue) via the transition mixing processes. However, from the phase diagram mentioned below, photographs f-1 could

not show the TRDP. As shown in photographs d-1, d-2, d-3, d-4, d-5, and d-6, the mixture solutions were fed into channels N2 at a flow rate of $10 \mu\text{L min}^{-1}$ and in channels N1 and N3 at flow rates ranging from 2.0 to $50 \mu\text{L min}^{-1}$. The volume ratios of the water–acetonitrile–ethyl acetate mixed solution in channel W were changed from 43:46:11 to 6.0:58:36 (the organic solvent-rich solution). With the TRDP, the mixing process changed from the transition mixing patterns to the patterns of the organic solvent-rich major inner phase (blue) and the water-rich minor outer phase (green). Various fluidic mixing processes of the solvents or fluorescent dyes were observed by varying flow rates and mixing ratios of the water–acetonitrile and the acetonitrile–ethyl acetate mixture solutions, based on the TRDP of the water–acetonitrile–ethyl acetate mixture in channel W. However, the ternary solvents in channel W did not always create the specific mixing process as described in the last section. The microfluidic mixing process of the solvents based on the TRDP is called “tube radial distribution mixing” (TRDM). The fluorescence photographs and profiles that had the same component ratios of the solvents (water–acetonitrile–ethyl acetate volume ratio are 10:57:33, 3:8:4, and 33:49:18) in Fig. 3 are rearranged with the residence times in channel W from the combining point (Fig. 4). The TRDM observed on the fluorescence photographs proceeded with increasing residence times or mixing times from the combining point.

Mixing process of two-component solvents in the microchannels The fluorescence photographs of the solvents that dissolved the dyes, hydrophobic perylene (blue) and relatively hydrophilic Eosin Y (green), were examined at a distance of 3 cm from the combining point in channel W by feeding two-component solvents, such as water–acetonitrile and water–ethyl acetate mixtures. The fluorescence photographs of the water–acetonitrile mixture in channel W were examined. Water containing 3.0 mM Eosin Y in channel N2 and acetonitrile containing 0.15 mM perylene in channels N1 and N3 were delivered at flow rates of $2.0 - 50 \mu\text{L min}^{-1}$, similar to those shown in Fig. 3. Eosin Y (green) flowed around the center of the channels and perylene (blue) flowed near both the side inner walls of the channels, according to the volume ratios of water and acetonitrile (Fig. 5). When hydrophobic perylene was deposited in channel W, i.e., in relatively water-rich solutions, the deposition disturbed a microfluidic flow in the channel. In these cases, fluorescence photographs are not presented in Fig. 5. The fluorescence photographs of the water–ethyl acetate mixture in channel W were also examined. Water containing 1.0 mM Eosin Y in channel N2 and ethyl acetate containing 0.1 mM perylene in channels N1 and N3 were delivered at flow rates ranging from 2.0 to $50 \mu\text{L min}^{-1}$, similar to those shown in Fig. 3. At relatively low flow rates, Eosin Y in water and perylene in ethyl acetate separated with vertical interfaces in channel W, while at high flow rates they separated with a horizontal interface (Fig. 6). No specific mixing process as observed with the ternary solvents solution in Figs. 2 and 3 were created using the two-component solvents, such as water–acetonitrile mixture or water–ethyl acetate mixture. The fluorescence photographs using the two-component

solvents were normal because of the nature of the solvents and dyes used: i.e., acetonitrile, hydrophilic; ethyl acetate; hydrophobic; Eosin Y, relatively hydrophilic; and perylene, hydrophobic.

Phase diagram for water–acetonitrile–ethyl acetate mixture solution and the component ratios required for TRDM caused by TRDP A phase diagram for the ternary mixture solvents of water–acetonitrile–ethyl acetate had been examined in a vessel at a temperature of 22 °C. The phase diagram is shown in Fig. 7. The dotted curve in the diagram indicates the boundary between the homogeneous and heterogeneous phases. The phase diagram showed that each component ratio of the solvents made either a homogeneous (one homogeneous phase) or a heterogeneous (two homogeneous phases) solution. As indicated in our previous paper, the TRDP was performed with specific homogeneous carrier solutions having the component ratios of the solvents positioned around the homogeneous-heterogeneous solution boundary curve in the phase diagram. Such carrier solutions caused the TRDP of the ternary solvents in a microflow through phase transformation from homogeneous to heterogeneous under pressure. The fluorescence photographs shown in Fig. 8 can be roughly classified into several typical mixing processes: three typical TRDM caused by the TRDP and two typical mixing patterns not based on the TRDP (Fig. 8). All the component ratios of the solvents in channel W in Fig. 3 are plotted in the phase diagram of Fig. 7, where open circles (○) and closed circles (●) indicate TRDM images and non-TRDM (or doubtful cases) images, respectively. The closed circle signals were far away from the dotted line of the homogeneous-heterogeneous solution boundary curve. The solutions of the component ratios of the solvents that were indicated by the closed circles did not show the TRDM at low flow rates of 0.1 – 1.0 $\mu\text{L min}^{-1}$ for channels N1 – N3, which provided long residence times or mixing times in channel W from the combining point. The plotted data in Fig. 7 were close to the previous data,^{15,17)} where the specific homogeneous carrier solutions having the component ratios of the solvents around the boundary in the phase diagram led to the TRDP.

In conclusion, the ternary solvents of water–acetonitrile–ethyl acetate mixture in the wide channel were prepared by combining the water–acetonitrile mixture and acetonitrile–ethyl acetate mixture through the narrow channels in the microchip. Some specific and interesting mixing processes of the solvents with the dissolved fluorescent dyes could be observed in the wide channel based on the TRDP of ternary solvents. This unique mixing process was denoted as “tube radial distribution mixing” (TRDM). The mixing process based on the TRDP was not observed using the two-component solvents, i.e., the water–acetonitrile mixture or the water–ethyl acetate mixture. The TRDM data visualized with the dyes are expected to be useful for developing a mixing technique to create a phase interface and a chemical reaction space in a microspace.

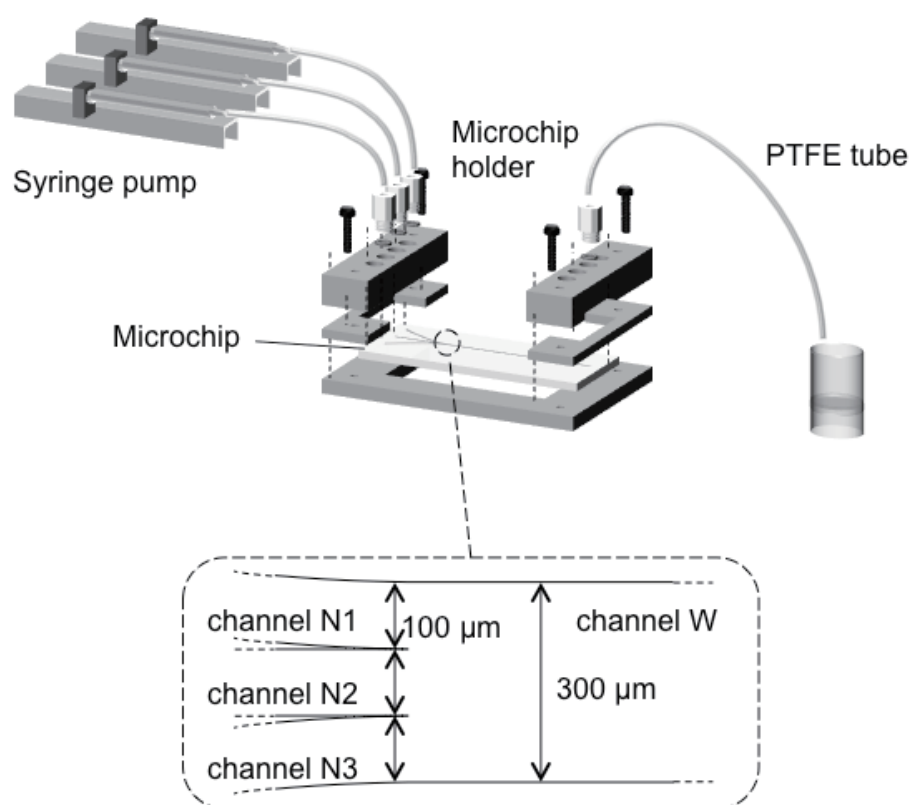


Figure 1. Schematic representations of the setup of the microchip in the microchip holder and the enlarged view of the microchip incorporating the three narrow channels combined to form one wide channel.

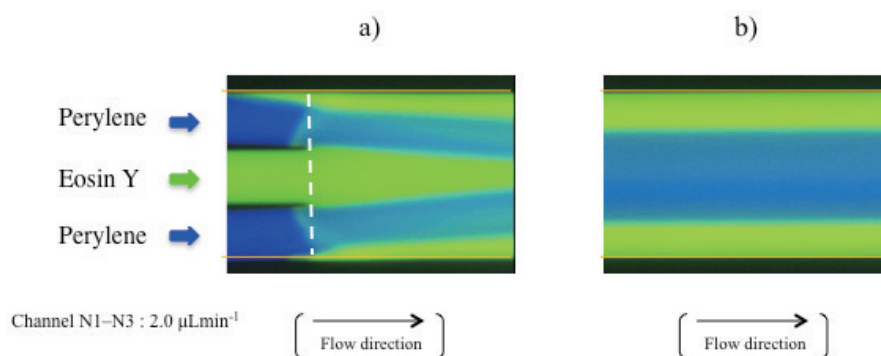


Figure 2. Fluorescence photographs of the solvents with the dissolved fluorescent dyes at a) the combining point of the channels and b) 3 cm from the combining point in channel W. The white dashed line indicates the combining point between channels N1 – N3 and channel W. Conditions: Carrier, water–acetonitrile (3:2, volume ratio) containing 3.0 mM Eosin Y in channel N2 and acetonitrile–ethyl acetate (3:2, volume ratio) containing 0.15 μM perylene in channels N1 and N3; flow rate, 2.0 μL min⁻¹ for channels N1 – N3. The volume ratio of water–acetonitrile–ethyl acetate in channel W is 3:8:4.

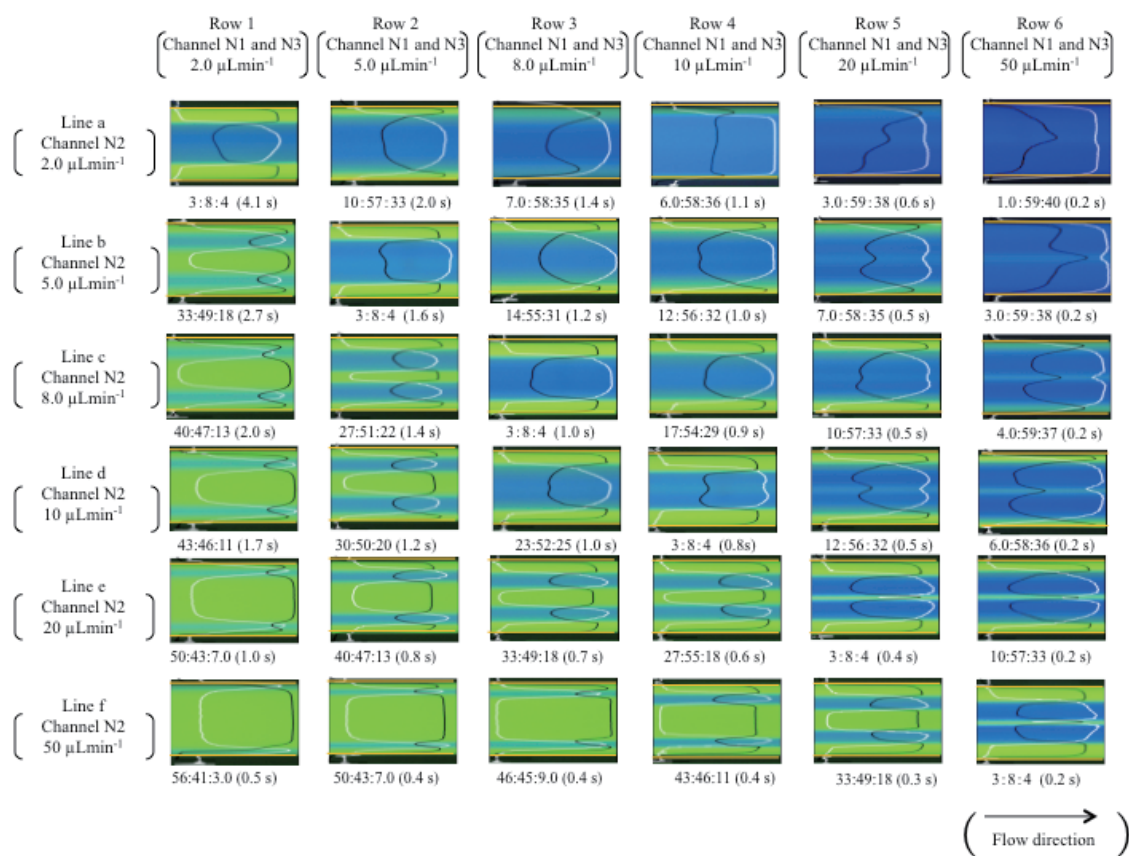


Figure 3. Fluorescence photographs and profiles of the solvents with the dissolved fluorescent dyes at 3 cm from the combining point in channel W where the water–acetonitrile–ethyl acetate mixture was fed with various mixing procedures. Conditions: Carrier, water–acetonitrile (3:2, volume ratio) containing 3.0 mM Eosin Y in channel N2 and acetonitrile–ethyl acetate (3:2, volume ratio) containing 0.15 mM perylene in channels N1 and N3; flow rates, 2.0 - 50 $\mu\text{L min}^{-1}$ for channels N1 - N3. The volume ratios of water–acetonitrile–ethyl acetate in channel W and the residence times from the combining point are indicated below each photograph.

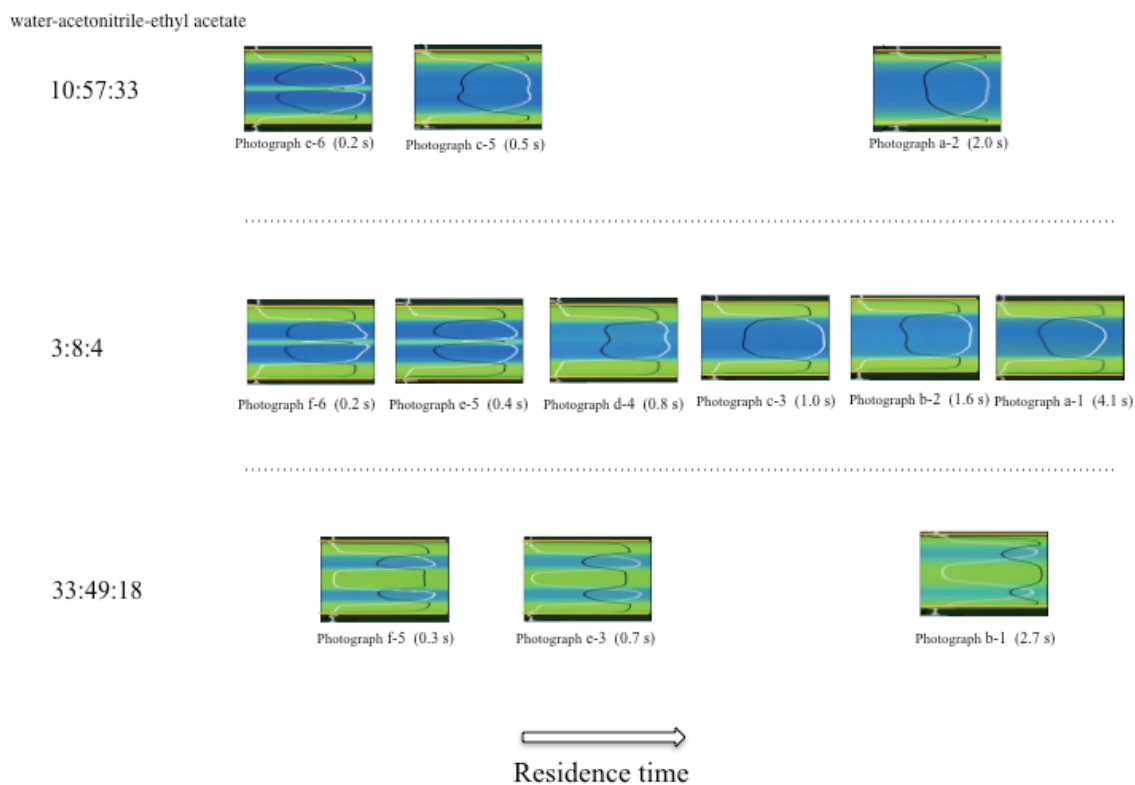


Figure 4. Fluorescence photographs and profiles of the solvents with the dissolved fluorescent dyes at 3 cm from the combining point in channel W where the water–acetonitrile–ethyl acetate mixture was fed with the same component ratios of the solvents. Conditions: Carrier, water–acetonitrile (3:2, volume ratio) containing 3.0 mM Eosin Y in channel N2 and acetonitrile–ethyl acetate (3:2, volume ratio) containing 0.15 mM perylene in channels N1 and N3. The volume ratios of water–acetonitrile–ethyl acetate in channel W are 10:57:33, 3:8:4, and 33:49:18. The photograph titles that are used in Fig. 3 and the residence times from the combining point are indicated below each photograph.

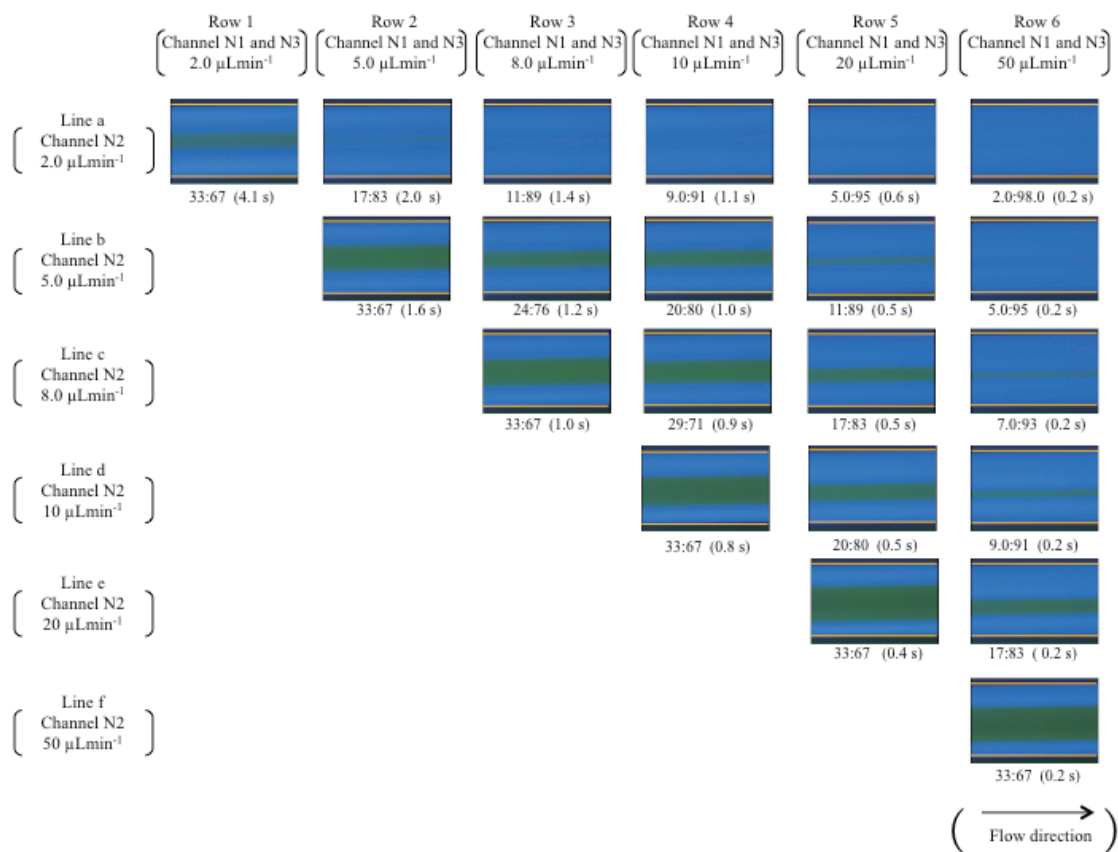


Figure 5. Fluorescence photographs of the solvents with the dissolved fluorescent dyes at 3 cm from the combining point in channel W where the water–acetonitrile mixture was fed. Conditions: Carrier, water containing 3.0 mM Eosin Y in channel N2 and acetonitrile containing 0.15 mM perylene in channels N1 and N3; flow rates, 2.0 – 50 $\mu\text{L min}^{-1}$ for channels N1 – N3. The volume ratios of water–acetonitrile in channel W and the residence times from the combining point are indicated below each photograph. When perylene was deposited in channel W, fluorescence photographs are not shown in the figure.

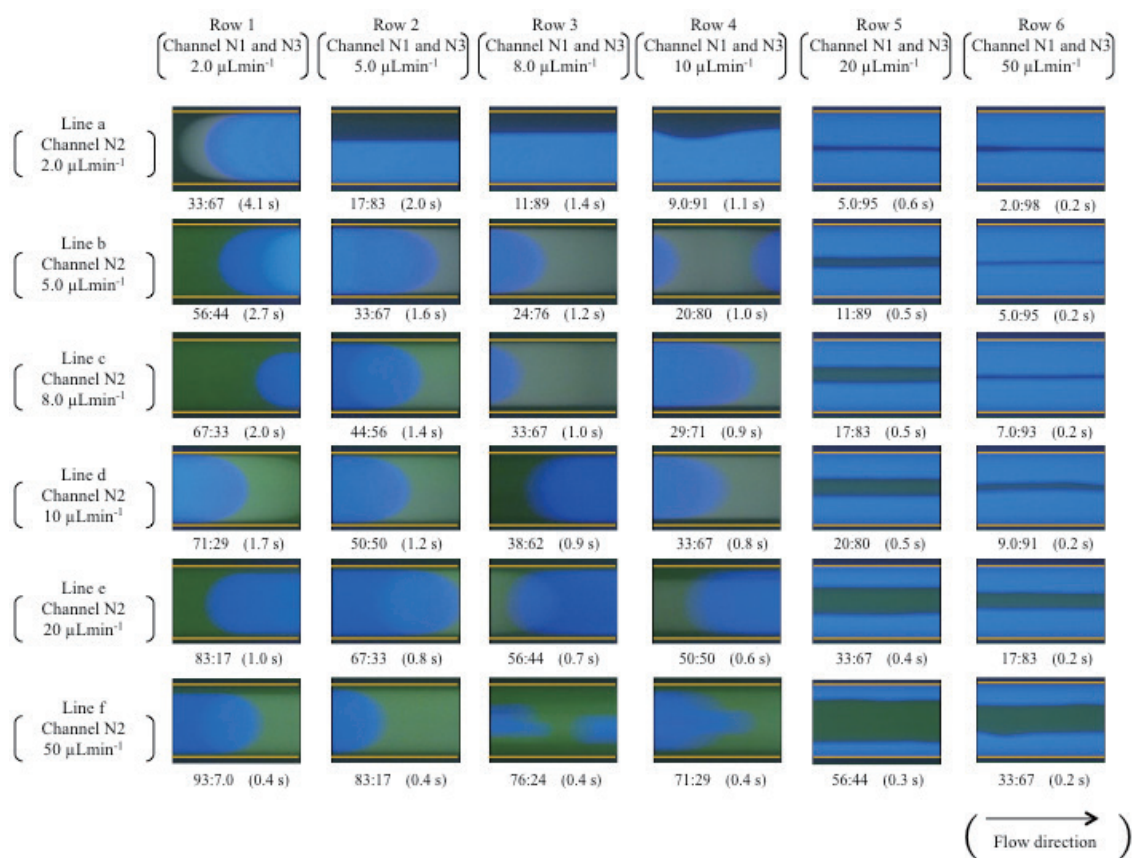


Figure 6. Fluorescence photographs of the solvents with the dissolved fluorescent dyes at 3 cm from the combining point in channel W where the water–ethyl acetate mixture was fed. Conditions: Carrier, water containing 1.0 mM Eosin Y in channel N2 and ethyl acetate containing 0.1 mM perylene in channels N1 and N3; flow rates, 2.0 – 50 $\mu\text{L min}^{-1}$ for channels N 1– N3. The volume ratios of water–ethyl acetate in channel W and the residence times from the combining point are indicated below each photograph.

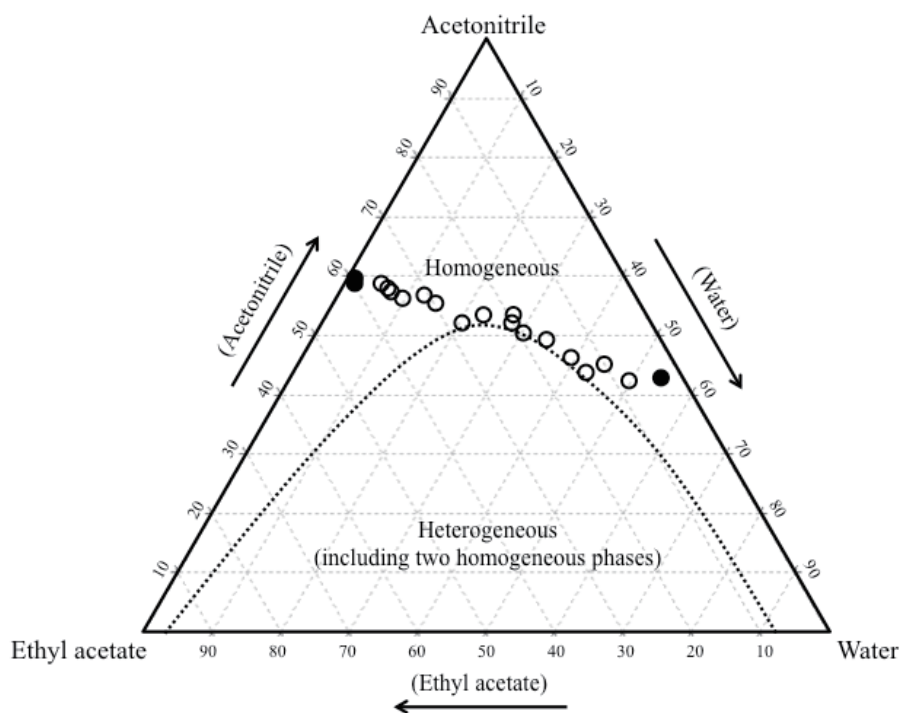
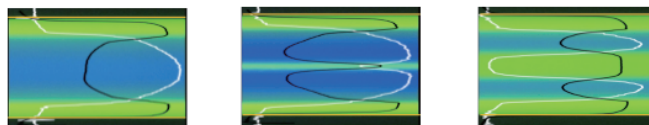


Figure 7. Phase diagram for a water–acetonitrile–ethyl acetate mixture and the component ratios of the solvents that provided the TRDM based on the TRDP in channel W. The dotted curve in the diagram indicates the homogeneous-heterogeneous solution boundary curve. The symbols \circ and \bullet indicate the TRDM photograph and the non-TRDM (or doubtful case) photograph, respectively.

Typical TRDM based on TRDP



Typical mixing patterns not based on TRDP

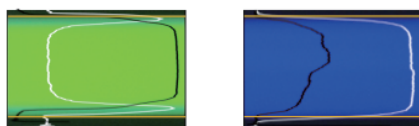


Figure 8. Typical TRDM photographs based on the TRDP and typical mixing patterns not based on the TRDP.

References

- [1] P. J. Asiello and A. J. Baeumner, *Lab Chip*, **2011**, *11*, 1420.
- [2] D. R. Reyes, D. Iossifidis, P. A. Auroux, and A. Manz, *Anal. Chem.*, **2002**, *74*, 2623.
- [3] Y. Kikutani, H. Hisamoto, M. Tokeshi, and T. Kitamori, *Lab Chip*, **2004**, *4*, 328.
- [4] A. Hibara, M. Tokeshi, K. Uchiyama, H. Hisamoto, and T. Kitamori, *Anal. Sci.*, **2001**, *17*, 89.
- [5] N. Kaji, Y. Okamoto, M. Tokeshi, and Y. Baba, *Chem. Soc. Rev.*, **2010**, *39*, 948.
- [6] H. Nakamura, Y. Yamaguchi, M. Miyazaki, H. Maeda, and M. Uehara, *Chem. Commun.*, **2002**, *23*, 2844.
- [7] H. Kawazumi, A. Tashiro, K. Ogino, and H. Maeda, *Lab Chip*, **2002**, *2*, 8.
- [8] G. Hefter, *Pure Appl. Chem.*, **2005**, *77*, 605.
- [9] G. R. Castro and T. Knubovets, *Crit. Rev. Biotechnol.*, **2003**, *23*, 195.
- [10] J. Niu and B. E. Conway, *J. Electroanal. Chem.*, **2003**, *546*, 59.
- [11] D. M. Ruiz and R. E. De Castro, *J. Ind. Microbiol. Biotechnol.*, **2007**, *34*, 111.
- [12] H. Ogino, K. S. Siddiqui, and T. Thomas, “*Protein Adaptation in Extremophiles*”, **2008**, Nova Science Publishers, Inc., New York.
- [13] M. Tjahjono, C. Huiheng, E. Widjaja, K. Sa-Ei, and M. Garland, *Talanta*, **2009**, *79*, 856.
- [14] M. K. Yeh, S. L. Lin, M. I. Leong, S. D. Huang, and M. R. Fuh, *Anal. Sci.*, **2011**, *27*, 49.
- [15] T. Maruyama, H. Matsushita, J. Uchida, F. Kubota, N. Kamiya, and M. Goto, *Anal. Chem.*, **2004**, *76*, 4495.
- [16] F. Torrens, *Chromatographia.*, **2001**, *53*, 199.

Chapter 12 Development of tube radial distribution reaction (TRDR)

A TRDP-based chemical reaction in a microspace, referred to as a tube radial distribution reaction (TRDR), has been performed as one of the applications of TRDP. The derivatization reaction of bovine serum albumin (BSA) with fluorescamine (FR), using the TRDR system, was evaluated and compared with conventional batch-based methods. The part of this chapter is constructed and rewritten based on related, published manuscripts.^{18,28)}

12.1 TRDR featuring the liquid-liquid interface created with TRDP

A micro-flow reaction system was developed in which liquid-liquid interface was created based on the tube radial distribution of ternary mixed carrier solvents. The system was constructed from double capillary tubes having different inner diameters (100 and 250 μm i.d.). The smaller tube was inserted into the larger one through a T-type joint. The reaction of a protein with a fluorescence derivatizing reagent was adopted as a model. A water–acetonitrile mixture (3:1 volume ratio) including bovine serum albumin (hydrophilic) was delivered into the large tube from the inside through the small tube and an acetonitrile–ethyl acetate mixture (7:4 volume ratio) containing fluorescamine (hydrophobic) as a derivatizing reagent was delivered from the outside through the joint. Solutions were mixed through the double capillary tubes to promote ternary mixed carrier solvents (water–acetonitrile–ethyl acetate; 1:2:1 volume ratio). The liquid-liquid interface was created based on the tube radial distribution of ternary solvents in the larger tube. The derivatization reaction was performed in the larger, or reaction, tube in the micro-flow system. The fluorescence intensity of the fluorescamine-derivatized bovine serum albumin obtained by the system, which specifically included the kinetic liquid–liquid interface in the tube, was greater than that obtained through a batch reaction using a homogeneous solution of water–acetonitrile (1:2 volume ratio).

Introduction

Micro-flow systems are an active area of research in chemistry and biochemistry. Novel components of micro-flow systems are frequently sought to improve performance for different types of uses and users [1-3]. Capillary tubes with inner diameters of less than several hundred micrometers, which provide a micro-flow, are also known to exhibit interesting and useful physical or hydrodynamic phenomena, such as electro-osmotic flow and laminar flow. The electro-osmotic flow in a capillary tube promotes capillary electrophoresis [4-6] and capillary electrochromatography [7], while the laminar flow conditions enable hydrodynamic chromatography [8,9].

Recently, our group reported on the tube radial distribution phenomenon of ternary mixed carrier solvents in a micro-flow, which we abbreviate as the “tube radial distribution phenomenon (TRDP).” When the ternary mixed carrier solvents of water–hydrophilic/hydrophobic organic solvent mixtures are delivered into a micro-space, such as a micro-channel or a capillary tube under laminar flow conditions, the carrier solvent molecules are radially distributed in the micro-space, generating inner and outer phases. A capillary chromatography system where the outer phase functions as a pseudo-stationary phase under laminar flow conditions has been developed based on the TRDP. We call this “tube radial distribution chromatography (TRDC)”.

There is much research interest in carrying out chemical reactions in aqueous–organic solvent mixtures [10,11], and at the liquid–liquid interfaces [12–14]; interesting and useful outcomes have been reported. TRDP creates a phase interface, i.e., it is a kinetic, not static, liquid–liquid interface in a micro-space under laminar flow conditions. Here, we applied the phase interface to a chemical reaction space in a micro-flow system. The formation of the liquid–liquid interface based on TRDP using double capillary tubes having different inner diameters was strictly confirmed through several experiments. Also, the results obtained with the present micro-flow reaction system were carefully compared with those of a batch reaction system. We briefly described preliminary results of this investigation in a previous communication.¹⁸⁾ A chemical reaction takes place in the micro-flow featured with the kinetic liquid–liquid interface created under the TRDP. The derivatization reaction of bovine serum albumin (BSA) with fluorescamine (FR) as a model was carried out in the present micro-flow reaction system.

Experimental

Apparatus and procedures A schematic diagram of the present micro-flow reaction system is shown in Fig. 1. The smaller tube (100 μm i.d.) was inserted into the larger one (250 μm i.d., 150 cm length) through a T-type joint. A water (10 mM borate buffer, pH 9.0)–acetonitrile mixture (3:1 volume ratio) including 25 μM bovine serum albumin (BSA) was delivered into the large tube from the inside through the small tube, and an acetonitrile–ethyl acetate mixture (7:4 volume ratio) including 1 mM Fluorescamine (FR) was delivered from the outside through the joint with micro-syringe pumps at various specified flow rates. The carrier solutions delivered from inside and outside into the larger tube were called Carriers A and B, respectively, as shown in Fig. 1. The carriers were fed at flow rates of 7.5, 12, and 15 $\mu\text{L min}^{-1}$ (Carrier A and B: 2.5 and 5 $\mu\text{L min}^{-1}$; 4 and 8 $\mu\text{L min}^{-1}$; and 5 and 10 $\mu\text{L min}^{-1}$, respectively). Carriers A and B were then mixed in the large tube to perform the derivatization reaction in the water–acetonitrile–ethyl acetate (1:2:1 volume ratio) solution. The solution including FR-derivatized BSA was collected at the outlet of the large tube until 1 mL was obtained for fluorescence spectroscopy (FP-6500, JASCO Corporation, Tokyo, Japan).

Fluorescence photographs A large capillary tube (250 μm i.d.) was set up for the fluorescence microscope-CCD camera system (Fig. 1) to confirm the tube radial distribution of the carrier solvents, i.e., TRDP. The water–acetonitrile mixture (3:1 volume ratio) including 1 mM Eosin Y and acetonitrile–ethyl acetate mixture (7:4 volume ratio) including 0.1 mM perylene solutions was delivered into the large capillary tube. The fluorescence in the capillary tube was mainly monitored from a position 30 cm from the outlet using a fluorescence microscope equipped with an Hg lamp, a filter, and a CCD camera.

Results and discussion

Tube radial distribution phenomenon of fluorescent dyes in a capillary tube Fig. 2 shows fluorescence photographs and profiles observed in the capillary tube (250 μm i.d.) at 20, 40, 80, and 120 cm positions from the smaller capillary outlet in which the fluorescent dye-containing aqueous–organic solvent carrier solution was delivered at a flow rate of 15 $\mu\text{L min}^{-1}$. The photographs and profiles showed that the hydrophobic perylene molecule (blue) was distributed around the middle of the tube and away from the tube inner wall, whereas the relatively hydrophilic Eosin Y molecule (green) was distributed near the tube inner wall. Thus, the kinetic liquid–liquid interface created through the TRDP was clearly confirmed in the present micro-flow system using double capillary tubes.

Effects of the flow rate on the tube radial distribution The effects of the flow rate on the tube radial distribution of the carrier solvents were examined using a fluorescence microscope-CCD camera system. Fig. 3 shows photographs taken at the smaller capillary tube outlet, where the water-acetonitrile mixture, including Eosin Y (green) from the inside and the acetonitrile-ethyl acetate including perylene (blue) from the outside, were mixed. As shown in Fig. 3, at all flow rates examined (7.5, 12, and 15 $\mu\text{L min}^{-1}$), the tube radial distribution started to form at the smaller tube outlet with an organic solvent-rich major inner phase (blue) and water-rich minor outer phase (green) based on the TRDP. That is, the water-rich solvents (green) and the organic solvents (blue) that were fed to the smaller tube outlet quickly changed from the inside and outside deliveries to the outer (green) and inner (blue) phases in the larger tube. We could observe the moment of TRDP creation at the smaller tube outlet for the first time. Fig. 4 shows fluorescence photographs and profiles of the dyes in the larger capillary tube 30 cm from the outlet at flow rates of 7.5, 12, and 15 $\mu\text{L min}^{-1}$. As shown in Fig. 4, TRDP was observed at all flow rates, and the outer water-rich phase became thicker with increasing flow rates.

Separation of 1-naphthol and 2,6-naphthalendisulfonic acid As described in the Introduction, the TRDC system has been developed based on the TRDP. We examined the separation performance of the TRDC using the present flow system with double capillary tubes of different inner diameters. The model analytes, hydrophobic

1-naphthol and hydrophilic 2,6-naphthalendisulfonic acid, were injected into the smaller capillary tube inlet by a gravity method (for 20 s from a height of 30 cm). Fluorescence detection was used. The thus obtained chromatograms are shown in Fig. 5 together with the analytical conditions. Since the water-rich outer phase acted as a pseudo-stationary phase in this case, hydrophobic 1-naphthol was first eluted near the average linear velocity, and second hydrophilic 2,6-naphthalendisulfonic acid was eluted with a lower velocity than the average linear velocity at all flow rates of 7.5, 12, and 15 $\mu\text{L min}^{-1}$. In more detail, the second peaks became broader and the resolution (R_s ; numbers in Fig. 5) decreased with increasing flow rates. The experimental data were consistent with the observation that the water-rich outer phase as a pseudo-stationary phase in the flow system became thicker, or included more organic solvents, with an increasing flow rate. It was suggested that the liquid-liquid interface based on TRDP in the capillary tube changes with the flow rates as a chemical reaction space, creating different fluidic property and component ratios of the solvents in the inner and outer phases.

Derivatization in batch reaction FR, which has no fluorescence itself before derivatization, is commonly used as a fluorogenic reagent in analytical chemistry. The reagent reacts readily under alkaline conditions with primary amines to form fluorescent substances, providing the basis for a rapid and sensitive assay of amino acids, peptides, proteins, and other primary amines [15]. FR is also quickly hydrolyzed in aqueous solution to become fluorescently inactive. The reaction schemes are shown in Fig. 6. An aqueous solution including a biomolecule, such as a protein, and an organic solution including FR are mixed and stirred for the derivatization reaction. FR, reacts competitively with BSA and water (hydrolysis) in an aqueous–organic solvent mixture solution. First, the derivatization reaction of BSA with FR was confirmed in a batch vessel using an aqueous–organic solvent solution in the usual manner as a reference. A 10 mM borate buffer solution (0.66 mL, pH 9.0) of 25 mM BSA was mixed with an acetonitrile solution (1.34 mL) of 1 mM FR, and stirred in the batch vessel (water–acetonitrile, 1:2 volume ratio and 8.3 mM BSA, 0.67 mM FR). The fluorescence due to the derivative in the solution was measured by fluorescence spectroscopy (ex 390 nm). The fluorescence spectrum exhibited a maximum at around 30 min after mixing, which then gradually decreased. The obtained spectrum at 30 min is shown in Fig. 7. The maximum intensity was ca. 200 (arbitrary units) (ex 390 nm, em 470 nm). The derivatization reaction of BSA with FR did not occur in a batch vessel using an aqueous–organic solvent solution (water–acetonitrile–ethyl acetate; 1:2:1 volume ratio) due to protein deposition.

Derivatization in tube radial distribution reaction The fluorescence spectrum of the solution collected through the capillary tube in the micro-flow reaction system (water–acetonitrile–ethyl acetate; 1:2:1 volume ratio and 8.3 mM BSA, 0.67 mM FR) is also shown in Fig. 7. The maximum intensities were ca. 340, 670, and 950 (arbitrary

units) (ex 390 nm, em 470 nm) at flow rates of 7.5, 12, and 15 $\mu\text{L min}^{-1}$, respectively. The fluorescence intensities, migration times in the large tube (140 cm from the small capillary tube outlet), and collection times up to 1 mL in a vessel are summarized in Table 1 together with the fluorescence intensities obtained in the batch reaction. The micro-flow reaction system with a flow rate of 15 $\mu\text{L min}^{-1}$ provided the highest fluorescence intensity, 950 (arbitrary units), among the experiments conducted. The reaction space created by the TRDP with 15 $\mu\text{L min}^{-1}$ must bring out a high derivatizing efficiency with the suitable fluidic property and composition of the solvents in the phases. The fluorescence intensity of the FR-derivatized BSA obtained under the present flow system in the capillary tube (950 arbitrary units) was about 4 times higher than that obtained in the batch-vessel using a water–acetonitrile homogeneous solution. Because the intensity of the fluorescence in the flow system did not increase in the collecting vessel, which is explained in the next section (Table 1 and Fig. 8), the greater fluorescence intensity in the system was attributed to the specific reaction area, i.e., the liquid-liquid phase interface created through the TRDP in the capillary tube where the hydrolysis of FR must be inhibited for the derivatization reaction to proceed. A chemical reaction that takes place in a micro-flow under the TRDP performance is called a “tube radial distribution reaction (TRDR)”.

Effects of the reaction time on the fluorescence intensity Figure 8 shows the relationships between the reaction times and the fluorescence intensities (ex 390 nm, em 470 nm) in a batch reaction. A reaction between BSA and FR was not carried out in the water–acetonitrile–ethyl acetate mixture solution because of protein deposition, due to ethyl acetate, which is shown with the plots (○) on the horizontal line in Fig. 8. The reaction between them occurred in the water–acetonitrile mixture solution with the maximum fluorescence intensity at ca. 30 min, as described above. To determine its influence on the reaction, ethyl acetate was added at 20 and 30 min after starting the reaction in a water–acetonitrile mixture solution. As shown in Fig. 8, the addition of ethyl acetate did not cause any marked changes in the fluorescence intensity in the aqueous–organic solvent mixture solutions. As shown in Table 1, the micro-flow reaction or TRDR system with a flow rate of 15 $\mu\text{L min}^{-1}$ required a migration time of 4.6 min in a capillary tube of 140 cm in length, and a collecting time of 67 min at the outlet of the tube. Although the migration time and the collecting time in the TRDR system were quite different from the reaction time of 30 min, which provided the maximum fluorescence intensity in the batch reaction system, the data in Fig. 8 showed no influence compared with the fluorescence intensity or derivatizing efficiency between the TRDR and batch reactor systems. This was because the fluorescence intensity in the flow system did not increase in the collecting vessel. Fig. 9 shows the relationship between the migration times and the fluorescence intensities in the TRDR system as well as the relationship between the reaction time and the fluorescence intensity in the batch reaction system. At all flow rates, the present TRDR system provided higher fluorescence intensity than that obtained by the batch reaction system

conducted for 30 min.

In conclusion, the TRDP creates a specific phase interface, i.e., a kinetic, and not static, aqueous–organic interface in micro-space under laminar flow conditions. We applied the phase interface created through the TRDP to a chemical reaction space in a micro-flow system. A chemical reaction that takes place in a micro-flow under TRDP performance is called a “tube radial distribution reaction (TRDR)”. The derivatization reaction of BSA with FR was carried out in the present TRDR system as a model. The fluorescence intensity of the FR-derivatized BSA obtained under the tube radial distribution phenomenon, which included a kinetic liquid–liquid interface, was greater than that obtained through batch reaction using a homogeneous solution of water–acetonitrile (1:2 volume ratio). The data obtained here will facilitate the development of novel micro-flow reactor devices.

Table 1 Fluorescence intensities in micro-flow reaction (tube radial distribution reaction; TRDR) and batch reaction (BR) systems as well as migration in a capillary tube and collection times up to 1 mL in a vessel in TRDR

Reaction	FL intensity [-]	Migration time [min]	Collection time [min]
TRDR			
H ₂ O(pH 9.0)-CH ₃ CN-EtOAc (1:2:1; v/v/v)			
15.0 μL min ⁻¹	954.1	4.6	66.7
12.0 μL min ⁻¹	670.7	5.7	83.3
7.5 μL min ⁻¹	340.8	9.2	133.3
.....			
BR			
H ₂ O(pH 9.0)-CH ₃ CN (1:2; v/v)			
	202.6	—	—
H ₂ O(pH 9.0)-CH ₃ CN-EtOAc (1:2:1; v/v/v)			
	5.2	—	—

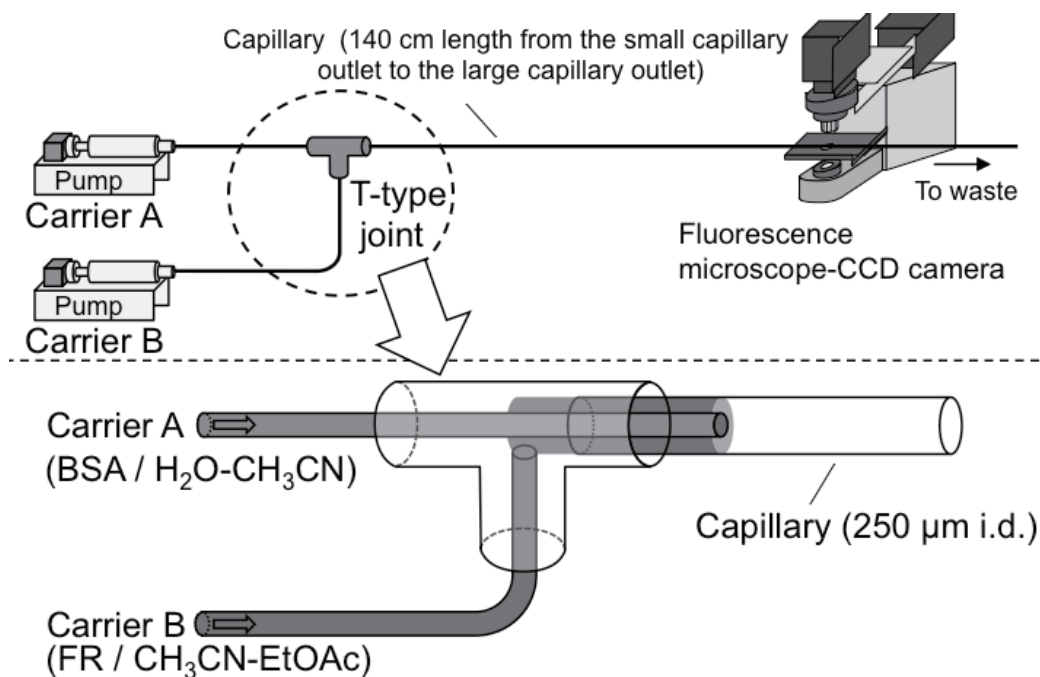


Figure 1. Schematic diagram of the present micro-flow system with a fluorescence microscope-CCD camera.

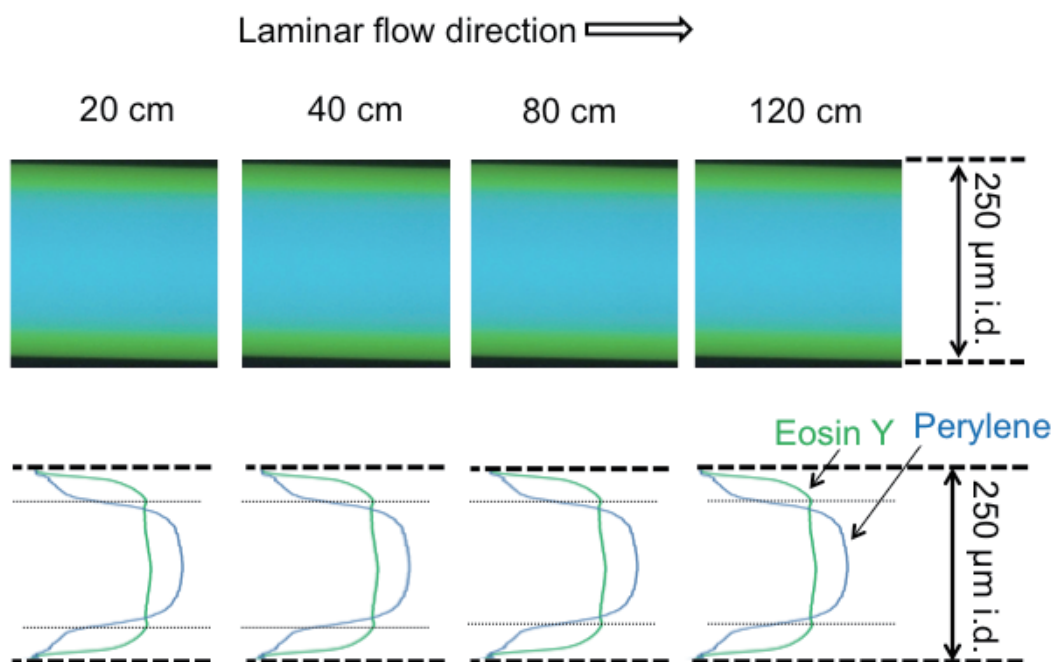


Figure 2. Fluorescence photograph and profiles of the fluorescent dyes dissolved in the ternary mixed carrier solvents at 20, 40, 80, and 120 cm from the smaller capillary outlet. Conditions: carrier, water–acetonitrile–ethyl acetate mixture (1:2:1, v/v/v), including 0.067 mM perylene and 0.33 mM Eosin Y; flow rate, $15 \mu\text{L min}^{-1}$.

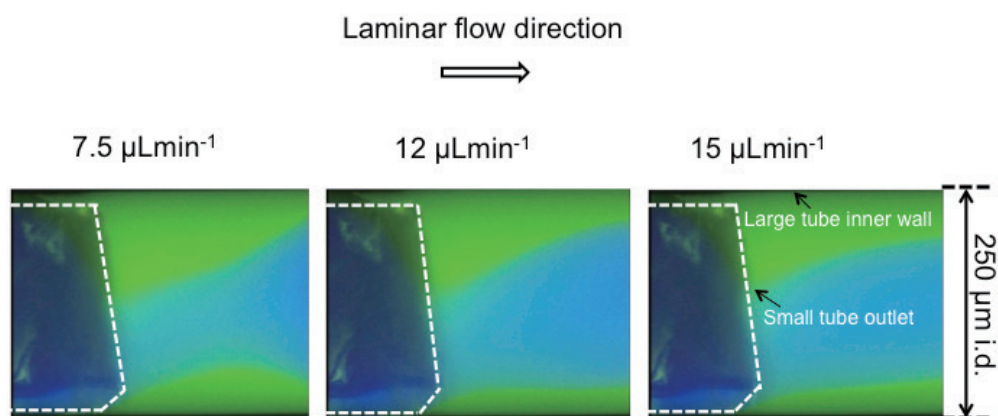


Figure 3. Fluorescence photograph of the fluorescent dyes dissolved in the ternary mixed carrier solvents around the smaller capillary outlet. Conditions: carrier, water–acetonitrile–ethyl acetate mixture (1:2:1, v/v/v), including 0.067 mM perylene and 0.33 mM Eosin Y; flow rate, 15 $\mu\text{L min}^{-1}$.

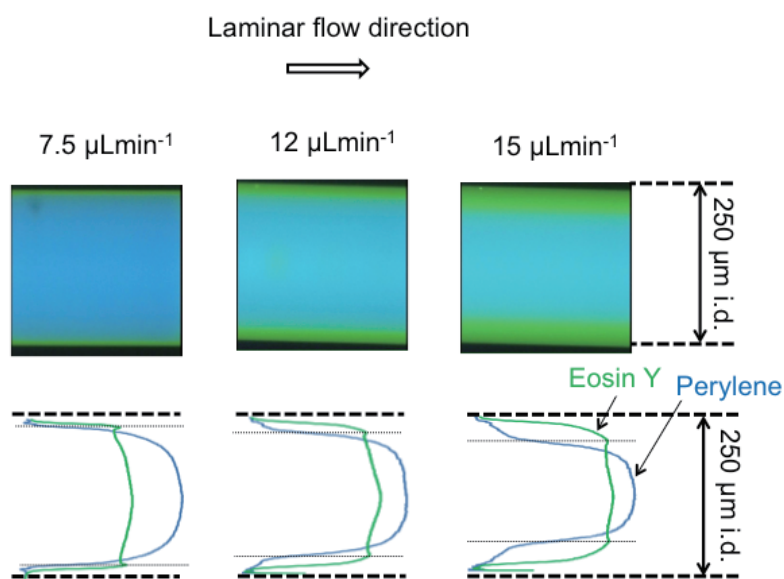


Figure 4. Fluorescence photograph and profiles of the fluorescent dyes dissolved in the ternary mixed carrier solvents at flow rates of 7.5, 12, and 15 $\mu\text{L min}^{-1}$. Conditions: carrier, water–acetonitrile–ethyl acetate mixture (1:2:1, v/v/v), including 0.067 mM perylene and 0.33 mM Eosin Y and observed point, 30 cm from the larger capillary outlet.

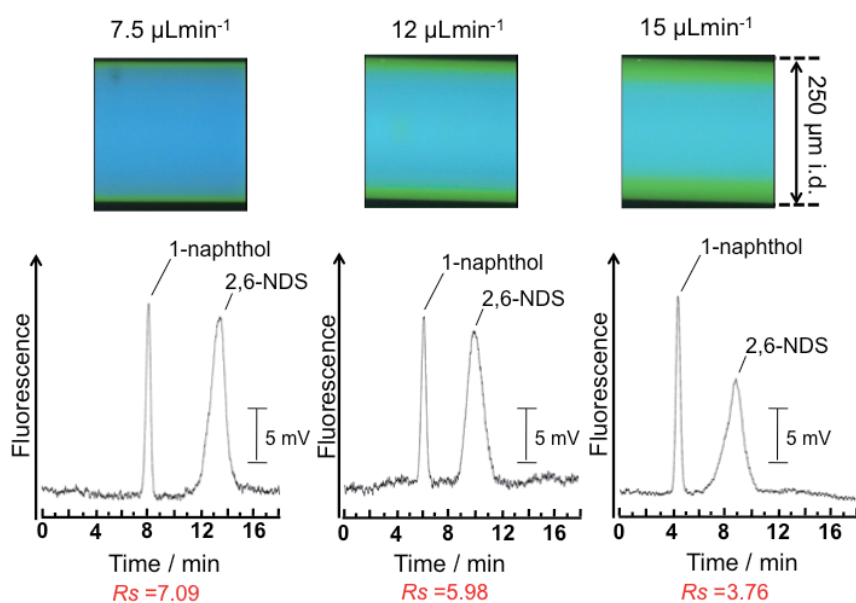


Figure 5. Chromatograms of 1-naphthol and 2,6-naphthalenedisulfonic acid by the micro-flow system using double capillary tubes of different inner diameters. Conditions: carrier, water–acetonitrile–ethyl acetate mixture (1:2:1, v/v/v); observed point, 30 cm from the larger capillary outlet; analyte injection, 20 s \times 30 cm height gravity method from the smaller tube inlet; detection (ex. 290 nm and em. 335 nm); analyte concentrations, 1 mM each.

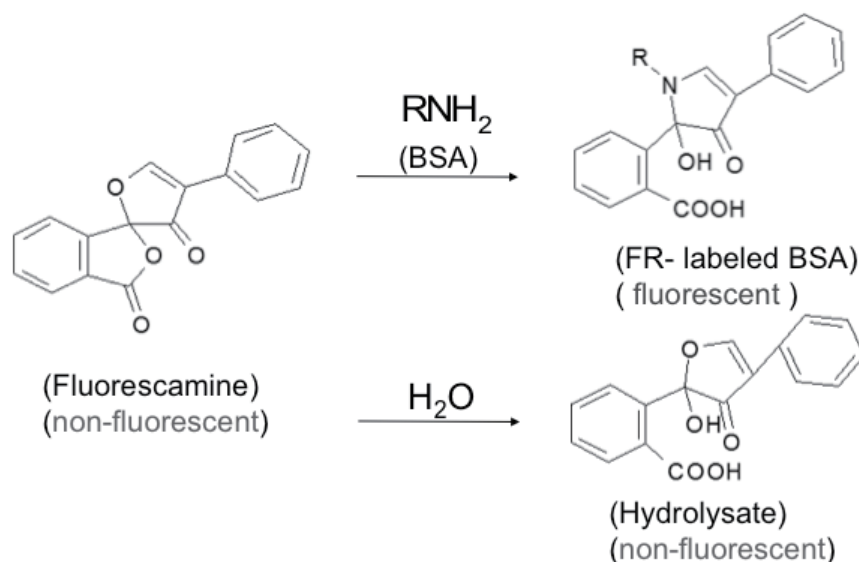


Figure 6. Reaction schemes of the derivatization of BSA with FR.

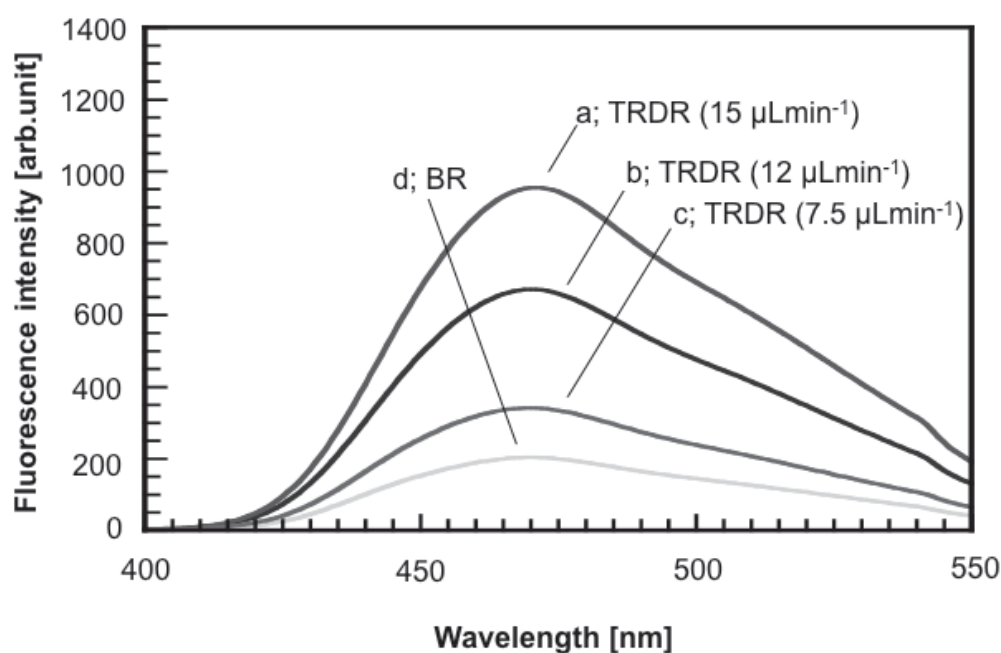


Figure 7. Fluorescence spectra of the FR-derivatized BSA. The solutions included 8.3 mM BSA and 0.67 mM FR for derivatization in the systems. Curves a), b), and c): micro-flow reaction (tube radial distribution reaction; TRDR) system (water–acetonitrile–ethyl acetate; 1:2:2 v/v/v) at 7.5, 12, and 15 $\mu\text{L min}^{-1}$, respectively. Curve d): batch reaction (BR) system (water–acetonitrile; 1:2 v/v).

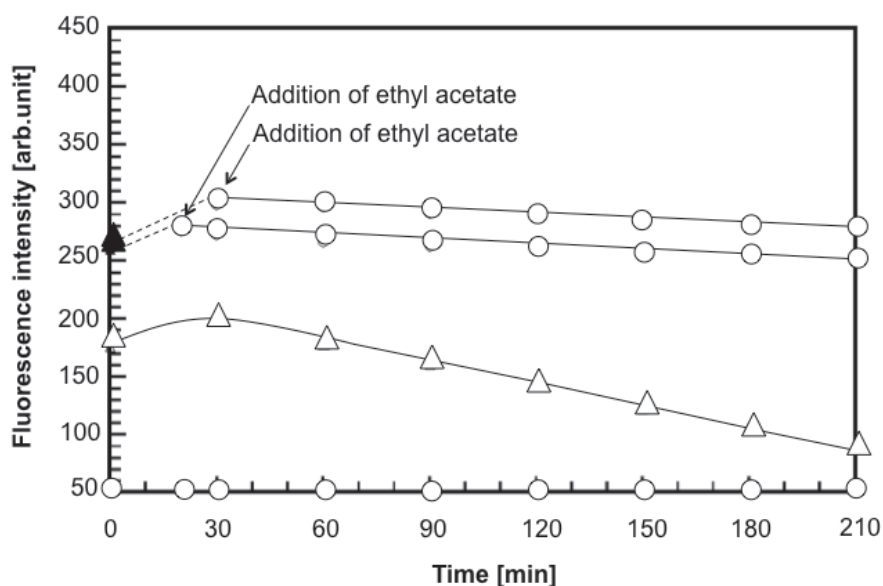


Figure 8. Relationships between the reaction times and the fluorescence intensities (ex 390 nm, em 470 nm) in the batch reaction system. ○, Water–acetonitrile–ethyl acetate (1:2:1 volume ratio; 8.3 μM BSA and 0.67 mM FR); △, water–acetonitrile (1:2 volume ratio; 8.3 μM BSA and 0.67 μM FR), and ▲, water–acetonitrile (1:2 volume ratio; 11 mM BSA and 0.88 mM FR).

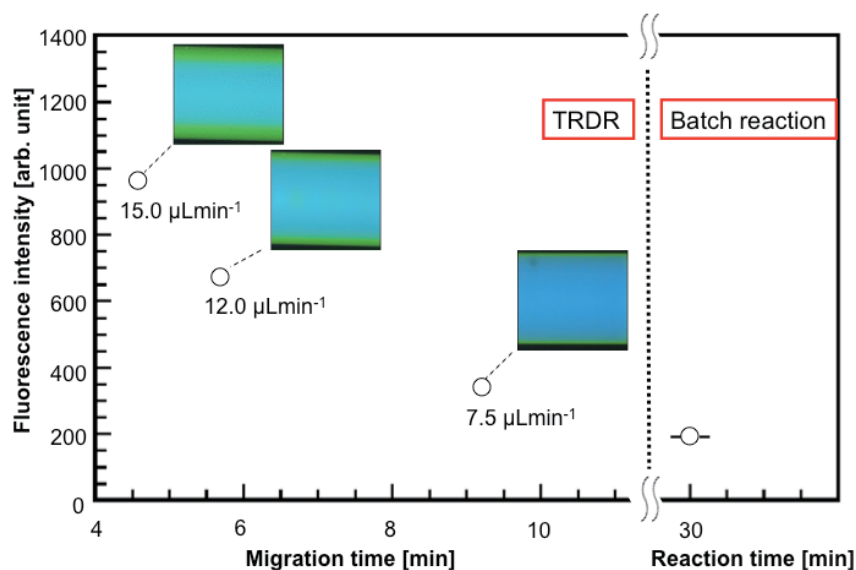


Figure 9. Relationship between the migration times and the fluorescence intensities in the micro-flow reaction (tube radial distribution reaction; TRDR) system as well as between the reaction time and the fluorescence intensity in the batch reaction system. The solutions included 8.3 μM BSA and 0.67 mM FR for derivatization in the systems. TRDR system (water–acetonitrile–ethyl acetate; 1:2:1 v/v/v) at 7.5, 12, and 15 $\mu\text{L min}^{-1}$ and batch reaction system (water–acetonitrile; 1:2 v/v).

References

- [1] M. H. Ghanim and M. Z. Abdullah, *Talanta*, **2011**, *85*, 28.
- [2] P. Hrnčirik and J. Nahlik, *Chem. Biochem. Eng.*, **2010**, *24*, 489.
- [3] C.-G. Yang, Z.-R. Xu, and J.-H. Wang, *Trends Anal. Chem.*, **2010**, *29*, 141.
- [4] E. Guihen and W. T. O'Connor, *Electrophoresis*, **2010**, *31*, 55.
- [5] S. Terabe, *Anal. Chem.*, **2004**, *76*, 240.
- [6] C. A. Lucy, A. M. MacDonald, and M. D. Gulcev, *J. Chromatogr., A*, **2008**, *1184*, 81.
- [7] K. Otsuka, *Chromatography*, **2007**, *28*, 1.
- [8] H. Small, F. L. Saunders, and J. Solc, *Adv. Colloid Interface Sci.*, **1976**, *6*, 237.
- [9] R. Umehara, M. Harada, and T. Okada, *J. Sep. Sci.*, **2009**, *32*, 472.
- [10] M. Tjahjono, C. Huiheng, E. Widjaja, K. Sa-Ei, and M. Garland, *Talanta*, **2009**, *79*, 856.
- [11] G. El-Subruiti, G. Younes, and M. Jaber, *Prog. React. Kinet. Mech.*, **2011**, *36*, 73.
- [12] Y. M. A. Yamada, T. Watanabe, T. Beppu, N. Fukuyama, K. Torii, and Y. Uozaki, *Chem.-A Eur. J.*, **2010**, *16*, 11311.

- [13] J. Jovanovic, E. V. Rebrov, T. A. Nijhuis, V. Hessel, and J. C. Schouten, *Ind. Eng. Chem. Res.*, **2010**, *49*, 2681.
- [14] K. Tsukagoshi, Y. Hattori, T. Hayashi, R. Nakajima, K. Yamashita, and H. Maeda, *Anal. Sci.*, **2008**, *24*, 1393.
- [15] K. Tsukagoshi, A. Tanaka, R. Nakajima, and T. Hara, *Anal. Sci.*, **1996**, *12*, 525.

Chapter 13 Two-phase separation systems of mixed solutions and TRDP

TRDP is caused by phase transformation of the two-phase separation systems of mixed solvent solutions, such as ternary water–hydrophilic/hydrophobic organic solvents, water–surfactant, water–ionic liquid, and fluorous–organic solvents, in a microspace under laminar flow conditions. The part of this chapter is constructed and rewritten based on related, published manuscripts.^{37,41,44,46,48)}

13.1 Two-phase extraction of metal ions using a ternary water-acetonitrile-ethyl acetate mixed solution

A ternary mixed-solvent solution of water-acetonitrile-ethyl acetate changes from a homogeneous (single-phase) to a heterogeneous (two-phase) system with changes in temperature and/or pressure. Here, we used this system in a batch vessel to extract metal ions. Water-acetonitrile-ethyl acetate at a volume ratio of 3:8:4 containing 8-hydroxyquinoline was used as a ternary mixed-solvent solution, changing from homogeneous at 25 °C to heterogeneous after 30 min at 0 °C. The two-phase system comprised an upper (organic solvent-rich) phase and a lower (water-rich) phase at a volume ratio of 6:1. Fe(III), Co(II), and Ni(II) were used as model metal ions dissolved in the homogeneous solution at 25 °C. The distribution constants and the extraction percentages were determined by measuring the metal ion concentrations in the upper and lower phases with inductively coupled plasma atomic emission spectroscopy. The metal ions were extracted through complexation with 8-hydroxyquinoline in the organic-rich phase with distribution constants and extraction percentage values, respectively, of 0.47 and 74 for Fe(III), 0.15 and 47 for Co(II), and 0.08 and 32 for Ni(II).

Introduction

The process of phase separation of aqueous systems containing polymers, micelles, and ionic liquid solutions has been well known and used in the fields of analytical chemistry and separation science since the last century [1-5]. For example, aqueous micellar solutions of some non-ionic surfactants separate into two distinct phases when heated above a certain temperature (the cloud point); that is, a temperature-induced phase separation occurs [6-10]. One phase is an almost micelle-free aqueous solution (the aqueous phase), while the other is a concentrated surfactant solution containing considerable amounts of water (the surfactant-rich phase). Hydrophobic compounds dissolved in the aqueous micellar solution are extracted into the surfactant-rich phase, while hydrophilic compounds remain in the aqueous phase.

Fluorous chemistry, which can undergo phase separation, has been heavily investigated since the seminal work of Horváth and Rábai in 1994 [11]. Two-phase separation of fluorous-organic solvent mixed solutions has been applied in separation science [12,13]. When cooled below a certain temperature [14], mixed solutions of fluorous-organic solvents separate into two distinct phases in a batch vessel; the lower phase comprising an almost pure fluorous solvent, and the upper phase comprising an organic solvent. Based on this two-phase system, liquid-liquid and liquid-solid extractions have been reported using a variety of fluorous solvents [15-17].

A novel two-phase separation system involving ternary mixed solvents has been reported by our group. A ternary mixed solvent solution of water-hydrophilic/hydrophobic solvents changes from a homogeneous (single-phase) to a heterogeneous (two-phase) system with temperature and/or pressure changes. This phenomenon causes a specific fluidic behavior in a microspace, such as a microchannel on a microchip or a capillary tube, leading to new types of open-tubular capillary chromatography and microreactors. Here, for the first time we have used a two-phase separation system comprising a ternary mixed-solvent solution in a batch vessel to extract metal ions.

Experimental

8-hydroxyquinoline (8-HQ), iron (1000 ppm, 0.275 M HNO₃), nickel (1000 ppm, 0.1 M HNO₃), and cobalt (1000 ppm, 0.1 M HNO₃) standard solutions were purchased from Nacalai Tesque, Inc. (Kyoto, Japan). A homogeneous ternary mixed-solvent solution of water-acetonitrile-ethyl acetate (at a volume ratio of 3:8:4) containing 8-HQ was prepared at 25 °C. Metal ions were dissolved in the homogeneous solution, and the solution was then cooled to 0 °C and held to obtain a heterogeneous solution including both upper (organic solvent-rich) and lower (water-rich) phases. The metal concentrations were determined in both phases. Each phase was subjected to evaporation, and the resultant residue was dissolved in 0.1 M nitric acid (10 mL) for inductively coupled plasma atomic emission spectroscopy (ICP, 8100-Type instrument, Shimadzu Co.). Distribution constants (D) and extraction percentages (E%) were calculated using the following equations:

$$D = C_o / C_w,$$

$$E(\%) = 100 D / (D + V_w/V_o),$$

in which C_o and C_w are the metal concentrations in the upper and lower phases, respectively; V_o and V_w are the volumes of the upper and lower phases, respectively.

Results and discussion

Phase diagram and tie line The phase diagram of the ternary mixed solvent solution of water-acetonitrile-ethyl acetate is shown in Fig. 1. The solid curve indicates the boundary between the heterogeneous and homogeneous systems at 25 °C. The dotted curve is the boundary between these systems at 0 °C. The plot (○) near the boundary curve at 25 °C locates the component volume ratio of 3:8:4 for water-acetonitrile-ethyl

acetate. The tie-line of the plot at 0 °C on the phase diagram was constructed using the solvent composition of the homogeneous solution at 25 °C, the water content of the lower phase in the batch vessel at 0 °C (where Karl Fischer moisture titrator (MKC-610; API Co.) was used), and the boundary curve at 0 °C. The volume ratio of the upper and lower phases at 0 °C in the batch vessel corresponds to the ratio of the line lengths, which are separated by the plotted point on the tie line. In this case, the volume ratio of the upper and lower phases was 6:1, as shown in Fig. 1. The phase diagram of the ternary mixed solvent solution containing 10 mM 8-HQ was similar to that shown in Fig. 1, although 10 mM 8-HQ was only sparingly dissolved in a mixed solvent solution containing water at less than ca. 50 vol%.

Preliminary extraction experiments Two preliminary experiments (Experiments 1 and 2) are illustrated in Fig. 2. In Experiment 1, a solution of ethyl acetate containing 10 mM 8-HQ and an acetic acid solution (pH 2.8) containing 0.34 mM metal ions (at a volume ratio of 6:1; total volume 15 mL) in a batch vessel was held for 30 min without stirring. This system, as might be expected, consisted of two phases. The metal concentrations of the two phases were then measured with ICP. D and E(%) were both zero for all metal ions (Fe(III), Co(II), and Cu(II)). That is, Experiment 1 showed no extraction behavior for these metal ions under the conditions used. In Experiment 2, the same conditions were used as in Experiment 1, but the system was well stirred in the batch vessel for 30 min, and then held without stirring for 30 min. The metal concentrations in the two phases were then measured by ICP. The D and E(%) values were, respectively, 0.46 and 73 for Fe(III), 0.15 and 47 for Co(II), and 0.08 and 32 for Ni(II) (the numbers were averages for 3 – 5 times measurements). Thus, as a general result, Experiment 2 showed extraction behavior for the metal ions. After 3 hours of stirring, D and E(%) remained constant at the above values for all metal ions.

Extraction experiment using the ternary mixed solvent solution Experiment 3 using the ternary mixed solvent solution was carried out as illustrated in Fig. 2. A homogeneous ternary mixed solvent solution of water-acetonitrile-ethyl acetate (volume ratio 3:8:4; total volume 15 mL) containing 10 mM 8-HQ and 0.34 mM metal ion solution in a batch vessel was cooled from 25 to 0 °C, and held for 30 min. The metal concentrations of the two phases were then measured by ICP. D and E(%) were, respectively, 0.47 and 74 for Fe(III), 0.15 and 47 for Co (II), and 0.08 and 32 for Ni(II) (the numbers were averages for 3 – 5 times measurements). That is, the two-phase system of the ternary mixed solvent solution performed similarly to the extraction system of Experiment 2. After 3 hours, D and E(%) remained constant at the above values for all metal ions. It is worth emphasizing that Experiment 3 using the two-phase system performed metal ion extraction with 8-HQ without stirring at almost the same D and E(%) values as those obtained in Experiment 2, although the extraction conditions, such as the pH values of the water-rich phase, have to be examined in detail in order to improve the extraction efficiency. The order of extraction performance obtained with

8-HQ in Experiments 2 and 3, Fe(II)>Co(II)>Ni(II), was consistent with that reported previously [18,19].

Extraction of mixed metal ions Mixtures of metal ions containing Fe(III) and Co(II), Fe(III) and Ni(II), and Co(II) and Ni(II) were extracted in the same way as in Experiment 3 (each metal concentration was 0.18 mM). The values of D and E(%) for the Fe(III) and Co(II) mixture were, respectively, 0.40 and 70 for Fe(III); 0.14 and 45 for Co(II). For the Fe(III) and Ni(II) mixture, the respective D and E(%) values were 0.33 and 66 for Fe(III) and 0.08 and 32 for Ni(II). Finally, the respective D and E(%) values for the Co(II) and Ni(II) mixture were 0.16 and 50 for Co(II) and 0.11 and 39 for Ni(II) (the numbers were averages for 3 – 5 times measurements). These values for the metal ions were very similar to those obtained in Experiments 2 and 3.

In conclusion, a two-phase separation system comprising a ternary mixed-solvent system was reported. The water-acetonitrile-ethyl acetate system changed from a homogeneous (single-phase) to a heterogeneous (two-phase) system with temperature and/or pressure changes. Here, for the first time, we used a two-phase separation system comprising a ternary mixed solvent solution in a batch vessel to extract metal ions. Model metal ions of Fe(III), Co(II), and Ni(II) were successfully extracted with the two-phase system. The experimental data obtained here suggest that the new phase separation system offers new capabilities in separation science, similar to other two-phase systems consisting of polymers, micelles, ionic liquids, and fluorosol solutions.

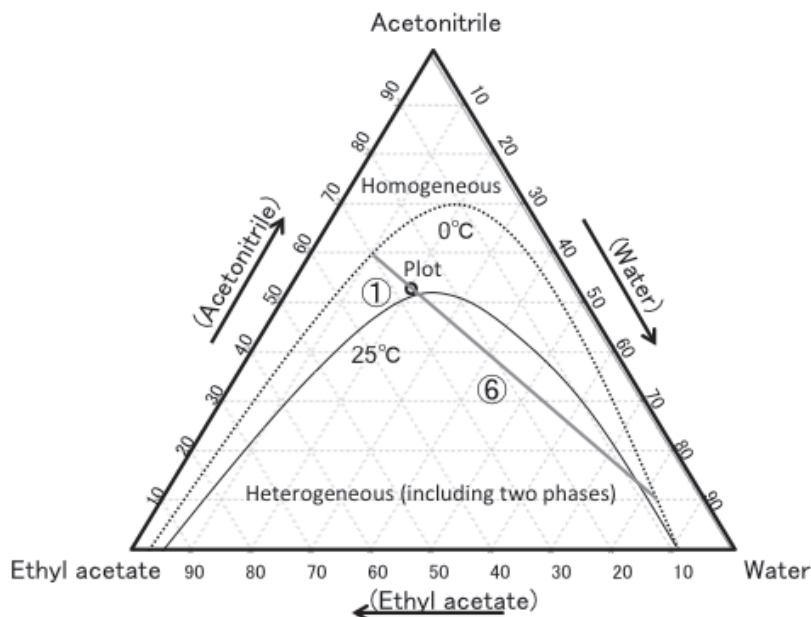
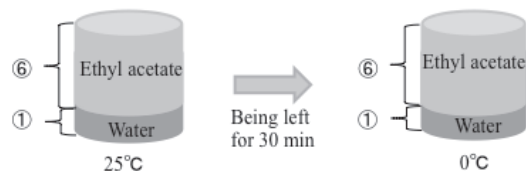
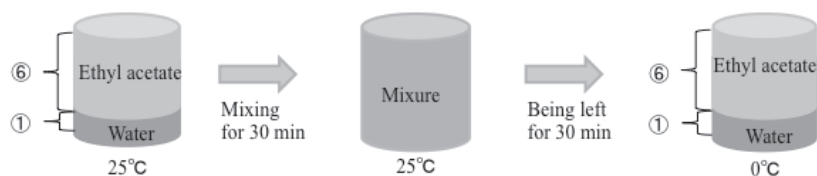


Figure 1. Phase diagram of the ternary mixed-solvent solution comprising water-acetonitrile-ethyl acetate. The solid curve represents 25 °C and the dotted curve represents 0 °C. The component ratio of water-acetonitrile-ethyl acetate for the plotted point (○) is a 3:8:4 volume ratio. The straight line on the plot represents the tie line at 0 °C.

Experiment 1; ethyl acetate containing 8-HQ - water (pH 2.8) containing metal ion (6:1, v/v).
Just being left.



Experiment 2; ethyl acetate containing 8-HQ - water (pH 2.8) containing metal ion (6:1, v/v).
Mixing and being left.



Experiment 3; water (pH 2.8) – acetonitrile – ethyl acetate (3:8:4, v/v/v) containing 8-HQ and metal ion.
Just being left.



Figure 2. Illustration of extraction experiments in the batch vessel. The extraction conditions are described in detail in Experiments 1–3 in the text.

13.2 TRDP created with an aqueous ionic liquid mixed solution

The tube radial distribution of solvents was observed in an aqueous ionic liquid mixed solution of 1-butyl-3-methylimidazolium chloride fed into a capillary tube. A phase diagram was constructed with 1-butyl-3-methylimidazolium chloride and potassium hydroxide, which included boundary curves between homogeneous and heterogeneous solutions at 15 and 20 °C. As an example, an aqueous ionic liquid mixed homogeneous solution, comprising the ratio of 1-butyl-3-methylimidazolium chloride : potassium hydroxide (24.0 : 20.0 wt/wt%), which were positioned near the boundary at 20 °C, were delivered into a fused-silica capillary tube (75 μm inner diameter, 110 cm length, 15 °C tube temperature) at a flow rate of 1.0 μL min⁻¹. The homogeneous solution changed to a heterogeneous solution with two phases: the inner (the ionic liquid-rich) and the outer (the aqueous phase merely containing the ionic liquid) phases, in the capillary tube. The radial distribution of the solvents in the aqueous ionic liquid mixed solution was observed through a bright-light microscope-CCD camera system.

Introduction

Since the last century, phase separation in aqueous two-phase systems of ionic liquids (ILs) has been well known in the field of analytical chemistry and separation science [1-5]. For example, aqueous solutions of ILs separate into two distinct phases when cooled below a certain temperature; that is, a temperature-induced phase separation occurs [12]. One phase is an almost IL-poor aqueous phase, while the other phase is a considerable IL solution (IL-rich phase). Also, as an application, it was reported that cytochrome c solubilized in the IL-poor aqueous solution are extracted into the IL-rich phase by taking advantage of the phase separation in aqueous two-phase systems of ILs [9].

Here, an aqueous IL mixed solution that showed phase separation as mentioned above was fed into a capillary tube to explore a new type of TRDP that is not used with the ternary mixed solvents of water-hydrophilic/hydrophobic organic solvents. The tube radial distribution of the solvents in the aqueous IL mixed solution was successfully observed in the capillary tube, indicating the kinetic liquid-liquid interface between the IL-poor aqueous and the IL-rich phases. This finding will expand the TRDP concept to a new research subject of microfluidic behavior, and allow the possibility of developing new types of chromatography, extraction, micro-reaction, and mixing process with the aqueous IL mixed solutions.

Experimental

The purity of potassium hydroxide (KOH) reagent was confirmed to be 87 wt% with titration. Acid Orange 10 was used as a dye for a bright-field microscope observation. A fused-silica capillary tube (75 μm i.d. and 150 μm o.d., 110 cm total length) was used. The microscopy was set up with a fused-silica capillary tube. Bright-light microscope observation in the capillary tubes was monitored at a length of 90 cm from the inlet

using a microscope equipped CCD camera. The part of the capillary tube for observation through the bright-field microscope was maintained at a temperature of 15 °C with a thermo-controller (MATS-555RO; Tokai Hit Co., Shizuoka, Japan).

Results and discussion

As described in the introduction, an aqueous solution of ionic liquid, 1-butyl-3-methylimidazolium chloride ([C₄mim]Cl), including a salt, such as potassium citrate, potassium carbonate, potassium phosphate, potassium hydrogenphosphate (K₂HPO₄) or KOH, separates into two distinct phases when cooled below a certain temperature. As preliminary experiments, we examined the aqueous solutions of [C₄mim]Cl (21.3 wt%)-K₂HPO₄ (13.7 wt%) mixture and [C₄mim]Cl (24.0 wt%)-KOH (20.0 wt%) mixture through the upper and lower phase separation in a batch vessel and the inner and outer phase separation in a capillary tube. Consequently, nearly the same separation or distribution behavior was observed for the two mixed aqueous solutions. Here, the aqueous solution of a [C₄mim]Cl-KOH mixture, where KOH had a simpler chemical construction than K₂HPO₄, was investigated in detail as a model.

A phase diagram was constructed between the KOH concentration and the [C₄mim]Cl concentration at 15 and 20 °C (KOH concentration was estimated based on the assumption that the purity level was 100%). The obtained phase diagram is shown in Fig. 1. The dotted curves are the boundary between homogeneous and heterogeneous solutions. The heterogeneous solution included two phases: an IL-poor aqueous and an IL-rich phase. The boundary at 15 °C is positioned slightly lower than that at 20 °C. The component ratios of [C₄mim]Cl and KOH in the homogeneous solutions for the symbols, ○, of Nos. 1 – 7 that were positioned almost on the boundary curve at 20 °C were as follows: (No. 1) [C₄mim]Cl:KOH, 52.3:6.5 wt/wt%; (No. 2) 44.8:9.3; (No. 3) 37.2:12.8; (No. 4) 30.5:16.5; (No. 5) 24.0:20.0; (No. 6) 18.4:24.0; (No. 7) 14.0:27.0. Phase separation in the homogeneous solutions of Nos. 1 – 7 by changing them from 20 °C to 15 °C in a batch-vessel is described below and shown in Fig. 1. The salt depositions were observed for Nos. 1 – 3 and also the volume ratios of upper and lower phases were not exactly estimated for Nos. 1 – 4. The viscosities of the upper and lower phases were examined qualitatively. The phase separation was carried out with an upper IL-rich solution and a lower IL-poor aqueous solution for Nos. 4 – 7. The volume ratios of the upper and lower phases for Nos. 4, 5, 6, and 7 were 80:20, 59:41, 30:70, and 21:79, respectively. Generally speaking, adding kosmotropic ions (OH⁻, HPO₄²⁻, etc.) into an aqueous IL solution leads to an increase in the interaction between ions and water molecules, generating the two separated phases [4]. However, through the interaction, it is difficult to know how many water molecules leave in the IL-rich phase, and how many water molecules move to the IL-poor aqueous phase. That is, the volume ratio of the upper and lower phase may be decided only with obtained experimental data.

Homogeneous aqueous solutions at 20 °C containing [C₄mim]Cl and KOH, Nos. 4 – 7, were delivered into the capillary tube which of the observation point was controlled

at 15 °C. The solution of No. 3 could not be fed into the capillary tube because of salt deposition. The TRDP in the tube was examined with a bright-field microscope for the solutions of Nos. 4 - 6. The homogeneous solutions of No. 4 and 7 did not create a TRDP with good reproducibility under the present conditions. Typical bright-field photographs of TRDP are shown in Fig. 2. The homogeneous solution of No. 5 created a TRDP with a major inner phase of the IL-rich solution, where Acid Orange 10 was mainly dissolved, and the minor outer phase of the IL-poor aqueous solution existed at a flow rate of 1.0 $\mu\text{L min}^{-1}$. However, the homogeneous solutions of No. 6 created the TRDP with a minor inner phase of the IL-rich solution, where Acid Orange 10 was mainly dissolved, and the major outer phase of the IL-poor aqueous solution existed at a flow rate of 3.0 $\mu\text{L min}^{-1}$ (the TRDP was partially created at a flow rate of 1.0 $\mu\text{L min}^{-1}$). Acid Orange 10 is soluble in water, but insoluble in ionic liquid, $[\text{C}_4\text{mim}]\text{Cl}$. Also it is scarcely soluble with a 50 wt% KOH aqueous solution. Thus, the distribution of Acid Orange 10 to IL-rich and IL-poor aqueous phases must be judged by comparing the yellow color depths in both phases. In the batch vessel, Acid Orange 10 was mostly soluble in the IL-poor aqueous phase in No. 4 solutions. However, in Nos. 5, 6, and 7 solutions Acid Orange 10 was very slightly soluble in the IL-poor aqueous phase, but was mostly soluble in the IL-rich phase, by judging the yellow color depth. The experimental data in the batch vessels consisted of the bright-light photographs shown in Fig. 2.

In the TRDP with ternary water-hydrophilic/hydrophobic organic solvents solutions reported by us previously, major inner and minor outer phases were observed in various types of capillary tubes. We did not observe minor inner and major outer phases in the TRDP with the ternary solvents solution. However, the observed TRDP pattern of the inner and outer phases in the aqueous IL mixed solution was not always consistent with the distribution pattern in the ternary mixed solvents solutions in our previous reports. The reason for the difference in the inner and outer formation patterns between the aqueous IL mixed solution and the ternary mixed solvents solution has not been clarified.

In conclusion, we have developed a new type of TRDP, i.e., a kinetic liquid-liquid interface, in a capillary tube, by the delivery of an aqueous homogeneous solution of IL, $[\text{C}_4\text{mim}]\text{Cl}$, including KOH. The previous TRDP using ternary mixed solvents of water-hydrophilic/hydrophobic organic mixtures have been examined from the viewpoints of chromatography,⁴ extraction, micro-reaction, and the mixing process. The new type of TRDP with the aqueous IL mixed solution will lead to further developments of both fundamentals and applications of TRDP and related technologies.

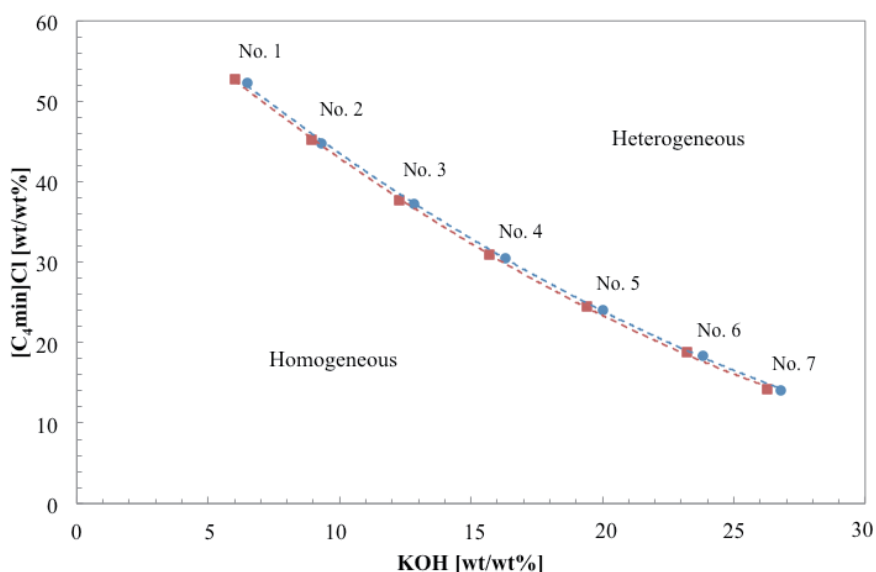


Figure 1. Phase diagram of an aqueous IL mixed solution consisting of $[C_4mim]Cl$ and KOH at 15 (■) and 20 °C (●). The phase separation in a batch vessel at 15°C is also illustrated along with the volume ratio of upper and lower phases in the figure; blue, IL-poor aqueous and yellow, IL-rich. The compositions of the homogeneous solutions (20°C), Nos. 1- 7, represented by the symbols (○) are (No. 1) $[C_4mim]Cl : KOH$, 52.3:6.5 wt/wt%; (No. 2) 44.8:9.3; (No. 3) 37.2:12.8; (No. 4) 30.5:16.5; (No. 5) 24.0:20.0; (No. 6) 18.4:24.0; (No. 7) 14.0:27.0.

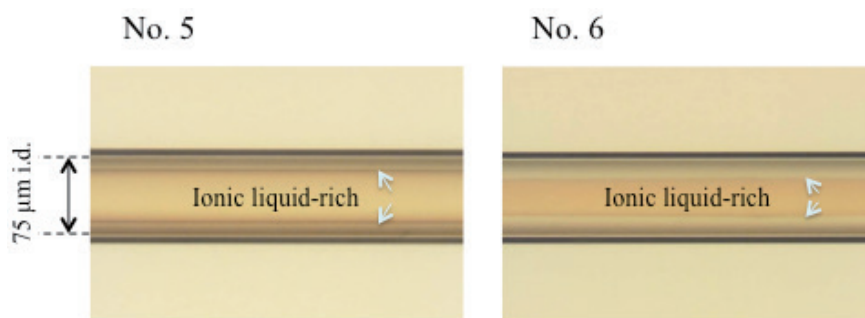


Figure 2. Typical photographs obtained with the bright-field microscope-CCD camera system for solutions of Nos. 5 and 6 at a tube temperature of 15 °C. The arrows indicate the interface between the IL-rich and IL-poor aqueous phases. Conditions: Capillary tube, 110 cm total length of 75 μm i.d. fused-silica; solution composition, (No. 5) $[C_4mim]Cl:KOH$, 24.0:20.0 wt/wt% and (No. 6) 18.4:24.0; flow rate, 1.0 $\mu L min^{-1}$ for No. 5 and 3.0 $\mu L min^{-1}$ for No. 6.

13.3 TRDP created with an aqueous non-ionic surfactant mixed solution

A new type of tube radial distribution phenomenon was observed in an aqueous micellar solution of non-ionic surfactant that was fed into a microspace. A homogeneous aqueous solution containing 2 wt% Triton X-100 and 2.0 M sodium chloride was fed into a microchannel (40 μm in depth and 200 μm in width) in a microchip at a flow rate of 4.0 $\mu\text{L min}^{-1}$, where the microchip was maintained at a temperature of 34 $^{\circ}\text{C}$. The homogeneous aqueous solution changed to a heterogeneous solution with two phases in the microchannel; the surfactant-rich phase was generated around the middle of the channel, while the aqueous phase merely containing the surfactant was formed near the inner wall. The radial distribution of the surfactant was observed through Rhodamine B dissolved in the aqueous micellar solution with a bright-field microscope-CCD camera system. An open-tubular capillary chromatographic system was also tried to develop using the fused-silica capillary tube (75 μm inner diameter and 120 cm length) as a separation column and the aqueous micellar solution as a carrier.

Introduction

Since the last century, phase separation in aqueous polymer or micellar solutions has been well known in the field of analytical chemistry and separation science [6-10,20]. Aqueous micellar solutions of some non-ionic surfactants separate into two distinct phases when heated above a certain temperature (clouding point), that is, a temperature-induced phase separation occurs [6-10]. One phase is an almost micelle-free aqueous solution (aqueous phase), while the other phase is a concentrated surfactant solution containing considerable amounts of water (surfactant-rich phase). Hydrophobic compounds that are solubilized in the aqueous micellar solution are extracted into the surfactant-rich phase, while hydrophilic compounds remain in the aqueous phase.

Here, an aqueous micellar solution of non-ionic surfactant that showed phase separation as mentioned above was fed into a microspace to explore a new type of TRDP that was not used with the ternary mixed solvents of water-hydrophilic/hydrophobic organic solvents. The tube radial distribution of the surfactant was successfully observed in the microchannel in a microchip and the capillary tube, indicating the kinetic liquid-liquid interface. We also tried to develop an open-tubular capillary chromatographic system, i.e., TRDC, using the fused-silica capillary tube as a separation column and the aqueous micellar solution as a carrier.

Experimental

Materials A microchip incorporating a straight-line microchannel (40 μm deep and 200 μm wide) was manufactured with Microchemical Technology (Kanagawa, Japan). The microchip was set up in a microchip holder. A fused-silica capillary tube (75 μm

inner diameter and 150 μm outer diameter) was used.

Bright-field microscope-CCD camera system The bright-field microscope-CCD camera system was setup with the microchip or the fused-silica capillary tube. The red dye, Rhodamine B, dissolved in the aqueous micellar solution of 2 wt% Triton X-100 and 2.0 M sodium chloride was observed using the microscope and CCD camera. The microchip or capillary tube was maintained at temperatures of 20 °C and 34 °C on a thermo-heater.

Open-tubular capillary chromatography The open-tubular capillary chromatography comprised mainly the microsyringe pump (Model 11 Single syringe 55-1199; Harvard Apparatus, Inc., Massachusetts, U.S.A), the analyte injector (17.7 nL injection volume) (Chemco Co., Osaka, Japan), the fused-silica capillary tube (150 cm total length and 100 cm effective length), the thermo-heater (20 °C and 34 °C) (Thermo Plate MATS-555RO; Tokai hit Co., Shizuoka, Japan), and the fluorescence detector (ex. 290 nm and em. 355 nm) (Fig. 1). An aqueous solution containing 2 wt% Triton X-100 and 2.0 M sodium chloride was used as a carrier solution. Model analyte solution of 1-naphthol and 2,6-naphthalenedisulfonic acid (1 mM each) that was prepared with the carrier solution was fed into the capillary tube at a flow rate of 2 $\mu\text{L min}^{-1}$.

Results and discussion

Phase diagram of aqueous micellar solution Clouding points of an aqueous solution containing 2 wt% Triton X-100 as a non-ionic surfactant were examined through inspection with various concentrations of sodium chloride, 0–3.0 M. The obtained data is shown in Fig. 2. The homogeneous and transparent solution at 20 °C changed through a clouding point to the heterogeneous solution including the two phases, the aqueous phase and the surfactant-rich suspension phase. The clouding points gradually decreased from 65 °C to 25 °C with increasing of sodium chloride concentration from 0 to 3.0 M as shown in Fig. 2.

Tube radial distribution of aqueous micellar solution in a microchannel A homogeneous aqueous solution containing 2 wt% Triton X-100 and 2.0 M sodium chloride possessed a clouding point at 34 °C as indicated in Fig. 2. The homogeneous solution that also included 5 mM Rhodamine B was fed into the microchannel in a microchip at a flow rate of 4 $\mu\text{L min}^{-1}$ under laminar flow conditions, where the microchip was maintained at temperatures of 20 °C or 34 °C. The bright-field photographs of the aqueous micellar solution were examined with the microscope-CCD camera system. The obtained photographs are shown in Fig. 3. At a temperature of 20 °C, which was under the clouding point, the homogeneous red solution due to Rhodamine B was observed at a flow rate of 4 $\mu\text{L min}^{-1}$. That is, the distribution of the surfactant in the microchip was not observed at a temperature of 20 °C (Fig. 3 a)). At a temperature of 34 °C and a flow rate of 4 $\mu\text{L min}^{-1}$, the solution phase containing the

surfactant was generated around the middle of the microchannel as an inner phase (the surfactant-rich phase) and the solution phase not containing the surfactant was formed near the inner wall as an outer phase (the aqueous phase) (Fig. 3 b)). Rhodamine B dissolved in the solution was distributed in the surfactant-rich phase (red) [21]. The homogeneous aqueous solution containing 2 wt% Triton X-100 and 2.0 M sodium chloride with a clouding point of 34 °C must bring about phase transformation to the heterogeneous solution with the aqueous phase and the surfactant-rich phase through the microchannel, the temperature of which was controlled at 34 °C.

Tube radial distribution of aqueous micellar solution under various conditions

Figure 4 shows the photographs of aqueous solution containing 2 wt% Triton X-100 and 2.0 M sodium chloride at 33 - 36 °C at various flow rates of 0.8 – 8.0 $\mu\text{L min}^{-1}$. The microchannel was suitable to the microscope observation because of the rectangle cross-section. At 33 °C, which was under the clouding point, the aqueous solution containing Rhodamine B indicated homogeneous red solution under all conditions. On the other hand, at 34, 35 and 36 °C, which were just over the clouding point, the TRDP was observed at 0.8 – 4.0 , 0.8 – 8.0, and 3.2 – 8.0 $\mu\text{L min}^{-1}$, respectively, although it was difficult to clearly distinguish between TRDP and non-TRDP in photograph observation. In the TRDP, the solution phase containing most of the surfactant was generated around the middle of the microchannel as an inner phase (the surfactant-rich phase) and the solution phase containing a small amount of the surfactant was formed near the inner wall as an outer phase.

Tube radial distribution of aqueous micellar solution in a capillary tube

The distribution of the surfactant and Rhodamine B in the aqueous solution containing 2 wt% Triton X-100 and 2.0 M sodium chloride was also observed in the capillary tube under and over the clouding point. The photographs are shown in Fig. 5; the TRDP is not observed at 20 °C and observed at 34 °C. The microfluidic flow in the capillary tube at 34 °C where gravity has little effect must produce a specific radial distribution of the surfactant featuring the surfactant-rich inner phase and the aqueous outer phase similar to that in the microchannels of a microchip. We developed a new type of TRDP, i.e., the kinetic liquid-liquid interface, in the capillary tube, by delivery of an aqueous micellar solution of non-ionic surfactant, Triton X-100, together with sodium chloride. Temperature control regarding the clouding point played an important role in the present TRDP using an aqueous micellar solution. The previous TRDP using ternary mixed solvents of water-hydrophilic/hydrophobic organic mixtures have been examined from the viewpoints of chromatography (TRDC), extraction (TRDE), mixing (TRDM), and as chemical reaction space (TRDR). The findings with the new TRDP of the aqueous micellar solution will lead to the further development of both fundamentals and applications of TRDP and related technologies, such as TRDC, TRDE, TRDM, and TRDR.

Open-tubular capillary chromatography Tentatively, we tried to develop the TRDC system using the fused-silica capillary tube as a separation column and the aqueous micellar solution containing 2 wt% Triton X-100 and 2.0 M sodium chloride as a carrier. Hydrophobic 1-naphthol and hydrophilic 2,6-naphthalenedisulfonic acid as a model mixture was subjected to the present TRDC system (Fig. 1). The obtained chromatograms are shown in Fig. 6. They were not separated at a tube temperature of 20 °C, while, they were separated and detected in this order at a tube temperature of 34 °C. The elution order was reasonable because of the distribution of the aqueous micellar solution generating the surfactant-rich inner phase (hydrophobic) and the surfactant-light outer phase (hydrophilic). The two peaks were identified with individual analyte analysis, although they did not show baseline separation under the present conditions.

In conclusion, a new type of TRDP was successfully created by feeding the aqueous micellar solution (containing 2 wt% Triton X-100 and 2.0 M sodium chloride) into the microspace over the clouding point. The TRDP generated the surfactant-rich inner phase and the surfactant-little outer phase. The TRDC system was also developed based on the TRDP. The new type of TRDP supported our consideration that the TRDP is generally caused through phase transformation from homogeneous to heterogeneous (including two phases) with some changes in pressure and/or temperature in a microspace.

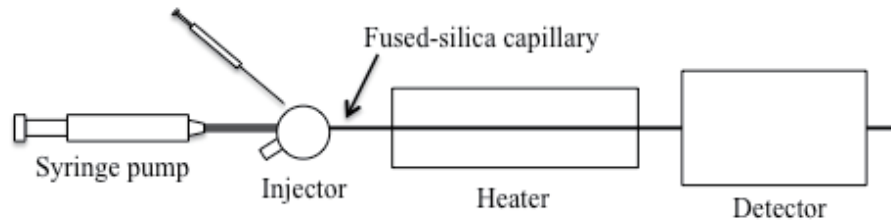


Figure 1. Schematic diagram of an open-tubular capillary chromatography.

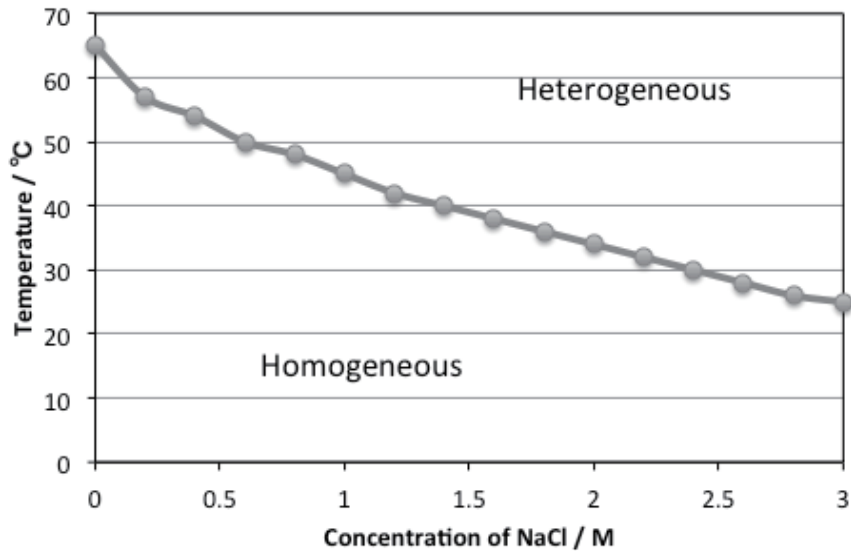


Figure 2. Phase diagram of an aqueous micellar solution containing sodium chloride. The solubility curve is constructed along the clouding points. The concentration of Triton X-100 is 2.0 wt%.

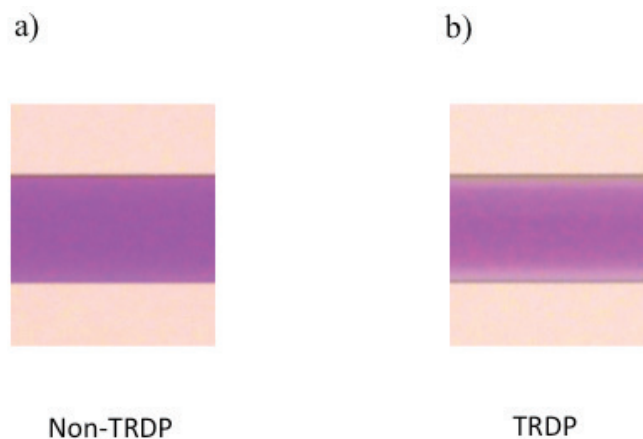


Figure 3. Bright-field photographs in a microchannel. a) 20 °C and b) 34 °C. The homogeneous aqueous solution containing 2 wt% Triton X-100, 2.0 M sodium chloride, and 5 mM Rhodamine B was fed at a flow rate of 4 $\mu\text{L min}^{-1}$ into the microchannel.

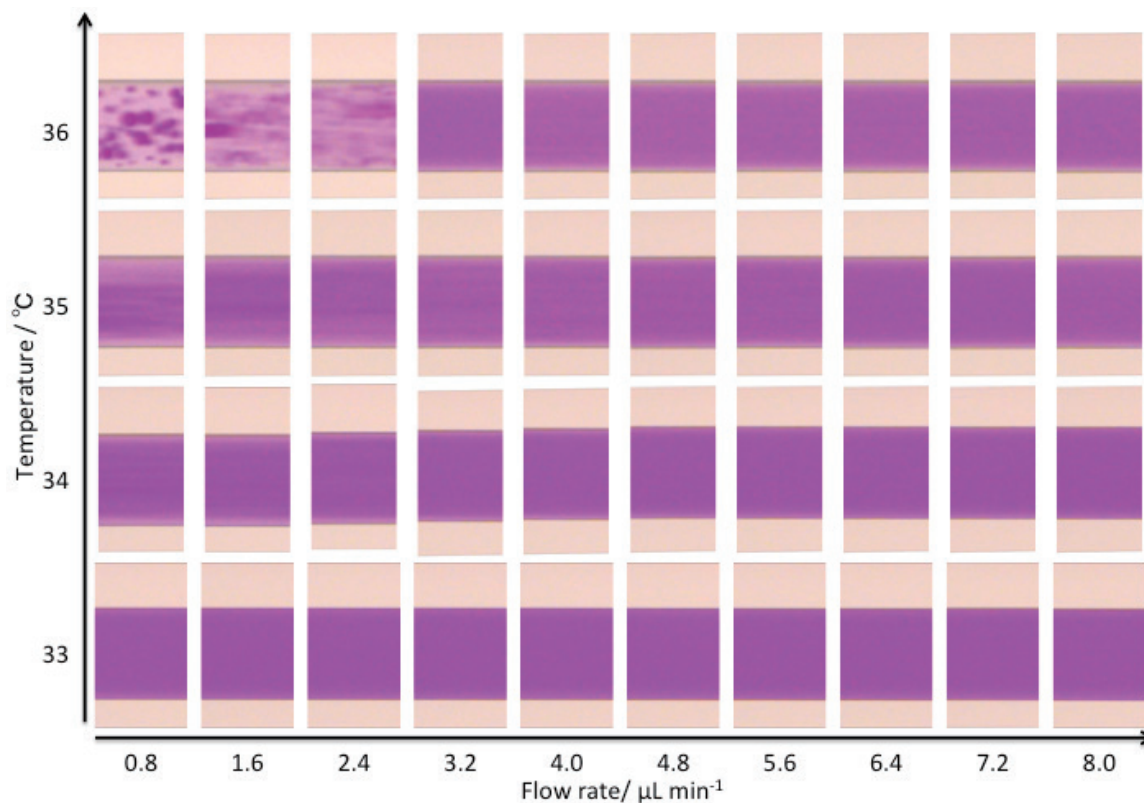


Figure 4. Bright-field photographs under various conditions. The temperature of 33 - 36 °C and the flow rates of 0.8 – 8.0 $\mu\text{L min}^{-1}$. The homogeneous aqueous solution containing 2 wt% Triton X-100, 2.0 M sodium chloride, and 5 mM Rhodamine B was fed into the microchannel.

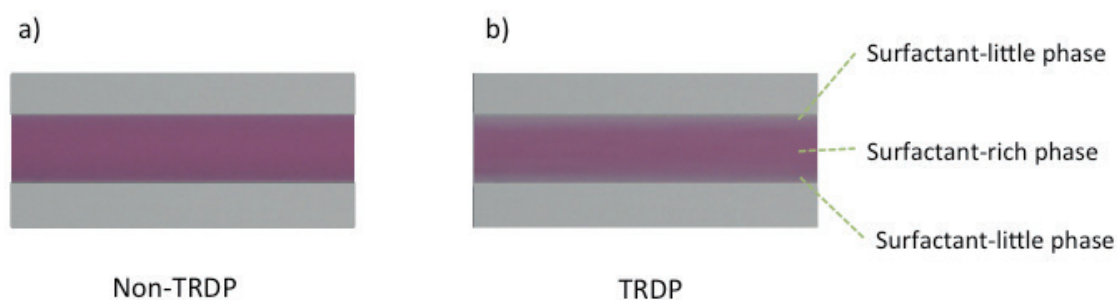


Figure 5. Bright-field photographs in a capillary tube. a) 20 °C and b) 34 °C. The homogeneous aqueous solution containing 2 wt% Triton X-100, 2.0 M sodium chloride, and 5 mM Rhodamine B was fed into the capillary tube (75 μm inner diameter and 120 cm long; the observed point was 100 cm from the inlet) at a flow rate of 2 $\mu\text{L min}^{-1}$.

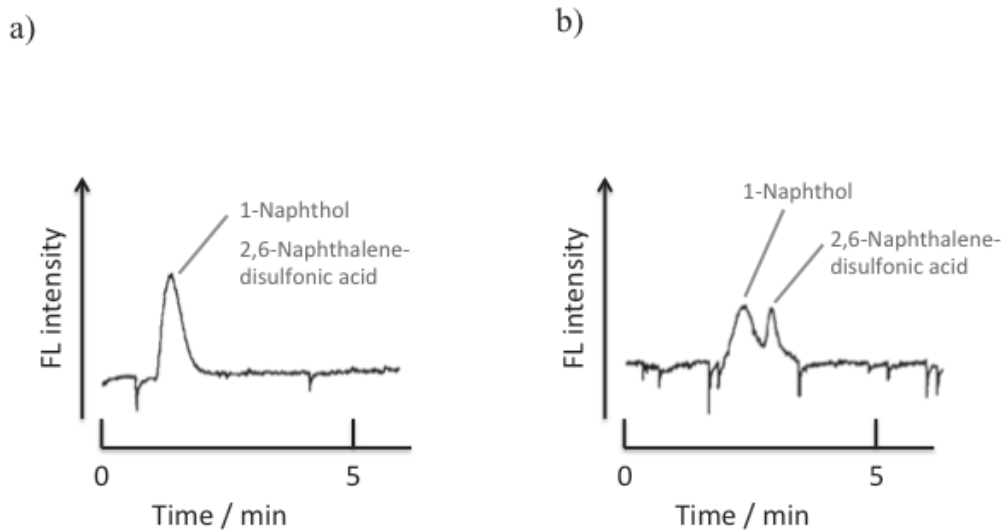


Figure 6. Chromatograms obtained by the present TRDC system. a) 20 °C and b) 34 °C. Capillary, 75 μm inner diameter, 150 cm total length and 100 cm effective length; carrier, aqueous solution containing 2 wt% Triton X-100 and 2.0 M sodium chloride; flow rate, 2 $\mu\text{L min}^{-1}$; and the analyte concentration, 1 mM each.

13.4 TRDP created with a fluorocarbon and hydrocarbon organic solvent mixed solution

A fluorocarbon and hydrocarbon organic solvent mixture is known as a temperature-induced phase-separation solution. When a mixed solution of tetradecafluorohexane as a fluorocarbon organic solvent and hexane as a hydrocarbon organic solvent (e.g., 71:29 volume ratio) was delivered into a capillary tube that was controlled at 10 °C, the tube radial distribution phenomenon (TRDP) of the solvents was clearly observed through fluorescence images of the dye, perylene, dissolved in the mixed solution. The homogeneous mixed solution (single phase) changed to a heterogeneous solution (two phases) with inner tetradecafluorohexane and outer hexane phases in the tube under laminar flow conditions, generating the dynamic liquid-liquid interface. We also tried to apply TRDP to a separation technique for metal compounds. A model analyte mixture, copper(II) and hematin, was separated through the capillary tube, and detected with a chemiluminescence detector in this order within 4 min.

Introduction

An investigation of fluorocarbon organic solvent solutions, or fluorous chemistry, has been reported since seminal work done by Horváth and Rábai in 1994 [11]. Two-phase separation in fluorocarbon and hydrocarbon organic solvent mixed solutions is known in the field of analytical chemistry and separation science [12,13]. Mixed solutions of fluorocarbon-hydrocarbon organic solvents separate into two distinct phases in a batch vessel when cooled below a certain temperature; that is, a temperature-induced phase separation occurs [14]. The lower phase is a fluorocarbon organic solvent phase, while the upper phase is a hydrocarbon organic solvent phase. Based on this two-phase system, liquid-liquid and liquid-solid extractions have been reported using different fluorocarbon organic solvents [15,16,17].

When ternary mixed solvents of water–hydrophilic/hydrophobic organic solvents (e.g., water-acetonitrile-ethyl acetate mixtures) are fed into a microspace, such as glass microchannels or capillary tubes (fused-silica, polyethylene, and PTFE for example) under laminar-flow conditions, the solvent molecules are radially distributed in the microspace. This “tube radial distribution phenomenon” (TRDP) creates inner and outer phases in the microspace, generating a specific dynamic liquid-liquid interface. The interface forms radially with a specific linear velocity in a capillary tube. We have investigated TRDP in the chromatography, extraction, chemical reaction, and mixing processes. The TRDP with the other two-phase separation aqueous solution systems, such as water-surfactant and water-ionic liquid mixed solutions, were also reported in our previous paper. However, these experimental data seemed to be just initial data in the field of the TRDP and related research, because TRDP involves a quite novel microfluidic behavior that has never been investigated. We must continue examining fundamental facts about the TRDP as much as we can. Here, a

fluorocarbon-hydrocarbon organic solvent mixed solution, not an aqueous solution, which showed two-phase separation in a batch vessel, was fed into a capillary tube to explore the TRDP, for the first time. The finding here is that it is important to know the TRDP capacity, and to expand the related technology.

Experimental

Reagents Tetradecafluorohexane (C_6F_{14} ; M_w 338.04 and density 1.67 g cm^{-3}) as a model fluorocarbon organic solvent and hexane (C_6H_{14} ; M_w 86.18 and density 0.66 g cm^{-3}) as a model hydrocarbon organic solvent were used. Also, cobalt(II) sulfate (Co(II)), copper(II) sulfate (Cu(II)), and hematin were used.

Fluorescence microscope-CCD camera system A fused-silica capillary tube ($75\text{ }\mu\text{m}$ inner diameter and $150\text{ }\mu\text{m}$ outer diameter) was used. A fluorescence microscope-CCD camera with a fused-silica capillary tube (100 cm total length) was set up. Capillary tube observations were monitored at a length of 80 cm from the inlet using a fluorescence microscope equipped with an Hg lamp and a filter. Blue fluorescence photographs were obtained because perylene emits light at 470 nm . The capillary tube used for observation was maintained at a temperature of $10\text{ }^\circ\text{C}$ with a thermo-controller (MATS-555RO; Tokai Hit Co., Shizuoka, Japan).

Separation system of metal compounds using an open-tubular capillary tube The microspace separation system of metal compounds was developed using an open-tubular capillary tube (100 cm length), a microsyringe pump, and a batch-type chemiluminescence (CL) detection cell. The mixed solution of tetradecafluorohexane and hexane ($71:29$ volume ratio) containing $50\text{ }\mu\text{M}$ luminol as a carrier solution was delivered into the tube at $1.8\text{ }\mu\text{L min}^{-1}$. The oxidant solution (40 mM hydrogen peroxide dissolved in 10 mM carbonate buffer solution, $\text{pH } 10.8$) was put in a CL detection cell equipped with an optical fiber [22]. The analyte solutions were prepared with the carbonate buffer solution-acetonitrile ($1:2$ volume ratio) and introduced directly into the capillary inlet side by the gravity method (from 20 cm height and for 20 s). The analytes, metal compounds, having catalytic activity for the luminol-hydrogen peroxide CL reaction, were mixed with the CL reagents at the tip of the capillary outlet in the cell to generate CL light. The CL was detected with the photomultiplier tube (PMT) (H5783-20, Hamamatsu Photonics K. K., Shizuoka, Japan).

Results and discussion

Phase diagram Tetradecafluorohexane-hexane mixture is a fluorocarbon-hydrocarbon organic solvent mixed solution; its phase-separation temperature is under ca. $30\text{ }^\circ\text{C}$ [14]. The phase diagram shown in Fig. 1, was constructed for varying the tetradecafluorohexane mole fractions. The curve in the diagram marks the boundary between homogeneous (single phase) and heterogeneous (two phases) solutions. The tetradecafluorohexane-hexane mixed homogeneous

solutions Nos. 1 – 9 in Fig. 1 were investigated. The heterogeneous solution includes two phases: the lower tetradecafluorohexane and upper hexane phases in a batch vessel. For example, the 0.36 mole fraction tetradecafluorohexane-hexane solvent mixed solution (No. 4) was cooled from 30 to 10 °C. Phase separation occurred at 10 °C, generating an upper hexane phase (blue solution with perylene) and a lower tetradecafluorohexane phase. The lower-to-upper phase volume ratio was estimated to be 8:9. Similarly, the volume ratios of the tetradecafluorohexane to hexane phases in the heterogeneous solutions were (No. 1) 15:65; (No. 2) 29:71, (No. 3) 42:58, (No. 4) 47:53, (No. 5) 50:50, (No. 6) 63:37, (No. 7) 71:29, (No. 8) 78:22, and (No. 9) 80:20. We also examined homogeneous mixtures of octafluorotoluene-toluene and trifluorotoluene-toluene with fluorocarbon organic solvent mole fractions of 0.3, 0.5, and 0.7 in the temperature range of 0 – 20 °C. Under these conditions, no two-phase system was observed. Consequently, in the present work we examined the TRDP in the tetradecafluorohexane-hexane mixture in detail.

TRDP creation The homogeneous tetradecafluorohexane-hexane solvent mixed solutions Nos. 1 - 9 were delivered into a capillary tube at a temperature of 10 °C and at flow rates of 0.5 – 20 $\mu\text{L min}^{-1}$. No tube radial distribution of the solvents was observed for solutions Nos. 1 – 6; the solvents were distributed in the axial direction, as shown in Fig. 2 a). On the other hand, for solutions Nos. 7 – 9 the tube radial distribution of the solvents was clearly observed in the capillary tube at all flow rates. The fluorescence images shown in Fig. 2 b) indicate that the TRDP creates inner major tetradecafluorohexane and outer minor hexane phases; perylene (blue) was dissolved in hexane, but little dissolved in tetradecafluorohexane. Fluorocarbon organic solvent does not mix with hydrocarbon organic solvent or water at a lower temperature. Then, the volume ratios of the two phases in a batch-vessel and a capillary tube at a lower temperature agreed with the mixing ratios of the solvents. Also, the TRDP creation was confirmed in the microchannel (100 μm width and 45 μm depth) on a microchip made of glass. Our TRDP for solutions Nos. 7 – 9 followed the same trend as the TRDP from a ternary mixed solvent solution of the water-acetonitrile-ethyl acetate previously reported; major solvents were distributed around the middle of the tube, whereas minor solvents were distributed near the inner wall, irrespective of whether the carrier solutions were organic solvent-rich or water-rich phases. The linear velocity in the radial face section of the capillary tube under laminar flow conditions is circular, indicating that the inside area of the tube has a lower velocity-change gradient than the outside area; however, the real velocity curve in an aqueous-organic solvent mixed solution may deviate from an ideal velocity curve. Fluidic stabilities based on linear velocity gradients in the radial profiles under laminar flow conditions infer that the major solvents must occupy the inside area instead of the outside area in the capillary tube. Because fluorocarbon organic solvents have high viscosities, stiff structures, and low surface tensions compared with hydrocarbon organic solvents, these specific properties might support TRDP, thus allowing for major inner fluorocarbon organic

solvent phase formation. The fluidic behavior of the TRDP was also in accordance with the viscous–dissipation principle, which postulates that the degree of viscous dissipation is smaller for a given flow rate. Thus, the high-viscosity fluid is located at the core of the tube, away from the inner wall [23-26]. However, why an axial distribution of the solvents occurs for solutions Nos. 1 - 6 has not yet been clarified.

Microspace separation system for metal compounds The retention times of Cu(II), Co(II), and hematin as model metal compounds were examined with the microspace separation system using the fused-silica capillary tube and the mixed solvent solution of tetradecafluorohexane-hexane as a carrier. The analyte solution of each metal compound was fed through the capillary tube and mixed with the reagents at the tip of the capillary outlet to generate CL. The retention times of Cu(II), Co(II), and hematin were 2.2, 2.2, and 2.7 min, respectively. The retention times of Cu(II) and Co(II) were the same; they were delivered with almost the average linear velocity, while, that of hematin was delayed; it was fed with a lower velocity than the average linear velocity. The analytes (Cu(II), Co(II), and hematin) were dissolved in the aqueous and acetonitrile mixture to prepare the analyte solutions. The Cu(II) and Co(II) were not dissolved by either tetradecafluorohexane and hexane, and then they were not distributed to the carrier solution in the capillary tube. The hematin was dissolved in hexane, but not dissolved by the tetradecafluorohexane. It was then distributed to the hexane outer phase in the capillary tube. In the TRDP with the tetradecafluorohexane and hexane mixed solvent, the hexane phase as an outer phase moved with much lower velocity than the average linear velocity which was easily estimated as being a parabolic curve in the tube under laminar flow conditions. Consequently, Cu(II) and Co(II) were eluted with the average linear velocity, followed by the elution of hematin with a lower velocity than the average linear velocity. Tentatively, the mixed analyte solution of Cu(II) and hematin was subjected to the present separation system. The obtained CL separation profile is shown in Fig. 3. They were completely separated; Cu(II) was first detected, and next hematin was detected. The separation in the capillary tube was performed without applying any high-voltage like capillary electrophoresis and using specific columns, such as monolithic and packed ones, like conventional capillary chromatography.

In conclusion, the tube radial distribution phenomenon (TRDP) with a phase-separated solution of a fluorocarbon (tetradecafluorohexane)-hydrocarbon organic solvent (hexane) mixture, for the first time, was successfully observed in a capillary tube under laminar flow conditions. A dynamic liquid-liquid interface between the inner tetradecafluorohexane and the outer hexane phases was generated. The separation system of metal compounds was also developed based on the TRDP with the fluorocarbon-hydrocarbon organic solvent mixed solution. The Cu(II) and hematin as model analytes were separated through the capillary in this order and detected with CL detection. Our findings expand the TRDP concept to investigate microfluidic behaviors,

and indicate the possibility of developing new types of separation technology, such as chromatography, extraction and micro-reaction, using a fluorocarbon-hydrocarbon organic solvent mixed solution in a microspace.

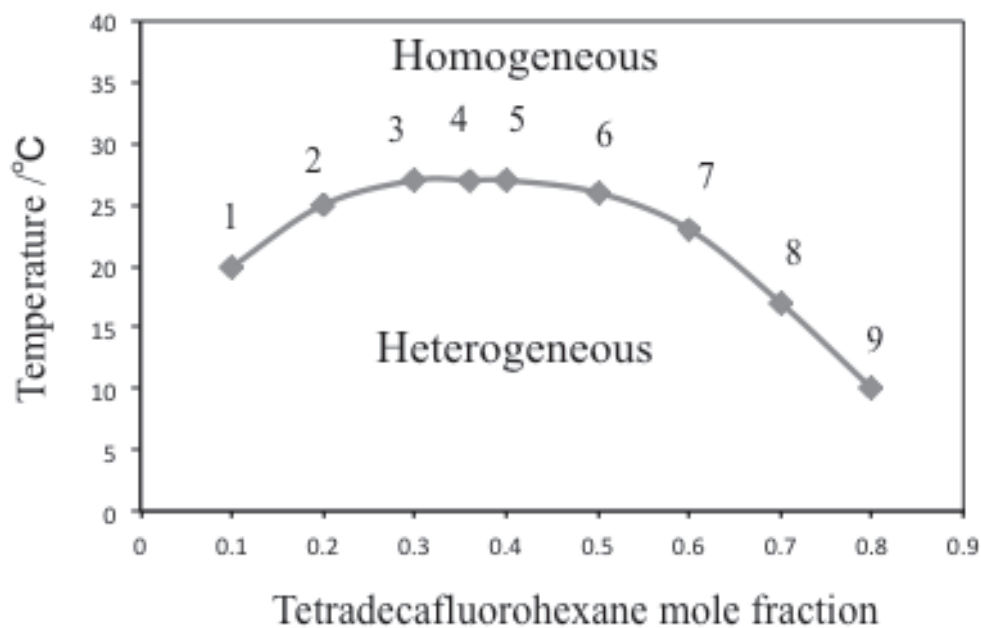


Figure 1. Phase diagram of a tetradecafluorohexane-hexane mixed solution that was examined in a batch vessel.

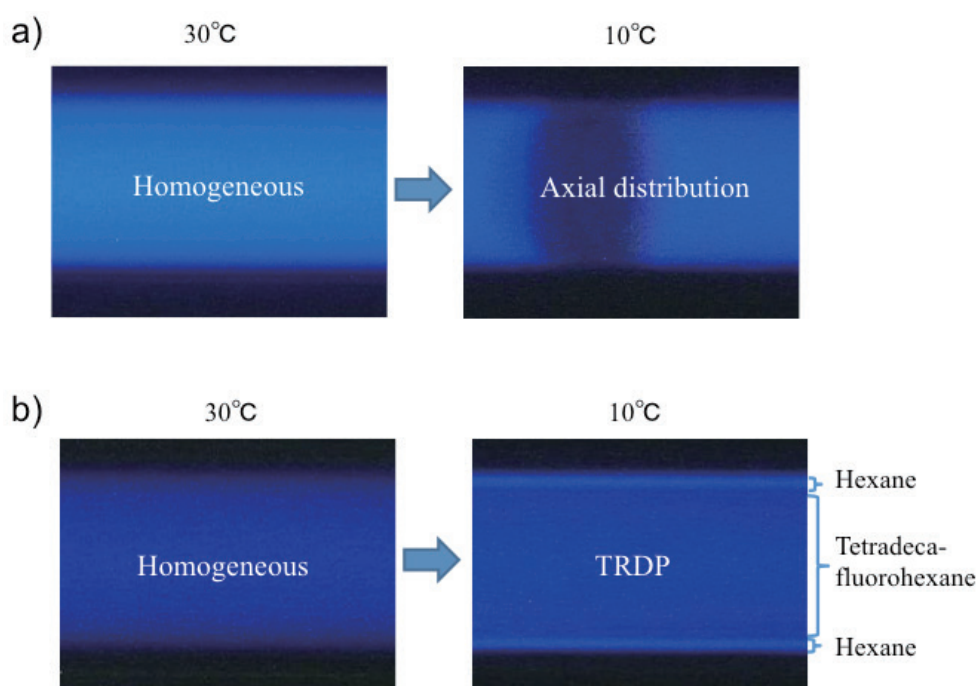


Figure 2. Fluorescence images of the microfluidic behavior of a tetradecafluorohexane-hexane mixed solution. a) Non-TRDP (No. 2 in Fig. 2, tetradecafluorohexane mole fraction 0.2) and b) TRDP (No. 7 in Fig. 2, tetradecafluorohexane mole fraction 0.6). Flow rate $5.0 \mu\text{L min}^{-1}$.

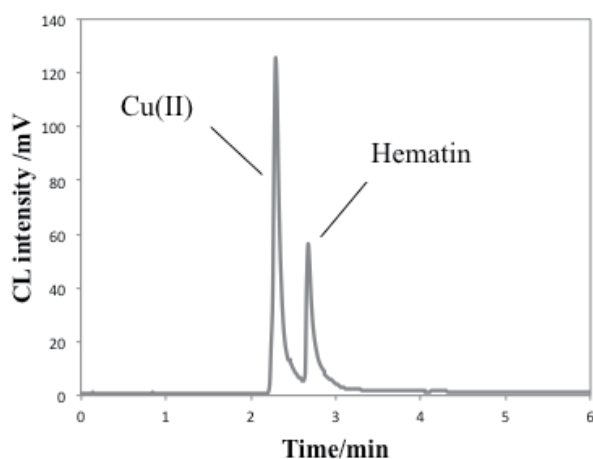


Figure 3. CL separation profile of Cu(II) and hematin.

Conditions: Capillary, fused-silica capillary tube of $75 \mu\text{m}$ inner diameter and 100 cm length; carrier, tetradecafluorohexane and hexane mixture (71:29 volume ratio) containing $50 \mu\text{M}$ luminol; the oxidant solution in the CL detection cell, 40 mM hydrogen peroxide dissolved in 10 mM carbonate buffer solution (pH 10.8); analyte injection, the gravity method (from 20 cm height and for 20 s); flow rate, $1.8 \mu\text{L min}^{-1}$; and metal compound concentration, 4.5 mM Cu(II) and $0.5 \mu\text{M}$ hematin.

13.5 TRDP created with a water-acetonitrile containing sodium chloride mixed solution

Open-tubular capillary chromatography was developed based on tube radial distribution of the water-acetonitrile mixture solvents containing sodium chloride under laminar flow conditions. The specific homogeneous carrier solvents were radially distributed in the capillary tubes, generating inner and outer phases. This distribution behavior was observed with a fluorescence microscope-CCD camera system and considered with the phase diagram constructed with the solvents composition and sodium chloride concentration. Hydrophilic 1-naphthol and hydrophobic 2,6-naphthalenedisulfonic acid as model analytes were separated in this order with the fused-silica capillary tube (100 μm inner diameter), while, in the reverse order with the PTFE capillary tube (100 μm inner diameter). The outer phase created in the capillary tube functioned as a pseudo-stationary phase in chromatography. The mixture solution including five analytes was examined with the present capillary chromatography. The opposite elution order was observed between the fused-silica and PTFE tubes.

Introduction

Until now, the TRDP has been investigated by using the ternary mixed solvents of water-hydrophobic/hydrophilic organic mixtures. The TRDP appears through phase separation from a homogeneous solution to a heterogeneous solution including the two phases with pressure and temperature change. The phase separation with their change makes an upper and lower phase in a vessel under the control of gravity. The phase separation introduces TRDP including inner and outer phases in a micro-flow where it is not under the control of gravity and laminar flow conditions. We were interested in water-acetonitrile mixture solvents. The homogeneous mixture solvents changed to heterogeneous including the two phases by adding sodium chloride (NaCl) in a vessel [27]. An open-tubular capillary chromatography was also reported by using the mixed solvents in the narrow-bored fused-silica tubes of 10 μm inner diameter [28]. Here the water-acetonitrile mixture containing NaCl instead of the water-hydrophobic/hydrophilic organic mixture was, for the first time, examined from the viewpoint of TRDP or TRDC by using wide-bore capillary tubes with fused-silica and PTFE (100 μm inner diameter each).

Experimental

Open-tubular capillary chromatography (TRDC system) Fused-silica and PTFE capillary tubes (100 μm inner diameter) were used. The present capillary chromatography system comprised of an open-tubular capillary tube, microsyringe pump, and absorption detector. The tube temperature was controlled by dipping the capillary tube in water maintained at a definite temperature in a beaker with stirring. Water-acetonitrile mixtures containing NaCl were used as carrier solutions. Analyte

solutions were prepared with the carrier solutions. 1-Naphthol, 1-naphthalenesulfonic acid (1-NS), 2,6-naphthalenedisulfonic acid (2,6-NDS), and 1,3,6-naphthalenetrisulfonic acid (1,3,6-NTS) were used as analytes. The analyte solution was introduced directly into the capillary inlet side by the gravity method (30 cm height \times 30 s; ca. 30 nL). After analyte injection, the capillary inlet was connected through a joint to a microsyringe. The syringe was set on the microsyringe pump. The carrier solution was fed into the capillary tube at a definite flow rate under laminar flow conditions. On-capillary absorption detection (254 nm) was performed with the detector.

Fluorescence microscope equipped with a CCD camera system We set up a capillary tube the same size as that of the TRDC system with absorption detection for the fluorescence microscope-CCD camera system. The tube temperature was controlled with a thermo-plate (MATS-555S, Tokai Hit Co. Ltd.; Shizuoka, Japan). Fluorescence in the capillary tube was monitored at approximately 100 cm from the capillary inlet using a fluorescence microscope equipped with an Hg lamp, a filter and a CCD camera. The carrier solution contained 0.1 mM perylene and 1 mM Eosin Y. We delivered the carrier solution into the capillary tube at a definite flow rate using the microsyringe pump.

Results and discussion

Phase diagram for water-acetonitrile containing NaCl A phase diagram for the water-acetonitrile mixture containing NaCl was examined in a vessel at a temperature of 20 °C. The obtained phase diagram is shown in Fig. 1. The curve in the diagram indicates the boundary between homogeneous and heterogeneous solutions including the two phases. The phase diagram showed that each composition of the solvents and NaCl made a homogeneous (one homogeneous phase) or a heterogeneous (two homogeneous phases) solution. Fluorescence photographs and chromatograms were examined with the solutions possessing compositions of (a) – (g) in the diagram as carrier solutions in the following sections. The compositions of (a) – (g) are noted in the caption of Fig. 1.

Fluorescence photographs and profiles in fused-silica and PTFE capillary tubes The fluorescence photographs and profiles of the fluorescent dyes, hydrophobic perylene (blue) and relatively hydrophilic Eosin Y (green), dissolved in the homogeneous carrier solutions, (a) – (e), were examined with the fluorescence microscope-CCD camera system. As the carrier solutions of (f) and (g) (acetonitrile-rich solution) did not dissolve Eosin Y, they were not used as carrier solutions for the fluorescence observation. With the fused-silica capillary tube the TRDP was observed for the carriers (d) and (e) (acetonitrile-rich solution), partially observed for (c), and not observed for (a) and (b) (water-rich solution) (Fig. 2 A)). The acetonitrile-rich inner

phase (blue) and the water-rich outer phase (green) were generated with the carrier solutions (d) and (e). The water-rich outer phase was suitable to the fused-silica inner wall. On the other hand, with the PTFE capillary tube, the TRDP was observed for the carrier solutions, (a) – (c) (acetonitrile-rich solution) and partially observed for the carriers (d) and (e) (Fig. 2 B)). The water-rich inner phase (green) and the acetonitrile-rich outer phase (blue) were generated with carrier solutions (a) – (e). The acetonitrile-rich outer phase was suitable to the PTFE inner wall.

Chromatograms obtained by using fused-silica and PTFE capillary tubes The chromatograms of hydrophobic 1-naphthol and hydrophilic 2,6-NDS, as model analytes, were examined with the present TRDC system with the homogeneous carrier solutions, (a) – (f). As the carrier solution of (g) (acetonitrile-rich solution) did not dissolve 2,6-NDS, it was not used as a carrier solution. With the fused-silica capillary tube the base-line separation of the analytes was observed for carriers (d), (e), and (f) (acetonitrile-rich solution), splitted separation for the carrier (c), and not separated for the carriers (a) and (b) (water-rich solution) (Fig. 3 A)). The hydrophobic 1-naphthol was first detected and then hydrophilic 2,6-NDS was detected with the carrier solutions of (c) – (f). Because 2,6-NDS was distributed in the outer phase (water-rich) as a pseudo-stationary phase. The separation information was expressed on the phase diagram; the symbols, \circ , Δ , and \times indicated baseline separation, splitted separation, and non-separation, respectively (Fig. 4 A)). Retention factor, theoretical number (EMG, exponential modified Gaussian, method was mainly used), and height of theoretical plate were calculated in the usual manner (Fig. 5 A)). On the other hand, with the PTFE capillary tube the baseline separation was observed for carrier (a) - (d), not separated for (e) and (f) (Fig. 3 B)). In this case the hydrophilic 2,6-NDS was first detected, followed by hydrophobic 1-naphthol detection with the carrier solutions of (a) – (d). Because 1-naphthol was distributed in the outer phase (acetonitrile-rich). The separation information was expressed on the phase diagram with the symbols, \circ and \times , respectively (Fig. 4 B)). Retention factor, theoretical number, and height of theoretical plate were calculated in the usual manner (Fig. 5 B)). The chromatographic data shown in Fig. 3 were well consistent with the fluorescent photographic ones shown in Fig. 2. The coincidence was also reasonable for the separation concept of the TRDC.

Effects of tube temperature on fluorescence photographs A phase diagram for the water-acetonitrile mixture containing NaCl was examined in a vessel at a tube temperature of 0 °C. The obtained phase diagram is shown in Fig. 6 together with that obtained at 20 °C. The curves at a tube temperature of 0 °C in the diagram also indicate the boundary between homogeneous and heterogeneous solutions. The compositions of (a') – (g') are noted in the caption of Fig. 6. Fluorescence photographs were further examined with the solutions possessing compositions of (h) – (n) in the diagram as carrier solutions at a tube temperature of 20 °C. The plots of (h) – (n) are shown in Fig. 7 and the compositions of the homogeneous solutions are noted in the caption of Fig. 7;

they are water-acetonitrile mixture (3 : 7 volume ratio) containing 0.129 – 0.0096 M NaCl. As the solution of water-acetonitrile mixture (3 : 7 volume ratio) containing 0.129 M NaCl created the TRDP and showed separation performance with the fused-silica capillary tube but did not with the PTFE capillary tube at a tube temperature of 20 °C as shown in Figs. 2-4, the fused-silica capillary tube was used in the following experiments. First, with the fused-silica capillary tube the TRDP was observed for the carrier solution (h) and not observed for the carrier solutions (i) – (n) (Fig. 8 A)) at a tube temperature of 20 °C. The acetonitrile-rich inner phase (blue) and the water-rich outer phase (green) were generated with the carrier solution (h). The water-rich outer phase was suitable to the fused-silica inner wall. Subsequently, at a tube temperature of 0 °C instead of 20 °C with the same fused-silica capillary tube the TRDP was observed for the carrier solutions (h) - (k), partially observed for the carrier (l), and not observed for the carriers (m) and (n) (Fig. 8 B)). The acetonitrile-rich inner phase (blue) and the water-rich outer phase (green) were generated with the carrier solutions (h) - (k). The water-rich outer phase was suitable to the fused-silica inner wall. The phase separation easily occurred from homogeneous solution to heterogeneous solution at 0 °C to lead the TRDP observation compared to 20 °C. The results were well consistent with the phase diagram of 0 and 20 °C shown in Fig. 7.

Effects of tube temperature on chromatograms The chromatograms of hydrophobic 1-naphthol and hydrophilic 2,6-NDS, as model analytes, were examined with the present TRDC system with the homogeneous carrier solutions, (h) – (n), at a tube temperature of 20 °C. With the fused-silica capillary tube the base-line separation was observed for the carrier (h) and not separated for the carriers (i) - (n) (Fig. 9 A)). The hydrophobic 1-naphthol was first detected and then hydrophilic 2,6-NDS was detected with the carrier. Because 2,6-NDS was distributed in the outer phase in the tube. The separation information was expressed on the phase diagram with the symbols of \circ and \times (Fig. 10 A)). On the other hand, at a tube temperature of 0 °C instead of 20 °C the baseline separation was observed for the homogeneous carrier solutions (h) - (m), not separated for the carrier (n) (Fig. 9 B)). The hydrophobic 1-naphthol was first detected, followed by hydrophilic 2,6-NDS detection with the carrier solutions of (h) – (m). The separation information was expressed on the phase diagram with the symbols, \circ and \times , respectively (Fig. 10 B)). The carrier solution (m) did not show the TRDP at the observation point (at 20 cm from the capillary outlet) in Fig. 8 B)), but the TRDP might be created, at least partially, in other parts of the capillary tube which were far away from the capillary outlet and were exposed with higher pressure. The phase separation easily occurred from homogeneous solution to heterogeneous solution at 0 °C to lead the TRDC separation compared to 20 °C. The results were well consistent with the phase diagram of 0 and 20 °C as shown in Fig. 7.

Separation of mixture solution including five analytes We examined a mixture analyte solution of 1-naphthol, Eosin Y, 1-NS, 2,6-NDS, and 1,3,6-NTS using the

present TRDC system with the fused-silica and PTFE capillary tubes. The obtained chromatograms are shown in Fig. 11 together with the analytical conditions. The elution times of the analytes were reversed when using the fused-silica and the PTFE tubes in the TRDC system. 1-Naphthol, Eosin Y, 1-NS, 2,6-NDS, and 1,3,6-NTS were eluted in this order with the fused-silica capillary tube and water-acetonitrile (3 : 7 volume ratio) containing 0.129 M NaCl carrier solution (Fig. 11 A)), although Eosin Y and 1-NS were not separated with baseline. The elution order seemed to be consistent with the hydrophilic or hydrophobic character of the analytes. With the PTFE capillary tube and water-acetonitrile (7 : 3 volume ratio) containing 1.23 M NaCl carrier solution, the comparatively hydrophilic compounds 1-NS, 2,6-NDS, and 1,3,6-NTS were not separated but were eluted together with almost average linear velocity, while the hydrophobic compounds Eosin Y and 1-naphthol were eluted in this order with velocity smaller than the average linear velocity (Fig. 11 B)), indicating a reverse elution order compared to that of the fused-silica capillary tube.

Difference in the TRDP between ternary water-hydrophilic/hydrophobic Carrier Solvents and Water-Acetonitrile Containing NaCl Carrier Solvents The ternary water-hydrophilic/hydrophobic carrier solutions are classified into two types, organic solvent-rich and the water-rich carrier solutions. The organic solvent-rich solutions generate the organic solvent-rich major inner phase and the water-rich minor outer phase, while, the water-rich solutions form the water-rich major inner phase and the organic solvent-rich minor outer phase. The tube radial distribution of the solvents brings out regardless with the tube materials, such as fused-silica, polyethylene, and PTFE, although the stability of the outer phase is influenced by the tube materials under some cases.²²⁾ On the other hand, in the TRDP with water-acetonitrile containing NaCl the organic solvent-rich carrier solution create the organic solvent-rich major inner phase and the water-rich minor outer phase with the fused-silica capillary tube. The water-rich carrier solution does not create the TRDP with the fused-silica capillary tube at least under the present analytical conditions. The water-rich carrier solution creates the water-rich major inner phase and the organic solvent-rich minor outer phase with the PTFE capillary tube. The organic solvent-rich carrier solution does not create the TRDP with the PTFE capillary tube. Judging from the information of fluorescence images, chromatograms, and phase diagrams, the TRDP with both carrier solutions of the ternary water-hydrophilic/hydrophobic mixture and water-acetonitrile mixture (hydrophilic) containing NaCl must be caused by the phase separation from homogeneous to heterogeneous solution in a microspace or not be influenced by gravity. However, the TRDP with the ternary mixed carrier solvents is little influenced by the inner wall materials in a microspace, while, the TRDP with the water-acetonitrile mixed solvents is influenced by the inner wall materials. The reason has not been clear yet. But, the carrier solvents with or without hydrophobic solvent (ethyl acetate) may play an important role in inner and outer phase generation. In other words, the carrier composition constructed with only water and hydrophilic solvents without hydrophobic

solvents may introduce sensitivity against the inner wall nature into the stable outer phase formation in the TRDP. The above description is consistent with our consideration of the TRDP proposed in our paper. The phase formation in a capillary tube under pressure due to laminar flow is estimated as follows, where it is not under the control of gravity. A specific homogeneous solution with a component ratio near the boundary between homogeneous and heterogeneous in the phase diagram is delivered under laminar flow conditions that produce a constant pressure to the radial face. The homogeneous solution first becomes an emulsion solution that includes minor solvent or tiny droplets. The tiny droplets start to aggregate near the inner wall where the linear velocity is lowest under laminar flow conditions. And then, the mixed solvent solution in a tube changes to a heterogeneous solution that includes a major inner solution and a minor outer solution, where it is not under the control of gravity. From the above viewpoint, the carrier composition constructed with only water and hydrophilic solvents without hydrophobic solvents may be sensitive against the inner wall nature for making an outer phase in the TRDP. That is, in the emulsion mentioned above, tiny water-droplets in a acetonitrile-rich carrier solution are suitable on a fused-silica inner wall to form the outer phase, while, tiny acetonitrile droplets in a water-rich carrier solution is suitable on a PTFE inner wall.

In conclusion, we tried to create the TRDP with water-acetonitrile containing NaCl carrier solution. The fluorescence photographs, chromatograms, and phase diagram information supported TRDP creation in the water-acetonitrile containing NaCl carrier solution through the fused-silica and PTFE capillary tubes. With the fused-silica capillary tube the TRDP created organic solvent-rich major inner and water-rich minor outer phases. With the PTFE capillary tube, water-rich major inner and acetonitrile-rich minor outer phases developed. The outer phase acted as pseudo-stationary phase in the capillary chromatography (TRDC system). 1-Naphthol and 2,6-NDS as model were separated in this order with fused-silica tube and in the reverse order with the PTFE tube. The obtained experimental data expanded concept and application, as well as provided new information in the TRDP and TRDC.

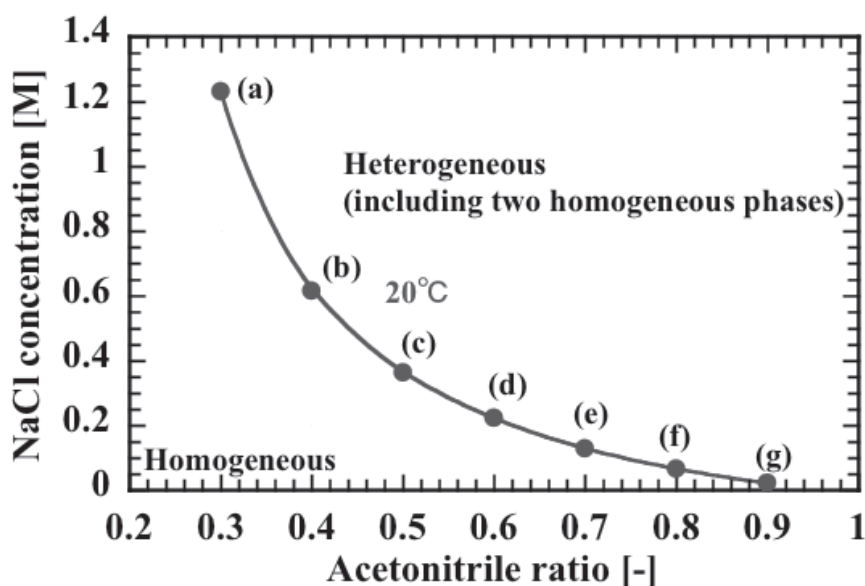


Figure 1. Phase diagrams for the water–acetonitrile containing NaCl mixture solution. The curve in the diagrams indicates the boundary between homogeneous and heterogeneous solutions (including two homogeneous phases). The solvents composition and NaCl concentration for the plots (a) – (g) that provide homogeneous solutions were positioned almost on the homogeneous–heterogeneous solution boundary curve of the phase diagrams. The solvents composition and NaCl concentration for plots (a) – (g) in the diagram are (a) water–acetonitrile of 7 : 3 volume ratio containing 1.23 M NaCl, (b) water–acetonitrile of 6 : 4 volume ratio containing 0.615 M NaCl, (c) water–acetonitrile of 5 : 5 volume ratio containing 0.364 M NaCl, (d) water–acetonitrile of 4 : 6 volume ratio containing 0.222 M NaCl, (e) water–acetonitrile of 3 : 7 volume ratio containing 0.129 M NaCl, (f) water–acetonitrile of 2 : 8 volume ratio containing 0.0667 M NaCl and (g) water–acetonitrile of 1 : 9 volume ratio containing 0.0227 M NaCl.

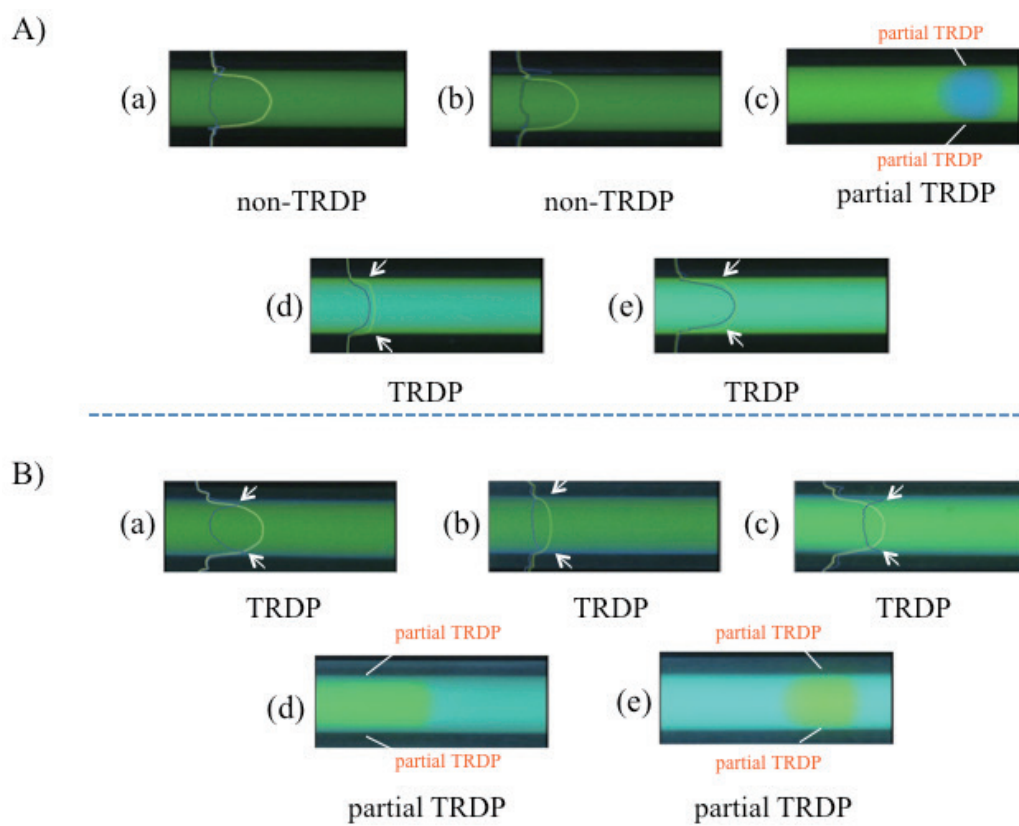


Figure 2. Fluorescence photographs and profiles of the mixture solution dissolved fluorescent dyes. A) Fused-silica and B) PTFE capillary tubes. The arrows point out the inflections on the fluorescence profiles of Eosin Y in fused-silica tube and perylene in PTFE tube. Conditions: Capillary tube, 110 cm (90 cm effective length) of 100 μm i.d.; carrier, water–acetonitrile mixture solution containing NaCl, (a) water–acetonitrile of 7 : 3 volume ratio containing 1.23 M NaCl, (b) water–acetonitrile of 6 : 4 volume ratio containing 0.615 M NaCl, (c) water–acetonitrile of 5 : 5 volume ratio containing 0.364 M NaCl, (d) water–acetonitrile of 4 : 6 volume ratio containing 0.222 M NaCl and (e) water–acetonitrile of 3 : 7 volume ratio containing 0.129 M NaCl; tube temperature, 20 $^{\circ}\text{C}$; flow rate, 0.8 $\mu\text{L min}^{-1}$; and dye concentration, Eosin Y 0.5 mM for (a) and (b), 1 mM for (c) – (e) and perylene 0.1 mM.

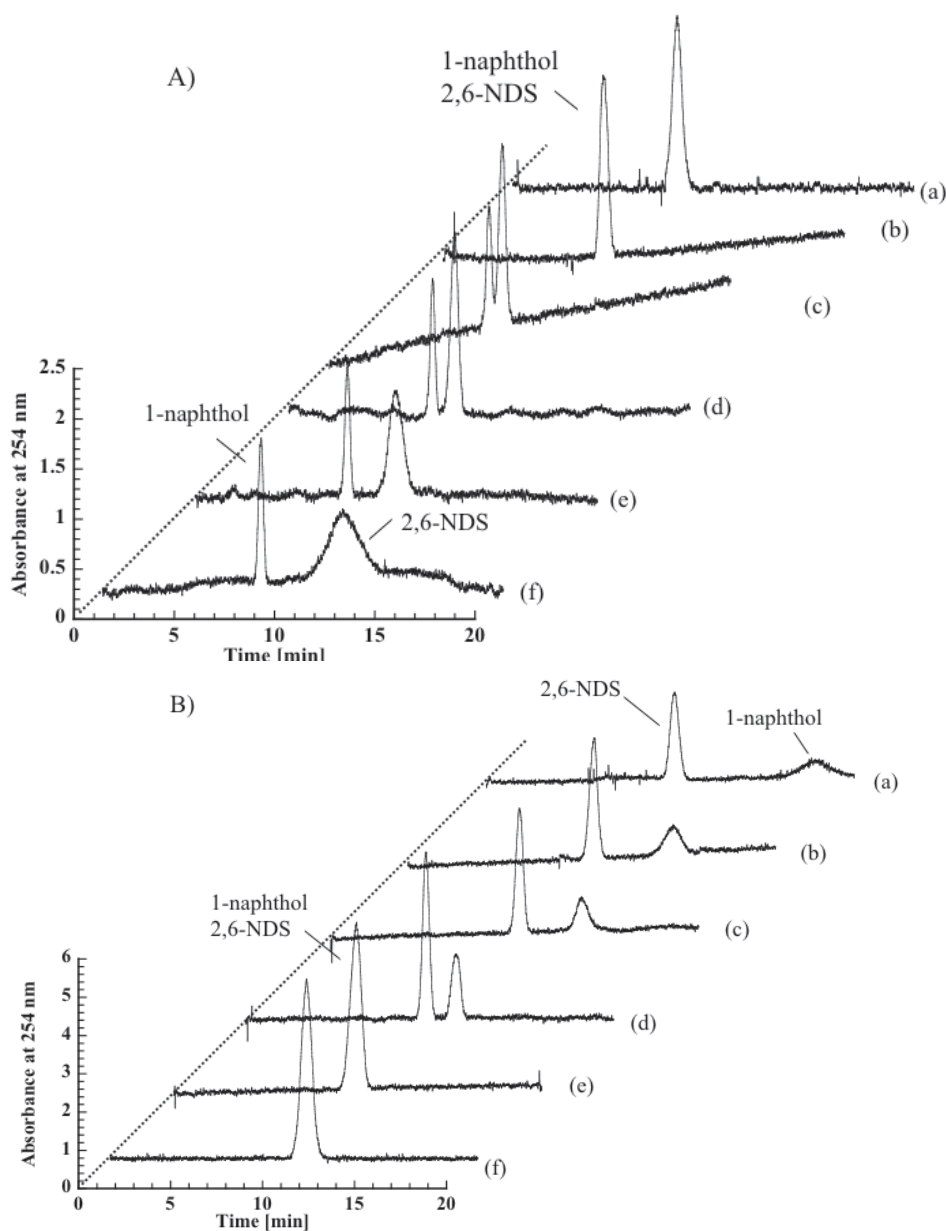


Figure 3. Chromatograms of 1-naphthol and 2,6-NDS. A) Fused-silica and B) PTFE capillary tubes. Conditions: Capillary tube, 110 cm (90 cm effective length) of 100 μm i.d.; carrier, water–acetonitrile mixture solution containing NaCl, (a) water–acetonitrile of 7 : 3 volume ratio containing 1.23 M NaCl, (b) water–acetonitrile of 6 : 4 volume ratio containing 0.615 M NaCl, (c) water–acetonitrile of 5 : 5 volume ratio containing 0.364 M NaCl, (d) water–acetonitrile of 4 : 6 volume ratio containing 0.222 M NaCl, (e) water–acetonitrile of 3 : 7 volume ratio containing 0.129 M NaCl and (f) water–acetonitrile of 2 : 8 volume ratio containing 0.0667 M NaCl; tube temperature, 20 $^{\circ}\text{C}$; sample injection, 30 cm height (gravity) \times 30 s; flow rate, 0.8 $\mu\text{L min}^{-1}$; and analyte concentration, 1-naphthol 1 mM and 2,6-NDS 0.5 mM.

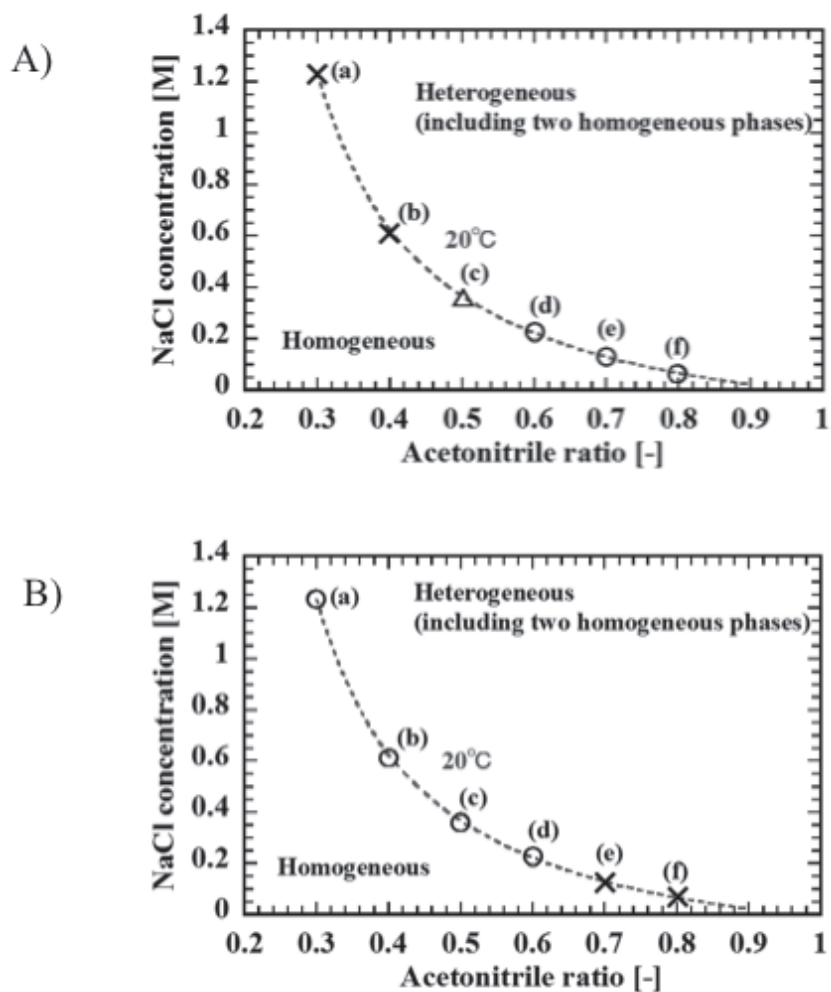
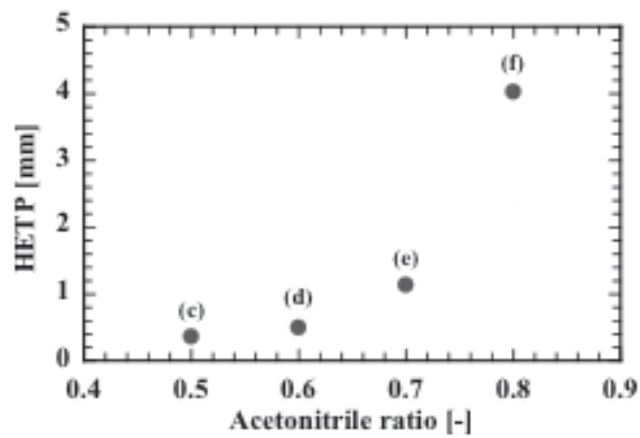
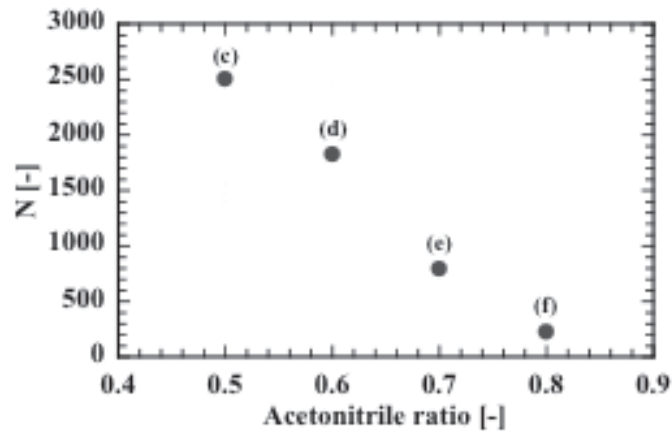
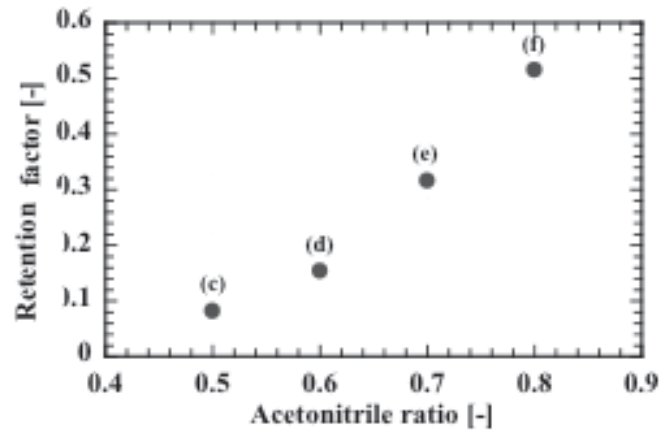


Figure 4. Phase diagram for water-acetonitrile mixture containing NaCl and the solvent composition and NaCl concentration for the chromatograms obtained with the TRDC system. A) Fused-silica and B) PTFE capillary tubes. The curve in the diagram indicates the homogeneous-heterogeneous solution boundary curve. The solvent composition and NaCl concentration of the carrier solvents, (a) – (f), for the chromatograms in Fig. 4 are plotted in the diagram with the symbols \circ , Δ , and \times , to express baseline-separation, split-separation, and non-separation, respectively, for the analytes.

A)



B)

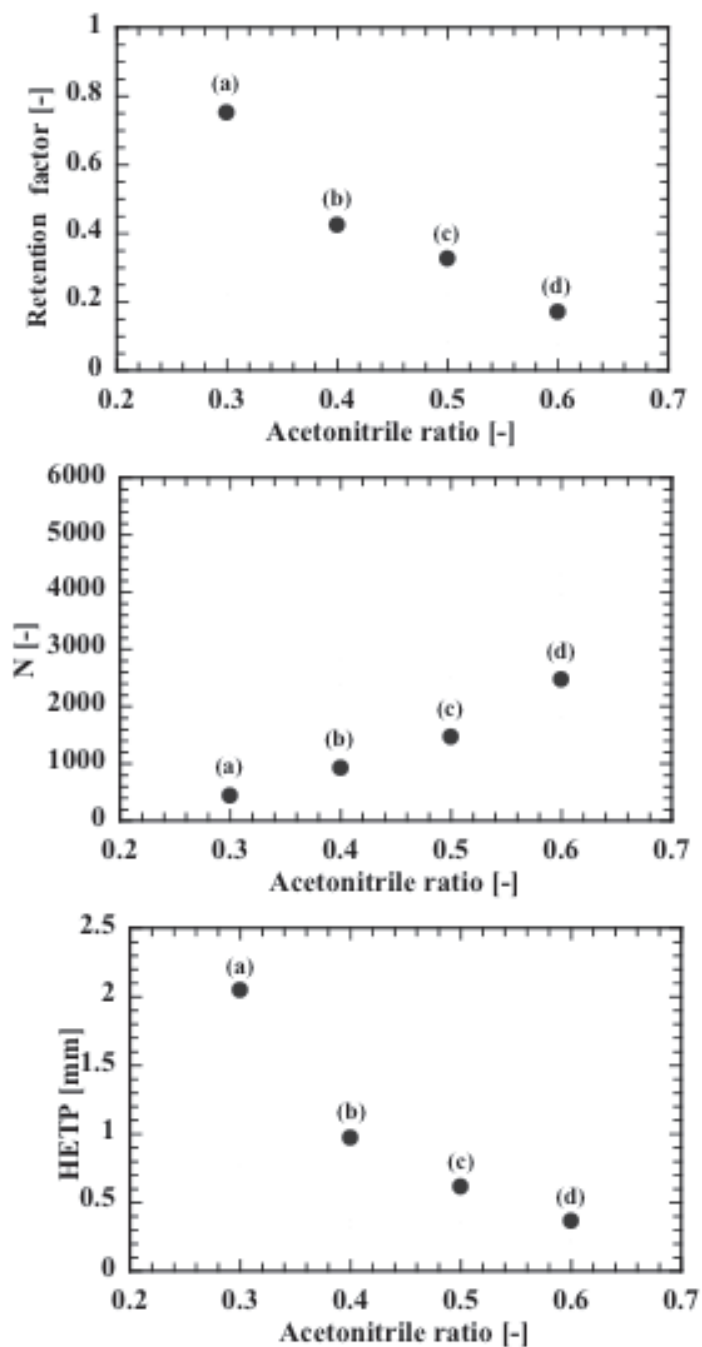


Figure 5. Retention factor, theoretical plate number (N), and height equivalent to the theoretical plate ($HETP$). A) Fused-silica and B) PTFE capillary tubes. They are calculated with the chromatographic data in Fig. 4 in the usual manner.

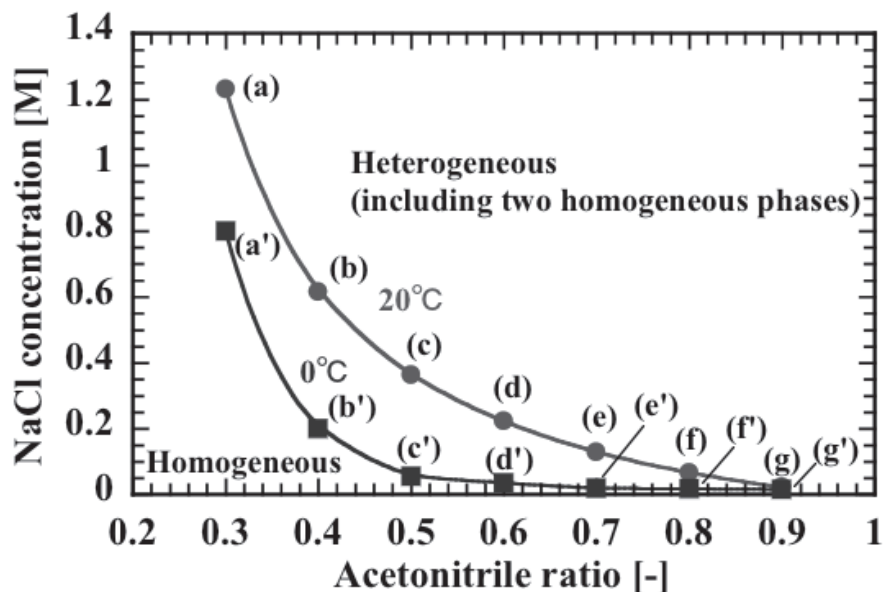


Figure 6. Phase diagrams for the water–acetonitrile containing NaCl mixture solution at 0 and 20 °C. The curves in the diagrams indicate the boundary between homogeneous and heterogeneous solutions (including two homogeneous phases) at 0 and 20 °C. The solvents composition and NaCl concentration for the plots (a') – (g') that provide homogeneous solutions were positioned almost on the homogeneous–heterogeneous solution boundary curve of the phase diagrams at 0 °C. The solvents composition and NaCl concentration for the plots (a') – (g') in the diagram are (a') water–acetonitrile of 7 : 3 volume ratio containing 0.800 M NaCl, (b') water–acetonitrile of 6 : 4 volume ratio containing 0.200 M NaCl, (c') water–acetonitrile of 5 : 5 volume ratio containing 0.0556 M NaCl, (d') water–acetonitrile of 4 : 6 volume ratio containing 0.0357 M NaCl, (e') water–acetonitrile of 3 : 7 volume ratio containing 0.0192 M NaCl, (f') water–acetonitrile of 2 : 8 volume ratio containing 0.0179 M NaCl and (g') water–acetonitrile of 1 : 9 volume ratio containing 0.0156 M NaCl.

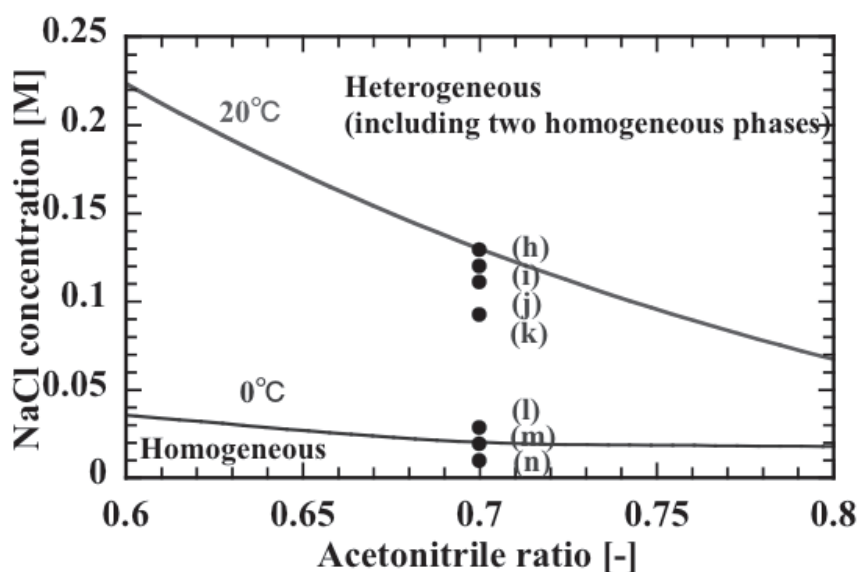


Figure 7. Enlargement of phase diagrams for the water–acetonitrile containing NaCl mixture solution at 0 and 20 °C around the mixtures of (e) and (e’). The curves in the diagrams indicate the boundary between homogeneous and heterogeneous solutions (including two homogeneous phases) at 0 and 20 °C. The solvents composition and NaCl concentration for the plots (h) – (n) that provide homogeneous solutions were positioned around the mixtures of (e) and (e’) of the phase diagrams of Fig. 7. The solvents composition and NaCl concentration for the plots (h) – (n) in the diagram are water–acetonitrile of 7 : 3 volume ratio (h) containing 0.129 M NaCl, (i) containing 0.120 M NaCl, (j) containing 0.111 M NaCl, (k) containing 0.0924M NaCl, (l) containing 0.0284 M NaCl, (m) containing 0.0192 M NaCl and (n) containing 0.0096 M NaCl.

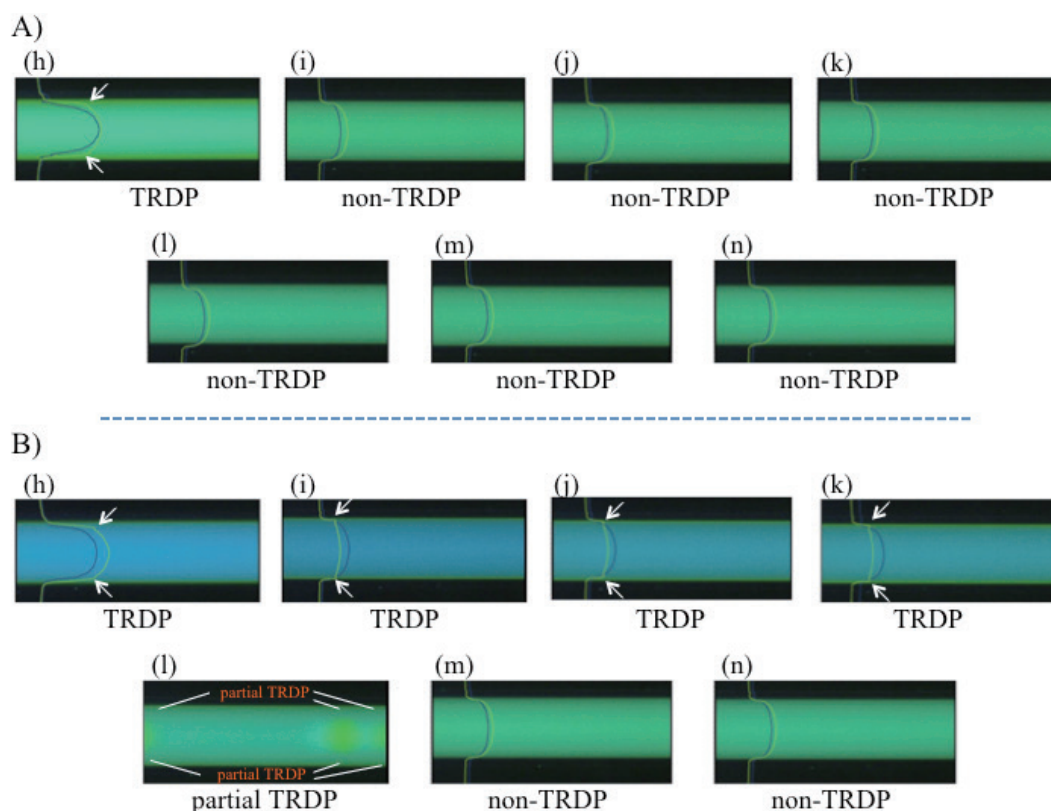


Figure 8. Fluorescence photographs and profiles of the mixture solution dissolved fluorescent dyes in the fused-silica capillary tube. Tube temperature of A) 20 °C and B) 0 °C. The arrows point out the inflections on the fluorescence profiles of Eosin Y in fused-silica tube. Conditions: Capillary tube, 110 cm (90 cm effective length) of 100 μm i.d. fused-silica; carrier, water–acetonitrile mixture solution containing NaCl, water–acetonitrile of 7 : 3 volume ratio (h) containing 0.1290 M NaCl, (i) containing 0.1199 M NaCl, (j) containing 0.1107M NaCl, (k) containing 0.0924M NaCl, (l) containing 0.0284 M NaCl, (m) containing 0.0192 M NaCl and (n) containing 0.0096 M NaCl; flow rate, 0.8 $\mu\text{L min}^{-1}$; and dye concentration, Eosin Y 1 mM and perylene 0.1 mM.

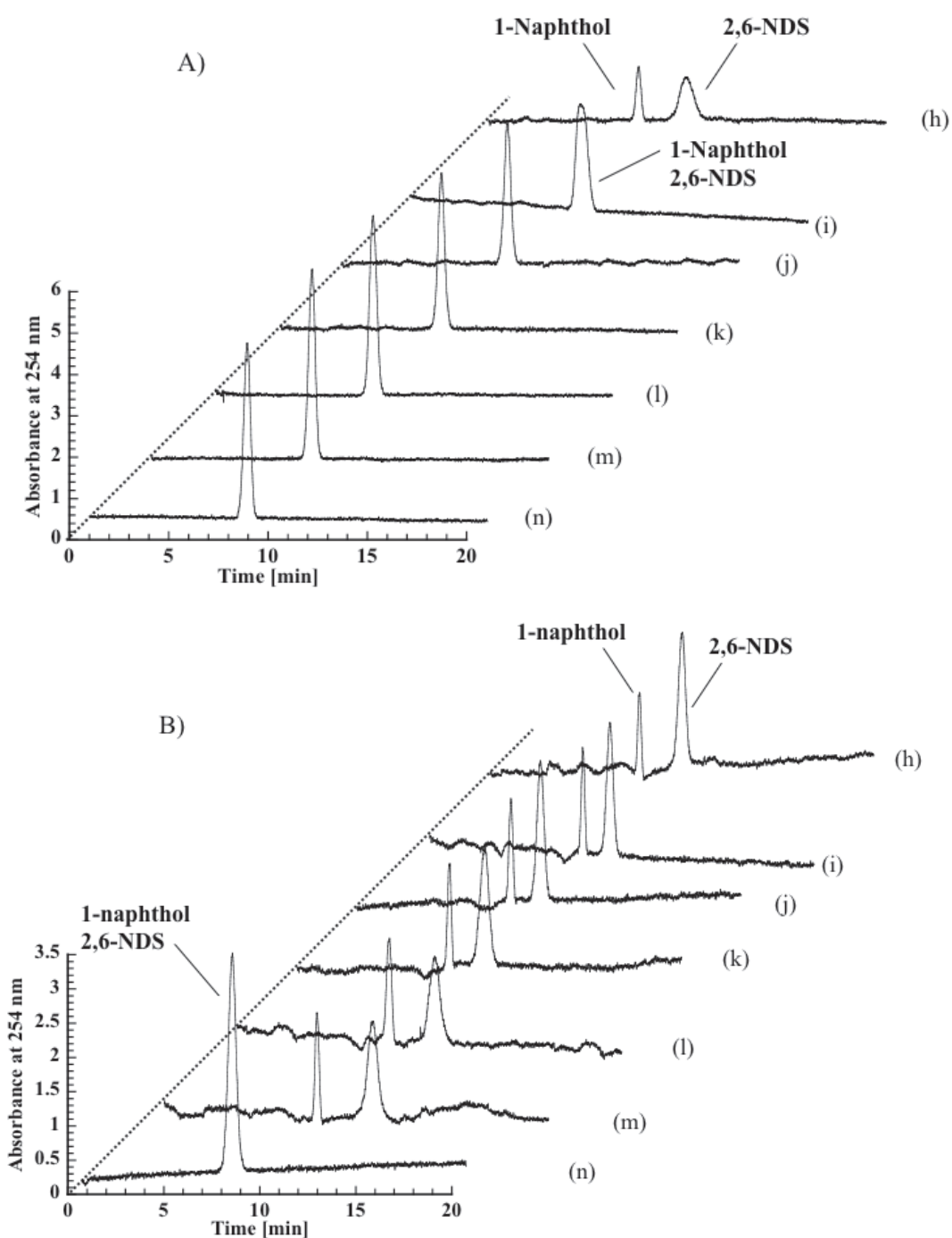


Figure 9. Chromatograms of 1-naphthol and 2,6-NDS. Tube temperature of A) 20 °C and B) 0 °C. Conditions: Capillary tube, 110 cm (90 cm effective length) of 100 μm i.d. fused-silica; carrier, water–acetonitrile mixture solution containing NaCl, water–acetonitrile of 7 : 3 volume ratio (h) containing 0.129 M NaCl, (i) containing 0.120 M NaCl, (j) containing 0.111M NaCl, (k) containing 0.0924M NaCl, (l) containing 0.0284 M NaCl, (m) containing 0.0192 M NaCl and (n) containing 0.0096 M NaCl; sample injection, 30 cm height (gravity) \times 30 s; flow rate, 0.8 $\mu\text{L min}^{-1}$; and analyte concentration, 1-naphtol 1 mM and 2,6-NDS 0.5 mM.

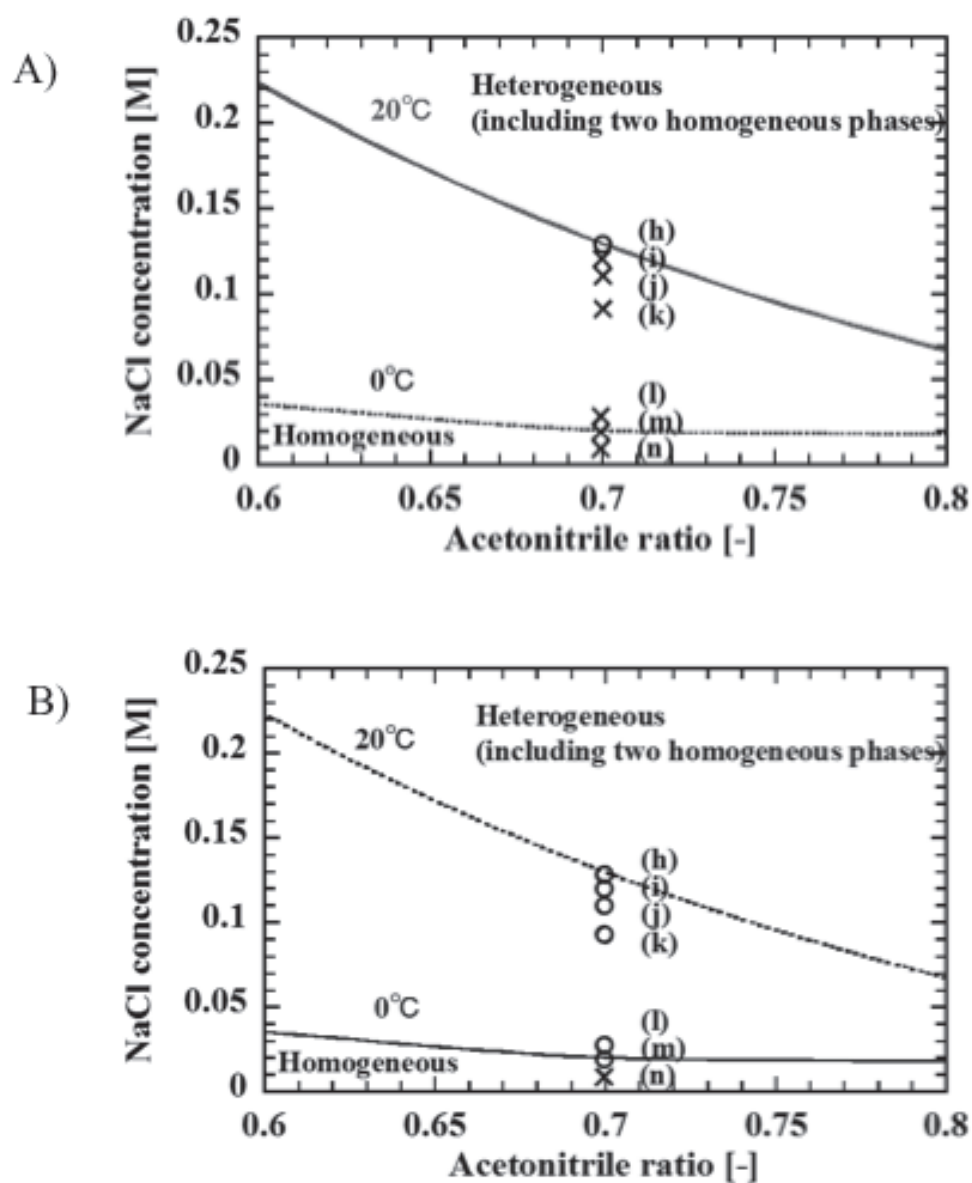


Figure 10. Phase diagram for water-acetonitrile mixture containing NaCl and the solvent composition and NaCl concentration for the chromatograms obtained with the TRDC system. Tube temperatures of A) 20 °C and B) 0 °C. The curves in the diagram indicate the homogeneous-heterogeneous solution boundary curves. The solvent composition and NaCl concentration of the carrier solvents, (h) – (n), for the chromatograms in Fig. 10 are plotted in the diagram with the symbols ○ and × to express baseline-separation and non-separation, respectively, for the analytes.

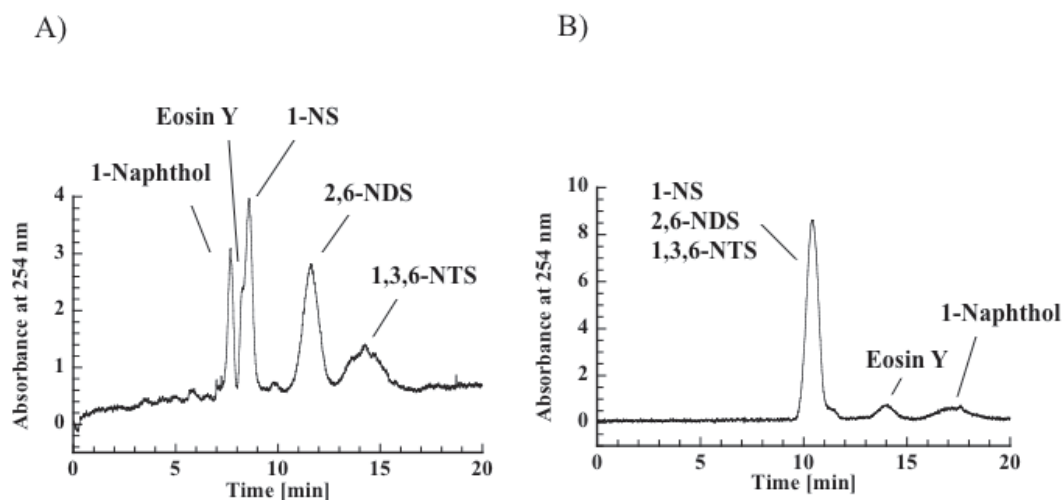


Figure 11. Chromatograms of 1-naphthol, 1-NS, 2,6-NDS, 1,3,6-NTS and Eosin Y. A) Fused-silica and B) PTFE capillary tubes. Conditions: Capillary tube, 110 cm (90 cm effective length) of 100 μm i.d.; carrier, water–acetonitrile of 3 : 7 volume ratio containing 0.129 M NaCl for A) and 7 : 3 volume ratio containing 1.23 M NaCl for B); tube temperature, 20 $^{\circ}\text{C}$; sample injection, 30 cm height (gravity) \times 30 s; flow rate, 0.8 $\mu\text{L min}^{-1}$; and analyte concentration, 1 mM 1-naphthol, 1-NS, 2,6-NDS, 1,3,6-NTS and 0.1 mM Eosin Y for A) and 1 mM 1-naphthol, 1-NS, 2,6-NDS, 1,3,6-NTS and 0.2 mM Eosin Y for B).

References

- [1] K. E. Gutowski, G. A. Broker, H. D. Willauer, J. G. Huddleston, R. P. Swatloski, J. D. Holbrey, and R. D. Rogers, *J. Am. Chem. Soc.*, **2003**, *125*, 6632.
- [2] Y. Lu, W. Lu, W. Wang, Q. Guo, and Y. Yang, *Talanta*, **2011**, *85*, 1621.
- [3] C. Wua, J. Wanga, H. Wanga, Y. Peia, and Z. Li, *J. Chromatogr., A*, **2011**, *1218*, 8587.
- [4] Z. Li, Y. Pei, H. Wang, J. Fan, and J. Wang, *Trends Anal. Chem.*, **2010**, *29*, 1336.
- [5] J. Han, Y. Wang, Y. Li, C. Yu, and Y. Yan, *J. Chem. Eng. Data*, **2011**, *56*, 3679.
- [6] K. Fujinaga, *Anal. Sci.*, **1993**, *9*, 479.
- [7] H. Watanabe and H. Tanaka, *Talanta*, **1978**, *52*, 585.
- [8] T. Saitoh, H. Tani, T. Kamidate, and H. Watanabe, *Trends Anal. Chem.*, **1995**, *14*, 213.
- [9] T. M. Z.-Moattar and R. Sadeghi, *Fluid Phase Equilib.*, **2002**, *203*, 177.
- [10] P. I. Trindade, M. M. Diogo, D. M. F. Prazeres, and C. J. Marcos, *J. Chromatogr., A*, **2005**, *1082*, 176.
- [11] T. I. Horváth and J. Rábai, *Science*, **1994**, *266*, 72.
- [12] K. Nakashima, F. Kubota, M. Goto, and T. Maruyama, *Anal. Sci.*, **2009**, *25*, 77.

- [13] J. Lim and T. M. Swager, *Angew. Chem. Int. Ed.*, **2010**, *49*, 7486.
- [14] H. Matsuda, A. Kitabatake, M. Kosuge, K. Tochigi, and K. Ochi, *Fluid Phase Equilib.*, **2010**, *297*, 187.
- [15] T. Maruyama, K. Nakashima, F. Kubota, and M. Goto, *Anal. Sci.*, **2007**, *23*, 763.
- [16] M. Masato, M. Hasegawa, D. Sadachika, S. Okamoto, M. Tomioka, Y. Ikeya, A. Masuhara, and Y. Mori, *Tetrahedron Lett.*, **2007**, *48*, 4147.
- [17] C. Dennis and Z. R. Lee, *Green Chemistry*, **2001**, G3.
- [18] A. Albert and A. Hampton, *J. Chem. Soc.*, **1954**, 505.
- [19] W. D. Johnston and H. Freiser, *J. Am. Chem. Soc.*, **1952**, *74*, 5239.
- [20] Taniguchi, Y., Suzuki, K., and Enomoto, T., *J. Colloid & Interface Sci.*, 1974, vol. 46, p. 511.
- [21] Pourreza, N., Rastegarzadeh, S., Larki, A., *Talanta*, 2008, vol. 77, p. 733.
- [22] K. Tsukagoshi, K. Nakahama, and R. Nakajima, *Anal. Chem.*, **2004**, *76*, 4410.
- [23] A. E. Everagae, *Trans. Soc. Rheol.*, **1973**, *17*, 629.
- [24] H. Sotjthernj and N. L. Ballmar, *Appl. Polymer Symp.*, **1973**, *20*, 175.
- [25] J. L. White and B. L. Lee, *Trans. Soc. Rheol.*, **1975**, *19*, 457.
- [26] D. L. Maclean, *Trans. Soc. Rheol.*, **1973**, *17*, 385.
- [27] M. Tabata, M. Kumamoto, J. Nishimoto, *Anal. Sci.*, **1994**, *10*, 383.
- [28] M. Tabata, Y. G. Wu, T. Charoenraks, S. S. Samaratunga, *Bull. Chem. Soc. Jpn.*, **2006**, *79*, 1742.

Chapter 14 Applications and related techniques with microfluidic behavior of mixed solvent solutions

The specific microfluidic behavior of the mixed solvent solutions, TRDP, has led to a unique and novel design of the respective analytical devices, such as for the chromatography, extraction, mixing, and chemical reaction spaces, in a microspace. The results obtained from them gave clues as to how to apply the TRDP to other applications and related techniques. The part of this chapter is constructed and rewritten based on related manuscripts that have been published previously.^{7,43,47,53)}

14.1 TRDP in bent and wound microchannels on microchips

The tube radial distribution of ternary solvents (water–hydrophilic/hydrophobic organic mixture) fed into bent and wound microchannels in a microchip was examined by fluorescence observation of dyes dissolved in the solvents under laminar flow conditions. Four kinds of microchips incorporating bent microchannels were used, together with a microchip with a straight channel. The microchannels had different bending times (2, 4, or 12 times), bending radii (0.8, 2.3, or 3 μm), and total channel lengths (80, 120, 200, or 500 mm). A water–acetonitrile (hydrophilic)–ethyl acetate (hydrophobic) mixture containing relatively hydrophilic Eosin Y (green) and hydrophobic perylene (blue) was delivered into the bent microchannels in the microchips. The fluorescence of the green and blue dyes enabled us to observe the specific radial distribution behavior of the ternary solvents in the bent micro channels at 0 °C, including liquid–liquid interfaces. Further, the radial distribution pattern of the solvents was clearly observed in the wound microchannel (bending radius, ca. 0.1 μm , real total channel length, 500 mm, and apparent straight channel length, 40 mm) at 20 °C (a room temperature) as well as 0 °C. It was found that radial distribution behaviors of the solvents were successfully generated in even the specific microchannels including various types of curves under the present conditions.

Introduction

Since the last century, the development of micro total analysis systems that include a microchip or microfluidic device has become an interesting and attractive area of analytical science [1,2]. It has been reported that microfluidics exhibit various types of fluidic liquid–liquid interfaces of solvents in a microchannel [3-6]; these liquid–liquid interfaces have been examined by varying the channel configurations and flow rates of the solvents, as well as by using various aqueous and organic solvent combinations. The fluidic liquid–liquid interface of solvents in a microchannel is related to the separation, diffusion, and reaction of the solutes. Information on the liquid–liquid interface of solvents is important and useful in the

design of microreactors or micro total analysis systems [3,5].

Various types of aqueous–organic solvent mixture solutions are used in dissolution [7], cleaning [8], preservation [9], and as reaction solvents [10]. Such mixtures are also useful in separation science [11,12]. When ternary mixtures of water–hydrophilic/hydrophobic organic solvents are fed into microspaces such as microchannels in microchips or capillary tubes under laminar flow conditions, the solvent molecules are radially distributed in the microspace; we call this the “tube radial distribution phenomenon” (TRDP).

Here, the microfluidic liquid–liquid interface of ternary solvents (water–acetonitrile–ethyl acetate mixture) was examined through observation of fluorescent dyes in bent and wound microchannels in microchips, in order to expand our knowledge of the TRDP in microchannels. We used commercial microchips that had single and Y-type channel ends. The ternary solvent solution was delivered into the microchannels from the single and Y-type channel ends.

Experimental

The microchips, incorporating microchannels, were made of glass (types ICC-SY05, ICC-SY10, ICC-SY15, ICC-SY200, ICC-SY500, and ICC-SY500MI, Institute of Microchemical Technology Co., Ltd., Kanagawa, Japan). The designs of the microchannels (100 μm width \times 40 μm depth) are shown in Fig. 1; the ICC-SY05, ICC-SY10, ICC-SY15, ICC-SY200, ICC-SY500, and ICC-SY500MI microchips, which are commercially available, are called Type A, Type B, Type C, Type D, Type E, and Type F, respectively, here. Also, the single, bent, or wound microchannels are called Channel M (the numbers in parentheses in Fig. 1 mean the total channel lengths). The radii of the bent parts in the microchannels are 3 mm for Type B and C, 2.3 mm for Type D, 0.8 mm for Type E, and ca. 0.1 mm for Type F, respectively. The microchip was set in a microchip holder for use here (Fig. 2). The microchip set in the holder was put on a stage for fluorescence microscope–charge-coupled device (CCD) camera observations. The water–acetonitrile–ethyl acetate mixture (3:8:4 volume ratio) containing 1.0 mM Eosin Y and 0.1 mM perylene was fed into the microchannel at a flow rate of mainly 2.0 $\mu\text{L min}^{-1}$ in Channel M, using microsyringe pumps. The fluorescence in the microchannel was monitored using a fluorescence microscope equipped with an Hg lamp, a filter, and a CCD camera. The fluorescence photographs mainly consisted of blue and green because perylene and Eosin Y emit light at 470 and 550 nm, respectively.

Results and discussion

Phase diagram of water–acetonitrile–ethyl acetate mixture solution and TRDP generation Our group reported that a ternary mixed solution of water–acetonitrile–ethyl acetate is a two-phase separated aqueous solution. Fig. 3 shows the phase diagram of the ternary mixed solution of water–acetonitrile–ethyl acetate at 0 and 20 $^{\circ}\text{C}$. The dotted curves show the boundaries between heterogeneous (inside) and

homogeneous (outside) regions. The ternary mixed solution of water–acetonitrile–ethyl acetate (3:8:4, volume ratio; organic-solvent-rich solution) is plotted in the diagram. When cooled to near 0 °C from 20 °C, the homogeneous ternary mixed solution changes to a heterogeneous solution. We viewed inner and outer phase formation in the TRDP, taking advantage of the above-mentioned phase diagram. A specific homogeneous solution, whose component ratio was near the boundary between the homogeneous and heterogeneous regions in the phase diagram, was cooled to below 20 °C in a batch vessel, in which it was under the influence of gravity. In an organic-solvent-rich solution (e.g., water–acetonitrile–ethyl acetate mixture; 3:8:4 volume ratio), the homogeneous solution changes to a heterogeneous solution that includes an upper major organic solvent-rich solution and a lower minor water-rich solution under the control of gravity. However, the phase formation of ternary mixed solvents in a microchannel under temperature changes is considered to not be greatly under the influence of gravity, as follows. In an organic solvent-rich solution, the ternary mixed solvent solution in a tube changes to a heterogeneous solution that includes major inner organic solvent-rich and minor outer water-rich phases (TRDP), where there is little control by gravity.

Delivery of ternary mixed solvents from single channel inlet The ternary mixture of water–acetonitrile–ethyl acetate was delivered from the single channel inlet in a microchip of Type A. Fluorescence photographs of the fluorescence dyes were examined in Channel M at 0 and 20 °C (a room temperature). At 20 °C, the TRDP was not observed, whereas at 0 °C, it was clearly observed; hydrophobic perylene (blue) was distributed around the middle of the channel, far from the inner wall, and the relatively hydrophilic Eosin Y (green) was distributed near the inner wall (Fig. 4). Fluorescence photographs in the bent microchips of Types B–E, at 0 and 20 °C, were also observed. The observation area and observation points (point 1–4) in the microchips are indicated in Fig. 5. As an example, the photographs of points 1–4 in the Type E microchip at 0 °C are also shown in Fig. 5. The TRDP was observed at every point of the microchip of Type E at 0 °C, but was not observed at 20 °C. The TRDP was similarly observed in the bent microchannels of microchips of Types B–D at 0 °C (Fig. 6), i.e., the TRDP was clearly generated at 0 °C, without any influence of bends in the channels, under the present conditions.

Delivery of ternary mixed solvents from Y-type channel inlet The ternary mixture of water–acetonitrile–ethyl acetate was delivered from the Y-type channel inlet in the microchip of Type A. Fluorescence photographs of the fluorescence dyes were observed in Channel M at 0 and 20 °C. At 20 °C, the TRDP was not observed, but it was clearly observed at 0 °C (Fig. 7). Fluorescence photographs were observed in the bent microchip of Type E, into which the ternary mixed solution was similarly delivered from the Y-type channel inlet. Type E was selected as a model for the experiment as the bending of the microchannels in all chips, Types B–E, showed no influence on the

TRDP, as described in the above section. The observation area in the Type E chip is shown in Fig. 8. The TRDP was not observed at 20 °C, but it was observed at 0 °C. The observed TRDP is also shown in Fig. 8. The TRDP was generated at 0 °C in the bent microchannel, without any influence of the channel inlets, single and Y-type, under the present conditions. Tentatively, using the Type E microchip, the TRDP was examined at other flow rates, i.e., 0.1 and 10 $\mu\text{L min}^{-1}$, at 0 °C, although the TRDP was observed at a flow rate of 2.0 $\mu\text{L min}^{-1}$ here. The TRDP was observed at flow rates of 0.1 and 10 $\mu\text{L min}^{-1}$ at 0 °C in the Type E microchip (Fig. 9, shows the data at a flow rate of 0.1 $\mu\text{L min}^{-1}$).

Delivery of ternary mixed solvents into wound microchannel in Type F microchip

The ternary mixture of water–acetonitrile–ethyl acetate was delivered into the wound microchannel from the single channel inlet and Y-type channel inlet in the Type F microchip (as shown in Fig. 10). Fig. 5 shows fluorescence photographs of the fluorescence dyes, observed in Channel M at 0 and 20 °C, from the single channel inlet (Fig. 11a) and from the Y-type channel inlet (Fig. 11b). As shown in the figures, the TRDP was observed for both flow directions at 0 and 20 °C, although the thickness of the outer phase in the TRDP seemed to change slightly at 20 °C. It was also confirmed that the TRDP appeared almost throughout the entire channels. We do not have any clear reason for TRDP generation at 20 °C in the wound microchannel. The specific mixing and pressure in the wound microchannel may generate the two separated phases, i.e., TRDP, even at 20 °C. We will continue to examine the TRDP in wound microchannels from various viewpoints.

In conclusion, a ternary mixture of water–acetonitrile–ethyl acetate (3:8:4, volume ratio) was delivered into bent and wound microchannels in microchips. Fluorescence photographs were observed using a fluorescence microscope–CCD camera system. The TRDP was clearly observed at 0 °C in the bent and wound microchannels, without any influence of the bends in the channels. The results obtained with the microchannels gave clues as to how to apply the TRDP to the design of analytical devices, such as for chromatography, extraction, and chemical reaction spaces, in microchips.

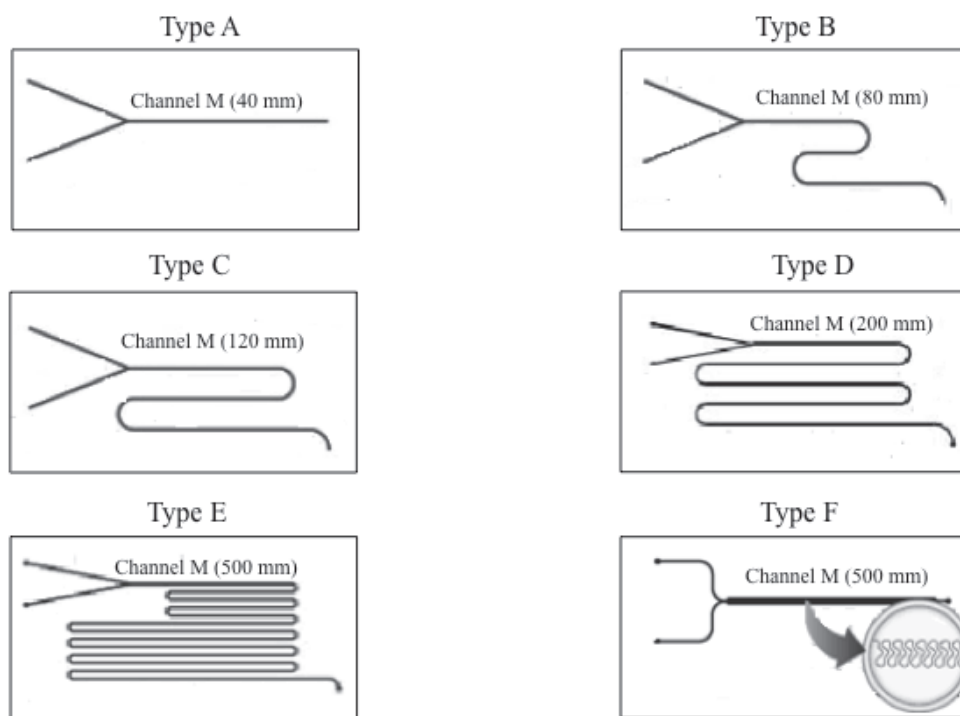


Figure 1. Designs of microchannels in microchips (Type A–F).

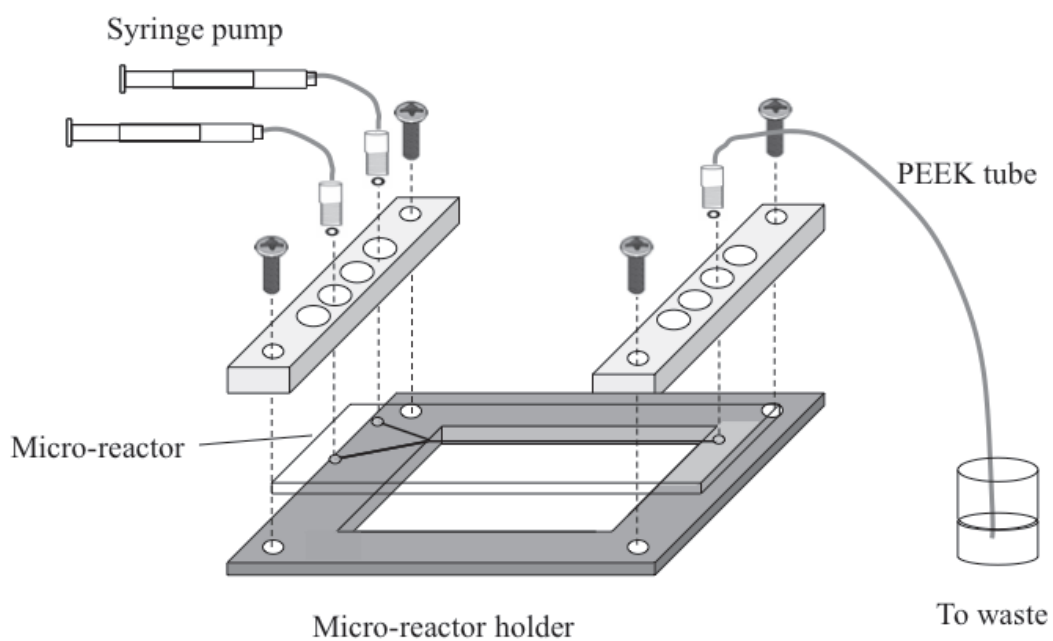


Figure 2. Schematic representation of a microchip in a microchip holder.

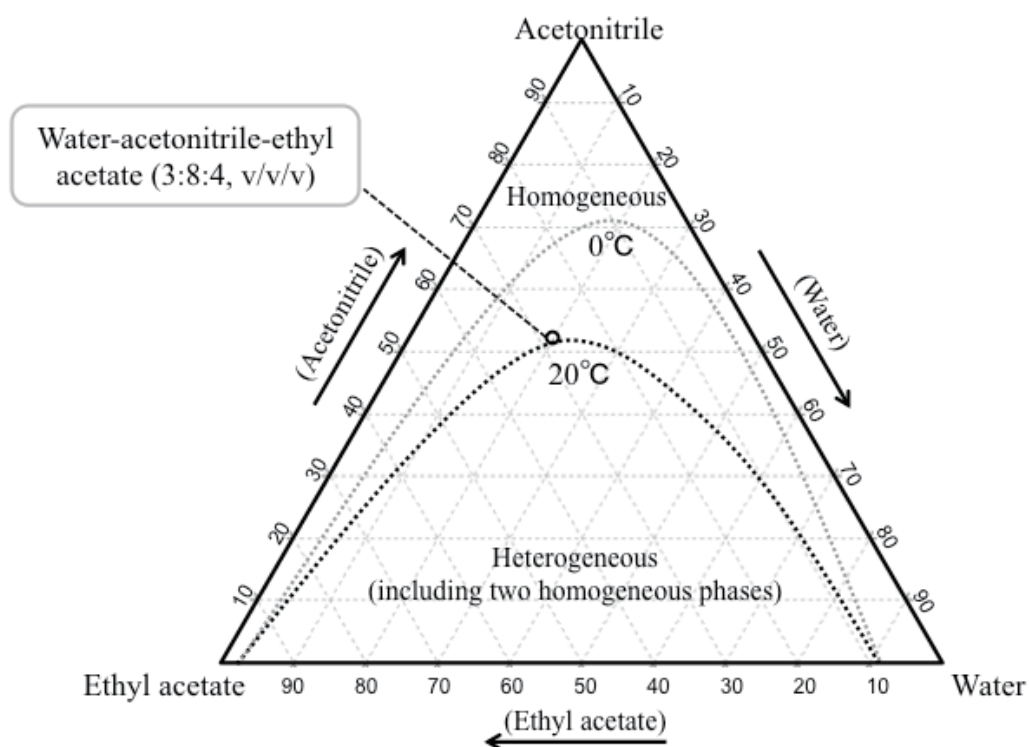


Figure 3. Phase diagram of a ternary mixed solution of water–acetonitrile–ethyl acetate at 0 and 20 °C. The dotted curves show the boundaries between heterogeneous and homogeneous solutions.

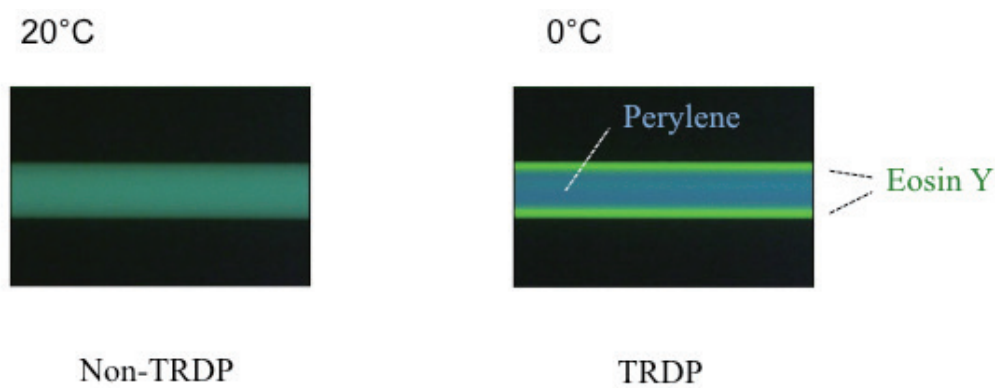


Figure 4. Fluorescence photographs observed in microchannel in Type A microchip at 0 and 20 °C. The ternary mixed solvent solution was delivered from the single channel inlet.

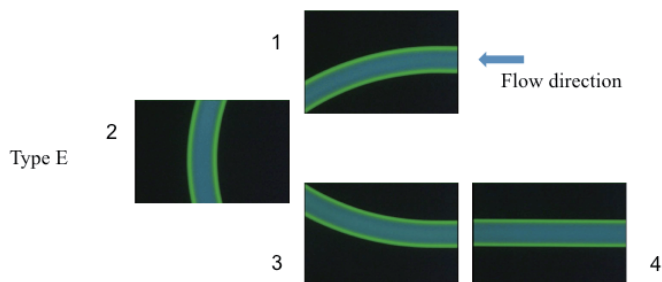
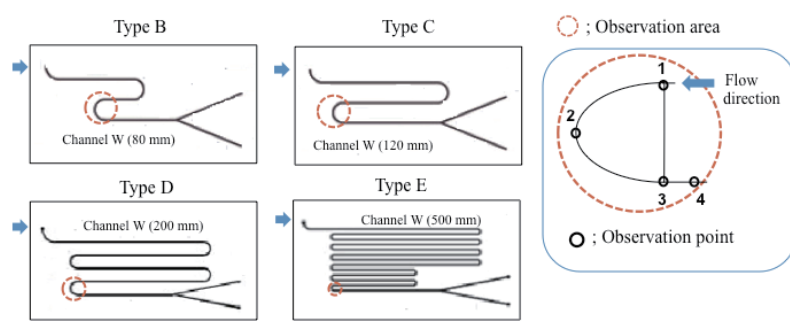


Figure 5. Observation areas and observation points in microchannels in microchips (Types B–E). Fluorescence photographs observed in microchannel in Type E at 0 °C. The ternary mixed solvent solution was delivered from the single channel inlet.

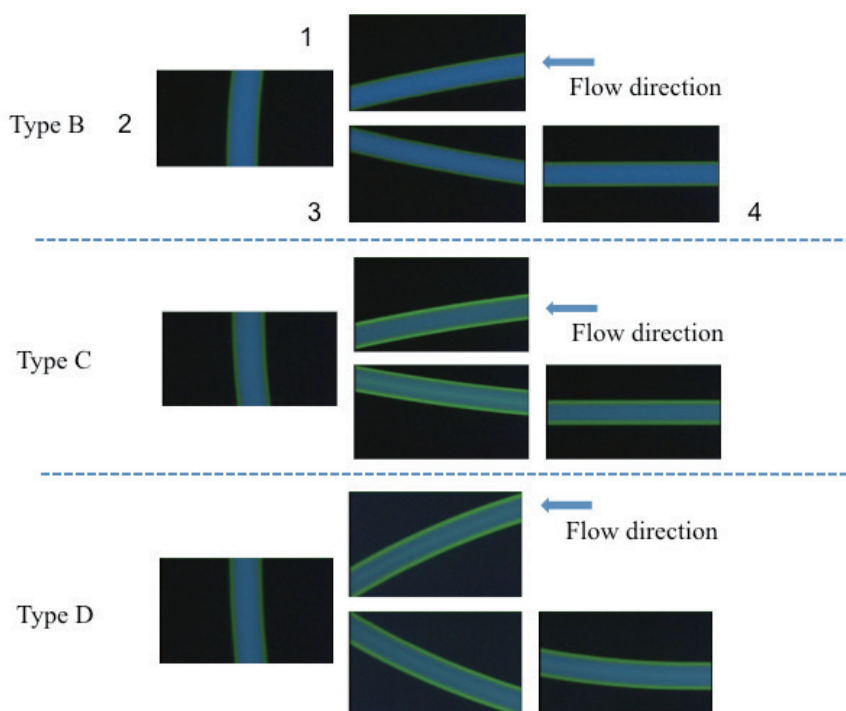


Figure 6. Fluorescence photographs observed in microchannels in microchips of Types B–D at 0 °C. The ternary mixed solvent solution was delivered from the single channel inlet.

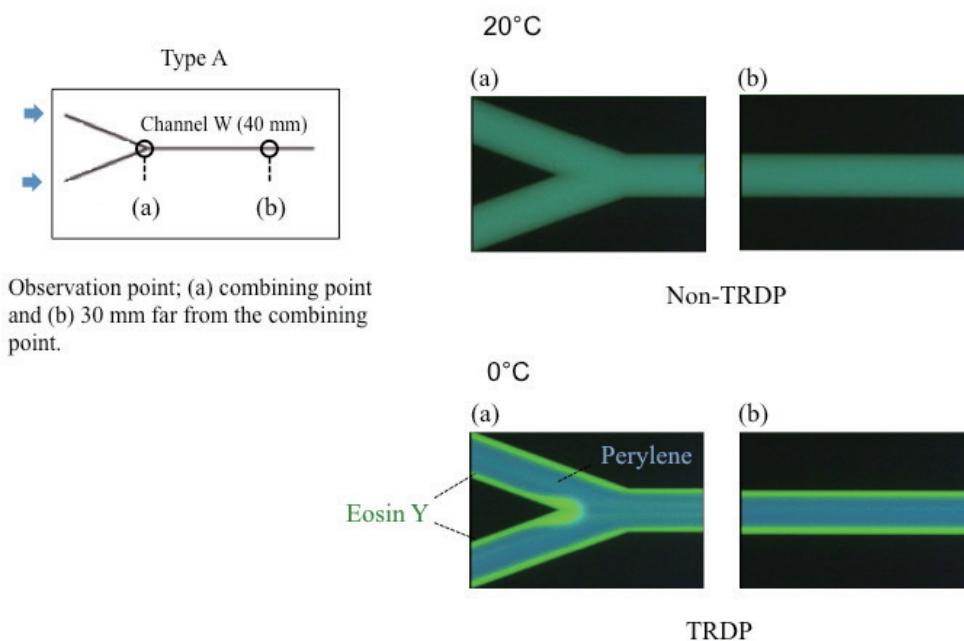


Figure 7. Fluorescence photographs observed in a microchannel in a Type A microchip at 0 and 20 °C. The ternary mixed solvent solution was delivered from the Y-type channel inlet.

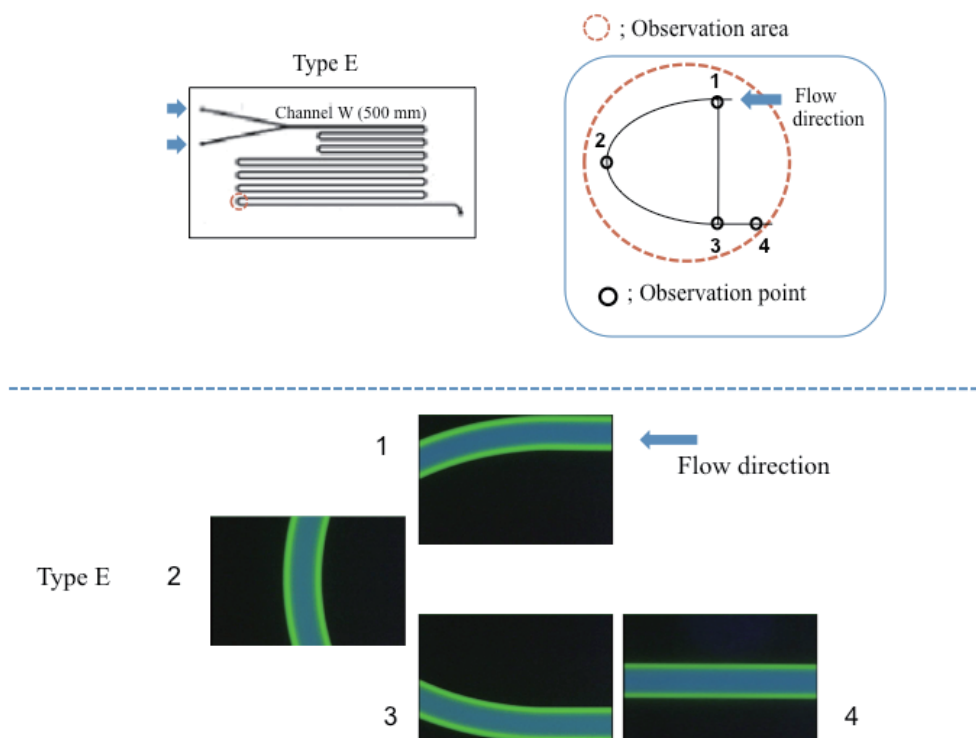


Figure 8. Observation areas and observation points in a microchannel in a Type E microchip. Fluorescence photographs observed in microchip Type E at 0 °C. The ternary mixed solvent solution was delivered from the Y-type channel inlet.

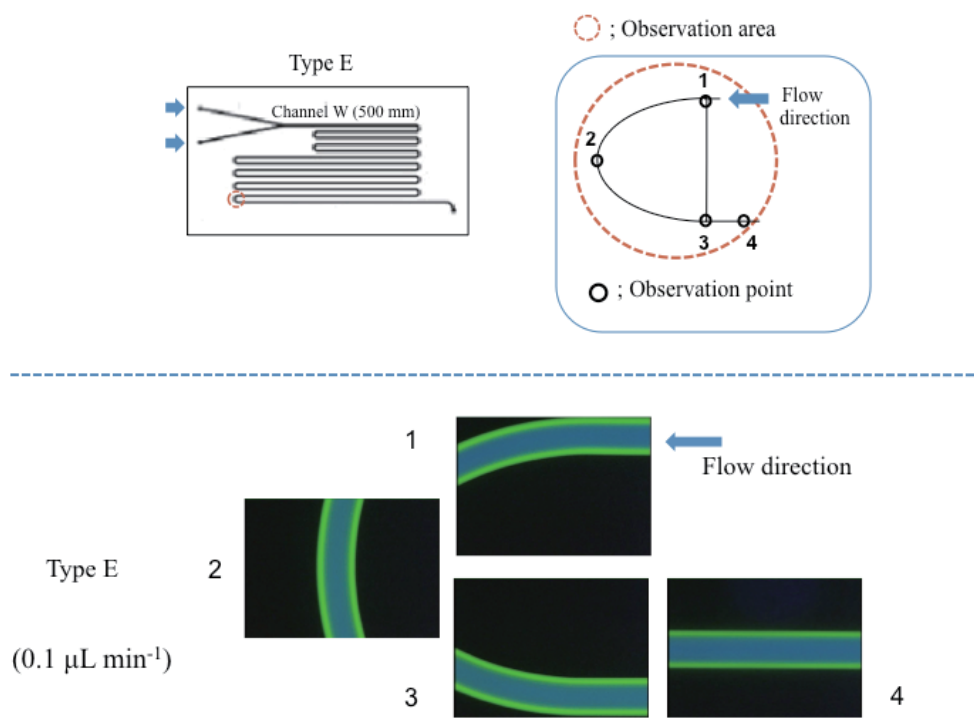


Figure 9. Fluorescence photographs observed in microchannel in Type E microchip at 0 °C at flow rate of 0.1 $\mu\text{L min}^{-1}$. The ternary mixed solvent solution was delivered from the Y-type channel inlet.

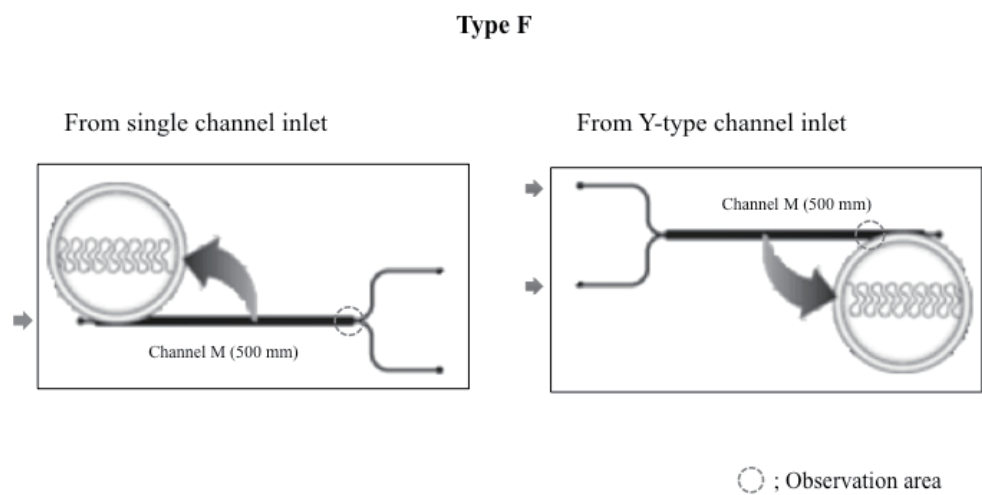


Figure 10. Observation areas and solution delivery directions in the microchannel of the Type F microchip.

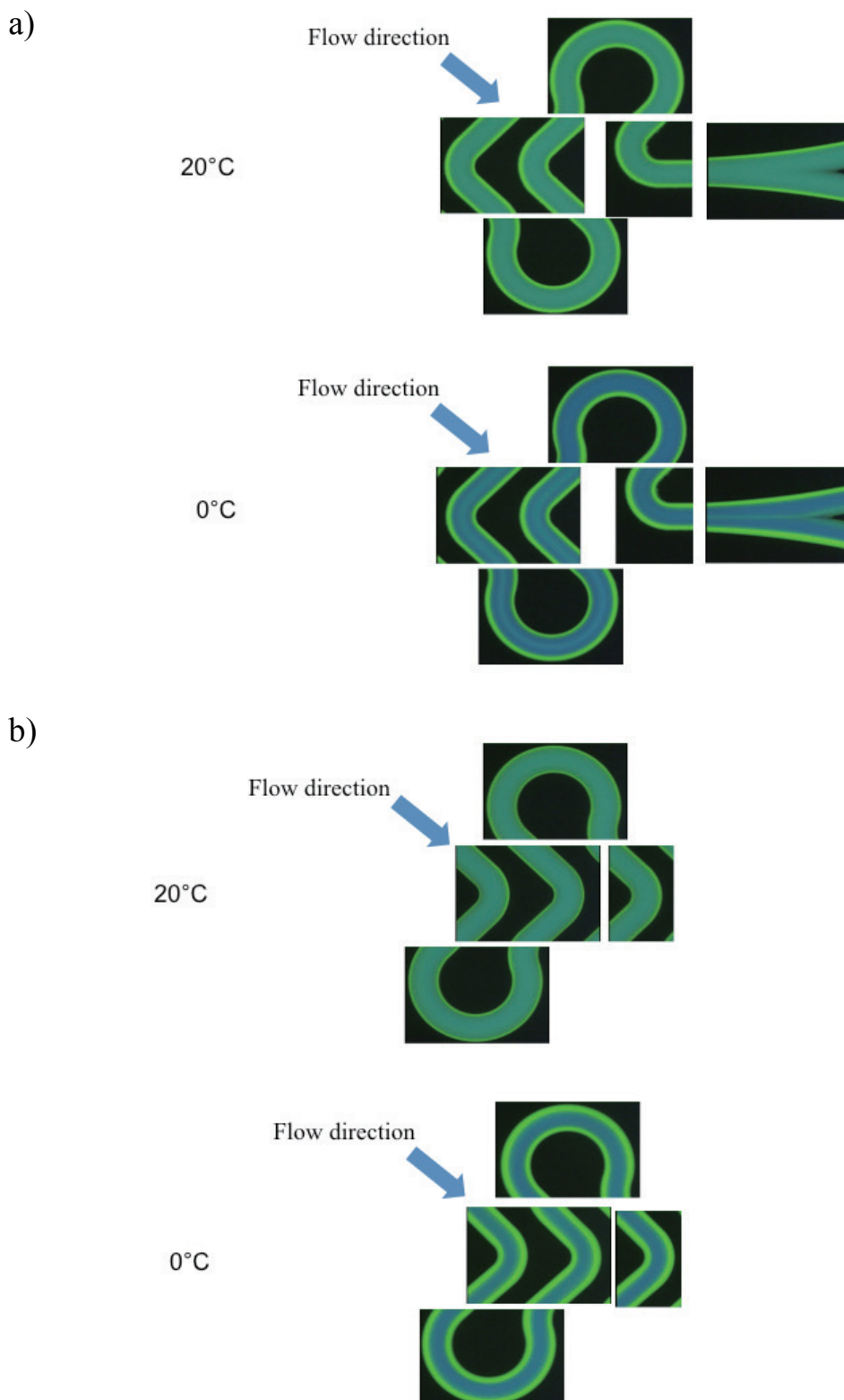


Figure 11. Fluorescence photographs observed in microchip Type F at 0 and 20 °C. The ternary mixed solvent solution was delivered from (a) the single channel inlet and (b) the Y-type channel inlet.

14.2 Introduction of double tubes having different inner diameters to TRDC system

We introduced double capillary tubes having different inner diameters to the tube radial distribution chromatography (TRDC) system. The tubes were fused-silica capillary tubes with 100 and 250 μm i.d.; the smaller tube was inserted into the larger one through a T-type joint. Water–acetonitrile mixture (volume ratio 3:1) and acetonitrile–ethyl acetate mixture (volume ratio 4:1) solutions were delivered into the large tube from the inside through the small tube and from the outside through the joint, respectively, and then mixed through the large tube to provide a water–acetonitrile–ethyl acetate carrier solution. The carrier solution was further fed into the large tube and then to an absorption detector. By changing the flow rates of the mixture solutions in both tubes, we could control the component ratio of carrier solvents in the carrier solution, yielding either organic solvent-rich, water–acetonitrile–ethyl acetate (volume ratio 3:33:8) or water-rich, water–acetonitrile–ethyl acetate (volume ratio 24:12:1). A model analyte-mixture solution of 1-naphthol and 2,6-naphthalenedisulfonic acid was eluted in this order with the organic solvent-rich carrier solution and eluted in the reverse order with the water-rich carrier solution. We discussed the chromatographic data together with the analytical conditions from the viewpoint of the tube radial distribution of the carrier solvents.

Introduction

Commercially available capillary tubes, e.g., fused-silica tubes, have uniform narrow bores, inert inner surfaces, and good flexibility, and are convenient for use with various analytical instruments. Among analytical techniques that make use of these tubes, various types of capillary chromatography, including capillary electrochromatography [13,14] and capillary high-performance liquid chromatography using packed and monolithic capillary columns [15,16], have attracted considerable attention for use in the fields of analytical chemistry and separation science. Capillary chromatography using open fused-silica capillary tubes has also been investigated and the results indicated interesting and unique characteristics [17-20]. Most capillary chromatography systems feature rapid measurements, easy procedures, inexpensive and small apparatus, small sample volumes, and low costs.

To date, in the TRDC system, aqueous–organic solvent carrier solutions were prepared with a water–acetonitrile–ethyl acetate mixture at various volume ratios to become homogeneous solutions, and were then delivered into a single capillary tube by a microsyringe pump. To change the component ratio of solvents in the carrier solution, we had to prepare the solution from the beginning and introduce it again into the TRDC system.

Here, we introduced double capillary tubes having different inner diameters to the TRDC system, instead of the single capillary tube just mentioned above. The double

tubes consisted of a small- and a large-inner diameter fused-silica capillary tube; the small tube was inserted into the large tube through a T-type joint. Water–acetonitrile mixture and acetonitrile–ethyl acetate mixture solutions were delivered into the large tube from the inside and outside, respectively, and then mixed through the large tube to provide a water-acetonitrile-ethyl acetate carrier solution. By controlling the flow rates of the mixture solutions in the two tubes, we could change the component ratio of a water-acetonitrile-ethyl acetate carrier solution, resulting in an organic solvent-rich solution and a water-rich carrier solution. We were thus able to separate and detect a model analyte-mixture solution of 1-naphthol and 2,6-naphthalenedisulfonic acid. Separation performance in the TRDC system was discussed based on the obtained chromatograms and the data concerning analytical conditions.

Experimental

Fused-silica capillary tubes (100 μm i.d. and 200 μm o.d. as well as 250 μm i.d. and 350 μm o.d.) were used. Fig. 1 shows a schematic diagram of the TRDC system comprising double capillary tubes, two microsyringe pumps, and an absorption detector; an enlarged image of the tubes and T-type joint is also shown (though the thickness of the tubes is not accurately expressed in the enlarged image). The tubes were fused-silica capillary tubes of 100 and 250 μm i.d. (called Capillaries A and B, respectively); Capillary A was inserted into Capillary B through a T-type joint. Water–acetonitrile mixture (volume ratio 3:1) and acetonitrile–ethyl acetate mixture (volume ratio 4:1) solutions (called Mixtures A and B, respectively) were delivered into Capillary B from the inside through Capillary A and from the outside through the joint, respectively, with the corresponding microsyringe pumps, then mixed through Capillary B. The resulting water–acetonitrile–ethyl acetate carrier solution in Capillary B was delivered to an adsorption detector; the distance from the outlet of Capillary A to the detector (the effective capillary length for separation) was 100 or 200 cm. The temperature of Capillary B having a 200 cm effective length was adjusted by dipping a part of the capillary tube (ca. 130 cm) in water maintained at a definite temperature in a vessel with stirring. By changing the flow rates of the mixture solutions (Mixtures A and B), we could control the component ratio of carrier solvents in the carrier solution that was fed into Capillary B. For example, an organic solvent-rich carrier solution (water–acetonitrile–ethyl acetate, volume ratio 3:33:8) was delivered at flow rates of 1.0 and 8.0 $\mu\text{L min}^{-1}$ for Mixtures A and B, respectively. A water-rich carrier solution (water–acetonitrile–ethyl acetate, volume ratio 24:12:1) was delivered at flow rates of 8.0 and 1.0 $\mu\text{L min}^{-1}$ for Mixtures A and B, respectively. An analyte-mixture solution of 1-naphthol and 2,6-naphthalenedisulfonic acid was prepared with Mixture A and introduced directly into the capillary inlet of Capillary A for 15 s from a height of 20 cm by the gravity method. After analyte injection, the capillary inlet was connected to a microsyringe set on the microsyringe pump. Mixtures A and B were fed at definite flow rates, respectively, to yield the desired organic solvent-rich or water-rich carrier solution

in Capillary B. On-capillary absorption detection (254 nm) was performed with the detector.

Results and discussion

Separation in the TRDC system Separation in the TRDC system was proposed in our paper, briefly repeated below. Water and organic solvent in the carrier solution do not disperse uniformly in the capillary, leading to the generation of a water-rich phase and an organic solvent-rich phase in the tube. A major solvent phase forms around the middle of the tube far from the inner wall as an inner phase, while a minor solvent phase is generated near the inner wall as an outer or capillary wall phase; when using a water-rich carrier solution, a major solvent phase or a water-rich phase forms around the middle of the tube as an inner phase, while when using an organic solvent-rich carrier solution, a major solvent phase or an organic solvent-rich phase forms as an inner phase. The tube radial distribution of the solvent molecules in the carrier solution is thus caused by the flow in the capillary tube under laminar flow conditions. Subsequently, the analytes are delivered through the tube, being distributed between the inner and outer (capillary wall) phases. The analyte lightly partitioned in the outer phase near the inner wall of the tube is eluted with near average linear velocity, while the analyte largely partitioned in the outer phase is eluted with a smaller velocity than the average linear velocity. The elution times of the analytes can be easily reversed by changing the component ratio of solvents in the carrier solution.

Analytical conditions The analyte-mixture solution must be injected into the capillary inlet of Capillary A, because the analyte zone in Capillary B is never formed exactly through the T-type joint if the analyte solution is injected into the inlet of Capillary B. Also, 2,6-naphthalenedisulfonic acid that was one of the analyte components was not enough dissolved with Mixture B (acetonitrile-ethyl acetate mixture), even not with acetonitrile alone, to show an absorption signal. Consequently, the analyte-mixture solution of 1-naphthol and 2,6-naphthalenedisulfonic acid dissolved with Mixture A (water-acetonitrile mixture) was injected into Capillary A and delivered toward Capillary B. Mixtures A and B were delivered at the flow rates of 1.0 and 8.0, 2.0 and 6.0, 4.0 and 4.0, 6.0 and 2.0, as well as 8.0 and 1.0 $\mu\text{L min}^{-1}$, respectively. The baselines monitored by the absorption detector were stable for the flow rates of 1.0 and 8.0, 4.0 and 4.0, as well as 8.0 and 1.0 $\mu\text{L min}^{-1}$ for Mixtures A and B. But they were not stable for the flow rates of 2.0 and 6.0 or for 6.0 and 4.0 $\mu\text{L min}^{-1}$. The carrier solution (water-acetonitrile-ethyl acetate mixture) provided by mixing Mixtures A and B at the end of Capillary A in Capillary B must be homogeneous for the stable baselines observed through absorption detection, while it must be heterogeneous for the unstable baselines. Furthermore, as a preliminary experiment, when Mixtures A and B were fed at the flow rates of 4.0 and 4.0 $\mu\text{L min}^{-1}$ respectively into the capillaries, the analytes in the mixture solution were not separated; the carrier solution obtained by the flow

rates comprised the water-acetonitrile-ethyl acetate mixture with the volume ratio of 3:5:1. The volume ratio that did not possess a large unbalance in water-organic solvent ratio must not lead to separation in the present system, although it could provide a stable baseline. As a result, we adopted the flow rates of 1.0 and 8.0 as well as 8.0 and 1.0 $\mu\text{L min}^{-1}$ for Mixtures A and B in the following experiments.

Effect of the temperature of Capillary B First, Capillary B having a 100 cm effective length for separation was used in the present TRDC system. This capillary length was very commonly used in our works, but we had not used a capillary tube of 250 μm i.d. (the largest inner diameter of the tube that we had used in the TRDC system was 200 μm of polyethylene tube). When Capillary B, with an effective length of 100 cm, was used, the obtained chromatographic data lacked reproducibility; therefore the details are not described here. Then, we tried to use Capillary B with an effective length of 200 cm, and dipped one part of it (ca. 130 cm) in water to control the capillary temperature. The data were obtained with good reproducibility at a capillary temperature of 15 - 20 $^{\circ}\text{C}$. In a large inner diameter tube of 250 μm i.d. that was necessitated for developing the double capillary tubes, the capillary temperature control must be useful for providing stable tube radial distribution of carrier solvents in the capillary tube. In addition the analytes were never separated at a capillary temperature of more than 25 $^{\circ}\text{C}$. The following experiments were carried out using Capillary B of 200 cm effective length at the capillary temperature of 15 - 20 $^{\circ}\text{C}$.

Separation performance Mixture A (water-acetonitrile mixture) and Mixture B (acetonitrile-ethyl acetate mixture) were delivered into the large Capillary B from the inside and outside, respectively, at the flow rates of 1.0 and 8.0 as well as 8.0 and 1.0 $\mu\text{L min}^{-1}$, and then mixed through the tube to provide a water-acetonitrile-ethyl acetate carrier solution. We could control the component ratio of carrier solvents in the carrier solution, that is, we could determine if the solution was organic solvent-rich or water-rich, by controlling the flow rates of the mixture solutions. The following component ratios of carrier solvents were demonstrated according to the flow rates mentioned above: organic solvent-rich (water-acetonitrile-ethyl acetate, volume ratio 3:33:8) and water-rich (water-acetonitrile-ethyl acetate, volume ratio 24:12:1). A model analyte mixture (1-naphthol and 2,6-naphthalenedisulfonic acid) was subjected to the TRDC system that was adjusted to feed the organic solvent-rich carrier solution. The two components were eluted in the order listed under laminar flow conditions and detected by the absorption detector. Similarly, the model analyte mixture was subjected to the TRDC system that was adjusted to feed the water-rich carrier solution. The two components were eluted in the reverse order. Obtained chromatograms for these two experiments are shown in Fig. 2. The components of the analytes, 1-naphthol and 2,6-naphthalenedisulfonic acid, in the chromatograms were confirmed with individual absorption signals. The elution times of the model analyte mixtures were easily changed

by altering the component ratio of the carrier solvents in the carrier solution. We altered the component ratio by adjusting the flow rates of the mixture solutions in the double capillary tubes. Additionally, instead of Mixture B of acetonitrile-ethyl acetate mixture, we attempted to use a solution containing acetonitrile alone that was fed into Capillary B. Such an analyte-mixture solution was never separated at any flow rates. Ethyl acetate (hydrophobic organic solvent) made an important role for separation performance in the TRDC system.

Tube radial distribution of carrier solvents It should be emphasized that analyte separation was achieved with even the organic solvent-rich carrier solution. Even when the water-acetonitrile (water-rich) solution was fed from the inner tube and the acetonitrile-ethyl acetate (organic solvent-rich) solution from the outside through the T-type joint, the organic solvent-rich carrier solution that resulted upon their mixing through Capillary B was delivered to the detector, providing that the organic solvent-rich phase formed in the middle of the tube far from the inner wall (the inner phase) and the water-rich phase formed near the inner wall of the tube (the outer or capillary wall phase). That is, the data obtained here supported that the tube radial distribution of carrier solvents in a carrier solution was appropriately performed under laminar flow conditions in the present TRDC system.

In conclusion, we have developed a TRDC system equipped with double capillary tubes having different inner diameters. We could change the component ratio of carrier solvents in the carrier solution by adjusting the flow rates of the two mixture solutions delivered into the tubes in the system, not preparing carrier solutions beforehand and exchanging them. A model analyte mixture solution of 1-naphthol and 2,6-naphthalenedisulfonic acid was eluted, in the order listed, with the organic solvent-rich carrier solution and eluted in the opposite order with the water-rich carrier solution. The demonstration shown here supported the specific solvent distribution in the capillary tube, i.e., the tube radial distribution of the carrier solvents, in the TRDC system together with the experimental data reported previously.

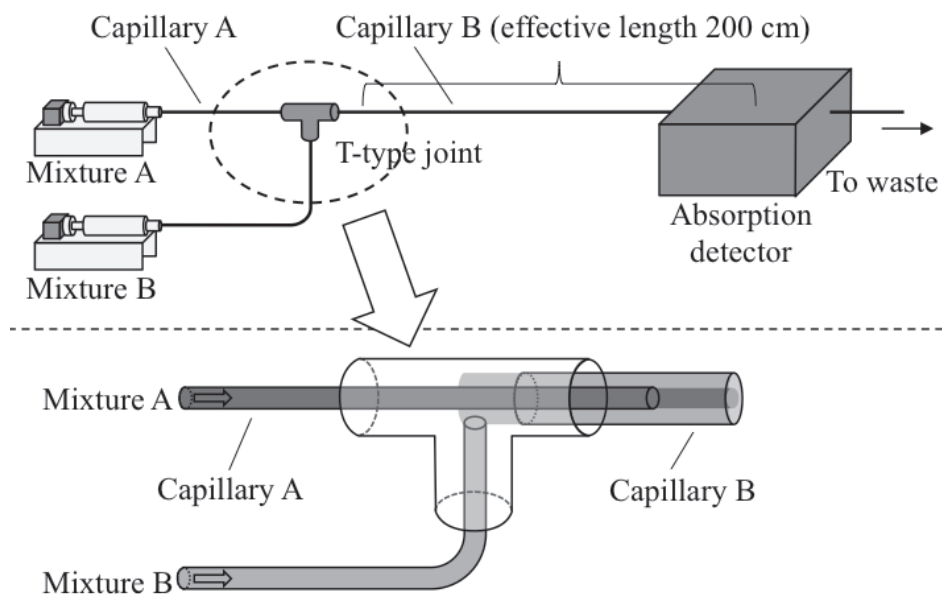


Figure 1. Schematic of the present TRDC system equipped with double capillary tubes.

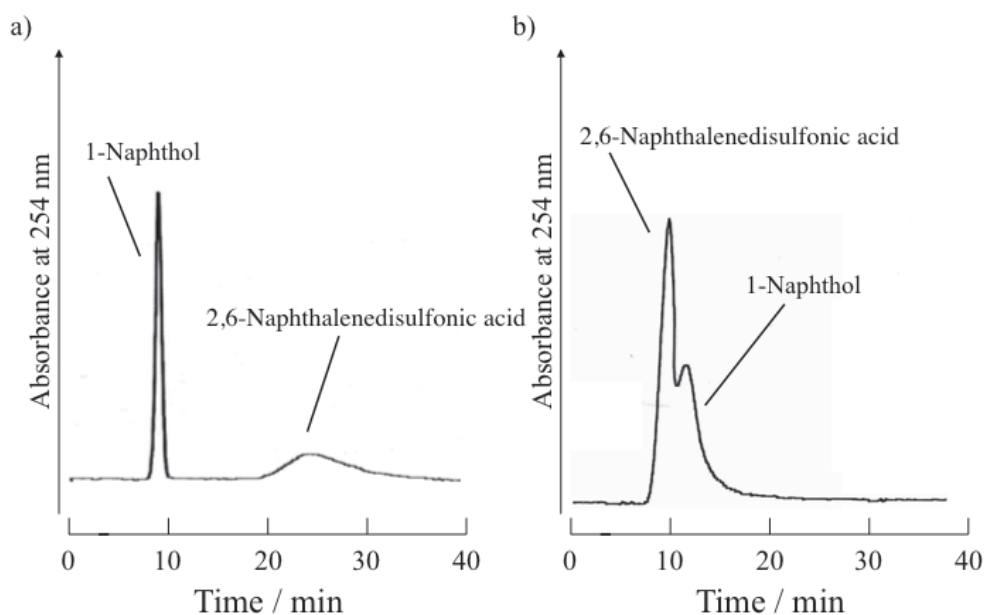


Figure 2. Chromatograms of a mixture of 1-naphthol and 2,6-naphthalenedisulfonic acid obtained using the present TRDC system equipped with double capillary tubes: a) Organic-solvent-rich carrier solution (water–acetonitrile–ethyl acetate, volume ratio 3:33:8), and b) water-rich carrier solution (water–acetonitrile–ethyl acetate, volume ratio 24:12:1). Analyte concentrations are each 2 mM.

14.3 Capillary chromatography using an annular and sluggish flow in the ternary water–acetonitrile–ethyl acetate mixed solution

An open-tubular capillary chromatography system was developed using an annular and sluggish flow system in a ternary water–acetonitrile–ethyl acetate mixed solvent as carrier solution. Fused-silica capillary tubes with different inner diameters of 75 and 200 μm were used. The smaller tube was inserted into the larger tube using a T-type joint. Water–acetonitrile and acetonitrile–ethyl acetate mixed solutions were delivered to the smaller and larger tubes, respectively, and then combined at the other end of the smaller tube located in the larger tube, generating annular and sluggish flows in the water–acetonitrile–ethyl acetate ternary mixed solution (2:5:3 and 2:4:3 (v/v/v), respectively). The annular flow comprised the organic solvent-rich inner and water-rich outer phases and the sluggish flow comprised the organic solvent-rich sluggish domain and water-rich continuous phases. A model analyte mixed solution of 1-naphthol (hydrophobic) and 2,6-naphthalenedisulfonic acid (hydrophilic) was injected into the smaller tube and proceeded to the annular or sluggish flow in the larger tube, where they were separated and detected in that order. As observed, the annular and sluggish flows in the microspace could be used for separation without any specific treatments such as tube packing or coating.

Introduction

The TRDP results in a dynamic liquid–liquid interface or inner and outer phases through phase transformation from a homogeneous (single phase) to a heterogeneous (two phases) mixed solution in a microspace. A capillary chromatography system based on the TRDP in which the outer phase acts as a pseudo-stationary phase under laminar flow conditions has been developed. Recently, an annular and sluggish flow system was investigated in a tube using immiscible organic and aqueous mixed solutions [21–24]. However, to our knowledge, capillary chromatography systems based on an annular and sluggish flow system in a microspace have not been reported yet. Also, a sluggish flow must be thought not to apply it to capillary chromatography, though it can be easily constructed in a microspace.

Here, an open-tubular capillary chromatography system was developed based on an annular and sluggish flow system in a microspace. The flows were generated using a dual capillary tube system with different tube inner diameters. The smaller tube was inserted into the larger tube. Water–acetonitrile and acetonitrile–ethyl acetate mixed solutions were separately fed to the small and large tubes, respectively. Both mixtures combined in the larger tube, generating an annular and sluggish flow in the water–acetonitrile–ethyl acetate ternary mixed solution serving as carrier solution. Model analytes were separated in the annular and sluggish flow in a microspace.

Experimental

Fused-silica capillary tubes (the smaller one: inner diameter, 75 μm and outer diameter,

150 μm ; the larger one: inner diameter, 200 μm and outer diameter, 350 μm) were used. The capillary chromatography system mainly comprised microsyringe pumps, capillary tubes, and a fluorescence detector. A schematic of the chromatography system is shown in Fig. 1. Water–acetonitrile and acetonitrile–ethyl acetate mixtures were delivered to the smaller (75 μm i.d.) and larger tube (200 μm i.d.), respectively. The mixtures were combined at the other end of the smaller tube located in the larger tube, generating a water–acetonitrile–ethyl acetate ternary mixed solution as carrier solution: a) annular flow, 2:5:3 (v/v/v) (water–acetonitrile, 3:2 and acetonitrile–ethyl acetate, 11:9); and b) sluggish flow, 2:4:3 (v/v/v) (water–acetonitrile, 2:1 and acetonitrile–ethyl acetate, 1:1). An analyte solution of 1-naphthol and 2,6-naphthalenedisulfonic acid (1 mM each) was prepared using the water–acetonitrile mixed solution. The analyte solution was directly introduced into the smaller capillary inlet using the gravity method (20 cm height for 20 s; ca. 0.9 mL). Following analyte injection, the capillary inlet was connected through a joint to a microsyringe on the microsyringe pump. The mixed solutions were fed to the capillary tubes at constant flow rates of 2.5 $\mu\text{L min}^{-1}$ (smaller tube) and 5.0 $\mu\text{L min}^{-1}$ (larger tube) under laminar flow conditions. Fluorescence detection of the analytes was performed with on-line capillary (effective length, 140 cm) using excitation (ex.) and emission (em.) wavelengths of 290 nm and 355 nm, respectively. The fluorescence in the larger capillary tube was monitored at approximately 140 cm from the smaller capillary outlet using a fluorescence microscope equipped with an Hg lamp, a filter, and a CCD camera.

Results and discussion

Figure 2 shows the phase diagram of the ternary water–acetonitrile–ethyl acetate mixed solvent. The diagram included the boundary curve between the homogeneous (single phase) and heterogeneous (two phases) regions. The component volume ratios of the ternary water–acetonitrile–ethyl acetate solution 2:5:3 and 2:4:3, as shown in Fig. 2, are denoted as a) and b), respectively. The mixed heterogeneous solutions a) and b) comprised an upper (organic solvent-rich) and lower (water-rich) phase solution in a batch vessel.

The water–acetonitrile and acetonitrile–ethyl acetate mixed solutions were respectively fed to the capillary tubes and combined to give the ternary water–acetonitrile–ethyl acetate solution in the larger tube. Fluorescence photographs of the ternary mixed solutions a) and b) in the larger capillary tube are shown in Fig. 3. The blue region corresponding to perylene (hydrophobic) revealed the organic solvent-rich solution and the green region corresponding to Eosin Y (hydrophilic) revealed the water-rich solution. As observed in Fig. 3, the heterogeneous solution a), whose component ratio is located near the boundary curve in the phase diagram, displayed two phases i.e., inner (blue, organic solvent-rich) and outer (yellow–green, water-rich) phases, generating an annular flow. In contrast, the heterogeneous solution b) resulted in two phases positioned along the axial direction, generating an organic

solvent-rich sluggish domain (ca. 510 μm length) and a water-rich continuous phase (ca. 150 μm length), resulting in a sluggish flow.

Separation of model analytes 1-naphthol and 2,6-naphthalenedisulfonic acid using the present system featuring an annular and sluggish flow system was investigated. The obtained chromatograms are shown in Fig. 4. 1-Naphthol and 2,6-naphthalenedisulfonic acid were separated and detected in that order, with both types of flows featuring microfluidic behaviors. The linear velocities in the tube are expressed as a parabolic function under laminar flow conditions. The outer phase of the annular flow of solution a) and the partial outer phase of the sluggish flow of solution b) moved at a very slow rate in the tube, and the outer phase acted as a pseudo-stationary phase in the current chromatography separation system. Hydrophobic 1-naphthol and hydrophilic 2,6-naphthalenedisulfonic acid were distributed in the organic solvent-rich inner phase region or sluggish region and in the water-rich outer phase region (pseudo-stationary phase), respectively. Consequently, 1-naphthol was eluted first at an average linear velocity and 2,6-naphthalenedisulfonic acid was subsequently eluted at a lower velocity than the average linear velocity, providing base-line separation on the chromatograms. The difference in separation performance between a) and b) in Fig. 4 may be caused by the difference of the component ratios of the solvents in the inner and outer phases.

The annular flow was successfully generated in a microspace using the ternary mixed heterogeneous solution water–acetonitrile–ethyl acetate. The inner and outer phase formation mechanism in a heterogeneous solution using an annular flow is relatively different from that in a homogenous solution under the TRDP. However, both systems are expected to feature the same chromatography separation mechanism. On the other hand, separation of the analytes in the sluggish flow was unexpected. Tentatively, we examined resolutions, theoretical plate numbers, and the height of equivalent theoretical plate for 2,6-naphthalenedisulfonic acid in the present system under sluggish flow conditions and varying capillary tube lengths (70, 105, 140, and 175 cm). 1-Naphthol and 2,6-naphthalenedisulfonic acid were separated and detected in that order, regardless of the capillary tubes studied under sluggish flow conditions. Separation systems employing capillary tube lengths of 70, 105, 140, and 175 cm achieved resolutions of 5.8, 8.0, 8.2, and 12, respectively. The corresponding theoretical plate numbers were 2400, 4000, 5600, and 6800. The associated height of the equivalent theoretical plate values were 0.23, 0.21, 0.19, and 0.20 mm. The resolutions and theoretical plate numbers increased with increasing capillary tube lengths, whereas the height of equivalent theoretical plate values remained mostly constant. These results implied that separation under sluggish flow conditions occurred in a similar way with conventional chromatography which of separation ability was independent of column length.

In conclusion, an annular and sluggish flow system was obtained under microfluidic flow conditions when heterogeneous ternary solution water–acetonitrile–ethyl acetate

was introduced into a capillary tube using a dual capillary tube system featuring different tube inner diameters. First, we would like to emphasize that the annular flow was easily generated in the capillary tube using the present system. Secondly, model analytes 1-naphthol and 2,6-naphthalenedisulfonic acid were separated into the outer phase of the annular flow and partial outer phase of the sluggish flow that acted as pseudo-stationary phase in the chromatography separation system. It is interesting to note that separation occurred in both the annular and sluggish flows, generated in a microspace. The current findings present a new concept towards the development of an open-tubular capillary chromatography system without any tube packing or coating requirements.

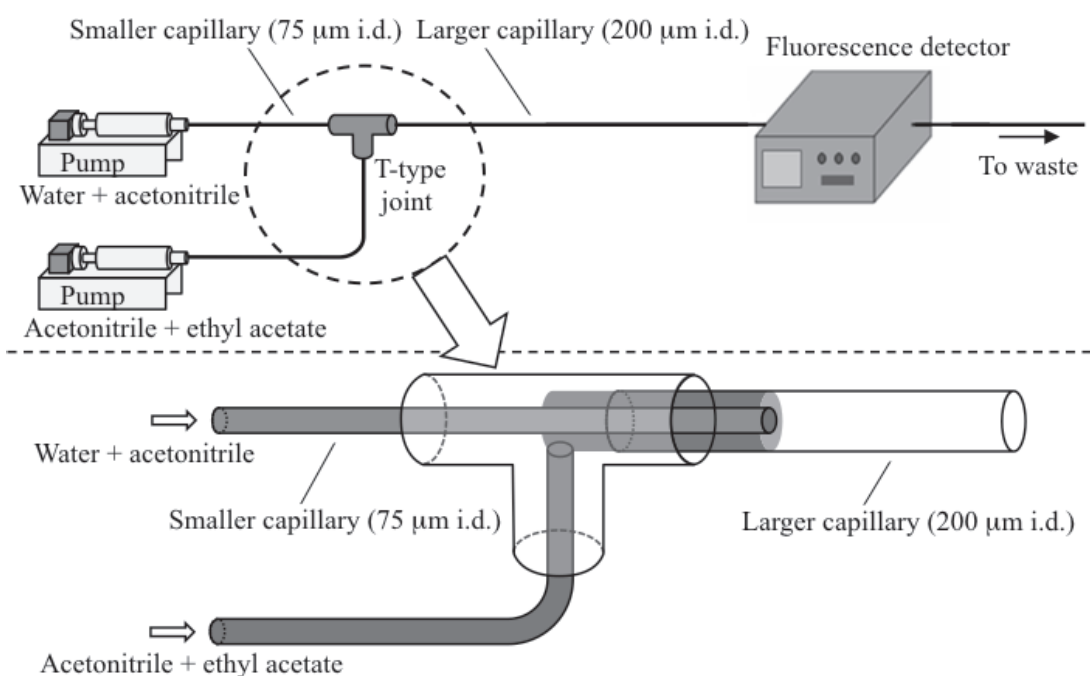


Figure 1. Schematic diagram of the present capillary chromatography system integrating a dual capillary tube system featuring different tube inner diameters.

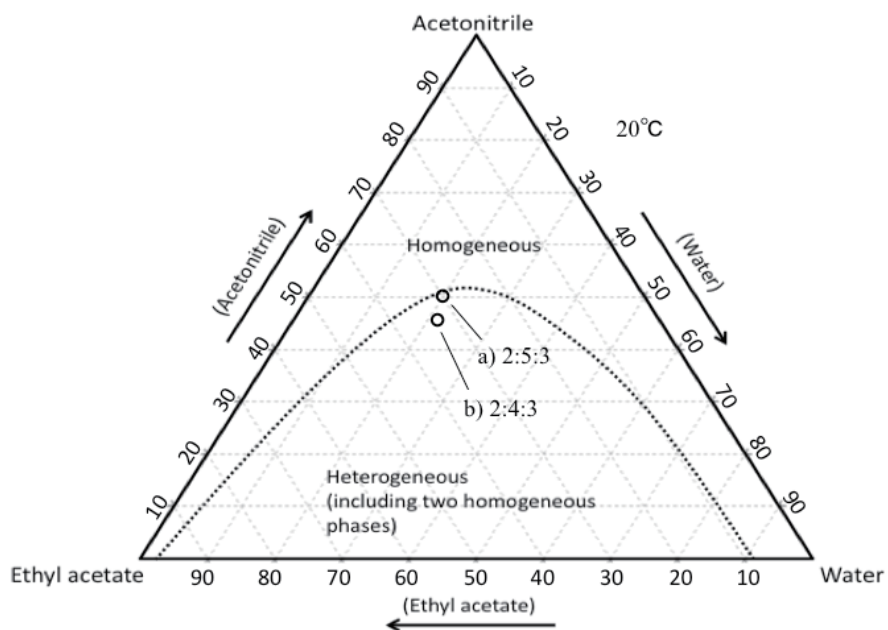


Figure 2. Phase diagram of the ternary water–acetonitrile–ethyl acetate mixed solvent at 20 °C.

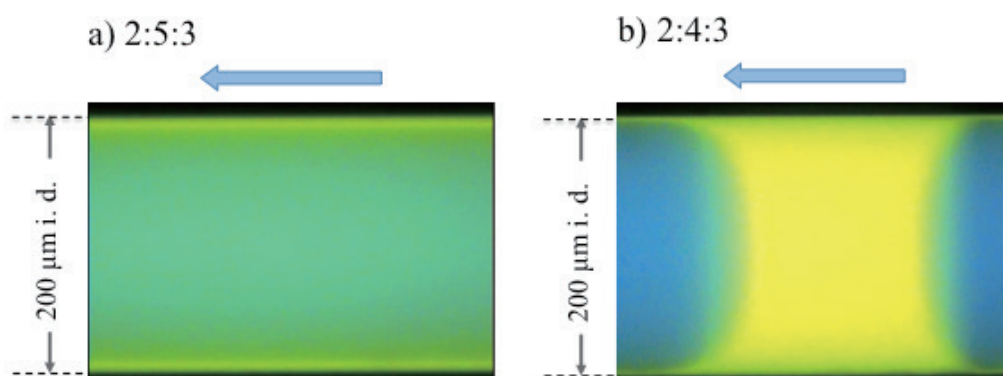


Figure 3. Fluorescence photographs of ternary water–acetonitrile–ethyl acetate mixed solution at volume ratios of a) 2:5:3 and b) 2:4:3.

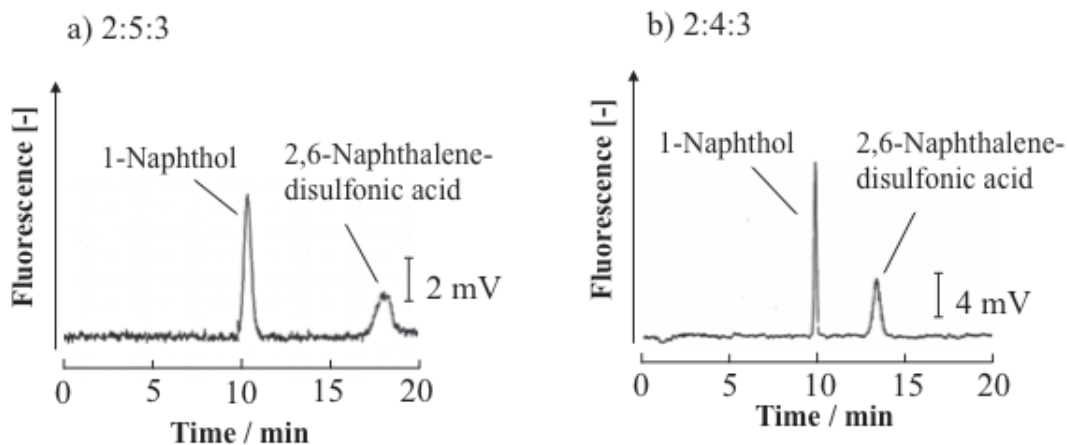


Figure 4. Chromatograms of 1-naphthol and 2,6-naphthalenedisulfonic acid mixtures obtained with the present system. The volume ratios of the ternary water–acetonitrile–ethyl acetate carrier solution are (a) 2:5:3 and (b) 2:4:3. The separation effective distance between the smaller capillary outlet and the detection point is 140 cm.

14.4 Microfluidic inverted flow of aqueous and organic solvent mixed solution in a microchannel

When two solutions are individually fed into two separated microchannels of a microchip that combine to form a single channel of a Y-type microchannel, the flows in the single channel are either parallel for immiscible solutions or initially parallel but become homogeneous through diffusion for miscible solutions. Nevertheless, a new type of microfluidic behavior was seen in the Y-type microchannel that was neither parallel nor homogeneous flow. Water-acetonitrile and acetonitrile-ethyl acetate mixtures, each marked by a distinctive dye, were delivered at the same flow rate into the Y-type microchannel under laminar flow conditions. Under different volume ratio mixtures, the two phases in the single channel were initially observed to flow in parallel but then swapped over to the opposite wall while still retaining parallel flow. We call this type of laminar flow “microfluidic inverted flow”.

Introduction

The development of the micro-total analysis system (μ -TAS) that includes microchip or microfluidic device technology is a very interesting aspect of analytical science [1,2]. Microfluidic solvents exhibit various fluidic behaviors in microchannels. Their flow patterns have been examined by varying the channel configuration and flow rate of the solvents, using aqueous–organic solvent mixtures, and introducing specific obstacles into microchannels [3,25,26]. Fluidic flow of solvents in microchannels is related to separation, diffusion, and reaction of solutes. Information regarding their microfluidic flow and interface formation is important and useful in designing microreactors or μ -TAS [1-3,25,26].

Various types of mixed solutions of aqueous–organic solvents are used in dissolution, cleaning, preservation, and as reaction solvents. Such mixtures are also useful in separation science [11,12,27]. However, to our knowledge, the use of ternary mixed solvents of water–hydrophilic/hydrophobic-organic solvents has not been examined in detail. When such ternary mixed solvents were fed into the microspace under laminar flow conditions, the solvent molecules radially disperse in the microspace through a phase transformation; this microfluidic behavior we call the tube radial distribution phenomenon (TRDP).

Here, the microfluidic behavior of two combining mixtures, water–acetonitrile and acetonitrile–ethyl acetate, was examined under the fluorescence of dyes Eosin Y (green) and perylene (blue) in the respective solutions. A microchip fabricated with a Y-type microchannel was used, in which two separated channels, labeled channels T1 and T2, combined to form a single channel, labeled channel S (see Fig. 1). Each channel was 100 μm wide \times 40 μm deep. The two mixtures to be combined were fed into the two separated channels. In the single channel, the combined mixture developed a specific fluidic behavior, i.e., microfluidic inverted flow, which depended on the solvents.

Experimental

The water–acetonitrile mixture (20:30 volume ratio) containing 2.0 mM Eosin Y and acetonitrile–ethyl acetate mixture (20:30 volume ratio) containing 0.2 mM perylene were fed at the same flow rate into channels T1 and T2, respectively, using a microsyringe pump. A microscope–CCD camera system was set-up to observe fluorescence from the dyes, Eosin Y and perylene, which emit light at 470 nm (green) and 550 nm (blue), respectively. The fluorescence was monitored near the combining point and in channel S using a fluorescence microscope equipped with an Hg lamp, a filter, and a CCD camera. The blue and green fluorescence images give a clear separation of the two flows. A distinctive feature to be noted is the microfluidic inverted flow in the Y-type microchannel with the water–acetonitrile and acetonitrile–ethyl acetate mixed solutions (Fig. 1); the flow conditions are indicated in figure captions. This inverted flow was unobserved with water and water, acetonitrile and acetonitrile, ethyl acetate and ethyl acetate, water and acetonitrile mixtures, as well as acetonitrile and ethyl acetate mixed solutions (miscible solutions); each of these combinations initially exhibited parallel flow and then homogeneous flow. The immiscible solutions of water and ethyl acetate mixtures produced parallel or sluggish flow, never inverted flow, in the Y-type microchannel. Only the ternary mixed solvent of water, acetonitrile, and ethyl acetate could bring about “microfluidic inverted flow”. This information will be useful for clarifying the creation of “microfluidic inverted flow” in the future.

Results and discussion

Here, with respect to our previous work on ternary mixed solvents of water-acetonitrile-ethyl acetate, we tentatively examined the composition ratios near the boundary curve in the phase diagram of the water-acetonitrile-ethyl acetate mixed solution (Fig. 2). The compositions of the water-acetonitrile-ethyl acetate mixed solutions were A; 14:43:43, B; 20:50:30, C; 43:43:11, and D; 52:37:11. The water-acetonitrile and acetonitrile and ethyl acetate mixed solutions were mixed so that compositions of A–F were produced in channel S. Mixed solutions with compositions A, B, and C (organic solvent-rich solutions) showed microfluidic inverted flow, whereas those of D, E, and F (water-rich solutions) exhibited a parallel-to-homogeneous flow evolution. Reasons for the microfluidic inverted flow for these mixed solutions remain unclarified.

Furthermore, we examined the effects of flow rates and channel lengths on the microfluidic inverted flow; the conditions are given in the captions. The fluorescence images were observed around the mixing point and in channel S at distances 1, 2, and 3 cm from the mixing point with flow rates 10, 20, and 100 $\mu\text{L min}^{-1}$ (Fig. 3). As flow rate increased, we observed various stages of inverted flow in the channel. Fig. 4 shows the inverted flow in a long single microchannel in a Y-type microchip. We also observed inverted flow in a long wooden microchannel.

Finally, we had a microchip fabricated that included three connecting Y-type mixing points (Fig. 5). The water-acetonitrile and acetonitrile-ethyl acetate mixed solutions

were fed into the microchannels via two of the Y-type microchannels (Fig. 5); see caption for conditions. Downstream from the first two Y-type mixing points, microfluidic inverted flows formed in the individual channels; the composition ratio of the water-acetonitrile-ethyl acetate was 20:50:30 in these sections of the channels. Subsequently, the two inverted flows were mixed at the third Y-type mixing point, from which TRDP formed in the microchannel; the composition ratio after mixing was 20:50:30 in this section channel. This unique microfluidic flow, evident in Fig. 5, has never been created in a microchannel by any other technique. Such a novel microfluidic flow pattern or liquid-liquid interface formation might lead to innovation of separation, extraction, mixing, and chemical reaction in a microspace.

In conclusion, ternary solvents of water–acetonitrile–ethyl acetate mixtures in a single channel were prepared by combining a water–acetonitrile mixture and an acetonitrile–ethyl acetate mixture fed from two separated channels in a Y-type microchannel of a microchip. A microfluidic inverted flow was a specific and interesting flow seen from the mixing of particular compositions of solvents in a single channel. This unique inverted flow was produced with the ternary mixed solvent of combining the two mixtures. The specific microfluidic flow was not observed using two-component solvents, i.e., a water–acetonitrile mixture or a water–ethyl acetate mixture. The data of the inverted flow, visualized under dye fluorescence are expected to be useful in developing a mixing technique to create a phase interface and a chemical reaction space in the microspace of a microchip.

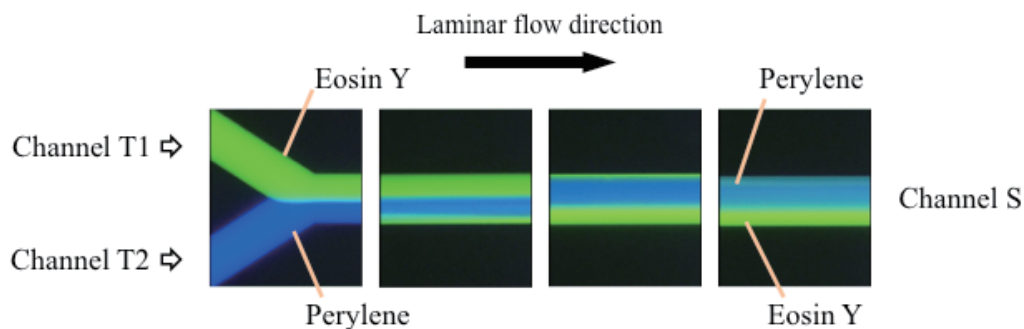


Figure 1. Typical microfluidic inverted flow observed in channel S of a Y-type microchannel. Channel T1, 2.0 mM Eosin Y dissolved in water-acetonitrile (20:30, v/v) and channel T2, 0.2 mM perylene dissolved in acetonitrile-ethyl acetate (20:30, v/v). Flow rate, $10 \mu\text{L min}^{-1}$ each at 20°C .

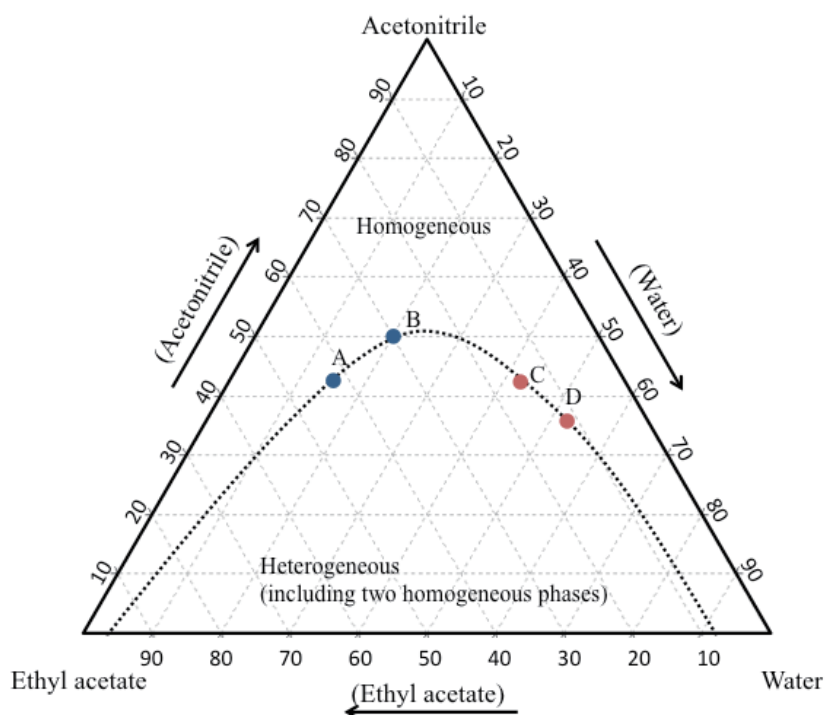


Figure 2. Phase diagram of ternary mixed solvents of water-acetonitrile-ethyl acetate mixture. The curve represents the boundary between homogeneous (single phase) and heterogeneous (two phases). The component ratios of water-acetonitrile-ethyl acetate; A; 14:43:43 B; 20:50:30, C; 43:43:14, and D; 52:37:11. 20°C .

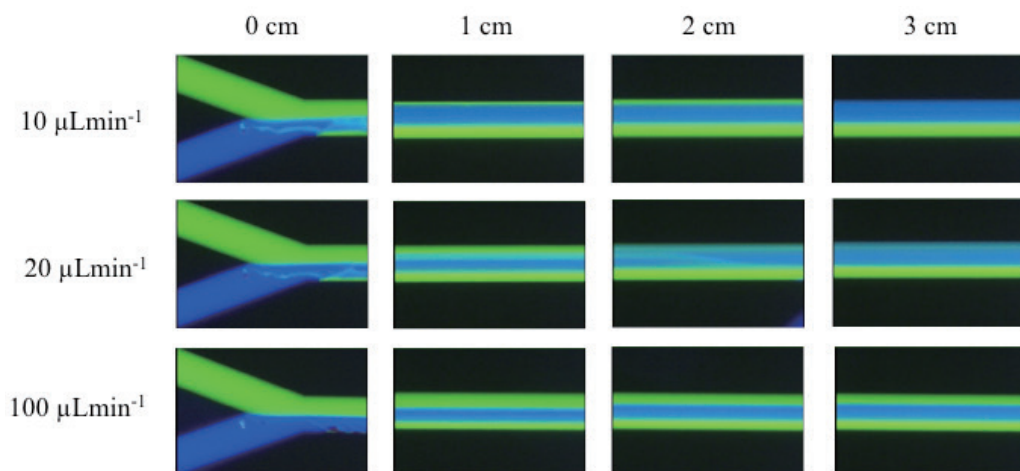


Figure 3. Effects of flow rate on the microfluidic inverted flow in channel S. Conditions in channels T1 and T2 are the same as in Fig. 1. 20 °C.

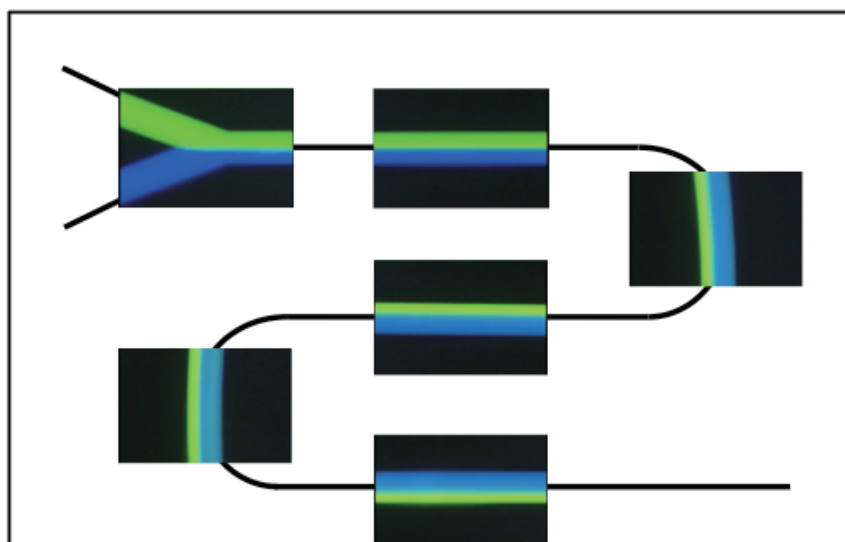


Figure 4. Effect of single-microchannel length on the microfluidic inverted flow in channel S. Conditions in channels T1 and T2 are the same as in Fig. 1. 20 °C. The single microchannel length is 12 cm and included the two bends.

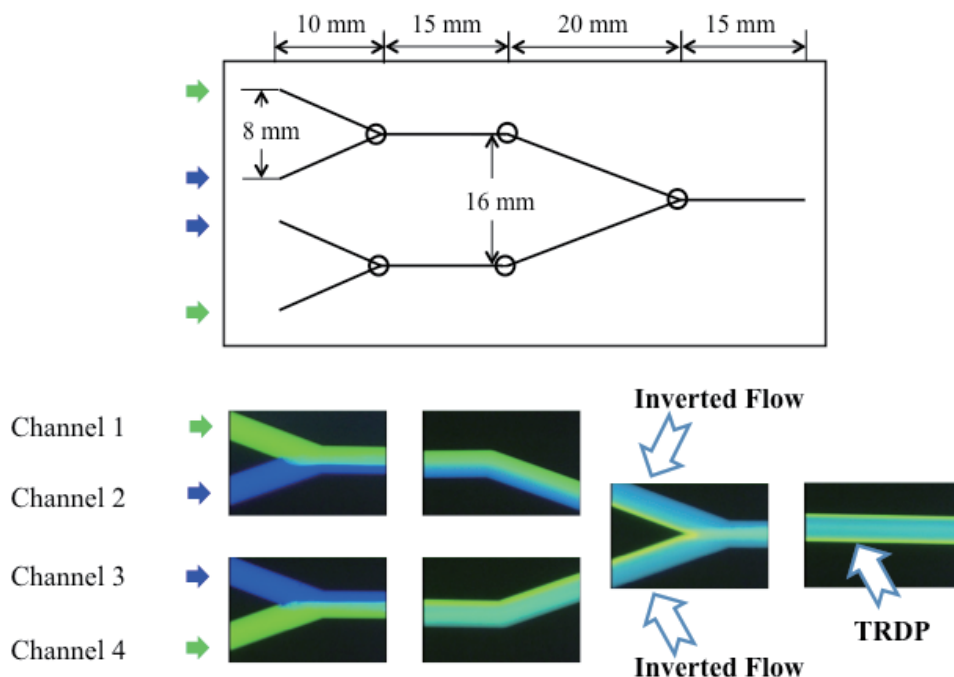


Figure 5. Schematic diagram of a microchip with three Y-type mixing points in the microchannel. Conditions in channels 1 and 4 are the same as in channel T1 of Fig. 1; channels 2 and 3 have the same conditions as for channel T2 in Fig. 1. Flow rate is 2.0 $\mu\text{L min}^{-1}$ each at 20 °C.

References

- [1] D. R. Reyes, D. Iossifidis, P. A. Auroux, and A. Manz, *Anal. Chem.*, **2002**, *74*, 2623.
- [2] P. J. Asiello and A. J. Baeumner, *Lab Chip*, **2011**, *11*, 1420.
- [3] A. Aota, A. Hibara, Y. Sugii, and T. Kitamori, *Anal. Sci.*, **2012**, *28*, 9.
- [4] A. Günther and K. F. Jensen, *Lab Chip*, **2006**, *6*, 1487.
- [5] T. Kitamori, M. Tokeshi, A. Hibara, and K. Sato, *Anal. Chem.*, **2004**, *76*, 52A.
- [6] J. G. Kralj, H. R. Sahoo, and K. F. Jensen, *Lab Chip*, **2007**, *7*, 256.
- [7] G. Hefter, *Pure Appl. Chem.*, **2005**, *77*, 605.
- [8] J. Niu and B. E. Conway, *J. Electroanal. Chem.*, **2003**, *546*, 59.
- [9] D. M. Ruiz and R. E. De Castro, *J. Ind. Microbiol. Biotechnol.*, **2007**, *34*, 111.
- [10] H. Ogino, K. S. Siddiqui, and T. Thomas, “*Protein Adaptation in Extremophiles*”, **2008**, Nova Science Publishers, Inc., New York.
- [11] M. K. Yeh, S. L. Lin, M. I. Leong, S. D. Huang, and M. R. Fuh, *Anal. Sci.*, **2011**, *27*, 49.

- [12] T. Maruyama, H. Matsushita, J. Uchida, F. Kubota, N. Kamiya, and M. Goto, *Anal. Chem.*, **2004**, *76*, 4495.
- [13] X. Wang, X. Lin, Z. Xie, and J. P. Giesy, *J. Chromatogr., A*, **2009**, *1216*, 4611.
- [14] I. Mikšik and P. Sedláková, *J. Sep. Sci.*, **2007**, *30*, 1686.
- [15] M. C. Jung, N. Munro, G. Shi, A. C. Michael, and S. G. Weber, *Anal. Chem.*, **2006**, *78*, 1761.
- [16] J. Urban and P. Jandera, *J. Sep. Sci.*, **2008**, *31*, 2521.
- [17] K. Otsuka and S. Terabe, *Trends Anal. Chem.*, **1993**, *12*, 125.
- [18] R. Koike, F. Kitagawa, and K. Otsuka, *J. Sep. Sci.*, **2009**, *32*, 399.
- [19] M. Tabata, Y. G. Wu, T. Charoenraks, and S. S. Samaratunga, *Bull. Chem. Soc. Jpn.*, **2006**, *79*, 1742.
- [20] T. Charoenraks, M. Tabata, and K. Fujii, *Anal. Sci.*, **2008**, *24*, 1239.
- [21] H. Foroughi and M. Kawaji, *Int. J. Multiphase Flow*, **2011**, *37*, 1147.
- [22] E. V. Rebrov, T. A. Nijhuis, M. T. Kreutzer, V. Hessel, and J. C. Schouten, *Ind. Eng. Chem. Res.*, **2012**, *51*, 1015.
- [23] M. Kashid and L. K. -Minsker, *Chem. Eng. Proces.*, **2011**, *50*, 972.
- [24] A. Ghaini, A. Mescher, and D. W. Agar, *Chem. Eng. Sci.*, **2011**, *66*, 1168.
- [25] M. Maeki, S. Yoshizuka, H. Yamaguchi, M. Kawamoto, K. Yamashita, H. Nakamura, M. Miyazaki, H. Maeda, *Anal. Sci.*, **2012**, *28*, 65.
- [26] N. Kaji, Y. Okamoto, M. Tokeshi, and Y. Baba, *Chem. Soc. Rev.*, **2010**, *39*, 948.
- [27] F. Torrens, *Chromatographia*, **2001**, *53*, 199.

Conclusions

Investigating the microfluidic behaviors of solvents is essential towards the design of highly efficient microreactors or micro-total analysis systems, since the microfluidic behavior of solvents in a microchannel is related to the separation, diffusion, and reaction of the solutes. In this book, we discussed an interesting and unique microfluidic behavior featured by mixed solvents confined in a microspace that we recently reported, and coined as TRDP. TRDP was observed in diverse mixed solvents systems, such as ternary water–hydrophilic/hydrophobic organic solvents, water–surfactant, water–ionic liquid, water-hydrophilic solvents containing salts, and fluoruous/organic solvents. The development of TRDP in a ternary mixed solvent solution instigated a two-phase separation system that was successfully exploited for chromatography separation, extraction, and mixing processes as well as for initiating chemical reactions. The respective developed TRDP-based systems showed great promise as efficient microreactors and micro-total analysis systems.

A list of the TRDP-related manuscripts reported by the author's group in chronological order

The part of this book is constructed and rewritten based on the following manuscripts together with new data and consideration.

¹⁾ Micro-Flow Separation System Using an Open Capillary Tube That Works under Laminar Flow Conditions; Naoya Jinno, Masahiko Hashimoto, and Kazuhiko Tsukagoshi, *Analytical Sciences*, **25**, 145-147 (2009).

²⁾ Capillary Chromatography Based on Tube Radial Distribution of Aqueous-Organic Mixture Carrier Solvents; Naoya Jinno, Minoru Itano, Masahiko Hashimoto, and Kazuhiko Tsukagoshi, *Talanta*, **79**, 1348-1353 (2009).

³⁾ Capillary Chromatography Based on Tube Radial Distribution of Aqueous-Organic Mixture Carrier Solvents: Elution Behavior of Carboxylated Polymer Particles in the System; Naoya Jinno, Masahiko Hashimoto, and Kazuhiko Tsukagoshi, *Journal of Chemical Engineering of Japan*, **42**, 767-770 (2009).

⁴⁾ Capillary Chromatography Based on Tube Radial Distribution of Aqueous-Organic Mixture Carrier Solvents: Effect of the Inner Wall Characteristics of the Fused-Silica Tube on Separation Performance; Naoya Jinno, Ko Hashimoto, Masahiko Hashimoto, and Kazuhiko Tsukagoshi, *Analytical Sciences*, **25**, 1369-1371 (2009).

- 5) Capillary Chromatography Based on Tube Radical Distribution of Aqueous-Organic Mixture Carrier Solvents: Introduction of Inner-Wall-Modified Capillary tube; Naoya Jinno, Katsuya Tsuji, Kaoru Shikatani, Masahiko Hashimoto, and Kazuhiko Tsukagoshi, *Journal of Separation Science*, **32**, 4099-4100 (2009).
- 6) Distribution of Fluorescent Dyes Dissolved in Ternary Mixed Solvent in a Micro-Channel under Laminar Flow Conditions; Mari Murakami, Naoya Jinno, Masahiko Hashimoto, Kazuhiko Tsukagoshi, *Chemistry Letters*, **39**, 272-273 (2010).
- 7) Capillary Chromatography Based on Tube Radial Distribution of Aqueous–Organic Mixture Carrier Solvents: Introduction of Double Tubes Having Different Inner Diameters to the System; Koju Yamada, Naoya Jinno, Masahiko Hashimoto, and Kazuhiko Tsukagoshi, *Analytical Sciences*, **26**, 507-510 (2010).
- 8) Separation of Optical Isomers in Capillary Chromatography Using a Poly(tetrafluoroethylene) Capillary Tube and an Aqueous-Organic Mixture Carrier Solution; Seiji Ishimoto, Naoya Jinno, Masahiko Hashimoto, and Kazuhiko Tsukagoshi, *Analytical Sciences*, **26**, 641-643 (2010).
- 9) Elution Behavior of Proteins in Capillary Chromatography Using an Untreated Fused-silica Capillary Tube and a Water-Hydrophilic-Hydrophobic Organic Mixture Carrier Solvent; Yuji Masuhara, Naoya Jinno, Masahiko Hashimoto, and Kazuhiko Tsukagoshi, *Chemistry Letters*, **39**, 688-689 (2010).
- 10) Analytical Conditions and Separation performance of Capillary Chromatography Based on the Tube Radical Distribution of Aqueous -Organic Mixture Carrier Solvents under Laminar–Flow Conditions; Naoya Jinno, Mari Murakami, Masahiko Hashimoto, and Kazuhiko Tsukagoshi, *Analytical Sciences*, **26**, 737-742 (2010).
- 11) Introduction of fluorescence and chemiluminescence detection to capillary chromatography based on tube radial distribution of water–hydrophilic–hydrophobic organic mixture carrier solvents; Seiji Ishimoto, Yudai Kudo, Naoya Jinno, Masahiko Hashimoto and Kazuhiko Tsukagoshi, *Analytical Methods*, **2**, 1377-1381 (2010).
- 12) Temperature Effect on Separation Performance in Capillary Chromatography based on Tube Radial Distribution of Aqueous-Organic Mixture Carrier Solvents; Naoya Jinno, Masahiko Hashimoto, and Kazuhiko Tsukagoshi, *The Science and Engineering Review of Doshisha University*, **51**, 168-172 (2010).
- 13) Metal Compound Analysis by Capillary Chromatography Using an Untreated Capillary Tube and Water-Hydrophilic-Hydrophobic Solvent Mixture as a Carrier Solution; Kazuma Yoshida, Naoya Jinno, Masahiko Hashimoto, and Kazuhiko Tsukagoshi, *The Science and Engineering Review of Doshisha University*, **51**, 198-201 (2011).
- 14) Fluorescence Observation Supporting Capillary Chromatography Based on Tube Radial Distribution of Carrier Solvents under Laminar Flow Conditions; Naoya Jinno, Mari Murakami, Kiyoshi Mizohata, Masahiko Hashimoto, and Kazuhiko Tsukagoshi,

Analyst, **136**, 927-932 (2011).

¹⁵⁾ Experimental Consideration of Capillary Chromatography Based on Tube Radial Distribution of Ternary Mixture Carrier Solvents under Laminar Flow Conditions; Naoya Jinno, Masahiko Hashimoto, and Kazuhiko Tsukagoshi, *Analytical Sciences*, **27**, 259-264 (2011).

¹⁶⁾ Extraction of Cu(II) Based on Tube Radial Distribution of Ternary Mixed Carrier Solution in Microchannels; Naoya Jinno, Masahiko Hashimoto, and Kazuhiko Tsukagoshi, *Chemistry Letters*, **40**, 654-655 (2011).

¹⁷⁾ Tube Radial Distribution Phenomenon of Ternary Mixed Solvents in a Microspace under Laminar Flow Conditions; Mari Murakami, Naoya Jinno, Masahiko Hashimoto, Kazuhiko Tsukagoshi, *Analytical Sciences*, **27**, 793-798 (2011).

¹⁸⁾ Derivatization of a Protein with Fluorescamine Utilizing the Tube Radial Distribution Phenomenon of Ternary Mixed Carrier Solvents in a Capillary Tube; Yuji Masuhara, Naoya Jinno, Masahiko Hashimoto, and Kazuhiko Tsukagoshi, *Chemistry Letters*, **40**, 804-805 (2011).

¹⁹⁾ Use of Tube Radial Distribution of Ternary Mixed Carrier Solvents for Introduction of Absorption Reagent for Metal Ion Separation and On-Line Detection into Capillary; Satoshi Fujinaga, Naoya Jinno, Masahiko Hashimoto, and Kazuhiko Tsukagoshi, *Journal of Separation Science*, **34**, 2833-2839 (2011).

²⁰⁾ Components of the Carrier Solvents and Separation Performance in the Tube Radial Distribution Chromatography Using a Fused-Silica Capillary tube; Naoya Jinno, Yoichiro Hashimoto, Masahiko Hashimoto, and Kazuhiko Tsukagoshi, *The Science and Engineering Review of Doshisha University*, **52**, 177-180 (2011).

²¹⁾ Influences of Analyte Injection Volumes and Concentrations on Capillary Chromatography Based on Tube Radial Distribution of Carrier Solvents under Laminar Flow Conditions; Yusuke Tanigawa, Naoya Jinno, Masahiko Hashimoto, and Kazuhiko Tsukagoshi, *Chromatographia*, **32**, 135- 140 (2011).

²²⁾ Effects of Tube Materials on Capillary Chromatography Based on Tube Radial Distribution of Ternary Mixture Carrier Solvents under Laminar Flow Conditions; Yudai Kudo, Naoya Jinno, Masahiko Hashimoto, and Kazuhiko Tsukagoshi, *Chromatographia*, **75**, 417-421 (2012).

²³⁾ Tentative Comparison of Tube Radial Distribution Chromatography and CZE; Kisuke Tabata, Naoya Jinno, Keiichi Noda, Masahiko Hashimoto, Kazuhiko Tsukagoshi, *Chromatographia*, **75**, 423-428 (2012).

²⁴⁾ Separation of Dansyl-DL-Amino Acids by Open Tubular Capillary Chromatography Based on Tube Radial Distribution Phenomenon of the Ternary Mixed Carrier Solvents; Yudai Kudo, Hyo Kan, Naoya Jinno, Masahiko Hashimoto and Kazuhiko Tsukagoshi, *Analytical Methods*, **4**, 906-912 (2012).

- ²⁵⁾ Biomolecule Analyses in an Open-Tubular Capillary Chromatography Using Ternary Mixed Carrier Solvents with Chemiluminescence Detection; Naoya Takahashi, Yuji Masuhara, Naoya Jinno, Masahiko Hashimoto, and Kazuhiko Tsukagoshi, *Analytical Sciences*, **28**, 351-357 (2012).
- ²⁶⁾ Mixing Process of Ternary Solvents Prepared through Microchannels in a Microchip under Laminar Flow Conditions; Kei Nishiyama, Naoya Jinno, Masahiko Hashimoto, and Kazuhiko Tsukagoshi, *Analytical Sciences*, **28**, 423-427 (2012).
- ²⁷⁾ Experiments and Considerations through the Phase Diagram in Open Tubular Capillary Chromatography Based on Tube Radial Distribution of Ternary Mixed Solvents Using a Fused-Silica Capillary Tube; Yusuke Tanigawa, Naoya Jinno, Masahiko Hashimoto, Kazuhiko Tsukagoshi, *American Journal of Analytical Chemistry*, **3**, 300-3005 (2012).
- ²⁸⁾ The Micro-Flow Reaction System Featured the Liquid-Liquid Interface Created with Ternary Mixed Carrier Solvents in a Capillary Tube; Yuji Masuhara, Naoya Jinno, Masahiko Hashimoto, and Kazuhiko Tsukagoshi, *Analytical Sciences*, **28**, 439-444 (2012).
- ²⁹⁾ Consideration of the Tube Radial Distribution of the Carrier Solvents in a Capillary Tube under Laminar Flow Conditions and Computer Simulation; Naoya Jinno, Yuji Masuhara, Tomoya Kobayashi, Naoya Takahashi, Yusuke Tanigawa, Masahiko Hashimoto, and Kazuhiko Tsukagoshi, *Analytical Sciences*, **28**, 527-530 (2012).
- ³⁰⁾ Elution Behavior of Lambda-DNA with Ternary Mixed Carrier Solvents in an Open-Tubular Capillary under Laminar Flow Conditions; Takahiro Nogami, Satoshi Fujinaga, Naoya Jinno, Masahiko Hashimoto, and Kazuhiko Tsukagoshi, *Analytical Sciences*, **28**, 617-620 (2012).
- ³¹⁾ Study of Outer Phases in Capillary Chromatography Based on Tube Radial Distribution of Carrier Solvents under Laminar Flow Conditions; Naoya Jinno, Mari Murakami, Kiyoshi Mizohata, Masahiko Hashimoto, and Kazuhiko Tsukagoshi, *Journal of Liquid Chromatography & Related Technologies*, **35**, 1750–1766 (2012).
- ³²⁾ Microfluidic Behavior of Ternary Mixed Carrier Solvents Based on the Tube Radial Distribution in Triple-Branched Microchannels in a Microchip; Naoya Jinno, Masahiko Hashimoto, Kazuhiko Tsukagoshi, *Journal of Analytical Sciences, Methods and Instrumentation*, **2**, 49-53 (2012).
- ³³⁾ Fluidic Behavior of Polymer Compounds in an Open-Tubular Capillary with Ternary Mixed Carrier Solvents under Laminar Flow Conditions; Takahiro Nogami, Satoshi Fujinaga, Masahiko Hashimoto, and Kazuhiko Tsukagoshi, *Journal of Flow Injection Analysis*, **29**, 21-24 (2012).

- 34) Influence of Adding Surfactants to an Analyte Solution on Separation Performance in Open-tubular Capillary Chromatography Based on the Tube Radial Distribution of Ternary Mixed Carrier Solvents; Katsuya Unesaki, Masahiko Hashimoto, and Kazuhiko Tsukagoshi, *Chemistry Letters*, **41**, 855-856 (2012).
- 35) Investigation into Tie Lines and Solubility Curves on Phase Diagrams in Open-Tubular Capillary Chromatography Using Ternary Mixed-Carrier Solvents; Yusuke Tanigawa, Satoshi Fujinaga, Masahiko Hashimoto, and Kazuhiko Tsukagoshi, *Analytical Sciences*, **28**, 921-924 (2012)
- 36) Chromatography Using Ternary Water-Acetonitrile-Ethyl Acetate Mixture as a Carrier Solution on a Microchip Incorporating Microchannels; Takafumi Matsuda, Naoya Jinno, Kenichi Yamashita, Hideaki Maeda, Akihiro Arai, Masahiko Hashimoto, and Kazuhiko Tsukagoshi, *Chemistry Letters*, **41**, 1448-1450 (2012).
- 37) Tube Radial Distribution of Solvents Observed in an Aqueous Ionic Liquid Mixed Solution Delivered into a Capillary Tube; Yuki Kawai, Masaharu Murata, Masahiko Hashimoto, and Kazuhiko Tsukagoshi, *Analytical Sciences*, **28**, 1029-1031 (2012).
- 38) Specific microfluidic behavior of ternary mixed carrier solvents of water–acetonitrile–ethyl acetate in open-tubular capillary chromatography and the chromatograms; Satoshi Fujinaga, Katsuya Unesaki, Shigeru Negi, Masahiko Hashimoto, and Kazuhiko Tsukagoshi, *Analytical Methods*, **4**, 3884-3890 (2012).
- 39) Capillary Chromatography Based on Tube Radial Distribution of Ternary Mixed Solvents: Construction of the Phase Diagram and the Separation Performance; Yusuke Tanigawa, Satoshi Fujinaga, Masahiko Hashimoto, and Kazuhiko Tsukagoshi, *The Science and Engineering Review of Doshisha University*, **53**, 167-172 (2013).
- 40) Microchip Chromatography Using an Open-Tubular Microchannel and a Ternary Water-Acetonitrile-Ethyl Acetate Mixture Carrier Solution; Takafumi Matsuda, Kenichi Yamashita, Hideaki Maeda, Masahiko Hashimoto, and Kazuhiko Tsukagoshi, *Journal of Separation Science*, **36**, 965-970 (2013).
- 41) Two-Phase Extraction of Metal Ions Using a Water-Acetonitrile-Ethyl Acetate Ternary Mixed-Solvent Separation System; Naoya Takahashi, Masahiko Hashimoto, and Kazuhiko Tsukagoshi, *Analytical Sciences*, **29**, 665-667 (2013).
- 42) Examination of Tube Radial Distribution Phenomenon and Its Function Appearance; Kazuhiko Tsukagoshi, *Bunseki Kagaku*, **62**, 393-407 (2013).
- 43) Specific Distribution Behavior of a Ternary Mixture of Solvents Fed into Bent and Wound Microchannels in Microchips; Kei Nishiyama, Masaharu Murata, Masahiko Hashimoto, and Kazuhiko Tsukagoshi, *Analytical Sciences*, **29**, 1003-1008 (2013).
- 44) Tube Radial Distribution Phenomenon Observed in an Aqueous Micellar Solution of Non-Ionic Surfactant Fed into a Microspace and Attempt to Capillary Chromatographic

Application; Naoya Jinno, Katsuya Unesaki, Masahiko Hashimoto, and Kazuhiko Tsukagoshi, *Journal of Analytical Chemistry*, **68**, 1197-1202 (2013).

⁴⁵⁾ Fundamental Research and Application of the Specific Fluidic Behavior of Mixed Solvents in a Microspace (Invited Review), Kazuhiko Tsukagoshi, *Analytical Sciences*, **30**, 65-73 (2014).

⁴⁶⁾ Tube Radial Distribution Phenomenon with a Two-phase Separation Solution of a Fluorocarbon and Hydrocarbon Organic Solvent Mixture in a Capillary Tube and Metal Compounds Separation; Koichi Kitaguchi, Naoya Hanamura, Masaharu Murata, Masahiko Hashimoto, and Kazuhiko Tsukagoshi, *Analytical Sciences*, **30**, 687-690 (2014).

⁴⁷⁾ Capillary Chromatography Using an Annular and Sluggish Flow in the Ternary Water–Acetonitrile–Ethyl Acetate System as Carrier Solution; Yuya Hamaguchi, Satoshi Fujinaga, Shunpei Murakami, Masahiko Hashimoto, and Kazuhiko Tsukagoshi, *Chemistry Letters*, **43**, 1318-1320 (2014).

⁴⁸⁾ Open-Tubular Capillary Chromatography Based on Tube Radial Distribution of the Water-Acetonitrile Containing Sodium Chloride Mixture Carrier Solvents; Tomoya Kobayashi, Hyo Kan, Kisuke Tabata, Masahiko Hashimoto, and Kazuhiko Tsukagoshi, *Journal of Liquid Chromatography & Related Technologies*, **38**, 44-53 (2015).

⁴⁹⁾ Investigation of the Composition for a Ternary Solvent System in Tube Radial Distribution Chromatography; Satoshi Fujinaga, Masahiko Hashimoto, and Kazuhiko Tsukagoshi, *Journal of Liquid Chromatography & Related Technologies*, **38**, 600-606 (2015).

⁵⁰⁾ Microflow-Extraction System Using Double Tubes Having Different Inner Diameters in Tube Radial Distribution Phenomenon; Katsuya Unesaki, Masahiko Hashimoto, and Kazuhiko Tsukagoshi, *the Solvent Extraction Research and Development, Japan*, **22**, 87-93 (2015).

⁵¹⁾ Estimation of the Dimensionless Weber Number in Tube Radial Distribution Phenomenon under Laminar Flow Conditions; Satoshi Fujinaga, Masahiko Hashimoto, and Kazuhiko Tsukagoshi, *Journal of Chemical Engineering of Japan*, in pressed

⁵²⁾ Investigation of Inner and Outer Phase Formation in Tube Radial Distribution Phenomenon Using Various Types of Mixed Solvent Solutions; Satoshi Fujinaga, Katsuya Unesaki, Yuki Kawai, Koichi Kitaguchi, Kosuke Nagatanu, Masahiko Hashimoto, Kazuhiko Tsukagoshi, and Jiro Mizushima, *Analytical Sciences*, in pressed

⁵³⁾ Microfluidic Inverted Flow of Aqueous and Organic Solvent Mixed Solution in a Microchannel under Laminar Flow Conditions; Shunpei Murakami, Satoshi Fujinaga, Masahiko Hashimoto, and Kazuhiko Tsukagoshi, *The Science and Engineering Review of Doshisha University*, submitted

Acknowledgements:

This publication was supported by a grant of Doshisha University for research results.

Education and Employment of Professor Kazuhiko Tsukagoshi

(Born : November 5, 1959)

B. S. : Doshisha University (1978-1982)

M. S. : Doshisha University (1982-1984)

Fuji Xerox Corporation: Regular member of research institute (1984-1986)

*D. S. : Doshisha University (1987-1990); Kogaku Hakushi (Doctor of Engineering),
Doshisha University, 1990*

Kyushu University: Research associate (1990-1993)

Kyushu University: Associate Professor (1993-1995)

[Indiana University in USA: Post Doctoral Researcher (1994, one year)]

Doshisha University: Associate Professor (1995-2001)

Doshisha University: Professor (2001-)

The book title; “Investigation of Tube Radial Distribution Phenomenon (TRDP) and Its Function Appearance”

The author name; Kazuhiko Tsukagoshi

The day of publication; September 25, 2015

Printed and published by Kimura Keibunsha,
110 Umezono-cho, Kawashima, Nishikyo-ku, Kyoto 615-8113, Japan
Tel: +81-75-381-9761, Fax: +81-75-381-1510
E-mail: keibunsha@nifty.com